Long-Term impact study for climate change in the shallow unconfined groundwater recharge in Ranger Uranium Mine

Mobashwera Kabir

Submitted to the Faculty of Engineering in fulfilment of the requirement for the Degree of Doctor of Philosophy

Faculty of Engineering, Department of Civil Engineering
Institute of Sustainable Water Resources (ISWR)
Monash University

September 2010

Declaration

I, Mobashwera Kabir, hereby declare that this thesis contains no material which has been accepted for the award of any degree or diploma in any university and that, to the best of my knowledge and belief, contains no material previously published or written by another person, except where due reference is made.

Signed……

Date:……..

Acknowledgements

I am profoundly indebted to my principal supervisor, Dr. Gavin M. Mudd, for his continuous guidance, encouragement and financial support. This is an unusual long journey where he used to continuously support and advise on the wide range of areas from analysing the numerical algorithms to improving the writing skill. I also owe gratitude to other co-supervisors Dr. Anthony R. Ladson and Dr. Edoardo Daly and other academic staff such as E. Weinman and J. Kodikara.

This research has been possible with generous data and other support from Alan Puhalovic from Energy Resources of Australia Limited (ERA) and Richard McAllister from the Office of the Supervising Scientist (OSS). I sincerely acknowledge the additional in-kind support from a range of ERA and OSS staff, as well as Gundjeihmi Aboriginal Corporation (especially Geoff Kyle).

This thesis was completed under an Australian Post-Graduate Award scholarship, courtesy of the Australian Research Council. Minor financial support was also provided by Gundjeihmi Aboriginal Corporation.

I must express my sincere gratitude to a significant number of scientists, researcher and scholars whose publications helped me significantly to initiate, develop and materialise my research. I did receive invaluable technical advices from S. W. Frank from the University of Newcastle, L. V. Alexander, N. Nicholls and Ian Cartwright of Monash University, S. Power and R. Colman of the Bureau of Meteorology, and K. Hennessy and C. Page of CSIRO, whose in-kind advice were critical in the development of my research work.

I would also like to acknowledge the support offered by the statistical services for postgraduate students of School of Mathematical Science of Monash University. I duly recognise the invaluable advice of Dr. Kais Hamza in particular.

Frank Winston from the hydraulics laboratory of Civil Engineering assisted with the preparation of laboratory work for the measurement of soil properties. Godwin Vaz provided invaluable technical support for the installation and use of a range of software. Mehedi Hasan for helping me with the writing the codes for extraction of result from the thousands of XML files to spreadsheet. Also I appreciate the editing services from Elite Editing for their support in formalising the structure, format, and writing style.

I would like to thank many other staff members of the Department of Civil Engineering and Faculty of Engineering for their cooperation at numerous stages of the work. My fellow postgraduate students from Monash University also were very helpful in many regards and shared the joy and pain of the research.

I am certain that without the persistent encouragement of my father I could not finish this research thesis.

I also wish to extent my gratitude to my other friends and associates for their technical, social and moral support.

Finally, I would like to announce my thankfulness to God of all of us, who has blessed me with my family (my husband Sagar, daughter Aishee and son Asif) who were there always my inspiration and everything. Thanks to you all for your contribution which you know better than me definitely!!

Abstract

The principal focus this research work is to model the response of shallow groundwater to changing and varying climatic conditions, using the Ranger uranium mine site as the case study.

There has long been recognised a relationship between shallow groundwater resources and local climatic conditions. The extent of this behaviour and relationship is dependent on seasonal trends, such as summer/winter, wet/dry periods, as well as on the geology, vegetation or other local aspects such as groundwater pumping, possible surface water interactions, etc.

The effect of climate change on water budgets is critical since shallow groundwater is often a vital component in supporting ecosystems and providing water for communities. Furthermore, governments and communities alike are demanding ever higher standards for the isolation of hazardous wastes. Thorough methods are therefore required to assess the effectiveness of different containment options, especially with respect to shallow groundwater behaviour – which in turn depends on climatic conditions.

In order to progress research on this topic, the Ranger uranium mine was adopted as the field site. This was due to two principal reasons – first, it has abundant data available; and second, but perhaps most crucially, the Ranger site is legally required to rehabilitate its tailings so that there are no environmental impacts from solutes for 10,000 years. The primary driver of solute transport in groundwater will be the hydraulic head – which in turn, of course, is strongly influenced by prevailing climatic conditions. Therefore, any assessment of rehabilitation requires a sound approach to modelling the long-term response of groundwater heads to changing and varying climatic conditions.

Therefore, this project has dual primary objectives and significance – firstly in developing more a advanced modelling framework for predicting the response of shallow groundwater to changing and varying climatic conditions, and secondly, in developing a sound technical basis to predict the long-term performance of the rehabilitation of the Ranger uranium mine.

After performing a wide-ranging review on the field of groundwater-climate relationships, with a main focus on modelling approaches to date, a review of the Ranger uranium mine and associated information was done. A detailed analysis of the climate and hydrology of

the Ranger area using various methods or models to quantify the principal components of the hydrologic cycle was performed. It was established that climate influencing groundwater recharge would be best represented by rainfall (R) minus actual evapotranspiration (AAET) – herein called 'net flux'. Time series statistics, a non-physics based approach, was used to model past climate-groundwater behaviour and make predictions about future groundwater response. This method is rarely used in groundwater research, and is a useful contrast to physical/numerical models.

A complex approach was developed and applied to generate future climate data sets, combining the issues as climate change trends from the Intergovernmental Panel on Climate Change (i.e. 5 global climate models and 7 emissions scenarios), climate variability phenomena (eg. El Nino/La Nina, Pacific Decadal Oscillation, Indian Ocean Dipole) and random variability. This leads to hundreds of replicates of 100 year net flux data sets for use in later modelling.

Using 26 years of historical data, an unsaturated flow model using net flux as the boundary condition was developed and calibrated. Models were developed for several groundwater bores, with all results analysed with respect to the primary research objectives. A total of 1,050 models were run, including 30 replicates of each GCM/emissions scenario combination (i.e. 5 GCMs, 7 scenarios and 30 random replicates). All results and the overall modelling are analysed in detail, demonstrating outcomes with respect to the primary research objectives. A major conclusion is that climate variability will clearly be the more dominant factor in governing the response of shallow groundwater heads to climatic conditions.

Overall, this project has developed a more advanced, hydrologically rigorous approach to predicting the response of shallow groundwater heads to climatic conditions. In addition, it has demonstrated a more thorough methodology for predicting the potential performance of the rehabilitation of the tailings from the Ranger uranium project – or any other site where such predictions are crucial in hazardous waste or groundwater management. On both counts, this makes a significant contribution to new knowledge in the field, and should also prove a valuable methodology at other sites with similar issues and needs.

Publications from this research

(The contents of the publications are given in Appendix J)

(Kabir and Mudd 2004; Kabir *et al.* 2006a; Kabir *et al.* 2006b; Kabir *et al.* 2007; Kabir *et al.* 2008a; Kabir *et al.* 2008b; Kabir *et al.* 2008c)

Kabir, M. and G. M. Mudd (2004). Modelling Long-Term Groundwater Rebound and Recharge at Ranger Uranium Mine, Kakadu National Park. Inaugural Australasian Hydrogeology Research Conference, Melbourne, December 2004. Poster Abstract.

Kabir, M., G. M. Mudd and T. Ladson (2006a). Understanding the groundwater recharge process with climate-GWT data. Joint Congress of: 9th Australasian Environmental Isotope Conference and 2nd Australasian Hydrogeology Research Conference. Adelaide, South Australia, Centre for Groundwater Studies.

Kabir, M., G. M. Mudd and T. Ladson (2006b). The application of time series techniques to groundwater and climate relationships. Joint Congress of: 9th Australasian Environmental Isotope Conference and 2nd Australasian Hydrogeology Research Conference. Adelaide, South Australia, Centre for Groundwater Studies.

Kabir, M., G. M. Mudd and A. R. Ladson (2007). Understanding the inconsistencies between two different sources of Morton's AAET data for Ranger Uranium Mine site, Northern Territory, Australia Victorian Universities Earth and Environmental Science Conference. La Trobe University, Bundoora Campus Geological Society of Australia. Abstract No 86.

Kabir, M., K. Hamza, G. M. Mudd and A. R. Ladson (2008a). Groundwater-Climate Relationships, Ranger Uranium Mine, Australia: 1. Time Series Statistical Analyses. Uranium, Mining and Hydrogeology - 5th International Conference, September 2008, Freiberg, Germany.pp 365 - 374.

Kabir, M., G. M. Mudd and A. R. Ladson (2008b). Groundwater-Climate Relationships, Ranger Uranium Mine, Australia: 2. Validation of Unsaturated Flow Modelling. Uranium, Mining and Hydrogeology - 5th International Conference, September 2008, Freiberg, Germany.pp 375 - 382.

Kabir, M., G. M. Mudd and A. R. Ladson (2008c). Groundwater-Climate Relationships, Ranger Uranium Mine, Australia: 3. Predicting Climate Change Impacts. Uranium, Mining and Hydrogeology - 5th International Conference, September 2008, Freiberg, Germany.pp 383 - 392.

List of Acronyms

Acronym	Definition/Description
AA	Advection Aridity
AAET	Areal Actual Evapotranspiration
ACF	Auto Correlation Function
AFFA	Agriculture, Fisheries & Forestry Australia
AHD	Australian Height Datum
AIC	Akaike Information Criterion
AICC	Akaike Information Criterion with Correction
AMO	Atlantic Multi-decadal Oscillation
AOGCM	Atmosphere/ Ocean/ sea-ice General Circulation Models
APET	Areal Potential Evapotranspiration
AR	Auto Regressive
ARMA	Auto Regressive Moving Average
ARR	Alligator Rivers Region
AQUAPAK	Model based on digital filter used to separate the base flow from total flow data of stream flow
AWBM	Australian Water Balance Model
BFI	Base Flow Index
BIC	Bayes Information Criterion
BoM	Bureau of Meteorology
BRANCH	One-dimensional unsteady flow model used in singular riverine or estuarine reaches and in networks or reaches composed of interconnected channels
BREATH	1-dimensional flow simulator for coupled heat and moisture flow. The simulator couples the Richards equation with diffusive vapour transport.
CCF	Cross Correlation Function
CCM1	GCM name outlined in section 7.2.2 of the thesis
CDMR	Cumulative Deviation from Mean Rainfall
CDR	Continuous Discharge Recharge
CLASS	Catchment scale multiple-Land use Atmosphere Soil water and Solute transport model
CLASS U3M	Catchment scale multiple-Land use Atmosphere Soil water and Solute transport Unsaturated Moisture Movement Model
CRAE	Complementary Relationship Areal Evapotranspiration
CRC	Cooperative Research Centre
CRCCH	Cooperative Research Centre for Catchment Hydrology
CRD	Cumulative Rainfall Departure
CRU	Climate Research Unit
CSIRO	Commonwealth Scientific and Industrial Research Organisation
CSIRO Mk2 CSIRO DARLAM	GCM names outlined in section 7.2.2 of the thesis

CVAP	Climate Variability in Agriculture R & D Program
CWD	Cumulative groundWater level Departure
DARLAM	GCM name outlined in section 7.2.2 of the thesis
DBM	Data Based Mechanistic Model
DMM	Daily Monthly Mixed
DPC	Dominant Processes Concept
ECHAM3, ECHAM4/OPY	GCM names outlined in section 7.2.2 of the thesis
EMIC	Earth Models of Intermediate Complexity
ENSO	El Nino Southern Oscillation
ER	Environmental Requirements
ERA	Energy Resources of Australia Ltd
ERDC	Engineering Research and Development Centre
ETCCDI	Expert Team on Climate Change Detection and Indices
EWLS	Earth-Water-Life Sciences Pty Ltd
FAO	Food and Agriculture Organisation
FORGE	FOcussed Rainfall Growth Estimation
GCM	General Circulation Model or Global Climate Model
GA10	Name of a groundwater bore (see ref. Yesertener 2005)
GFDL	GCM name outlined in section 7.2.2 of the thesis
GIS	Geographic Information System
GLUE	Generalised Likelihood Uncertainty Estimation Model (Monte Carlo Simulation based)
GMS	Groundwater Modelling System
GRAPHIC	Groundwater Resources Assessment under the Pressures of Humanity and Climate Change
GROWA	GIS based water balance model for determination of mean long-term groundwater recharge
GSSHA	Grided Surface Subsurface Hydrologic Analysis (USACE ERDC) Scientific Software Group
GS##	Name of stream flow measuring station (gauging station) in Magela Creek e.g. GS821009
GW	Groundwater
GWT	Groundwater Table
GWL	Groundwater Level
HADCM2, HADCM3	GCM names outlined in section 7.2.2 of the thesis
HC	Hydraulic Conductivity
HELP	Hydrologic Evaluation of Landfill Performance model (US EPA) (US Army Corps of Engineers)
HGU	Hydro Geo-morphological Unit
HRU	Hydrologic Response Units
HUMUS	Hydrologic Unit Model for the United States

HYDRUS-2D, HYDRUT-2D	Simulating the movement of water, heat, and multiple solutes in variably saturated media
IAEA	International Atomic Energy Agency
IOD	Indian Ocean Dipole
IPCC	Intergovernmental Panel on Climate Change
IPO	Interdecadal Pacific Oscillation
ISO	Intra - Seasonal Oscillation
LARS-WG	Stochastic weather generator for simulating time series of daily weather for climate scenarios of GCMs
LIZA	Land cover for the Intensive use Zone for Catchment Hydrology
MA	Moving average
MAE	Mean Absolute Error
MAR	Multivariate Autoregressive
MC##	Name of well in the WTLA site of Ranger
MIKE SHE	Comprehensive, distributed, and physically based modelling system capable of simulating all major hydrological processes in the land phase of hydrological cycle (UK)
MLAA	Magela Land Application Area
MODFLOW	MODular three-dimensional finite-difference ground-water FLOW model (USGS)
MOHISE	Integrated hydrological model considering most of the hydrologic processes particularly groundwater flows using spatially distributed finite element approach
NAO	North Atlantic Oscillation
NCAR	GCM name outlined in section 7.2.2 of the thesis
NF	Net Flux
NF##	Net Flux computed using various methods e.g. NF1
NINO3	Index that measures the strength of an ENSO event. The sea surface temperature anomalies averaged over (5S, 5N) and (150W, 90W) i.e. in the eastern equatorial Pacific.
OB##	Name of the monitoring bores e.g. OB1A
OSS	Office of the Supervising Scientists
Ozclim	CSIRO source of GCM climate data for 100 years from 2001 to 2100
PCA	Principal Component Analysis
PDF	Probability Distribution Function
PDO	Pacific Decadal Oscillation
PNNL	Pacific Northwest National Laboratory (USA)
PPD	Patched Point Dataset (SILO)
PPET	Point Potential Evapotranspiration
PTF	Pedo Transfer Function
PRECIS	Providing Regional Climates for Impact Studies
RCM	Regional Climate Model
RE	Richard's Equation
REA	Representative Elementary Area
RIRDC	Australia's Rural Industries Research & Development Corporation

RL	Relative level to Australian Height Datum
RMSE	Root Mean Square Error
ROSETTA	Model to estimate water retention parameters according to van Genuchten (1980), saturated hydraulic conductivity, unsaturated hydraulic conductivity parameters according to van Genuchten (1980) and Mualem (1976) (USSL)
RP#	Retention Pond #
RPA	Ranger Project Area
RRL	Rainfall Runoff Library (CRCCH)
RUEI	Ranger Uranium Environmental Inquiry
RUM	Ranger Uranium Mines Pty Ltd
SACF	Sample auto correlation function
SAO	Southern Atlantic Ocean
SCCF	Sample Cross Correlation Function
SCL	Stochastic Climate Library (CRCCH)
SDSM	Statistical Downscaling Model
SEEP2D	2D finite-element flow model for confined, partially confined, and unconfined flow situations, both the saturated and unsaturated flow is simulated and the phreatic surface determined and for soils that are non-homogeneous and anisotropic. However SEEP2D is a steady-state flow model. (Scientific software group of US)
Seep/W	Finite element software product for analysing groundwater seepage and excess pore-water pressure dissipation problems within porous materials such as soil and rock for saturated-unsaturated time-dependent problems. Used in analyses and design of geotechnical, civil, hydrogeological, and mining engineering projects. (GEO SLOPE).
SHPA	Soil Hydrological Properties of Australia (CRCCH)
SILO	Electronic resource of information available from BoM
SIMHYD	Daily conceptual rainfall-runoff model (CRCCH)
SLP	Sea Level Pressure
SMAR	Soil Moisture and Accounting Model (CRCCH)
SPACF	Sample Partial Auto Correlation Function
SO	Southern Oscillation
SRES	Special Report on Emission Scenario (IPCC)
SSR	Supervising Scientist Report
SST	Sea Surface Temperature
SUFT3D	Saturated Unsaturated Flow and Transport groundwater model in 3 Dimension to integrate water quality and quantity data. A finite element model used for contaminant transport.
SVAT	Soil Vegetation Atmosphere Transfer scheme
SVFLUX	Finite element seepage analysis program for saturated and unsaturated flow incorporating Richard's Equation. Developed by SoilVision Systems Ltd.
SWAGSIM	Soil, Water, and Groundwater Simulation Model (CSIRO, used with salinity problem)
SWAT	Soil and Water Assessment Tool (USDA Agricultural Research Service)
SWCC	Soil Water Characteristics Curve

SWIM	Soil Water Infiltration and Movement Model (CSIRO)
TAR	Third assessment report (IPCC)
TD	Tailings Dam
TFN	Transfer function noise
TOC	Top of collar
UNSAT-H	Simulate the one-dimensional flow of water, vapour, and heat in soils**.** The code addresses the processes of precipitation, evaporation, plant transpiration, storage, and deep drainage.
UNESCO–IHP	United Nations Educational, Scientific and Cultural Organization – International Hydrological Programme
UNFCCC	United Nations Framework Convention on Climate Change
UNSODA	Database of Unsaturated Soil hydraulic properties (USSL)
USAV	Upper South Alligator Valley
US EPA	United States Environmental Protection Agency
USACE	United States Army Corps of Engineers
USDA	United States Department of Agriculture
USDA-ARS	United States Department of Agriculture-Agricultural Research Service
USGS	United States Geological Survey
USNRC	United States Nuclear Regulatory Commission responsible for storage and disposal of nuclear material and waste
USSL	United States Salinity Laboratory
Vadose/W	Finite element model for analysing flow from the environment, across the ground surface, through the unsaturated vadose zone and into the local groundwater regime (GEO SLOPE).
VAMOS	An automotive simulation framework with emphasised thorough physical modelling and C++ design.
VWC	Volumetric Water Content
VSWC	Volumetric Soil Water Content (same as VWC)
VS2DH	Model for simulating water flow and energy transport in variably saturated porous media (USGS) (good for teaching) (finite difference/ central)
VS2DT	Model for simulating water flow and solute transport in variably saturated porous media (USGS) (good for teaching) (finite difference/ central)
WAVES	1-dimensional daily-time step model that simulates the fluxes of mass and energy between the atmosphere, vegetation, and soil (CSIRO)
WG1	Working Group 1 (IPCC)
WGEN	Weather Generator
WMO	World Meteorological Organization
WTLA	Water Treatment Land Application
ZFP	Zero Flux Plane

Contents

List of Figures

List of Tables

1. Introduction

1.1. Background

The largest reservoir of fresh water resources on Earth is groundwater and the recharge of groundwater plays a major role in the water cycle. Groundwater resources around the world are widely recognised to be under significant stress with respect to quantity and quality (Alley *et al.* 1999; Morris *et al.* 2003; Taylor and Tindimugaya 2008). The recharge of groundwater takes place through the vadose (or unsaturated) zone, where complex interactions between thermal, hydrological, geochemical and biological processes affect water quantity and quality (Glassley 2003). Groundwater recharge, in turn, is influenced by the long-term changes in mean temperature, mean precipitation, precipitation variability, land use, and sea levels: all of which are expected to be impacted by climate change (Faye *et al.* 2008; Miguel *et al.* 2008).

The relationship between climatic conditions and groundwater resources, especially the vadose zone and unconfined shallow groundwater, is critical in understanding numerous environmental processes. For example, shallow groundwater can provide base flow to streams and wetlands, water to deep-rooted vegetation and water supply for people. The ability to understand and model this relationship has many important outcomes. In recent years, there has been increasing research into the relationship between shallow groundwater and climatic conditions (Chen *et al.* 2002; Eckhardt and Ulbrich 2003; Chen *et al.* 2004; Cheng *et al.* 2006; Hiscock *et al.* 2008; Kundzewick and Doll 2008; Kundzewicz *et al.* 2008; Taniguchi *et al.* 2008; Goderniaux *et al.* 2009; Ludwig *et al.* 2009; Wang *et al.* 2009b). The influence of a changing climate on shallow groundwater resources significantly influences the sustainability of existing ecosystems and communities.

The seasonal variation of climate, such as precipitation and temperature, cause temporal and spatial changes in the water flow components in a hydrological catchment at a regional scale. The annual groundwater level fluctuation is one of the indications of this variation. The other scales of variation could be interannual, decadal or multi-decadal. The process of climate change, which leads to changes at the multi-decadal and centurial time scales, will certainly lead to changes in groundwater resources and behaviour.

However, the response of groundwater to climate change will not be identical for all regions on Earth. For instance, the annual precipitation will increase in some locations and decrease in others. Average ground surface temperatures and timing of precipitation are also important in local or regional water cycles and resources. Other factors could be related to geographical, geological or topographical characteristics or based on human interventions for various land use patterns. There is a clear need to develop techniques and models to link shallow groundwater with climatic conditions, especially to predict the expected impacts of climate change on groundwater resources.

The primary focus of this thesis is the development of techniques and models to predict the potential impact of climate change on shallow unconfined groundwater resources.

1.1.1. Practical Importance

Some of the major impacts of projected climate change consist of changes in precipitation patterns, average and maximum temperatures, mean sea level, and altered frequencies and intensities of extreme weather. More specifically, the impacted areas are wide ranging and include fresh water resources, ecosystems, food, fibre and forest products, (biodiversity and agriculture), energy supply, coastal systems and low-lying areas, industry, health, settlement and society (Rosenzweig et al. 2007). The impact of climate change is an important issue in the planning of the future development activities for the sustainability of the environment and society.

The concept of sustainable development was defined by the World Commission on Environment and Development in 1987 as 'development that meets the needs of the present without compromising the ability of future generations to meet their needs' (Brundtland *et al.* 1987). The essence of sustainable development is meeting fundamental human needs in ways that preserve the life support systems of the planet (Kates *et al.* 2000). Water is one of the key focus areas for the United Nation's (UN) Millennium Development Goals to help guide countries and humanity towards sustainable development.

Given that water resources are a fundamental component of sustainable development, the practical importance of developing improved techniques and models for assessing the potential impacts of shallow unconfined groundwater resources is clear.

1.2. Kakadu National Park and the Ranger Uranium Mine

The Kakadu National Park is a world heritage-listed property on the northern tip of the Northern Territory (NT) of Australia, colloquially known as the 'Top End'. The region contains major uranium deposits excised from the park, namely Ranger, Jabiluka and Koongarra. The Ranger mine started production in 1981 and was authorised in 2000 for a further 26 years (Senate 2003). The mining of uranium in such an environmentally and culturally sensitive region has always been controversial. In reality, the mining leases are linked with the important ecological and cultural values of Kakadu.

Kakadu is of significant cultural and environmental significance, protecting various habitats of northern Australia and one-third of the country's bird species, and preserving an important record of nature and Aboriginal history in extensive galleries of rock art (Press et al. 1995). The region has a typical wet-dry monsoonal climate, whereby most of the rain occurs between November and April (the wet season) with virtually no rain between May and October (the dry season).

The safe containment of radionuclides and other contaminants will depend almost entirely on the levels (or height) of the groundwater as the driving force for flow, which in turn relies on and is linked to recharge from the climate (i.e. rainfall). The hazards of declining groundwater levels (GWLs) are that unsaturated conditions will leave uranium mine waste exposed to higher rates of radioactive radon gas emanation. Conversely, the implications of rising GWLs are the potential transport of contaminants by seepage and/or runoff.

The study site adopted for this thesis is the Ranger uranium mine: due to the need to contain uranium mill tailings within a region surrounded by the world-heritage Kakadu National Park. The Ranger Project Area (RPA) is located approximately 250 km east of Darwin at position $132^{0}55$ ` E latitude and $12^{0}43$ ` S – $12^{0}40$ ` S longitude, occupying 79 km^2 in the upper reaches of the Magela Creek catchment (Press et al. 1995). Creeks surround the Ranger mine, with Magela, Djalkmarra and Georgetown Creeks to the east, Corridor and Gulungul Creek to the south, Gulungul Creek to the west and Coonjimba and Magela Creeks to the north. The four small tributaries, namely Georgetown, Djalkmarra, Coonjimba and Gulungul Creeks, collect runoff from the mine area and drain out to Magela Creek.

Following mine rehabilitation, groundwater levels inside the mined landforms of the site will be the principal driver of seepage and contaminant transport to the shallow unconfined aquifer (i.e. water table). The legal requirements for the Ranger project include a clause that requires that solutes derived from the radioactive mill tailings 'will not result in any detrimental environmental impacts for at least 10,000 years' (clause 11.3 ii; Senate 2003). The groundwater in the immediate vicinity is therefore vulnerable to contamination by the radioactive mine waste and could influence the ecological sustainability of the flora and fauna of the environment significantly. The prediction of the long-term rebound and behaviour of groundwater following the mine site rehabilitation is a fundamental issue to address for a sustainable environment.

A number of past and present studies at Ranger have shown that there are strong links between surface waters and shallow groundwater, dependent on topography and localised geology (Salama and Foley 1997; Salama et al. 1998). Whitehead (1980) and Vardavas (1993) have shown that the tropical wet-dry climate leads to an annual cycle of saturated-unsaturated flow condition in the shallow soils and rocks. The regolith consists of variable thickness of weathered soils overlying complex geologic formations, which mainly consist of fractured rock aquifers. The extent of hydraulic connection between these shallow and deep units is considered minimal. Therefore, in this thesis, it is assumed that the primary groundwater-climate relationship relevant for mine rehabilitation design will be that between the shallow unconfined aquifer and surface climatic conditions.

1.3. Groundwater-climate Relationship for the Site

In the water cycle of the hydrologic processes, the net infiltration of water after a rainfall event passes through the shallow unconfined soil layer and reaches the saturation zone or water table. With subsequent rainfall, the GWL or the level of saturation rises and with the absence of rainfall, the GWL declines because of the evaporation and transpiration from the soil surface and vegetation. Figure 1.1 shows the typical water balance components in the shallow unconfined layer of the soil stratum to which the present research is targeted.

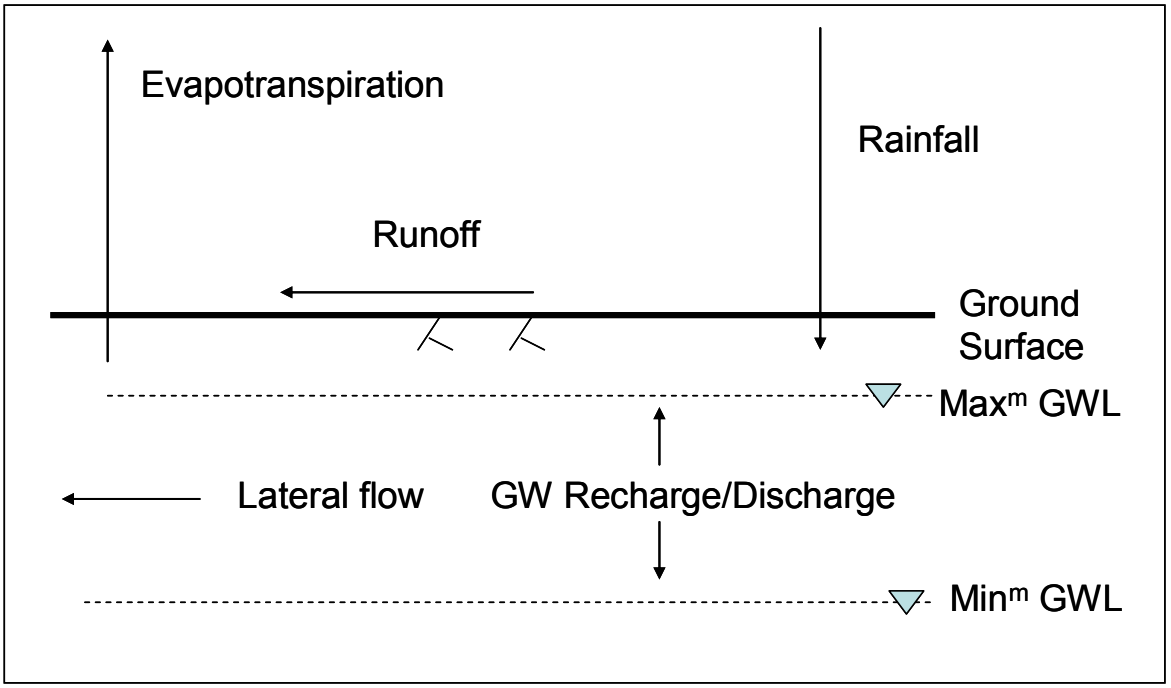

Figure 1.1 The water balance components in the shallow unconfined soil layer

The groundwater hydrograph, or GWLs over time, has a clear interaction with the climate, more specifically, with the annual rainfall hyetograph and evapotranspiration pattern. These variables influence the rate of groundwater recharge and thus the GWLs. The extent of interconnectivity depends on the physical characteristics of the catchments and distribution of rainfall in time and space. A year of lower rainfall can lead to a decline in the water table, while an above average rainfall year can lead to an increase in the water table. A key issue in assessing the long-term performance of uranium mine rehabilitation is the understanding and prediction of the rise and fall of the groundwater with respect to the climate system.

The changes in hydrologic processes such as precipitation, evaporation, transpiration, infiltration, runoff, interception and surface storage are response to hydro-climatic processes. The configuration of the future climate at any specific location in the Earth's surface includes both climate variability and climate change. The two different concepts represented by climate change and climate variability need to be addressed explicitly to study the impact of climate change on the system.

1.3.1. Climate Change and Climate Variability

The process of climate change is the continual evolution of the average climate in a given region. Climate change can be either natural in origin, or, more recently, it is now strongly driven by anthropogenic interference in the climate system due to growing emissions of greenhouse gases such as carbon dioxide (CO_2), nitrous oxide (N_2O) and methane (CH_4). As atmospheric concentrations of these major greenhouse gases continue to rise due to human emissions sourced from coal and oil combustion, agriculture and land use change, the pace of climate change is predicted to increase (Meehl *et al.* 2007). The results are projected to include higher surface temperatures, changing rainfall patterns and intensities, and rising sea levels.

Climate change is caused by increasing greenhouse gas emissions and concentrations, whereas climatic variability is considered natural in its origin. The influence of climate change on this natural climate variability remains an unresolved area of scientific understanding.

The climate change caused by rising temperature would be responsible for the increased number of occurrence of extreme events in terms of magnitude and intensity (Solomon *et al.* 2007). There is evidence that the trends of the most extreme events of both temperature and precipitation are changing more rapidly in relation to corresponding mean trends than are the trends for more moderate extreme events (Alexander et al. 2007). There is an increasing recognition that rising temperature is exacerbating (increasing severity) the impact of any rainfall reduction (Cai 2007).

The existing climate variability in the Top End is understood to be related to the El Nino Southern Oscillation (ENSO) index, which has a range of possibilities from high intensity rainfall to during the wet season in one side and longer spell of extreme temperature during summer on the other. In regards to the Ranger site, Hennessey et al. (2004) indicate that there will be an increased number of dry days with increased suction in soil during the dry season and a higher number of wet days with increased seepage head in the wet season. The predicted effects of climate change in relation to the site are characterised by exaggerated results of climate variability. The question of sustainability of a rehabilitated

uranium mine site concerning the exaggerated climatic variability imposes an additional necessity for this kind of investigation.

1.4. Research Question

The research aims to resolve one fundamental question. The question is 'how can a modelling framework be developed to study the long-term impact of future climate on shallow groundwater?' To address this question in relation to a specific site, some site-specific questions need to be addressed. For example, in relation to radioactive mine site rehabilitation facilities, the slow decay of many transuranic waste products, modelling efforts must be concerned with potential changes in boundary conditions in the long-term. The changed boundary conditions can be represented by future replicates of climatic fluxes as an input to a groundwater or unsaturated-saturated flow model.

For the present thesis, the framework of the investigation consists of several consecutive steps, each building on the previous work. The traditional approach of conceptual modelling and exploratory methods of data analyses are performed first. This gives rise to application of subsequent methods such as time series techniques and physically based modelling, leading to a gradual increase in the complexity of the understanding and ability to model the processes of groundwater-climate interactions. This robust framework is especially important for challenging sites such as a radioactive waste containment facility in the wet-dry tropics surrounded by a world heritage-listed national park in the face of climate change and climate variability. The specific research questions could be listed as follows (each generally being a thesis chapter, and justified further following the literature and site review):

- How can the significant net flux of water be represented (recharge/discharge) into a shallow unconfined groundwater system as a response to the hydrologic processes (such as rainfall and runoff) in a specific site? (Chapter 5)
- Can statistical methods provide a useful approach to assess the response of GWLs to the net flux of water to the system, especially considering factors such as the unsaturated zone thickness or the annual wet and dry seasons? (Chapter 6)
- How can the trends of climate change predictions be combined with natural climatic variability to obtain future replicates of net flux of water to the system of a specific site? (Chapter 7)

- Which groundwater model should be selected and validated to perform the physically based computation for the purpose of long-term prediction? (Chapter 8)
- What are the possible scenarios of long-term GWLs in response to the future replicates of net flux of water to the system? What is the relative importance of trends of changing climate and naturally varying climate? What is the uncertainty of the predictions? (Chapter 9)

One of the challenges for the sound development of the methodology for this research is the required time scale of investigation. While the centurial time scale predictions are highly uncertain, making predictions for 10,000 to 100,000 years will be extremely uncertain (Jyrkama and Sykes 2007). Specifically, there is a lack of fundamental understanding about how climate change-induced changes in hydro-morphology will interact with ecology (Wilby et al. 2006a). Therefore, in this thesis, the focus is on the centurial time scale only, as this is also more practically applied to rehabilitation designs of sites such as the Ranger uranium project.

2. Literature Review

This chapter will present a review of the basic scientific concepts that must be addressed to understand and predict the groundwater-climate relationship. The water cycle is described very briefly to identify the typical physical processes that are the basic elements of the modelling for understanding and predicting the groundwater-climate relationship. Starting from hydrology, the process of groundwater recharge is introduced as an integral part of the water cycle. The estimation procedures of all the hydro-climatic parameters are described. For predicting groundwater recharge as a future hydrologic process, both statistical and physical process-based approaches are investigated. In a physical process-based approach, a brief section introduces the fundamental concepts of human-induced climate change and natural climatic variability that influence the water cycle. Recent researches on groundwater modelling for climate change, natural climatic variability and land use changes are broadly reviewed. The key issues that impede the novel scientific investigation for the long-term prediction of the groundwater-climate relationship are identified. While reviewing the previous work, the necessity for developing a new and up-to-date modelling framework has been established for the long-term modelling of groundwater recharge in shallow unconfined vadose zone with changing and variable climate utilising the available timeframe and other necessary resources.

2.1. Water Cycle

The movement of water in solid, liquid or gas form throughout the Earth is called the water cycle or the hydrologic cycle. Ideally, the water cycle consists of precipitation, interception, surface/depression storage, surface runoff, evaporation, evapotranspiration, infiltration, percolation, subsurface runoff, deep percolation, base flow, and stream flow, as shown in Figure 2.1. The immense water engine that is fuelled by solar energy, driven by gravity and Earth's movement proceeds endlessly in the presence and absence of human activity (Maidment 1993). To solve some practical and complex problems, it is reasonable to assume simplifications of the processes that should not contribute to significant deviation from the ideal situation. Before performing the simplification for a specific problem, it is logical to provide a very brief description about the representation and estimation of all the processes. The following section is provided in here to build the scientific basis of the basic physical processes for development of the conceptual model of the groundwater

system though the subject matter is quite standard and could be found in any textbook on hydrology.

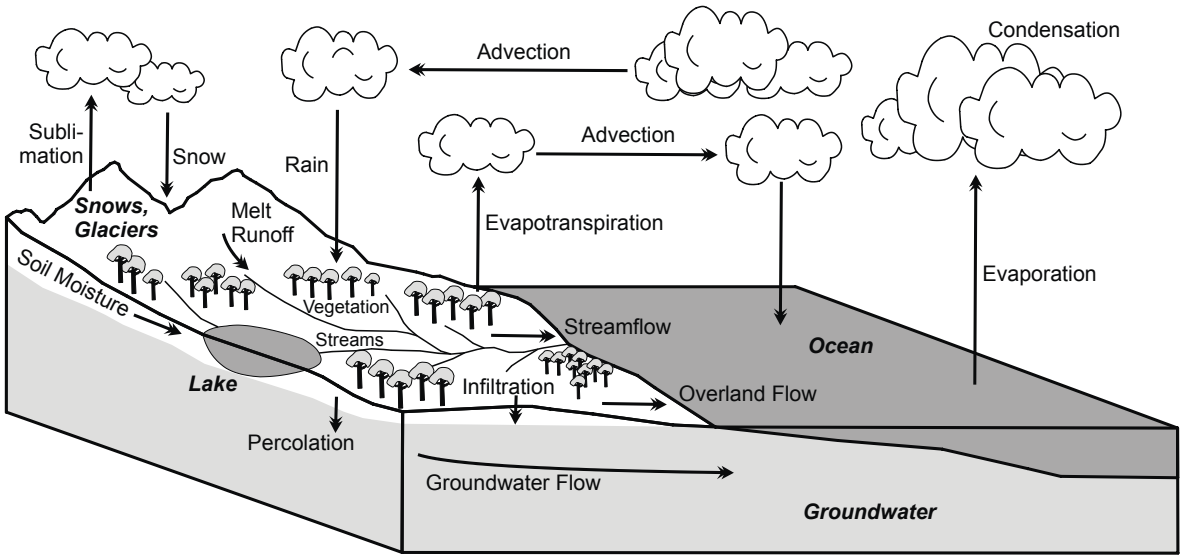

Figure 2.1 Water cycle (Ladson 2008)

2.1.1. Representation and Estimation of Hydro-climatic Parameters

The inflow components in a catchment consist of precipitation P, surface inflow I_s, subsurface inflow I_g. The outflow components consist of evaporation E, transpiration T, which are commonly combined into one single term called evapotranspiration, subsurface outflow Q_g, stream flow Q, and diversion D. The difference between the total inflow and total outflow contributes to the change of storage in the catchment. The storage type can be represented as surface storage S_s, soil moisture storage S_{sm}, groundwater storage S_g, vegetation S_v, rivers and channels S_r, snow and ice S_i (Ladson 2008). Combining the inflows, outflows and storages in the water balance equation the following general representation can be obtained, as shown in Equation 2.1:

$$\left(P + I_s + I_g\right) - \left(Q + ET + D + Q_g\right) = \Delta S_s + \Delta S_{sm} + \Delta S_g + \Delta S_v + \Delta S_r + \Delta S_i \qquad \text{Equation 2.1}$$

where Δ are indicating variations of the storages during the time step interval of the computation. The more elaborate representation of the evaporation could be detailed as sublimation and condensation, and the same for precipitation could be interception, depression storage, infiltration and runoff.

In the absence of perfect knowledge about all the processes, the dominant processes concept (DPC) as suggested by Grayson and Bloschl (2000a; 2000b) and Woods (2002) is incorporated in the formulation of the conceptual model of the problem under consideration. A similar technique is applied to the present research while characterising the research site. The long-term average values of the flow components are considered and the insignificant flow components are assumed to negligible for the scale of space and time of the modelling study. The identification of the dominant processes is also conducted by the judgment of the physical factors that influence the phenomena. For example, the point scale runoff can contribute to the catchment scale groundwater in relation to ephemeral rivers of humid climate. In that situation, runoff can be neglected for a time scale (for example, a month) that is significantly greater than the storm duration (for example, hours or days). Therefore, the issue of modelling scale is also important in the selection of significant hydro-climatic processes.

The simplification of the various processes typically results into three to four dominant processes depending on the relative quantity of flow in the annual water balance. For example, Morton (1983) compares the various seasonal water balances for six river basins in six different environments in North America, as presented in Figure 2.2. The significant components considered consist of rainfall, evapotranspiration, runoff and storage. In fact, these four processes are typical to any catchment scale water balance study.

As to the typical hydrologic processes in the catchment scale water balance studies for long-term modelling, the four significant hydro-climatic processes are reviewed in the context of the modelling purpose. The four processes are:

- precipitation
- evapotranspiration
- groundwater recharge
- runoff

The other processes of the general water balance equation are assumed negligible as far as the modelling context is concerned.

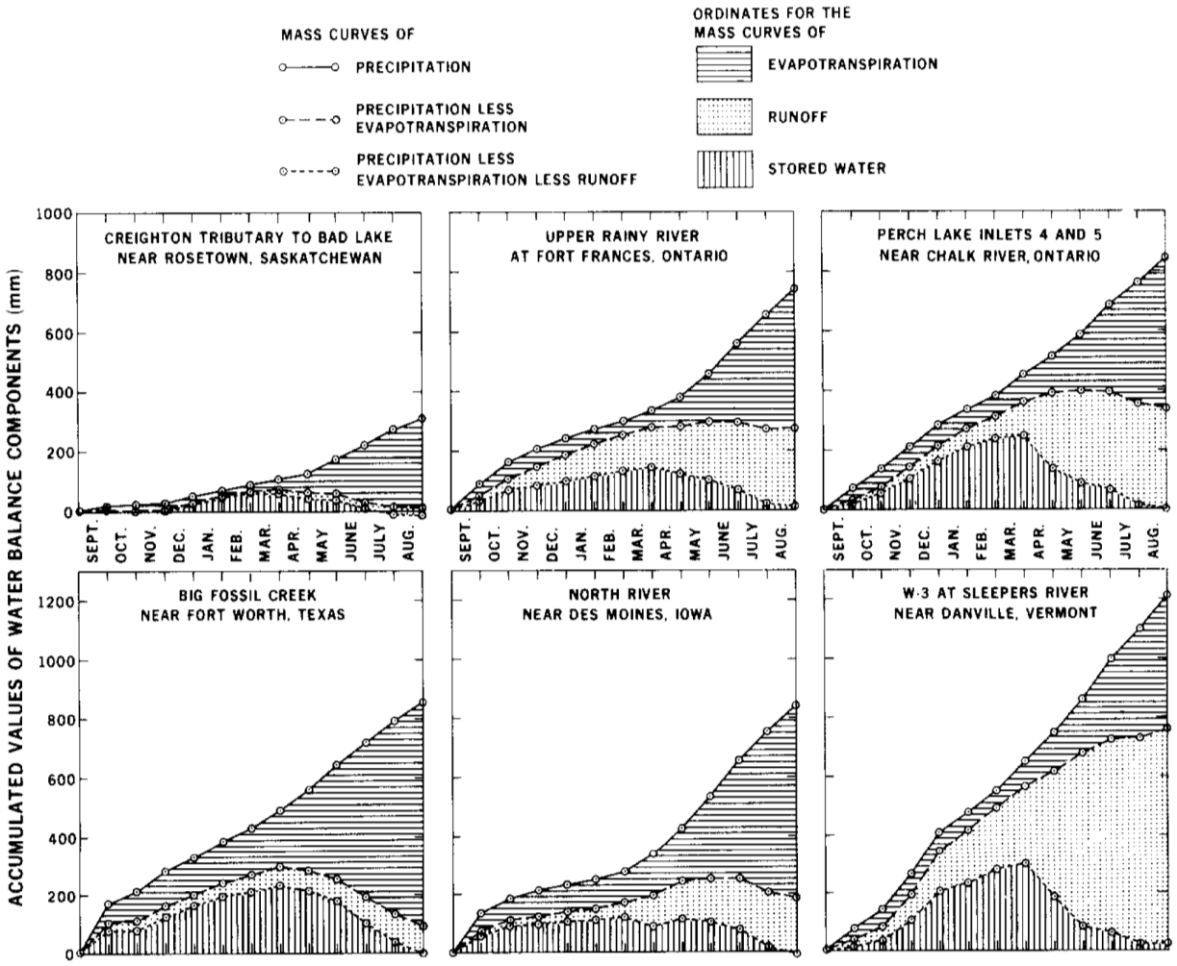

Figure 2.2 Seasonal water balance for six basins in North America (Morton 1983)

Precipitation: Precipitation is represented by any form of water such as rainfall, snowfall, hail or sleet originating from atmosphere and reaching the Earth's surface. When the form of precipitation is rain, it is typically measured in a rain gauge, for example a tipping bucket type rain sensor. Although the measurement of rainfall is direct and straightforward, the wide range of variation of rainfall at temporal and spatial scale can contribute significant deviation from reality while generalising the hydrologic processes at catchment scale. For this research, since the study is about understanding groundwater-climate relationship at catchment scale, the long-term average rainfall should adequately represent the system. However, in the predictive analyses, thousands of replicates of future rainfall need to be generated to encompass the natural variability and changing climate scenarios.

Evapotranspiration: Evapotranspiration is the combination of evaporation from the soil surface and free water surfaces and transpiration from vegetation. It consists of the transfer of water in vapour form from the ground surface to the air and it includes evaporation from

open water bodies and soil surfaces, sublimation of frost, ice and snow, and transpiration from vegetal cover (Ladson 2008). The annual average precipitation over the land surface of the Earth returns to the atmosphere in the form of evapotranspiration by two thirds of its total amount (Chiew *et al.* 2002). Over the continent of Australia, evapotranspiration is more than 90% of precipitation.

However, the scale of temporal and spatial variation of the vegetation characteristics, hydro-climatic and hydro-geologic factors that are responsible for the variation of evapotranspiration process is very wide and highly complex due to the interaction among the factors. The direct measurement of evapotranspiration is difficult, and therefore, often a large number of methods are used for estimation of evapotranspiration. Consequently, the results derived from those methods are also varying.

Unlike rainfall data that is a measured data, the evapotranspiration data is usually estimated, and a range of methods and variables is introduced to represent this. In terms of data availability for the historical value, there can be a number of sources. Therefore, selection of the appropriate evapotranspiration estimation method, appropriate variable and reliable data provider source are the imperative issues that need to be addressed with due consideration. Relevant discussions have been provided in Section 2.1.2 in this regard. The specific estimates of evapotranspiration performed by earlier investigators in the region of the site analysed in the present research will be discussed in much more detail in Chapter 5.

Groundwater recharge: If the water balance equation for a catchment is considered, the status of groundwater level would indicate the amount of storage of water in the subsurface region. Although the soil moisture content in the unsaturated soil also constitutes some part of water storage, the existence of groundwater level (GWL) would indicate fully saturated condition underneath the GWL. For a one-dimensional vertical flow system, any additional input to the system would cause rising levels of groundwater. In the event of rainless condition, the evapotranspiration losses would cause falling levels of groundwater. Therefore, in annual scale of time, groundwater recharge is the amount of water that enters into the saturated zone from rainfall. However, in broader context, recharge could be defined as water that reaches an aquifer from any direction (down, up or laterally) (Lerner 1997).

There are some other variations with the definition of recharge. For instance, uniform recharge from irrigation or precipitation is referred as *diffuse recharge* or *direct recharge,* whereas concentrated recharge from local depressions, such as streams, lakes, and playas, are referred to as *focused or localised recharge or indirect recharge.* Rushton (1997) distinguishes *actual recharge*, estimated from groundwater studies and that reaches the water table, from *potential recharge,* estimated from surface water and unsaturated zone studies, and that is water that has infiltrated that may or may not reach the water table because of unsaturated zone processes or the ability of the saturated zone to accept recharge. In the intended research, the vertical flow of water in the soil, which eventually reaches water table or groundwater level, is meant by the term 'recharge'. In many instances, the representation of recharge as a percentage of rainfall is used by hydrologists in water balance study and is termed as 'recharge coefficient'. The various techniques for the estimation of groundwater recharge have been listed briefly later. An example of a shallow groundwater response to rainfall and climatic conditions is given in Figure 2.3.

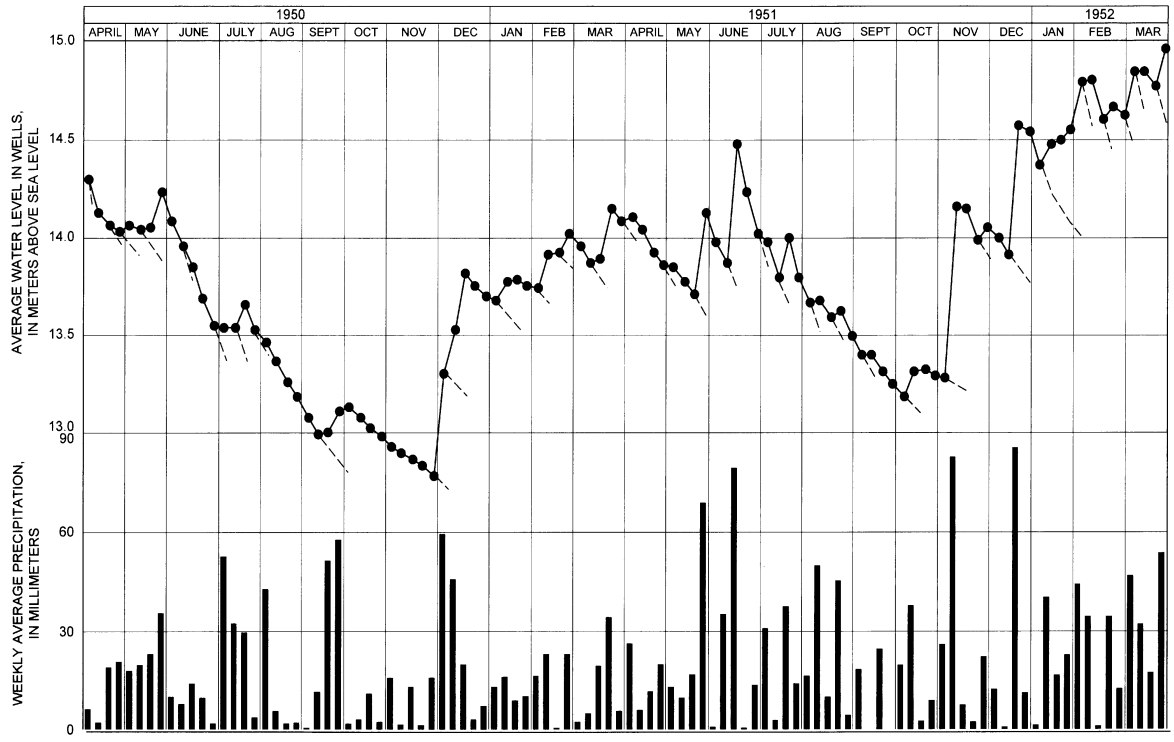

Figure 2.3 Average groundwater levels and weekly rainfall at the Beaver dam Creek basin, Maryland, US (Healy and Cook 2002)

Runoff: The incorporation of runoff as a significant water flow component in the water balance equation for a catchment depends on the areal extent of the catchment boundary,

surface imperviousness or vegetal cover, rainfall intensity, soil moisture status, soil hydraulic conductivity (HC), hydraulic gradient and overall the relative quantity of the other flow components (Ladson 2008). The representation of runoff in the water balance is governed by its relative value with the other hydrological flow. For instance, the water balance in the Murray-Darling Basin shows 5% runoff while that of Lake Eyre Basin shows 1% runoff of the annual rainfall in the regions (Ladson 2008). Runoff coefficient, which is the ratio between runoff and rainfall related to a particular catchment, is widely used to represent the component of flow in the hydrologic system. The catchment and storm characteristics influence the runoff coefficient and there is wide range of variability of its value in relation to time and space (Merz *et al.* 2006; Merz and Bloschl 2009).

Summary water balance: The equation of continuity for the control volume can be written as inflow-outflow to be equal to change in storage. The groundwater recharge or discharge is represented by the net flux, which is the algebraic summation of rainfall, runoff and evapotranspiration, while rainfall is considered to be of positive value, and runoff and evapotranspiration to be as negative value.

2.1.2. Estimating Evapotranspiration

The factors that govern open water evaporation such as energy supplies and vapour transport also govern evapotranspiration. In addition, a third factor enters the picture, the supply of moisture at the evaporative surface. The various methods of estimation of evapotranspiration are based on the basic physical processes in conjunction with some modifications obtained from experiment-based empirical methods. Broadly categorising the methods of estimation can lead to the following approaches:

- Pan evaporation method (Chow et al. 1988)
- Penman-Monteith (FAO 56) method (Allen et al. 1998). This method supersedes Penman's (FAO 24) method (Maidment 1993)
- Morton's method (Morton 1983)

The pan evaporation method estimates crop evapotranspiration by combining pan evaporation and crop factor. The pan evaporation is directly measured in the weather stations. The calculation of evaporation from open water is also alternatively performed by a number of methods such as energy balance method, aerodynamic method (Thornthwaite and Holzman 1939), combination method (Penman 1948) and Priestly-Taylor method (Priestley and Taylor 1972), as reported in Chow et al. (1988).

The Penman-Monteith method estimates reference crop evapotranspiration and uses a crop coefficient to estimate real crop evapotranspiration. The reference crop evapotranspiration is estimated as a combination of potential evapotranspiration and some function of soil moisture deficiency (Nash 1989). The potential evapotranspiration is estimated by solving for the potential evapotranspiration equilibrium temperature, the temperature that satisfies both the energy balance equation and the vapour transfer equation for a moist surface meaning unlimited water supply (Morton 1983).

The methods reviewed in detail for this thesis other than Morton's method are the pan evaporation method as described in Doorenbos and Pruitt (1977), Tindall and Kunkel (1999), Penman method, i.e. FAO-24 method described in Doorenbos and Pruitt (1977), Penman-Monteith method, i.e. FAO-56 method described in Allen et al (1998) and also described in Van Bavel (1966), Monteith (Monteith 1980) and Chiew et al. (1995a). Collectively, it is certain that these estimation methods incorporate the term potential evapotranspiration (PET), which may be defined as evapotranspiration that would take place, under the condition of unlimited water supply. Then, crop factor or crop coefficients are used to transform the potential evapotranspiration to actual evapotranspiration for a specific crop.

The brief description of Morton's method is given in Appendix A and the critical comparison of the other estimation procedures has been performed here to select the appropriate method of estimation of evapotranspiration.

Morton's ET: Morton's method of estimation is based on a large number of climate data such as temperature, solar radiation, location, vapour pressure and atmospheric pressure in which the measured pan evaporation data use is deliberately excluded. The method proposes three evapotranspiration variables such as Areal Actual Evapotranspiration (AAET), Areal Potential Evapotranspiration (APET) and Point Potential Evapotranspiration (PPET). Citing directly from Chiew et al. (2002) page 2, the definitions of the three-evapotranspiration variables as used in Morton's method are as follows (Morton 1983; Chiew and Leahy 2003).

- AAET is the evapotranspiration that actually takes place, under the condition of existing water supply, from an area so large that the effects of any upwind

boundary transitions are negligible and local variations are integrated to an areal average.

- APET is the evapotranspiration that would take place, under the condition of unlimited water supply, from an area so large that the effects of any upwind boundary transitions are negligible and local variations are integrated to an areal average.
- PPET is the evapotranspiration that would take place, under the condition of unlimited water supply, from an area so small that the local evapotranspiration effects do not alter local air mass properties. It is assumed that latent and sensible heat transfers within the height of measurement are through convection only.

Morton's method is widely known as the Complementary Relationship Areal Evapotranspiration (CRAE) model (Doyle 1990). From the analogy of potential evaporation as evaluated by Nash (1989), it can be said that potential evapotranspiration is represented by Morton in two ways: firstly, as the energy available for evapotranspiration under the condition of unlimited water supply; and secondly, as the negative index of actual evapotranspiration under the condition of limited water supply. Mathematically, this means the AAET and PPET are inversely proportional under the condition of limited water supply. This concept of negativity in the relationship between potential and actual values were firstly proposed by Bouchet (1963) and then applied by Morton explicitly in his CRAE model. Thus, according to the Morton's method of estimation of evapotranspiration, in its complementary relationship, it is stated that the 'sum of AAET and PPET is equal to twice the APET' (Morton 1983).

The physical significance of the three variables could be explained in the following way. Under dry conditions, there is no water to evaporate, AAET = 0 and PPET is at its maximum rate. As water becomes available, AAET increases. This increase in AAET causes the overpassing air to become cooler and more humid (reducing the vapour pressure deficit at a point), producing an equivalent decrease in the PPET. Finally, when the soil water has increased sufficiently, the values of AAET and PPET converges to that of the APET (Morton 1983; Chiew and Leahy 2003). The APET as shown in Figure 2.4 indicates the wet environment areal evapotranspiration. The dry environment potential evapotranspiration is indicated by twice the APET at zero water supplies.

It should be noted that the graphical plot of the historical monthly average rainfall along the X axis and PPET and AAET values along the Y axis have been found to generate similar scatter of Figure 2.4, as described in Chapter 5. Some additional analyses have been provided in Chapter 5 to show the adequacy of Morton's AAET in relation to various estimates of evapotranspiration, soil porosities and lateral subsurface flows. Therefore, it can be agreed that Morton's AAET should adequately represent the outgoing flux from the system under consideration.

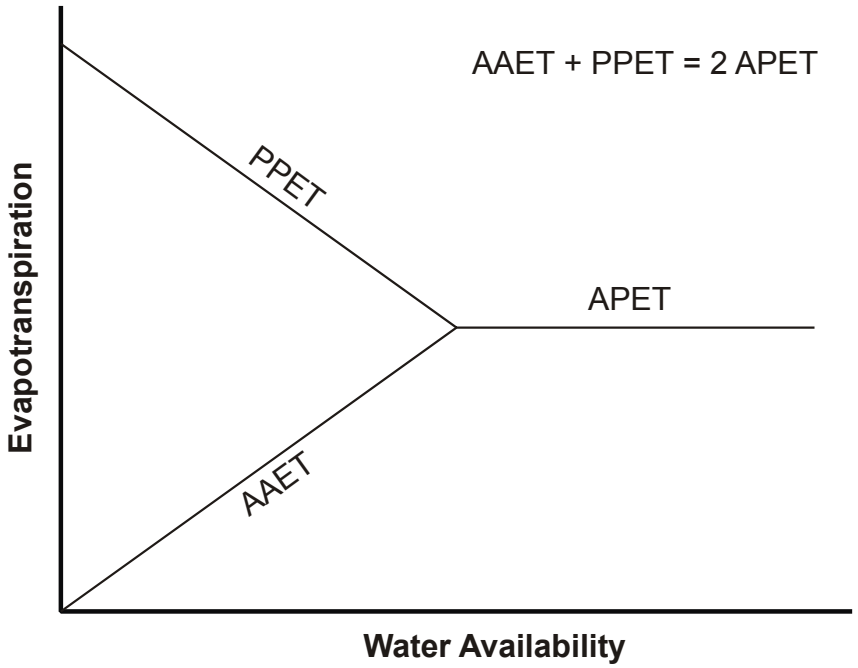

Figure 2.4 Complementary relationship between AAET and PPET (Morton 1983; Chiew *et al.* 2002)

Comparison between Penman-Monteith and Morton: Similar to the Penman-Monteith method of estimation, both the vapour transfer and energy balance equations are considered in Morton's method. However, the application is more comprehensive in the sense that rather than solving for one single variable called 'potential evapotranspiration equilibrium temperature', two key evapotranspiration variables such as PPET and APET are simultaneously solved in the procedure of Morton and the complementary relationship is used to estimate the required evapotranspiration variable AAET. Nash (1989) explicitly elaborates the superiority of complementary relationship in relation to the traditional methods of estimation of actual evapotranspiration from potential values. Morton's contribution in top of Penman's method though these are not conflicting but Morton adds some value. For a clear understanding, in the computational steps followed in the two

methods such as Penman and Morton, it is observed that while Penman uses a single potential value to combine with factor/coefficients for estimating actual value, Morton calculates two sets of values (PPET and APET) to calculate AAET for each time step. Morton suggests the feedback mechanism that acts on the factors influencing potential values (Morton 1983; Nash 1989). Both the Penman methods and pan evaporation method are relevant for a specific type of crop and on shorter (for example, daily) time scale. Morton's method does not consider any specific crop type and the time scale is longer (for example, monthly).

Superiority of Morton's evapotranspiration in the modelling context: The introduction of crop factor in the estimation of evapotranspiration makes it less universal for a range of vegetation. Both the Penman-Monteith method and Pan Evaporation method have this limitation. Morton's method does not consider any specific crop type. Therefore, considering the context of the catchment scale model where a range of vegetation should exist rather than a specific type of crop, Morton's method is more appropriate for the estimation of evapotranspiration.

The other factor relates to the dependency of estimated evapotranspiration on pan evaporation. One measure of goodness of the estimation of evapotranspiration is the good correlation of the estimated potential evapotranspiration with pan evaporation data. For example, Chiew et al. (1995a) have used pan evaporation data to estimate potential evapotranspiration when the necessary climate data were unavailable in performing their investigation to find the relationship between various estimates of evapotranspiration in Australia. However, the correlation between daily estimates of Penman's PET and pan evaporation data have been found to be poor for Australia (Chiew and McMahon 1992). Therefore, it is better to avoid the estimates of evapotranspiration that are based on pan evaporation data.

Jeffrey et al. (2001) also have shown that out of a number of measured climatic variables, the pan evaporation data has the largest value of mean absolute error (MAE) in relation to that of the other variables. Therefore, the methods that are based on pan evaporation values are also susceptible to error.

Therefore, for Australia, Penman's method and thereby Penman-Monteith methods are less desirable than Morton's method, which does not compute pan evaporation as initial step for estimation of evapotranspiration. From the evidence of field investigation, it is suggested that Morton's method of estimation of evapotranspiration is more appropriate for Australia than other estimates.

Representation of wet dry tropic by Morton's ET: The applicability of the Penman's method in comparison with Morton's method in rainfall-runoff modelling for Australia has been investigated by Chiew and McMahon (1991). In rainfall-runoff modelling, the condition of wet environment prevails. Morton's wet environment evapotranspiration and Penman's potential evapotranspiration have been found to provide similar magnitudes of only the upper limit of actual evapotranspiration at moderate climatic condition (Chiew and McMahon 1991). This indicates that during the wet season, both the methods are equally applicable and can be used interchangeably in rainfall-runoff modelling application and during the dry season, these two methods give different result because of the complementary relationship between evapotranspiration variables being considered in Morton's method.

In the context of present research, the distinct wet-dry tropic region is subjected to significant wet and dry conditions in the annual cycle. The recharge to a groundwater system during the wet season ultimately becomes discharge to the stream by base flow and evapotranspiration for the dry season. Thus, the dry season's water balances are equally significant. To represent the whole annual cycle of wet and dry conditions, Morton's estimates of actual evapotranspiration is more representative than Penman's potential evapotranspiration. As Penman's method has been found to be insufficient, as stated in Chiew and McMahon (1992). Morton's method should be more reasonable, due to its more physically-based estimation methodology.

The natural processes that correspond to a certain combination of PPET and AAET are considered unique. The summation of PPET and AAET is constant for any set of physical condition in terms of water availability and that summation is equal to the twice of APET. The use of complementary relationship in Morton's method makes the transformation of potential evapotranspiration to actual evapotranspiration more realistic.

Scientific superiority of Morton's method: Doyle (1990) has shown that the Bouchet-Morton approach, the CRAE model, provides a valuable alternative to the empiricism of the Thornthwaite-style (Thornthwaite and Holzman 1939) reduction of actual evaporation from potential evaporation, but this is achieved at a high cost, which means the introduction of a strong degree of empiricism into the process of advection modelling. But Hobbins et al. (2001) suggest that there is clear indication about the superiority of CRAE model with respect to the Advection-Aridity (AA) model (Brutsaert and Stricker 1979), as the later one needs to be recalibrated before it could be used successfully on a regional basis, whereas the CRAE model accurately predicts monthly regional evapotranspiration. It should be indicated that the AA model is based on the concept that the degree of non-availability of water for evapotranspiration is deduced from regional advection of drying power of the air in the atmospheric environment (Brutsaert and Stricker 1979). However, the CRAE model considers the atmospheric environment directly in the estimation of PPET, as found in Morton (1983).

Granger and Gray (1990) show that Morton's method for evaporation estimation has several deficiencies such as the assumption water transfer coefficient is not dependent on wind speed, and calculation of albedo may lead to significant errors. However, these deficiencies lead to poor performance of Morton's method while used for smaller time scale but for a larger time scale, estimates are more reliable. In the present research, the time scale considered is monthly and the use of Morton's estimates of evapotranspiration would be accepted.

Summary: Concerning all the discussions above, the various methods of estimates of evapotranspiration, the selection of the Morton's method is justified from the following considerations:

- Theoretical basis of CRAE is stronger than empirical models
- Not dependent on pan evaporation, which is not preferable for Australia
- Adequately represent the dry season flow as well as wet season by CRAE model
- The universal vegetation type can be represented
- The monthly time step is better for Morton's method while daily values are better with other methods. In the present context, monthly values are needed

2.2. Groundwater Recharge

The interaction of climate, geology, morphology, soil condition, and vegetation determines the Groundwater (GW) recharge process. In general, the influence of the near-surface conditions in semi-arid or arid areas is relatively more prominent in governing the recharge process than that in humid areas. In humid areas, the deep percolation is subjected to the control of surplus precipitation in excess of potential evapotranspiration, infiltration capacity of the soil, and the storage and transport capacity of the subsurface soil. In semi-arid areas, it has been found that potential evapotranspiration on average exceeds rainfall. Therefore, the recharge in semi- arid areas particularly depends on rainfall events of high intensity, when there is possibility of accumulation of rainwater in local depressions and streams exists and the rainwater can escape the loss by evapotranspiration while flowing quickly by percolation through the cracks, fissures/faults or solution channels. Recharge is retarded by vegetation, thick alluvial soils, which allow high retention storage during the wet season and extraction by vegetation during the dry season. In contrast, a poor vegetation cover on a permeable soil near the surface accelerates the rate of recharge (Vries and Simmers 2002). Duah and Xu (2008) have shown the relative extent of recharge significance of various types of recharge for different climate regions as shown in Figure 2.5. The variation of direct recharge with annual precipitation in this diagram is analogous to the Morton's CRAE model as applied for representation of evapotranspiration process.

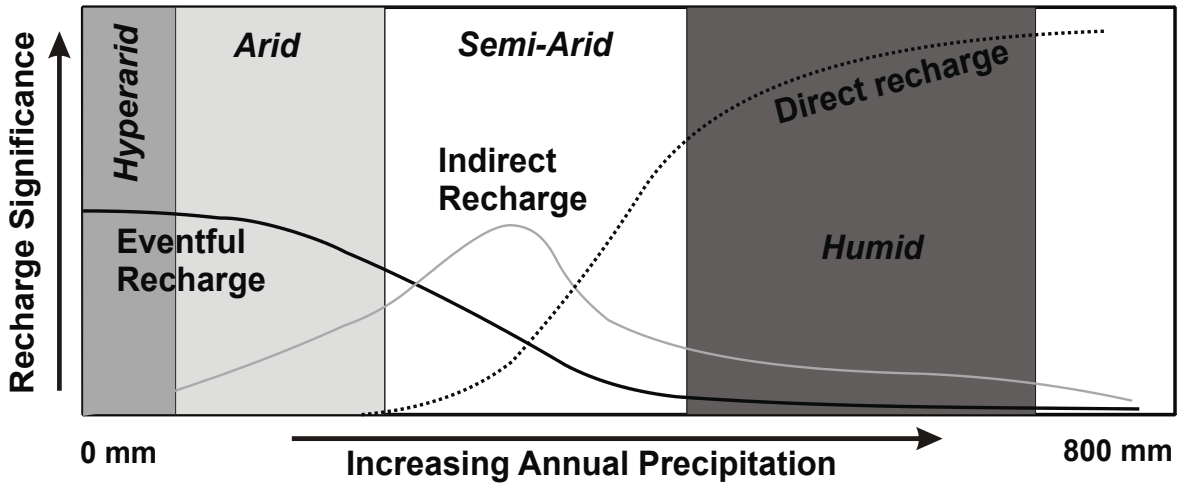

Figure 2.5 A diagram showing different types of recharges in different climate areas (Duah and Xu 2008)

In the present context, the region is of tropical climate with distinct wet and dry spell in the annual cycle, as will be discussed in more detail in Chapter 3. The following sections are provided to review the methods of estimation of recharge and to select the most appropriate method of conceptualising and predicting the groundwater recharge process for the site.

2.2.1. Estimation of Recharge

The methods used for estimating recharge can be broadly classified into the following categories (Hatton 1998):

- Chemical methods based on indicators of recharge processes (existence of Chloride, Tritium and Chlorine-36, Carbon-14 and Chlorofluorocarbons in groundwater);
- Physical methods based on soil properties (Zero flux plane, Darcy's law and Lysimetry);
- Hydrologic methods based on catchment scale (water balance for surface water and subsurface water in the catchment along one, two or three dimensions);
- Observed groundwater response related to hydraulic and geologic property of aquifer;
- Soil water tracer based on movement of tracer (artificial, historical or environmental tracer); and
- Electromagnetic method based on electrical conductivity of soil water.

The methods of estimating recharge can be overviewed with another perspective. The techniques are subdivided into three categories based on the location or zone where the processes occur or interact: surface water zone, unsaturated zone and saturated zone or groundwater. Within each zone, the techniques are generally classified into physical, tracer or numerical modelling approaches (Scanlon *et al.* 2002). Looking in this way will help to select the appropriate technique for the proposed research or to justify the selection of an approach for the understanding of the site condition.

A detailed study shows the important aspects of each approach when choosing appropriate techniques, such as the space/time scale, range of flow, climatic quality and reliability of estimate (Scanlon *et al.* 2002). Figures 2.6, 2.7, 2.8 and Table 2.1 describe broad guidelines for the selection of techniques.

From the integrated review of the related characteristics of the site and the broad guidelines as stated, it is certain that the study of recharge for the site under consideration must encompass both saturated and unsaturated flow conditions together as far as the one-dimensional analysis is concerned. Both saturated and unsaturated flows have distinct significance as related to the environmental safety of the mine site. However, the surface water flow has to be considered if it is concerned with two-dimensional analyses.

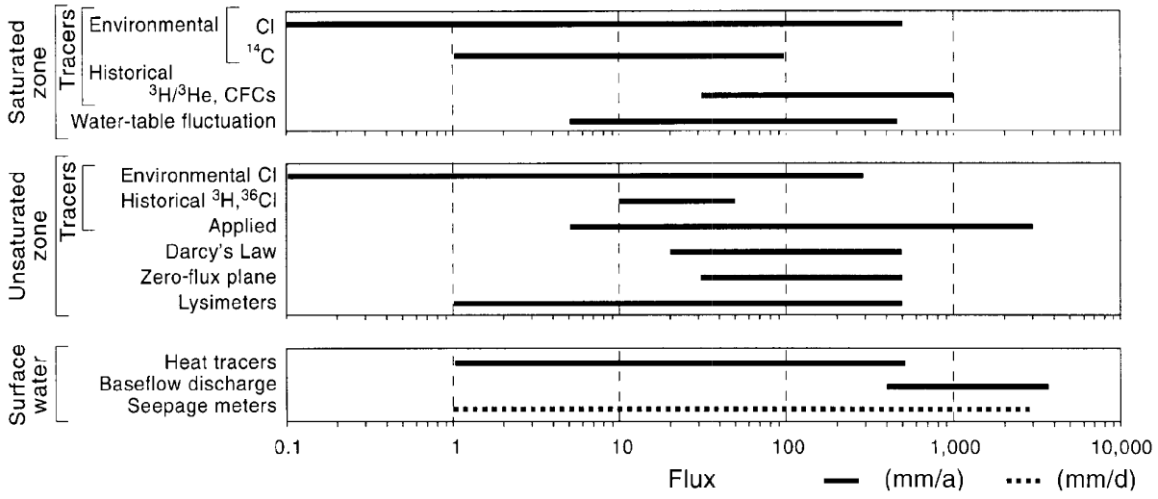

Figure 2.6 Range of fluxes that can be estimated using various techniques (Scanlon *et al.* 2002)

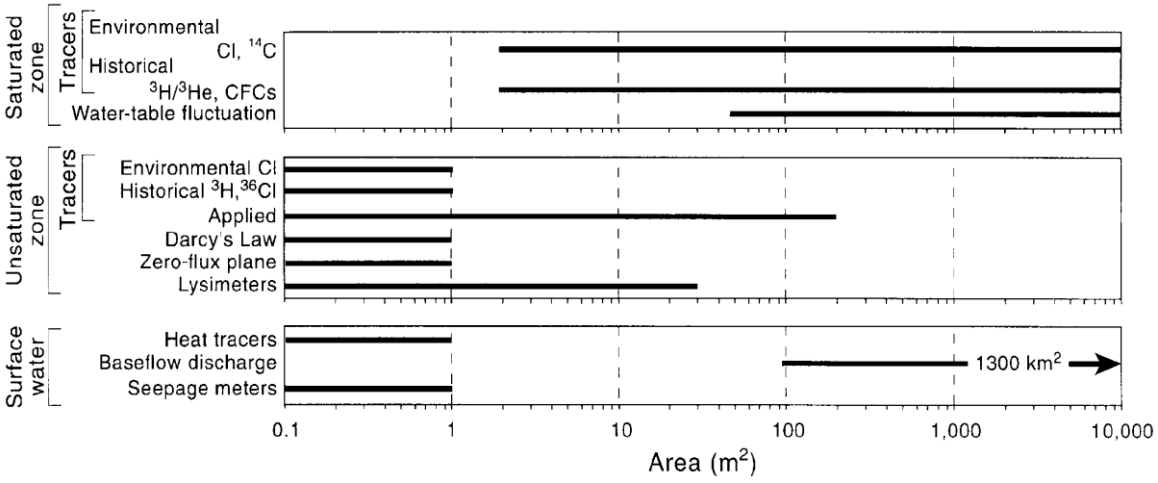

Figure 2.7 Spatial scales represented by various techniques for estimating recharge. Point-scale estimates are represented by the range of 0 to 1 m (Scanlon et al. 2002)

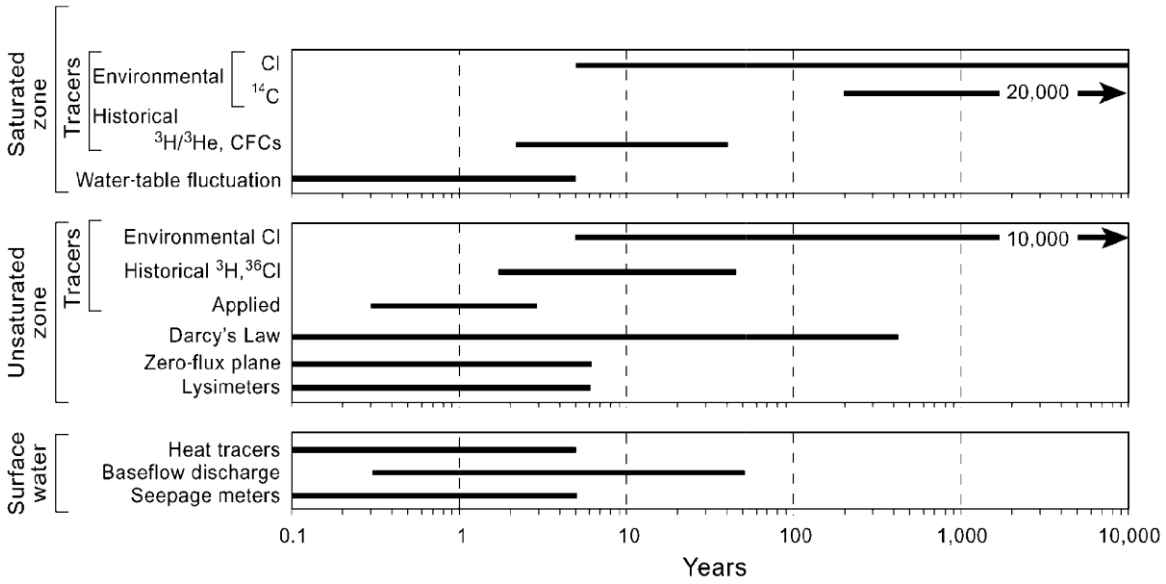

Figure 2.8 Time periods represented by recharge rates estimated using various techniques. Time periods for unsaturated and saturated zone tracers may extend beyond the range shown (Scanlon et al. 2002)

Table 2.1 Appropriate techniques for estimating recharge in regions with arid, semi-arid, and humid climates (Scanlon *et al.* 2002)

Hydrologic zone	Technique	
	Arid and semiarid climates	Humid climate
Surface water	Channel water budget Seepage meters Heat tracers Isotopic tracers Watershed modelling	Channel water budget Seepage meters Base flow discharge Isotopic tracers Watershed modelling
Unsaturated zone	Lysimeters Zero-flux plane Darcy's law Tracers [historical ^{36}Cl, ^{3}H, environmental (Cl)] Numerical modelling	Lysimeters Zero-flux plane Darcy's law Tracers (applied) Numerical modelling
Saturated zone	Tracers [historical (CFCs, $^{3}H/^{3}He$), environmental (Cl, ^{14}C)] Numerical modelling	Water table fluctuations Darcy's law Tracers [historical (CFCs, $^{3}H/^{3}He$)] Numerical modelling

2.2.2. Selection of Technique for Recharge Estimation

Three different methods of investigation for recharge estimation have been reviewed and the range of the past investigations have been classified in terms of the methods of investigation and the zone of groundwater recharge as shown in Table 2.2. From the three major categories of available techniques for recharge study, which may be physical process-based, tracer-based or numerical modelling-based, it can be conceived that numerical modelling is the most versatile. The only limitation of numerical modelling is that it requires some observed data for model validation. Therefore, the available record of climate data and groundwater level data builds the scope of physical process-based modelling for evolution of the best conceptual model.

There are instances when either the physical process-based technique or the tracer technique is combined with numerical modelling in the framework of result validation stage of the investigation. Jimenez-Martinez et al. (2009) use the physical process-based measurement technique with the numerical technique. Other researchers such as Smerdon et al. (2009) use either of the three techniques, such as numerical modelling when adequate time series data are available and physical process-based analyses when insufficient data are available, in which case only annual lumped estimates of the flow components are used.

The review of the previous investigation for estimation of recharge in the site is conducted in detail in Chapters 3 and 5. The significant physical processes for the site include precipitation, evapotranspiration and groundwater storage as established earlier in this chapter. Detailed data-based analyses are also performed in Chapter 5. The method of investigation for prediction of future recharge in the future climate can be easily performed with numerical computation if the future climate data are available. In this regard, the other two methods of estimation are of very limited capacity.

Table 2.2 Classifications of techniques/models for recharge estimation

Zone	Techniques	Names of methods with references
Surface water studies	Physical techniques	Channel water budget: (Lerner et al. 1990; Lerner 1997; Rushton 1997) Seepage meters: (Kraatz 1977), (Lee and Cherry 1978) Base flow discharge: (Meyboom 1961; Rorabough 1964; Mau and Winter 1997; Rutledge 1997; Halford and Mayer 2000; Herrmann *et al.* 2009)
	Tracer techniques	Heat tracer:(Stallman 1964; Lapham 1989; Constantz *et al.* 1994; Healy and Ronan 1996; Ronan *et al.* 1998) Isotopic tracer:(Stuyfzand 1989; Taylor *et al.* 1989; Taylor *et al.* 1992)
	Numerical modelling	Lumped: (Kite 1995; Tilahun and Merkel 2009) hydrologic-response units (HRUs) or hydrogen-geomorphologic Units (HGUs): (Salama *et al.* 1993), (Leavesley and Stannard 1995) SHE (Mudgway et al. 1997), MIKE-SHE (Smerdon *et al.* 2009) BRANCH (Schaffranek 1987) GSSHA (Ogden 2000; Nelson 2001; Ogden and Y 2002) AWBM, SIMHYD (Podger 2004) GROWA (Herrmann *et al.* 2009)
Unsaturated - zone studies	Physical techniques	Lysimeters: (Brutsaert 1982; Allen et al. 1991; Young et al. 1996) Zero – flux plane: (Cooper *et al.* 1990; Sharma *et al.* 1991) Darcy's law: (Sammis *et al.* 1982; Stephens and Knowlton 1986; Healy and Mills 1991; Nimmo *et al.* 1994)

	Tracer techniques	Applied tracers: (Athavale and Rangarajan 1988; Kung 1990; Flury *et al.* 1994; Cresswell *et al.* 1997; Aeby 1998; Forrer *et al.* 1999) Historical tracers: (Nativ *et al.* 1995; Sibanda *et al.* 2009)
	Numerical modelling	Soil water storage routing: bucket model (Flint *et al.* 2002; Walker *et al.* 2002) Quasi-analytical: (Kim *et al.* 1996; Simmons and Meyer 2000) HELP (Schroeder *et al.* 1994; Stephens and Coons 1994), Numerical solution to Richards equation: BREATH (Stothoff 1995), HYDRUS – 1D, HYDRUS -2D (Simunek et al. 1996), SWIM (Verburg *et al.* 1996), VS2DT (Lappala et al. 1987), (Hsieh et al. 2000), WAVES (Dawes and Short 1993), UNSAT – H (Fayer 2000), VAMOS (Bornhoft 1994), CLASS U3M (Tuteja *et al.* 2004). Pedotransfer Function (Wang *et al.* 2009a)
Zone	Techniques	Names of methods with References
Saturated zone studies -	Physical techniques	Watertable fluctuation: (Meinzer and Stearns 1929; Rasmussen and Andreasen 1959; Gerhart 1986; Hall and Risser 1993; Healy and Cook 2002; Sibanda *et al.* 2009) Darcy's law: (Theis 1937; Belan and Matlock 1973; Nativ *et al.* 1995; Sibanda *et al.* 2009)
	Tracer techniques	Groundwater dating by historical tracer: (Allison and Hughes 1977; Egboka *et al.* 1983; Robertson and Cherry 1989) Environmental tracers: (Johnston and Needham 1999; Cook et al. 2001)

	Numerical modelling	Analytic element method: (Strack 1989) Inverse modelling: (Reilly *et al.* 1994; Szabo *et al.* 1996; Portniaguine and Solomon 1998) SMAR(Tan and O'Connor 1996) SWAGSIM (Prathapar et al. 1994) Surface water and groundwater: SWAT and MODFLOW (Sophocleus and Perkins 2000) Arc GIS and MODFLOW (Ajami *et al.* 2007) saturated and unsaturated zone: Seep/W (Krahn 2004b), Vadose/W (Krahn 2004a).

2.3. Physical Process-based Models for GW Recharge

To predict the behaviour of seepage and GW recharge of any catchments using numerical models, it is essential that adequate consideration is given to the underlying theories based on which the model has been programmed. There has been a general understanding of numerical models that simplicity and accuracy do not go in a body. It is conventional to start with a simpler water balance model to conceptualise the significant processes in the system and then apply that understanding to represent the more complex processes such as unsaturated flow condition together with the saturated flow system. A range of approaches exists for modelling and a very brief description of the classification of the models is reviewed. Following this, only the relevant approaches are detailed.

2.3.1. Classification of Models

The three basic features useful for distinguishing approaches to modelling are:

- The nature of the basic algorithms (empirical, conceptual or process-based);
- Whether a statistical or deterministic approach is taken to input or parameter specification; and
- Whether the spatial and temporal representation is lumped or distributed.

There has been a range of work related to classifications of model. Some of the following classifications are reported from the toolkit resource of Cooperative Research Centre for Catchment Hydrology (CRC for CH) (CRCCH 2005).

Empirical, regression or 'black-box' models: The first question of classification is whether any attempt is made to represent the basic processes. Models that simply calibrate a relationship between inputs and outputs are known as empirical, regression or 'black-box' models.

Conceptual-empirical models: The next step in complexity is conceptual-empirical models; in the case of catchments modelling, the basic processes such as interception, infiltration, evaporation, surface and subsurface runoff are separated to some extent.

Physically-based or process-based models—complex conceptual models: As the quest for deeper understanding of hydrological processes has progressed, models based on the

fundamental physics and governing equations of water flow over and through soil and vegetation have been developed.

Stochastic or deterministic representations: Another basic distinction between models is whether stochastic or deterministic representations and inputs are used. Most models are deterministic, meaning that a single set of input values and a single parameter set are used to generate a single set of outputs. In stochastic models, some or all of the inputs and parameters are represented by statistical distributions, rather than single values.

Physical models or analog models: The laboratory representation of field conditions is a physical model and the conceptual models based on analogy of the physical processes are analog models.

Lumped or distributed models: Spatially lumped models treat the modelled area (such as sub-catchments) as a single unit and average the effects of variability over that unit. Spatially distributed models separate the region to be modelled into discrete units, enabling different model inputs or parameters to be used to represent spatial variability.

Temporally lumped and distributed models: Some models are designed to provide output that represents 'average' or 'long-term' values may be called 'temporally lumped', whereas others are 'time stepping' models in which output is produced at regular intervals such as hourly, daily or monthly may be called temporally distributed.

Finite difference and finite element models: Depending on the temporal and spatial discretisation and solution technique, there may be finite difference models, finite element models or analytic element models.

1-2-3 dimensional models: Depending on the spatial description of the location to be modelled, it may be one-dimensional, two-dimensional or three-dimensional. A three-dimensional modelling approach is the most adequate way to capture the subsurface complexity of most geologic settings, which can lead to improved hydro-geologic appraisals in the context of an integrated approach.

In the following sections, only the theories of the process-based models (saturated and unsaturated flows) and then the representation and solution techniques (finite element and finite difference) are highlighted. By considering the current research objective and available resources of modelling software in terms of data requirement and physical basis, the most appropriate models are selected for detailed analyses.

2.3.2. Water Balance in Saturated Flow

The relationship between the ongoing processes for any control volume in a hydrologic system can be described by the water balance equation. The equation states that the difference between inflow and outflow to and from the system should be equal to the change in storage, as is demonstrated in Equation 2.1. Some of the variables are represented by measured or estimated values while others are represented by equations, most of which are empirically developed. The number of unknowns that could be solved is to be equal to the number of equations available. Therefore, the appropriate modelling approaches are developed so that the number of unknowns is reduced to match the purpose of modelling with availability of data and other issues related to practical conveniences.

The catchment and climate characteristics determine the relative importance of all those components of water balance equations. For example, the intensity of rainfall and potential infiltration capacity of soil determines whether there will be surface storage or surface runoff.

The two examples of saturated flow models commonly used by the hydrologist community in Australia for surface water modelling and groundwater modelling are the Australian Water Balance Model (AWBM) (Podger 2004) and the Modular Three-dimensional Finite Difference Groundwater Flow Model (MODFLOW) (McDonald and Harbaugh 1988).

AWBM: AWBM is a catchment water balance model that can relate runoff to rainfall. It does not consider unsaturated flow. The flow to groundwater resources from rainfall is estimated grossly by introducing the Base Flow Index (BFI), which is an empirical value ratio between base flow and total stream flow (Podger 2004). The estimation of groundwater recharge by using this model is highly dependent on the reliability and representativeness of runoff data for a particular site. In Chapter 5, this issue will be discussed in relation to the site under consideration.

MODFLOW: The MODFLOW model considers the three-dimensional movement of groundwater of constant density through porous material by using Darcy's equation and finite difference as the solution technique (McDonald and Harbaugh 1988). It is a saturated flow model. The MODFLOW model can be used to compute the water balances for extreme weather conditions like flood. However, the unsaturated flow condition is not adequately represented in MODFLOW. The 'recharge coefficient' is used to represent the inflow of water to the soil system. This value is a percentage value of rainfall for a site and is estimated from annual water balance components of the site under consideration. Recent investigators are using this model in combination with unsaturated flow models and packages for considering evapotranspiration flow in combination with rainfall (Twarakavi *et al.* 2008; Doble *et al.* 2009).

The AWBM is used for developing a conceptual model of the site because unlike MODFLOW, it does not require soil property data. In addition, MODFLOW is a three-dimensional model whereas AWBM is a data-based empirical model. Therefore, at the preliminary stage of saturated flow modelling, a less data-intensive model is used. For further detailed modelling for unsaturated conditions, other models are considered, which will be discussed shortly. However, before looking at the models, the formulation of unsaturated flow equation must be introduced.

2.3.3. The Richard's Equation in Unsaturated Flow

One-dimensional vertical flow of water through isothermal, rigid, saturated soil is governed by Darcy's law (Darcy 1856; Buckingham 1907) in Equation 2.2:

$$q = -K \frac{\mathrm{d}H}{\mathrm{d}z} \qquad \text{Equation 2.2}$$

where

q = water flux density = volumetric water flow per unit cross-sectional area per unit time [cm^3 volume of water/cm^2 area of soil/h time]

K = hydraulic conductivity [cm^2 water/cm soil/h]

H = hydraulic head [cm water]

z = distance into the soil [cm soil]

As long as soil can be treated as a continuum, Darcy's law has been proven valid. The continuity of flow path is interrupted as moisture content falls below saturation, i.e. in unsaturated flow. In a flow situation where flow, conductivity and head vary in space and time, the equation of continuity or equation of conservation of mass is to be combined with Darcy's law to describe the flow mechanism in a more representative way. For incompressible flow, the combination of these two basic equations, named Richards' equation (RE) (Richards 1931), is written as Equation 2.3:

$$\frac{\partial \theta}{\partial t} = \frac{\partial}{\partial z}\left(K \frac{\partial H}{\partial z}\right) + S \qquad \text{Equation 2.3}$$

where

θ = volumetric water content [cm^3/cm^3]

t = time [h]

S = source or sink strength [cm^3 water/cm^3 soil/h]

In rigid, unsaturated or saturated soil, in which the gas pressure is always atmospheric (i.e. air can move freely) the hydraulic head (H) is the sum of gravitational potential (z) and the matric potential (Ψ). The RE then becomes Equation 2.4:

$$\frac{\partial \theta}{\partial t} = \frac{\partial}{\partial z} K\left(\frac{\partial \psi}{\partial z} + 1\right) + S \qquad \text{Equation 2.4}$$

This equation is highly non-linear whereby K and Ψ change over several orders of magnitude with change in θ. The RE-based representation is a more accurate simulation of the water balance components of the system of the vadose zone groundwater and soil surface.

2.3.4. Solution Techniques of RE

There are numerous codes written for the purpose of solving the RE by the method of finite difference or finite element techniques. They are always being updated due to the development of the computing technologies and industries. Some of the currently available packages relevant to the proposed research are investigated in this work. For finite difference techniques, the models considered are Soil Water Infiltration and Movement

(SWIM) (Verburg *et al.* 1996), and Catchment Scale Multiple-Land use Atmosphere Soil Water and Solute Transport Model (CLASS) (Vaze et al. 2005). For finite element techniques, the models considered are Seep/W (Krahn 2004b) and Vadose/W (Wilson 1990).

SWIM: Soil Water Infiltration and Movement (SWIM) is a software package developed within the CSIRO Land and Water for simulating infiltration, evapotranspiration, and redistribution. It combines water movement with transient solute transport and accommodates a variety of soil property descriptions and flexible boundary conditions (Verburg *et al.* 1996) .

This is based on a numerical solution of the RE and the advection-dispersion equation. Soil water and solute transport properties, initial conditions and time dependent boundary conditions (such as precipitation, evaporative demand, solute input) need to be supplied by the user in order to run the model.

Using a hyperbolic sine transform of Ψ, as shown in Equation 2.5, for dry range unsaturated flow with $\Psi_0 < \Psi_1$ as:

$$-\frac{\psi-\psi_0}{\psi_1} = \sinh p \qquad \text{Equation 2.5}$$

and linear transform of Ψ, for wet range saturated flow with $\Psi_0 > \Psi_1$, as in Equation 2.6:

$$-\frac{\psi-\psi_0}{\psi_1} = p \qquad \text{Equation 2.6}$$

RE can be written as Equation 2.7:

$$\frac{\partial\theta}{\partial t} = \frac{\partial}{\partial x} K\left(\frac{\mathrm{d}\psi}{\mathrm{d}p}\frac{\partial p}{\partial x} + \frac{\mathrm{d}z}{\mathrm{d}x}\right) + S \qquad \text{Equation 2.7}$$

where Ψ_0 is the shifting parameter and Ψ_1 is the scaling parameter for the transformation. Appropriate choice of Ψ_0 allows the inverse hyperbolic sine transform to be applied for dry range and linear transform for wet range.

Use of this transform allows SWIM to deal with unsaturated and saturated flow and dry soils with relatively large space steps in the solution. SWIM uses finite difference methods such as backward differencing in time and central differences in space for RE and for solving, uses the Newton-Raphson method (Verburg *et al.* 1996).

CLASS: CLASS is a physically-based distributed eco-hydrological modelling framework that can be used to predict land-use effects at paddock, hill slope and catchment scales. Effects of climate scenarios predicted by stochastic climate models as well as the effects of spatio-temporal climate variations within a catchment can be analysed (Vaze et al. 2005). The RE is explicitly solved by the finite difference method.

The model uses adaptable sub-daily simulation time steps by sensing the transient nature of the atmospheric conditions and attempts to overcome the divergence problems usually associated with solution of the RE. The vertical flux computations are implemented at a shorter time interval than that of the horizontal. Hydraulic diffusivity $D(\theta) = K / (d\theta/d\Psi)$ is considered another parameter, similar to vapour diffusivity (Verburg *et al.* 1996) in the soil as used in SWIM to consider isothermal vapour flow, to address the unsaturated hydraulic property (Tuteja *et al.* 2004).

Seep/W: In Seep/W, the solution of the partial differential equation is achieved by using the finite element method (Krahn 2004b). The RE is written in a two-dimensional form. Applying the Galerkin method of weighted residuals to the RE, the following finite element for two-dimensional seepage is derived, as in Equation 2.8:

$$[K]\{H\} + [M]\{H\},t = \{Q\} \qquad \text{Equation 2.8}$$

where

[K] = the element characteristic matrix for hydraulic conductivity

{H} = the vector of nodal heads (hydraulic head)

[M] = the element mass matrix (soil mass for moisture storage)
t = time derivative of
{Q} = the element applied flux vector (source or sink).

Seep/W uses the backward difference method for temporal integration of the time variant section of the finite element equation. Gaussian numerical integration is used for the evaluation of *[K]* and *[M]*. The integrals are evaluated by sampling element properties at specifically defined points and then summed together for the entire element. The integrals for source or sink term are solved by closed-form solutions for two-dimensional analyses.

Vadose/W: In Vadose/W, the basic equations for water flow are written in terms of pressure head (P) in place of total hydraulic head (H) to consider the findings of Wilson (1990) regarding the relationship of potential and actual evaporation with pore water pressure in a proper way. The hydraulic property of unsaturated soil drastically changes with the increase of soil suction, which depends on the amount of flow of water, which is again a function of hydraulic property and *vice versa*. Thus, to simulate the behaviour of unsaturated soil, flow of mass (liquid water and water vapour) and flow of energy (heat) are coupled together to conserve both mass and energy (Krahn 2004a). The finite element formulation of the coupled flow of mass and energy can be generalised in brief as follows.

The finite element equation for mass (liquid water and water vapour) transfer is shown in Equation 2.9 and finite element equation for energy (heat) transfer is demonstrated in Equation 2.10:

$$[K_w]\{P\}+[K_{wt}]\{T\}+[M]\{P\},t=\{Q\} \qquad \text{Equation 2.9}$$

$$[K_t]\{T\}+[K_{tw}]\{P\}+[M_t]\{T\},t=\{Q_t\} \qquad \text{Equation 2.10}$$

Therefore, these two equations can be combined to form Equation 2.11:

$$\begin{bmatrix} K_w K_{wt} \\ K_{tw} K_t \end{bmatrix}\begin{Bmatrix} P \\ T \end{Bmatrix}+\begin{bmatrix} M0 \\ 0M_t \end{bmatrix}\begin{Bmatrix} P \\ T \end{Bmatrix},t=\begin{Bmatrix} Q \\ Q_t \end{Bmatrix} \qquad \text{Equation 2.11}$$

where $[K_w]$ and $[K_{wt}]$ are the relevant element characteristics matrices (hydraulic conductivity and thermal conductivity) for mass flow and $[K_t]$ and $[K_{tw}]$ are the relevant element characteristics matrices for heat flow.

2.3.5. Selection of Unsaturated Flow Model

In the water balance equation, as mentioned previously, some of the parameters such as rainfall, infiltration, evaporation, transpiration, and surface runoff are assumed to be known while the seepage and deep drainage are the parameters to be determined. The solution of this water balance equation requires saturated hydraulic conductivity of soil as long as flow is saturated. However, as the flow may be unsaturated as well, the variable hydraulic conductivity should be defined as a function of suction. In such a case, quantification of flow of water through soil requires the hydraulic property function of soil. Therefore, to analyse a range of physical conditions, a number of numerical models are investigated.

All of the unsaturated flow models require the basic hydraulic properties such as porosity, soil moisture characteristics, or volumetric water content function or parameters to define the relationship of hydraulic conductivity, soil moisture content and soil suction. However, specific factors that differ depending on the model are as follows:

- The SWIM model requires coefficients related to soil property and solute transport, which in turn involves hysteresis function, adsorption isotherm and dispersion coefficients. Moreover, the boundary conditions require vegetation characteristics and water management practices in addition to soil and solute properties (Verburg *et al.* 1996).
- CLASS requires data for land use pattern involving the vegetation characteristics such as physical and physiological properties of root and leaf (Vaze et al. 2005).
- Vadose/W requires the thermal conductivity function of the soil in addition to the hydraulic conductivity function for the representation. The thermal conductivity function is not required for Seep/W.

The ultimate purpose of the current research is to investigate the centurial scale response of GWLs with multiple numbers of scenarios. These include the Special Report on Emission Scenarios (SRES) of the Intergovernmental Panel on Climate Change (IPCC) and considering the thousands of replicates of natural climatic variability, such as ElNino

Southern Oscillation (ENSO) events. Therefore, the ease of application with regard to numerous ranges of input data is another selection criterion of the physically-based model. With the appropriate combination of theoretical basis, data requirement and ease of application, Seep/W model is selected for modelling the saturated-unsaturated flow condition.

2.4. Statistical Techniques in Hydrology

It was reported earlier that numerical models based on physical processes are an appropriate method for estimation of recharge. Numerical models can also be based on non-physical processes, statistical process-based models are one example. Statistical methods have been traditionally applied to hydrological processes by many investigators. Klemes (1978), and Salas and Smith (1981) provided a review of the research on the physical foundations of stochastic models used in hydrology (Hipel and McLeod 1994). In many instances, the complexity of the physical processes or inadequacy of the observed data for the preferred spatial and temporal scale hinders the applicability of the traditional upward or reductionist approach in hydrological prediction (Bloschl and Sivapalan 1995; Sivapalan *et al.* 2003). Through the synthesis of the traditional upward or reductionist approach (based on the laws of physics) with the downward approach (based on systematic learning from data), significant progress can be achieved in the representation and prediction of hydrologic systems. The application of time series analysis techniques is thus intended as a complementary approach to the physically-based computational modelling work. For example, Mayer and Congdon (2007) used time series analyses with seasonal decomposition to groundwater levels to identify the climate and anthropogenic effects. Some of the relevant theories for the application of the time series method to the present research are reviewed in Appendix B.

2.4.1. Time Series Techniques

A time series is a set of observations generated sequentially in time. If future values of a time series are estimated by some mathematical functions then the time series is *deterministic*. If the future values can be described only in terms of a probability distribution, the time series is non-deterministic, or simply a *statistical* time series (Box and Jenkins 1976). The statistical time series method is incorporated into the current research. It was stated by Gaspar (1984) that ‘time series analysis consists of all the

techniques that, when applied to time series data, yield, at least sometimes, either insight or knowledge, and everything that help us choose or understand these procedures'.

The observed time series is an actual realisation of an underlying time series process. The term 'realisation' refers to a sequence of observed data points, not just a single observation (Vandaele 1983). With regard to the present research, the yearly variability and seasonality in each year's climate and the various relevant activities in the site are to be considered simultaneously to represent the response of groundwater table. The past record of climate and GWLs should be considered to be the time series realisation of the underlying time series processes.

The reasons for studying time series often consist of determination of the most appropriate method of investigation to be used, achieving an overview of some basic steps of exploratory analyses, and performing the forecasting and control of the time series processes (Vandaele 1983). The specific objectives of the time series analyses are as follows:

1. To obtain a concise *description* of the features of a particular time series process;
2. To construct a model to *explain* the time series behaviour in terms of other variables and to relate the observations to some structural rules of behaviour;
3. Based on the results of 1 and 2, to use the analysis to *forecast* the behaviour of the series in the future, based upon knowledge of the past; and
4. To *control* the process generating the series by examining what might happen when we alter some of the parameters of the model.

Possibly, the most important objective in this study of time series modelling is to help uncover the dynamical law governing its generation. Obviously, a complete uncovering of the law governing its generation demands a complete understanding/representation of the underlying physics, chemistry and biology. When the underlying theory is far from complete (because of too many complex processes acting together) and the problem is presented with not much more than the data themselves, the previously mentioned approach is reasonably acceptable (Tong 1990).

With regard to the present research, the aforementioned objectives could be explicitly described as follows. The primary objective of the time series modelling is to examine the

inherent components (deterministic and stochastic) of the climate and GWL time series, and to investigate the possibility of representing the process using different statistical models (see Appendix B for details). The possibility could be a representation of the univariate model, the multi-variate model, the transfer function model (Brockwell and Davis 2002) and the rational distributed lag transfer function model (Pankratz 1991), which is represented as a multiple regression model. The secondary objective is to represent the dependent variable as a function of the independent and intermediate variables, which restrengthens the necessity of including most of the variables in the physically-based model of the system (Seep/W). In a more philosophical way, the objective can be phrased as 'understanding the physics with the help of statistics'. The tertiary objective is prediction of future response of dependant variables (such as GWLs) with the corresponding change in independent variables (such as rainfall and net flux).

The relationship of the variables in time series models could be represented as independent and dependent types. *Independent* variables denote a predictor variable that is used to predict another variable and *dependent* variable refers to a predicted variable. These two roles are not mutually exclusive; an *intervening* variable plays both roles, being an independent variable in one component of the prediction and a dependent variable in another (Hildebrand et al. 1977). This incorporation of bilateral behaviour of the key variables is important in the representation of the system.

2.4.2. Application of Time Series Analyses in the Research

The most important application of statistical techniques in the present research is related to exploratory analyses. Slimani et al. (2009) can be cited as a typical example of using time series statistics to explain the spatio-temporal variability of groundwater levels as influenced by climatic and geological forcings, Chapter 6 provides a detailed description. The other application includes the long-term forecast of climate and GWL data. This forecast is based purely on historical data and thereby a completely non-physical approach is taken. This can be applied as a comparative assessment of the uncertainty limits of physical and non-physical methods.

There are numerous instances in which time series models are used for hydrological forecast and uncertainty analyses. For instance, while estimating the uncertainty of these forecasts, Monatanari and Grossi (2008) use Auto Regressive Moving Average (ARMA)

models for synthetic data generation in their study. Therefore, the comparative analyses of the confidence intervals of statistical methods with physical methods would be a more comprehensive way of evaluating the uncertainties of this type of investigation. More detailed application-based reviews have been provided in the later sections.

2.5. Climate Change and Groundwater Recharge

The use of numerical methods for the representation and prediction of groundwater recharge as a response to long-term future climate has been partly reviewed in the earlier section while considering the non-physical techniques. However, the physically-based techniques used for the same purpose are much more scientifically significant and possess stronger acceptance from the scientific community. The prediction of groundwater recharge as impacted by changing climate has been attempted by many recent investigators such as (Dibike and Coulibaly 2005; Scibek and Allen 2006a; Wilby *et al.* 2006a; Scibek and Allen 2006b; Wilby *et al.* 2006b; Wilby and Harris 2006c; Jyrkama and Sykes 2007; Scibek *et al.* 2007; Herrera-Pantoja and Hiscock 2008; Hiscock *et al.* 2008; Steele-Dunne *et al.* 2008). These all utilise physical process-based numerical modelling. A more critical appreciation of these investigations is performed in Chapter 7 while generating the future climate data.

The use of the numerical model for the prediction of recharge in the future climate is primarily dependent on the selection of the right conceptual model of the present groundwater flow system. The manifestation of the conceptual model is always relevant to a specific set of climate data. With regard to the present research, the numerical model based on physical process is used for the validation of historical groundwater level data. The prediction of future response is performed by using the data of changed variable future climate. Thus, the prediction of future recharge, which is the function of future climate, should embrace the challenge of prediction of future climate. Therefore, the future climate prediction is another issue that must be addressed.

The task of future climate prediction does not only rely on the climate prediction scenarios but also the consideration of natural climatic variability. To encompass a range of natural climatic variability, the future climate data are to be generated considering all the possible interactions of the ocean-atmospheric circulations surrounding the research site. The ocean-atmospheric circulations are believed to be responsible for natural climatic

variability of annual, multi-annual, decadal and multi-decadal time scales. A detailed description of this issue is conducted in Chapter 7.

The literature for understanding the scientific basis of prediction of future climate is reviewed here to investigate the strengths and weaknesses of the relevant issues.

2.5.1. Climate

The term 'climate' is commonly used by a wide range of disciplines. The meaning of the term varies among users and in various contexts. The classification of climate is also performed according to a range of criteria. Therefore, it is imperative that a reasonably accepted definition of the term and related concepts should be considered and used. In Sections 2.5.1, 2.5.2, 2.5.3 and 2.5.4, unless otherwise specified, most of the contents elaborate on the definitions and concepts that have been obtained from IPCC reports (Houghton *et al.* 2001; Solomon *et al.* 2007).

Climate is usually defined as the 'average weather', or as the statistical description in terms of the mean and variability of relevant quantities over a certain period. The average period is 30 years, as defined by the World Meteorological Organisation (WMO). However, in times of insufficient data, it is acceptable to use 20 years of data as indicated in Solomon et al. (2007). These quantities mainly consist of surface variables such as temperature, precipitation and wind.

In a more comprehensive sense, climate could be manifested as the state comprising of a statistical description of the various physical processes of climate system. Thus, climate system should consist of the significant components such as atmosphere, hydrosphere, cryosphere, land surface and biosphere. With the influence of its own internal dynamics of the various processes and the external forcing, which could include volcanic eruptions, solar variations, and human-induced forcing in the atmosphere, land and water, the system is in the continuous process of evolution with respect to time.

It should be mentioned here that in the context of the present research, the climate data as used to indicate the hydro-climatic variables responsible for causing flow of water to and from the surface and subsurface soil water system consist of rainfall, runoff and evapotranspiration processes only. The influence of other hydro-climatic variables such as

temperature, humidity, atmospheric pressure, radiation and wind speed are assumed to be represented indirectly by the rainfall and evapotranspiration process.

2.5.2. Climatic Variability and Climate Change

As defined in the IPCC report (Solomon *et al.* 2007):

> Climate change refers to a change in the state of the climate that can be identified (e.g., by using statistical tests) by changes in the mean and/or the variability of its properties, and that persists for an extended period, typically decades or longer. Climate change may be due to natural internal processes or external forcing or to persistent anthropogenic changes in the composition of the atmosphere or in land use.

Climate change in IPCC usage refers to any change in climate over time, whether due to natural variability or human activity. This usage differs from that of the United Nations Framework Convention on Climate Change (UNFCCC). The UNFCCC defines climate change as 'a change of climate which is attributed directly or indirectly to human activity that alters the composition of the global atmosphere and which is in addition to natural climate variability observed over comparable time periods.' A distinction as made by UNFCCC is that 'climate change' is attributable to human activities altering the atmospheric composition, and 'climate variability' is attributable to natural causes.

There have been numerous documentations regarding the evidence of changing climate in concurrent scientific publications. The increase in global temperature as the cause of reduction of snow cover has been addressed by investigators from the last decade (Serreze et al. 2000). Hinzman et al. (2005) give a wide range of descriptions of the impact of climate change in the hydrologic cycle and biogeochemical cycle for northern Alaska and other Arctic regions. Very recently, a number of studies have examined the extent of change in stream flow and snow cover in relation to climate change (Adam *et al.* 2009; Jong *et al.* 2009; Schmidt *et al.* 2009; Schoner *et al.* 2009).

Both climate change and climatic variability of a particular region are influenced by its geographical characteristics such as the sea or water body, ground surface and atmospheric interactions, solar activities and human interventions. The ongoing processes, such as physical, chemical, biological, biochemical or any other, are specific for each location. The evidence of climate change and variability in various locations and time is being increasingly investigated by the researchers to understand, predict and control the processes.

The sufficient spatial and temporal resolution of these prediction processes needs extensive computational work. The resolution of the scale (temporal and spatial) of computation and the complexity of the ongoing scientific processes that are to be represented in the computation are two opposite areas of endeavour. In all modelling studies, one is compromised for the sake of the other. Therefore, the complexities of the processes, scale of area and time period need to be optimised. With regard to the long-term impact analyses of future climate in groundwater for a specific site, exploration and use of the relevant understanding of climate change and climatic variability has to be combined optimally to generate the future replicates of climate by formulating an appropriate statistical process. The incorporation of statistics into this type of future predictive study is a well-established method. A detailed discussion of this topic can be found in Chapter 7.

2.5.3. Climate Prediction

A climate prediction or climate forecast is the outcome of an attempt to estimate the evolution of the climate in the future at various time scales, such as seasonal, interannual, decadal or long-term. It is different to climate projection in some ways. For example, climate projection is the projected response of the climate system to emission or concentration scenarios of greenhouse gases and aerosols, or radiative forcing scenarios, which are based upon simulations by climate models. Therefore, the climate scenario is a plausible and often simplified representation of the future climate, based on an internally consistent set of climatological relationships that are constructed for investigating possible consequences of human-induced climate change. The scenarios are represented in terms of mean values of the variables with specific and clear trends that are devoid of the natural variability.

The prediction of weather is reliable as it is predicted for a few days from the present but prediction of climate is questionable because of its scale of time, space and underlying internal dynamics and external forcing. A poor understanding of the carbon cycle and feedback from clouds (trapping or reflecting heat) are still reported as the two biggest unknowns by the top 150 top climate modellers of the world. Another limitation is the relative inadequacy of the computing power to deliver detailed information at a local level by the General Circulation Models (GCMs).

With all of these shortcomings in the field of climate prediction, significant progress in the understanding of the scientific basis has been achieved with increased confidence on the climate change phenomena as reported by the IPCC 2001 and 2007 reports (Solomon *et al.* 2007). The incorporation of multiple numbers of climate models with all the available prediction scenarios should result in better confidence of the predicted results. This technique is followed in the present research. The description about the climate models and the possible emission scenarios considered in the present study are described in Chapter 7. In the following section, some basic concepts of the climate models are introduced.

2.5.4. Global Climate Model/General Circulation Model

GCMs are numerical representations of the climate system based on the physical, chemical, and biological properties of its components, their interactions and feedback processes, and accounting for all or some of its known properties. Some of the important features of GCMs can be listed as follows. They incorporate equations of motion for atmosphere and ocean, take account for fluid flow and heat transports and account for partitions of energy between internal reservoirs. The equations to be solved are highly non-linear and cannot be solved analytically hence are solved numerically (Risbey *et al.* 2000; Hennessy *et al.* 2004). The various processes represented in a GCM are illustrated schematically in Figure 2.9.

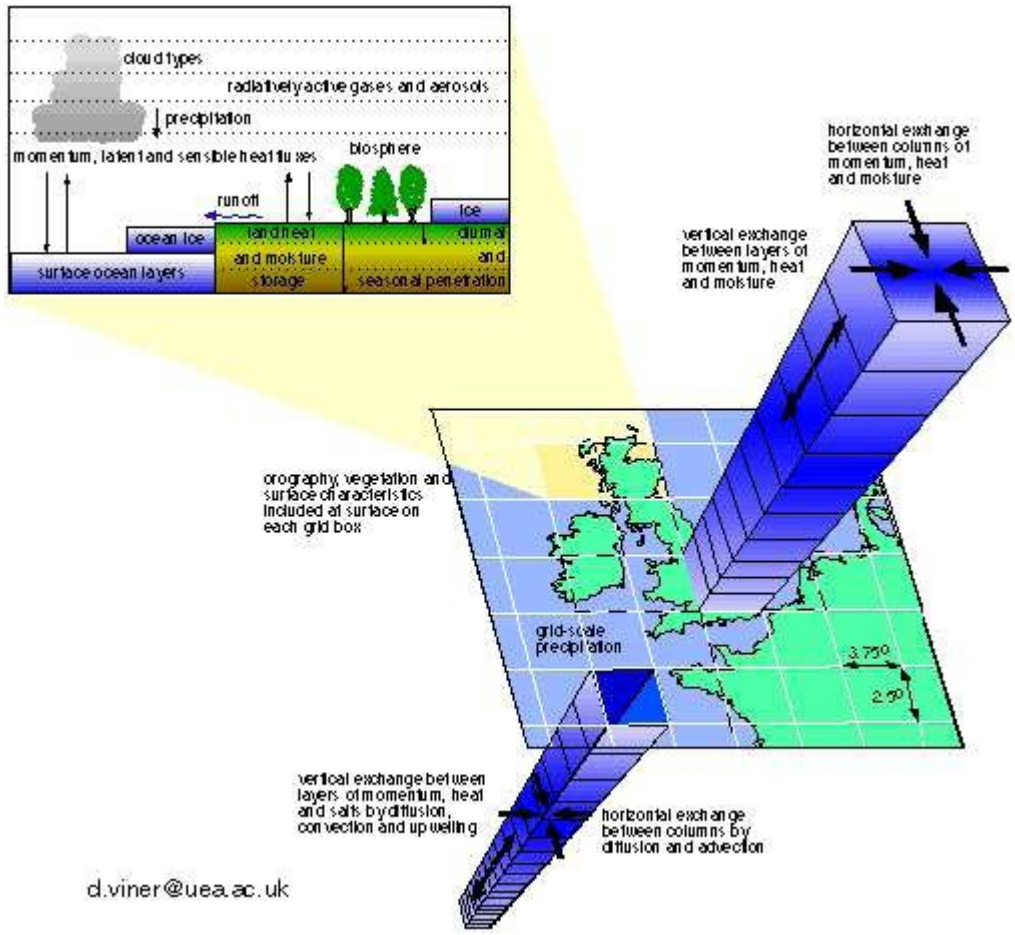

Figure 2.9 Process representation by GCM (Risbey *et al.* 2000)

Models of varying complexity and coupled Atmosphere/Ocean/Sea-ice General Circulation Models (AOGCMs) provide a comprehensive representation of the climate system. These models are applied as a research tool to study and simulate the climate and also for operational purposes, including monthly, seasonal and interannual climate predictions (Risbey *et al.* 2000; Houghton *et al.* 2001). GCMs are not calibrated to reproduce the current climate but may be tuned to fit observed data as closely as possible. Future climate is estimated simply by changing the composition of the model atmosphere (Arnell 2002). In the present research, a number of GCMs output of 100-year monthly climate data are used as a deterministic (non-stochastic) indication for the predicted climate change impact to the hydro-geologic system of the site. This is discussed in detail in Chapter 7.

2.5.5. Climate Influencing GW

During the last 100 years, global climate has warmed by an average of 0.6^{o}C, which has been caused primarily by greenhouse gas emissions from human activities (Houghton *et al.* 2001; Solomon *et al.* 2007). If global greenhouse gas emissions are not reduced

significantly, the climate models project an increase in temperature of another 1.4^{o} to 5.8^{o}C in the next century. This change in temperature is much higher than the past change of 2^{o}C, which occurred during the one millennium since the last ice age (Houghton *et al.* 2001; Solomon *et al.* 2007). Though there are areas of inadequate understanding, such as the role of the carbon cycle and cloud feedback, as indicated in Solomon et al (2007), climate change will significantly impact the hydrologic cycle. The impact of climate change on the water cycle is expected to be different in various locations, depending on their latitude (Herrera-Pantoja and Hiscock 2008; Kundzewicz *et al.* 2008). A hotter climate will lead to increased evapotranspiration, increased humidity, increased precipitation and increased frequency of extreme events such as flood and drought.

The relationship between groundwater and climate is explicitly documented in any standard textbook on hydrology (Chow *et al.* 1988; Maidment 1993). Climate change, in terms of the variation of temperature and quantity and intensity of precipitation, could change groundwater recharge in any particular location, either increasing or decreasing with time (Eckhardt and Ulbrich 2003; Scibek and Allen 2006b). The groundwater recharge patterns, including the quantity and quality, will be affected by the changes in the hydrologic processes (Sophocleous 2004). During positive net flux in the wet season, when rainfall is greater than evapotranspiration loss, the groundwater storage increases and during negative net flux, the opposite condition applies. Therefore, with the predicted changes of climate, which relates to the change in precipitation and evapotranspiration, as suggested by the IPCC (Solomon *et al.* 2007), climate scenarios, the groundwater storage and thus the groundwater levels of a particular location may change in the future. Increased net flux will lead to raised groundwater level and *vice versa*.

2.6. Previous Studies on Recharge Prediction for Future Climate

From earlier sections, it has been demonstrated that the prediction of groundwater recharge given future climate scenarios should encounter two basic challenges. The first challenge is the representation of the existing physical processes in an optimally constructed hydrologic/groundwater model based on past data. The second challenge is the representation of future physical conditions, encompassing climate change, climate variability and other possible changes of the environment, such as land use change. In the present context of the research, only the climatic factors are considered for the prediction though the other environmental factors should be also investigated (if appropriate). For

instance, Holman (2006) has analysed the potential effects of changed soil and landscape caused by different socio-economic scenarios under future climate change on groundwater recharge.

In this section, the studies related to the representation of the physical processes are reviewed. This allows the selection of the most suitable hydrologic/groundwater model to represent the significant processes of a given system, thereby facilitating assessments of the potential impacts of climate change and variability on that system. Next, the studies related to prediction methods of the future climate processes, such as downscaling of global climate data, are reviewed to identify their utility and possible limitations. The necessity of a comprehensive and novel modelling approach is thereby established for predicting the groundwater recharge with future climate scenarios.

A wide range of studies has been published recently about the impact of climate change, specifically on groundwater. In the next section, the studies relating to climate change and the various hydrologic processes forming the water balance at catchments scale are evaluated in terms of the:

1. Physical process representation;
2. Evidences cited for past data-based studies; and
3. Future prediction-based findings.

2.6.1. Process Representation

To represent the impact of climate change on groundwater recharge, the influence of increased temperature on the hydrologic processes are to be analysed. Typically, those hydrologic processes consist of precipitation, evapotranspiration, runoff and groundwater recharge at a catchment scale. At a global scale, the increase of snowmelt, glacier retreat, rise of sea level are the processes that operate significantly. In the present context of the research, only the processes significant at a catchment scale are considered. The storm characteristics, such as intensity, duration, frequency, together with temporal and spatial variability are also important at a relatively shorter time scale of investigation. The other non-climatic factors that influence the groundwater recharge are catchment characteristics such as topography, hydrogeology and connectivity of the subsurface flow, source and process of recharge, and land use patterns. However, these non-climatic factors are not absolutely free from influence of climate change since the physical processes are always

connected each another. In the present context, only the following processes and factors are considered to obtain a workable understanding for the process representation and predictive analyses of the groundwater-climate relationship:

- Hydrologic processes such as precipitation, evapotranspiration, runoff and groundwater recharge for modelling
- Influence of temperature change in relation to snowmelt, glacier retreat, and sea level rise for evidence-based discussion
- Topography, hydrogeology, land use and various mechanisms and sources of groundwater recharge

Relative to surface water resources, the potential consequences of climate change on groundwater have not received as much attention (IPCC 2001b). This is because the direct impact of climate change is more easily recognised in the surface water system than that of groundwater. In contrast to surface water resources, a groundwater-based study is required to be fully dependent on the scientific understanding of the ongoing processes since the flow is difficult to estimate, as it is not physically seen without investigation. Therefore, more in-depth scientific investigations are required for groundwater study, as far as the understanding of the process is concerned.

In 2004, the United Nations Educational, Scientific and Cultural Organization – International Hydrological Programme (UNESCO–IHP) initiated the project Groundwater Resources Assessment under the Pressures of Humanity and Climate Change (GRAPHIC), which was launched to promote and advance sustainable groundwater management in the face of climate change and linked human effects (Taniguchi *et al.* 2008). This is a platform for exchanging information through case studies, thematic working groups, scientific research and communication.

Some studies are enlisted in this section according to the processes they considered to represent the groundwater-climate relationship. This demonstrates the challenges of representing climatic and non-climatic issues in climate change studies. The climatic factors are rainfall, evapotranspiration and groundwater recharge, as influenced by temperature. Although runoff is a significant hydrologic process, it is excluded in the review process because a linear relation is assumed between rainfall and runoff. The non-

climatic factors such as geology, topography, source and process of recharge are also discussed.

Rainfall: The relationship between groundwater and rainfall can never be overemphasised. Numerous studies have demonstrated the response of groundwater level with the events of rainfall or precipitation at various temporal and spatial scales. Some are cited here to show the diversity of the representation method by the investigators.

Chen et al. (2002) have demonstrated the simple, strong and positive correlation between rainfall and groundwater level while analysing observed data of 82 wells for the past 63 years (1938–1999) in Manitoba, Canada. 60% of the wells had correlation coefficients better than 0.95. They have estimated recharge as the algebraic summation of positive rainfall, negative outflow (similar to runoff) and evapotranspiration. Serrat-Capdevila et al. (2007) have used the following equation to estimate recharge from the predicted precipitation for San Pedro Basin of Arizona, US in order to predict the future recharge as impacted by climate change.

$$\text{Log}(Q_{rech}) = -1.40 + 0.98 * \text{Log}(P-8)$$

where P is annual precipitation and Q_{rech} is annual recharge (both in inches). This equation simply indicates that with the increase of precipitation there will be an increase in recharge. The validity of this type of equation for the specific catchment was verified by the previous investigators as claimed by Serrat-Capdevila et al. (2007). Kirshen (2002) has discovered that drought reduces the annual recharge and lowers GWLs while predicting potential impacts of global warming on groundwater in eastern Massachusetts. Cheng et al. (2006) have also showed the evidence of influence of precipitation on the GWLs at a range of locations in the catchment of south-west Goulburn, Victoria. These investigations collectively demonstrate the relationship between groundwater and rainfall, which is the most significant hydro-climatic process for a particular site.

Evapotranspiration: The second significant hydro-climatic process is evapotranspiration. Traditionally, this was represented as a function of temperature and/or rainfall, with the assumption that a simple linear relationship exists between evapotranspiration and temperature. However, the availability of water and energy are other factors that were

considered with the advancement of the scientific knowledge of the processes. A number of studies have been conducted in which the evapotranspiration has been represented in a wide range of complexities, starting from simple empirical equations based on temperature to experimentally measured estimates of the processes. For the impact analyses, these simple representations of the process were adopted to explain the influence of changing temperature on the evapotranspiration process. In this section, the simple equation-based studies are cited to show their limitation in comparison to the current state of the art estimation process of evapotranspiration as suggested by Morton (1983).

Kruger et al. (2001) estimate recharge by using temperature and precipitation data and the Turc formula (Turc 1954) for determination of evaporation. This is an empirical and dimensionless formula used to estimate annual evaporation from mean annual temperature and annual precipitation. This is also a very simplified representation of the evaporation and it has very limited application for a temperature range of 0 to 25^{o}C. Chen et al. (2002) also consider the evapotranspiration to be linearly dependent on temperature only. In the estimation of recharge, Aguilera and Murillo (2008) use the difference between precipitation and actual evapotranspiration. However, the estimation of evapotranspiration is simply an exponential function of temperature. Collectively, they do not consider all other climatic and dynamic factors, such as equations of energy balance or mass balance, for estimation of evapotranspiration and thus an overly simple model is used.

Other studies relate temperature and rainfall to estimate evapotranspiration. Collison et al. (2000) studied the influence of temperature and rainfall on evapotranspiration by using a one-dimensional hydrologic model. They discovered that increased temperature and rainfall would lead to increased evapotranspiration in south-east England. Ranjan et al. (2006a) introduced the aridity index to represent the variations in precipitation and temperature. They observed that deforestation leads to increased groundwater recharge in arid areas because deforestation leads to reduced evapotranspiration, even though it favours runoff. Kirshen (2002) has estimated annual actual evapotranspiration by correlation with annual potential evapotranspiration and precipitation while studying the groundwater impact for global warming in Massachusetts, USA. Bouraoui et al. (1999) found that rainfall reduction is less sensitive and evaporative demand is more sensitive to increased CO_2, and thereby GW recharge reduced with the impact of climate change.

In the estimation of actual evapotranspiration in the water balance model, Xu (1999) has used the equation in his conceptual model, which considers the minimum value between 'water available' and potential evapotranspiration. Scientifically, the 'water available' represents only the concept of water balance; but for the actual evapotranspiration to occur many other environmental factors are to be satisfied, which are dependent on energy balance as well. The equation considers some model parameters to estimate the 'water available'. They are empirically estimated parameters based on the validation for specific catchments. Therefore, the applicability of this model requires calibration of those model parameters.

In relation to the above mentioned work of Aguilera and Murillo (2008), a more scientific study was conducted by Chiew et al. (1995b) at an earlier time. They calculated the actual evapotranspiration from potential evapotranspiration by using soil moisture store, which is estimated from soil wetness multiplied by a model parameter representing the maximum plant controlled rate of evapotranspiration. The estimation of actual evapotranspiration is based on the assumption that a climatic factor such as temperature is not the only factor to influence evapotranspiration. The soil moisture content of the crop type should also be considered. This method of estimation is more accurate than those in which only temperature is used for estimation of evapotranspiration. It has been established earlier that Morton's method is the best as far as the physical processes are concerned.

Sea level rise: Sherif and Singh (1999) considered three ranges of sea level rise taken from previous references. They did not consider any rainfall process since the aquifer is in an arid region. A hydro-chemical investigation was used for salinity intrusion. They found that increased temperature would increase sea level and seawater intrusion in coastal aquifers.

Geology: The influence of geology is another factor that should be carefully considered. Van Roosmalen et al. (2007) have demonstrated the variable impact of climate change on the groundwater recharge due to variable geology of two sites in Denmark. They have found that precipitation, temperature and potential evapotranspiration were predicted by GCMs to be increased. However, the resulting recharge was predicted to increase in sandy soils in the Jylland area, while only minor changes were predicted to the GWLs in Sjaelland areas with low permeability topsoil and a thick clay layered aquifer. Van der

Kamp et al. (2004) have shown that the different responses of groundwater levels of different aquifer types in response to climatic variability during the past 40 years in the northern Prairies of North America. They discovered unconfined aquifers and shallow fractured glacial till are relatively more sensitive and deep, confined aquifers are less sensitive to climate variation.

Topography: The influence of topography is the other factor that influences the response of hydrologic processes differently for the same storm event at different locations of a particular catchment. The investigations in relation to surface runoff are much more numerous and comprehensive than those of groundwater recharge. The studies of Slimani et al. (2009) indicate the differential impact of the multi-annual and multi-decadal climate on the different locations of the catchment in France. The responses of GWLs in the upper regional locations were quick and varied sharply while those in the lower regions were slow and attenuated. Similar results are reported by Cohen et al. (2006) for different locations of water divide, valley and hills of a catchment in Minnesota, USA. Bores in the lower positions in the catchment have smaller amplitude and higher frequency of GWLs and *vice versa*. Both studies analysed past data from previous decades. Fendekova and Fendek (2006) have demonstrated the complexity of the physical system consisting of climatic and hydrological factors together with geology, altitude, duration of freezing period and topography that determine the response of groundwater regime at a catchment scale for the High Tatra Mountains in Slovakia and Poland. Brouyere et al. (2004) have demonstrated that catchments with prominence of fast runoff over base flow due to groundwater are more sensitive to climate change than other catchments. This result is related to the influence of geology and topography of a particular catchment.

Cheng et al. (2006) identify the variations in the responses of groundwater levels of bores located at various locations, such as the upper, middle and lower slopes of the Mount Camel Range area of the south-west Goulburn region of northern Victoria (see Figure 2.10). Variable trends of falling groundwater levels in different bores, one in the mid-slope with some weak trends and another in the lower slope with almost flat long-term trends have been reported. The system is impacted differently by the same climate changes and the same extraction program of GW.

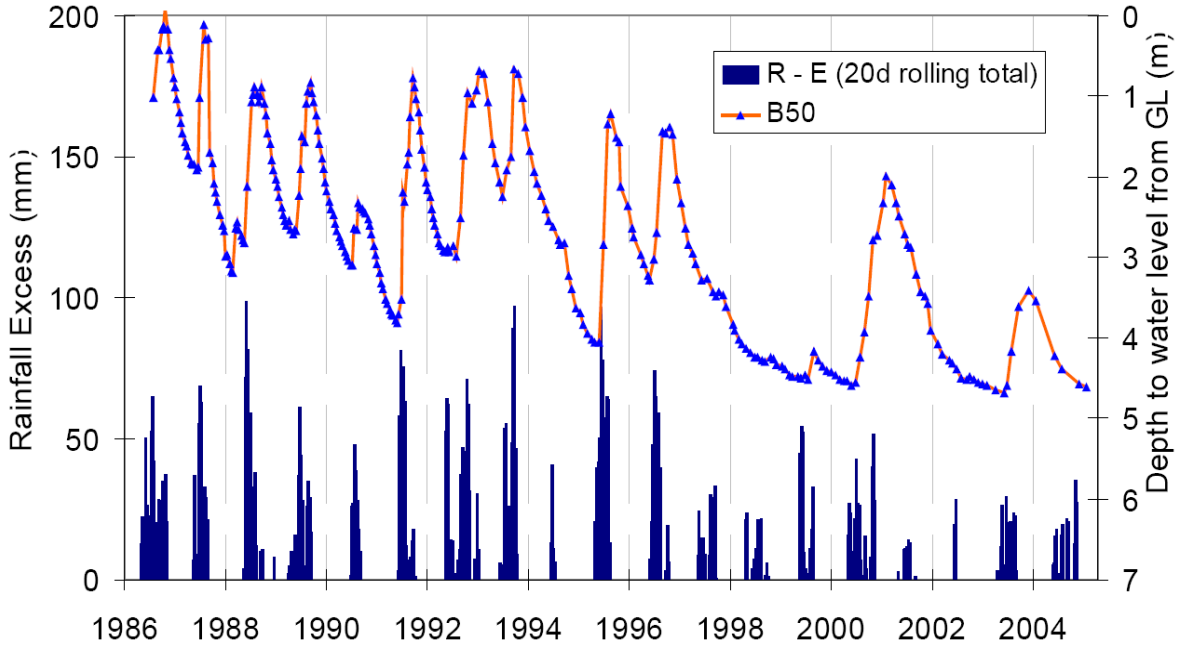

Figure 2.10 The groundwater level hydrograph and 20 day rolling total of the rainfall – evaporation in Bore 50 in the mid-slope of Mt Camel Range (Cheng et al. 2006)

Source/process of recharge: The process of groundwater recharge, whether it is direct or indirect, is susceptible to varied impact by changing temperature and/or precipitation. Gavigan et al. (2008) argue that the behaviour of indirect localised recharge is influenced more severely by increased temperature than increased precipitation, as found in Uganda. The other complexity relates to the relative extent of precipitation and evapotranspiration in a specific catchment (Wolaver 2007), snowmelt-induced recharge (Earman 2007) . Over many areas, groundwater recharge is projected to increase in the warming world, but many semi-arid areas that suffer from water stress may already face decreased groundwater recharge (Yohe *et al.* 2007; Kundzewick and Doll 2008). Issar (2008) has shown how different the climate change responses of the groundwater system can be at the two ancient cities of Arad and Jerico, located in central Israel. These cities are located less than 100 km apart in an arid zone. However, as the sources and processes of recharge were different, the responses were different with regard to the climate change of the warm period that occurred during 4000 BP in the Mediterranean region.

Conclusion:

- The representation of evapotranspiration, which is a very important and sensitive hydrologic variable in relation to temperature, is not adequate in any of the investigations.
- The currently available SILO AAET data would be a very appropriate source for representation of outflow component from the system.
- The representation of non-climatic factors such as geology, topography and the overall process and source of recharge should be carefully studied in order to be represented in the physically-based model.

2.6.2. Evidences from the Past

The studies identified in this section primarily provide the evidence of climate change on GWLs, as reported by various investigators in various regions of the world by considering rainfall and temperature as the major variables. The influence of climate change on other factors such as runoff, GW extraction and land use change is also discussed , as the processes are inter-related while influencing the groundwater-climate relationship for any specific site.

Edmunds and Tyler (2002) demonstrate a correlation between rainfall and groundwater recharge rate in Senegal while considering 108 years of records, as illustrated in Figure 2.11. They have used Cl profiles together with ^{3}H profiles and records of rainfall and river gauging to show the relationship between groundwater recharge and rainfall. However, they have also explored the inadequacy of the Cl profile method to study the preferential flow occurring in unsaturated zone for a long-term study.

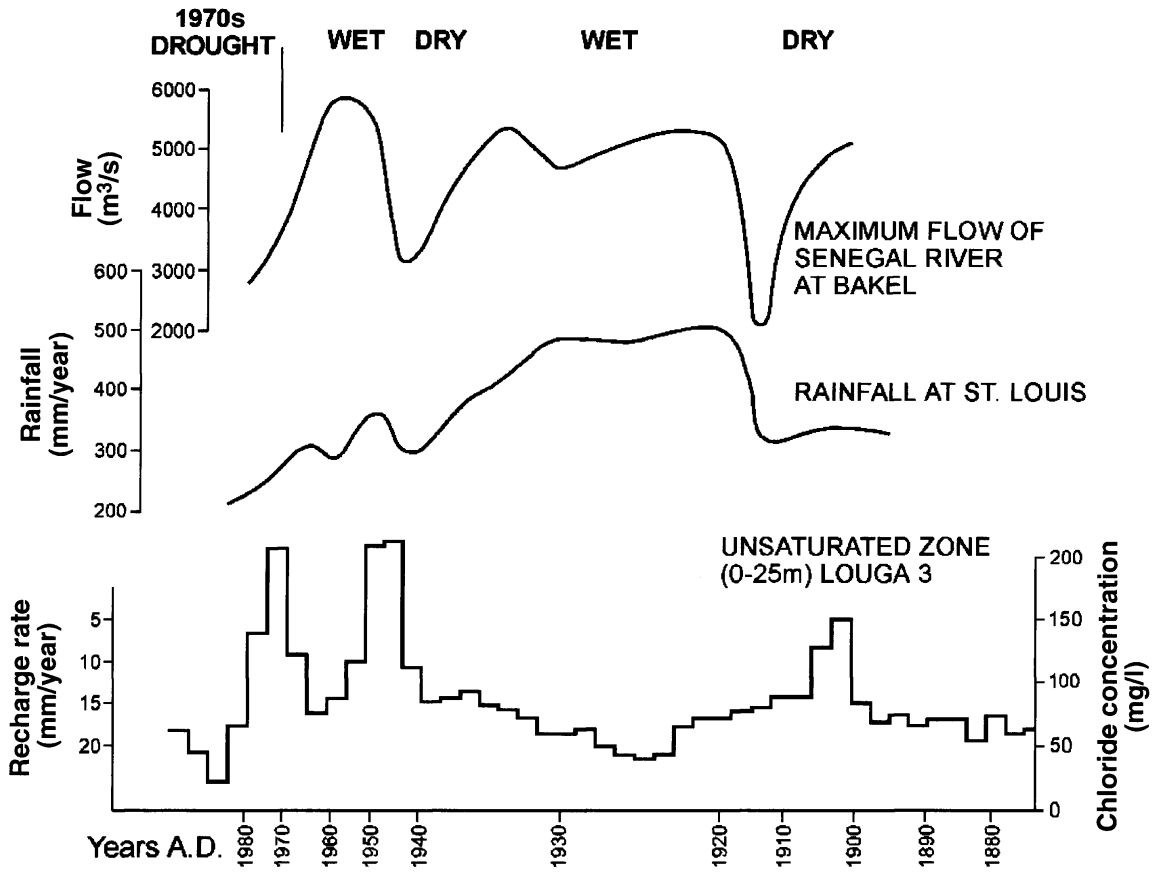

Figure 2.11 Groundwater recharge and climatic variability at the centurial time scale, Senegal (Edmunds and Tyler 2002)

Chen et al. (2003) demonstrate the evidence for change of groundwater levels caused by climate change in the North China Plain. They have demonstrated the drop of shallow GWLs from decreasing rainfall during a drought from 1971 to 1999 and thus extraction of groundwater by over-pumping. Chen et al. (2004) used the past 105 years to show the relationship between GWLs and temperature and precipitation. They discovered that GWLs are highly correlated with temperature and precipitation. Shallower GWLs were more sensitive to temperature than were deeper GWLs. They also concluded from their study that increased temperature would reduce GW recharge.

Michaud et al. (2004) developed a model by analysing the past fifteen to 30 years' data of GWLs in the wells and 100 years data of precipitation, temperature and stream flow in Quebec and the Atlantic Provinces of Canada. The developed model demonstrated a strong correlation between the separated base flow (which is supposed to be contributed by groundwater to the river), component of the stream flow and GWLs at the nearest well. From the GWLs, the recharge at a regional scale was estimated. In their analyses, both

temperature and precipitation seem to have increased during the past 100 years (twentieth century), while annual recharge was either stable or gently decreasing over time. The decrease of recharge was attributed to the increase of evapotranspiration and runoff as influenced by the increase of temperature and changed land use (increase of impervious surfaces) and precipitation patters. An increase of precipitation intensity allows less water to infiltrate for recharge and more runoff.

In south-east Spain, Aguilera and Murillo (2008) have analysed the past 100 years of data of precipitation, temperature, groundwater extraction, GWLs and storage coefficient and have predicted the future 100 years response of mean annual recharge without incorporating any GCMs or Regional Climate Models (RCMs) into the prediction. They use the 100-year time series of monthly temperature and precipitation to generate the groundwater recharge and the corresponding estimated GWLs. The GWLs were calibrated and validated against the observed values. The simple water balance equation was used for the estimation of GWLs. The series was processed and tested to identify the trend. They claim the effect pertains to climate change effects on natural water recharge at the four aquifers in south-east Spain. The logarithmically decreasing trend was found for every case.

Ludwig et al. (2009) have studied the impact of changing climate in Western Australia on the hydrologic processes over recent decades (before and after 1975) and non-proportional impacts on hydrological aspects were found where proportionality is often presumed. They have shown that since 1970, there has been an 11% decrease in rainfall during the period of May to October, and a 20% decrease in rainfall in June and July. This reduction in rainfall has caused a 95% reduction of deep drainage, i.e. groundwater recharge. The reason of the non-proportional reduction of recharge is attributable to the fact that during June and July, the rainfall is greater than the crop demand and significant deep drainage occurs during that time. Since this rainfall is reduced, deep drainage is also reduced.

Separation of climatic and non-climatic processes: The observations of groundwater levels are mostly performed as an imperative part of monitoring the groundwater extraction programme. Therefore, climate change impact studies on groundwater systems that are free from any direct influence of human intervention, such as groundwater extraction, are rare. As groundwater extraction reaches close to its sustainable limit, it is possible that a small incremental change in inflow, outflow or storage can cause environmental consequences.

Mayer and Congdon (2007) have argued that human-induced changes in hydro-geologic systems may be on the scale of natural variability. As most of the groundwater systems that are examined for climate change impact studies have already been altered by human activities, the changes in groundwater levels are not necessarily related to climate change alone (Green *et al.* 2007b).

Therefore, there are some cases in which the various components of the driving forces are split. For example, Yesertener (2005) studied the declining groundwater levels on the Gnangara Groundwater Mound in Perth, Australia due to changes in climate, land and water use (see Figure 2.12). With regard to the groundwater level variation curve, the clearing of land indicates an increased portion of rainfall to get into recharge. Thus, the groundwater level rises with the decrease of rainfall. However, after a certain amount of time with a persistent decrease of rainfall value, the groundwater level starts to fall. Ideally, the long record of climate data and monitoring bore data, which correspond to locations away from any human intervention, should build the basis of this kind of investigation. Therefore, the physical process-based model should adequately represent all of these processes and be capable of simulating the past observation of data.

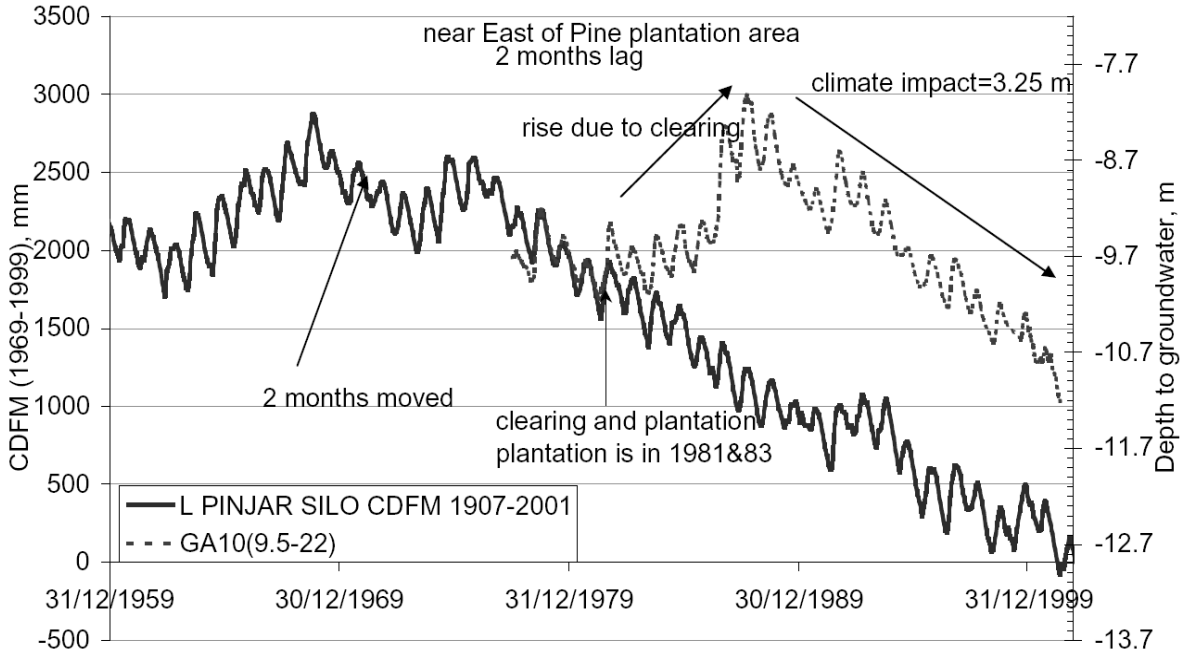

Figure 2.12 Cumulative Deviation from Mean Rainfall (CDMR) graph and separation of various impacts such as climate, land clearing and bush fire on groundwater level at bore GA10 (Yesertener 2005)

Conclusion:

- The relationship between groundwater recharge and precipitation is universally recognised and temperature heavily influences the recharge process as well. Since temperature plays an important role influencing the various forms of precipitation and the process of evapotranspiration, the relation between rainfall and recharge is not always linear.
- The other non-climatic factors such as land use change, geology and topography could also be susceptible to climate change. The representation of the physical processes and catchment features are crucial for modelling the impact of climate change.

2.6.3. Future prediction-based findings

The impact studies for climate change typically consist of developing the physically process-based model of the system in which climate is an independent variable and impact in a specific process is the dependent variable. After adequate calibration and validation with past data, that model is run with future replicates of climate data. The results are then evaluated from various perspectives. In this section, some of the studies that were

performed in various location of the world, such as Australia, Europe, USA, and Canada, are reviewed to explore the range of variations of the predicted impacts.

Chiew et al. (1995b) have analysed the sensitivity of runoff and soil moisture in relation to some arbitrary changes of temperature and precipitation for 28 catchments throughout Australia. When a change in rainfall occurs, amplified changes occur with runoff. The amplification factor is higher for drier catchments compared to wetter ones. In addition, wet catchments experience less change in soil moisture. Temperature change is the only factor that has negligible affects on runoff and soil moisture. However, the percentage change in soil moisture levels can be higher than that of rainfall in drier catchments.

Chiew et al. (1995b) also studied the predictions for GCMs scenarios for 2030. The wide range of predictions indicates the level of uncertainty. The predicted changes in runoff varied from a 50% increase to a 50% decrease for the western coast of Australia, a 10% increase for Tasmanian catchments and a 35% decrease in the South Australian Gulf.

Wang et al. (2009b) have studied the sensitivity of water balance of a catchment in south-east Australia in relation to climate change. They discovered the interrelationship of the influencing factors and responses. They have shown that a $1^{o}C$ increase in temperature would cause a 10% decrease in rainfall. They have also demonstrated that a CO_2 increase would cause reduced evapotranspiration and increase deep drainage, i.e. groundwater recharge.

Herrera-Pantoja and Hiscock (2008) presumed that climate change is expected to have negative effects on water resources, such as shorter precipitation seasons and an increase in hydrological extremes, such as floods and droughts. They studied three locations of Britain. A decrease of 20%, 40% and 7% were predicted for potential groundwater recharge in Coltishall, Gatwick and Paisley by the end of this century. The variability of the impact was also different for the three locations.

Kruger et al. (2001) have established that with the predicted rise in mean temperature, the statistical model simulates decreasing precipitation in Germany. Both effects contribute to a reduction of groundwater recharge. While in the mountainous areas of the catchment the groundwater recharge change is small, in the planes a reduction of up to 30% of the current

groundwater recharge is predicted. Krysanova et al. (2005) predicted that climate change caused by increasing temperature in the Elbe basin of Germany would most likely result in the mean groundwater recharge decreasing.

Panagoulia and Dimou (1996) showed that a temperature increase in Greece would cause reduced precipitation, a large reduction of runoff and an increase of evapotranspiration during the spring and summer months. Panagoulia and Dimou (1996) have discovered increased interaction between surface water and groundwater during spring and summer and reduced interaction during winter.

Serrat-Capdevila et al. (2007) have used seventeen GCMs data for modelling climate change impact and uncertainty on the hydrology of the San Pedro Basin of Arizona. They have found the range of predicted precipitation will vary from 100 to 500 mm/year at the end of the year 2100, starting from a baseline value of 400 to 425 mm/year during the year 2000. From the seventeen GCMs initially considered, they have used four models that were selected based on their capacity to best simulate the historical record of annual precipitation. This large range of predicted precipitation is provided in terms of annual average values with a clear linear trend of increase or decrease. However, the natural variability of the actual hydrologic processes were not considered.

Sensitivity of impact study: There have been reports of variable impacts of climate change on recharge for a specific site during winter and summer because of the combination of rainfall, snowfall or snowmelt as the source of recharge in the system. Amplification of the seasonal cycle of groundwater recharge, such as an increase in winter recharge or decrease in summer recharge, can be caused by increased temperature in the winter as reported by Eckhardt and Ulbrich (2003) with regard to Germany. A similar result has been reported by Steele-Dunne et al. (2008) for Ireland. In the United Kingdom (UK), the existing gradient of effective rainfall at a regional scale, i.e. greater precipitation in the north-west and smaller precipitation in south-east, are reported to have been exaggerated during last 20 years due to climate change, as reported by Price (1998).

The predictions from climate change scenarios indicate annual winter and summer flow will decrease in southern Britain, leading to reduced recharge of groundwater as reported by Arnell (1998). Climate change will affect both the amount of water available for

recharge and the duration of the recharge season for the UK (Arnell 2002). Scibek and Allen (2006b) have also shown a predicted recharge increase in spring, rather than summer in the unconfined aquifer of Grand Forks in south-central British Columbia, Canada. In a concurrent study, Scibek and Allen (2006a) have predicted a very small but observable decrease of GWLs due to climate change during the 2010–2039 period. Two aquifers were studied, one aquifer (in south-west British Columbia) was predicted to experience a decreased recharge while the other (in south-central British Columbia) was predicted to increase in the future. The variation is due to factors such as timing (winter *versus* spring) and the source of recharge (rainfall *versus* snowmelt). They have also shown the influence of river-aquifer interaction in the impact of climate change on groundwater recharge at a regional scale of Abbotsford-Sumas aquifer of south-west British Columbia, Canada and northern Washington, USA. The responses are obviously the combination of many factors such as geology, hydrogeology, meteorology, vegetation, and topography (Person et al. 2004). The incorporation of future variability of natural climatic process in conjunction with climate change predictions could not be found in any of these impact studies. However, the question of the future response to this natural climate variability due to global warming needs to be addressed. The necessity of incorporating climate variability with climate change projections has been reviewed in detail in Chapters 4 and 7.

Conclusion: All these studies lead to a general understanding that the spatial and temporal variability of the hydrologic processes, physical characteristics of land surface, and soil profile of a catchment are the significant influencing factors to be considered in order to obtain a reasonable compromise between model complexity and computational practicality for the representation and prediction of the system. The proper representation of evapotranspiration, which primarily occurs in unsaturated zones, and the large-scale uncertainty of the future predictions related to different physical conditions as well as various GCMs, their climate change scenarios and downscaling methods, also need to be further addressed.

Therefore, the key areas of research requiring further investigation are as follows:

- The representation of unsaturated flow
- Net flux to consider evapotranspiration
- Selection of GCMs and climate scenarios for encompassing the range of uncertainty and consideration of climate variability
- Integration of statistical methods for addressing the uncertainty of predictions

2.6.4. Representation of Unsaturated Flow

The significance of geology and topography has been addressed in an earlier section. Therefore, the representation of the unsaturated flow zone is important and has to be represented adequately in the physical process-based groundwater model. The unsaturated flow modelling for long-term climate change impact studies has specific implications on the rehabilitation facilities design (Jyrkama and Sykes 2007). The previous works related to unsaturated flow modelling are described in the following section as this discussion raises the most important research question of the present research. The unsaturated flow is the area of least investigation as far as the present state of existing knowledge is concerned. The most relevant study in this area is considered here to identify the specific weakness of the work and to formulate a better modelling framework with regard to the available data problem.

The impact study review has found that most of the studies that use MODFLOW for representing the groundwater flow system only consider the saturated flow condition, such as Scibek (2004; 2006a; 2006b; 2007; 2008). Van Roosmalen et al. (2007) use a distributed hydrologic simulation based on MIKE-SHE (Abbott *et al.* 1986) code to study the regional climate change effects on groundwater recharge in Denmark. In MIKE-SHE, groundwater flow is based only on the saturated condition described by the Darcy type relationship. The recent study by Twarakavi et al. (2008) includes unsaturated flow in the vadose zone by using a HYDRUS-based flow package (Simunek *et al.* 2005; Simunek *et al.* 2008) with MODFLOW.

From the aforementioned review, it is found that most of the studies have been undertaken where the climate change issue affects the water availability in aquifers or flood risk in rivers. Thus, the investigations are mostly concerned with the saturated condition of flow (Woldeamlak et al. 2007). However, flow in the unsaturated zone and atmospheric interactions play very important roles in most of the geo-environmental problems such as land fill covers, drainage and desiccation of tailings deposited by aqueous methods in mine waste impoundments, and overall groundwater recharge in response to infiltration (Benson 2007). The following studies are considered here to establish the influence of unsaturated thickness in the climate groundwater relationship for any catchment.

While predicting the groundwater recharge in mountainous watersheds in the Okanagan Basin in British Columbia, Canada, Smerdon et al. (2009) report that groundwater recharge varies from 0 to 20 mm/yr at lower elevations and 20 to 50 mm/yr at higher elevations. These variations in recharge correspond to the variation of the unsaturated thickness of the locations under consideration. Similarly, Hunt et al. (2008) have demonstrated that areas with a thin unsaturated zone (less than 1 m) have a smaller time lag between the time of infiltration and recharge, while areas with thicker unsaturated zone (15 to 26 m) have lags of several months between occurrence of infiltration and recharge to groundwater levels in humid climates. More specifically, Viswanathan (1984) demonstrated that the assumption of variable rates of time dependency of recharge parameters produced better estimates of groundwater levels compared to that of constant recharge parameters. Variable rates of time dependency corresponded to the variable thickness of unsaturation while performing the field tests at Tomago Sandbeds, Newcastle, Australia.

While comparing the annual variability and multi-year variability of piezometric levels in the chalk aquifer, Slimani et al. (2009) have shown how the thickness of surficial formations and underlying aquifers strongly influence the relative range of the two variabilities at two time scales. Therefore, long-term prediction of the system should encompass the variability of annual, multi-year and multi-decadal time scales.

Seiler et al. (2008) has shown that groundwater flow is significantly controlled by the hydraulic properties of the aquifer system and it does often contain a transient flow component affected by natural hydrologic processes. He has demonstrated that at low recharge rates, a transient condition of flow exists and at high recharge rates, a steady-state flow prevails. The negligence of transient response of groundwater resources in sensitive recharge/discharge areas can lead to a significant deviation of the assessment from the actual condition (Seiler *et al.* 2008). The transient flow condition is related to the unsaturated thickness above the groundwater level. Moreover, Cartwright et al. (2009) have shown the transient relationship of dynamic hydraulic connectivity (effective porosity) with unsaturated thickness. Their findings were consistent with previous research under a steadily rising or falling shallow water table and under periodic flow conditions. Therefore, the representation of the unsaturated, unconfined layer in the groundwater system is very important.

A specific study recently performed by Cohen et al. (2006) explores some very important and relevant understandings about the long-term response of GWLs located in the areas of watershed divide. Their study has established that responses of lake water levels located at topographically different locations of large catchment areas are different. On a millennial time scale during 4400 and 7000 years BP, they have found evidence of differential responses of water levels of two lakes: Moody Lake, located at river confluence and Lake Mina, located at watershed divide. The water level fell by 4 m and 15 m respectively with regard to climate change during that period. Cohen et al. (2006) argue that these findings are consistent with analytical calculations that indicate the magnitude of water table and lake level fluctuations will be greatest near water table divide. The study indicates two important understandings; the first is related to the different ranges of annual fluctuation of groundwater levels at different topographical locations in the same catchment, the second regards the differential impact of climate change on those locations.

Green et al. (2007a) have developed and demonstrated a method for simulating climate change effects on vegetation and soil-water regimes affecting groundwater recharge at two sites in Australia with Mediterranean and subtropical climates where the WAVES (Zhang *et al.* 1996) model is used for incorporation of unsaturated flow. Variably saturated flow condition based physical models WAVES, as also used by Green et al. (2008), is analysed in light of its capability in relation to the long-term climate change scenarios and generation of climatic variability in their study.

WAVES is a one-dimensional daily-time step model that simulates the fluxes of mass and energy between the atmosphere, vegetation and soil (Zhang *et al.* 1996). This model provides an equivalent physically-based simulation of water and energy, including plant dynamics. It emphasises the importance of transpiration in water budget and addresses the necessity of considering plant response to the changing climate. The water balance equation is RE's, which is common in WAVES and Seep/W. However, the carbon assimilation and respiration from roots, stems and leaves are represented by empirical equations, which should be dependent on the specific plant type and relative availability of light, water and nutrients. The Penman-Monteith equation, as used for energy balance, is also a combination of physically-based thermodynamics and experimental-based empirical parameters. Therefore, they had to design a model that needed seventeen numbers of

vegetation parameters for each of the four types of vegetation in addition to different soil hydraulic parameters.

The adaptation of the plant communities to the changing climate would also change the values of those vegetation parameters, thus increasing the level of uncertainty as indicated by Green et al. (2007a). Therefore, the WAVES model is a data-intensive model while Seep/W is relatively simpler in terms of input data. The solution technique of Seep/W is also better, being a finite element model, while the WAVES is a finite difference model. The numerical accuracy of a finite element model is better than that of a finite difference model. Therefore, the use of the Seep/W model for predicting long-term response is preferable to the WAVES model.

In comparison to Green et al. (2008), the present scope of research is based on very small areal extent so far as the availability of monitoring data of groundwater level is concerned. However, a much broader range of GCMs outputs with all the seven emission scenarios has been considered to obtain a comprehensive picture of the future response of the system. In addition, the weather generator (WGEN) is programmed for fully stochastically generated data and the GCMs used do not explicitly simulate the ENSO, tropical cyclones, rain depressions, extratropical lows and cold fronts, which are sources of widespread, heavy rains at their site of consideration. Therefore, this investigation, which is the most relevant study to the intended research, has a number of limitations. The required method for performing the current study needs to be designed with due consideration to these limitations.

In another study of unsaturated flow representation, the SUFT3D (Carabin and Dassargues 1999) model is used by Brouyere et al. (2004). However, the limitation of SUFT3D is that it can handle only unidirectional flow of water from top to bottom. Goderniaux et al. (2009) is one of the most recent and best investigations of the interdependent processes such as recharge, evapotranspiration and other climatic variables. They use the 3D variably saturated finite element model HydroGeoSphere (Therrien *et al.* 2009) specifically to assess the climate change impact on groundwater reserves of the Geer Basin of Belgium.

The difficulty in representing the unsaturated flow equation lies in the uncertainty and unpredictability of highly variable hydraulic characteristics of various soils, as shown in

Figure 2.13 and Figure 2.14 (O'Kane *et al.* 2002). The volumetric water content (ψ) and hydraulic conductivity (K), as used in Equation 2.4, vary in the order of magnitude with the variation of pore water pressure. The measurement of these properties of various soils is also difficult because of the uncertainty of the hydraulic connectivity along the soil mass during the process of drying. Since the unsaturated flow is difficult to represent by basic equations of flow of mass, the empirical equations are generally used to quantify the incoming or outgoing fluxes. This approach is mostly used in physical process-based models.

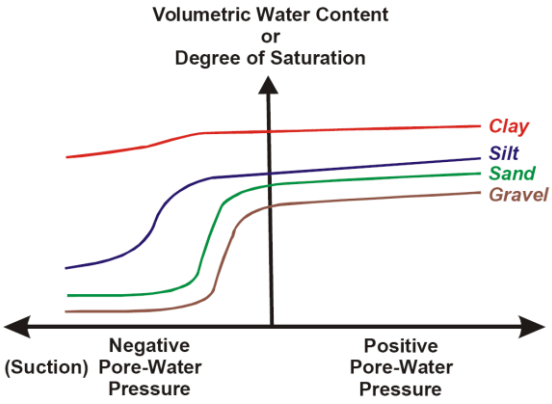

Figure 2.13 Qualitative curves of soil moisture characteristics (volumetric water content as a function of pore-water pressure) for clay, silt, sand and gravel (O'Kane *et al.* 2002)

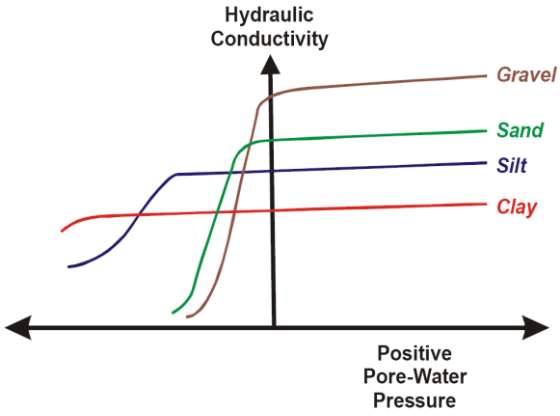

Figure 2.14 Qualitative curves of soil moisture characteristics (hydraulic conductivity as a function of pore-water pressure) for clay, silt, sand and gravel (O'Kane *et al.* 2002)

By incorporating the scientific advancement in computational capabilities and programming software, more accurate representations and predictions of the unsaturated flows could be performed. The Seep/W is considered state of the art for modelling unsaturated flow for the following reasons:

- The accepted physically based model (Seep/W) incorporates the soil water characteristics curve and hydraulic conductivity characteristics curve as input functions for material property of the system.
- The time variant inflow or outflow of water to or from the system can also be represented by the boundary condition function for the elements of the system.
- Calibration of the parameters for the characteristics curves to validate the modelled groundwater level with the monitored data can be achieved with this software.

Conclusion:

- In comparison to other models, Seep/W is an optimum model for long-term impact studies.

2.6.5. Representation of Climate by Net Flux

The studies using MODFLOW when representing groundwater flow systems consider the flow into the system mostly by recharge coefficient, as in Scibek (2004; 2006a; 2006b; 2007; 2008). Very recently, some effort has been initiated by Twarakavi et al. (2008) and Doble et al. (2009). They include unsaturated flow in the vadose zone by using HYDRUS-based flow packages (Simunek *et al.* 2005; Simunek *et al.* 2008) or continuous discharge recharge (CDR) function (Doble *et al.* 2009) to model evapotranspiration and recharge with MODFLOW. The CDR function is similar to the 'net flux' as would be used in the present research. The incorporation of the CDR function (Doble *et al.* 2009) to model evapotranspiration and recharge with MODFLOW is another significant improvement in modelling .

Cohen et al. (2006) studied the effect of geology, land surface topography and watershed size, which influence GWL fluctuation, wetland formation, evapotranspiration and runoff by developing a transient saturated-unsaturated hydrologic model (HYDRAT2D) (Yakirevich *et al.* 1998) that couples surface-subsurface hydrologic cycles. The evapotranspiration is computed from the potential evapotranspiration, based on the Priestly and Taylor (1972) method, and the sink-term method of Feddes et al. (Feddes *et al.* 1978) in which a crop factor is used.

As mentioned previously, the unsaturated flow representation by the SUFT3D (Carabin and Dassargues 1999) model can handle only a unidirectional flow of water from top to bottom, not the reverse (Brouyere *et al.* 2004). The study was conducted on the Geer Basin in Belgium. An improved study was subsequently conducted on the same basin by Goderniaux et al. (2009).

Although the variably saturated flow is considered in the groundwater flow model of HydroGeoSphere by Goderniaux et al. (2009), they use a correlation between potential evapotranspiration and temperature to estimate evapotranspiration values for future

scenarios. The use of a single correlation with temperature in representing the complex process of evapotranspiration, which is influenced by many other climatic and environmental variables such as humidity, wind, solar radiation, vegetation, soil type and geology. Again, it is vulnerable to being overly simplified with regard to the complex physical system. Therefore, a physically based model must be selected critically.

None of the models reviewed thus far have used AAET, which is used by following Morton's method. When the AAET is estimated by Morton's method, whose superiority has already been established in an earlier section of this chapter, the net flux of water for the system is a more accurate representation of the actual physical processes. 'Net flux' in the present study, as represented by the algebraic summation of rainfall and AAET, is scientifically more acceptable and better representation of the physical system. This input is significantly better for any GW model than the input by 'recharge coefficient', which is simply a percentage of rainfall (determined empirically). The use of similar variables as net flux has been reported in a number of separate studies but none are related to climate change impact on the GWL. A more detailed description is provided in Chapter 5.

There is also one limitation of using net flux as well. That is related to the data source of future climate as used in the present study. In the present study, during the time of data extraction from GCMs (CSIRO 2006), AAET data were not available and the PPET values were available. Those PPET values need to be converted to AAET values for estimation of future net flux. However, this limitation has been recovered in the latest version of the data source of GCMs (CSIRO 2010).

Conclusion:

- There will be a higher level of uncertainty in the case of long-term predictions while too many model parameters are incorporated, as stated in the earlier studies (such as WAVES).
- The 'recharge coefficient' in the other studies is too simple (such as MODFLOW).
- Optimum compromise between the two extreme cases of model complexity and computational efficiency is the 'net flux', the best representation of the climate system for the GW model.

2.6.6. Uncertainty of Predictive Studies

The future climate is a combination of climate change and climate variability. The other significant physical factor that would influence the hydrologic processes leading to change of groundwater recharge is land use change. In fact, land use change can be a result of climate change itself. For the predictive analyses, all of these factors are to be considered for the downscaling of climate data from the GCMs scale to the catchment scale. Numerous studies analyse the impact of climate change, climate variability and land use change combined or individually on the various hydrologic processes of various vulnerable regions of the world at varied time scale as well as spatial scale, as has been stated in previous sections. The consideration of the physical process-based conceptual model for a specific location is one way to handle the range of complexities for the system under consideration.

Xu (1999) has studied the appropriateness of the conceptual model, which should be developed for a climate change impact study. He has expressed the need for the model to be able to demonstrate 'fitness for the said purpose', which would indicate the possible deviation of the climate condition from the past observed period and future predictions. Since the predictions from scenarios and GCMs vary widely, it is important to encompass all possible ranges of change to the system. For prediction of runoff, Xu (1999) calibrates and validates the observed runoff data for past years for the conceptual model, which was developed for predicting runoff for future climate change. By drawing the analogy, it is logical for groundwater level predictions; the groundwater model should be calibrated and validated for observed GWLs. In relation to all other hydrological processes (such as stream flow or runoff process), the response of groundwater is the most difficult.

As reported by Green et al. (2008), the impacts of climate change and modified climate variability on groundwater resources, soil water, agriculture, and human life are relatively unknown in most areas. Key sensitivities could be explored by a low-cost approach of identifying geographical analogues between hydrologic/climatic regions around the world. Gravity Recovery and Climate Experiment (GRACE) satellite gravity data and GCMs are used for climate change projection scenarios. The stochastic weather generator WGEN (Richardson and Wright 1984) is used for downscaling and the hydrologic model WAVES (soil-vegetation-atmosphere numerical model) (Zhang *et al.* 1996) is used for simulating

soil moisture and vegetation cover as impacted by climate change in a number of hydrological analogous regions of the world. Other works are enlisted briefly to indicate the respective models used in their predictive studies:

- GCM and MODFLOW used by Kirshen (2002), Croley II and Luukkonen (2003), and Hiscock et al. (2008)
- GCM and spatially distributed hydrologic model MOHISE (Brouyere *et al.* 2004) used by Brouyere et al. (2004)
- GCM and Hydrologic Evaluation of Landfill Performance model HELP3 (Schroeder *et al.* 1994) used by Jyrkama and Sykes (2004)
- GCM, stochastic weather generator WGEN (Kilsby *et al.* 2007) such as SDSM (Wilby *et al.* 2002) or LARS-WG (Semenov *et al.* 1998; Semenov and Barrow 2002) or principal component analysis (PCA) method for downscaling, HELP for recharge estimation, surface water model BRANCH (Schaffranek 1981) for river water levels and MODFLOW for groundwater flow used by Scibek et al. (2004; 2007; 2008) and Scibek and Allen (2006a; 2006b)
- Stable isotope to link rainfall to recharge used by McGuffie et al (2004)
- GCM, Hydrologic Unit Model for the United States (HUMUS) (Srinivasan et al. 1993) and Soil and Water Assessment Tool (SWAT) (Arnold *et al.* 1998) hydrologic model used by Rosenberg et al (1999)
- GCM, SDSM, LARS-WG, HELP and soil unsaturated hydraulic property model ROSETTA (Schaap *et al.* 2001) used by Allen and Toews (2007)
- GCMs and soil moisture balance model (Allen *et al.* 1998) of Food and Agriculture Organization (FAO) in the estimation of potential groundwater recharge used by Hiscock et al. (2008) who compare the responses in five locations in southern and northern Europe. The sensitivity of groundwater recharge was performed for three periods, the 2020s, 2050s and 2080s, with one SRES named A1F1. An additional number of GCM-based works have been cited in Chapter 4, 7 and 9.

These attempts are highly resource-oriented in terms of data availability and instrumentation. From a broad review of this kind of investigation, as indicated by Fowler and Kilsby (2007), it is understood that investigations involving the extraction of GCMs data and applying them to catchment scale models are typically based on numerical

modelling in terms of future climate data generation by incorporating GCMs, and RCMs. For an impact study of climate change in the context of the present research, the steps involved typically consist of the following:

- Selection of emission scenarios and GCM for obtaining climate data as output from GCM
- Downscaling that climate data of GCM to RCM or catchment scale hydrologic model incorporating synthetic weather generators
- Developing, calibrating, validating the hydrologic model with historical climate data
- Forecasting with the synthetically generated climate data for sufficient number of replicates

By evaluating the possible sources of uncertainty in each of the steps of the impact analyses, the issues of concern could be listed as climate change (incorporating 'change factors' (Mitchell 2003)) for various GCMs and scenarios), climate variability (incorporating natural variability of multi-decadal spells of wet or dry years) and the downscaling technique (incorporating statistical methods for converting GCM scale climate data to catchment scale). Some studies undertaken in the past are categorised in Table 2.3 with regard to the downscaling techniques to show their inadequacy of incorporating future climate variability. Fully stochastic generation of climate data can preserve some statistical property of historical data but the future response of the natural variability as influenced by climate change will be certainly missing in that generated data. The number of GCMs used and scenarios considered are also listed in Table 2.3 in relation to the study methodology and findings.

From the studies as mentioned below, it is found that all of the studies downscale the GCM data by statistical methods based on past climate data at the local scale but the response of future climate variability is not considered. In fact, no study could be cited to have performed this kind of investigation since the variability due to the ENSO type of events are still an open problem and vary widely at different climatic regions of the world.

Table 2.3 List of some studies incorporating the various ranges of methods for impact analyses

Investigations	Downscaling technique	Number of GCM	Number of scenario	Finding/processes considered
Vaccaro (1992)	Synthetic weather generator	3	2	Groundwater recharge sensitive to irrigation (land use)
Bouraoui (1999)	Local weather generator	1	2 (doubling CO_2)	Rainfall and potential evapotranspiration generated, GW recharge reduced with increased CO_2
Kirshen (2002)	Statistical generation from historical data	1	2 sensitivity levels and 4 climate change scenarios	20 year drought assessed as one extreme dry year for generation of scenarios
(Ranjan *et al.* 2006b)	Use aridity index as a predictor	1 (HadCM 3)	2 (A2 and B2)	Loss of fresh groundwater due to climate change in the coastal regions
(Scibek and Allen 2006b)	LARS-WG	1	4	'Change factors' used for climate change
(Scibek and Allen 2006a)	SDSM and LARS-WG	1	1	Predictions of small reduction in recharge
(Brouyere *et al.* 2004)	3 GCMs, scenarios detail not reported in the reference. Uses historical climate data combined with monthly 'change rates' from the GCMs as downscaling technique.			Predictions show decrease of GWLs at various climatic conditions in Belgium.

More importantly, the relative impacts of the various factors such as climate change, climate variability, land use and environmental change have been found to be different in different investigations, as reported by Zheng et al. (2009), Li et al. (2009) and Ma et al. (2008) in their study of stream flow and other hydrologic processes as impacted in China. These impacts have also been highlighted by van Roosmalen et al. (2009) in their study of hydrologic processes in Denmark. The uncertainty arising from impact studies as reported

by the investigators are categorised here according to the three major issues such as climate change, climate variability and downscaling techniques.

Climate change (GCMs and scenarios): Wilby et al. (2006b) have confirmed the large uncertainty in climate change scenarios and impacts in hydrologic systems due to choice of GCMs in the impact study of climate change for River Kennet, UK. Kirshen (2002) has demonstrated that higher, similar and significantly lower recharge rates result from different climate scenarios used for an impact study. Croley II and Luukkonen (2003) have shown the increase or decrease of GWLs depending on the GCM used.

The incorporation of 'change factor' in impact studies is a representation of predictions for climate change by long-term linear trend, as discussed in Mitchell (2003). As a result of using the predicted linearity in future climate changes, since the GCMs predictions are varying in magnitude and directions, the impacts are also found to be widely varying. Therefore, it is important to consider as many GCMs and scenarios as possible in any impact study.

Climate variability (multi-decadal time scale): Timilsena et al. (2009) have demonstrated how the interdecadal and interannual climate variability are associated with the hydrologic processes of the Colorado river basin during the past 500 years. More recently, White et al. (2007) relate groundwater hydrology to droughts associated with ENSO climate variability. Hanson and Dettinger (2005) have simulated the past GWLs from 1950 to 1993 by developing a physically-based regional groundwater model for California to estimate the GWLs from precipitation. They used the GCMs output of rainfall for that period and imparted the ENSO and Pacific Decadal Oscillation (PDO) related events at the top of the GCMs output of rainfall for that period. They obtained agreement between modelled GWLs and recorded GWLs. However, the future prediction of this natural variability could not be found in any impact study of this kind.

It should be mentioned that the non-stationarity in hydrological processes, especially precipitation, occurs due to the multi-annual and multi-decadal spells of wet or dry climate, such as ENSO events. However, the prediction of this ENSO event is still an open problem for a given catchment of a climatic region. Though a number of studies do correlate the climate variability with ocean atmospheric circulation (see Chapter 7) for a given climatic

region, the association of climate variability with the climate change prediction is least investigated, especially in impact studies.

Downscaling: While examining the implications of climate uncertainties in hydrological systems in the Thames catchment in the UK, Manning et al. (2009) have reported in their study that different downscaling methods produce significantly different predictions of hydrologic processes. Wilby and Wigley (1997) have identified the difficulty of representing regional or local variability of the hydrological processes at any time scale and non-stationarity of the key relationship in the future while reviewing the various downscaling methods. Dibike and Coulibaly (2005) have used two different downscaling techniques, stochastic and regression-based. The increasing trend was obtained with regression-based analyses but no trend was obtained in stochastic generation-based analyses. They obtained the increasing trend of rainfall prediction with the increasing trend of temperature as downscaled from GCMs prediction.

The uncertainty associated with downscaling techniques is related to the incorporation of climate variability in the prediction process. The exclusion of the natural variability, which is susceptible to be influenced by any future climate change due to global warming, is a serious but unavoidable limitation of the existing downscaling techniques. An attempt is initiated in this respect to address this shortcoming in the present research.

Conclusion: There are significant issues with the generation of future climate data, which are to be extracted from GCMs or RCMs and downscaled to catchment scale studies. The predictability of climate variability with climate change is an area of least investigation. The difficulty in performing the impact study of groundwater response to climate change and climatic variability should be handled by considering the following issues:

- The typical framework for impact study should be based on the development of an appropriate hydrologic groundwater model.
- That model should be calibrated and validated with observed GWLs.
- The natural variability of regional climate as influenced by ocean atmospheric oscillation should be combined with climate change prediction scenarios for a more comprehensive impact study.
- Future climate replicates should be generated considering the maximum possible combination of GCMs and scenarios.

2.6.7. Integration of Physical and Statistical Techniques

The complex interaction of the physical, chemical and biological processes involved in the reality and the simplification of them for modelling work have given rise to uncertainties in the predictions. To handle the uncertainty in the prediction by physical process-based models, statistical methods have also been investigated. The areas of uncertainty in modelling impact of climate change can never be overemphasised.

The interaction between climate forcing and response of the environment consists of positive and negative feedback. These include water-vapour feedback, cloud feedback, surface albedo, soil moisture, vegetation feedbacks and aerosol feedback (Loaiciga 2003). An increase in temperature leads to an increase in both evaporation and transpiration, which in turn may decrease aquifer recharge (Michaud *et al.* 2004). However, increased evaporation can result in increased precipitation. Thus, feedback from cloud remains the biggest 'known unknown'. For example, Weng and Yu (2010) have addressed the influence of ocean-atmosphere circulations by considering two sets of feedback such as wind-evaporation-SST and cloud-radiation–SST with three sets of air-sea couplings to explain the intraseasonal variability in the Indo-Pacific region.

For the numerical representation of any physical process, there are two different approaches used by the modeller: statistical method-based models and physical process-based models. The physical process-based modelling approaches are reviewed in this chapter for representation and forecast of groundwater levels in relation to climate. The detailed reviews for the statistical methods have been provided in Chapter 6 in which hydrologic processes are represented by time series statistics. It should be mentioned that very few examples could be cited in which statistical methods are used in the long-term impact analyses for climate change on groundwater (Kruger *et al.* 2001; Aguilera and Murillo 2008).

Kruger et al (2001) use the statistical model to study the impact of increased temperature caused by climate change on groundwater recharge in Germany. Temperature is considered as the single climate variable to represent the past variability of the hydro-climatic processes during 30 to 50 years of observations. Based on the past temperature statistics,

and observed precipitation and temperature data, future predictions of the variability for precipitation and temperature are conducted.

Aguilera and Murillo (2008) use the combination of hydrologic modelling and statistical modelling to represent the past 100 years GWLs and also predict the future 100 years recharge. They represent the system with hydrology and calibrate, validate and predict by statistics.

One of the practical advantages of using the statistical method in predictive analyses is that the level of uncertainty of the analyses is explicitly described in terms of variance or standard deviation. To provide a similar level of explicitness from physically-based modelling, a large volume of computations is required for the model runs with sufficient number of replicates of future climate. It is clearly understood that uncertainty in both methods exists and needs to be addressed. Therefore, integration of the two methods of modelling is a novel approach.

Conclusion:

- The integration of statistical modelling with physical process-based study in the climate change impact investigation eases the demonstration of the uncertainty of analyses.
- Though these two approaches are fundamentally different, the final output of both studies should be consistent.

2.6.8. Summary

The limitation of existing methods of investigation to quantify long-term impact of climate change and natural climatic variability on groundwater is identified and the methodology for more appropriate technique is introduced. Four areas of scientific inadequacy could be listed from the review of the studies in this section, which are as follows.

1. Among the studies that use the output of GCMs in the impact analyses, most only consider one or two GCMs and one or two emission scenarios. The maximum number of GCMs considered is four and maximum number of scenarios is four as by Hiscock et al (2008) for generation of climate data. This is inadequate in regards to the possible changes in the long-term future.

2. The limitation of stochastic weather generators used by most of the investigators is that they do not consider the natural climatic variability in light of the ocean atmospheric circulation and the possible interaction of climate change predictions with the historical climate variability. The generation of future climate data should be based on the existing understanding of these two phenomena and should encompass all possible interactions in the future.

3. For the representation of groundwater flows, most of the models use MODFLOW, which is a saturated flow model that does not incorporate unsaturated hydraulic properties of soil. However, for performing the impact study of climate on groundwater, the importance of unsaturated soil in the system representation should be recognised. The inadequacy in the representation of the physically-based model should be handled properly.

4. In the hydrologic model HELP or groundwater model MODFLOW, the input for climate flux is represented by a 'recharge coefficient', which is simply a percentage of rainfall estimated on the basis of annual water balance components for any particular site. Therefore, the influence of variable intensity and duration of rainfall, temperature, humidity, wind speed, solar radiation and atmospheric pressure (i.e. all other climatic factors that influence inflow or outflow of water from the soil) is grossly represented by the water balance equation.

The first two limitations are related to the adequacy of the generated future climate data as should be used as input to the physically-based model. A more comprehensive review of the scientific investigations related to downscaling techniques has been provided in Chapter 7. However, the third and fourth limitations are more fundamental in the sense that they address the representativeness of the physically-based model itself. The integration of the statistical method with the physical method would add extra value to the prediction in terms of uncertainty of the predictions.

2.7. Conclusion

Detailed reviews have been conducted of the ongoing work performed with various time scales, at different locations and with consideration to a range of hydrologic processes. The

review process leads to the understanding that the impacts in the groundwater system by the changes in climate are complex and different. Globally, the rising temperature influences the hydrologic processes in different ways in different local contexts. Therefore, the understanding for one region should not necessarily contribute to the understanding of another, which is different in climate, topography and geology. Therefore, there are various views from different communities of researchers in this regard. The structuring of the scientific reports addressing the different regions of the world by IPCC indicates the importance of this diversity.

From a scientific perspective, the study of the impact of the changing climate on groundwater requires some fundamental issues to be addressed. These include the identification of the significant flow components by considering a number of conceptual models, representation of the shallow vadose zone hydrogeology by the unsaturated flow model, consideration of various climate change prediction scenarios and interaction with the natural climate variability based on the understanding of the climatic system of the region. The integration of physically-based modelling with time series models is a new modelling framework, which is the best of its kind with regard to the current problem and resources.

2.7.1. Intellectual Significance of the Research

While performing the literature reviews on the long-term impact study of climate change and climate variability on groundwater levels, the following issues were identified to be significant challenges and provided scope for performing the intended research work:

1. Scarcity of data on groundwater levels, which are solely impacted by climate only and free from any human intervention such as abstraction, artificial recharge or modified hydrologic system
2. Complexity of the groundwater-climate relationship, which is subject to a range of factors such as topography, climatic region, land use pattern, source and process of recharge, hydrogeology and hydro-climatic configuration
3. Difficulty of representation of the complex unsaturated flow system in the predictive studies for the varying and highly uncertain soil water properties
4. Inadequate consideration of various GCMs and emission scenarios to encompass the whole range of possible changes to the long-term average climate

5. Incorporation of a fully stochastic method to generate future climate data with little consideration to the natural climatic variability as influenced by ocean atmospheric circulation in the surrounding climatic regions; the method should not be fully stochastic and would be better represented by a quasi-stochastic process
6. Inadequate representation of climate by 'recharge coefficient' in most of the significant studies as used in the HELP and MODFLOW models
7. Missing integration of the two modelling approaches as used by hydrologists and statisticians to represent and forecast the natural hydrological processes

Of these limitations, the available monitoring data and established conceptual model for the research site eases the first two limitations, as is described in Chapters 3 and 5 respectively. The incorporation of an appropriate physically based model sufficiently represents the unsaturated flow system as is described in Chapter 8. The future climate change and climatic variability are incorporated with appropriate scientific judgement as is described in Chapter 7. The modelling approaches followed by statisticians for representing hydrologic systems are incorporated in Chapter 6. The final integration of the two approaches is described very briefly in the Chapter 9. These are the key issues, which make the work a significant contribution to the development of an integrated approach for the modelling of a long-term impact study for groundwater by the changing and variable climate.

3. Site Review: Ranger and Kakadu

This chapter presents a brief review of the location of the Ranger uranium project and its development history, climatic characteristics, geology and hydrogeology, sources of data and long-term monitoring results. As such, the chapter presents the basic information about the Ranger project with respect to understanding subsequent hydrologic, time series and groundwater modelling, especially the link between climate conditions and groundwater behaviour. It is demonstrated that with a reasonable record of groundwater levels of unimpacted bores, the Ranger site is ideal for a study of the climate-groundwater relationship as well as being required for sound rehabilitation of radioactive uranium mill tailings.

3.1. Regional Geography and Historical Background

The Alligator Rivers Region (ARR) study area is located in northern Australia, in the central northern region of the Northern Territory, commonly known as the 'Top End'. The region contains Kakadu National Park and extends into western Arnhem Land, an area reserved for indigenous people since 1931, as shown in Figure 3.1.

The ARR includes the catchments of the East, South and West Alligator rivers and comprises an area of 25,000 km^2. Its geomorphologic sub-regions are mainly classified into three types, which are the Arnhem Land Plateau or Escarpment, the lowlands and the floodplains (Press *et al.* 1995). All the major streams in the ARR have their head waters in the Arnhem Land Plateau and traverse the gently undulating lowlands before spreading out over floodplains, which are inundated during the wet season and merge with tidal flats along the northern coastline (see Figure 3.1) (Press *et al.* 1995).

Kakadu is listed as world heritage for significant cultural and environmental values, protecting various habitats of northern Australia and one-third of the country's bird species, as well as preserving an important record of living Aboriginal history in extensive galleries of rock art (Press *et al.* 1995). Before European settlement, this was one of the most intensely populated areas in the continent, with Arnhem Land being home to a large number of language groups (Mulvaney and Kamminga 1999). The Arnhem Land escarpment meanders 200 kilometres to the east, separating Kakadu National Park in the west from the Aboriginal-owned land in the east (Press *et al.* 1995).

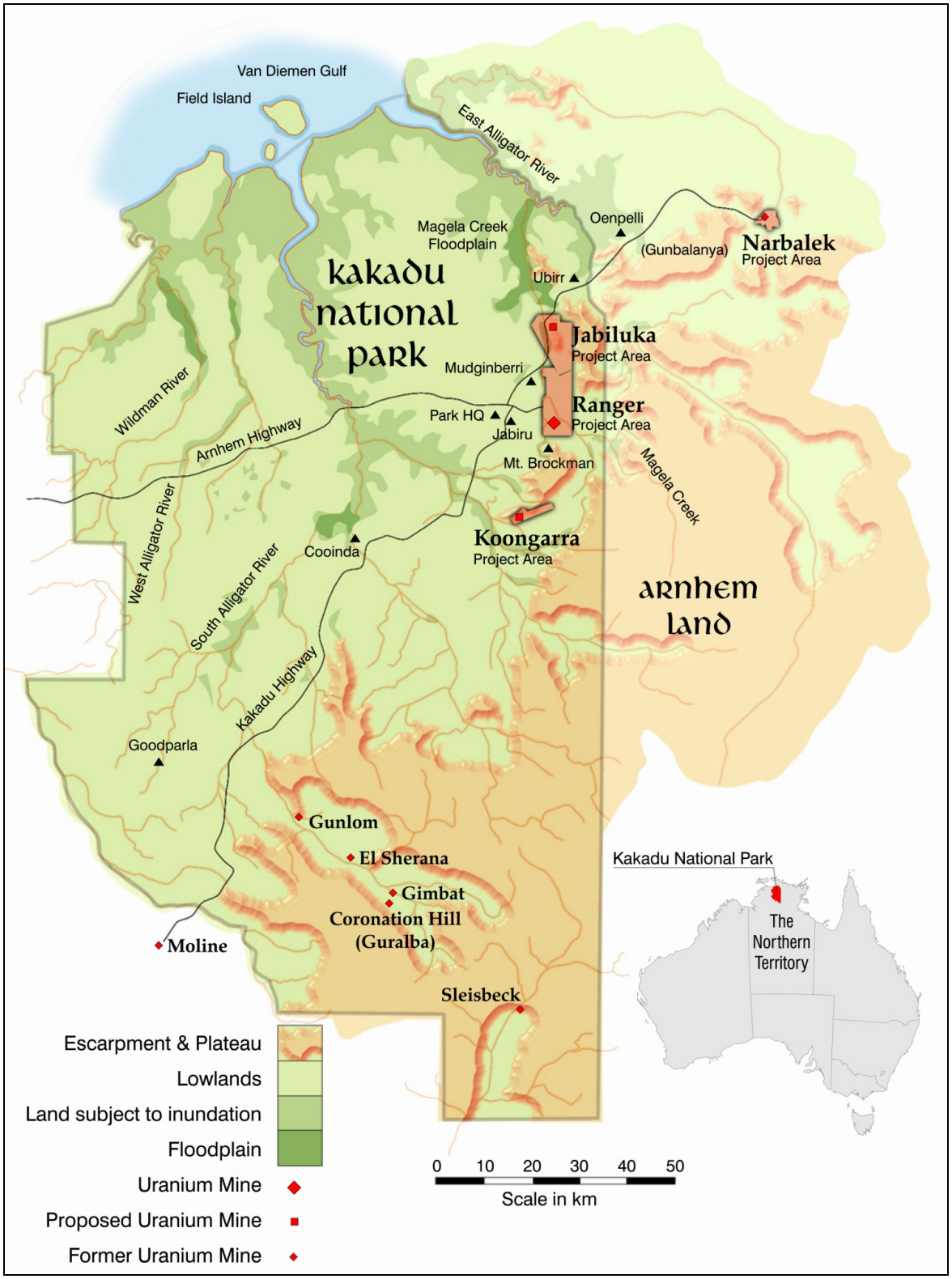

Figure 3.1 Location of Kakadu National Park and the outline of Ranger Project Area(RPA) in the Alligator River Region, Northern Territory, Australia (Courtesy: Scott Ludlam)

Until the 1950s, the ARR had seen very little European development, with the area predominantly being used for traditional indigenous living. However, from this time, the

region has undergone rapid change, with the introduction of uranium mining in the Upper South Alligator Valley (USAV) in the 1950s (now southern Kakadu) and new pastoral stations at Mudginberri and Munmarlary in the 1960s on the northern ARR plains, east of the South Alligator River. A proposal to make the escarpment country a national park of equal status to the USA's Yellowstone or Yosemite was first raised in 1964 by former USAV uranium miner Joe Fisher, though no progress was forthcoming. In 1969, a new phase of large-scale base metals and uranium mineral exploration began with remarkable success, finding some of the world's largest uranium deposits at Ranger, Jabiluka, Nabarlek and Koongarra from 1969 to 1973.

Throughout the 1970s, there was major national controversy over the recognition of indigenous land rights in the area, conservation via national parks and especially nuclear issues and uranium mining. In 1975, the Whitlam Labour Government instituted the Ranger Uranium Environmental Inquiry (RUEI), a major public inquiry to assess nuclear power issues broadly and uranium mining in the ARR, especially the Ranger project. After passage of the land rights legislation in 1976 (the *Aboriginal Land Rights [Northern Territory] Act 1976*), the RUEI was also made the Lands Commissioner for the purposes of hearing the indigenous land claims for the ARR.

After two major reports by the RUEI (Fox *et al.* 1976 ; Fox *et al.* 1977), the Fraser Liberal Government approved the development of Ranger, the establishment of Kakadu National Park and granted freehold title to a significant portion of the region to indigenous land trusts. The Fraser Government also established a major research and advisory group to oversee uranium mining in the region, based on the recommendations by RUEI, called the Office of the Supervising Scientist (OSS). A critical issue identified by the second RUEI report was long-term containment of uranium mill tailings, of which groundwater was recognised as the most important pathway, assuming tailings were placed in former pits.

The Ranger project began commercial production in August 1981, with Nabarlek operating from 1980 to 1988. To date, the Jabiluka and Koongarra uranium deposits have yet to be commercially developed. A detailed history of the region is given by (Lawrence 2000).

3.2. Ranger Uranium Project: A Brief Overview

3.2.1. Topography

The RPA, as shown in Figures 3.1 and 3.2, is located approximately 250 km east of Darwin at about 132^0 55` E latitude and $12^0$ 43` S – 12^0 40` S longitude and occupies 78.6 km^2 in the upper reaches of the Magela Creek catchment, some 70 km south of Van Diemen Gulf (Press *et al.* 1995).

Several creeks or billabongs surround the RPA, including Magela Creek and Georgetown Billabong to the east, Corridor, Georgetown and Gulungul Creeks to the south, Gulungul Creek to the west and Coonjimba and Magela Creeks to the north (Djalkmarra Billabong and Creek were recently excavated by Pit #3 over the last five years) (see Figure 3.2).

The Magela Creek is a major tributary of the East Alligator River, contributing about 10% of the flow (Fox *et al.* 1977). Its southern catchments cover an area of approximately 1,000 to 1,500 km^2 and include the major uranium deposits at Ranger and Jabiluka. Downstream of the RPA, the Magela consists of a series of stream channels, billabongs and floodplains. The paperbark-lined channels and floodplains are in close proximity to the sandstone escarpments of the Jabiluka outlier (Wasson 1992) .

The RPA site is located on the recognised traditional lands of the Mirarr-Gundjeihmi clan, who are members of the Gagadju Land Trust, established to manage the freehold indigenous title to the region, including the central core of Kakadu National Park ((Lawrence 2000).

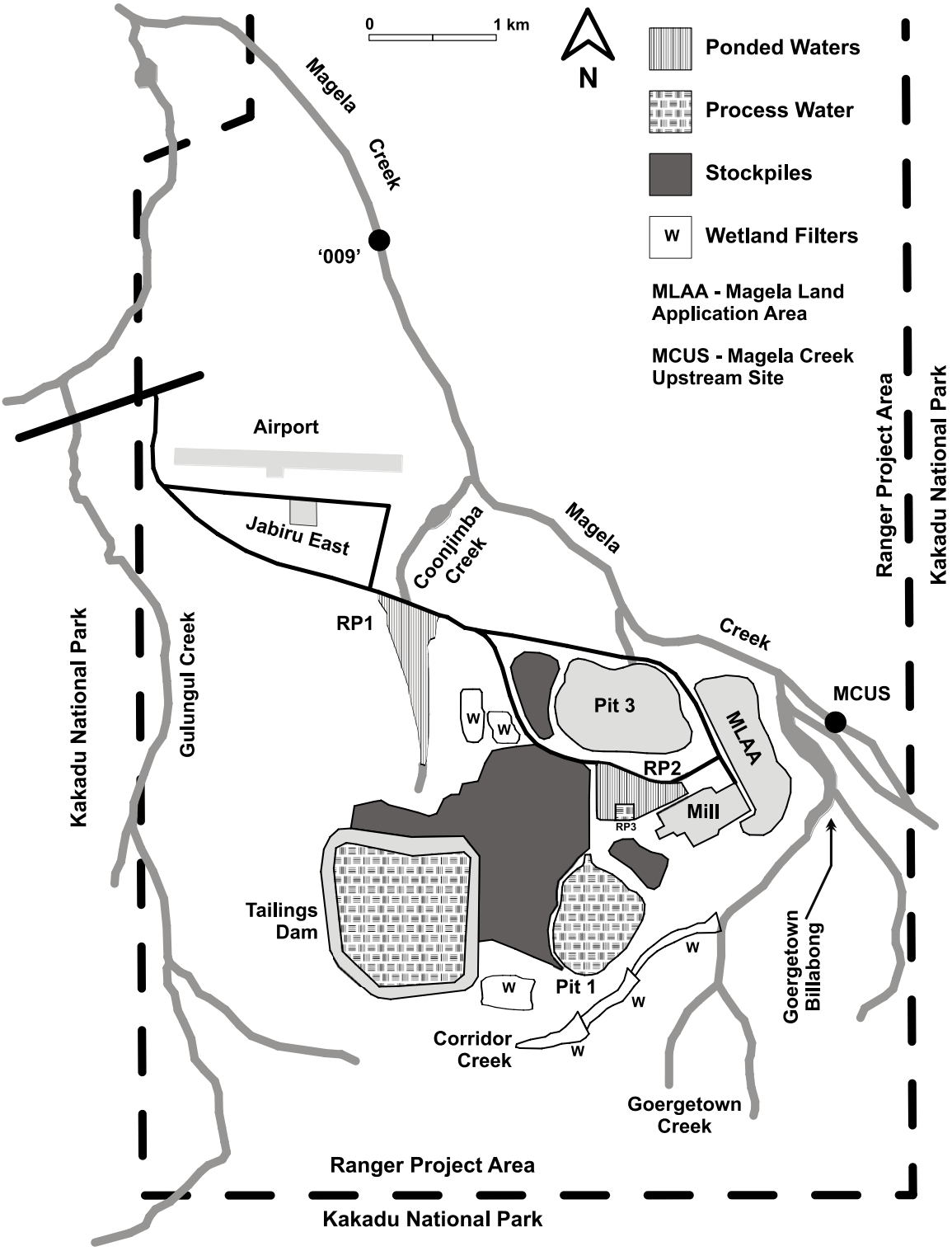

Figure 3.2 Site layout of the Ranger Uranium Mine

3.2.2. Time Line of Development and Mining

Uranium mineralisation was first proven at the Ranger site in late 1969, with subsequent exploration work proving it to contain several uranium deposits. Each deposit or prospect was given a number, with Rangers 1 and 3 being the largest deposits. After extensive

investigation, public debate and assessment, especially by the RUEI (1975-1977), the Ranger project received government approvals in August 1977. Mining agreements, required under the land rights act, were then negotiated between the indigenous owners, Ranger and the government, and signed in November 1978. The Ranger project was formally approved under the *Atomic Energy Act 1953* in January 1979 for a period of 21 years, with construction starting immediately. Based on the land rights agreements and formal approvals, a series of 'Environmental Requirements' (ER's) were mandated for Ranger, covering areas such as water and tailings management, rehabilitation, radiation exposure, cultural heritage and mining royalties.

The first deposit mined by open cut was Ranger 1 ('Pit #1'), operating from 1980 to 1994 (when the deposit was exhausted). Following approvals in 1995, Pit #1 became the major facility to receive tailings from mid-1996. Open-cut mining began at Ranger 3 in 1996 ('Pit #3'), and on present plans are expected to continue until 2012 (underground mining may begin past this date but is not yet approved). The major features of the site over this period (1980 to late 2000's) include the mill, tailings dam, retention ponds, ore, low-grade ore and waste rock stockpiles, as shown in Figure 3.2. A montage of aerial photographs showing the evolution of the Ranger site is provided in Figure 3.3.

In January 2000, the Ranger project was re-authorised for a further operating period of 21 years, followed by a five-year period of rehabilitation and expected lease relinquishment in January 2026. A new set of ERs were also incorporated at this time. One of the major clauses in the revised ERs related to tailings management and stated that all tailings were to be transferred to former pits before rehabilitation to ensure that long-term management was below natural ground surface. This was considered by the RUEI as the most appropriate solution for tailings due to the release of radioactive radon gas from the tailings and the intensity of the tropical climate leading to major risks of erosion and seepage if the tailings were rehabilitated in the tailings dam above natural ground surface. Additionally, a major criteria included in this clause was that after rehabilitation, solutes derived from tailings were not to lead to unacceptable environmental impacts for at least 10,000 years[1] (clause 11.3 ii).

[1] Environmental Requirements of the Commonwealth of Australia for the Operation of Ranger Uranium Mine. Appendix A, Section 41 Authority Under the Atomic Energy Act 1953 (Commonwealth of Australia).

~1985

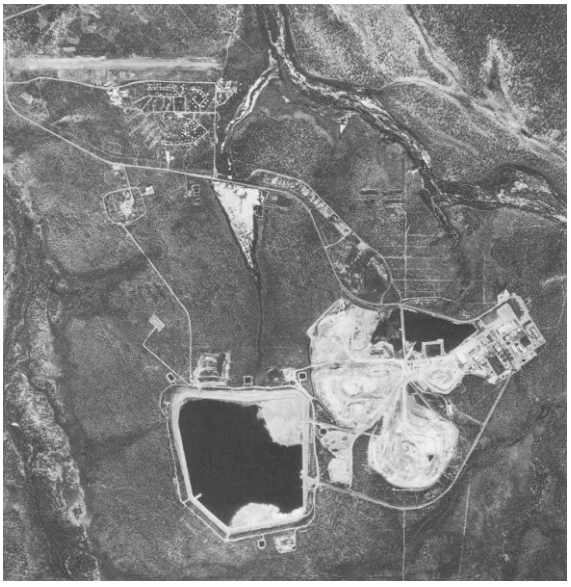

~1988

~1991

~ 1995

~1999

~2008

Figure 3.3 Aerial view of the development of the Ranger uranium mine (OSS var.); 2008 Edition, (ERA var.-a); 2008 Edition , (ERA var.-b)

The Ranger mine is owned and operated by Energy Resources of Australia Ltd (ERA), of which 68.4% is owned by Rio Tinto Ltd. At present, there is the possibility of underground mining beneath Pit #3 being actively investigated by ERA. A proposal for a major heap leach facility at the Ranger project is also being investigated and undergoing environmental assessment.

3.2.3. Practical Importance of Long-term Impact of Climate Change

Ideally, the design criteria for a rehabilitated mine should ensure a sustainable environment surrounding the waste containment site. The design of rehabilitation should prevent the transport of contaminants through surface runoff or seepage. Therefore, the level of saturation, or groundwater level, should be contained to a certain range on a long-term basis to achieve this outcome.

The rehabilitation of the radioactive waste from the mining and milling at Ranger clearly requires such long-term containment. Ideally, the rehabilitated landform is intended to isolate and contain these wastes, physically, chemically and biologically, for many thousands of years, if not millions. The long-term containment is necessary due to the long half-life of radionuclides such as radium-226 (^{226}Ra) at 1,600 years, thorium-230 (^{230}Th) at 75,000 years and uranium-238 (^{238}U), the parent of the radioactive decay sequence, at 4.5 billion years (IAEA 1981; IAEA 1992). According to current regulatory requirements, the rehabilitation of the Ranger mine site must ensure that tailings and associated contaminants are effectively contained for a period of at least 10,000 years.

The primary objective of this study is to develop a physically based modelling technique that can be used to assess the long-term groundwater recharge (infiltration) at the Ranger site. The varying climatic conditions and predicted changed climate scenarios over the long-term (i.e. 10,000 years) should be sufficiently represented in the modelling framework. It should be able to provide a more realistic basis for assessing the environmental performance of the rehabilitation of the Ranger site considering the ranges of uncertainties of future climatic conditions and possible scenarios.

3.3. Geology and Hydrogeology

The Ranger uranium deposits occupy Early Proterozoic metasediments (about 1,800 million years in age) consisting of quartz and mica schists, amphibolite, calc-silicate and

carbonate (Kendall 1990). The underlying basement rocks are Archaean in age and comprise granite, gneiss and schist, ranging in age from 1,800 to 2,470 million years (Kendall 1990). The overlying Kombolgie sandstone, dated at 1,830 million years, acts as a cover to the Proterozoic rocks containing the uranium mineralisation (Kendall 1990). The sandstone provides the spectacular escarpments and land forms of the Kakadu and Arnhem Land regions. A geological map and cross-section are shown in Figure 3.4.

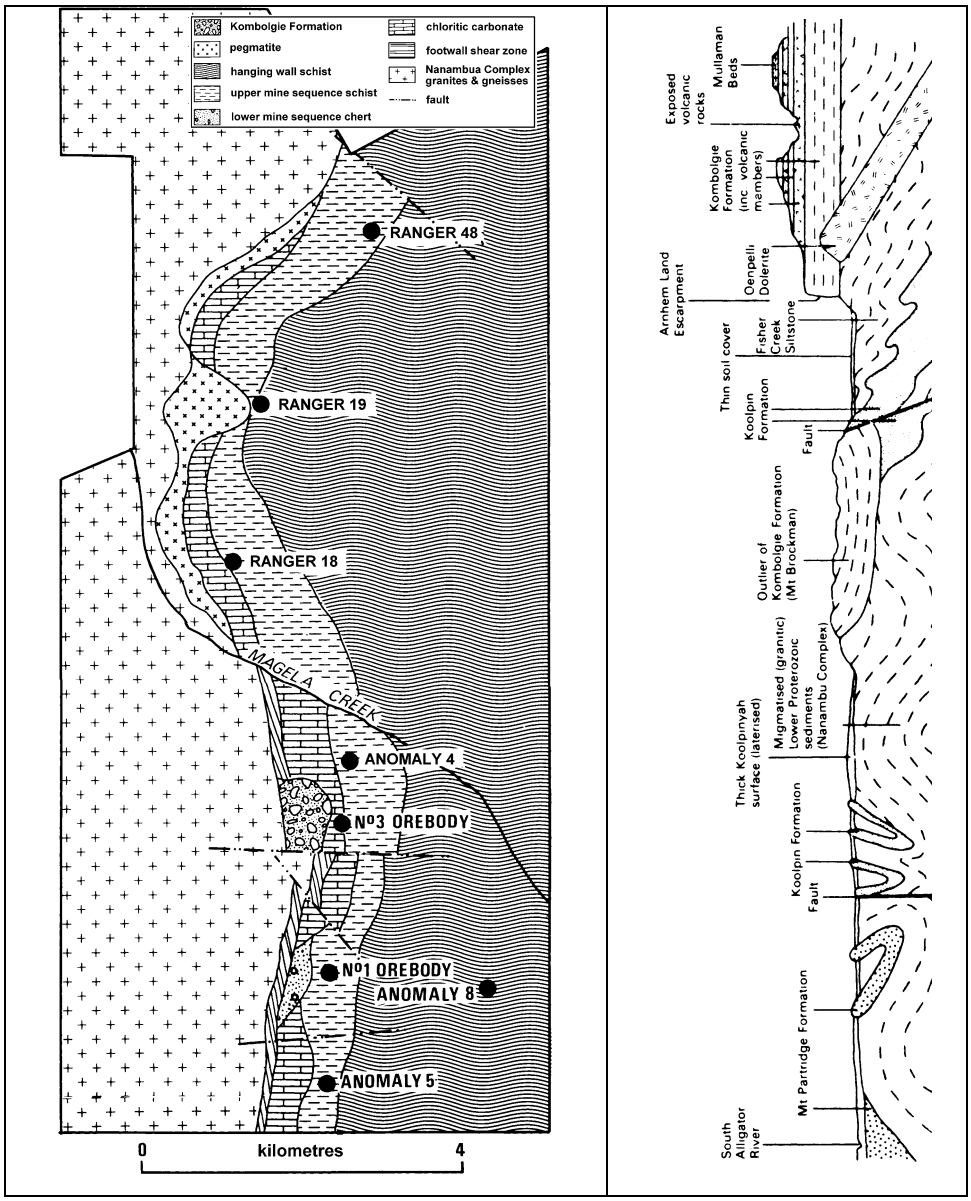

Figure 3.4 Left: Geology of the RPA (Kendall 1990), right: Conceptual Regional Geological Cross-Section (RUM 1974)

The extent of weathering of the near-surface rocks is variable across the mine area, ranging from a few metres up to 35 metres (Eupene *et al.* 1975; Morton 1976; Ahmad and Green 1986). Regionally, weathering has been noted to depths of tens of metres (Needham 1988).

The hydrogeology of the Ranger mine area is complex and is generally described as consisting of three basic formations (as illustrated schematically in Figure 3.5) (Ahmad and Green 1986): alluvial sands and gravels ('Type A'), weathered soils ('Type B') and fractured rocks ('Type C'). The nature and extent of each aquifer in a particular area will depend on local geology and weathering history.

The interconnection of the different aquifers will largely be controlled by the presence of semi-confining clay layers; although it is probable that all three types are hydraulically connected due to similar pressure levels (Ahmad and Green 1986). The fractured nature of the sandstones and escarpments and the occurrence of springs at their base suggest abundant recharge, flow and good quality groundwater (Christian and Aldrick 1975).

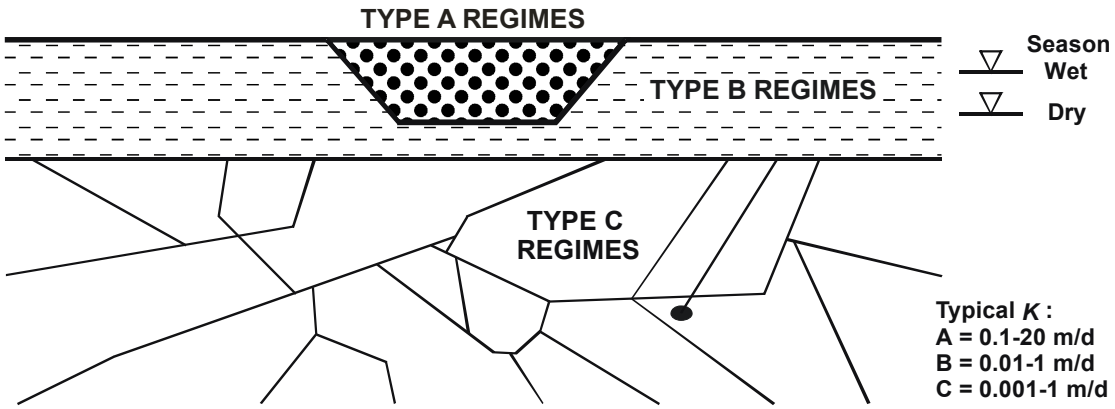

Figure 3.5 Conceptual hydrogeology of the RPA, adapted from (adapted from (Ahmad and Green 1986)

The groundwater levels (i.e. height) in all types of aquifers are usually related to gullies and hills (surface topography). They undergo a seasonal fluctuation of up to 5 m or more, related to recharge during the wet season and evaporation and transpiration during the dry season (Ahmad and Green 1986). The wet and dry seasons in the region are typically indicated on a half-yearly basis as described in the following section.

3.4. Kakadu/ARR Climate and Annual Water Balance

The Kakadu/ARR region has a typical monsoonal wet season (November–April) and dry season (May–October). The distribution of rainfall, pan evaporation and annual fluctuation of groundwater level are illustrated in Figure 3.6.

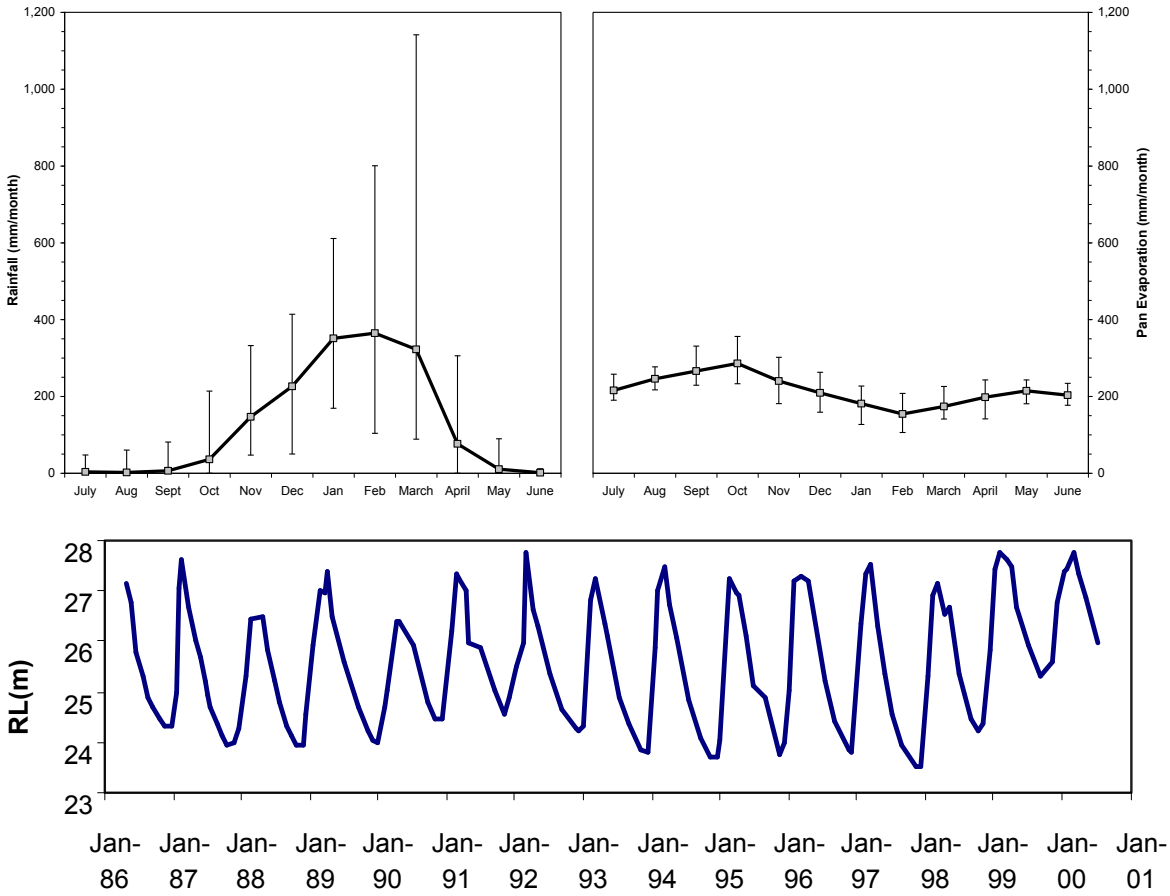

Figure 3.6 Top: Average monthly rainfall and pan evaporation for Jabiru East, including minimum and maximum (years 1972 to 2008) (Data Courtesy: ERA, OSS, BoM); Bottom: Typical seasonal groundwater level fluctuations around the RPA, (2001 Edition, (ERA var.-b)

The average annual rainfall at Jabiru East (1971–2008) is 1552 mm, but it has varied from approximately 1032 to 2623 mm with a standard deviation of 367 mm (data courtesy: ERA, OSS, BoM). The variability of rainfall is relatively high, as demonstrated in Figure 3.6 Figure 3.6. One example is late February 2007, when some 750 mm of rain fell in less than 72 hours, leading to extensive flooding in the region (including the Ranger site).

The average annual pan evaporation at Jabiru East is 2588 mm; it has varied from 2237 to 2900 mm with a standard deviation of 161 mm. Pan evaporation is relatively uniform throughout the year (see Figure 3.5). Table 3.1 shows the monthly pan factors for estimating evapotranspiration in the region.

Table 3.1 Pan coefficients to estimate evapotranspiration from pan evaporation data (Chiew and Wang 1999)

Sep	Oct	Nov	Dec	Jan	Feb	Mar	Apr	May	Jun	Jul	Aug
0.66	0.66	0.75	0.84	0.92	0.92	0.95	0.77	0.70	0.70	0.66	0.64

Pan evaporation indicates the rate of water loss from the free water surface of a region. However, evapotranspiration is a better representation of the outflow of water from the regional hydrologic system, which is a combination of free water surface and land surface. Evapotranspiration includes evaporation from soil and water surfaces and transpiration from vegetation, and is considered the net influx to and from the soil surface. Further analyses of evapotranspiration are presented and discussed in Chapter 5.

3.5. Data Sources

The information about the site consists of some time series data and some time independent data. The time series data considered are rainfall, evapotranspiration, stream flow or surface runoff, and groundwater level. The time independent data consists of lithology and hydraulic properties of weathered soils and rocks. The topography in the direct mining area is also changing over time, as the open cut expands, tailings dam is increased in height and new waste rock and low-grade ore stockpiles are created.

The sources and types of data used in this work are shown in Table 3.2. The specific descriptions about the data sources are also mentioned. Some of the data are measured and other data are estimated as described in the various subsections. The temporal intervals of measured values vary from 6-minutes to few months. The analyses are performed on a daily, monthly or annual basis.

Table 3.2 Description of data analysed

Data type	Time period	Frequency	Source
Climate (Rainfall and Evapotranspiration)	1900-2008	Daily	PPD of SILO of BoM weather station 14198 Jabiru East*
Surface Runoff	1971-2005	Daily**	OSS, gauge station GS821009
Groundwater level, Groundwater Chloride	1980-2008	Daily and Monthly	ERA, OSS
Lithology		Time invariant	ERA, OSS

*SILO is an electronic resource of information available from BoM (SILO 2006)

** Data is available on a 6-minute basis, but daily average is used in the thesis

PPD: Patched Point Data; BoM: Bureau of Meteorology

3.5.1. Climate

The measured climatic data considered in this research consists of rainfall and the estimated climate data is evapotranspiration. The Jabiru East weather station is used as the source of these data, since it is located within a short distance (<5 km) from the site. It was first established in 1971. The nearest weather stations are located at a considerable distance (such as Oenpelli/Gunbalanya, Darwin) such that the Jabiru East station alone is assumed to represent the areal average value of the climatic variables (Chiew and Wang 1999). The rainfall data are measured (or interpolated when measured data is missing) in the weather station, while the evapotranspiration data are estimated using the measured climate data (such as temperature, vapour pressure, solar radiation and atmospheric pressure) by following the methods described by (Morton 1983).

Two additional rainfall stations are located in the RPA and operated by ERA. They are the tailings dam and the Pit #3 sites. In those stations, only rainfalls are recorded and not pan evaporation or other climate data. Evapotranspiration data is available from Jabiru East only. The Jabiru East meteorological station started operating in 1971. From 1971 to 1989, it was operated by ERA. From 1990 to present, it is operated by the BoM. The historical data for the period before 1971 was estimated by SILO PPD data (SILO 2006). The detail climate data as collected from SILO are provided in Appendix C.

3.5.2. Rainfall

For the purpose of representing historical rainfall in any catchment in Australia, Patched Point Data (PPD) (SILO 2006) data are developed by the Queensland Department of Natural Resources and Water, which is available via the Internet (Ladson 2008). This dataset provides daily values for 4650 meteorological stations in Australia, starting from January 1889. The missing data in terms of period or location have been interpolated with sufficient accuracy (Jeffrey *et al.* 2001). Given that monitoring has been direct at Jabiru East since 1971, apart from some minor gaps, PPD has been adopted as the primary source for rainfall statistics.

3.5.3. Actual Areal Evapotranspiration (AAET)

The estimation of Morton's actual areal evapotranspiration over land (AAET) is conducted by SILO (SILO 2006). The basis of selection of the appropriate evapotranspiration variable has been discussed in Sections 2.1.2 and 2.1.3. The climate data are available in daily basis and the monthly subtotals are estimated from daily values.

The Evapotranspiration Map of Australia (Chiew *et al.* 2002) is another source of long-term average evapotranspiration variables (AAET, PPET and APET) with water balance corrections for the hydrologic catchments of all of Australia. Of the three evapotranspiration variables (AAET, PPET, and APET), AAET is selected as the best representation of evapotranspiration processes for the current project (this issue is discussed in detail in Section 5.3.3).

3.5.4. Groundwater Levels

The available data of groundwater level in a number of monitoring bores surrounding the Ranger mine site have been supplied by ERA. The record of the data is a combination of daily, weekly or monthly values with regular or irregular intervals for 21 monitoring bores. Two bores were located inside Pit #3, with missing data since this pit began but provide useful data until this time. Other bores are impacted by seepage from the retention ponds or tailings facilities. However, there are numerous bores whose GWL fluctuation is solely related to natural processes. These are selected for subsequent analyses. Also excluded are the open bores that do not have any screen and extend to the deep aquifer of 100 to 150 m below ground surface. Other factors for the selection of bores included encompassing a large areal extent, varied elevation of ground surface and varied depths of unsaturated soil

above the GWL. The irregular interval GWL data were converted to monthly GWL data by the outlook function in Microsoft Excel in the case of having too much dense data, and linear interpolation was used when data was too sparse.

Details about the location, period of record, annual groundwater fluctuation, screen location and unsaturated thickness are presented in Table 3.3. Complete information for all bores, including lithology, monitoring graphs and other details, are given in Appendices D1 and D2. From these 21 bores, a selected number were chosen for this thesis, which is discussed in Section 3.6.

Table 3.3 Relevant information of all the 21 bores

Bore	Mine Features Nearby	Length of record (years)	Highest GWL (m AHD)	Annual GWL Fluctuation (m)	Unsaturated Zone Thickness (m)	Bore Depth (m)[#]	RL ToC and also datum AHD (m)
OB19A	TD	83-03	33.516	6.26	[##]	51.2	33.096
OB1A	TD	81-03	30.08	6.58	0	31	30.08
OB20	South of TD	82-03	20.402	5.61	1.28	36.18	21.682
OB21A	South of TD	82-03	27.003	6.98	2.96	43.13	29.963
OB23	North of TD	82-03	27.94	11.37	0	51.3	27.94
OB24	North of TD	82-03	24.15	10.38	1.34	36.5	25.49
OB27	Georgetown	81-88, 03-05	10.37	3.46	3.8	40	14.17
OB29	Orebody #3	81-03	15.13	29.71	[##]	50.47	15.09
OB2A	TD	81-03	30.327	6.41	0	31.51	30.327
OB30	Pit #1	82-05	18.82	27	0	47.5	18.82
OB31	TD	83-88	31.896	5.56	1.31	50.2	33.206
OB34	TD	84-88, 93-98	29.958	4.37	0.15	22	30.108
OB35	TD & Pit #1	86-88	28.9	4.56	5.17	15	34.07
OB36	TD & Pit #1	86-88	25.63	2.68	1.23	12	26.86
OB37	TD & Pit #1	86-88	25.63	2.7	1.03	5	26.66
OB38	Orebody #3	86-88, 90-96	18.591	13.07	0.99	168	19.581
OB41	RP1	88-05	16.198	3.63	0.09	25	16.288
OB42A	RP1	92-05	16.405	2.98	0.14	12	16.545
OB43	RP1	88-03	16.602	3.6	0.18	22	16.782
OB44	North of TD	88-02	19.69	4.814	0.01	16.1	19.7
79/6	Orebody #3	80-88, 90-02	11.75	6.04	1.23	116	12.98

[#] assuming the bore depth is measured from Top of Collar (ToC) of the bore, [##] Data discrepancy as found from the source.

TD = Tailings Dam, Orebody #3 = Pit #3, RP1 = Retention Pond 1.

3.5.5. Runoff

All stream flow data is collected from gauging station GS821009 in Magela Creek, located about 3 km downstream of the Ranger mine site, as shown in Figure 3.7. The discharge at GS821009 arises from a catchment of about 600 km^2. The depth of runoff at the RPA, which is located as near as 4 km upstream of the station, is assumed to be same as that of the whole 600 km^2 catchment of the station GS821009 (ARRI 1991). Runoff depth is estimated as flow discharge per unit catchment area of the station. The historical record of daily rainfall and runoff are shown in Figure 3.8 and Figure 3.9. There are also a number of other gauging stations along the Magela Creek (see Figure 3.7), which are used later in Chapter 5.

To convert the discharge data in to depth of flow, uniform spatial distribution of rainfall in the catchment has been assumed. For a catchment of 600 km^2, the assumption is reasonable, since a significant similarity in the distribution and magnitude of average annual rainfall has been reported by Vardavas (1992) while analysing the rainfall data of stations located at 50 to 300 km from Jabiru East (namely Darwin, Oenpelli, Pine Creek and Katherine).

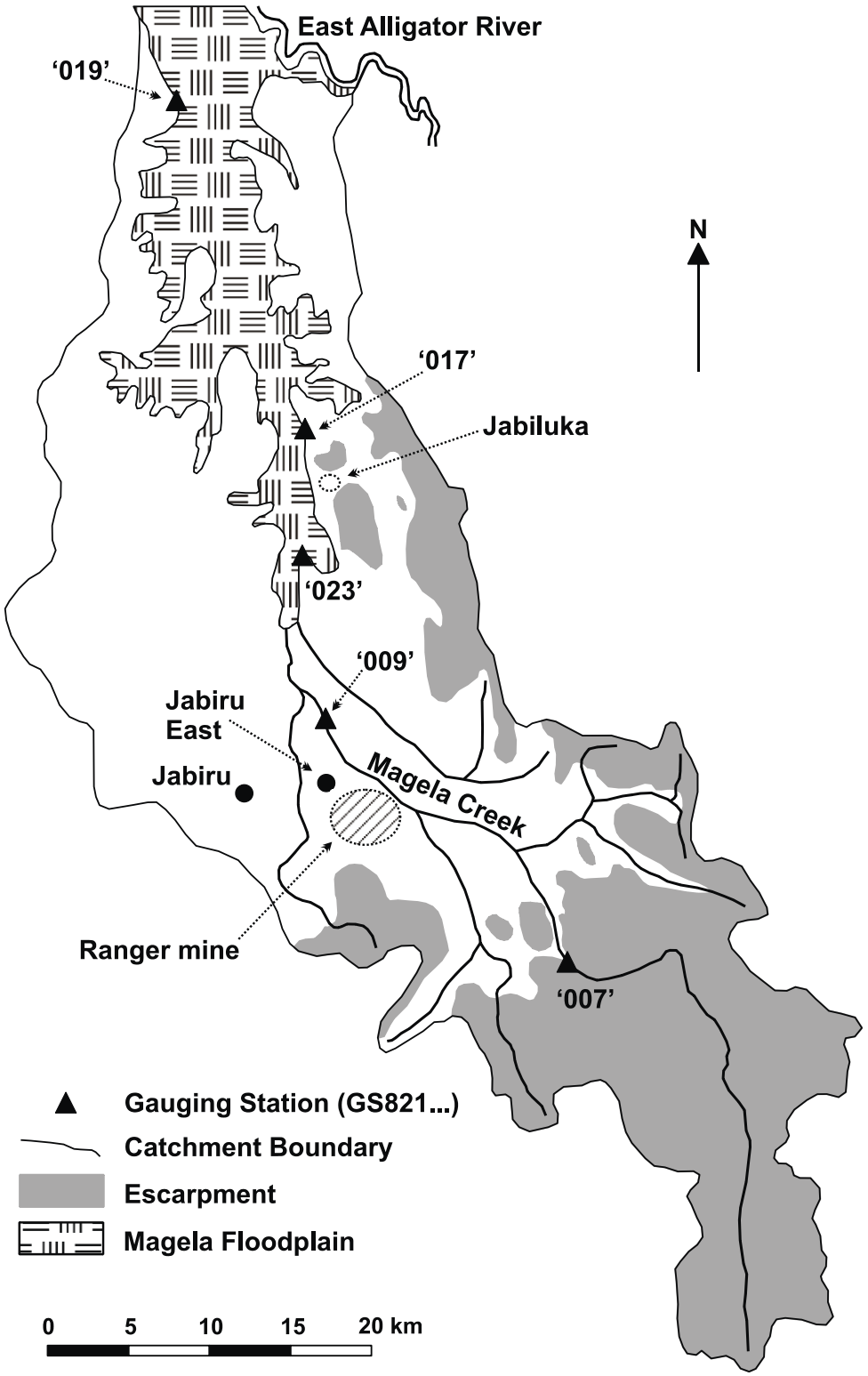

Figure 3.7 Location, topography and catchment area of Magela Creek in the Northern Territory, adapted from (Hart et al. 1987a)

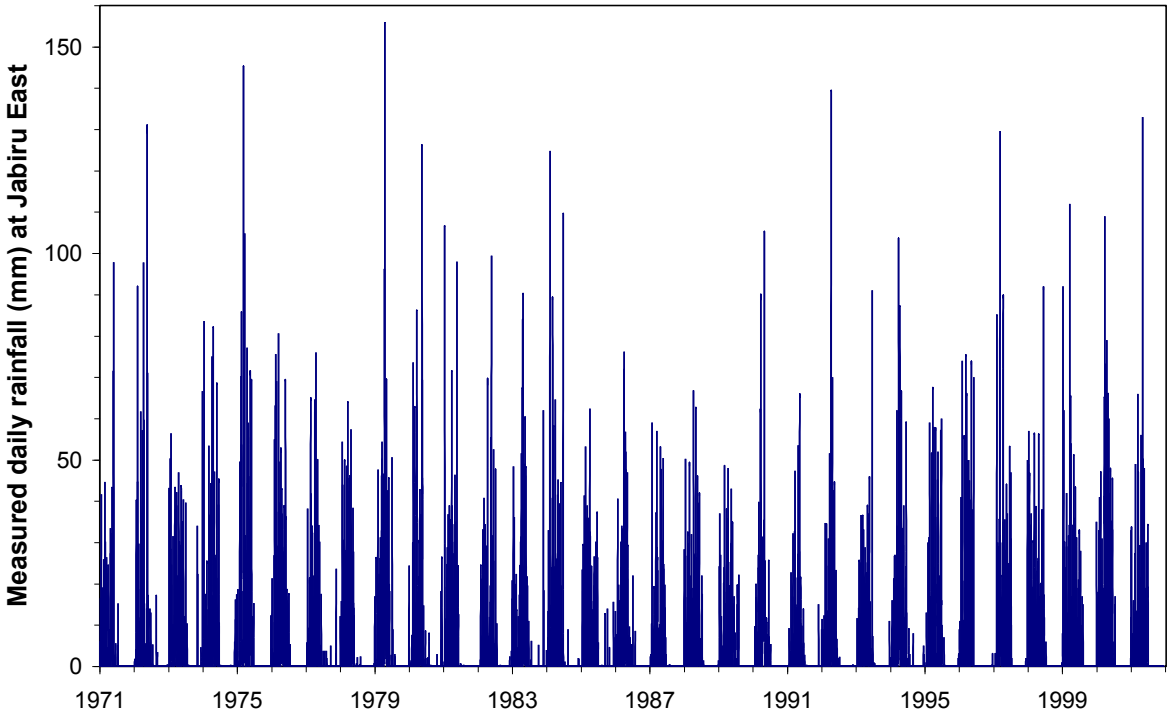

Figure 3.8 Historical record of measured daily rainfall

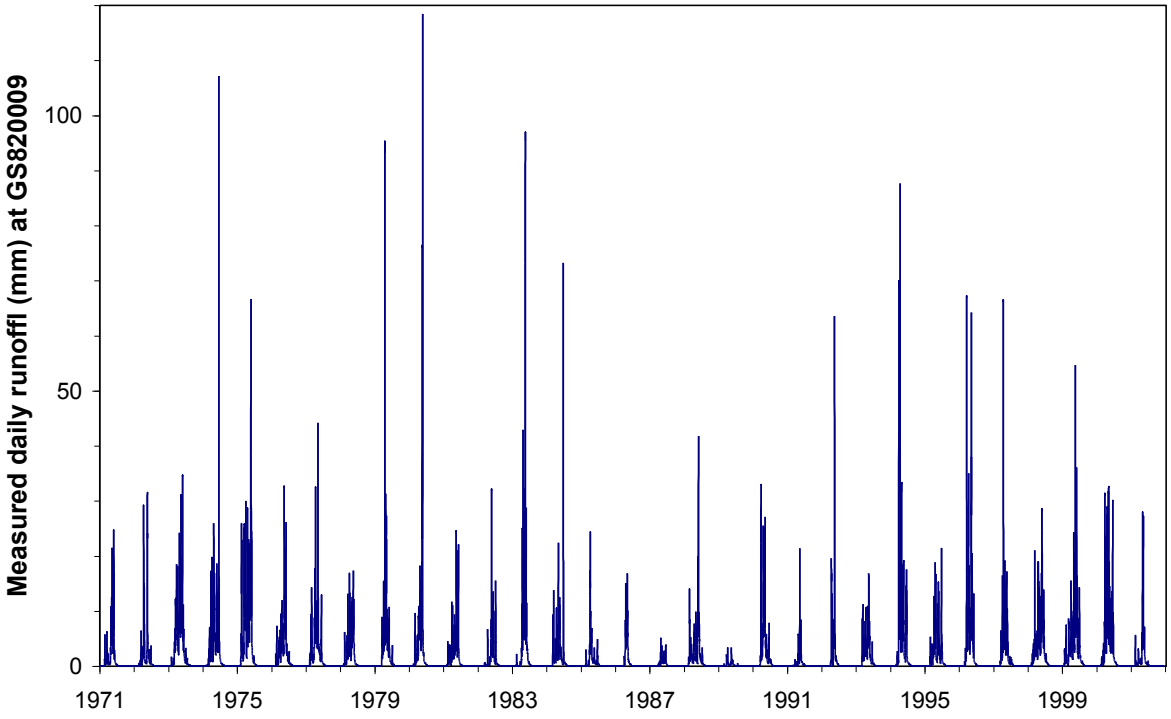

Figure 3.9 Historical record of measured runoff

3.6. Selection of Bore for Investigation

The locations of the significant operational features around the site and monitoring bore locations for GWL data for Ranger are illustrated in Figure 3.10.

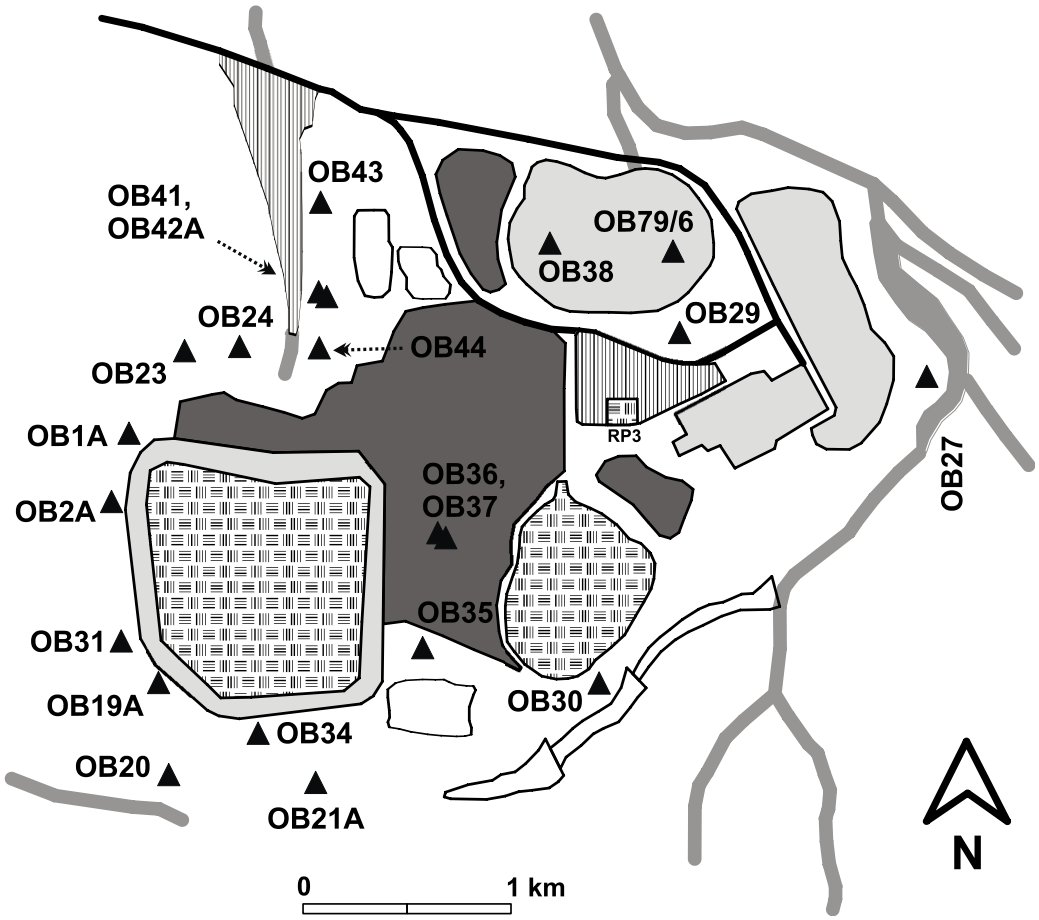

Figure 3.10 Locations of the monitoring bores in the site

The bores surrounding Pit #1 (OB30), or inside or near Pit #3 (OB29, OB38 and 79/6) are directly impacted by mining activity, as shown in Figure 3.11. OB38 and OB79/6 are excluded from consideration because these were deep open bores with no casing (at 150 m to 200 m in depth) rather than screens in the shallow unconfined aquifer (up to 50 m deep). Other bores, such as OB35, OB36 and OB37, do not have a record of GWLs of more than two years, while OB23 and OB24 are impacted by tailings dam seepage, as shown in Figure 12. Therefore, the bores located at the southern sides of the pits are investigated in more detail. Certain bores located around the perimeter of the tailings dam, such as OB1A, OB2A, OB20, OB21A, OB41 and OB43, are considered for detail investigation. The bore OB27, located in the east of the region, is also considered for further investigation.

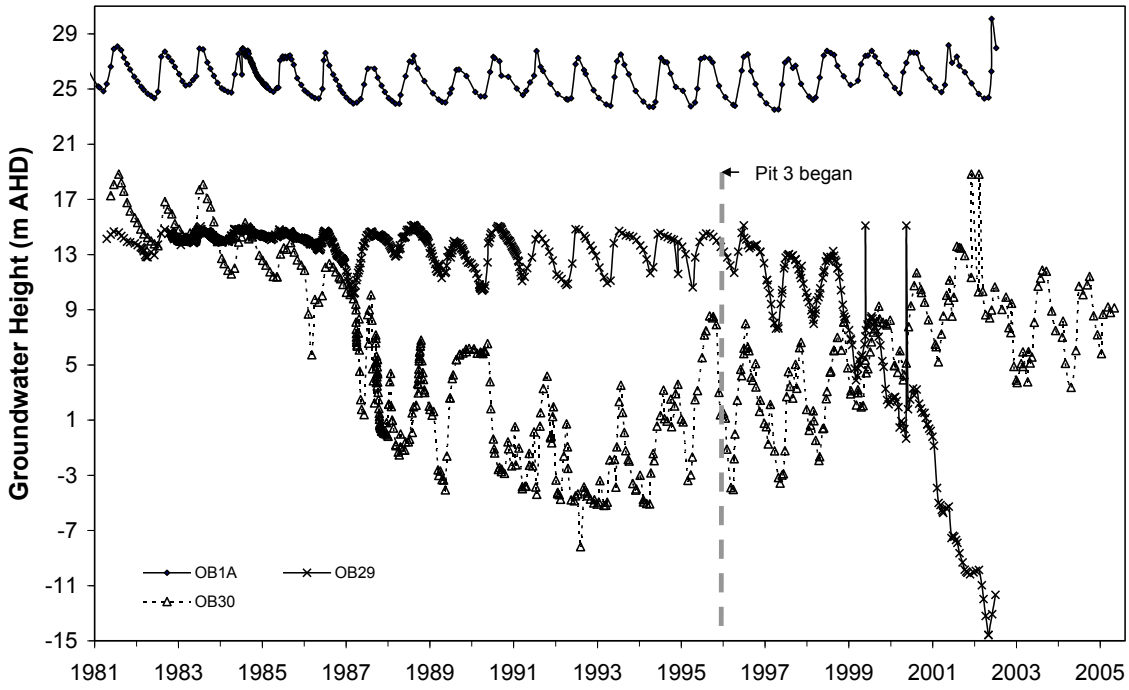

Figure 3.11 The bore OB1A is relatively unaffected by mining activity while bore OB30 is influenced by mining and filling in Pit #1 from 1981 to 1994 and 1995 to 2001. Similarly, OB29 started to become influenced by mining in Pit #3 from 1996

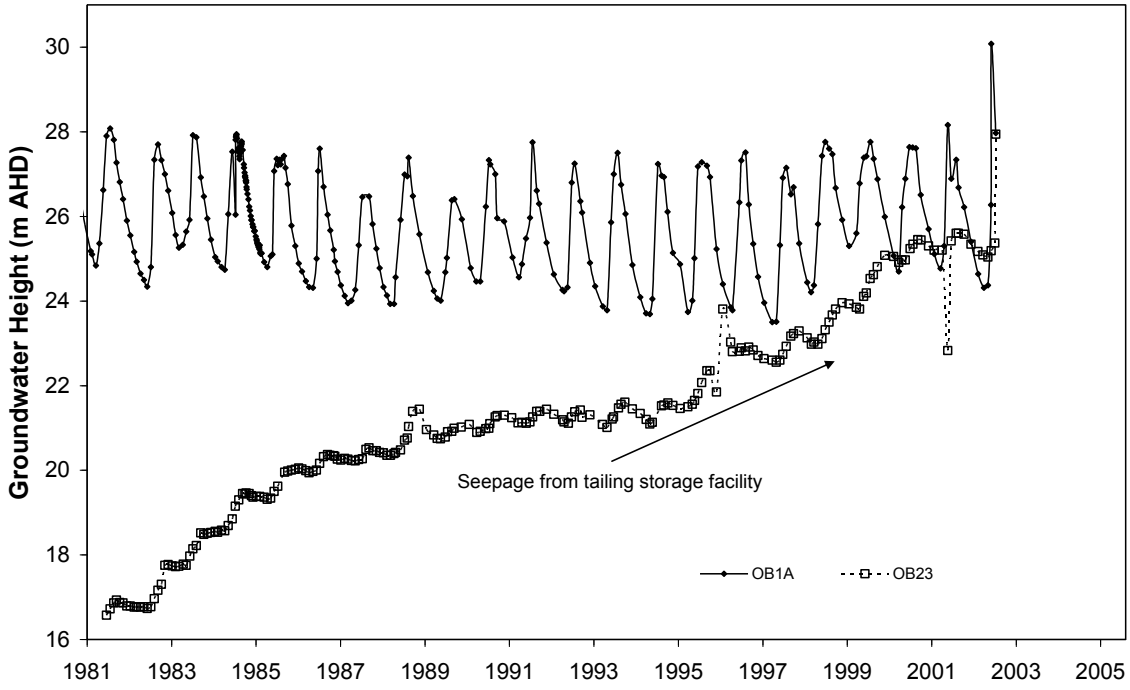

Figure 3.12 Bore OB23 impacted by seepage

The natural surface generally consists of flat slopes (see Figure E-1, Page 107, 2000 Edition, (ERA var.-b). Considering the measured GWLs at various surface elevations, annual GWLs are found to fluctuate in the zone of the upper unconfined layer of the site. The unsaturated layer thickness varies from approximately 0 to 5 m throughout the year. Based on GWLs around the Ranger site, GWL contours generally follow the land surface profile (Mc Quade 1991; Willett *et al.* 1991; ERA var.-b). Further detailed analyses of various bores are presented in later chapters, particularly Chapters 5, 6 and 8.

3.7. Conclusion

It is established in this chapter that the Ranger mine site is required to monitor groundwater levels within their mining area to demonstrate their adherence to the existing guidelines (i.e. various legislation and statutory conditions). This is to ensure that no detrimental environmental impact occurs on the surrounding world heritage-listed Kakadu National Park. The rehabilitation of the Ranger project is required to demonstrate physical and chemical containment of the radioactive tailings for at least 10,000 years. This will ensure that the environment is protected from contaminant transfer either by surface flow or by groundwater seepage. An important practical need for (and use of) the research conducted at this site is thus the assessment of the rehabilitation structures' performance.

Given the available historical data of hydro-climatic processes (rainfall, evapotranspiration, runoff and groundwater level) available for Ranger, this will allow the development of a suitable groundwater-climate response model. This site has the privilege of being equipped with the relevant data and has a crucial need to understand and model climate-GWL relationships. Thus, it is thereby selected for the research.

4. Research Question and Proposed Methodology

Having reviewed the literature and introduced the proposed site for this research, this chapter introduces the research question and proposes the sequence of steps to be followed to obtain the answer. All the deficiencies relevant to the objective of long-term prediction of groundwater levels, as identified in the concluding section of Chapter 2, can be summarised into two fundamental components. The first is the spatial and temporal scale of data acquisition, while the modelling framework is the second. An overall approach and systematic methodology is proposed to answer the research question.

4.1. Research Question

The fundamental aim of this research is to understand and model the relationship between shallow groundwater and climate. This gives rise to the following primary research question:

- **What is an appropriate framework to model the response of groundwater to varying and changing climate at the Ranger site?**

To address the aforementioned primary research question, a number of secondary technical questions emerge, which are consequently answered in the following chapters of the thesis:

- How to develop the best conceptual model for the site in order to model the groundwater recharge in the shallow unconfined aquifer? What is the best approach to represent the evapotranspiration process for the site under consideration? What is the relative significance of runoff in relation to the selected evapotranspiration data to explain the water balance for the region? What is the significance of unsaturated zone in the process of wetting and drying in the tropical climatic region? (Chapter 5)
- How can the statistical methods explain the physical processes? What are the possible methods to represent and forecast the groundwater-climate relationship in the long-term? (Chapter 6)
- With the GCM predictions incorporating the future trend of average climate, how to combine the natural climatic variability with the climate change predictions of GCMs? What is a possible method to predict the ENSO events at the site of investigation? (Chapter 7)

- What should be the best criteria for validation of groundwater models? What is the influence of geology in the long-term response of the process of groundwater recharge? (Chapter 8)
- Are decadal scale events of wet or dry spells (influence of climatic variability) more important than the predicted trends of climate change? What are the ranges of uncertainty for the predictions by time series methods and physically-based groundwater modelling? (Chapter 9)

This framework will include a sequence of independent models in which the output of one model will be used as the basis for the following model. The physical process-based modelling and statistical modelling are two fundamentally different ways to solve this problem. Examples of physical process-based models include conceptual hydrologic models (i.e. water balance models), groundwater response models, and models of climatic conditions, trends and variability. In contrast, statistical models could include time series techniques.

As discussed previously in Chapter 3, the Ranger uranium project is required by law to prevent impacts from solutes derived from its radioactive tailings for 10,000 years. The long-term driver of solute transport in groundwater will be the hydraulic head, which in turn is governed by the recharge rates driven by climatic conditions. Therefore, to demonstrate no environmental impacts of solutes derived from tailings containment over 10,000 years, a clear understanding of the relationship between groundwater heads and climatic conditions is required. Thus, this thesis proposes to address the fundamental research question by using the Ranger uranium mine as a case study, since there is a need to solve this problem at this site as well as the ready availability of all relevant data.

4.2. Methodology

The sequence of the proposed modelling framework, incorporating physical process-based and non-physical (statistical) models, is shown in Figure 4.1. The overall approach makes extensive use of historical groundwater and climate data for the Ranger site to validate the various proposed models.

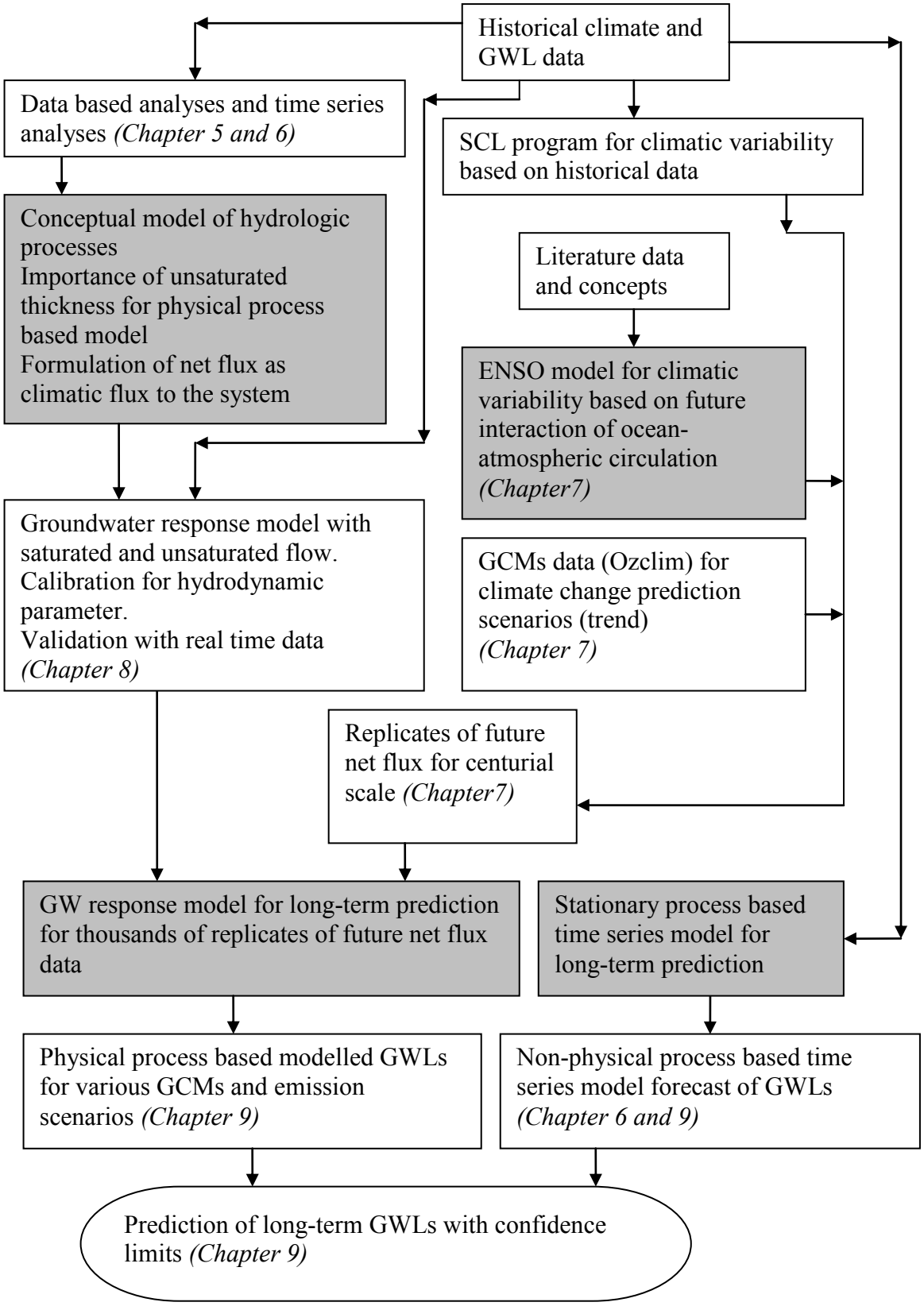

Figure 4.1 The sequence of physical and non-physical models in the developed framework as described in the various chapters of the thesis

First, exploratory analyses of climate and groundwater level data have been performed to understand the most significant hydrologic and hydro-geologic processes, leading to a conceptual water balance approach to link groundwater response with climate. Appropriate time series analyses have also been performed to complement the understanding of physical processes, such as the variable thickness of unsaturated soil. The available data from GCMs have been combined with algorithms for climatic variability to generate replicates of future climate data. Based on the water balance model, a physical process-based model using unsaturated flow has been developed by calibrating the soil hydraulic properties to reach a reasonable agreement between modelled and measured groundwater levels at several bores. The calibrated models for each bore are then run using the future climate replicates to predict the response of groundwater to changing and varying climatic conditions. Results are then presented and analysed, with a special focus on uncertainty, including a comparison to predictions under time series methods.

The atmospheric, hydrologic, and terrestrial components of the Earth's systems operate on different temporal and spatial scales. Therefore, resolving these scaling incongruities as well as understanding and modelling the complex interaction of land surface processes at the different scales represents a major challenge (Feddes 1995a). Data acquisition is a challenge when forecasting the future climate, while the downscaling technique is commonly used for transferring GCMs data to catchment scale application.

There are instances of numerous investigations (Groves *et al.* 2008; Lopez *et al.* 2009; Raje and Mujumdar 2009; Rotstayn *et al.* 2010), which are significantly resourced in terms of computational capability, human resources and time. Those attempts are not comparable to the present research. For example, Rotstayn et al. (2010) have attempted to incorporate ENSO-related rainfall variability in GCM to simulate the Australian climate with an interactive aerosol treatment. It can be anticipated that the prediction of groundwater response at a particular site due to long-term climate change response involves gradual transformation of GCMs output to RCMs, which is then used as the input to a physical process-based groundwater flow model.

The outputs from GCMs continue to evolve and retain a certain degree of uncertainty with respect to their applicability to catchment scale hydrological analyses. Manning et al.

(2009) have demonstrated that different downscaling methods produce significantly different flow predictions of the hydrological processes. Similarly, Qian et al. (2010) have compared the influence of downscaling methods on the climate simulations for the western United States (US) by using two different dynamic downscaling schemes. They have found that RCMs are better than GCMs at representing hydro-climate as far as downscaling is concerned. Holman et al. (2009) have identified that uncertainty with the selection of downscaling techniques is greater than that of selection of emission scenarios. While assessing the impact of climate change on water resources in Iran, Abbaspour et al (2009) have shown that variation for uncertainty in hydrological models is greater than that of variation of emission scenarios. Therefore, there exist all ranges of uncertainty related to downscaling techniques, hydrologic models and emission scenarios. Thus, it is imperative that all the possible emission scenarios are encompassed with the best possible hydrologic model. Nevertheless, the downscaling of GCM data for the site has been performed by Ozclim (CSIRO 2006). Selection of the GCM for the site has been based on the study conducted by Hennessy et al. (2004).

Overall, this leads to a logical and substantive methodology, which allows the response of groundwater to be modelled with respect to a changing and varying climate, thereby answering the research question and addressing an important problem concerning the rehabilitation of the Ranger uranium project.

4.3. Conclusion

The key issues are identified as: representation of the annual water balance components for the site; consideration of unsaturated flow in controlling recharge to the shallow unconfined aquifer (or water table); consideration of the climate change predictions for the range of future socio-economic development scenarios; interaction of climate change with the natural climate variability and link to extreme weather events; and the variation of the responses of groundwater system for the full range of climate change scenarios. It is concluded that this study is unique in this mutli-disciplinary area of science and engineering. Therefore, it should make a distinctive contribution to the advancement of knowledge in addressing such challenges. It should also contribute to the understanding and modelling of groundwater-climate relationships, the potential impacts of climate change on groundwater resources, and the ability to inform rehabilitation design of uranium mill tailings sites such as Ranger.

5. Estimation of Hydrologic Processes

The primary objective of this chapter is to develop a hydrologic process-based conceptual groundwater-climate model, which will represent the hydro-geological behaviour of the site in terms of the historical climatic record and groundwater monitoring data. The latest available data of climate and GWLs, which are obtained for the present research, are analysed to develop a sound understanding of the flow processes in a comprehensive manner.

In the first sections of this chapter, the scale issue for data acquisition and system representation for the research site is critically considered for the implementation of the modelling work. The existing hydrologic models are briefly reviewed with regard to the representation of evapotranspiration processes. Three sets of available sources of evapotranspiration data are considered from which the most appropriate set of data is selected for use in the study. The insignificant flow components such as horizontal subsurface flow of the system are numerically established to be negligible and a one-dimensional vertical flow model is derived. The representation of the GW climate relationship with the help of 'net flux' has been established by performing various methods of analyses. Four different conceptual models, the correlation model, the AWBM, the chloride balance model and the classical decomposition models, are developed and compared for estimated values of groundwater recharge. Monthly Data Based Mechanistic (DBM) models are used to verify the relationships between rainfall and the rest of the flow components such as evapotranspiration, runoff and soil moisture storage in relation to the previous investigations undertaken for this site. Consequently, the updated version of the conceptual model is also proposed.

5.1. Scale Issue

For development of the hydrologic model, estimation of the hydrologic processes is required in order to examine the relative significance of each of the possible components. All the flow components are estimated to select the relevant input variable to represent the climatic flux to the soil water system. The subsequent modellings are performed based on the findings of the significant flows of the system.

The scale of occurrence of a hydrologic process, scale of possible observation of that process and the scale of required information about that process may vary widely in context to space and time. Cushman (1984; 1987) has discussed the relationship between the process scale and observation scale and highlighted that sampling involves filtering. Figure 5.1 provides a more intuitive picture of the effect of sampling.

Depending on the scale of representation, the meaning of an analysis can vary. The processes that are normally larger than the coverage appear as trends in the data, whereas processes that are smaller than the resolution appear as noise in the data. Therefore, while combining two unequal scales of data is necessary, awareness of the possible consequences for designing the modelling framework is required. From this general understanding, the relevant hydrologic processes are reviewed with regard to the current problem.

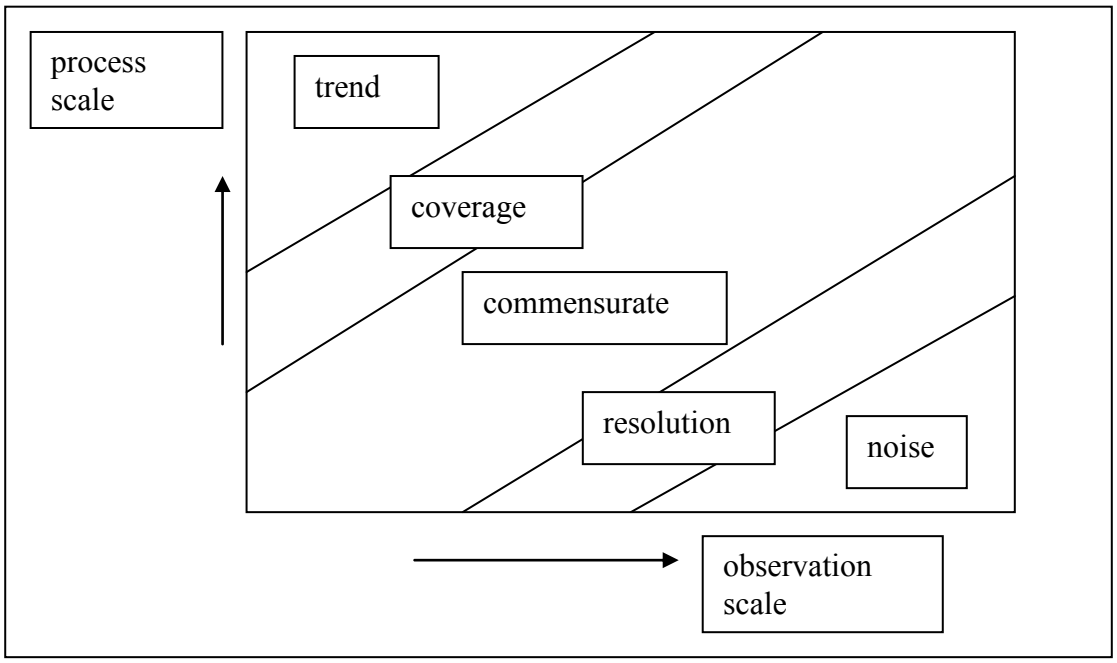

Figure 5.1 Relationship between process scale and observation scale (Cushman 1984)

'To scale' means to zoom, to reduce or to increase in size. In a hydrological context, upscaling and downscaling refer to transferring information to a larger or smaller scale (Gupta *et al.* 1986). Measuring hydraulic conductivity in a borehole and assuming it applies to the surrounding area involves upscaling. In addition, estimating a 100-year flood from a ten-year record involves upscaling. Conversely, using runoff coefficients derived from a large catchment for culvert design on a small catchment involves downscaling (Mein 1993).

Regionalisation involves the transfer of information from one catchment (location) to another (Kleeberg 1992). In some cases, this may be satisfactory if the catchments are similar; however, it can be error-prone if they are not (Pilgrim 1983). Once the data about the dominant processes are gathered (Grayson and Bloschl 2000a; Grayson and Bloschl 2000b; Woods 2002), it is imperative that the variability of hydrological processes are explored and represented in the relevant resolution as determined by the data availability and purpose of the analyses of the system. Factors that cause scaling to be difficult include the variability of hydrological processes and the heterogeneity of catchments (Bloschl and Sivapalan 1995).

The time-based variability is considered by involving time series methods of analyses, as it is applicable for long-term prediction. The Chapter 7 discusses the prediction of climatic variability in combination with climate change predictions for generating the centurial scale replicates of climate flux. For the future projection of the system at the centurial time scale, the estimates are derived from the output of Ozclim (CSIRO 2006). Starting from the base year of 1990, projections are computed until the year 2100 with monthly values of rainfall and PPET in the grid spacing of about 25 km over Australia by the Ozclim. Relevant conversions are performed to estimate AAET from PPET, as will be discussed in Chapter 7.

In addition to the areal extent of the site, the scale of observation and the scale of the required information need to be assessed in order to achieve the highest quality result. Therefore, the guidelines for varied observation scale and working scale are reviewed. After considering the key issues of the research and application of the scaling technique to the available data, an appropriate modelling framework has been developed. The scale issue is introduced here at a fundamental level. The concepts of catchment heterogeneity and representative elementary area (REA) are introduced here to provide an adequate scientific basis of the modelling approach.

To model the catchment recharge in heterogeneous systems, the spatial pattern of the variation is obtained in two ways. First, the catchment is divided into land units in which recharge can be expected to respond similarly to climate (disaggregation recharge modelling). Second, the individual controls on recharge are independently distributed and

serve as input for spatially explicit water balance model yielding recharge (distributed parameter recharge modelling) (Hatton 1998). The schematic representation of a typical heterogeneous and anisotropic groundwater flow system is illustrated in Figure 5.2.

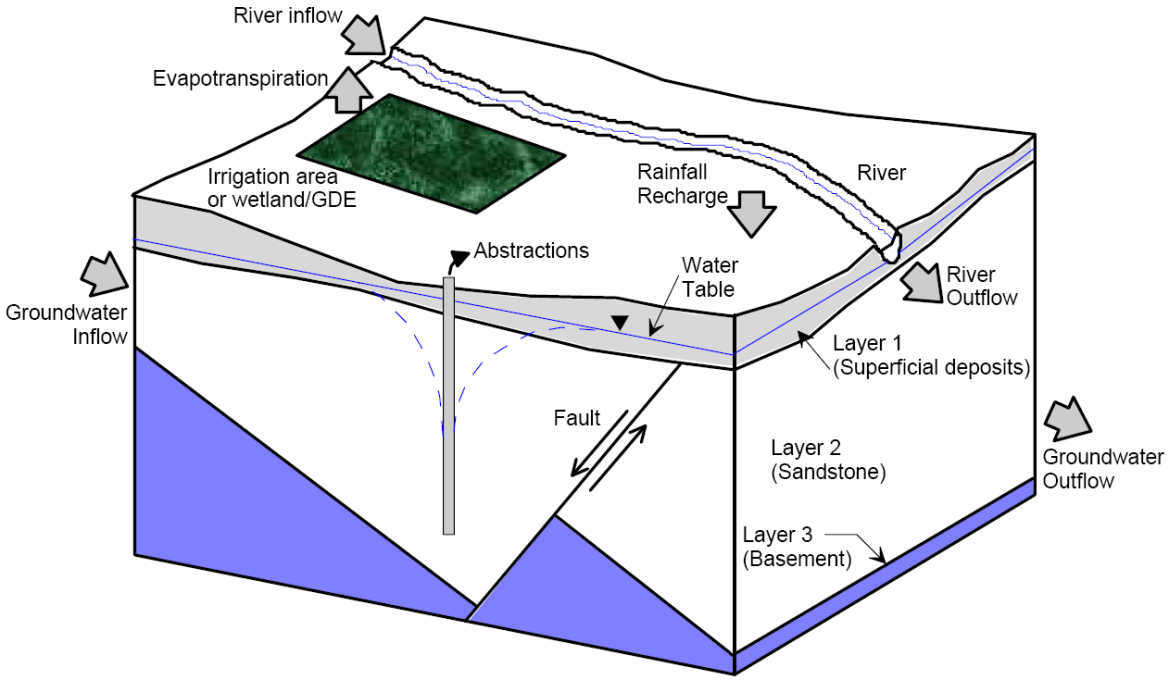

Figure 5.2 The complex system of groundwater flow in a typical three-dimensional multilayered groundwater model (Middlemis et al. 2001)

Both approaches are selected for the project site during the investigation. The land units are primarily partitioned based on the existence of groundwater divides, then subdivided based on the availability of groundwater level data and geology. In this case, the controls of recharge consist of rainfall and evapotranspiration. These two flow processes are combined as net flux to the system. The remaining lateral flow components such as surface runoff and lateral subsurface flow have been analysed with historical data and measured soil hydraulic properties. The surface runoff is included in estimated evapotranspiration and lateral flow is so small it is negligible.

5.1.1. Variability in Hydrologic Processes

Ideally, processes should be observed at the scale they occur. Often, the interest lies in large-scale processes while only small-scale point samples are available and *vice versa*. In addition, hydrological processes operate simultaneously at a range of scales (Bloschl and Sivapalan 1995).

From the guidelines of the spatial scale of hydrologic models, as provided by Refsgaard (2001) in Table 5.1, the site area under consideration falls in the boundary between catchment scale and field of hill slope scale. In the field of hill slope scale, the runoff is accumulated at different locations of its pathway in the proportion of the respective catchment areas, if the steady state situation exists along the pathway. For the point scale, hill slope scale and catchment scale, the water balance equations could be simplified as demonstrated in Equations 5.1, 5.2 and 5.3:

Rain – Runoff – ET = Infiltration (Point scale) Equation 5.1

Rain – Δ Runoff – ET = Infiltration (Hill slope scale) Equation 5.2

Rain – ET = Infiltration (Catchment scale) Equation 5.3

This simplification is also supported by Sivapalan and Kalma (1995). Therefore, the catchment scale equation is acceptable for the site and this simplification is supported by real time data of the site as is detailed in later sections of this chapter.

Table 5.1 Definition of spatial hydrological modelling scales (Refsgaard 2001; Scanlon *et al.* 2002)

Spatial scale	Characteristics	
	Length	Area
Point scale	<10 cm (Refsgaard 2001), <100 cm (Scanlon *et al.* 2002)	
Field of hill slope scale	100 m	
Catchment scale	3–100 km	$10–10^4$ km^2
Regional scale	100–1000 km	$10^4–10^6$ km^2
Continental or global scale	>1000 km	$>10^6$ km^2

Other classifications of the areal scale have been suggested by Dooge (1995), Henderson-Sellers et al. (1995) and Becker (1995), as shown in Table 5.2. The values correspond to the REA of the catchment as used by Wood et al. (1988) .

The modelling or working scale, which is agreed upon by the scientific community in context to the relevant processes and application, as suggested by Dooge (1982; 1986) might not necessarily be the same as the observation scale. For example, typical spatial modelling scales are the local (1 m), the hill slope (reach) (100 m), the catchment (10 km) and the regional (1000 km). Similarly, in terms of time, typical modelling scales are the event (1 day), the seasonal (1 year) and the long-term (100 years).

Table 5.2 Classification of scales of models as used by hydrologists and meteorologists

Investigator	Scales with the related scientists and subjects of consideration			
J. C. I. Dooge	Particle Scale (10^{-6}–10^{-3}) m	Pedon Scale (10^{-2}–10^{0}) m	Field Scale (10^{3}-)m	
A. Henderson-Sellers and others	Particle scale 10^{-5} km	Pedon scale 10^{-2} km	Microscale (1–5) km	Micromet/hydro Pedologists
			Mesoscale (10–50) km	Hydrologists
			Macroscale (100–500) km	Meteorologists and Global Modellers
A. Becker	Microscale (≤10) m			Patches, ecotopes, single plant, soil columns, pedons, single leave
	Mesoscale-γ (1-5) km			
	Mesoscale-β (3-30) km			Heterogeneous landscapes, biomes, complex river basins, planetary boundary layer
	Mesoscale-α (30-1000) km			Regional climate, single GCM grid
	Macroscale (>100) km			Global atmospheric circulations models (GCMs)

Sivapalan and Kalma (1995) indicate that for smaller basins, the response is mainly related to basin characteristics; for larger basins, the response is related to precipitation. It will be

demonstrated later that as the site area is large enough in relation to the REA of the catchment, it is reasonable to represent the climatic flux for long-term impact analyses of groundwater for the site by the records of the Jabiru East weather station. The catchment heterogeneity of both surface water (for catchment morphology) and groundwater (for hydro-geologic configuration) are important for the present research. The following sections explain the practical considerations based on which the downscaling of data has been performed with due consideration to catchment heterogeneity.

5.1.2. Surface Water Context of Heterogeneity

Surface water context relates to the data availability of flow components of water through and along the ground surface. The two factors that need to be considered for appropriate analyses of the flow components, are:

- The spatial variability of hydrological processes such as rainfall, runoff and evapotranspiration; and
- The availability of measuring stations in context with space and time.

Deen (1983a) has demonstrated that rainfall patterns in the ARR are characterised by intense, highly localised rainfall events. Heavy rainfall only occurs over larger areas, such as tropical cyclonic storms that cause high flood flows. The study was conducted on a reasonably dense network of rain gauges and the time scale was a few years only. However, for long-term predictive analyses, a larger resolution of space and time is more appropriate.

The spatial variability of the rainfall and evapotranspiration in the tropical region of Australia appears to be smaller with respect to monthly averages and total annual values. The entire coastal belt spanning hundreds of kilometres is in the same range. The variability of rainfall data in the region is described by Chiew and Wang (1999). For the purpose of the development of the hydrologic model in which the runoff data is also needed, the period is confined to start from 1980 because minimal records of runoff estimates are available before that time.

Relatively sparsely located stations in the surrounding area (especially to the south-east) of the Magela catchment confine the study to the Jabiru East weather data. Therefore, rainfall and evapotranspiration are sourced from Jabiru East Airport weather station for a historical record, as stated in Chapter 3. It may be mentioned that the Jabiru East Airport weather station commenced operation in 1973 and SILO data for this region for the period before

1973 is estimated from the other existing stations such as Darwin, Oenpelli, Pine Creek and Katherine.

The project site area under consideration is a sub-catchment of a bigger natural catchment. The area of the sub-catchment is 78.6 km^2 surrounded by a natural catchment area of 600 km^2. The Ranger mine site area is bigger than the REA (Wood 1995) for a natural catchment. The REA of the catchment is in the range of 5–10 km^2 according to Wood (1995) and 1 km^2 according to Wood et al. (1988). Therefore, the hydrological processes can be adequately represented by the statistical values such as monthly averages. Hence, simple downscaling is the only option to bridge the gap between observation and working scale.

5.1.3. Groundwater Context of Heterogeneity

Groundwater context relates to the data availability of groundwater levels in the shallow, unconfined soil layer in the site. The historical time span of the record is the same as that of the surface water context (as far back as 1980). The heterogeneity of the groundwater system has been addressed by considering a number of bores located at different geologic configurations and nearby structural features of the Ranger mine project.

The modelling scale is usually much larger or smaller than the observation scale. To bridge the gap, a combination of an upward and downward approach is required. For example, van Geer and Zuur (1997) use 24 wells in an area of 6 km by 10 km, in which they use spatial interpolation for regional analyses, and 21 bores are considered in an area of 3km by 3.5 km. The detailed information about the bores and their groundwater level data are analysed in the Chapter 3.

The REA for fractured aquifer as found by the investigators appears to be in the range of 200 to 300 m, as indicated by Wellman and Poeter (2005). However, for an unconfined, shallow aquifer, the groundwater system is essentially one-dimensional and the response of groundwater levels is mostly influenced by the unsaturated depth of the soil layer. The locations of the bores selected are about 1 to 3 km apart and the relatively unimpacted bores show a similar pattern of annual fluctuation. Hence, the result of each of the bores should be considered as a representation of the ongoing system.

A moderate upscaling is used while performing the physical process-based analysis by using the bore GWLs and hydraulic conductivity to represent the surrounding value. Moreover, with regard to the impact analysis in the regional scale, the adequate number of replicates should be critically considered, while the accuracy of each of the simulations could be a secondarily important issue. Thus, the careful upscaling and regionalisation in the interpretation of the results will be necessary.

5.1.4. Selection of the Time Step

The observation scale of the available climate data is daily for the time scale and 50 to 100 km for spatial distances. The justification of representing climate by the data of one single weather station (Jabiru East Airport), which is relatively nearby to the site in relation to the spatial distances of the available stations is detailed in Sections 3.5.1. and 3.6.4.

At a given location on the Earth's surface, climatic processes vary from one season to another. These changes across seasons are largely dependent on the rotation of the Earth about the sun, along with the accompanying changes in the tilt of the Earth's axis. In other words, the geographical location determines the hydrological process at annual time scales (Hipel and McLeod 1994). Therefore, for the purpose of the long-term prediction of the processes, the seasonal hydrological data with monthly intervals are used as the time series.

Hipel et al. (1977), Vecchia (1985), Tankersley and Graham (1993; 1994), Xu (1999), Arnell and Reynard (2000), Von Asmuth et al. (2002), Grigor'ev and Trapenznikov (2002) are examples of the investigations based on a monthly time step of climate variables. The lumping of daily climate data into monthly totals is a well-established practice in long-term predictive studies. Robins et al. (2002), Rajasooriyar et al. (2002), Kirk and Herbert (2002), Lubczynski (2006), Mackay et al. (2006), Morabito et al. (2006), Tang et al. (2006), Somura et al. (2006) and Prasad et al. (2006) use a monthly time step in modelling the sustainability of the environment and ecosystem. To represent the periodicity in the yearly climate and stream flow, Mondal and Wasimi (2005; 2006) developed a specific type of time series model based on each of the twelve months. Bidwell and Morgan (2002) use the lumped monthly time series from daily data in a study area of 2000 km^2. The lumping of daily data to monthly values is thus a reasonable modification for predicting the centurial time scale behaviour.

The primary purpose of the present research is to obtain the understanding of groundwater-climate relationships. Climate is represented in terms of water flow to the GW system by rainfall and AAET. The variability of AAET is subject to the natural availability of water in the soil-water system. The availability of water in the soil-water system is dependent on rainfall. Therefore, the climatic variable as a net flux for developing a physically-based model is a reasonable representation of the system in terms of the natural variability.

The representation of net flux of water entering or leaving the soil water system is thereby indicated by the algebraic summation of rainfall and AAET. The subsurface lateral flow is negligible as indicated in Section 5.2.2 and surface runoff components are taken care of by the soil moisture available for dry season AAET, which is detailed in Section 5.2.3, while analysing two sources of AAET variables.

5.2. Hydrologic Processes

The representation of the hydrologic processes by an appropriate model largely depends on the determination of the significant flow components in the soil-water system. To determine the flow, some variables are measured and others are estimated. The measured variables such as rainfall, pan evaporation, runoff, and groundwater are relatively easy to quantify while the estimated variables such as evapotranspiration are subject to more complexity.

There have been some studies focusing on quantifying and modelling the seasonal groundwater recharge processes in the northern Kakadu region. A climatically-based water balance-depletion model for the Magela Creek catchment was developed by Vardavas (1993). The main process considered was the seasonal variation of the water table as a function of infiltration and evapotranspiration. A review of mine rehabilitation with regards to long-term infiltration to groundwater was performed by Woods (1994). This was largely conceptual and contained no modelling of the links between climate and groundwater recharge. At the Ranger mine, some field and modelling studies have been conducted to date on the hydrogeology, largely related to tailings management (Whitehead 1980; Ahmad and Green 1986; Salama et al. 1993; Salama and Foley 1997; Salama et al. 1998). There is evidence that the site does have a preferential component of groundwater flow (Brown et al. 1998). Collectively, these studies have demonstrated the importance of

local geological features as preferential flow paths, fault zones, high permeability weathered zones and fractured rocks (though not all fracture zones are permeable).

In general, the studies have shown the complexity of the system, especially with regard to geologic faults and the depth of weathering. There are also strong links between surface water systems and groundwater, dependent on topography and localised geology as shown in Figure 5.3.

The topsoil is the unconfined layer and GWL fluctuates annually within this layer. The lithology data of the bores were also analysed and the complex geology along the depths of all 21 bores are listed in Appendix D. However, the topsoil cover at the top of weathered rocks and/or fractured rocks was identified as being the same. Therefore, the topsoil cover is presented as an unconfined aquifer system with GWL fluctuating within that layer.

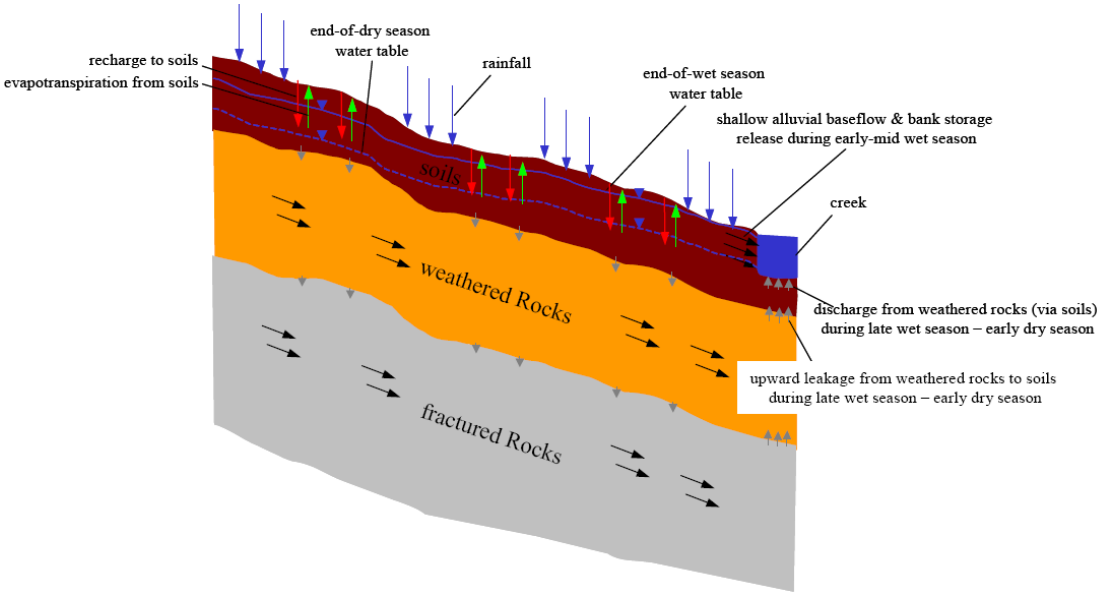

Figure 5.3 A recently developed hydrogeological model of the site (Pillai 2005)

Hatton et al. (1995) have demonstrated that a one-dimensional lumped model such as the vertical Soil-Vegetation-Atmosphere-Transfer schemes (SVATs) may not be adequately representative when lateral transport of water by overland or subsurface flow occurs. Becker (1995) has added that for catchments with complex sloping terrains and groundwater tables, a vertical domain like SVAT has to be coupled with either a process or a statistically-based scheme that incorporates lateral transfer (Feddes 1995b). However, Zhang et al. (1996) argue that the soil-water balance of many Australian land systems does not have to be treated with a fully three-dimensional model but may be approximated with

a one-dimensional treatment. Jimenez-Martinez et al. (2009) have used one-dimensional modelling for estimating recharge from irrigated areas in south-east Spain using HYDRUS-1D (Simunek *et al.* 2005) software, which simulates water, heat and solute movement in variably saturated porous media. It can be noticed that HYDRUS-2D (Simunek *et al.* 1996) software, which is a two-dimensional model, was not used as a one-dimensional model seemed more appropriate.

It should be considered that the best choice for a particular situation for recharge estimation depends upon the spatial and temporal scales being considered and the intended application of the recharge estimate (Scanlon *et al.* 2002). Sequential description of the measurement and estimates of the various hydrologic processes starting from rainfall, runoff to lateral subsurface flow and evapotranspiration are provided here. A one-dimensional vertical flow system is proposed for consideration after the scientific judgement.

5.2.1. Measurement of Rainfall and Runoff

The rainfall values are measured in the Jabiru East weather station BoM 14198 and runoff is measured at gauge station GS821009. The measuring sites were described in Chapter 3. The annual average rainfall and runoff from 1980 to 2005 was 1498 mm and 514 mm respectively. A representation of the average monthly flow components is provided in Figure 5.4. The annual average of observed runoff at station GS821009 from 1980 to 2005 was 514 mm, and from 1972 to 2002 was 595 mm. The result reported by Vardavas (1988) for long-term average runoff is 696 mm for the same catchment.

Data analysis shows the average monthly runoff in the station is of significant value during December, January, February, March and April. This occurs one month later than the wet months, as the typical start to the wet season is November. This one-month delay may represent the time of travel for the runoff from the points of initiation to the measuring location. The catchment area considered is 600 km^2, situated in a south-east direction from the Magela Creek gauging station GS821009. Vardavas (1989) has also reported that Magela Creek begins to flow a month after the commencement of the wet season and flow ceases by the end of April. He analysed the data of twelve continuous years from 1974 to 1986 for the water budget of Magela flood plain. This one-month lag is common to both

the previous study with a shorter record length and the present study with a longer record length.

Estimation of runoff coefficient: A runoff coefficient is the fraction of rainfall that becomes runoff; the value of the coefficient is 0.34 (514/1498 = 0.34). This runoff coefficient is greater than 0.25 as suggested by Hart et al. (1987b). However, the study conducted by Vardavas (1988) shows a four-year average measured value of 0.34, modelled value of 0.39 and fifteen-year average measured value of 0.44. The AWBM computed value is also 0.39, which will be demonstrated later. Hence, the estimated runoff coefficient is comparable with these other investigations. The spatio-temporal variability of runoff coefficients is recognised by many investigators at various scales of time and catchment size (Merz *et al.* 2006; Merz and Bloschl 2009; Merz *et al.* 2009). However, Merz et al. (2009) have shown that data analyses for a 5-year duration is adequate to capture the hydrological variability of the processes in any specific catchment. Therefore, the data analysed in this study can be assumed adequate in sample size.

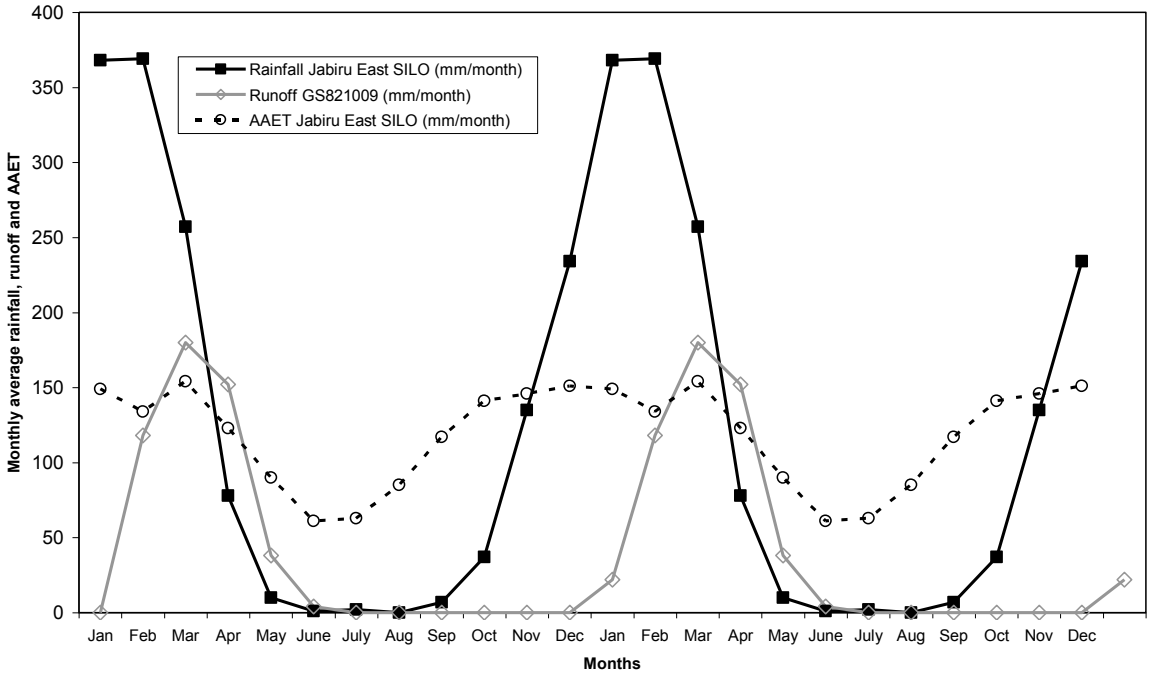

Figure 5.4 Average monthly rainfall, runoff and evapotranspiration (mm/month)

5.2.2. Estimation of Lateral Subsurface Flow (1 D Model)

In order to achieve a better understanding of the processes, an appreciation and understanding of scaling hydrologic parameters is essential. However, Beven (1995)

argued that it is unlikely any general scaling theory could be developed because of the dependence of hydrological systems on historic and geological perturbations (Hatton 1998). Therefore, site-specific insight is important for the best conceptualisation of the particular catchment's behaviour.

During September 1986, Water Treatment Land Application (WTLA) was occurring while a number of field investigations were conducted relating to the rate of flow or drainage capability of the site soil. In the present work, some of those field data has been used to compute the probable horizontal flow in the subsurface region. The rate of water entering from irrigation was 10 mm/day (Mc Quade 1991). Assuming an effective porosity of 10%, a seepage velocity of 0.1 m/day was obtained.

The flow along the five directions has been considered, generating from a relatively upper-elevated well to lower wells, as found in Willett et al. (1991) and Chartres et al. (1991). While considering the flow from well MC32 to the other five wells, MC21, MC23, MC28, MC15 and MC33 (see Figure 5.5), a variation of flow velocities from 0.001 to 0.014 m/day was discovered (see Table 5.3). Based on Dupuit's assumption of flow through unconfined aquifers, the flow velocities are estimated and found to be overestimated for higher gradient paths as it is more likely deviate from horizontal paths (Todd 1980).

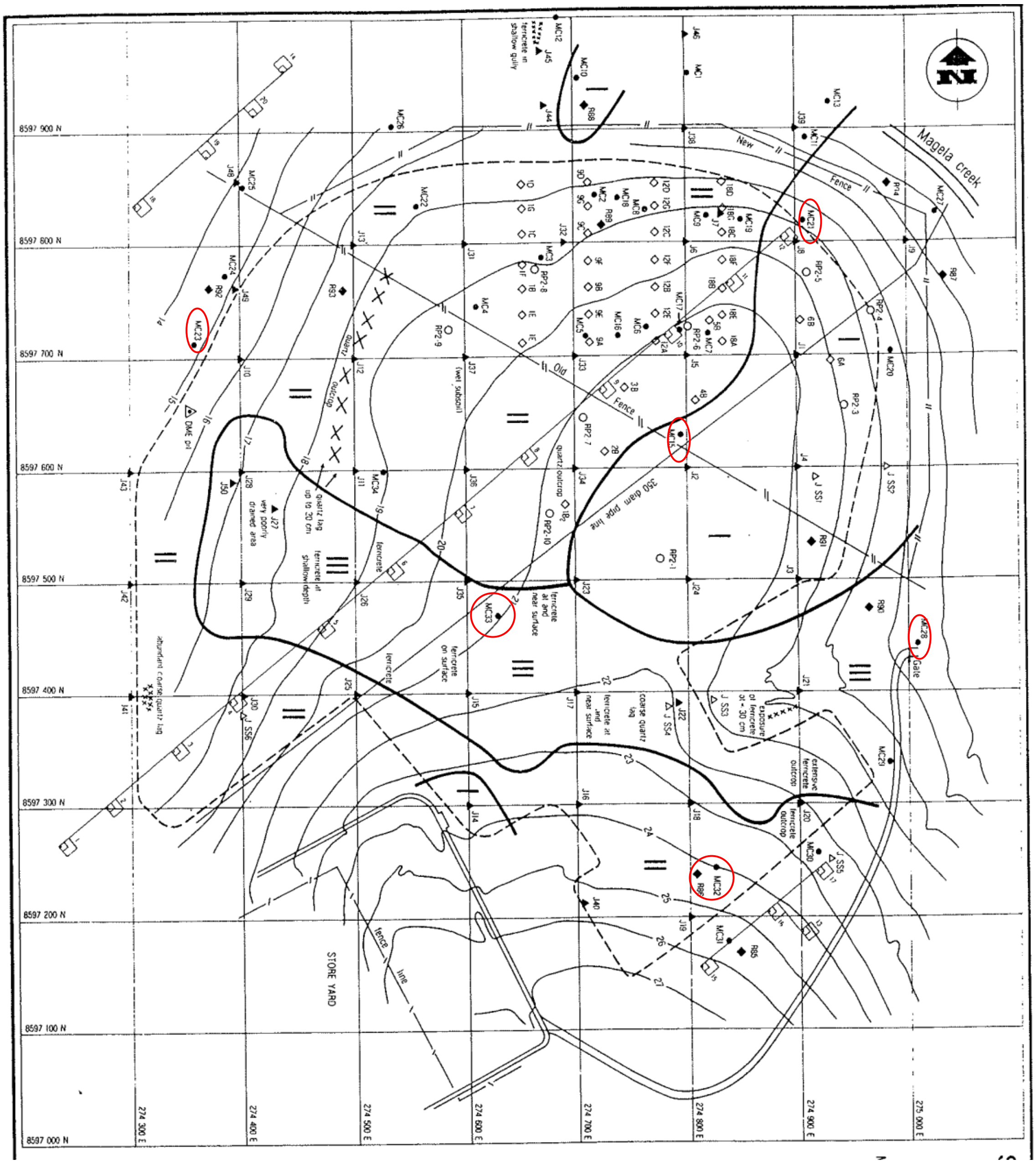

Figure 5.5 The location of the wells with the contour levels as used for horizontal flow computations

Table 5.3 Computation of horizontal flow in WTLA during September 1986 (Chartres *et al.* 1991).

Mapping Unit	Test well no.	Ground surface elevation (m AHD)	Well depth (m)	Static water level (m below ground surface)	Elevation of static water level (m)	Horizontal Hydraulic Conductivity (m/day)	Distance between MC32 and the well considered (m)	Average hydraulic conductivity (m/day)	Hydraulic Gradient	Velocity of flow (m/day)
Col (I)	Col (II)	Col (III)	Col (IV)	Col (V)	Col (III) – Col (V) = H_d	K_d *	L	$K_{avg} = (K_o + K_d)/2$	$(H_o - H_d)/L$	$V = K_{avg} \times (H_o - H_d)/L$
I	MC21$_d$	19	4	0.8	18.2	0.55[a] - 0.69[b]	600	0.46	0.005833	0.00268
II	MC23$_d$	15	3.9	1	14	0.90[a] - 1.75[b]	675	0.8125	0.011407	0.009268
II	**MC32$_o$**	**24**	**3.6**	**2.3**	**H_o = 21.7**	**K_o = 0.3[b]**				
III	MC28$_d$	17.5	4.1	1.7	15.8	1.02[b]	275	0.66	0.021455	**0.01416**
I	MC15$_d$	21.4	3	1.2	20.2	0.72[a] - 0.38[b]	400	**0.425**	0.00375	**0.001594**
III	MC33$_d$	21	3.1	0.5	20.5	2.40[a] – 4[b]	300	1.75	0.004	0.007

o = origin well for lateral flow

d = destination well for lateral flow

a = data source (Mc Quade 1991)

b = data source (Chartres *et al.* 1991)

* = for computation of K_d equal weighages were used (average) for the data, which have both sources, Mc Quade and Chartres et al.

Along the paths of higher hydraulic gradient (such as along MC32 to MC28 or MC23), the flow velocity (0.014, 0.009 m/day) is approximately 10% of incoming flow in a vertical direction. The hydraulic gradient is higher because of two reasons. First, the topography, which is sharper slope along MC32 to MC28. Second, the existence of preferential flow (Brown et al. 1998) along other paths, such as MC32 to MC15 or MC33, causes the difference in hydraulic head to be comparatively less. Therefore, the land slope and soil property act in similar ways to cause a non-uniform horizontal flow of water in the unconfined aquifer. The minimum hydraulic gradient (MC32 to MC15) gives the minimum flow velocity of 0.00159 m/day, which is 1% of incoming flow in the vertical direction.

The distribution of K values was found to range over two orders of magnitude in the 29 bores tested during September 1986. If a sample of data is determined to come from a log-normally distributed population, the geometric mean and the geometric standard deviation may be used to estimate confidence intervals akin to the way the arithmetic mean and standard deviation are used to estimate confidence intervals for a normally distributed sample of data (Hull 2005). The geometric mean value of hydraulic parameter yields the estimation of drawdown such that the estimated values are in the middle of the range indicated by arithmetic mean and harmonic mean value of the same hydraulic property (Morel-Seytoux 2001). Hence, the geometric mean value was found to be 0.38 m/day (Chartres *et al.* 1991). This value is nearest to that of the MC15 bore (0.425). Thus, it is assumed that bore MC15 represents the WTLA in terms of horizontal flow.

On a catchment scale basis, this horizontal flow velocity can be computed for other locations such as between OB41 and OB43. From observing the topography and GWL charts, as illustrated in Figure 5.6, it can be found that there exists very little hydraulic gradient between these two points, as the difference in groundwater levels of the two bores at a particular time is as small as 0.1 to 0.2 m. This indicates a very small hydraulic gradient and thus very small horizontal flow. Therefore, the similar heights of groundwater levels in both bores indicate negligible lateral flow of subsurface water. Conversely, the annual change of groundwater levels in these bores varies between 2 to 3 m. This indicates the existence of significant vertical flow. Therefore, the lateral flows in the unconfined aquifer vary in the range of 1 to 10 % of vertical flow. Thus, the one-dimensional vertical flow model is a valid representation of the system. In the next section, the selection of

AAET data source is elaborated since there are multiple sources of AAET data, such as SILO daily data and long-term average monthly AAET map data of BoM.

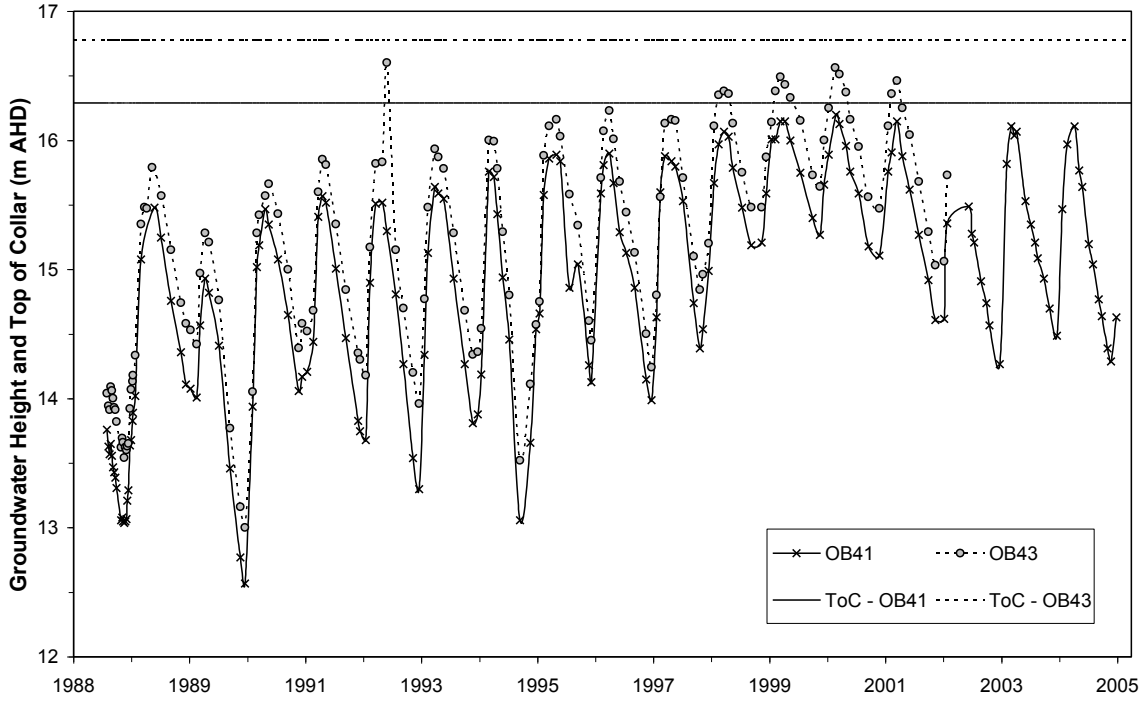

Figure 5.6 The variation of measured GWLs of OB41very similar to that of OB43

5.2.3. Estimation of Evapotranspiration

The estimation of evapotranspiration becomes especially important where the region is subjected to sharp variation of climatic conditions such as temperature, humidity, wind speed and solar radiation with respect to space and time. For given climatic conditions, the basic rate is the reference crop evapotranspiration (Doorenbos and Pruitt 1977; Chow et al. 1988), which is multiplied by crop coefficient and soil coefficient to account for type of vegetation and soil (Chow et al. 1988). However, if pan evaporation data is available, estimates of evapotranspiration can be made using pan factor (Chiew and Wang 1999; Tindall and Kunkel 1999).

It should be mentioned that the use of pan factors and crop factors for the estimation of evaporation and transpiration have been replaced by the estimated AAET of Morton (Morton 1983) as available in SILO (2006) and Chiew et al. (2002). The appropriate evapotranspiration variable (AAET) presented in Sections 2.1.2 and 2.1.3, and the selection of an appropriate source of AAET (SILO) presented in this section have been discussed in detail.

There are two sources of AAET data available for Australia: SILO AAET daily data and the evapotranspiration map of Australia . The applicability of the two sources are carefully judged as available for Jabiru Airport weather station of BoM, in order to select the best AAET estimate for the specific method of investigation. For these analyses, the numerical values of average annual AAET from the two sources are compared. Another source of evapotranspiration estimates conducted by Hutley et al. (2000) are reviewed in this study since the evapotranspiration coefficients are based on measured values in the tropical region of Australia, located at Howard Spring near Darwin. The evaporation from the storage in the Jabiluka site was investigated by Chiew and Wang (1999) and those values are included here for a relative comparison.

After comparing the numerical values of these estimates, some additional analyses are performed considering monitored GWLs to examine the capability of these estimates to explain the water balance of the region at a daily time scale and a multi-decadal time scale. Based on these analyses, the best source of evapotranspiration estimates is selected for further analyses.

Estimated historical AAET data by SILO: For the purpose of estimating historical AAET data in any catchment in Australia, PPD data (SILO 2006) are developed by the Queensland Department of Natural Resources and Water, which is available via the Internet (Ladson 2008; SILO 2009). This dataset provides daily values for 4650 meteorological stations in Australia starting from January 1889. The estimation of AAET, as provided in 2006 by SILO, is based on Morton (1983).

The detailed steps of estimation of AAET as followed by SILO are also described in Appendix A. The vegetation of the site consists mainly of open woodland. Therefore, the regional evapotranspiration could be represented adequately by AAET. The representation of the evapotranspiration process by AAET as an outgoing component of water from the system as a time series process is the best available estimate as far as the long-term analyses of the groundwater-climate relationship are concerned. This is because the estimation of AAET by SILO considered a number of data quality checks as described in Jeffrey et al. (2001).

The historical data starting from January 1889 demonstrated a discontinuity of records in terms of time and location. This missing data have been interpolated with sufficient accuracy (Jeffrey et al. 2001). From 1957, with the availability of an increased number of neighbouring stations, the interpolated values were of better quality. Jeffrey et al. (2001) describe the detailed interpolation technique that was followed during construction of the long historical climate data of Australia. They performed some very important and relevant checks with the interpolated data to ensure the quality of the synthetic data. For example, they used a thin plate smoothing spline to interpolate daily climate variables. Ordinary kriging was used to interpolate daily and monthly rainfall. Independent cross-validation for a number of climate variables was performed to analyse the temporal and spatial error of the interpolated data. Maximums and minimums, systematic overestimations and underestimations, operator error and observer errors were identified at the possible locations and checked.

Estimated monthly average AAET map data by BoM: Using the duration of the World Meteorological Organisation (WMO) standard period 1961–1990, 713 stations' climate data were used to estimate long-term monthly averages of evapotranspiration variables as represented in the evapotranspiration map (Chiew *et al.* 2002) . The computations were performed by following Morton's method (Morton 1983). The locations of the stations of the BoM are illustrated in Figure 5.7. Thus, the evapotranspiration map data is a source of long-term average for the three evapotranspiration variables: AAET, PPET and APET. It is not representable as a time-series process. The map data is provided after annual water balance corrections for surface runoff have been applied to the different hydrologic catchments of Australia. Of the three evapotranspiration variables (AAET, PPET, and APET), AAET is selected for the representation of the evapotranspiration process in the system under consideration.

Figure 5.7 Locations of stations used in evapotranspiration analyses by Morton's Method (Chiew *et al.* 2002). The location of the site is indicated by 'X' in the map

Although the evapotranspiration map of Australia presented by Chiew et al. (2002) allows rapid and approximate estimates of evapotranspiration (Ladson 2008), these values are subject to error from a number of sources. The basic input data used are subject to measurement error. The estimates of AAET means are subject to sampling error due to limited record lengths. The mapping of AAET estimates is affected by the spatial coverage of the climate stations available, and by the interpolation and mapping techniques used. In addition, there is model error in deriving the AAET estimates and some degree of professional judgement in adjustments made to the estimates (Wang et al. 2002).

Site related limitation of map AAET: As to the SILO (SILO 2006) PPD of AAET for the station of Jabiru Airport (BoM station number 14198), the station did not exist during 1961. The selected 713 meteorological stations used in the basic climate data and 60 stations

used for comparing the evapotranspiration variables of the evapotranspiration map, do not include the Jabiru Airport. The surrounding region of the Top End in the NT is characterised by sparsely located stations. The stations in the northern part of the NT are sparsely located in comparison to those located in the south-east regions of Australia. Thus, the influences of local hydrological catchment characteristics contributing to the regional water balance were not taken into consideration directly. Those factors were indirectly subject to the measured basic climate data such as temperature, humidity or vapour pressure, wind speed and radiation values of the sparsely located stations. Therefore, it can be conceived as a way of covering hydrological heterogeneity under the shadow of climatic homogeneity.

For better use of this data source, Chiew et al. (2002) suggest the seasonal adjustment and water balance adjustments to the evapotranspiration map data. The requirement of the adjustments is validated by checks on the limits of AAET. With regard to the present research, the map AAET is not investigated for any detail in relation to those corrections. This is because the map AAET data are not used for analyses since the values are only long-term averages and do not constitute time-series data sources as available in SILO.

Estimated evapotranspiration by Hutley's coefficients: Estimates of evapotranspiration based on Hutley's coefficients are values calculated using the pan coefficient suggested by Hutley et al. (2000) for a site near Darwin (Howard Spring). This site is highly vegetated and near the coast along the Howard River (Cook *et al.* 1998). As detailed in Chapter 3, estimates of evapotranspiration are particularly difficult at Ranger because it is a mine site with a great deal of heterogeneity in the surface characteristics. One section of the area consists of free surface water, another is not vegetated and another is vegetated mainly with spear grass that grows up to 3 m during the wet season. Ranger is presumably a combination of these three estimates because it has a varied surface.

Figure 5.8 illustrates averages of monthly rainfall and different estimates of evapotranspiration. Two sources of evaporation data such as pan evaporation and evaporation from Jabiluka storage by Chiew and Wang (1999) are also plotted.

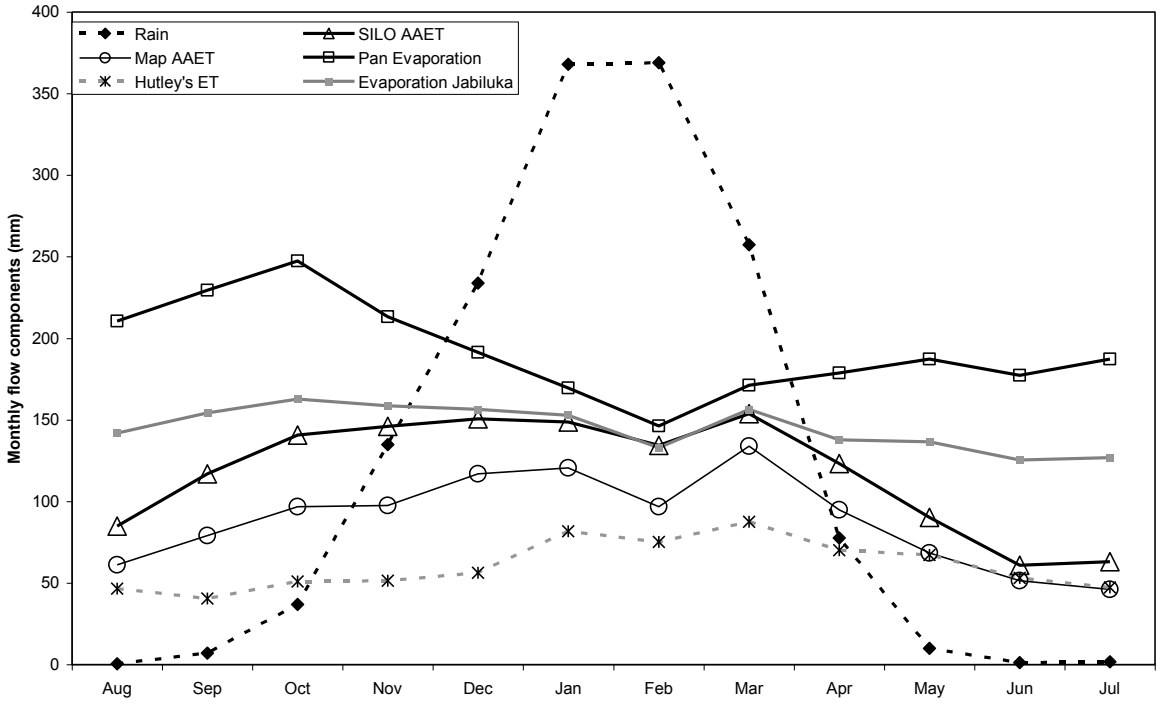

Figure 5.8 Graphs visually represent the relationship between rainfall and evapotranspiration

The three sources of evapotranspiration data are SILO AAET (SILO 2006), map AAET (Chiew *et al.* 2002), and pan evaporation combined with Hutley's coefficient (Hutley *et al.* 2000). In general, the SILO AAET values are consistently greater than map AAET and map AAET values are greater than Hutley's evapotranspiration values during most of the year, except May, June and July when the difference among the evapotranspiration sources almost diminishes.

With this preliminary comparison, the following analyses are performed to build confidence with regard to selecting the optimum source of evapotranspiration, which is SILO AAET. SILO AAET started to become available in early 2006. Recently, a number of scientific investigations (Ludwig *et al.* 2009; Wang *et al.* 2009b) based on hydro-climatic data use this SILO historical and real time daily climate data. The capability of SILO AAET data to explain the water balance of the region under consideration is also elaborated in the following sections at daily time scale, multi-decadal time scale and annual average estimates. From these analyses, the selection of SILO AAET is also established scientifically.

5.2.4. Comparison of Evapotranspiration Estimates for Water Balance

a) Daily Time Scale: A comparative analysis of evapotranspiration estimates was conducted to observe the rates of depletion of soil moisture during dry spells of the year when negligible rainfall and runoff occur. The rate of depletion of soil moisture is solely dependent on the rate of evapotranspiration from saturated and unsaturated soil.

From the various bores' GWLs, it is observed that OB1A has a record of very closely recorded data of GWLs during the dry months of 1985 (16 April 1985 to 31 October 1985). Computations are performed using the daily GWLs data and various estimates of evapotranspiration to estimate the depletion of soil moisture content in the top unsaturated zone. The GWLs data are selected for checking the performance of various evapotranspiration estimates such as Map AAET, SILO AAET and Hutley's evapotranspiration. In addition, the influence of soil storage characteristics as influenced by porosity is investigated. The influence of lateral subsurface flow is also studied in the analyses. The loss of water from unsaturated soil and saturated soil is estimated separately and added together to match with the data-based estimates of evapotranspiration losses from the various methods.

Influence of evapotranspiration estimates: For a porosity of 20%, the following results were obtained for three different estimates of evapotranspiration. The initial degree of saturation (S1) was assumed to be at field capacity of the soil and was taken to be 65%. Rainfall is assumed to be zero for the days of 16 April 1985 to 31 December 1985 (the dry season).

The degree of saturation at the end of each consecutive day (S2) of the dry season is computed according to Equation 5.4:

$$S2 = (Zu1.S1.n - ET - n(Zw2-Zw1))/n.Zu2 \qquad \text{Equation 5.4}$$

S1, S2 = degree of saturation at t1 and t2 time

Zu1, Zu2 = unsaturated depths at t1 and t2 time

Zw1, Zw2 = GWLs at t1 and t2 time

n = porosity

ET = evapotranspiration estimates by various methods.

The water losses from the unsaturated soil zone are ascertained from the difference in the degree of saturation. The water losses from the saturated soil zone are obtained from the difference in GWLs elevation during the period of 16 April 1985 to 31 October 1985. The data-based estimates are acquired through the summation of daily evapotranspiration from the three sources of data. Figure 5.9 illustrates the result of the estimates of water losses during a dry spell in 1985.

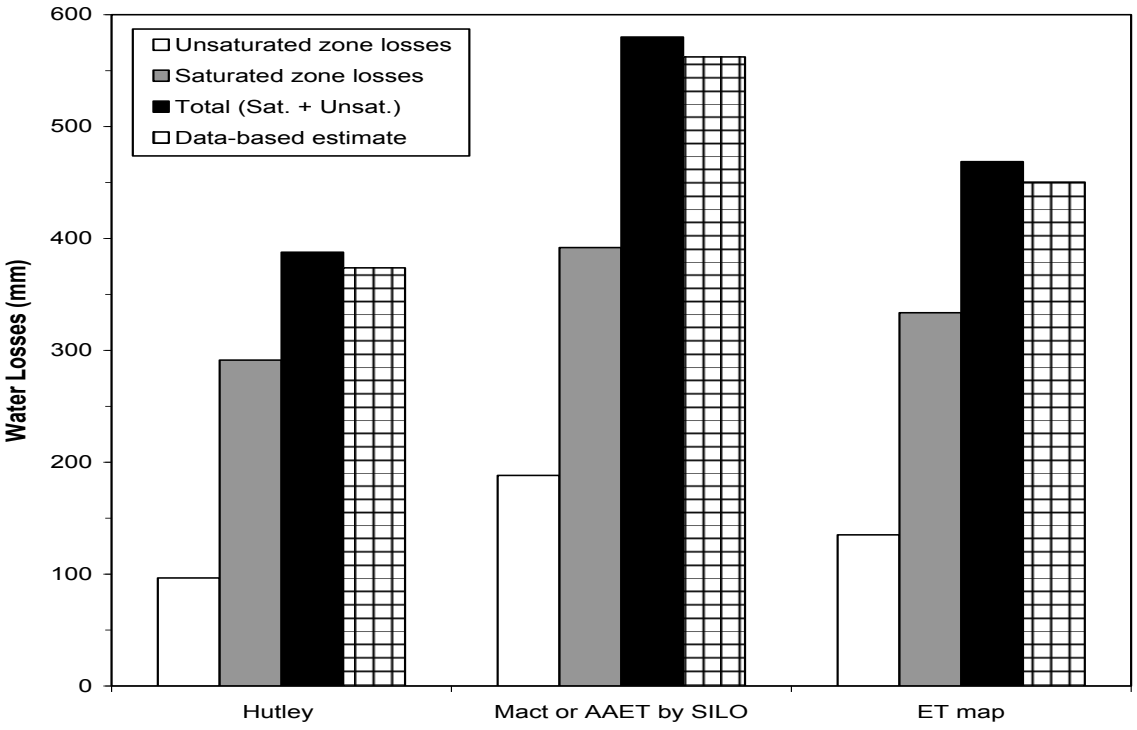

Figure 5.9 The estimations of water losses from saturated and unsaturated soil as compared with data-based estimates of evapotranspiration following Hutley's evapotranspiration, SILO and evapotranspiration map data sources for porosity

Influence of porosity: The influence of porosity was investigated for a single source of evapotranspiration data (the estimates of evapotranspiration map data) on the rate of depletion and final soil moisture content. The rate of depletion of soil moisture content is observed to be sensitive to porosity. Soil with a higher porosity is less sensitive and *vice versa*. This result is consistent with the water balance concept for the water content in the storage.

The initial degree of saturation is assumed to be 65%, which is the standard value of field capacity of silty soil. The gradual depletion of the degree of saturation is computed using Equation 5.4 and estimated on a daily time step basis. Figure 5.10 illustrates the gradual depletion of soil moisture, which is the function of a degree of saturation with time for a range of soil porosity varying from 0.3 to .05 for the map AAET data. A similar result could be obtained using SILO AAET or Hutley's evapotranspiration. However, the uncertainty with the soil property and the evapotranspiration estimates are determining factors that influence the loss of water by the evapotranspiration process and thus the GWLs.

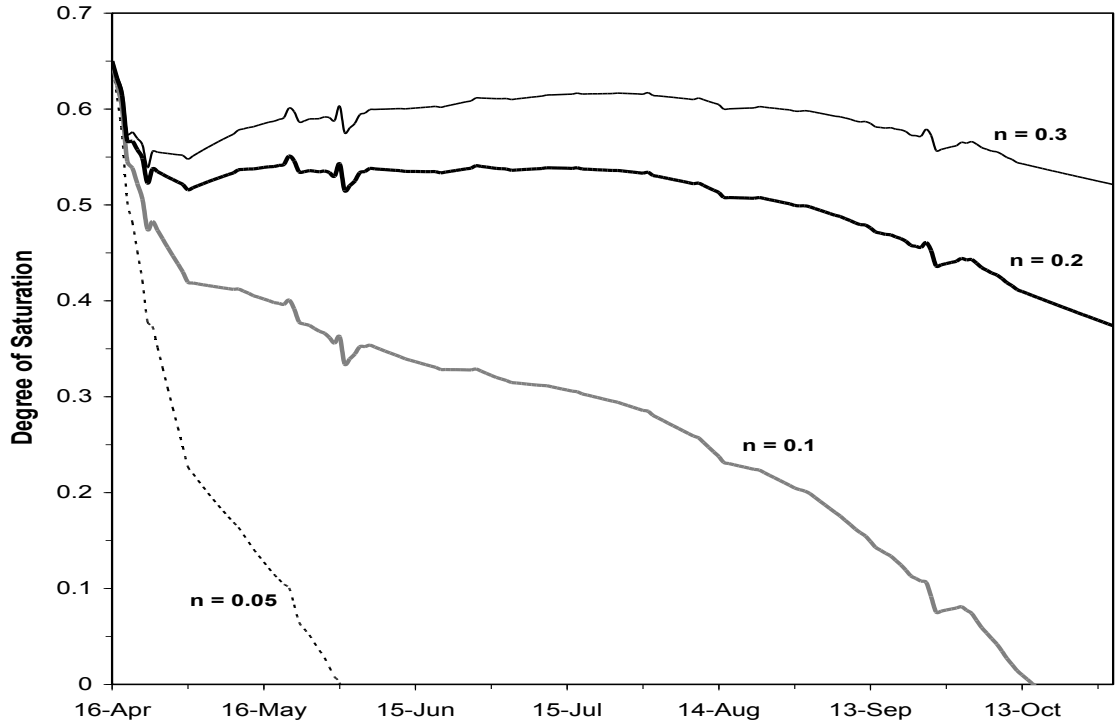

Figure 5.10 The depletion of degree of saturation as computed from map AAET data source for various values of soil porosity

Influence of lateral flow: The influence of lateral flow was investigated by varying the amount to be 5% of the vertical groundwater flow. The 5% reduction in vertical flow was considered in the water balance equation (see Equation 5.5):

$$S2 = (Zu1.S1.n - ET - n(Zw2-Zw1)\ (.95))/n.Zu2 \qquad \text{Equation 5.5}$$

The 5% was taken based on an average lateral flow of 1 to 10% of vertical flow, as was estimated in Section 5.2.2. The influence of this amount of lateral flow was found to be insignificant.

Conclusion: In relation to the selection of the best method to estimate evapotranspiration for the site situation, the SILO AAET are the largest estimates, followed by the map AAET and Hutley's estimates are the smallest. The following section compares the capability of these estimates in relation to the multi-decadal trend of groundwater level fluctuation for the region by using the analogy of average GWLs as an indication of annual water balance.

b) Multi-decadal Time Scale: This section attempts to examine the capacity of various estimates of net flux to explain the water balance of the site for multi-decadal time scale in combination with the observed groundwater levels in the relatively unimpacted bore.

The GWLs of OB20 and OB21A demonstrate a similar trend. Detailed assessment will indicate that OB21A has a more enhanced trend (increasing) than that of OB20, while OB1A has the minimum trend and is mostly stationary. These are the ranges of dissimilarity with all other bores. However, the common patterns of all these bores are a convexity, a concavity and a convexity from 1980 to 2005. Overall, there is a mildly increasing trend for this period. In addition, this pattern is selected as a gross measure of the true representation of accumulated net flux as shown in Figure 5.11. The net flux (NF) is calculated as the algebraic summation of rainfall, inflow and runoff combined with evapotranspiration as outflow. 'Accumulated' refers to summation of positive and negative net flux values, as shown in the figures below. Ferdowsian et al. (2001) use the similar concept of accumulated net flux in their study of groundwater level hydrograph as a function of rainfall.

Various estimates of runoff such as measured runoff or runoff coefficients from literature values are used in the computations. The estimates of evapotranspiration such as SILO AAET, map AAET and Hutley's evapotranspiration are used in the computations. In the first set of computations, only the extent of variation of the multi-decadal water balance for SILO AAET and Hutley's evapotranspiration are shown in Figure 5.12. The measured runoff is about 34% of rainfall. Thus, if runoff is reduced to 25% (as applicable for map data) or 5% (as comparable to SILO AAET data), Hutley's curve will be heading upwards. Therefore, Hutley's estimates are the worst to use for explaining annual water balance.

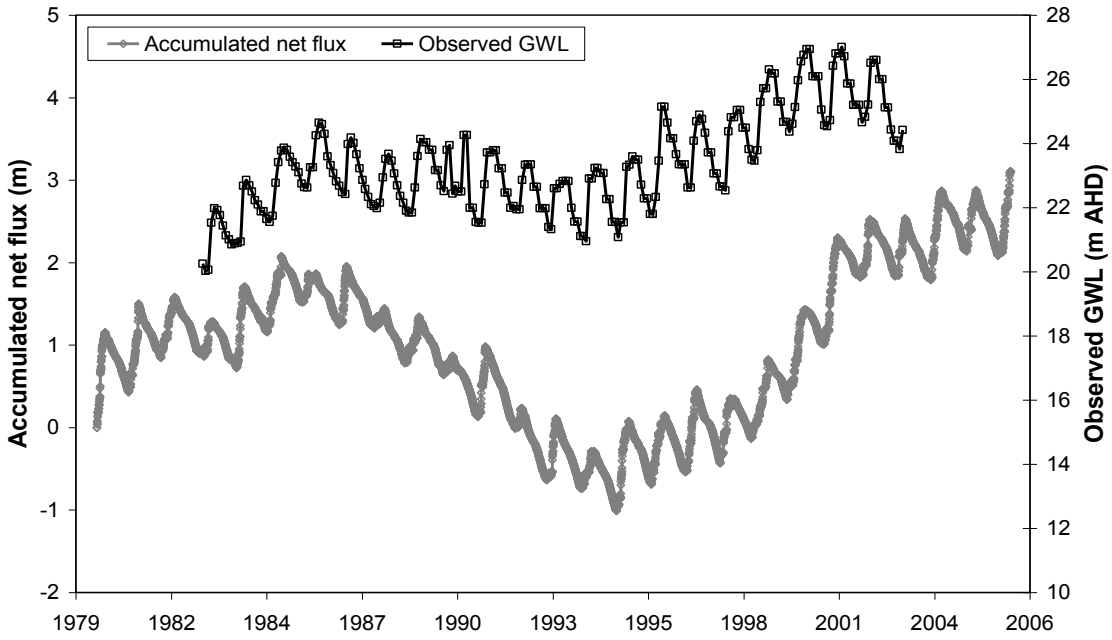

Figure 5.11 Accumulated net flux estimated based on (NF = rain – SILO AAET) compared with bore GWLs of OB21A

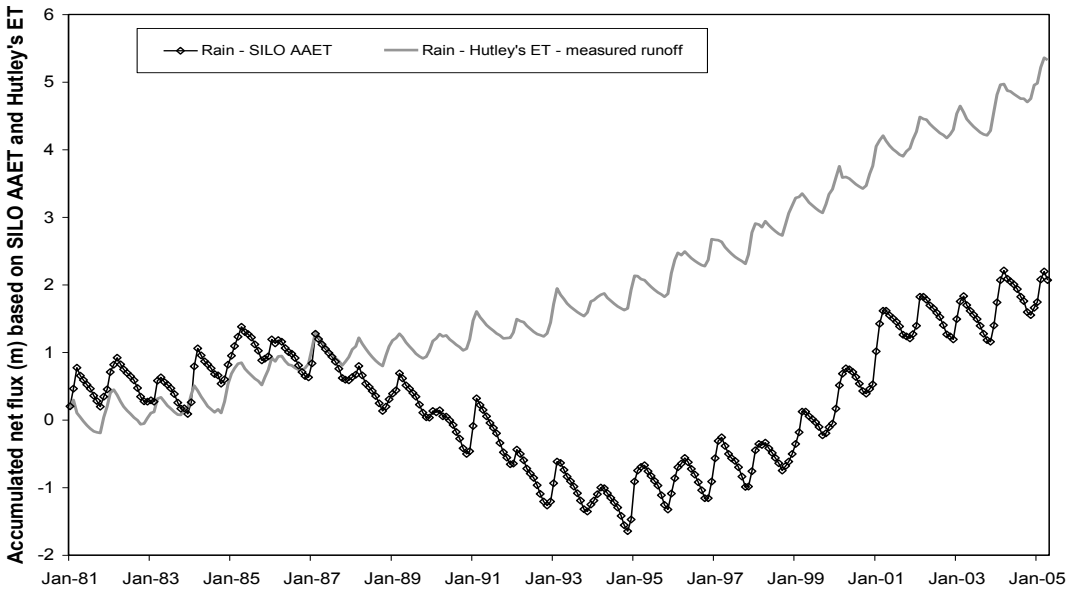

Figure 5.12 The net flux based on Hutley's pan coeff (2000) and measured runoff data (34% of average annual rainfall). NF = rain – Hutley pan coeff X pan evaporation – measured runoff

Comparison of SILO AAET and map AAET: In Figure 5.12, four sets of net flux data are computed using SILO AAET and map AAET with measured runoff data. The graphs for Rain – SILO AAET and Rain – map AAET – Runoff are better performing than the remaining two, since these are similar to the overall trend of GWLs curve as shown earlier.

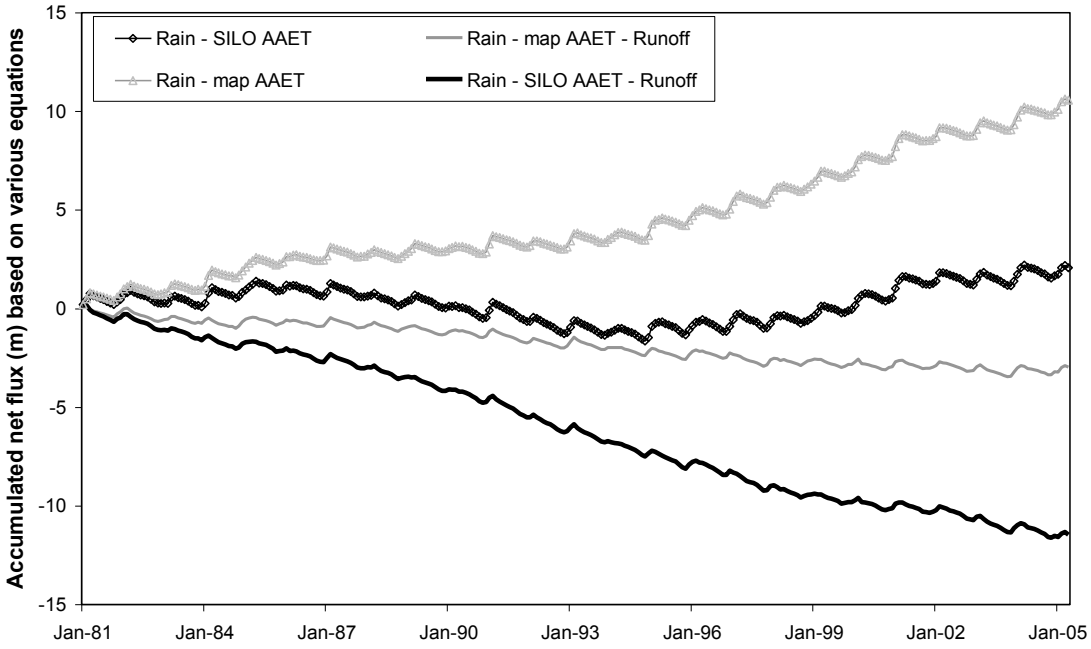

Figure 5.13 The two extreme deviations are caused by considering only map AAET (NF3) and SILO AAET with runoff (NF4). However, NF2 is comparable since it is using map AAET and runoff data

The top graph has an increasing trend while the bottom graph has a decreasing trend. Even if the runoff coefficient is considered to be 0.05, the graph of accumulated net flux using SILO AAET data deviates qualitatively from the observed GWLs. If the net flux is computed neglecting runoff while using SILO AAET data, the graph of accumulated net flux matches significantly with the observed GWLs. Therefore, neglecting runoff in the estimation of net flux is reasonable while outflow is represented by SILO AAET data.

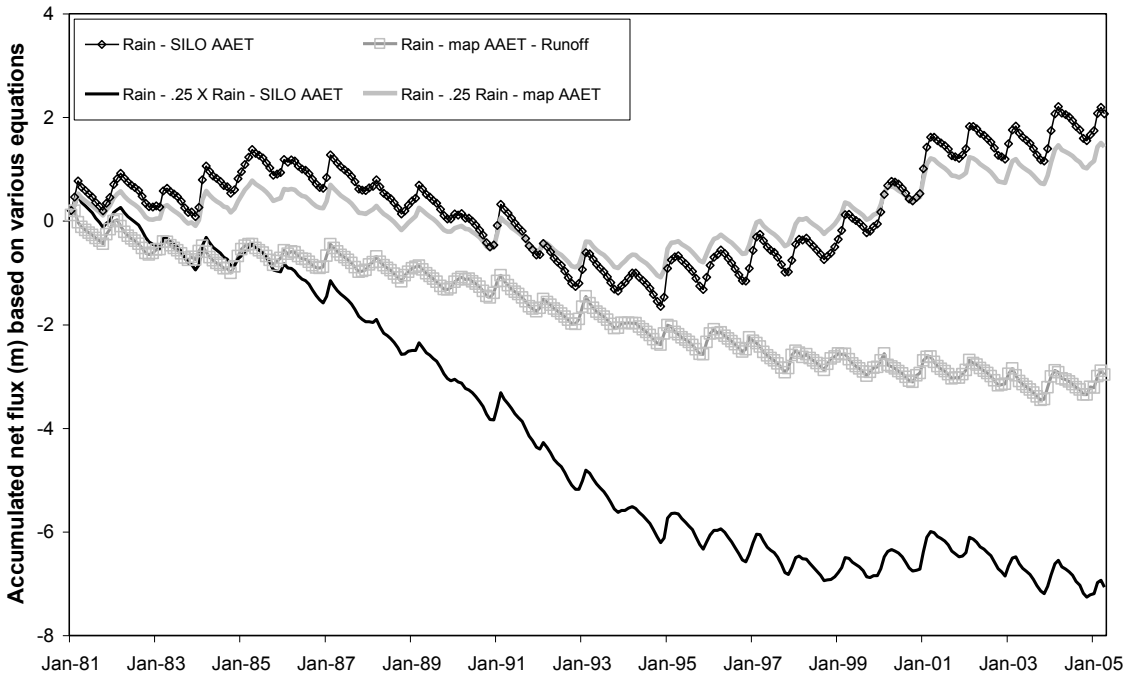

Figure 5.14 The 25% runoff coefficient represents the system reasonably while used with map AAET data and 0% to less than 5% runoff coefficient represent the system while used with SILO AAET data

However, map AAET is further investigated for better fitting by trying various runoff coefficients, as shown in Figure 5.14. The net fluxes considering two options were found to represent the system best. Those were as follows:

NF_{SILO} = rainfall – SILO AAET

NF_{map} = rainfall – map AAET - 0.25 X rainfall (as runoff).

NF_{SILO} was better than NF_{map} for the following reasons:

1. NF_{SILO} reasonably explains the annual water balance. The future data of AAET can be obtained from the future data of PPET. In contrast, map AAET is not a time-series data source; it is an estimate of long-term average. NF_{SILO} would be preferable than NF_{map} for the predictive study of the system at the centurial time scale.

2. The limitation of using runoff coefficient in estimating net flux is that it can underestimate the net flux during the start of the rainfall event/season. This is because no runoff is generated when the intensity of rainfall is less than soil

infiltration capacity, or when runoff is stuck in the soil moisture on its way to remove the catchment due to lowered GWLs and existence of soil moisture storage. Conversely, it can overestimate the net flux when the GWLs are at the surface of the soil. In reality, more runoff is leaving the system than the percentage of runoff coefficient. However, on average these effects neutralise each other over the long-term. Therefore, for the purpose of the long-term impact study of groundwater levels in the site, the NF_{SILO} is preferred over NF_{map}.

3. In the figure for the accumulated net flux estimations based on NF_{SILO} and NF_{map}, the relative fluctuation is more for NF_{SILO} than NF_{map}. The selection of net flux should be based on the criteria of capturing the wider ranges of flow of water from and to the system. From that perspective, NF_{SILO} is preferable to NF_{map}.

Therefore, NF_{SILO} is selected for boundary conditions of GW-response modelling.

If the GW model were validated with net flux data containing unreliable runoff values, it would lead to greater uncertainty. Historical runoff data should be avoided because it does not represent the local site condition. In addition, the generation of the future runoff component in the net flux estimation would be more cumbersome and add more uncertainty.

c) Annual Time Scale: It has been shown that of the various estimates of evapotranspiration, only SILO AAET data and map AAET with runoff component perform comparably with better results, as indicated by NF_{SILO} and NF_{map}. Therefore, the extended analyses are performed only for these two sources of AAET data.

The average annual rainfall and AAET from SILO 2006, source of the Jabiru East Airport site, for the period 1980 to 2005 were 1498 mm and 1414 mm respectively. The average AAET for the same site from the evapotranspiration map of Australia (Chiew *et al.* 2002) is 1064 mm. The evapotranspiration map is based on the period 1961 to 1990. Therefore, the AAET from SILO 2006 source for the Jabiru East Airport site is also estimated for the same period (1961 to 1990) and is 1361 mm. Thus, it is found that the SILO data source consistently overestimates the AAET and the evapotranspiration map of Australia underestimates the AAET.

To understand this inconsistency, detailed information on the evapotranspiration map is reviewed. It has been found that the evapotranspiration map values are modified for catchments with stream flow hydrologic system and the values of the site are provided after water balance modifications for annual time scale have been performed. Therefore, the consideration of annual runoff (514 mm) in annual water balance (Runoff + AAET = Rain) fits better with map data in comparison to SILO data, as shown in Table 5.4.

The water balance equation in a smaller scale of areal extent could be written as
Rain = Runoff + AAET

An imbalance of 430 mm per year for SILO data can be assumed approximately equal to the annual runoff of 514 mm as shown in Table 5.4. The map evapotranspiration variables are provided after taking care of the runoff phenomenon.

Table 5.4 Monthly average values of hydrologic data (mm)

Month	Runoff GS821009	Rainfall Jabiru East	Morton's AAET Jabiru East SILO data	Morton's AAET Jabiru East Map data	Imbalance with annual flow (rain-runoff - AAET)	
					SILO data	Map data
Nov	0	135	146	121		
Dec	22	234	151	97		
Jan	118	368	149	134		
Feb	180	369	134	95		
Mar	152	257	154	68		
Apr	38	78	123	51		
May	4	10	90	46		
June	0	1	61	61		
July	0	2	63	79		
Aug	0	0	85	97		
Sep	0	7	117	98		
Oct	0	37	141	117		
Total	514	1498	1414	1064	-430	82

Therefore, the map data can be interpreted as based on point scale annual water balance. If runoff is considered as a one-way point flow (as in rainfall-runoff modelling), map evapotranspiration should be used, as would be used in the AWBM (Podger 2004). When runoff is used as a reversible flow (as dry season soil moisture in groundwater flow modelling) SILO AAET should be used. SILO AAET data takes care of the runoff phenomenon as a component within the catchment. Therefore, the SILO data can be recognised as being based on the catchment scale seasonal water balance.

The runoff acts as a sink for wet season rainfall and source for dry season AAET in the form of soil moisture. Thus, the runoff component should be considered as part of rainfall and AAET in the entire annual water budget of the catchment according to the following interpretations.

During the wet season:
Rain – (Runoff and/or groundwater recharge) = AAET (wet season).

During the dry season:
Rain + (Runoff and/or groundwater discharge in the form of soil moisture) = AAET (dry season).

Thus, the SILO AAET values satisfy the annual water balance as Rain = AAET with runoff being included in the SILO AAET estimates. The representation of net flux as Rainfall – AAET becomes positive and negative making the annual summation zero. Similar results are reported by Vardavas (1987; 1989) for this site, such that the average annual rainfall to be 1551 mm while the average annual pan evaporation rate is about 2000 mm. Therefore, in the present research, SILO estimates of AAET are used for the outflow component from the system. Therefore, the net flux time series is estimated as the algebraic summation of positive rainfall and negative AAET.

5.2.5. Representation of Significant Flow Components by Net Flux

The relative significance of the hydrologic flow components such as rainfall, runoff, evapotranspiration and lateral subsurface flow for the site have been analysed in terms of numerical analyses in the earlier sections. In this section, some physical factors are considered to strengthen the outcome of the earlier analyses.

The representativeness of measured runoff at GS821009 of Magela Creek is analysed in terms of the physical factors such as catchment characteristics and site condition of the research site. The catchment area of 600 km^2 consists of a steep slope (i.e. hill slope region) in the upstream areas, whereas the area near Ranger is relatively flat at the downstream region. It is arguable that the runoff coefficient for a steeper slope should be greater than that of flatter slope. Hence, the runoff coefficient of 0.34 should be assumed to be the combination of hill slope values and flat slope values. Since the Ranger site is located at the flat slope region in relation to the hill slopes at the upstream parts of the catchment, the actual percentage of rainfall contributing to the runoff should be much less that the runoff coefficient of the whole catchment, i.e. less than 0.34. Conversely, the runoff coefficient for the hill slope region should be greater than 0.34.

The runoff hydrograph clearly has a one-month lag from the rainfall hydrograph, based on the long-term average measured values, as discussed previously. The travel time of surface runoff from the remote locations of this 600 km^2 area, from where significant runoff is being generated, may be causing this one-month lag. The lateral subsurface flow or base flow phenomenon may be the other ongoing significant process that is responsible for the lag. Therefore, the runoff in the flat topography at Ranger is infiltrated into the soil and contributes to dry season evapotranspiration.

However, irrespective of the real value of the runoff for Ranger, since the annual water balance is sufficiently explained by the equation Rainfall = AAET, the net flux at monthly the time step is adequately represented as rainfall – AAET, when the data used is SILO (SILO 2006). Therefore, the monthly difference in rainfall and evapotranspiration becomes positive during the wet season and negative during the dry season. The river nearby the site is an ephemeral type and the catchment area of that river is much larger than the area of the site under consideration. It is presumed that the flow in the river is largely contributed from the upstream catchment while the runoff generated from the site is relatively insignificant. The dense vegetation, highly pervious soil surface and roughness, minimum imperviousness and flat topography constitute favourable factors, which conclude that the runoff at catchment scale analyses could be negligible. Therefore, it is assumed that runoff measured in GS821009 is contributed by hill slope regions of the catchment and the local runoff is represented as wet season soil moisture and dry season AAET for the site because of its flat topography.

In relation to the present research, hydro-climatic parameters such as precipitation, evapotranspiration, and groundwater storage are only considered applicable for long-term groundwater flow modelling in the shallow unconfined aquifer of a region in tropical climate with flat topography. The runoff components of the water balance equation are assumed negligible in the long-term modelling framework at catchment scale study as far as the SILO AAET data is used to estimate evapotranspiration. The ultimate representation of the net climate flux to the system consists of rainfall and evapotranspiration only as the runoff being absorbed in the process of evapotranspiration.

The use of net flux as the fundamental climatic factor in hydrologic modelling is common and can be found in the study by Knotters and Bierkens (2000). Cheng (2006) uses the

‘effective rainfall’ as a 20-day average rainfall minus pan evaporation in studying the influence of climatic variation on groundwater. Knotters and Bierkens (2000) use ‘potential precipitation excess’ and represent input term to be precipitation minus potential evapotranspiration and another variable to represent the difference between potential and actual evapotranspiration. These two variables combine to represent precipitation minus actual evapotranspiration, which is used to forecast water table depths.

Similarly, Bidwell and Morgan (2002), and Bidwell (2005) use ‘land surface recharge’ to represent monthly totals estimated from a daily water balance model, which implicitly includes rainfall and evapotranspiration. Parlange et al. (1992) represent the ‘change of amount of water stored’ as the difference between applied water events and evaporation for modelling soil water content by time series technique. Lubczynski (2006) uses ‘net recharge’ as the difference between recharge and groundwater evapotranspiration. Xu (1999) uses ‘active rainfall’ as the difference between rainfall and evapotranspiration in validating the conceptual hydrologic model for modelling climate change impacts. In addition, Misstear et al. (2009) use ‘effective rainfall’ as rainfall minus actual evapotranspiration in estimation of groundwater recharge using multiple approaches for an aquifer in Ireland. Therefore, in this thesis, net flux will be applied in a similar manner to numerous other researchers.

5.3. Estimation of Groundwater Recharge

Estimation of groundwater recharge is an iterative process that is highly dependent on climate, surface and subsurface conditions, as noted by many investigators (Middlemis et al. 2001) (Vries and Simmers 2002). Based on information about the research site that is more comprehensive, multiple types of models are developed, which are based on different assumptions. They are analysed to obtain a comprehensive understanding of the catchment scale recharge process. The practical reasons for selecting the methods could be attributed to the availability of rainfall, runoff, evapotranspiration, groundwater level, groundwater salinity and rainfall salinity data for the site.

However, the real scientific basis of considering all these methods lies in the fact that each has its own strengths and weaknesses. A more comprehensive modelling is always better at the beginning stage of any investigation. The most appropriate model is then selected for long-term prediction. The use of various conceptual models for hydrologic processes to

explore the impact of climate change has increased recently (see Chapter 2) in comparison to earlier trends of research in the field of modelling of water resources systems (Xu 1999). The four types of conceptual models are investigated to understand the GW climate relationship from different perspectives. Based on the best representation, the physical process-based saturated-unsaturated model is developed for long-term prediction of the groundwater response with climate change. The four types of models are as follows:

- Correlation model: correlating GW levels with single climatic variable
- Water balance model: rainfall-runoff modelling with multiple climatic variable
- Chloride balance model: mass balance for chloride in rainfall, runoff and GW
- Extraction of seasonal component by classical decomposition: exploratory analyses for dynamic relationships in GW and climate

5.3.1. Correlation Model for Understanding GW Climate Relationship

The correlation model can be described as the simple application of the continuity equation to the control volume of soil in the shallow, unconfined aquifer of the site under consideration. For example, a unit area of soil surface with a specific depth of soil containing the GWL within the depth. The equation of continuity as applied to the control volume of soil has been stated in Equation 2.1. The left-hand side refers to difference between inflow and outflow, which is net flux. Change of GWL should represent the right-hand side of the equation if the one-dimensional flow is considered. Therefore, the climate data and GWL data are analysed to identify the probable correlation between monthly net flux and changes in GWL. The monthly time step is investigated in combination with a half-yearly time step to explore the best correlation between net flux and change of GWL.

Correlation performance for various time steps: The correlation analyses have been conducted to establish the cause-effect relationship between climate and groundwater. Kashyap and Rao (1976) have shown the comparison for various scales of time step discretisation in the model representation and have suggested that different models with various levels of discretisation have to be constructed so that the correct model for the given task can be selected. Therefore, a range of methods has been tested with variation of dependent and independent variables. Various definitions of wet and dry seasons were set for the analyses, as indicated in method 1, 2 or 3, as shown in Table 5.5. The respective

amount of the wet or dry season's climate flux and the amount of rise or fall of the GWL of the bores were also estimated accordingly.

Table 5.5 Key features of the methods used for correlation between net flux and GWL

Net flux data	Factor indicating the duration of wet season	Computation of independent variable	Computation of dependant variable	Comments	Method
Daily flux summed up for a certain duration	Wet season from trough of previous season to peak of following season of GWL of each bore	Summation of daily flux for the relevant wet season.	Difference in elevation of GWL from trough of previous season to peak of following season	Each bore had different seasonal flux data. Individual bore analysed.	1
Monthly flux summed up for certain duration	Wet season when the monthly flux values are positive as the wet and dry seasons are distinct	Summation of previous dry season flux and following wet season flux as the cause for rise of GWL.	Difference in elevation of GWL from trough of previous season to peak of following season	All the bores had the same seasonal flux data. Grouped as well as individual analysis done.	3
Monthly flux summed up for certain duration	Wet season from the month of maximum negative flux to the month of maximum positive flux	Maximum monthly flux of a season.	Peak GWL of that season	All the bores had the same seasonal flux data. One single bore analysed	2

The time step of the analyses were too big and thus overly lumped (approximately half a year); hence, a relatively poorer correlation was found. In some years, there was a negative value of wet season flux, which contributed to a very poor result of all the correlation analyses based on the wet/dry season. One sample result of correlation (method 1) is given in Table 5.6. The length of data is different for different bores and the bore with less data obviously had a better correlation. However, bores with larger data sizes yielded insignificant correlation. The other two methods returned similar results with poor values of R^2. Further analyses were conducted with a smaller time step such as monthly net flux *versus* monthly change of GWLs.

Table 5.6 Result of correlation method 1 (wet-dry season based)

Bore	Data size (No of years)	R^2 for rise	Slope 'm' of (y = mx+c) **Positive** for ideal case	R^2 for fall	Slope 'm' of (y=mx+c) **Negative** for ideal case
OB19A	19	0.03	Positive	0.05	Negative
OB1A	22	0.19	Positive	0.09	Negative
OB20	20	0.26	Positive	0.04	Negative
OB21A	19	0.41	Positive	0.03	Positive
OB23	19	0	Negative	0	Negative
OB24	20	0.15	Positive	0.01	Positive
OB27	7	0.04	Positive	0.51	Negative
OB29	20	0.23	Positive	0.28	Positive
OB2A	22	0.02	Positive	0.31	Negative
OB30	23	0.02	Positive	0.05	Negative
OB31	5	0.25	Positive	0.63	Negative
OB32	3	0.97	Negative	0.54	Positive
OB33	3	0.9	Negative	0.4	Positive
OB34	9	0.28	Positive	0.06	Negative
OB35	2	1	too few data	1	too few data
OB36	2				
OB37	2				
OB38	8	0.4	Positive	0.15	Positive
OB41	17	0.01	Positive	0.12	Negative
OB42A	14	0.08	Positive	0.43	Negative
OB43	14	0	Negative	0.07	Negative
OB44	14	0.01	Positive	0.16	Negative
79/6	20	0.02	Positive	0.09	Negative

From the record of monthly GWL data, the monthly change of GWL indicated by Δ GWL is computed by Equation 5.6:

$$\Delta GWL = GWL_{i} - GWL_{i-1} \qquad \text{Equation 5.6}$$

where GWL_i means groundwater level elevation in the i^{th} month. Figure 5.15 shows the definition of monthly change and annual fluctuation of GWLs as Δ GWL and Δ H respectively.

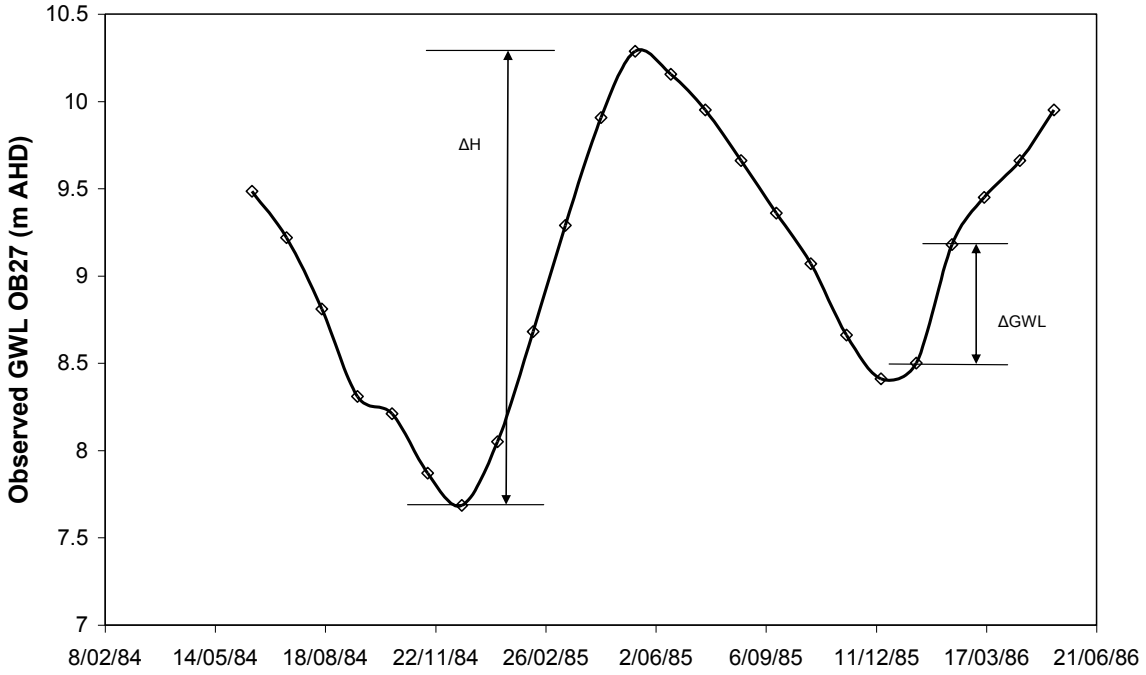

Figure 5.15 The definition sketch of monthly change of GWL indicated by Δ GWL and annual fluctuation of GWL indicated by Δ H

With a monthly time step for net flux and change of GWLs, the correlation was improved as is demonstrated in Table 5.7. Of the 21 bores located in the Ranger site, four have been found relatively unimpacted by mining activities. The bores were selected based on location, trendline of GWL, correlation between GWLs and climate, and lag analysis, which are described in detail in Chapter 3. The use of a monthly time step to discretise a continuous hydrological process is considered acceptable (Hipel *et al.* 1977; Von Asmuth *et al.* 2002). An extension of a monthly time step-based correlation was performed by splitting the period of record into pre- and post-mining term to demonstrate the influence of mining activities on net flux-GWL relationship. Thus, the selections of monthly time step for data analyses were justified.

Table 5.7 Improved correlation with monthly time step data

Bore	R^2
OB1A	0.33
OB20	0.4
OB27	0.5
OB43	0.29

The GWL varies significantly and shows a distinct seasonal cycle. Monthly net flux explains approximately 50% of the variance in monthly changes in GWL elevation as the equation of correlation and R^2 value indicate in Figure 5.16.

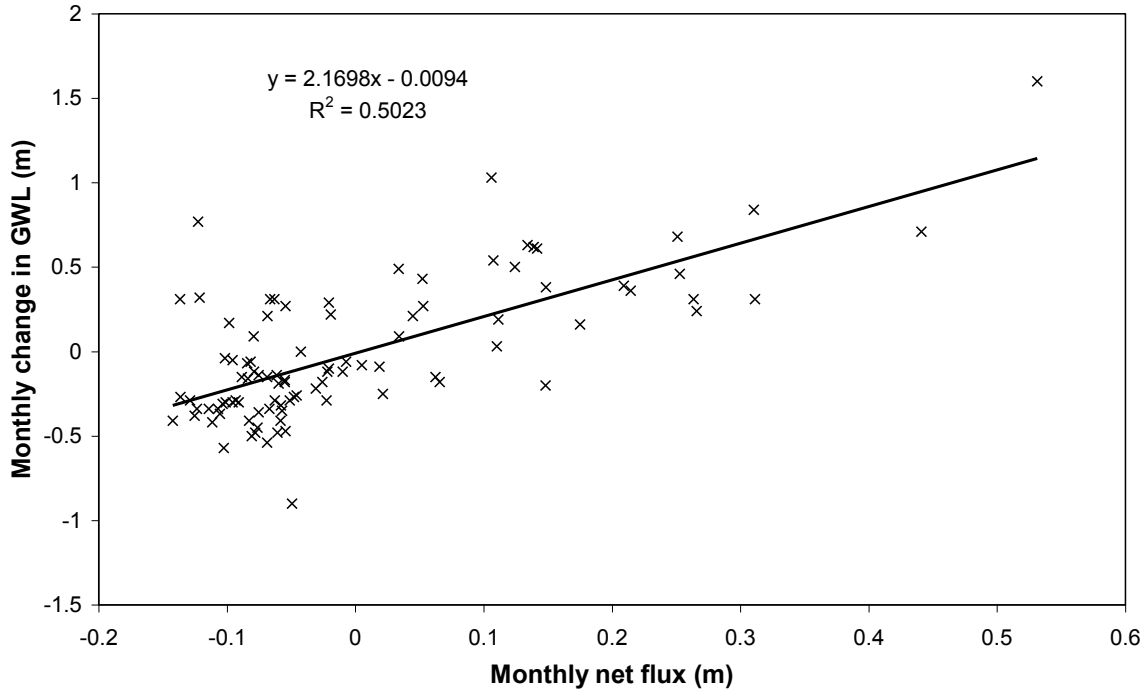

Figure 5.16 Monthly time step-based correlation between net flux and changes in GWLs

Estimation of recharge with monthly bore data: The monthly changes of GWL for bores OB1A, OB20, OB27 and OB43 were analysed, as shown in Table 5.8. The average annual fluctuation could be estimated from the mean value of normally distributed data. A range of duration is considered for monthly data to investigate the statistical property of the frequency distribution. For normally distributed data, more than 95% of the area under the probability distribution curve is contained within the range of mean plus/minus two standard deviations. Therefore, if the data were normally distributed, mean plus/minus

twice the standard deviation of the monthly data should be accepted as the range of variation of monthly change of GWL with 95% confidence (Devore 1999). However, as the data are not normally distributed, as shown in Figure 5.17, the aforementioned approach of using mean monthly change of GWL for estimating average annual fluctuation of GWL has been rejected. An alternative lumped approach verified by time series analysis is used for that purpose.

Table 5.8 The statistical data analyses of monthly change of GWL (mm) of four selected bores as meant for normally distributed data

Bore name	Number of months (Year)	Min value of Δ GWL (mm)	Max value of Δ GWL (mm)	Mean value of Δ GWL (mm)	Std. Deviation of Δ GWL (mm)
OB1A	263 (1980-2002)	-1490	3190	-1.4	758.4
OB20	251 (1981-2002)	-3680	4390	6.5	487.9
OB27	95 (1981-1988)	-900	1600	-6.9	407.6
OB43	174 (1988–2003)	-1030	1460	9.7	391.3

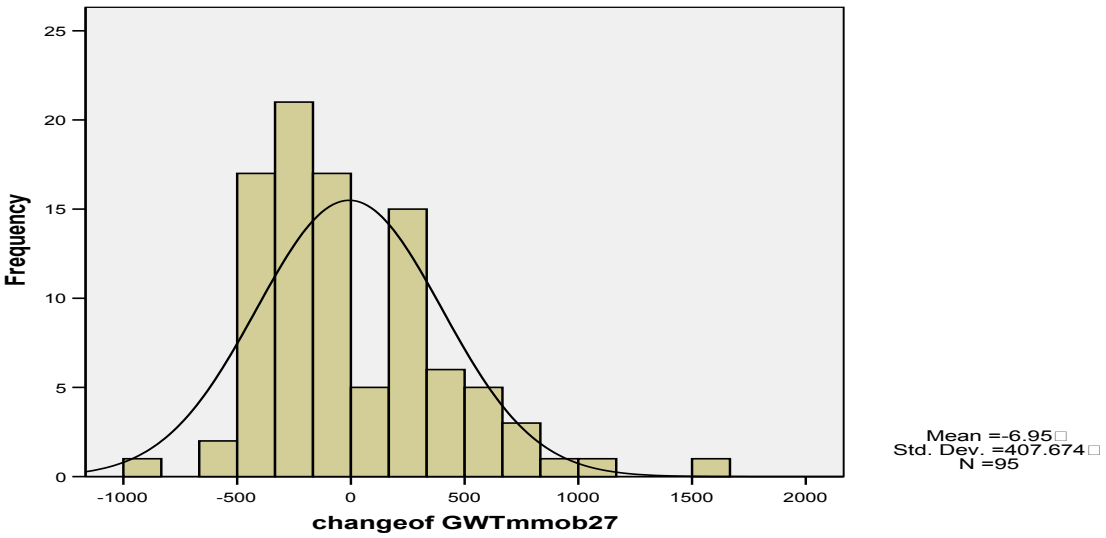

Figure 5.17 Histogram of monthly change of GWL (mm) of ob27 during 1981-1988

Estimation of recharge by annual fluctuation of bore data: The average annual recharge is considered to be represented by the average annual fluctuation of GWL (ΔH). Average annual fluctuation is represented by the difference in elevation between the highest and lowest GWL during the wet and dry season respectively. This ΔH value varies

between years and bores due to climatic variability and complex geology. The average annual fluctuation of GWL has been estimated by directly considering the GWL fluctuation charts. The average annual fluctuation for these four bores is demonstrated in Table 5.9.

Table 5.9 The estimated average annual fluctuation of GWL from GWL fluctuation charts

Name of bore	Year of data analysed	Average annual fluctuation (ΔH) (mm)
OB1A	1982-2002	3173.5
OB20	1983-2002	1669.0
OB27	1983-1988, 2004-2005	1859.6
OB43	1989-2002	1665.3

There is considerable variation of OB1A data with the rest bores as highlighted in Table 5.9. A similar variation of monthly change of GWL (mm) is found within the bores (with OB1A being effected by seepage from tailing dam) by comparing the standard deviation values in Table 5.8. Assuming the regional fluctuation GWL to be the average, the value becomes 2.09 m.

Considering the method of estimation of recharge from observed GWL, the equation used by Armstrong and Narayan (1998) is written in Equation 5.7:

Average annual recharge (mm) = (ΔH) (mm) * effective porosity Equation 5.7

From the aforementioned relationship, it is critical that the regional estimation of average annual recharge using groundwater level fluctuation is highly sensitive to the estimation of soil property, which is liable to vary along the three dimensions around the point of observation.

For instance, porosity of 0.20 is considered normal for unsorted gravel size material at depths below the biomantle. Hence, average annual fluctuation of GWLs by 2.09 m would lead to a recharge value of between 418 mm and 836 mm for porosity of 0.2 to 0.4. However, if the porosity is 0.1, the recharge becomes 209 mm/year, which is 13% of the

annual rainfall. This indicates the very high sensitivity of estimated recharge with soil property. This kind of variation in estimation of recharge is practiced with reasonable acceptance in similar studies. For example, Lautz (2008) uses diurnal water table fluctuations in a semi-arid riparian zone for estimating groundwater evapotranspiration (i.e. losses of water from GWLs). The specific yield value is used for the estimation of losses and found to increase from 7 to 30%, causing groundwater evapotranspiration to increase by 4.3 times.

To compensate for the weaknesses of estimation of this method, more techniques are considered to improve confidence levels regarding the accuracy of the result. The following sections discuss these other methods.

5.3.2. Australian Water Balance Model

There exist a wide range of water balance models and selection of a specific model depends largely on the input-output data and calibration facilities. The AWBM (Podger 2004), a lumped conceptual model, which is widely used in rainfall-runoff analysis in Australia, has been selected for the study. The model selection is conducted based on the data requirement of the model and its inbuilt calibration facilities. In the water balance study of the catchment, the site is considered as a surface water hydrologic system. As the climate is tropical, in which distinct wet and dry seasons exist throughout the year, the recharge to an unconfined aquifer during the wet season is represented by the base flow recharge, (see Appendix E).

According to Lerner (1997), recharge can be defined as water that reaches an aquifer from any direction (down, up, or laterally). This is what is considered for the present study. Therefore, groundwater recharge is defined as the amount of water that enters into the saturated zone. In the application of surface water balance method for recharge estimation, Zhang et al. (1998) have suggested the assumption that groundwater runoff or base flow is represented by that portion of infiltrated rainfall that reaches the water table and then discharges into the streams. Thus, recharge to a groundwater system can ultimately become discharge to the stream to form part of the total runoff. This analogy has been used in the construction of AWBM, in which the term ‘Base Flow Recharge’ will simulate the required groundwater recharge of the intended study.

Many investigators have worked on this technique in terms of evaluation and applicability. For instance, Scanlon et al. (2002) suggested that the base-flow discharge in a surface water system is a typical representation of groundwater recharge. According to their recommendation, the representation is valid for up to 1300 km^2 of catchment area and for up to 50 years of data. Tilahun and Merkel (2009) used a GIS-based distributed water balance model to estimate groundwater recharge in Dire Dawa, Ethiopia. Szilagyi et al. (2003) also used BFI to quantify the recharge to groundwater with the convenience being that the method does not require complex hydrogeologic modelling or detailed knowledge of soil characteristics, vegetation cover or land-use practices. Herrmann et al. (2006) use a physically based runoff generation model to study surface-shallow groundwater relationships and environmental systems with regard to global warming and climate change. For a similar reason, AWBM is used for the estimation of groundwater recharge using only rainfall, evapotranspiration and runoff data in the catchment area.

As estimated earlier, the lateral flow in the Ranger area with the highest hydraulic gradient (near WTLA) and a wide range of variability in hydraulic conductivity is less than 10% of vertical flow. As shown in the structure of AWBM, the 'Base flow' will simulate the lateral flow component of the region. The 'Surface Runoff' will simulate the observed runoff at the measuring station. The equations of water balance in AWBM are represented as follows. The detail conceptual framework of AWBM, the data requirement and calibration methods are described in Appendix E.

Output result: The base flow (lateral flow), computed runoff and base flow recharge (groundwater recharge) computed in Model Run 3 are shown in Table 5.10. The graphical representation of the flow components are demonstrated in Figure 5.18 and Figure 5.19. The scatter plot of the observed and modelled runoff values are illustrated in Figure 5.20. The analysis of the result and performance of the model are discussed in the following sections.

Table 5.10 Flow components estimated by AWBM

Variable	Total (mm) for 11119 days	Mean (mm/day)	Std Dev (mm)	Skewness (mm)
Observed Runoff	18134	1.63	5.08	8.43
Base flow	9063	0.82	1.75	2.97
Routed surface runoff	9054	0.81	2.54	5.18
Computed runoff (Base flow +Routed surface runoff)	18117	1.63	4.09	4.08
Base flow recharge	9054	0.81	3.70	7.73
Input rainfall	46330	4.17	11.57	4.63
Effective rainfall	35111	3.16	10.51	5.33

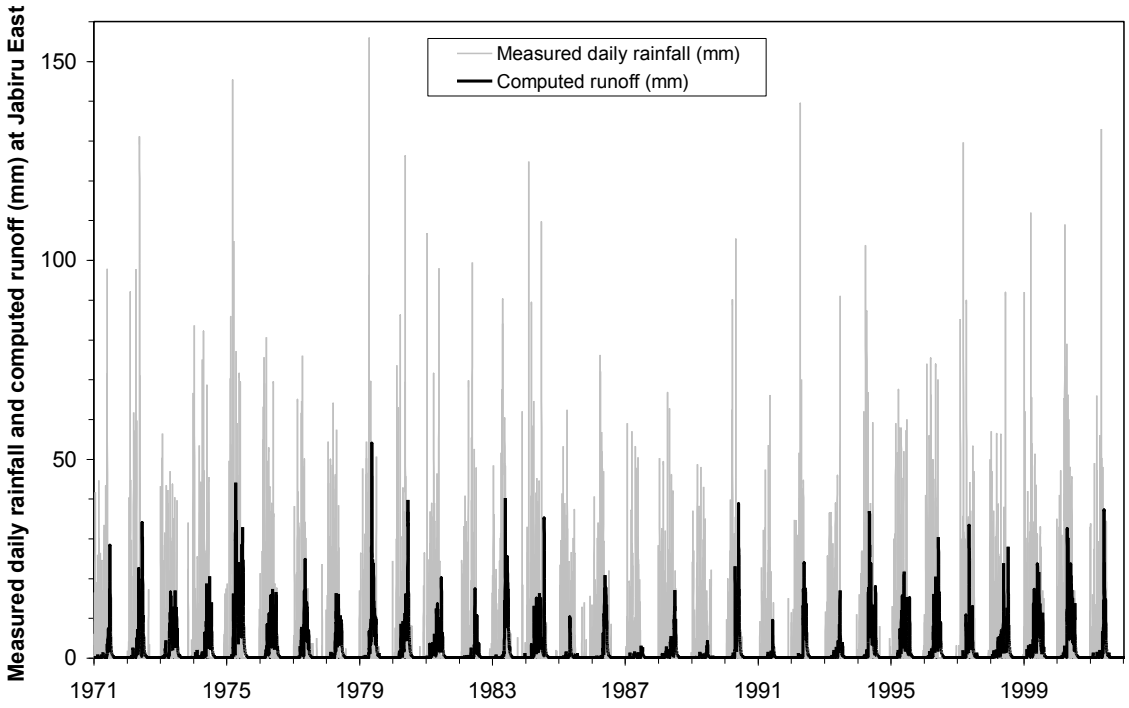

Figure 5.18 Rainfall and runoff with time

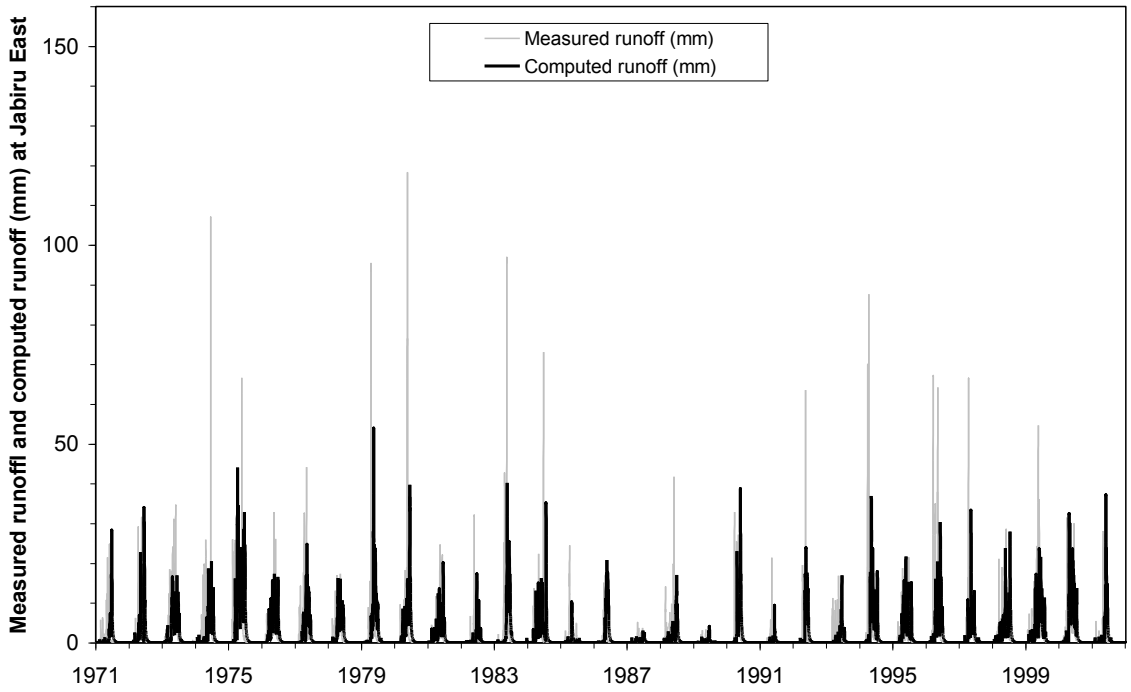

Figure 5.19 Measured and computed runoff with time

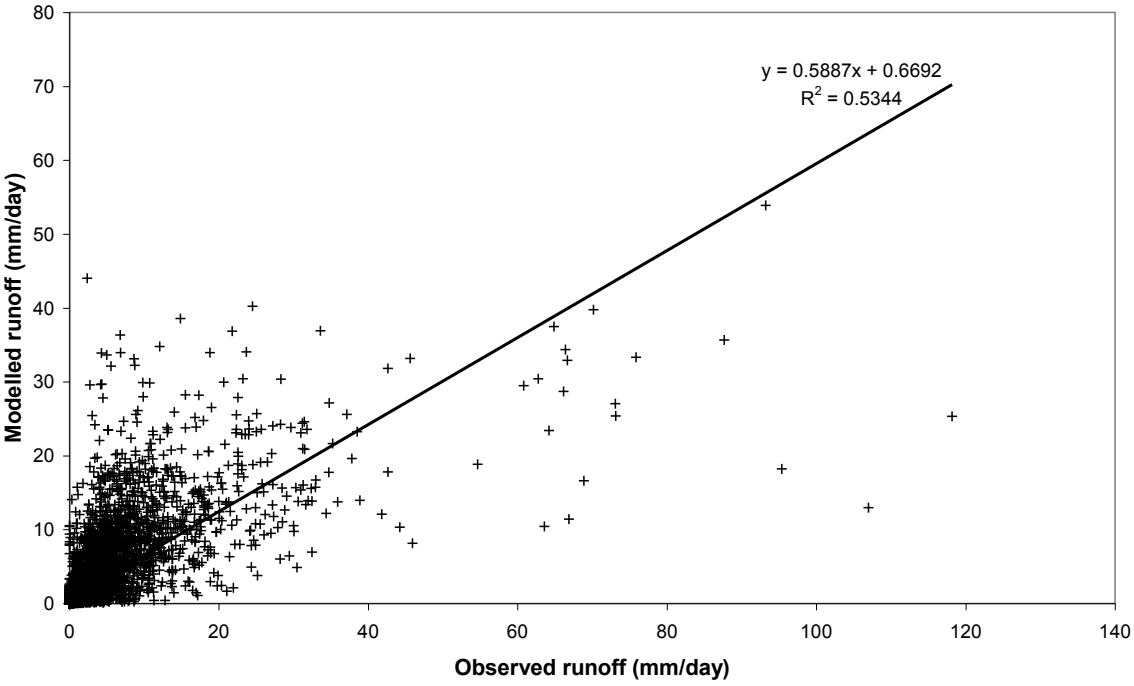

Figure 5.20 Calibration results scatter plot

Statistics of the model performance: The result comparison is represented in Table 5.11 in terms of different performance criteria. For monthly data of calibration run and verification run, the Nash-Sutcliffe coefficients are 0.860 and 0.841 respectively.

Table 5.11 Statistical performance of calibration and verification

Variable	Length	Relative Difference	Absolute Difference	Nash-Sutcliffe	Correlation
Calibration Runoff	11119	-0.094%	-17.045	0.529	0.731
Verification Runoff	735	18.506%	212.739	0.521	0.774

Comparison of water balance components: The water balance components computed from the model runs are analysed in this section with relevant references. Of the many components of the computed flows, the most important flow component for the study is base flow. The ratio of base flow to the total flow is termed as BFI. In the following analyses, the BFI values of various methods of computations are compared.

a) Comparison of Separated Base Flow by Digital Filter: From the knowledge of conventional methods of hydrograph analyses, as described in Nathan and McMahon (1990), a number of available techniques are used to estimate base flow from surface flow, and hydrograph generated from rainfall runoff. Most are graphical and require various subjective decisions to be made such as the point at which surface runoff ceases and what would be the actual shape of the base flow hydrograph (Grayson et al. 1996).

A program named AQUAPAK (Gordon et al. 2006), based on a digital filter is used to separate the base flow from total flow data (daily discharge) measured at Magela Creek station GS821009. The digital filter separates base flow in the same way that high frequency noise is filtered out from sound waves. This technique is introduced to compare the estimated BFI as obtained from AWBM.

The method in the analysis has been widely used with daily data. The equations that relate the quick flow, original stream flow (i.e. runoff) and base flow are stated in Equations 5.8 and 5.9:

$$q_f(i) = \alpha q_f(i-1) + (q(i) - q(i-1))\frac{(1+\alpha)}{2} \text{ for } 0 \le q_f(i) \qquad \text{Equation 5.8}$$

$$q_b(i) = q(i) - q_f(i)$$ Equation 5.9

where

$q_{f(i)}$ = filtered quick flow response for the i^{th} sampling instant

$q(i)$ = original stream flow for the i^{th} sampling instant

α = filter parameter for which a value of 0.925 is recommended for daily data (Nathan and McMahon 1990)

$q_{b(i)}$ = base flow

There are adequate analogies between stream flow and sound wave and selection of the appropriate value of the filter parameter α is particularly significant as there is no physical basis of the selection procedure. Based on the relationship $k = e^{-\alpha}$, the value of the filter parameter α used in the computation is 0.925, which led recession constant k to be 0.3965. The filter was selected based on the work of Nathan and McMahon (1990). Three passes were used to smooth the data (Grayson et al. 1996).

The results from a two-year period are shown in Figures 5.21 and 5.22. The ratio of accumulated base flow to that of total flow is provided in Table 5.12.

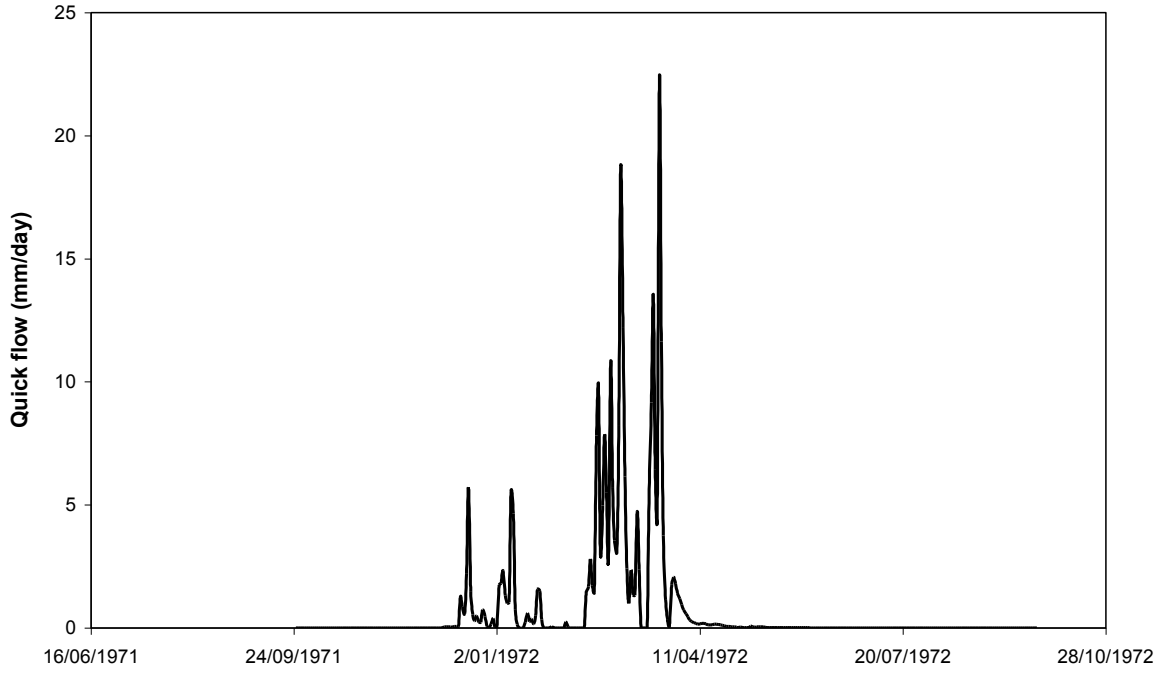

Figure 5.21 The separated quick flow computed from the measured runoff in station GS821009 from 1971 to 1972

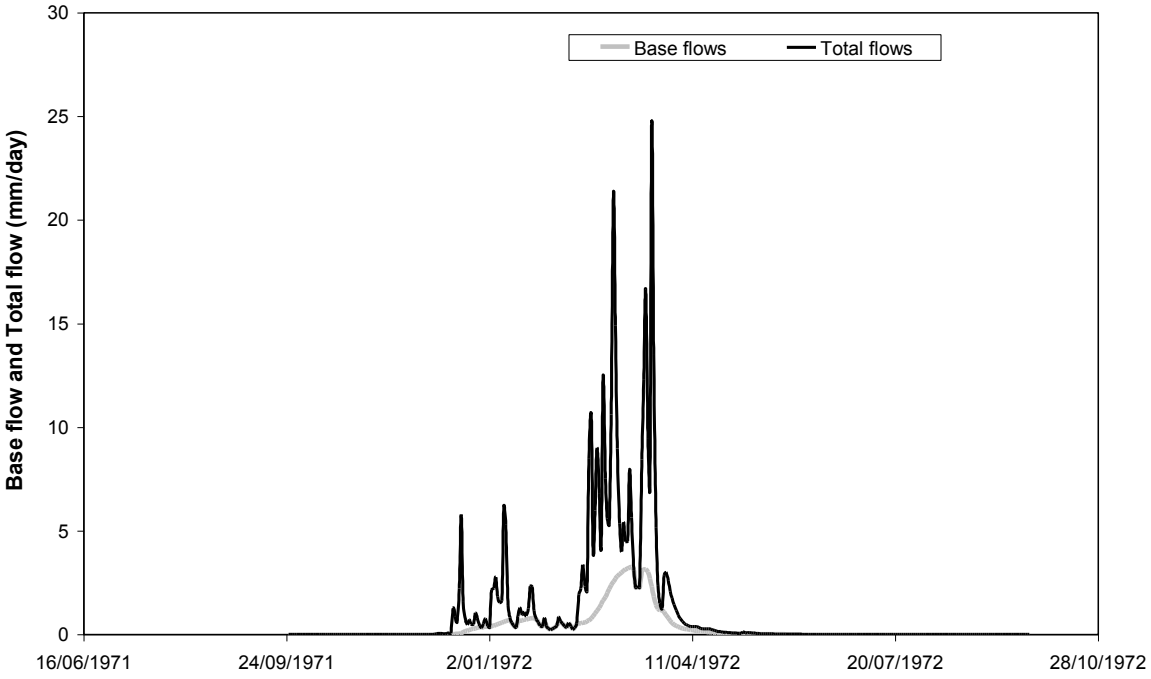

Figure 5.22 The separated base flow computed from the measured runoff as total flow in station GS821009 during 1971 to 1972

Table 5.12 The result of computation using AQUAPAK (Nathan and McMahon 1990) for separation of base flow from total flow (daily discharge in mm) measured at Magela Creek Station GS821009 from 1971 to 2005

Accumulated base flow (mm)	Accumulated quick flow (mm)	Accumulated total flows (mm)	BFI
7235.78	12893.95	20129.73	0.359

The BFI from the analysis lie within the range (0.091–0.670) and close to the average BFI (0.35) from the manual technique for five catchment areas having an areal extent of 4.2 km^2 to 210.0 km^2 as conducted by Nathan and McMahon (1990). The results of similar investigations are provided in Table 5.13.

Table 5.13 Comparison of digital filter and water balance estimates of daily recession coefficients and BFI with existing references

Names of investigators and present study	Recession Coeff for surface flow	Recession Coeff for base flow	BFI	Coeff of Variance of annual flow
(Klaasen and Pilgrim 1975)	0.2-0.8	0.93-0.995		
(Nathan and McMahon 1990)			0.091-0.670	0.15-1.41
Digital filter (Gordon et al. 2006)	0.3965 (used)		0.36 (computed)	0.48 (computed)
AWBM Model Run 3	0.61	0.92	0.49	0.48

Therefore, the result of AWBM in terms of BFI can be considered acceptable.

b) Comparison of Surface Runoff: The computed runoff is used to estimate the runoff coefficient in order to compare it with the previously investigated values of Hart et al. (1987b) of the Ranger site. As the runoff coefficient is the ratio of runoff to rainfall (Chow et al. 1988), there can be two different estimates, which is defined as the ratio of observed runoff and computed runoff to rainfall over a given time period. All computation steps and values are listed in Tables 5.14 and 5.15. These values are close to 0.25, as suggested by Hart et al. (1987b).

Table 5.14 Computation of average annual runoff

Sources of value	Annual average runoff (mm)
Observed	(18134/11119)*365 = 595
Computed (Model Run 3)	(18117/11119)*365 = 595

Table 5.15 The comparison of runoff coefficients with earlier investigator (Hart et al. 1987b)

Average annual rainfall (mm)	Average annual runoff from observed and computed value (mm)	Runoff coefficient (observed runoff/rainfall)	Runoff coefficient (Hart et al. 1987b)
(46330/11119) X 365 = 1521	595	0.3910	0.25

c) Comparison of Lateral Flow: The computed lateral flow from the field test data varied from 1 to 10% of vertical flow. For example, when irrigation occurs at a rate of 10 mm/day, the flow in lateral direction, considering an effective porosity of 0.1, is between 0.1 mm/day and 1.0 mm/day. This value is comparable to the computed base flow value of 0.82 mm/day (9063/11119 = 0.82) for the AWBM Model Run 3 as shown in Table 5.16.

Table 5.16 Computation of average annual base flow

Sources of value	Annual average base flow (mm)	% of average annual rainfall
Model Run 3	(9063/11119)*365 = 298	(298/1521)*100 = 19.56

d) Comparison of Recharge: The computation steps and values are given in Table 5.17. The base flow recharge computed by AWBM is assumed to represent recharge and is equal to 19.54% of average annual rainfall.

Table 5.17 Computation of average annual recharge

Sources of value	Annual average recharge (mm)	% of average annual rainfall
Model Run 3	(9054/11119)*365 = 297	(297/1521)*100 = 19.54

Conclusion of AWBM: By using AWBM, some data-based annual average estimates of base flow (19.56%), runoff (39.10%) and recharge (19.54%) components as percentage of annual average rainfall of the site have been achieved. This AWBM has its assumptions and limitations, which have been stated previously. To strengthen the understanding of the

site, an additional number of simple modelling techniques based on different perspectives are considered. In the following sections, chloride balance methods and data-based mechanistic methods are described with their results.

5.3.3. Chloride Balance Model

Many investigators such as Scanlon et al. (2002) and Refsgaard (2001) have reviewed the methods of estimating recharge with the perspective of range of fluxes, spatial scale of area and time period of representation. The chloride balance method is an appropriate recharge estimation technique for an area of 2 m^2 to more than 10,000 m^2 (Scanlon et al. 2002). Hence, the chloride balance method is selected to estimate recharge for the catchment scale of spatial extent. This method is widely used by investigators. Gates et al. (2008) use the chloride balance technique to estimate recharge in a desert environment in a study area of several hundred km^2. Edmunds and Tyler (2002) use chloride concentration as a tool for the estimation of recharge at the centurial time scale.

Theory: The general mass balance equation for chloride content in a control volume in the environment should be considered. Specifically, a unit area of soil, exposed to atmosphere in its top surface and groundwater table at the bottom. If the wind and air are considered as the primary medium of chloride flux in the soil, then the chloride balance in the soil can be represented as in Equation 5.10:

$$WF_c + RW_c * RW = GW_c * GW + \Delta(SS_C) + ET_c * ET + SR_c * SR \qquad \text{Equation 5.10}$$

where WF_c is the mass of chloride accumulated in the soil by wind flow, RW_c is chloride concentration (mg/L) in rainwater, RW is the depth of annual rainfall (mm), GW_c is chloride concentration (mg/L) in groundwater, GW is the depth of annual recharge (mm), SS_c is the mass of chloride existing in the soil stratum and Δ represents the annual change in the soil (if there is any). The ET_c is the concentration (mg/L) of chloride in the evapotranspiration process. Evapotranspiration is the annual amount (mm) from the soil stratum. Similarly, SR_c and SR represent the chloride concentration (mg/L) in surface runoff and depth of annual surface runoff (mm) respectively, from the soil surface under consideration.

Assumptions:

1. The contribution of chloride per unit area of the catchment (chloride coming from the wind blow and evaporative residue) is uniform in the entire catchment area. In the present study, this is represented by the term 'soil wash'.
2. As the total area of the Magela Creek catchment has been divided with respect to a number of gauging stations, as reported by Deen (1983b), it is considered that the runoff from an area of approximately 20 km^2 is flowing through the Ranger site. The imaginary delineation of the area is bordered by Mount Brockman in the south and an irregular rectangular shape of 5 km in a north-south direction and 4 km in an east-west direction.
3. The measured runoff chloride content represents the average value of the respective catchment area. Hence, the seasonal and annual variations have been lumped into a steady state condition.
4. For point scale (1 km^2) of chloride balance, the following equation represents the horizontal profile:

   Runoff incoming + soil wash per 1 km^2 area = Runoff out going

5. For point scale (1km^2) of chloride balance, the following equation represents the total of horizontal and vertical profile:

   Rainfall * 1 km^2 area = Runoff * (chloride from rainwater + chloride from soil wash) * 1 km^2 area + Recharge * 1 km^2 area

If it is assumed that runoff is 25% of rainfall, as suggested by Hart et al. (1987b), and if the concentration of chloride due to wind blow and evaporative residue is washed by runoff each year, such that no change of chloride occurs in the soil, then the chloride balance equation can be written as Equation 5.11:

$$RW_c * RW = GW_c * GW + SR_c * 0.25 * RW \qquad \text{Equation 5.11}$$

According to the assumptions stated above, SR_c is the summation of RW_c and soil wash chloride, which is estimated in the following sections. The runoff coefficient has been

alternatively estimated from the measured runoff at station GS 82 1009 during the period 1978 to 1998 and compared with the rainfall during that period. The runoff coefficient is 0.32; however, when the computed surface runoff from AWBM for the period 1972 to 2002 is compared with rainfall, it is 0.39.

Chloride content in soil depth: Soil samples were analysed for physical and chemical properties at seven sampling pits with 9 to 10 m intervals and a total depth of approximately 50 to 100 cm. The weight ratios of chloride contents with soil were less than 20 mg/5 kg (4/1000000), i.e. consistently in all locations and depths (Chartres *et al.* 1991). Hence, the soil profiles and the land area may be assumed homogeneous with respect to chloride content with this limited range of information.

Evapotranspiration consideration: The ongoing evaporation is supposed to cause increased concentration of chloride in surface coming from rainwater to the soil with time (Walker 1998). The top 100cm soil was found have a minimal amount of chloride with no sign of gradient. As there is no gradient of chloride content along depth, the transient method is not necessary as it considers the gradient of chloride content along depths of soil (Walker 1998).

Groundwater data evaluation: The chloride data in groundwater was collected during the period of September 2000 to July 2001, covering almost one year. There were data from different locations of the site and different structures, such as pumping station, sump, weir and dam wall. From all those data, the groundwater bores, which are located at the relatively outer periphery of the site such as OB20, OB21A, OB28, OB29, OB30, OB41 and OB42A are considered for the estimation of average annual recharge by the method of chloride balance (see Table 5.18).

The concentrations of chloride were measured during November (start of the wet season, deepest GWL) and May (start of the dry season, shallowest GWL). It was observed that in the month of November, the concentration is higher, which results in an accumulation of chloride. During May, the concentration is lower meaning dilution by incoming recharge. With this typical cycle of variation in all of the bores, the average concentration can be considered for the estimation of recharge.

However, the complex geology of the site is always a barrier to the assumption that the mean value will be the representative value. The chloride contents vary significantly even within the closely located bores, such as between OB20 and OB21 or between OB28 and OB29. The other two bores OB41 and OB43 only show similarity in the value of concentration and can be assumed representative of the site. Gates et al. (2008) report Cl concentrations in groundwater ranging from 63 mg/L to 383 mg/L, which is of a much greater variation with respect to the present site situation.

Table 5.18 The groundwater chloride data of selected bores

Site	Date	Chloride (mg/L)	Depth of GW from Datum (m)
OB20	27/11/2000	5.3	1.14
	29/05/2001	4.8	0.62
OB21A	27/11/2000	8.9	5.4
	23/05/2001	7.8	3.25
OB28	16/11/2000	8.6	No Data
	21/05/2001	9.1	
OB29	24/11/2000	5.5	14.17
	25/05/2001	2.5	13.54
OB30	04/09/2000	3.3	13.88
	16/11/2001	7.4	12.8
	15/02/2000	2.7	9.54
	25/05/2001	2.4	8.58
OB41	27/11/2000	4.84	1.02
	25/05/2001	4.8	0.53
OB43	27/11/2000	4.4	1.14
	25/05/2001	2.9	0.62
Average	Annual	5.32	
Average	Annual	4.23 (considering OB41 and OB43)	

Runoff consideration: The consideration of runoff is regarded as significant when runoff is received from surrounding areas. The issue becomes insignificant when the length of

runoff path, i.e. scale of the recharge area under consideration, is relatively small (Walker 1998). The groundwater chloride data are collected from bores that are located within an areal extent of approximately 10 km^2 (see Figure 3.10) whereas the surrounding runoff catchment area of Magela Creek at the nearest location (GS 821009) is approximately 600 km^2 (see Figure 3.7). The site is surrounded by Gulungul Creek (west and north), Corridor Creek (south), Georgetown Creek (east), Djakmara Creek (north) and Coonjimba Creek (north). All of the creeks drain into Magela Creek. The period of rainwater data collection by Hart et al. was during the 1982–1983 wet season (November–May), when the tailing dam at the Ranger site was being constructed, as described in Table 5.19.

Table 5.19 Construction stages of the tailing dam (Salama and Foley 1997)

Stage of construction	Year	RL (m)
I	1979–1980	26.17
II	1983	39.0
III	1985	41.0
IV	1990	44.5

Hence, the natural runoff generated in the Magela catchment adjacent to the Ranger site can be assumed to be travelling through Gulungul Creek to the west and Georgetown Creek to the east towards Magela.

The point of initiation of the particular runoff water that is travelling though the Ranger site is 5 km (approximately) south from Ranger, where the Mount Brockman escarpment ends. The length of travel (distance from point of initiation) of this runoff water is estimated from the Magela Creek catchment map of Hart et al. (1987a). The data of Hart et al. (1987a), who had measured rainwater quality and runoff water quality, i.e. chloride concentration at points such as GS 821009, GS 821023 (Island Billabong), GS 821017 (Jabiluka) and GS 821019, is used in the analyses. The catchment areas of the gauging stations are available from Deen (1983b). The catchment area of the Ranger site is located at the south of the site and bounded by Mount Brockman, an area of 15 to 20 km^2 (3 to 4 km wide and 5 km long). These data are now used to estimate the runoff water chloride concentration (see Table 5.20).

Method used to estimate runoff chloride at Ranger: From the guidelines regarding the spatial scale of the hydrologic model, as provided by Refsgaard (2001) (see Table 5.1, the site area under consideration falls in the boundary between catchment scale and field of hill slope scale. In the field of hill slope scale, the runoff is accumulated at different locations of its pathway in the proportion of the respective catchment areas if the steady state situation exists along the pathway.

Table 5.20 Chloride concentration and catchment areas of gauging stations of Magela Creek

Location/Station	Distance from the point of initiation or length of travel of runoff (km)	Catchment Area (km^2)	Main wet-season waters chloride concentration (mg/L) (measured)	Rainwater chloride concentration (mg/L)
Ranger	5	15–20		0.5 (0.2–1.1)
GS 821009	10	600	1.7	
GS 821023 (Island Billabong)	20	986	3.1	
GS 821017 (Jabiluka)	30	1134	3.2	
GS 821019	52	1565	6	

Estimation of soil washes chloride: Table 5.20 demonstrates that the concentration of chloride increases with the increase in size of the catchment area. The assumption that the surface area of the runoff catchment is uniformly contributing to the chloride content is thus valid. Therefore, from correlation analysis between length of travel, catchment area and chloride concentration of the different locations, the concentration at the Ranger site will be estimated.

The rainwater with an existing amount of chloride content is assumed to accumulate the chloride from the surface soil, from the point of generation to the points of measurement such as GS 821009 (Jabiru), GS 821023 (Island Billabong), GS 821017 (Jabiluka) and GS 821019 (see Figures 5.23 and 5.24). It should be mentioned that Walker and Wong (1999)

used a similar approach to develop a relationship between wet mass of gross pollutant with runoff flow.

From the fitted equation for the catchment area, the chloride content in the Ranger runoff is 0.821 mg/L based on the area of the generating catchment (see Figure 5.23). The other estimation is 1.681 mg/L, based on length of travel (see Figure 5.24). This is much greater than 0.821. However, the travel length is estimated based on the approximation from the map, which contains errors, whereas the catchment areas are measured values. Hence, the equation relating catchment area with chloride concentration should be accepted.

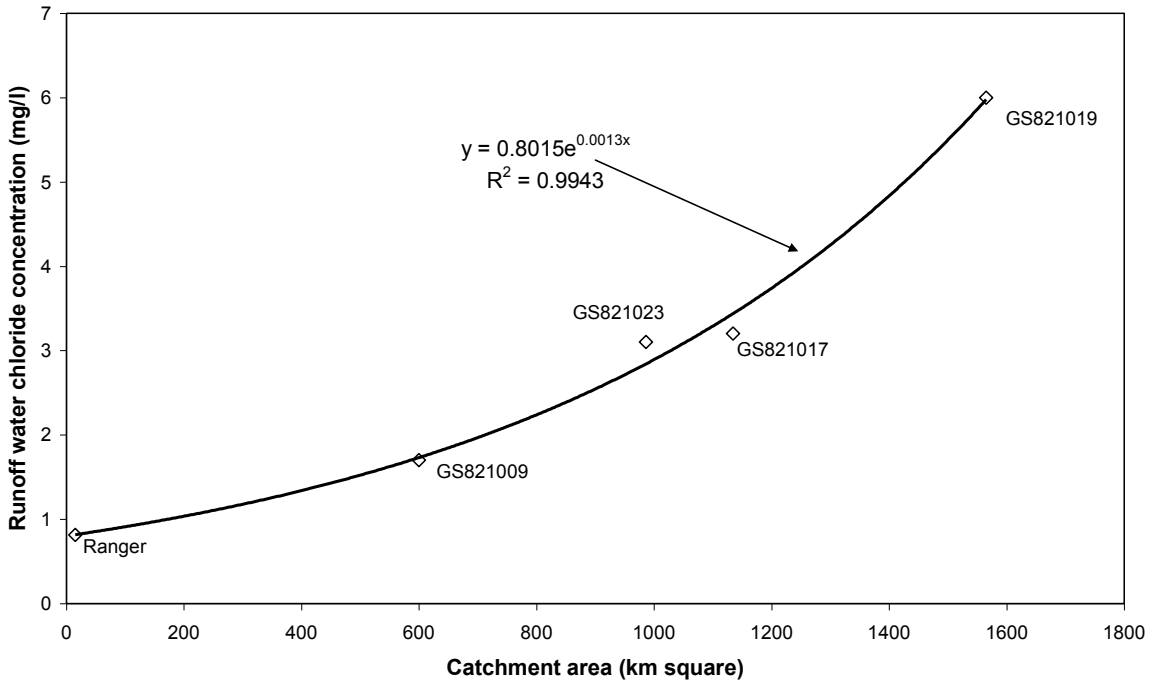

Figure 5.23 Extrapolating the runoff chloride content at Ranger from four measured values at downstream gauging stations of Ranger

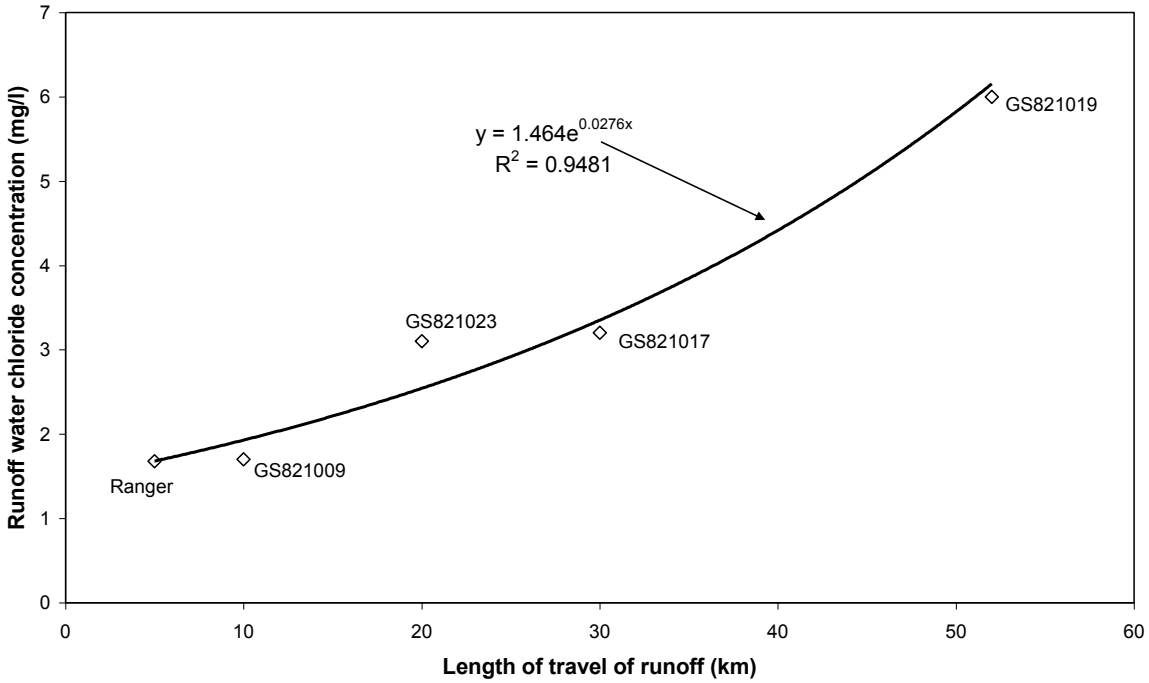

Figure 5.24 Extrapolating the runoff chloride content at Ranger from four measured values at downstream gauging stations of Ranger (less accurate than Figure 5.23, as the distances are approximate)

If it is assumed that the runoff in Ranger contains 0.821 mg/L chloride, the rainwater contribution is 0.5 mg/L and the remaining 0.321 mg/L is a result of runoff from the 20 km^2 area. If the remaining 0.321 mg/L chloride is being washed from 20 km^2 areas, then the 0.016 mg/L of chloride is assumed to be coming per 1 km^2 area. Hence, the soil wash chloride is 0.016 mg/l per km^2 area at Ranger. Thus, the concentration of runoff from the soil surface of Ranger should be considered a summation of rainwater concentration and soil wash per unit area.

Method used to estimate rainwater chloride: To estimate the concentration of chloride in rainwater, samples were collected at six sites located within a radius of 30 km in the catchment of Magela Creek. There were sixteen to 20 samples at each site and the total number of samples was 107. The volume-weighted means was 0.5 mg/L with a range of 0.2 to 1.1. The wet season of 1982–1983 was selected for sampling by Hart et al. (1987a), as shown in Figure 5.25. The average rainfall for the area under consideration is assumed to be 1527 mm (Chiew and Wang 1999). The actual rainfall during 1982–1983, which was a strong El Nino year is 1198 mm only. The actual rainfall during 2000–2001, the year of

groundwater chloride data collection, is 2052 mm. Hence, the long-term annual average of 1527 mm is used in the estimation process.

The other source of rainfall chloride data are from Noller and Currey (1990). The data was collected for ARR during the wet season of 1982–1083 (i.e. November 1982 to May 1983). The average of all daily rainwater chloride was found to be 7.3 micro equivalents per litre with a standard error of 0.9. This is equivalent to (7.3/1000) x 35.45 = 0.26 mg/L.

Both of these data were collected during 1982–1983. The groundwater data relates to 2000–2001. Hence, another method for a reasonable estimation of rainwater chloride content is used. For the sites where no data exist about the rainwater chloride content record, Equation 5.12 was developed by Hutton (1976) and can be used to estimate chloride fallout:

$$\left[Cl^{-}\right] = 35.45(0.99 / d^{0.25} - 0.23) \qquad \text{Equation 5.12}$$

where $[Cl^{-}]$ is the chloride concentration (mg/L) and d is the distance from the ocean (km). From Figure 5.25, it can be observed that the spatial distribution of rainfall in the Top End is uniform up to a distance of 200 to 300 km from the ocean. Hence, if the Indian Ocean is considered as source of chloride in the rainfall, then the concentration becomes 0.28 mg/L for a distance of 300 km and 0.67 for a distance of 250 km. These values are demonstrated in Table 5.21. Therefore, the rainfall chloride content is estimated to be 0.5 mg/L. There are instances of wide ranges of variation in the rainfall solute concentrations also. For instance, Gates et al. (2008) report rainwater Cl concentrations in the range of 0.5 mg/L to 36.5 mg/L in the Badain Jaran Desert of northern China.

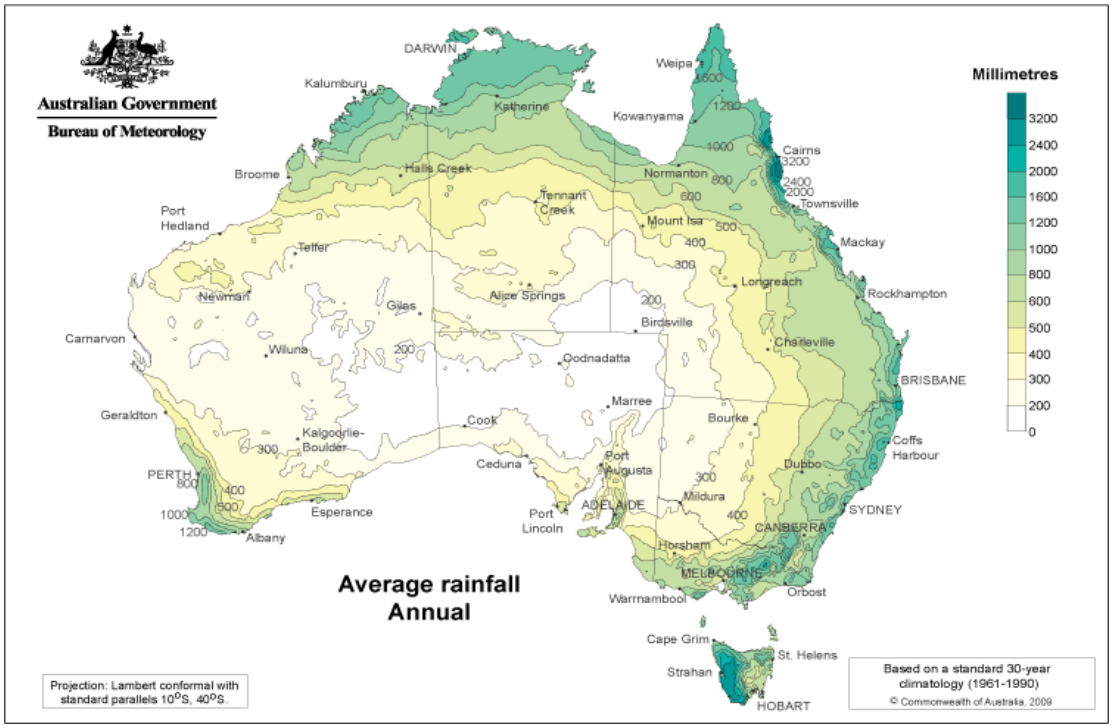

Figure 5.25 The scale of variability of average annual rainfall in the Top End is relatively small surrounding Ranger than other locations in Australia

Table 5.21 Chloride concentration estimates in rainwater from different sources

Method or Investigators	Relevant Features	Chloride Concentration in Rainwater (mg/L)
Estimated from Hutton 1976 equation	For d = 300km	0.28
	For d = 250 km	0.67
Measured value by Hart et al. 1987	1982-1983 wet season in Magela Creek Catchment	0.50 (average)
Measured value by Noller and Currey 1990	1982-1983 wet season in Alligator River Region	0.26 (average)

Application of chloride balance method: The value of the parameters as considered for Equation 5.11 are as follows:

RW_c = 0.5 mg/L (Hart et al. 1987a)

RW = 1527 mm/year (Chiew and Wang 1999)

GW_c = 4.23 mg/L (ERA 2005)

GW = groundwater recharge to be estimated

SR_c = (0.5 + 0.016) mg/L

The groundwater recharge to be estimated becomes 134 mm/year that is 9% of the annual rainfall.

5.3.4. Recharge Estimation by Extraction of Seasonality from GWLs

To obtain an estimate of groundwater recharge by performing an appropriate exploratory analysis of hydrologic time series data of net flux and groundwater level, the classical decomposition (Brockwell and Davis 2002) technique is selected to estimate the seasonal components of the two time series. The scientific basis behind selecting this method of obtaining the seasonal component of any hydrologic time series data is discussed in Chapter 6.

The time series analysis result for a cycle of twelve months is presented in Figure 5.26. The GWL values are the decomposed seasonal components estimated from the transformation of the monthly GWL elevation data by classical decomposition procedure. The result is similar to that of Table 5.9. Hence, these values are considered for recharge estimation.

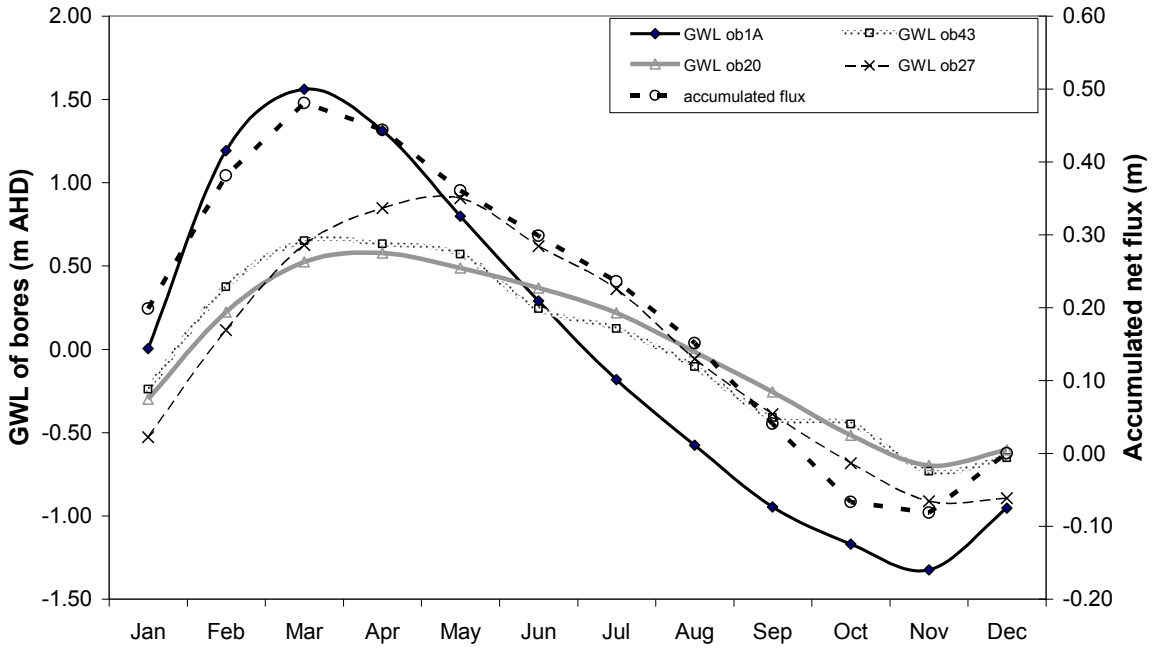

Figure 5.26 After classical decomposition of time series of GWL elevation of different bores, the seasonal components are plotted for a cycle of twelve months

The seasonal components' values of the groundwater level data of bore OB1A and monthly net flux data after performing classical decomposition are demonstrated in Table 5.22.

Table 5.22 The accumulated values of the seasonal components of monthly (accumulated) flux and seasonal components of groundwater levels of ob1A (GWL ob1A) for the respective months

Month	Net flux (mm)	Accumulated net flux (mm)	GWL ob1A (mm)
Jan	198	198	4
Feb	183	381	1192
Mar	100	481	1560
Apr	-37	444	1312
May	-83	361	797
Jun	-62	299	289
Jul	-63	236	-182
Aug	-84	151	-577
Sep	-111	40	-947
Oct	-107	-67	-1170
Nov	-15	-82	-1324
Dec	82	0	-954

The accumulated flux values are the summation of net flux values. The scatter plot of GWL with respect to accumulated flux is illustrated in Figure 5.27.

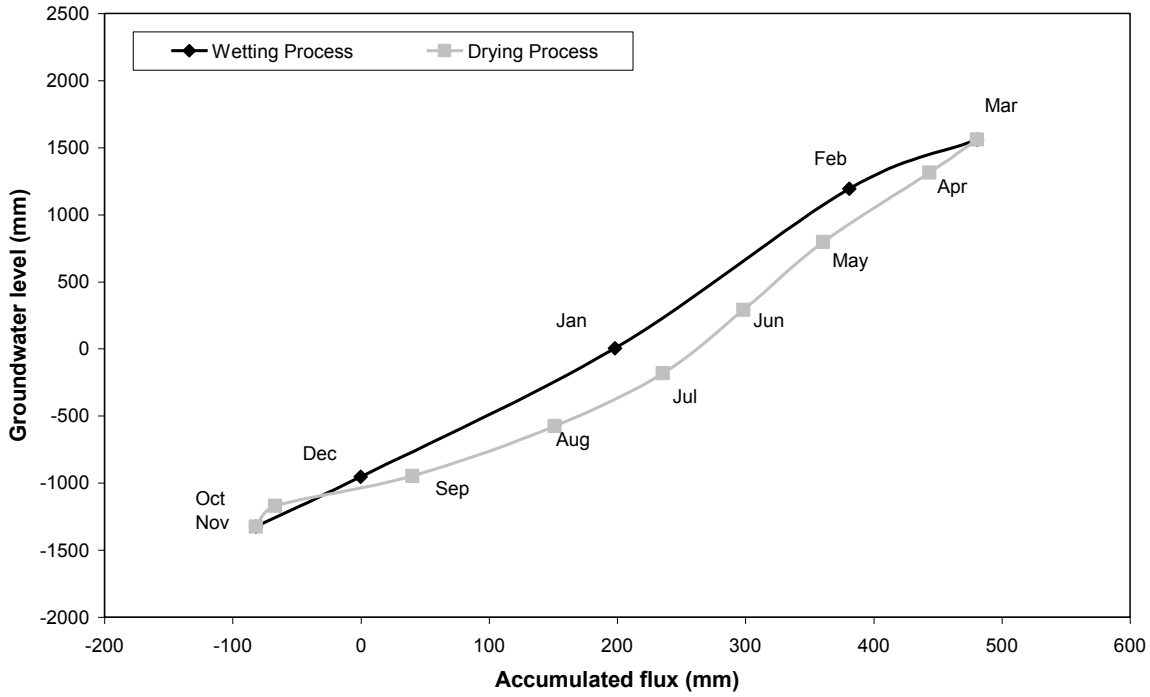

Figure 5.27 The seasonal components of monthly flux added consecutively from January to obtain the accumulated flux along the X axis and groundwater level along the Y axis. The rise in the graph starts in November and ends at March, the fall in the graph starts in April and ends in October

The line demonstrates the annual fluctuation of groundwater level to be 1560 mm to -1324 mm and the accumulated net flux range to be 481 mm to -82 mm. (1560-[-1324]) = 2884 mm of annual fluctuation of groundwater level is found in the analysis. Assuming 10% effective porosity, the annual recharge is estimated to be 288.4 mm. If other bores such as OB20 with annual GWLs fluctuation of 1280 mm, OB27 with 1820 mm and OB43 with 1380 mm are selected, the average value is 1840 mm, as indicated in an earlier section on the correlation model.

The annual fluctuation of groundwater level is comparable with Vardavas (1988; 1993), who estimates an average seasonal variation of in the water table of approximately 4 m and also refers to the regional estimate of 3 to 5 m provided by Ahmad and Green (1986). The lower value of negative accumulated flux results from the limited evapotranspiration during the dry season and higher value of positive accumulated flux results from relatively unbounded rainfall value. Thus, it is clear that a more variable climate would cause a higher fluctuation of the groundwater level.

5.3.5. Summary of Recharge Estimates

The estimates of recharge by the correlation method, water balance method, chloride balance method and extraction of seasonal fluctuation of GWLs are compared in this section. The average annual recharge as a per cent of annual rainfall is demonstrated in Table 5.23. These values are much less than 25% of the annual rainfall as conceived in the initial conceptual model, as represented in earlier sections of this chapter. Thus, the groundwater recharge is estimated to be ten to 15% of annual rainfall. The result of AWBM gives the recharge values in the range of 13 to 15% for the other sets of data such as pan evaporation with pan factor or potential evapotranspiration with evapotranspiration ratio

.

Table 5.23 Summary of the average annual recharge estimates

Methods of estimation of recharge	Average annual recharge (mm)	% of average annual rainfall
Correlation model (Observed annual GWLs fluctuation)	209	13
AWBM	297	19.54
Chloride balance model	134	9
Extracted seasonal fluctuation of GWLs (time series)	184	12

The estimation by correlation method and DBM is based on 10% porosity. It should be mentioned that the use of 5% porosity at the regional scale may be found in Vardavas (1993). Secondary porosity exists in the region and thus a consideration of 10% porosity is reasonable.

Vardavas (1993) finds the 3 m variations of observed head between dry and wet season. He uses the groundwater level in the bore RN20383 located 1 km downstream of Coonjimba billabong. He analysed the data of 1980–1981, 1981–1992, 1982–1983, and 1983–1984. He suggests that with an effective porosity of 5%, 3 m annual variation in the observation bore head is consistent with the soil store capacity of 200 mm predicted by the daily rainfall-runoff model of Magela Creek (Vardavas 1988). Thus, the amount of rainfall that

is required to recharge the groundwater store over the wet-dry seasonal cycle is approximately 150 mm/year.

The use of various recharge estimation methods results in various ranges of values. For example, in the investigation by Risser et al. (2009), the investigators found the annual groundwater recharge to vary between 229 and 357 mm. This was 45% of the mean of all their estimates while they were using 1994 to 2001 data for two locations in east central Pennsylvania, US and used four methods of estimation. Sibanda et al. (2009) use the chloride mass balance method, water table fluctuation method, Darcian flownet method, ^{14}C age dating method and groundwater modelling where the recharge values were 19–62 mm/year, 2–50 mm/year, 16–28 mm/year, 22–25 mm/year and 11–26 mm/year respectively for a semi-arid area of Nyamandhlovu in Zimbabwe. Therefore, the ranges of fluctuation with regard to estimated recharge values as found in the present investigation are reasonably accurate. This acceptance also establishes the representativeness of net flux to be worth a single significant flow component caused by climate to the groundwater system.

5.4. Verification with Previous Investigations by DBM

Some previous investigations in relation to the water balance components are considered in this section to build a stronger basis for the use of net flux as the single significant flow component to the groundwater response model. It should be mentioned that the water balance components estimated by AWBM have been verified with those of previous studies in Section 5.3.2. The key hydrologic components analysed in AWBM were daily data-based analysis. In this section, rainfall, evapotranspiration, runoff, soil moisture storage (unsaturated conditions) and groundwater recharge are considered in long-term monthly-based estimated values. Therefore, it may be considered a more lumped representation than that of AWBM. The AWBM does not use any GWLs data and the record is from 1971 to 2005. However, in this monthly data-based mechanistic (DBM) model, the monitored groundwater level data is also considered, its monitoring period commences in 1980. Therefore, the period of analyses is 1980 to 2005.

5.4.1. Comparison of Key Flow Components

Monthly rainfall and evapotranspiration: The monthly rainfall, evapotranspiration and net flux are plotted in Figure 5.28. It can be observed that there is a positive correlation

between rainfall and evapotranspiration. The historical estimates of monthly AAET and measured rainfall data are analysed in Figure 5.29. Similar results are reported by the previous investigation (Chiew and Wang 1999) and have been reported in Section 3.2 and Figure 3.6. The variability of annual rainfall among the existing weather stations in the Top End of Australia is consistent (Chiew and Wang 1999). However, the variability of monthly rainfall is very high and that of AAET is relatively small. The AAET values are estimated and rainfall values are measured. Therefore, in the present context of analyses, the event of rainfall is relatively independent whereas the process of AAET is relatively dependent on many other factors.

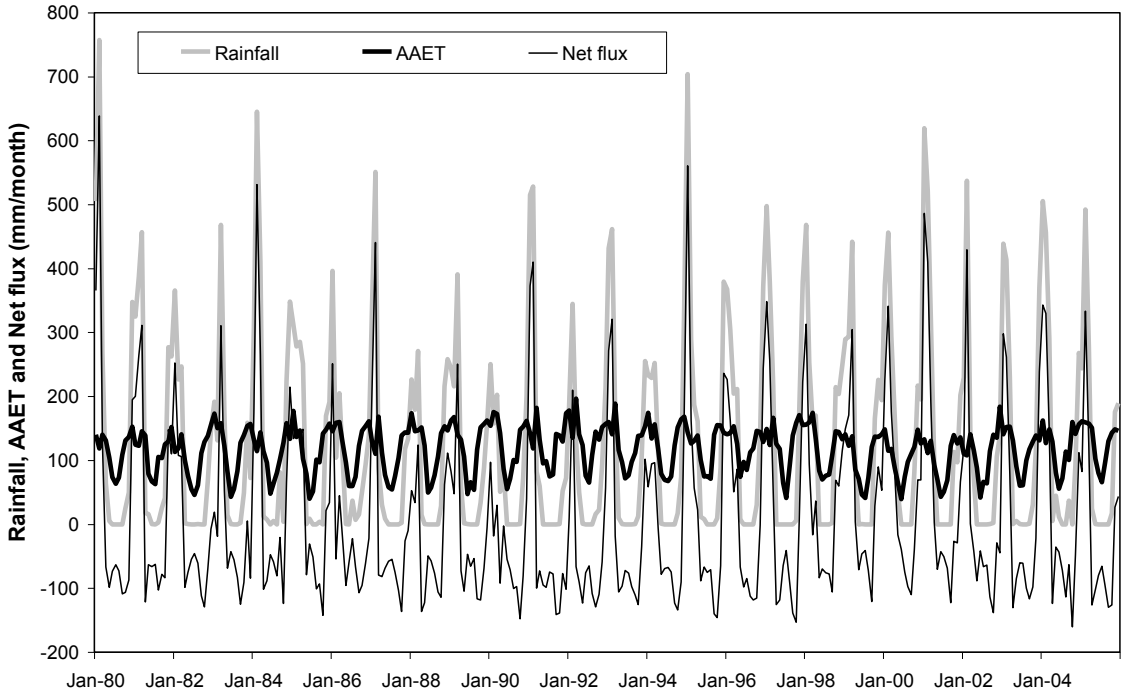

Figure 5.28 Average (1980–2005) monthly rainfall, AAET and net flux in the site

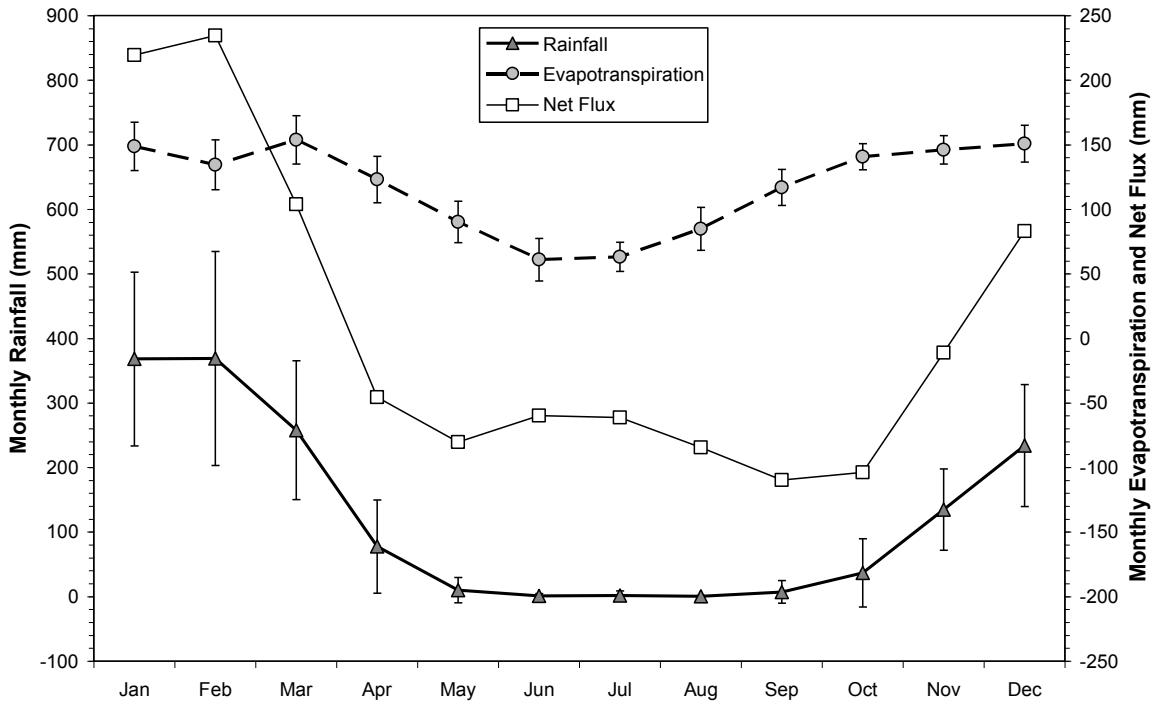

Figure 5.29 Mean monthly rainfall, evapotranspiration and net flux with standard deviations of rainfall and evapotranspiration

The monthly average rainfall values are close to the previously reported values of Chiew and Wang (1999), and Vardavas (1989). Figure 5.29 illustrates the typical climate for the region in terms of AAET of SILO 2006 data as summarised in Table 5.24. Using the latest available AAET estimates of Morton from SILO in contrast to map evapotranspiration or other estimates of evapotranspiration, a better consistency has been attained between the other components of hydrologic cycle such as runoff, soil moisture and lateral subsurface flow, which are discussed later.

Table 5.24 Typical climate at the Ranger site from 2006 SILO data

Months or seasons	Annual rainfall (mm)		AAET(mm) from SILO 2006
November–April	1498	96% of annual rainfall	857 (57% of annual rainfall)
May–October		4% of annual rainfall	557 (37% of annual rainfall)

Verification of runoff generation: The monthly average rainfall and evapotranspiration are represented in Figure 5.30 as a scatter plot with the name of the months indicating the wetting and drying processes. It is assumed that the rainfall comes in as soil moisture and goes out as evapotranspiration. The amount of rainfall is less than evapotranspiration at the

starting months of the wet season. Rainfall then increases and becomes equal to evapotranspiration. When the rainfall exceeds evapotranspiration, runoff is generated. It is assumed that when rainfall is equal to evapotranspiration, the soil moisture storage capacity of the region has been filled.

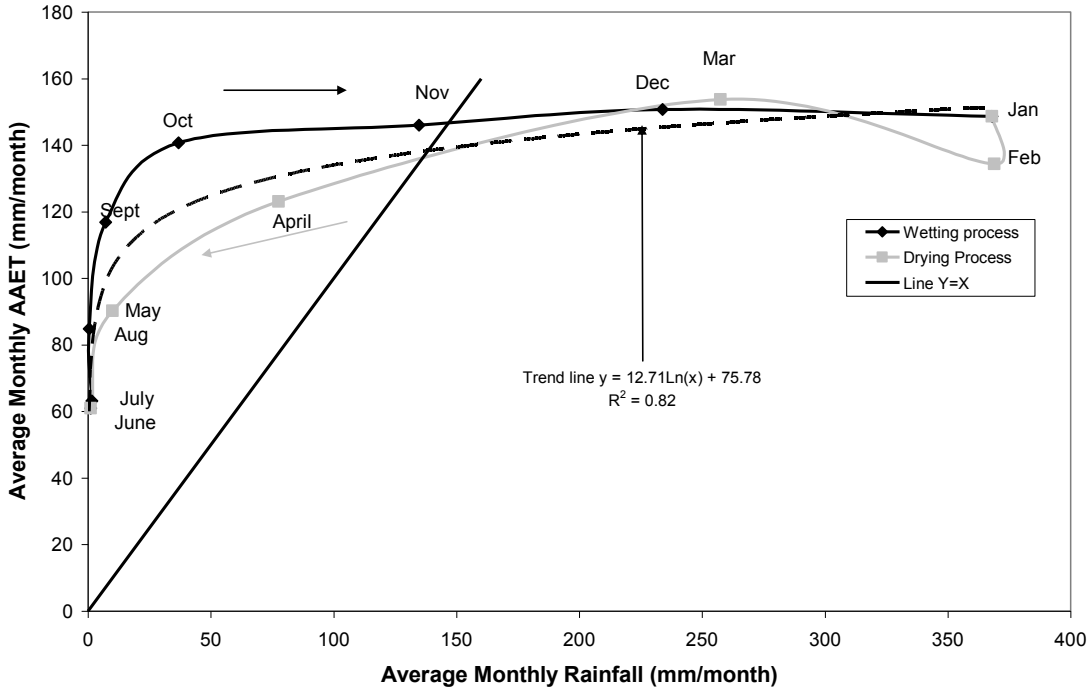

Figure 5.30 The monthly average evapotranspiration as a function of monthly average rainfall and the distinct processes of wetting and drying showing the non-unique relationship between rainfall and evapotranspiration

Therefore, the equation y = x is combined with the best-fit trend line and solved for the value of x. Here, 'x' represents the monthly rainfall; 'y' represents the monthly evapotranspiration. The rainfall required to achieve the condition of equilibrium, meaning 'rain = evapotranspiration', is approximately 140 mm. This value can also be obtained by geometrically drawing a line Y = X or algebraically solving the equation of trend line as X = 1271 ln (X) + 75.78 for the value of X.

Hence, the months that receive this amount of rainfall or higher are November, December, January, February and March, the wet season months of the year. During these months, runoff is expected to be generated. This timing of runoff generation can be compared with

the observed runoff data in a stream flow measuring station downstream of the site (see Figure 5.4).

The accumulated rainfall up to this point in the year includes the rainfall of September, October and November, which makes a value of (7+37+135) 179 mm. This value is comparable to the requirement of containment of first runoff of the wet season to prevent the waste from travelling beyond the site. That particular value is 200 mm of rainfall, as reported by Vardavas (1991; 1993), which needs to be contained so runoff with the waste does not spread across the boundary.

Vardavas and Cannon (1991) demonstrated that for all wet seasons during 1978–1979 and 1985–86, there was little catchment runoff until the cumulative rainfall exceeded 200 mm. The same amount of soil storage was found at the end of dry season. Vardavas (1993) also refers to the prediction of soil store capacity by the daily rainfall-runoff model for Magela Creek to be same. Thus, from this analysis, the generation of runoff for saturated soil moisture leads to the accumulated rainfall of 180 to 200 mm, starting in the wet season (September, October and November).

Verification of Morton's AAET, APET, and PPET relationship: The shape of the lines in Figure 5.30 is similar to the representation of AAET and APET during dry and wet conditions as described by Morton (1983). During the driest part of the year, the soil moisture supports average monthly evapotranspiration of at least 75 mm per month. During the wet season, the average monthly evapotranspiration become constant at 140 to 150 mm per month, which is twice the dry season value. From the theoretical consideration, this is the condition when AAET, PPET and APET are all equal and the complementary equation of AAET + PPET = 2 APET is fully satisfied. Figure 5.31 represents the theoretical lines and computed points of the relationship between AAET, PPET and APET of Morton. This is a verification of authenticity of SILO, incorporating the complementary equation while estimating the three variables of evapotranspiration.

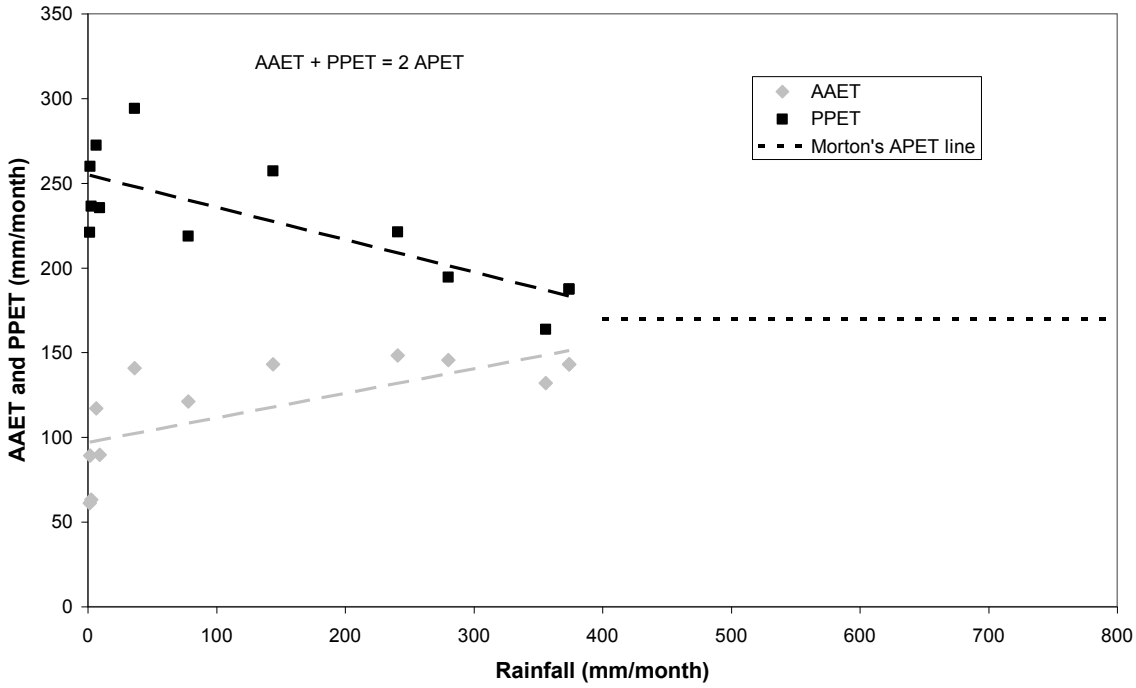

Figure 5.31 Average monthly AAET and PPET values in relation to Morton's APET line

5.4.2. Dynamics of the Hydro-climatic Relationship

Rainfall and evapotranspiration relationship: The non-unique relationship between rainfall and AAET during drying and wetting processes is discussed in this section. The underlying physical processes are considered a function of soil moisture content and corresponding hydraulic property.

October/November: After a dry spell, underlying soil is unsaturated, the deep percolation rate is small and the available soil moisture supports higher evapotranspiration. During the initial stage of the wet season, the evapotranspiration is near the potential value. The evapotranspiration is greater than rainfall because the surface store is evaporated instantaneously; water cannot easily infiltrate into unsaturated soil.

April/May: After a wet spell, underlying soil is saturated, the deep percolation rate is bigger and less soil moisture exists for evapotranspiration. In the final stage of the wet season, the evapotranspiration is also greater than rainfall due to the available soil moisture and elevated groundwater table.

As shown in Figure 5.30, evapotranspiration during the wet season reduces in the month of February. Three probable reasons have been established for the reduced AAET in February:

- The duration of February is shorter than that of January or March. Thus, the monthly value is reduced by a factor of 28.25/31 on average.
- The condition of saturation exists throughout the depth. The wet season causes the underlying soil to be saturated. Saturation causes higher hydraulic conductivity of the soil. Hence, a higher rate of deep percolation occurs and less water is available for evapotranspiration.
- Increased humidity and cloudiness and reduced solar radiation causes less evapotranspiration. The maximum relative humidity occurs in the month of February in the region (Press *et al.* 1995). Moreover, the inverse relationship between rainfall and evaporation has been addressed previously by many investigators for this particular site.

After the saturation level reaches a higher elevation, moisture is again available and evapotranspiration rises during March.

As shown in Figure 5.4, from July to October, the monthly rainfall increase is (37 – 2) = 35 mm but the monthly evapotranspiration increase is (141 – 63) = 78 mm. Hence, during this period of the dry season, approximately 40 mm of water has been supplied for evapotranspiration and sourced from soil moisture through internal flow. By this process, the groundwater table decreases in November. This soil moisture contributes to evapotranspiration from July to October, which makes the slope of evapotranspiration line sharper than that of the rainfall line.

In the early dry season, the reverse occurs. From April, the slope of the evapotranspiration line is flatter (123 – 61) = 62 mm for two months and the slope of the rainfall line is sharper (78 – 1) = 77 mm in the same period of two months. The soil moisture with higher groundwater level is the source of water for evapotranspiration during that time. It is clear that the soil moisture keeps the evapotranspiration rate steadier during the drying phase and makes the evapotranspiration rate higher than available rainfall during the start of wetting phase.

The variation of the rate of evapotranspiration during the drying phase has also been specifically addressed and represented by Vardavas (1988). In the initial part of the dry season (April–May), the rate of evapotranspiration is defined by equation (a) but in the middle of the dry season (June–July), the rate of evapotranspiration is defined by equation (b) as shown below. During the final period of the dry season, when the soil is unsaturated, all of the pre-monsoon rainwater is available to be evaporated.

From the relative comparison between the two equations, it can be easily perceived that the rate of evapotranspiration is higher during the initial period of the dry season, is relatively smaller during the middle of the dry season and is higher again at the end of the dry season:

Equation (a) = > $E_T = ES/S_m$

Equation (b) = > $E_T = EG/(G_m+S_m)$

where E_T is the rate of evapotranspiration, E is the rate of potential evaporation, S is the soil store, S_m is the saturation soil store capacity (range of variation 100-300 mm), G is the groundwater store and G_m is the groundwater store capacity (range of variation 500–2000 mm). In this model, the soil store and groundwater store are considered the two-layered subsurface system. Therefore, the variation of the rainfall AAET relation exists during the wet and dry seasons, which can be explained with the underlying configuration of the transient soil hydraulic property.

Rainfall and runoff relationship: The hydrographs of monthly average rainfall, AAET and runoff are shown in Figure 5.4. The average monthly net flux, computed as an algebraic summation of rainfall and AAET, is plotted along the vertical axis and the runoff is plotted along the horizontal axis in Figure 5.32. The sequence of wetting and drying processes are illustrated by joining the monthly points in the graph.

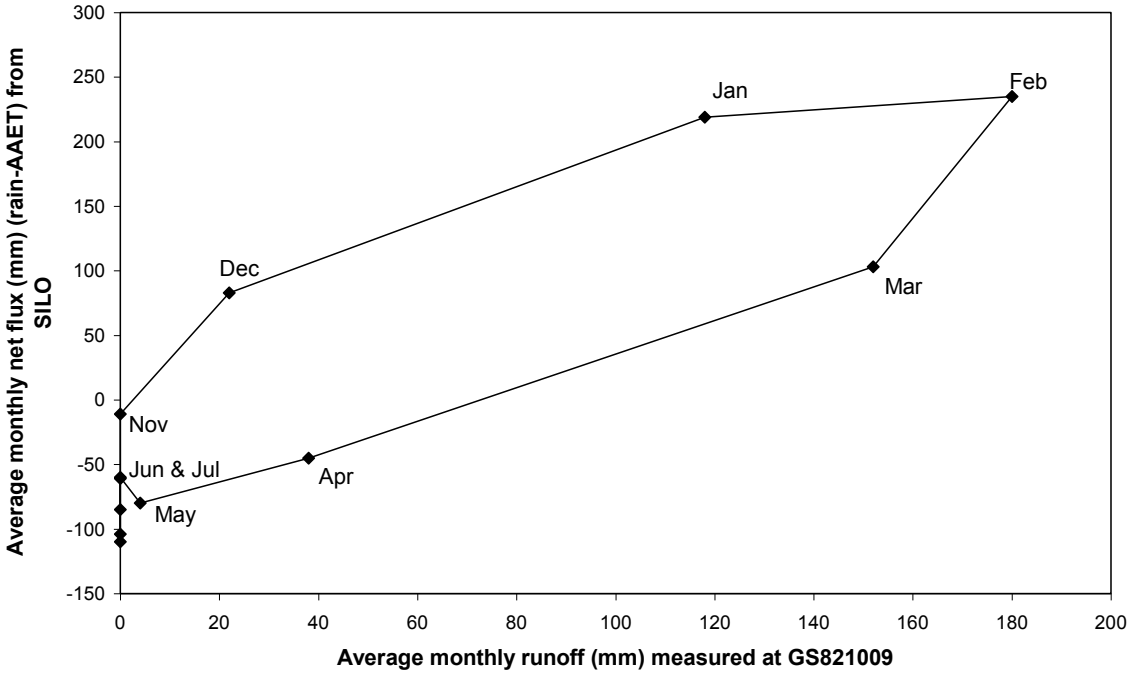

Figure 5.32 The typical wetting and drying phases in the scatter plot of the inflow and outflow data points analogous to the water budget model result (Vardavas 1989)

The loop of wetting and drying processes was demonstrated by plotting the stage discharge relationship that resulted for the same catchment, as illustrated by Vardavas (1989). The analogy can be drawn between the loop of the rating curve and that in the net flux-runoff scatter plot. In the study conducted by Vardavas over four wet seasons: 1974–1975, 1977–1978, 1980–1981 and 1983–1984, the inflow point was the GS821009 and the outflow point was GS21019. The concepts of the distinct processes of wetting and drying in the soil of the wet and dry tropic near the Ranger uranium mine were demonstrated. A similar loop of wetting and drying is demonstrated by plotting the rainfall component contributing to runoff and measured runoff at the station (see Figure 5.32).

The positive net flux starts in December when runoff also commences. The negative net flux starts in April but the runoff continues for another two months. It can be assumed that the summation of the runoff (514 mm) is represented by the summation of positive net fluxes (640 mm) or summation of negative net fluxes (-556 mm).

During the wetting time, a significant amount of water from rainfall is lost into unsaturated soil of the catchment from U/S point to D/S point. Therefore, the X values are less than Y values, i.e. the rainfall does not generate runoff. During drying time, water is not lost into

soil, as a saturated condition prevails. Runoff is generated from soil storage even if there is no rainfall.

The small catchment of present research at the Ranger Uranium Mine (RUM) site is much smaller than the catchment considered by Vardavas. It is also located downstream of the sub-catchment of the RUM site under consideration. However, the typical phenomenon of wetting and drying are clearly represented in the present work in spite of the smaller scale.

5.5. Proposed Hydrologic Model

The difference in physical processes that occur during the wetting months and drying months in light of the DPC (Grayson and Bloschl 2000a; Grayson and Bloschl 2000b; Woods 2002) have been elaborated by considering the work of Vardavas (1987; 1988; 1989; 1993) in parallel to the current data-based approach. The annual water balance has been revised (see Figures 5.33 and 5.34) to improve the conceptual model, which will be used in physically-based unsaturated flow modelling for predicting the long-term response of groundwater. The runoff coefficient is revised as being 30 to 35% instead of 25% as in the preconceived model. The positive net flux (640 mm) or negative net flux (-556 mm) or runoff (514 mm) (considering the rainfall AAET runoff relationship) is therefore approximately 35% of annual rainfall. This 35% of rainfall is the source for runoff during the wet season; it is stored in soil storage and is the source of evapotranspiration during the dry season. The 100% rainfall occurs in the wet season and wet season AAET is 55%. The water infiltrated from rainfall during the wet season is 65%. Thus, 10% is deep percolated to GW. This 10 to 15% GW recharge and 30 to 35% soil storage makes 40% AAET during the dry season. In general, it can be concluded that the annual recharge in the region is in the range of 10 to 15% of annual rainfall based on 10% effective porosity. If porosity is larger, the recharge is larger also.

Incorporating longer periods of historical data in the DBM means the underlying hydrologic processes are better understood. Most of the results are consistent with the prior investigators in the region.

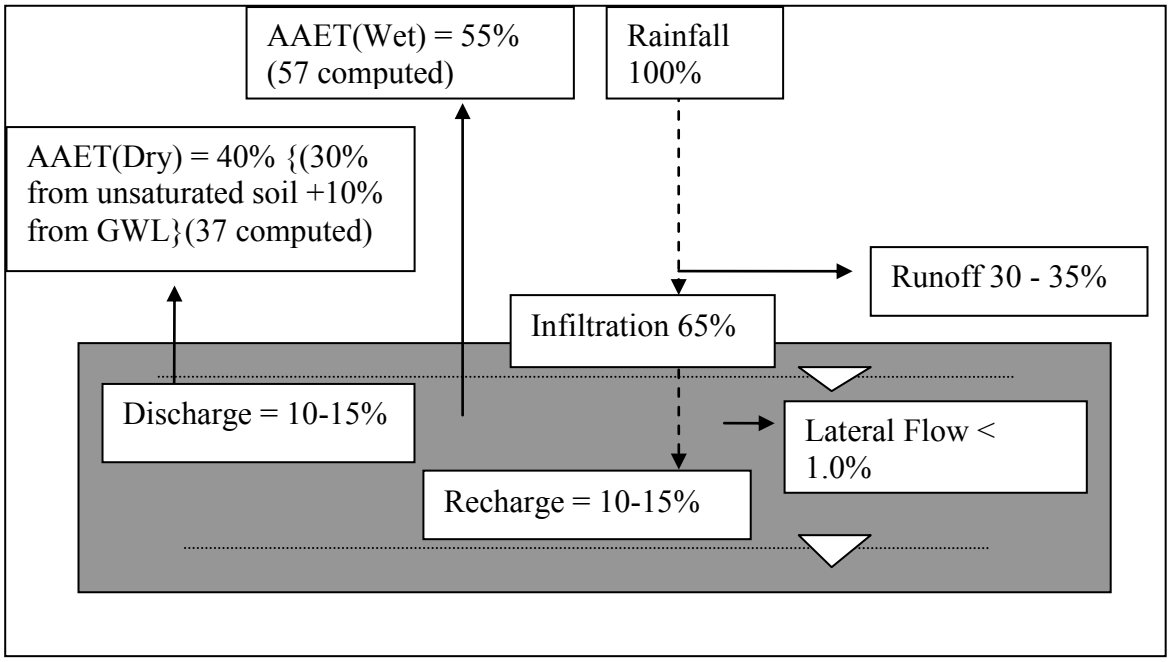

Figure 5.33 Revised conceptual model of the hydrologic processes of the region (seasonal)

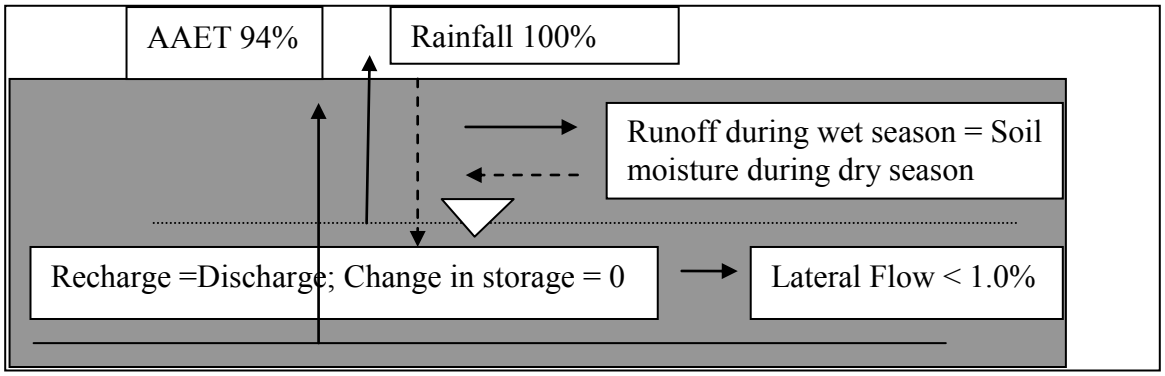

Figure 5.34 Revised conceptual model of the hydrologic processes of the region (annual)

5.6. Conclusion

In this chapter, the selection of net flux for representing the influence of climate on the groundwater system has been justified by addressing the physical processes from multiple perspectives. The selected net flux is used as the key variable both in physical and non-physical process-based modelling. Recharge estimation has been conducted using various techniques and a modified conceptual model is proposed based on the recharge estimates and verification with previous investigations in the relevant field for the site.

With this achievement, the physically-based unsaturated flow model Seep/W for the site will be developed. The input into the Seep/W model is given as monthly net flux and the

monthly groundwater level elevations are obtained as output. The time series technique, which is a special type of data-based modelling approach, conventionally used for the forecast of hydrologic processes, is applied to the historical time-series data of monthly net flux and GWLs. The time series analysis techniques described in the following chapter are used in multiple approaches, such as understanding the mechanism of groundwater responses with climate, representing the system with historical data of net flux and GWLs at a multi-decadal time scale, and predicting the responses at the centurial time scale.

6. Time Series Modelling

This chapter builds upon previous work in the region by applying time series statistical methods to groundwater-climate relationships. The outcome is an ability to understand the degree of dependency between these two sets of variables and future prediction of groundwater by using climatic data.

The statistical techniques are used to explain some of the significant physical processes. The significance of unsaturated thickness in the relationship of net flux and GWLs is analysed with the help of classical decomposition transformation, which separates the trend and seasonal component of the processes. Identification of the predictor is also selected by building a number of models with varied climatic variables such as rainfall series and net flux series. A number of time series models are also investigated to represent and predict the long-term response of the groundwater-climate relationship. The estimated parameters (such as Phi values of MAR models) are examined to explain the physical significance of the representation of the processes.

Some important concepts relevant to the time-series statistics incorporated in hydrological studies are reviewed Chapter 2. In this chapter, the various approaches to the application of time series statistics to the exploration, representation and prediction of the physical processes are analysed. By analysing the various issues such as model fitness, physical representativeness, and computational efficiency, the best model with the best variable as a predictor for further modelling are suggested in this chapter.

6.1. Motivation

In the 1980s, time series analysis was introduced in groundwater modelling. Adamowski and Hamory (1983) analysed groundwater level fluctuations predominantly affected by stream flow. There are many instances of this kind involving specific time series modelling techniques such as the ARMA mode and Transfer Function Noise (TFN) models (Parlange et al. 1992).

The real time data of the climate and groundwater levels in the research site show strong seasonality, which is typical for a tropical climate. Given the available monthly record of these hydro-geologic variables at a multi-decadal time scale, time series modelling is

chosen as an additional method of investigation and prediction for the groundwater-climate relationship. The exploration of the physical processes builds the sound basis of performing groundwater modelling. Prediction by the time series supports and complements the predictions from the groundwater models in terms of the range of uncertainty of the long-term predictions. The approach of physical process-based modelling involves downscaling. To combine this approach with upscaling (Gupta *et al.* 1986), a time series prediction technique that is based on non-physical or statistical process is employed.

6.2. Application of Time Series Technique

Numerous methods exist in the realm of time series process representation. When selecting the appropriate time series technique in representation of the process, the first step is to perform exploratory analyses. In exploratory data analysis, simple graphical methods are used to uncover the basic statistical characteristics of the data. In the confirmatory analysis, an appropriate time series model or group of models are constructed for process representation and prediction. Exploratory data analyses have been performed by Tukey (1977). According to the author, to learn about data analysis, it is right that everyone should try many things that do not work—that to tackle more problems than making expert analyses at the first instance of investigation. In the process of exploratory analyses, new understandings have arisen, which contribute to subsequent decisions regarding the technique selection. Thus, the selection of the time series technique for forecasting has to be justified by the sequence of the exploratory analyses and subsequent understanding. It is imperative that a reasonable basis exists to justify the application of the particular technique in place.

6.2.1. Selection of Technique

The identification of the technique of analysis is primarily because the present research work considers hydrogeologic parameters, which are obviously varying in the space and time domains. Hence, the exploratory and confirmatory data analyses are necessary for understanding the processes and answering the future responses with regard to the changing environment. The task is not straightforward at its initial stage, as the technique seems increasingly different with the knowledge learnt from the application of different techniques. In the following section, the identification of appropriate variables for the various models are performed by conducting some physically-based computations. Various

exploratory analyses are then elaborated for a deeper understanding of the physical processes and the application of time series modelling for representation and forecast.

6.2.2. Identification of Variable

To select a suitable set of variables representing the groundwater-climate relationship, a number of methods are reviewed in the previous chapters and a number of analyses are conducted in this chapter. The selection of an exogenous variable as climate and an endogenous variable as GWLs must be specified in terms of numeric data of the hydrologic processes. The rainfall and evapotranspiration are the two significant hydrologic processes as has been established previously. Measured rainfall data is available; however, because of a lack of information about soil moisture and the plant groundwater usage, it becomes very difficult to use evapotranspiration data as an outflow of water from the system for the analysis. However, the selection of SILO AAET has been well documented in Chapter 5, in which other possible sources of the evapotranspiration data are compared in relation to their capacity to explain water balance in the region at a varied time scale. Given the information, the reliable data that are decided to be useful are rainfall and groundwater levels and SILO AAET. Therefore, it is assumed an exogenous variable is related to climate, such as monthly rainfall and monthly net flux, which is the algebraic summation of rainfall, AAET and accumulated net flux.

The physical significance of net flux is much better than that of rainfall, as net flux represents both positive and negative flow of water while rainfall represents only positive flow. Therefore, net flux is selected to be a better predictor than rainfall. To obtain more confidence in selecting the net flux, the prediction performance of both predictors (rainfall and net flux) have been investigated in Section 6.6.2.

The endogenous variable is related to GWLs and monthly changes of GWL. An endogenous variable is selected based on the statistical performance of the two time series, such as monthly GWLs time series and time series of monthly changes of GWLs. From the water balance equation, the climatic net flux, which is a flow of water per unit time, should be correlated to the change of storage in the soil. Therefore, if the monthly net flux time series is an exogenous variable in a model, the time series of monthly change of GWLs should be an endogenous variable. However, models built on net flux *versus* GWLs perform better that the models built on net flux *versus* change of GWLs. A stronger

association is found between net flux and GWLs time series and less association with change of GWLs time series. Therefore, the time series of GWLs is selected as the endogenous variable for the study.

In multiple regression models, a third category variable representing the antecedent soil storage is used, which is called an intermediate variable. Ideally, the soil storage capacity influences the wetting-drying process both ways. Hence, soil storage influences net flux and GWLs. However, for simplicity, it is considered to be in the cause component of the process and effect component is neglected. The antecedent available soil storage and quantification of this parameter is ideally subjected to two variables: unsaturated thickness and available storage capacity of soil. However, for simplicity of the representation, the antecedent soil storage is represented by only the numerical value of the depth of unsaturated soil of the antecedent time step.

6.3. Exploratory Analyses

Based on the understanding of the physical processes, the possibility of identifying a long-term trend in GWL data is investigated. The trend in GWL data might be caused by mining activities including a rising trend caused by seepage from ponding of process water in the retention ponds, falling trend caused by excavation in the mining pits, or naturally, by climatic variations.

The trend line analyses using Microsoft Excel is performed to isolate impacted bores from unimpacted bores by the mining activities. The trend in the past climate is also plotted to compare the similarity of GWL graphs of the bores with climate. By using a simple visual assessment of the graphical plots of the GWL data, the bores with maximum range of missing data and mining impacts are excluded for further analyses. The responses of all the bores' GWLs are plotted in Appendix F. The bores selected for time series analyses are OB1A, OB20, OB27 and OB43. The location of OB27 is farthest from the structural features of the site; this bore is selected even though it has missing data for a few years. However, for obtaining a preliminary idea of the underlying factors influencing the groundwater-climate relationship, some additional exploratory analyses, such as correlation analyses, were performed on all the bores.

The correlation analyses have been performed to establish the cause-effect relationship between climate and groundwater as described in Chapter 5. To assess the complexity of the influence of geology, nearby features and topography on the timing of the response of different bores with the same net flux data, lag analyses are performed. Lag here refers to the time gap between peak net flux and peak GWL. For example, the five bores located within a distance of 1 km show significant variation in the magnitude of annual fluctuation of GWLs and lag (see Figure 6.1). Yesertener (2005) also showed similar amounts of lag between climate (Cumulative Deviation from Mean Rainfall, (CDMR)) and groundwater levels with the bore PM3 (see Figure 6.2).

OB1A and OB2A responses are similar, such as having approximately 4 m fluctuation and quicker response with net flux. Those of OB19A and OB34 are also similar (2 m fluctuation and quicker response); however, OB34 is different (1 m fluctuation and slower response). The annual fluctuation and the lag are different for OB34 compared with the other four bores. These complexities of responses of the bores indicate the influence of unsaturated thickness. To explore the complexity with the help of time series analyses, some specific techniques appropriate for hydrological processes are employed herein.

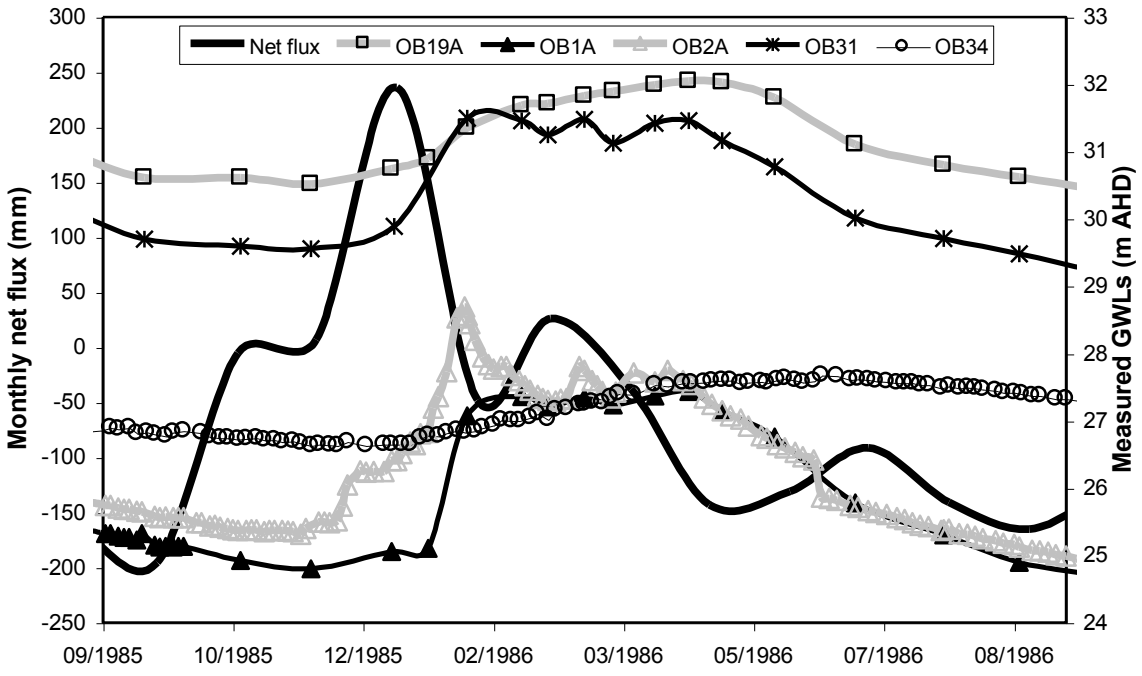

Figure 6.1 Variations in timing and magnitude of GWL responses of a number of bores for the cause of net flux to the system

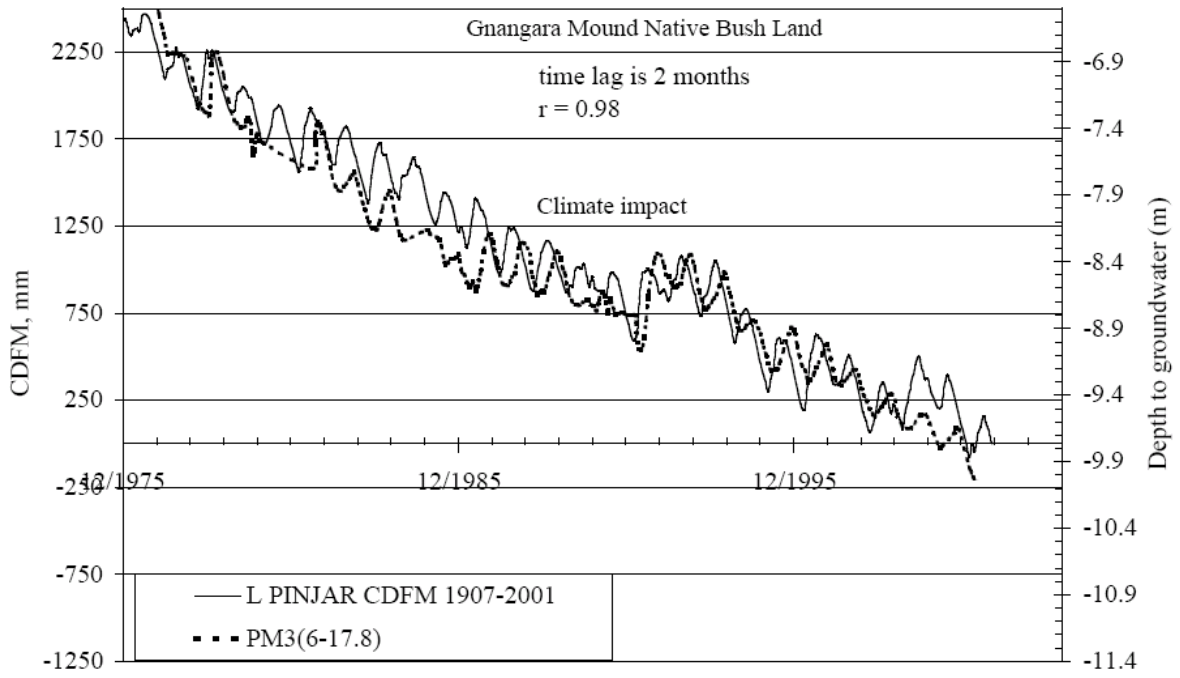

Figure 6.2 Cumulative Deviation from Mean Rainfall (CDMR) graph and declining groundwater levels in bore PM3 (Yesertener 2005)

6.3.1. Identification of Seasonality

As discussed in the description of the site, because of the tropical climate, the historical monthly totals of rainfall, evapotranspiration, AAET, net flux and monthly GWLs are found to be fluctuating in the annual cycle. The clear seasonality in the climate and thus GWLs are prominent. This typical characteristic is exploited in the following section to understand some very important physical relationships between the climate and various bore's GWLs. Four bores have been selected (OB1A, OB20, OB27 and OB43), which are relatively unimpacted by mining activity, have a maximum period of data records and are sparsely located to encompass the whole region of the mining site.

Autocorrelation analyses are performed to identify periodic seasonality in each of the time series data such as net flux and GWL. The various sample size of GWLs of the bores yield various limits of 95% confidence. The Autocorrelation Function (ACF) of net flux and GWLs of all the four bores show significant seasonality with a cycle of twelve months, which is indicated by the number of lags in Figures 6.3 and 6.4.

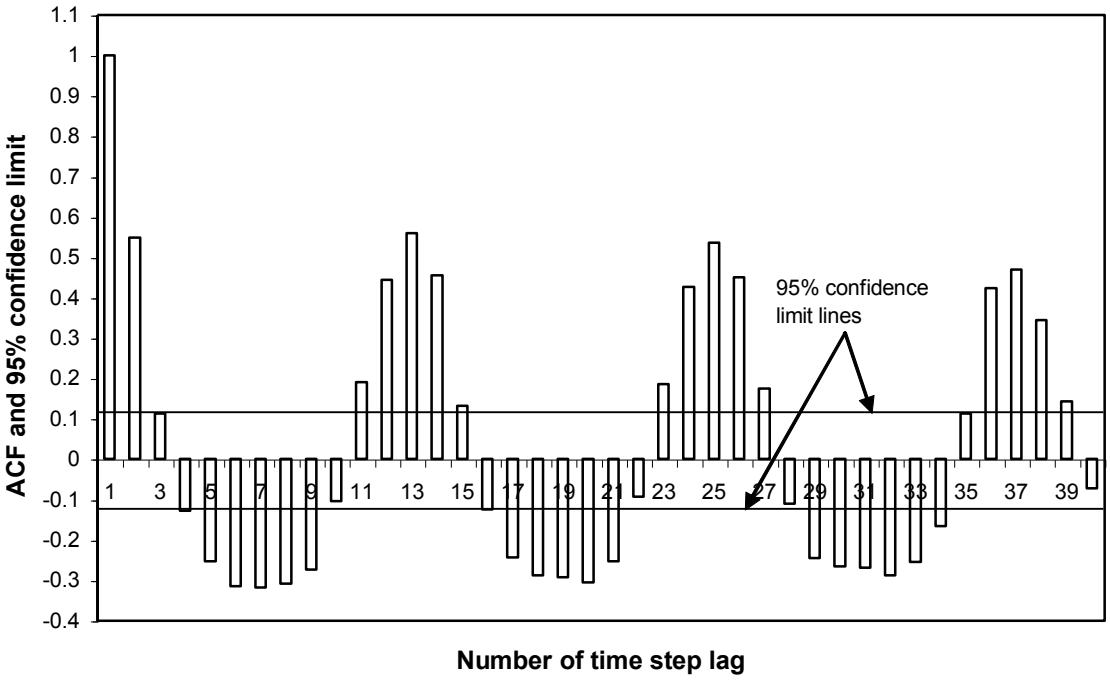

Figure 6.3 ACF of net flux

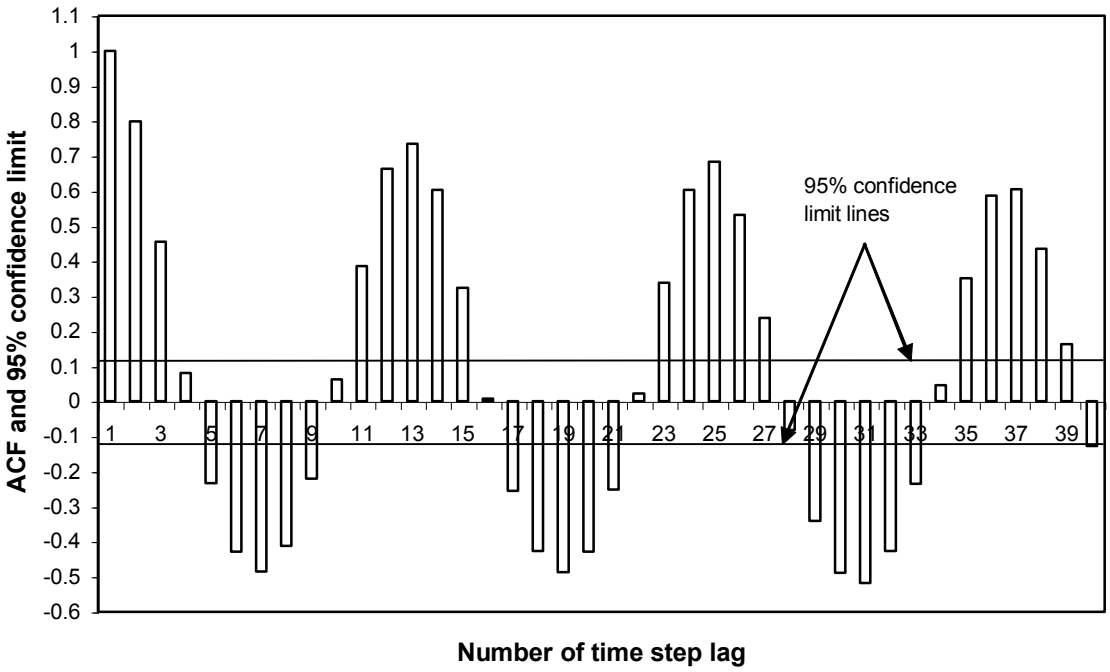

Figure 6.4 ACF of GWLs of bore OB1A

As both net flux and GWLs time series are auto-correlated, this indicates that both series have significant periodic seasonality. The univariate ARMA representation is very much appropriate for these time series. At the same time, the possibility of multivariate AR

representation should be investigated because the underlying physical processes indicate that variation in net flux causes the variation in GWLs. Therefore, cross-correlation analyses are also performed for estimating the statistically significant lag between the net flux and GWL. The significant lag is four to six months for various bores. When similar analyses are conducted for net flux and change of GWLs, the lag is one to two months.

6.3.2. Influence of Unsaturated Thickness

With the assumption that unsaturated thickness of different bores influences the variations of significant lag, some additional analyses were performed. The variable 'unsaturated thickness' is employed to represent the depths of GWLs from ground surface at bore locations. In addition to cross-correlation function (CCF) analyses, a rational distributed lag model was developed by representing the change of GWLs as a function of the previous month's unsaturated thickness and net flux of earlier months. Thus, in the construction of a rational distributed lag model or multiple regression model, the number of lagged net flux time series found to be statistically significant to influence change of GWLs are as shown in Figure 6.5.

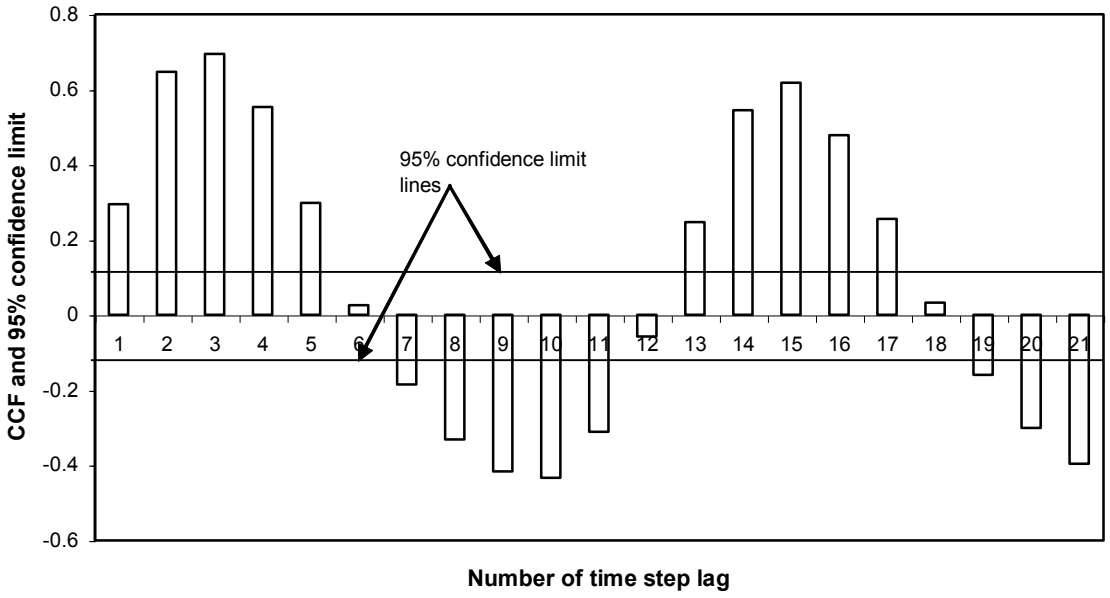

Figure 6.5 CCF for Net flux and GWLs of OB1A. The CCF of GWLs at (t+h) time with net flux at t time. The lag 'h' varies from approximately 1 to 20

The results of multiple regression analyses and CCF analyses are the same with regard to number of months of net flux that influence the change of GWLs of the different bores as shown in Table 6.1.

Table 6.1 Lag between net flux and GWLs, changes in GWLs estimated from CCF analyses and distributed lag models

	Significant lag (months) between net flux and GWLs from CCF analyses	Significant lag (months) between net flux and change in GWLs from CCF analyses	Significant lag (months) between net flux and change in GWLs from rational distributed lag (multiple regression) model
OB1A	4	1	1
OB20	6	2	2
OB27	5	2	2
OB43	5	2	2

The 'Beta' values of multiple regressions for each of these bores are analysed to compare the relative importance of unsaturated thickness on the response of GWLs of different bores. A higher value of 'Beta' of a specific independent variable indicates a stronger relationship of the that independent variable with respect to the other remaining independent variables in a particular set up of multiple regression analysis (Kerr *et al.* 2002). Figure 6.6 illustrates that the value of 'Beta' is highest for the bore OB1A with the smallest unsaturated thickness and lowest for the bore OB27 with largest unsaturated thickness. This indicates that the shallower GWLs are more strongly influenced by net flux than are deeper GWLs.

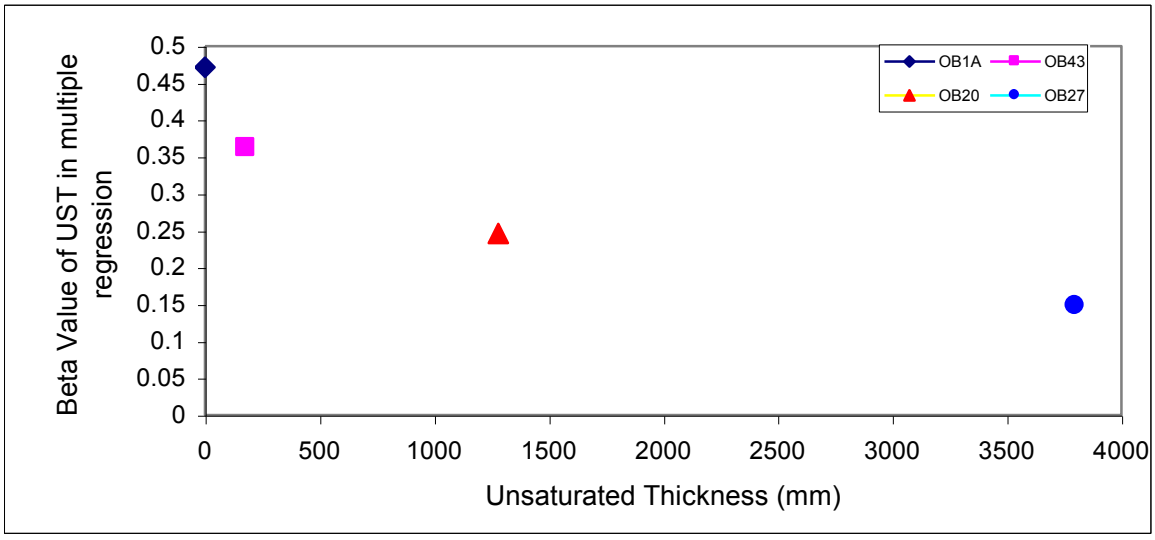

Figure 6.6 The Bete values of unsaturated thickness in multiple regression of various bores

By comparing the signs of regression coefficients of multiple regressions for describing GWLs of OB1A as function of antecedent unsaturated thickness and current months net flux, it has been established that it is negative (-0.83) for antecedent unsaturated thickness and positive (0.372) for net flux, with the R^2 value of 0.765. This is consistent with the relationship shown in Figure 6.6. The Beta value of unsaturated thickness in the multiple regression is given in Table 6.2. This finding contributes to a better understanding of the physical processes that relate the rate of response of GWL to net flux.

Table 6.2 The relationship between unsaturated thickness and Beta value

Bore	Unsaturated thickness (m)	Beta value of UST in multiple regression
OB1A	0	0.471
OB43	0.18	0.362
OB20	1.28	0.246
OB27	3.8	0.148

Due to the presence of a periodic seasonal component being found statistically significant, and to analyse the seasonal components of net flux and GWL time series of a number of bores, transformation is performed using classical decomposition techniques (Brockwell and Davis 2002).

The results of autocorrelation and cross-correlation analyses also formed the basis of selecting a univariate ARMA model for each of the time series and multivariate AR models for net flux-GWL time series for the purpose of representation and forecast of the ongoing processes with specified prediction bounds. In general, the ultimate purpose of the time series analyses is to forecast and control; therefore, the best possible model for this purpose is considered.

Being equipped with the understanding of the underlying physical processes, a special type of multivariate time series model is decided upon, which is similarly efficient both scientifically and computationally to the multivariate AR model. It is the Transfer Function Noise (TFN) model (Brockwell and Davis 2002). The details of most of the techniques and computational performances are described below.

6.3.3. Classical Decomposition for Separation of Seasonality and Trend

Time series analysis performed for computing the seasonal components of hydrologic data can serve as a powerful technique for exploring the physical processes. For hydrologic time series data, which has both the trend and seasonal component embedded within, a specific type of transformation, known as classical decomposition, makes the data zero-mean stationary process (Brockwell and Davis 2002). From the inspection of the graphs of the data, the existence of the trend component, seasonal component and random noise components were realised. The classical decomposition model is a univariate time series model, which is used for the data that contains both long-term trend and seasonality with the random noise. This model is applied to monthly net flux and monthly groundwater level data for the extraction of their seasonal components. Those seasonal components are then analysed to obtain an overall understanding of the probable relationship between the two sets of variables.

Classical decomposition of any time series $\{X_t\}$ is based on the model:

$$X_t = m_t + s_t + A_t \qquad \text{Equation 6.1}$$

where $EA_t = 0, s_{t+d} = s_t, and \sum_{j=1}^{d} s_j = 0$

In Equation 6.1:

X_t= the numerical value of the variable (i.e. monthly net flux and monthly GWL) at time *t,* where *t* varies from 1 to *n*,

m_t= the long-term trend component

s_t = the seasonal component

A_t = the random noise component, which is a zero-mean stationary process

EA_t = the expected value of A_t

d = period of seasonal components

The seasonal component is computed in such a way that with the period length of *d* number of time steps, the values become the same ($s_{t+d} = s_t$). For example, with monthly data, at a 12-time step interval, the seasonal components of the time series are the same. In addition, the algebraic summation of the twelve months seasonal components becomes zero (summation of s_j, where *j* varies from 1 to *d* becomes zero). This requirement

indicates that the seasonal components of net flux and groundwater level comply with the annual water balance.

Observations of monthly net flux values and GWL are available in the record of data source of the research. Either of these two time series is assumed $\{x_1, x_2 \ldots xn\}$. From each of the series, the trend is estimated by applying a moving average filter chosen to eliminate the seasonal component and to reduce the noise. If the period d is even (twelve months) and $d = 2r$, r being the half of the period, then the trend component is estimated $\hat{m}_t$ in the following equation:

$$\hat{m}_t = (0.5x_{t-r} + x_{t-r+1} + \ldots + x_{t+r-1} + 0.5x_{t+r})/d, \text{ where } \quad r < t \le n - r \quad \text{Equation 6.2}$$

The seasonal component is estimated in the next step. For each $k = 1, \ldots, d$, the average of the deviations w_k as $\{(x_{k+cd} - \hat{m}_{k+cd}), \; r < k+cd \le n-r \}$ is computed. Since these average deviations do not necessarily sum to zero, the seasonal component $\hat{s}_k$ is estimated as:

$$\hat{s}_k = w_k - d^{-1}\sum_{i=1}^{d} w_i \text{ , where } k = 1, \ldots, d, \quad \text{Equation 6.3}$$

and $\hat{s}_k = \hat{s}_{k-d}$, $k > d$

These steps of computations are well documented (Brockwell and Davis 2002).

The seasonal components $\hat{s}_k$ of the net flux and groundwater level data are analysed in the following section to explore the significance of unsaturated zone thickness in the relationship of net flux and GWLs.

6.3.4. Result of Classical Decomposition

The seasonal components of monthly net flux and groundwater level data are plotted in sequential order in Figure 6.7. For the groundwater level hydrograph, the peak corresponds to the highest level due to positive flux; the trough corresponds to the lowest level due to negative flux. The lag varies along the year from two to four months. The lag is greater when the groundwater level drops and is smaller when the groundwater level rises. This means that a longer time is required to propagate a longer way for the soil moisture. It is

shown that during the wet season (November to April) the lag is two months (for AA/ January to March) but during the dry season (for BB/ June/July to October) the lag is four months. It has been established that June to July is the driest time by critically examining the result described below. For identification of the driest month, it is seen that the monthly net flux hydrograph has two peaks (January and June/July) and two troughs (May and September) in the cycle of twelve months. The dry season net flux shows the typical fluctuation of a two-trough system.

For the net flux hydrograph, starting from January, the first positive peak corresponds to maximum positive net flux and the first trough corresponds to maximum negative flux after the end of the wet season. The first trough occurs during May when the rainfall is reduced; due to available soil moisture, evapotranspiration attains one maximum, which may be represented as wet environment APET.

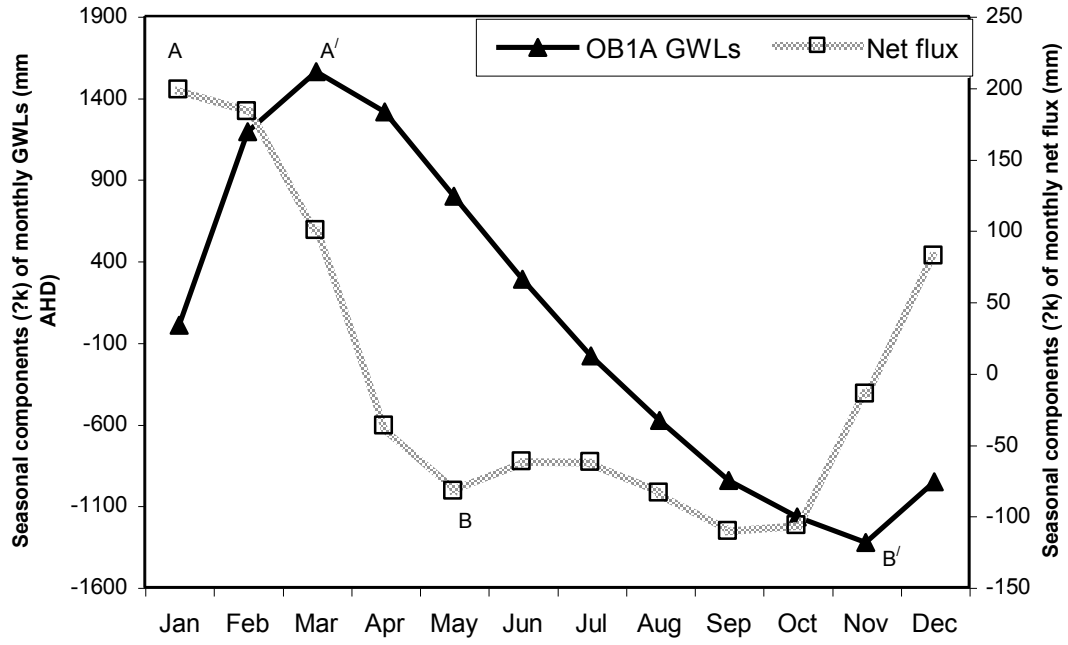

Figure 6.7 Seasonal components of GWLs of OB1A and monthly flux extracted from classical decomposition (Brockwell and Davis 2002)

The second trough occurs during September-October, when the rainfall has started and the evapotranspiration attains its second maximum, with soil moisture being available from the early wet months. This is also the stage of APET. In between these two troughs, there is a very flat peak during June-July, when evapotranspiration is limited due to the minimum soil moisture available, as indicated by AAET in Morton's estimation method of

evapotranspiration as described in Morton (1983). In brief, it can be concluded that, even if the net flux hydrograph is a two-trough system, the time in the middle of the two-trough period represents the driest condition of soil, even evapotranspiration is not at its maximum in its numerical value.

The seasonal components of groundwater levels of multiple bores data have been estimated by classical decomposition. As shown in Figure 6.8, a wide range of variation of annual groundwater levels are found for the different bores with the same net flux. The deepest water levels in bore OB27 respond with a larger lag and shallower water levels in bore OB1A respond quicker. Slimani et al. (2009) have shown the influence of variable thickness of surficial formations on the relationship between the climatic influx and piezometer responses at a multi-decadal time scale in the chalk aquifer of Upper Normandy in France (see Figure 6.9).

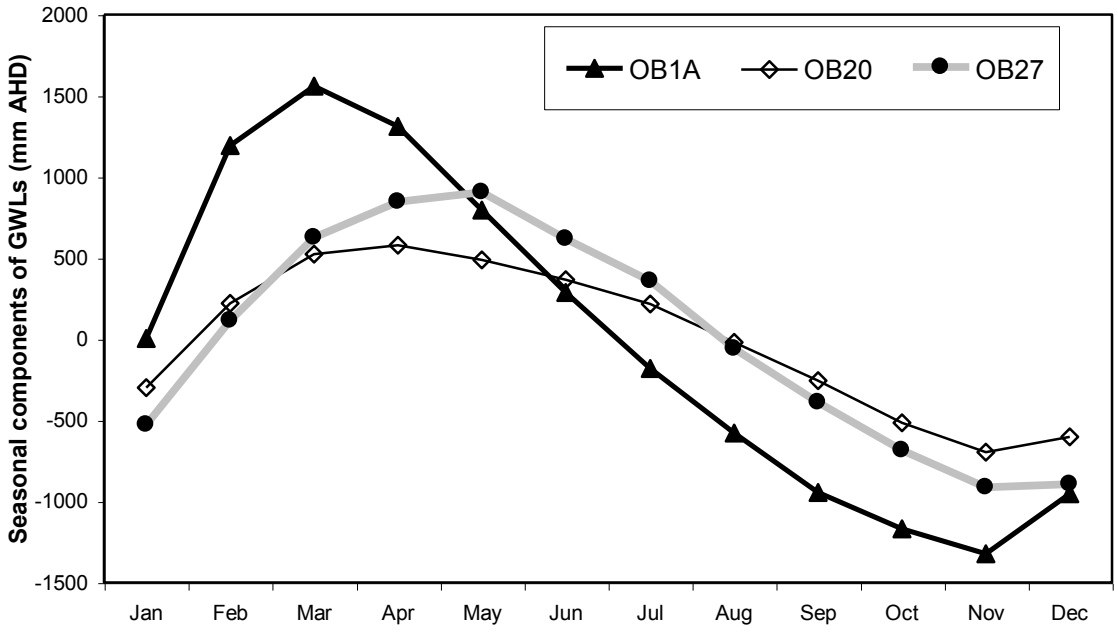

Figure 6.8 Variations of seasonal components of the GWLs of three different bores with different thicknesses of unsaturation compared to show the different lags of the responses

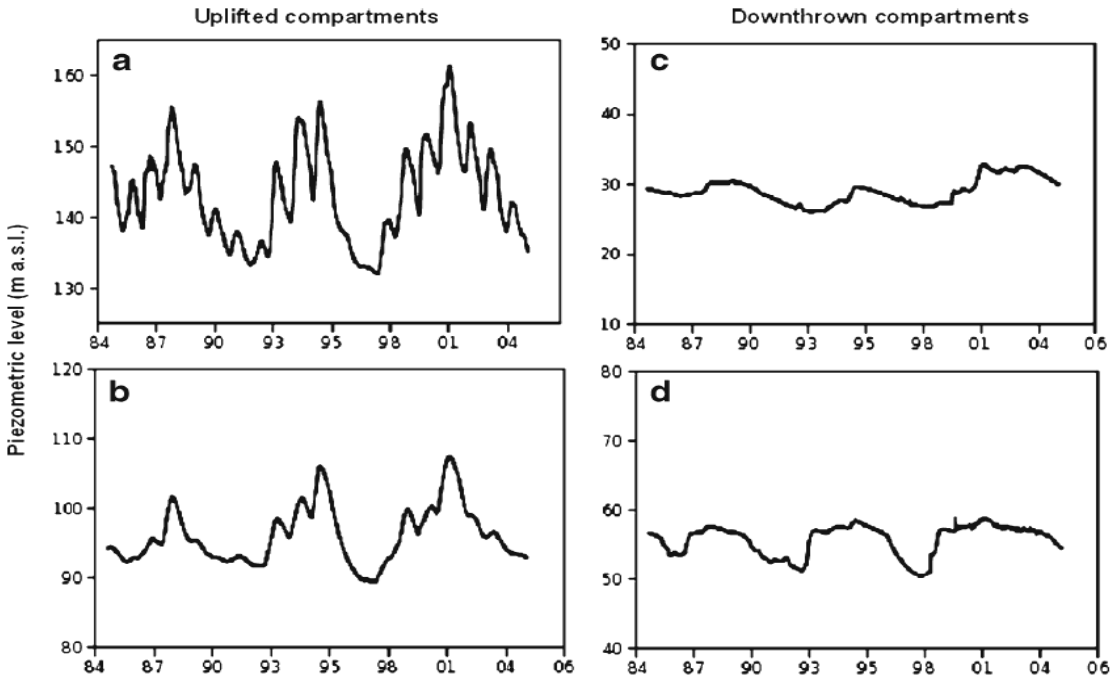

Figure 6.9 Piezometric level for four different compartments in Upper Normandy, France: a. Roquemont, b. Hattenville, c. Vaupaliere, d. Auberville. The regions of a. and b. are in the region of a thinner layer of surficial formation and those of c. and d. are in the region of thicker formation

The use of classical decomposition for various bores' GWLs give exactly the same understanding of the physical processes in the unsaturated zone, which are traditionally observed and investigated by earlier investigators involving *in situ* measurement techniques, such as those performed by Wu et al. (1996). By measuring soil-moisture contents at various depths with various events of rainfall, they have found that when groundwater is relatively deep, the correspondence between individual rainfall and recharge events is usually more obscured by the increases of time lag between rainfall and groundwater response.

Similar studies have been performed by Mutiibwa (2008), in which the investigation of human and climate influences on groundwater levels are related to periodic components and long-term trends of groundwater level data. They also relate the time lag between rainfall event and recharge to the geology of the site. Therefore, these complexities in the physical process form the basis of undertaking physically based computational modelling, which is the ultimate goal of the ongoing research.

The statistically significant lag was found to be several months between monthly net flux and change of groundwater level, while multiple regressions with distributed lag concept and cross-correlation analyses were performed. The cross-correlation analyses are described in detail in a previous section of this chapter.

Dynamics of GW climate relationship: The result demonstrates that the climate does have a predictor rule over the response of groundwater level; however, it takes time for the response to occur. During the wet months ($AA^{/}$), the time lag is approximately two months but during the dry months ($BB^{/}$), the lag is more than four months. Hence, the incorporation of the TFN model for representing the relationship between these two sets of data becomes complex at the point of assigning the lag between two variables. It should be mentioned that models for hydrological time series are characterised by parameters that may stay constant or may change over time (El-Shaarawi and Esterby 1981). A modified approach is investigated herein to overcome this complexity by using seasonal the TFN model in parallel to monthly TFN models. However, because of the lack of data for the seasonal model, the result is not significant in comparison with the monthly model.

It can be concluded that there is a difference in lag between GWLs and net flux during the wet ($AA^{/}$ two months) and dry ($BB^{/}$ four to six months) seasons (see Figure 6.7). The rate of rise is relatively quicker (four months, December to March) while the rate of fall is slower (eight months, April to November). This indicates the saturated and unsaturated flow conditions with variable hydraulic conductivities. The unsaturated thickness of the bores acts as a barrier to the climate GWLs relationship. The three bores, OB1A, OB20 and OB27, have the unsaturated thicknesses of 0 m, 1.28 m and 3.8 m respectively. The unsaturated thickness is defined here as the differences in elevation between the NS and maximum measured GWLs in the bores. The greater the thickness, the more lagged the response (see Figure 6.8), though the response also depends on soil hydraulic properties. It is observed that OB27 has the largest value of unsaturated thickness, while OB1A has the smallest value. These values are consistent with their responses. The process of development of a physically based model as described in the next chapter is thereby justified in light of these exploratory analyses.

The wetting process starts from the surface; when the wetting front reaches groundwater level, the rise of groundwater level is accelerated. The drying process starts from the

surface and the process slows as the unsaturated thickness increases. Thus, the upward movement of the saturation level takes four months whereas the downward movement takes eight months. The rate of rise is twice the rate of fall. The rising period is governed by the saturated flow condition and the falling period is governed by the unsaturated condition.

The process of groundwater recharge involves water falling as rainfall, moistening soils and infiltrating down to the water table. As the depth of the unsaturated zone increases, the water table reacts with an increasing delay to fluctuations in climate and influences of human activities (Gehrels *et al.* 1994). As the local geology indicates differential weathering across the east-west profile and the response of the water table should be different with regard to timing and range.

As illustrated in Figure 6.10, it can be seen that for a particular value of accumulated flux, the groundwater level (saturation level) in the rising section is higher than that of the falling section. In other words, for a particular value of groundwater level, the accumulated flux required in the wetting process is smaller than that during the drying process. This indicates the physical configurations of saturation and unsaturation processes. The drying process requires the soil moisture to be progressively dried for the downward movement of the saturation level. The wetting process requires progressively less additional water for the upward movement of the saturation level. Therefore, for a particular level of saturation, accumulated flux is less for the wetting process and more for the drying process.

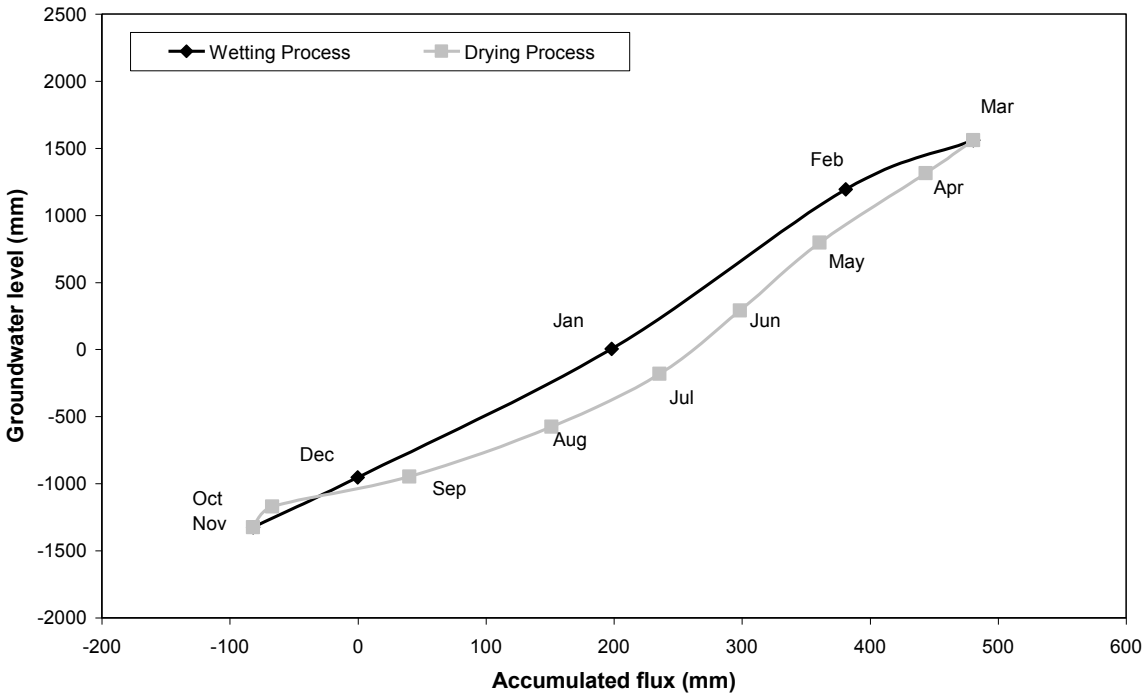

Figure 6.10 The seasonal components of monthly flux added consecutively from January to obtain the accumulated flux along the X axis and groundwater level along the Y axis. The rise starts from November and ends in March, the fall starts in April and ends in October

6.4. Univariate Autoregressive Moving Average (ARMA) Representation

The suitability of various types of seasonal models for describing seasonal data has been investigated and monthly autoregressive (AR) models have been suggested as a viable class of models for fitting monthly time series (Hipel and McLeod 1994). It is recommended that ARMA models fit to annual geophysical time series because these models readily account for the Hurst phenomenon (Bloschl and Sivapalan 1995). The Hurst phenomenon is used to indicate long-term persistence of a process, unlike a Markov process, in which an event is dependent only on the preceding event. Vecchia (1985) used the ARMA model for representing river flow with strong periodic seasonality of monthly data. Woodward and Gray (1993), Fendekova (1999), and Von Asmuth and Knotters (2004) use ARMA models for representing GWL.

The ACF and Partial Autocorrelation Function (PACF) are generally used to select the appropriate order of the ARMA model for data representation (Brockwell and Davis 2002). This means that the ACF (of the data), which is smaller in absolute value than $1.96/\sqrt{n}$ for lags greater than '*q'*, suggests a multivariate autoregressive (AR) model of order less than or equal to *'q'*. This means that the previous *'q'* number of residuals have dependence on

the current residual of the stationary process. The suggestion about the PACF is that the process whose PACF is smaller in absolute value than 1.96/√n for lags greater than *'p'* should be dealt with an AR model of order less than or equal to *'p'*. This means that the previous *'p'* number of data have dependence on the current data of the process.

The ACF and PACF are estimated to demonstrate the seasonality in the time series data of historical net flex and GWL of bores. Next, the scope of representing the historical data of monthly net flux and GWLs of bores OB1A, OB20, Ob43 and OB27 by the ARMA model are investigated. Using classical decomposition for determination and elimination of trend and seasonality from the data, an appropriate univariate ARMA model is used for representation. The following models shown in Table 6.3 are found to fit for the time series of monthly net flux and GWLs of the four bores.

Table 6.3 The orders of ARMA models for the net flux and GWLs after classical decomposition for a twelve-month seasonality and long-term linear trend

Name of time series data analysed	ARMA model order
Monthly net flux	(3,1)
OB1A	(3,2)
OB20	(1,0)
OB27	(1,0)
OB43	(2,1)

6.4.1. Test of Goodness of Fit

To test the goodness of fit of the selected ARMA model, the randomness of the residual has been tested with the incorporation of a number of plots and tests such a: ACF plot of residuals; QQ plot of residual with normal distribution; histogram plot; Kolmogorov-Smirnov cumulative periodogram test; Ljung-Box statistic p-value test; and Order of Min AICC, Information criterion of Akaike (1973) and Hurvich and Tsai (1989), YW Model for Residuals test. ACF plots for the residuals of ARMA models of monthly net flux and GWLs of OB1A are shown in Figures 6.11 and 6.12.

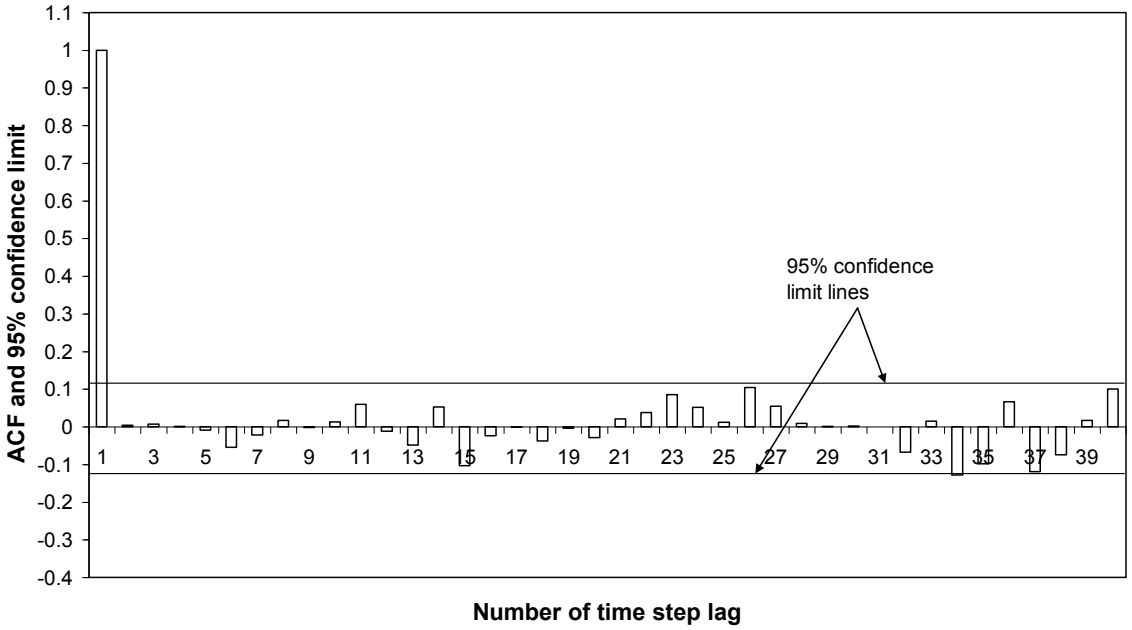

Figure 6.11 ACF of residuals of univariate ARMA model of monthly net flux

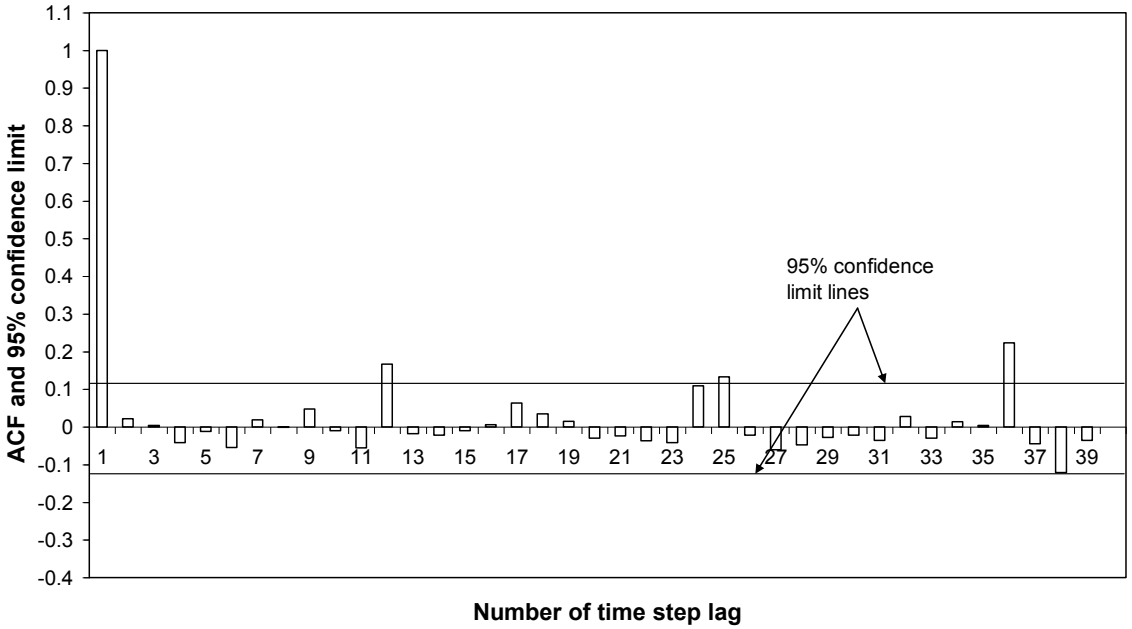

Figure 6.12 ACF of residuals of univariate ARMA model of GWLs of OB1A

The univariate ARMA model forecast for 20 years are shown in Figures 6.13 and 6.14 for monthly net flux and GWLs of OB1A. The result of the same forecast performed by the multivariate AR model is given in the next section. For all the numerical computations the Interactive Time Series Model (ITSM) software of Brockwell and Davis (2002) is used.

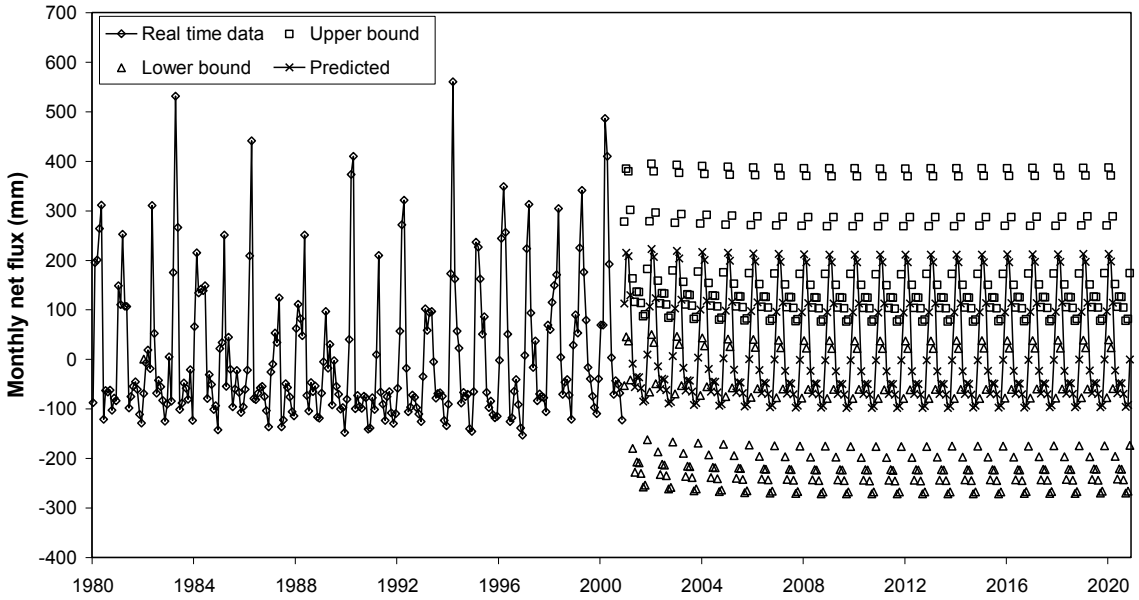

Figure 6.13 Univariate ARMA forecast of monthly net flux

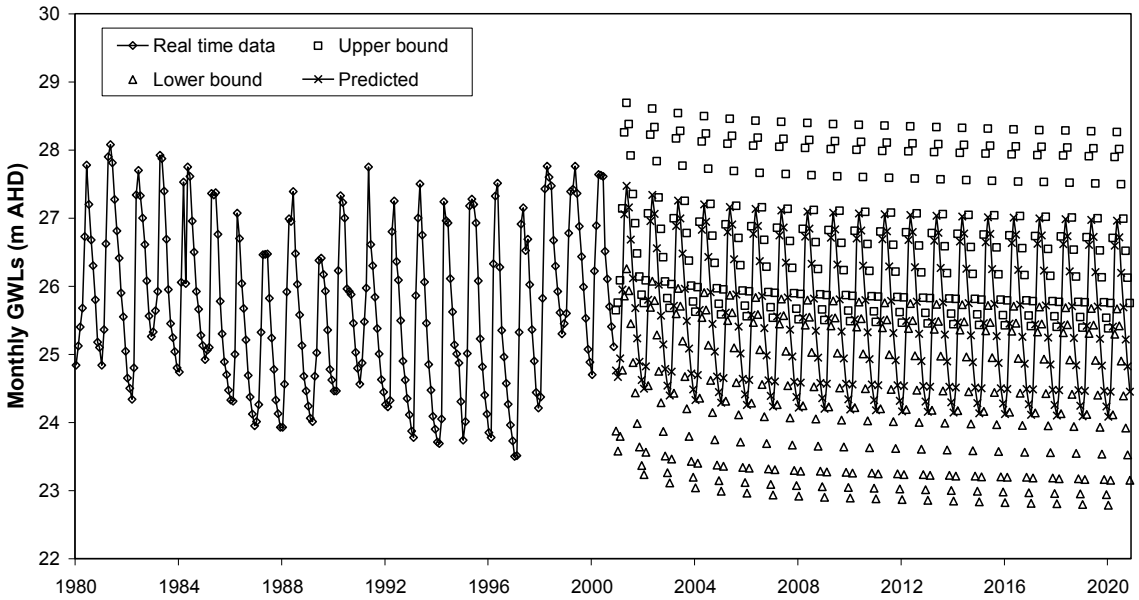

Figure 6.14 Univariate ARMA forecast of GWL of OB1A

6.5. Multivariate Autoregressive (AR) Representation

The appropriateness of applying the multivariate ARMA model for groundwater-climate relationship was investigated by estimating CCFs between the time series of net flux and GWLs in the bores. While examining the CCF values, statistically significant lag was found between GWLs and net flux. Therefore, the physical approach of Tong (1990) was considered while multivariate ARMA modelling was performed to represent the relationship of GWL and net flux. Two-way relationships between net flex and GWL is

assumed in the modelling. Hence, net flux causes GWL and GWL causes net flux. From the physical perspective, this is true because the position of GWL determines the soil moisture and thus the rate of evapotranspiration and net flux.

The logical justification is to represent the GWL and net flux relationship by two-way relation. The MAR model could be established by referring the dynamic feedback between vegetation type and water balance at a regional scale, as suggested by numerous investigators (Naumburg *et al.* 2005; Scanlon *et al.* 2005; Miguez-Macho *et al.* 2008; Jiang *et al.* 2009; Schymanski *et al.* 2009; Yeh and Famiglietti 2009).

The theory of AR process is available in any standard time series textbook such as Brockwell and Davis (2002). Though there are serious obligations imposed to identify co-integration before doing the multivariate time series analyses (Brockwell and Davis 2002), the concept of co-integration is not relevant here because the data series selected for the time range in the present work has been pre-whitened by suitable transformation before the model development. Co-integration is an econometric technique for testing the correlation between non-stationary time series variables. If two or more series are themselves non-stationary, but a linear combination of them is stationary, then the series are said to be co-integrated (Engle and Granger 1987).

6.5.1. Comparison between Univariate and Multivariate Models

The AR model has been estimated using the AICC criteria. The method of estimation is the Yule-Walker method as described in Brockwell and Davis (2002). The multivariate AR model forecast for 20 years are shown in Figures 6.15 and 6.16 for monthly net flux and GWLs of OB1A respectively. From a visual assessment, the multivariate AR model forecast seems better than that of the univariate AR model, as shown in Figures 6.13 and 6.14. The longer forecast should have a broader limit for a certain confidence interval. This is reflected in multivariate forecast but not present in the univariate forecast. The physical basis of multivariate representation is also better than univariate because the two time series (net flux and GWL) are not independent of each another.

Therefore, the difference in the representation can be attributed to the difference in the result of predictions, which is obvious. However, the comparison is performed to assess the range of variation that can result between general (multivariate AR) and specific (TFN)

forms of statistical methods. To perform this comparison, the TFN model is applied to the same set of time series data in the following section.

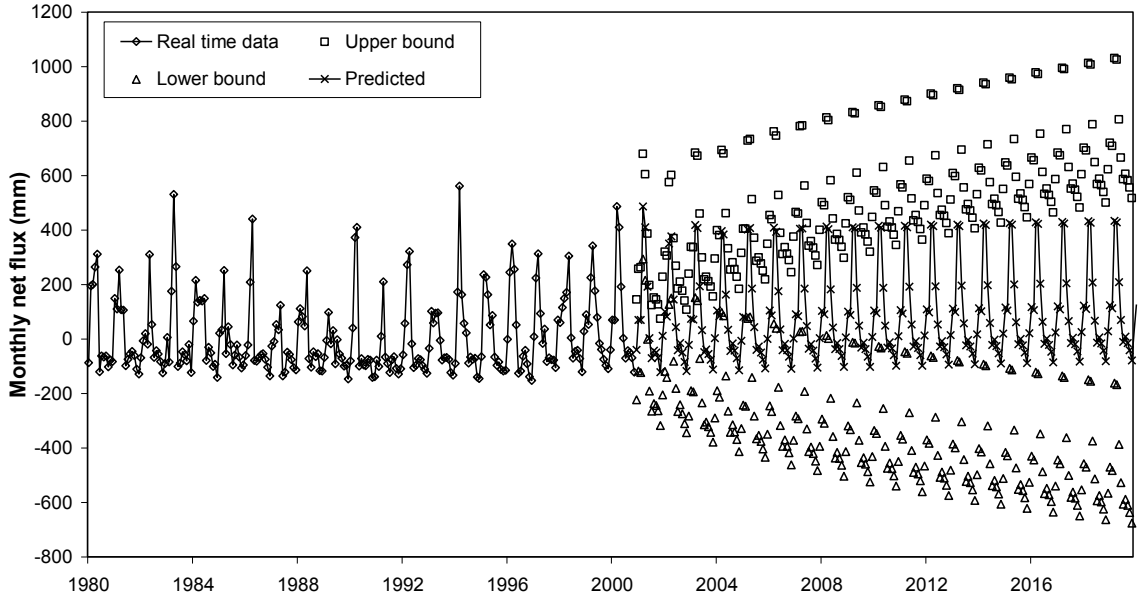

Figure 6.15 Multivariate AR forecast of monthly net flux

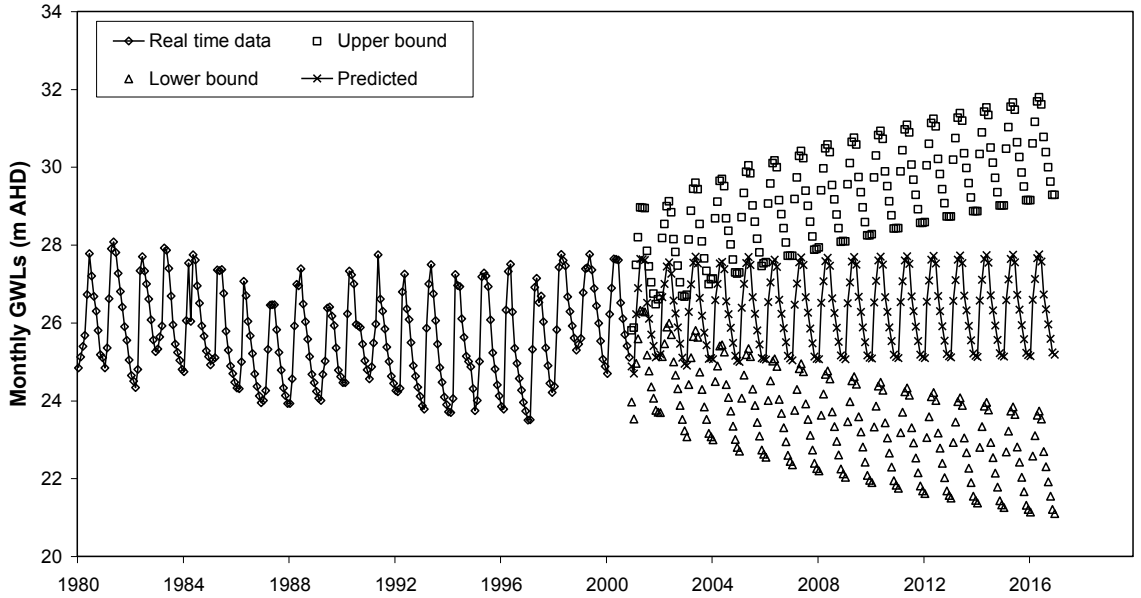

Figure 6.16 Multivariate AR forecast of GWLs of OB1A

6.6. Transfer Function Noise (TFN) Representation

The theory of multivariate AR model considers mutual dependence of all the series of the process. For instance, the net flux at time t+1 is represented as function of net flux at t, t-1, t-2, … together with groundwater level at t, t-1, t-2…as well and a noise component.

However, in the TFN representation, the previous values of the groundwater level series are not considered explicitly. From the scientific perspective, there exists a strong causal relationship between net flux and groundwater level, but the relationship is not two-way. Therefore, net flux influences groundwater level but groundwater level does not influence net flux to that extent. The evaporative flux depends on soil moisture content, which is influenced by the proximity of the groundwater level to the soil surface. However, this variable is much less important than other variables that influence the evaporation and transpiration process such as intensity and duration of radiative energy, relative humidity, temperature gradient, thermal conductivity of the soil surface, wind speed and vegetation type.

Hydrological applications of TFN models include rainfall-runoff modelling, stream flow modelling and forecasting, urban water-use modelling, and reservoir modelling (Berendrecht 2004). The work of Maidment et al. (1985) in urban water use, the work on rainfall-runoff modelling by Cooper and Wood (1982), Thompstone et al. (1985) and Jakeman et al. (1990), and water quality modelling by Hirsch (1983), Whitehead et al. (1986) and Jakeman et al (1989) are some examples. Welsh and Stewart (1991) use the TFN approach to represent the turbidity of a lake as a function of river flow and rainfall in the catchment. Mondal and Wasimi (2006) developed methods that can be applied to monthly rainfall and river flow data to capture the seasonal variability and forecast.

Van Geer and Defize (1987), and Gehrels et al. (1994) included precipitation excess and an artificial trend in a TFN model for detection of natural and artificial causes of groundwater fluctuations. Bidwell and Morgan (2002) used a TFN model relating recharge to groundwater level. Tankersley and Graham (1993) compared forecast accuracies for groundwater fluctuations of univariate and TFN models. Tankersley and Graham (1994) applied a TFN model to generate a control strategy for the purpose of managing groundwater fluctuations at ecologically vulnerable locations. Welsh and Stewart (1991) used a TFN approach to represent the turbidity of a lake as a function of river flow and rainfall in the catchment. Grigor'ev and Trapeznikov (2002) used a TFN model for relating lake water level with climate changes.

Some investigators have compared the performances of multiple regression models, ARMA models and TFN models (Thompstone *et al.* 1985; Welsh and Stewart 1991;

Tankersley and Graham 1993; Tankersley and Graham 1994). The concept of comparing the models with a different physical basis and statistical efficiencies is followed in the present study. From the physical perspective, there exists a strong causal relationship between net flux and groundwater level. A transfer function model would be more appropriate in those situations in which a causal relationship exists between or among variables in particular directions. The theory of TFN models is discussed here with specific consideration to the important issues relating to the estimation steps of the model parameters.

6.6.1. Theory of Transfer Function Model

The two sets of time series observations such as monthly net flux {U(t)} and monthly groundwater level {V(t)} are transformed to generate zero-mean stationary processes as input and output. The transformation required for the generation of the stationary series has to be determined by inspection of the data. For annual time series data, differencing by one time step lag might be appropriate whereas the monthly time series data might need to be differenced by twelve time steps. In addition, classical decomposition transformation is applicable for the monthly data with periodic cycle of twelve time steps.

The input or independent variable {X(t)} and output or dependent variables {Y(t)} are thus represented by a relationship, as shown in Equation 6.4:

$$Y(t) = T(B)X(t) + N(t) \qquad \text{Equation 6.4}$$

where the transfer function, *T (B)*, is a causal time-invariant linear filter and *N(t)* is a zero-mean stationary process, uncorrelated with input process *X(t)*. The transfer function, *T (B)* is assumed to have the form of Equation 6.5:

$$T(B) = \sum_{J=0}^{\alpha} \tau(J)B^{J} = \frac{B^{l}(u_o + u_1 B + \cdots u_q B^{q})}{1 - v_1 B - \cdots - v_p B^{p}} \qquad \text{Equation 6.5}$$

where the exponent *l* of back shift operator *B* corresponds to the lag between the input series and output series and known as 'delay parameter'. The other exponents *q* and *p* are respectively the orders of the moving average (MA) part and autoregressive (AR) part of

the transfer function representation of the relationship between input and output series. The parameters $u_0, u_1 \ldots u_q$ are the coefficients of the MA part and the parameters $v_1, v_2 \ldots v_p$ are the coefficients of the AR part of the transfer function representation.

The algebraic expansion of the numerator and denominator of the right-hand side of Equation 6.5 results an infinite polynomial of B and the respective coefficients are indicated by τ.

{N (t)} is an ARMA process uncorrelated with *{X (t)}*, such that:

$$\phi_N(B)N(t) = \theta_N(B)W(t), \{W(t)\} \approx WN(0, \sigma_W^2) \qquad \text{Equation 6.6}$$

and the input process *{X (t)}* is assumed to be another ARMA process:

$$\phi_X(B)X(t) = \theta_X(B)Z(t), \{Z(t)\} \approx WN(0, \sigma_Z^2) \qquad \text{Equation 6.7}$$

The parameters of ϕ and θ with subscripts X and N are the coefficients of the ARMA processes used to represent the input model *{X (t)}* and noise model *{N (t)}* respectively. *{W (t)}* and *{Z (t)}* are white noise processes corresponding to the ARMA representations of the noise model *{N (t)}* and input model *{X (t)}* respectively. The white noise processes are represented as zero-mean and variance σ_w^2 and σ_z^2 respectively.

The parameters in the last three equations are all to be estimated from the given observations of *(X (t), Y (t))*.

The back shift operators B, as used in the equations, are used to indicate the following relationship between the variable under consideration:

$$B^J X(t) = X(t - J) \qquad \text{Equation 6.8}$$

Therefore, when the back shift operator B^J is applied to *X(t)*, it corresponds to the value of X at *t-J* instant of time.

Computational steps: The successful and correct implementation of the transfer function model involves three distinct steps of computation such as model identification, parameter estimation and diagnostic checking (Hipel and McLeod 1994; Brockwell and Davis 2002).

Model identification: When designing a TFN model, the number of parameters required in each of the operators contained in the dynamic and noise transfer functions must be identified. Three different procedures for model identification have been reviewed. The first being empirical approaches, which has been used when modelling hydrological time series by Hipel et al. (1977; 1982; 1985). The other two techniques are that of Haugh and Box (1977), which use the residual CCF and Box and Jenkins (1976), which is based on the suggestions by Bartlett (1935). The latter two methodologies rely heavily upon the results of cross-correlation studies and often the first procedure is used in conjunction with either the second and third approaches (Hipel and McLeod 1994). However, with regard to the scope of the study, an interactive technique is followed to identify the model and that technique directly or indirectly incorporates all of these approaches. The steps of identification process followed in the work are discussed in detail (Brockwell and Davis 2002).

Parameter estimation: Following the identification of one or more plausible transfer function models, maximum likelihood criteria are used for parameter estimation. Often, more than one TFN model is identified. As recommended by Hipel (1994), a combination of the first and second approaches for preliminary estimation of TFN parameters has been used. Subsequent to estimating the model parameters separately for each model, automatic selection criteria such as the Akaike Information criterion (AIC) (Akaike 1969) and Bayes Information Criterion (BIC) (Schwarz 1978) are utilised to assist in selecting the most appropriate model. The doctrines of both ‘good statistical fit’ and ‘model parsimony’ are simultaneously considered in the formulation of AIC and BIC (Hipel and McLeod 1994).

Diagnostic checking: The white noise components are assumed identical and independently distributed. A recommended procedure for checking the whiteness assumption is to examine a plot of the residual ACF along with confidence limits (Hipel and McLeod 1994; Brockwell and Davis 2002). Residual correlations and cross-correlations are then computed for model checking. Although a plot of residual ACF is the best whiteness test to use, other tests that can be employed include the cumulative

periodogram test and the modified Portmanteau test, as described in Brockwell and Davis (2002).

In general, a number of different methods exist for the class selection of statistical models. The most commonly used methods are the likelihood approach, hypothesis testing, recursive (or Real Time) prediction and best fitting. Among all the methods, the likelihood approach is versatile, theoretically sound, and appears to give reasonable results in practice. Often, the best fitting models from the classes chosen by this rule pass all validation tests and give reasonable forecasts (Kashyap and Rao 1976).

Hence, the AIC value of the fitted model is computed for model comparisons. Forecasts of Y (t) and of the original output series V (t) are computed from the fitted model. In addition, validation of the predicted data by the TFN Model and AR Model are plotted in chart for more generalised recognition of the quality of the result.

6.7. Selection of Predictor and Model Type

The predictor is selected by comparing the prediction performances of two sets of models. One is based on rainfall as the predictor and the other is based on net flux as the predictor. The model type is selected by comparing the two types of models such as TFN models and MAR models. These comparisons are performed to select the best predictor and best model for the long-term prediction of the groundwater-climate relationship.

6.7.1. Selection of Predictor

The incorporation of the net flux-based TFN model in parallel to the rainfall-based TFN model is justified by the fact that this involves physical process-based modelling of the system in which the boundary condition should be represented by positive flux during the wet season and negative flux during the dry season of the year. Since rainfall time series is representing only positive flux to the system, a negative flux representation would be necessary to represent the negative flux from the system. That negative flux is incorporated by considering the net flux as an independent variable to the system. The procedure followed in the modelling consists of classical decomposition for separation of trend and seasonality followed by the development of the models. Within the scope of available data, the records of March 1981 to June 2001 were used for model development and those of

July 2001 to February 2003 were used for performance evaluation of the predictions. The number of predicted times step was 20.

To assess the performance of TFN models developed for rainfall-based representation and net flux-based representation, the average difference between observed and model results are determined. It is found that the average difference is 286 mm for the net flux-based model and 360 mm for rainfall-based model. Figure 6.17 shows the closeness of agreement between the predictions of the rainfall-based TFN model and net flux-based TFN model. Since the predictions by the two models are similar, the net flux is selected for long-term prediction since this predictor has some physical process-based advantage over rainfall.

The model performance is indicated by the AICC value, less AICC corresponds to a better model. It was found that all the AICC values are comparable for both the TFN and Multivariate AR (MAR) models, based on rainfall and net flux data (see Table 6.4).

Table 6.4 AICC values for the net flux and rain based TFN and MAR models

.636881E+04	for NF-based TFN model
.635250E+04	for NF-based MAR model
.634081E+04	for rain-based TFN model
.631971E+04	for rain-based MAR model

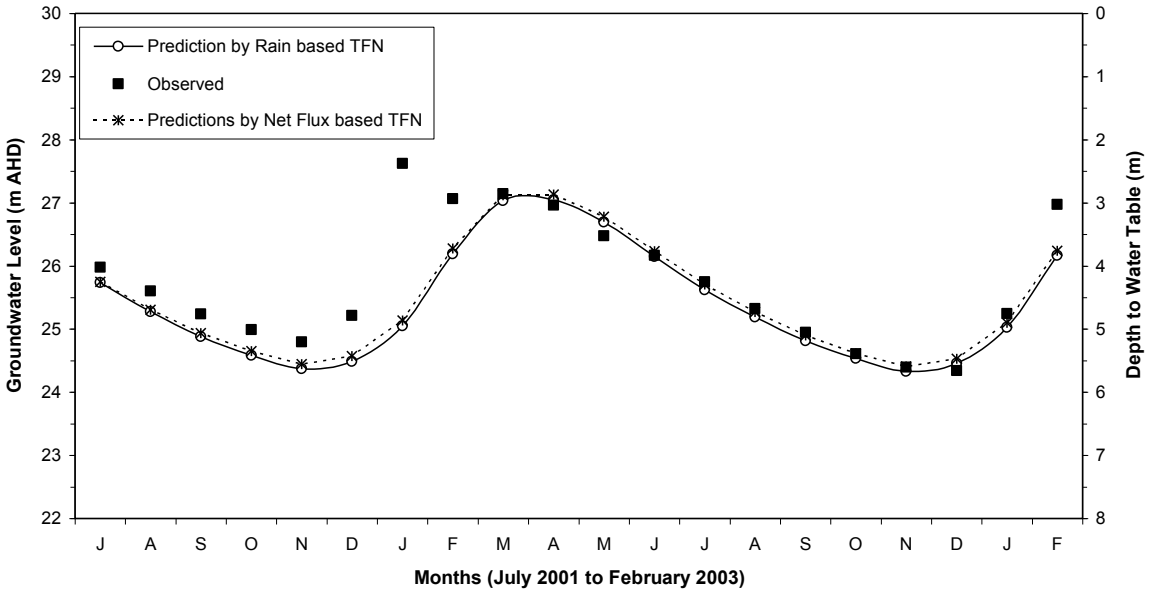

Figure 6.17 Comparison of rain-based TFN and net flux-based TFN

Figure 6.18 illustrates the predictions made by the TFN model and MAR models based on rainfall data. From the comparison of the coefficients as estimated from the MAR models, it has been found that the correlation coefficient indicating GWL as a function of rainfall (or net flux) is significantly higher. Conversely, the correlation coefficient indicating rainfall (or net fluxes) as a function of GWL is significantly lower. This result can be attributed to the physical processes involving the flow of water in the vadose zone in terms of the cause and effect relationship.

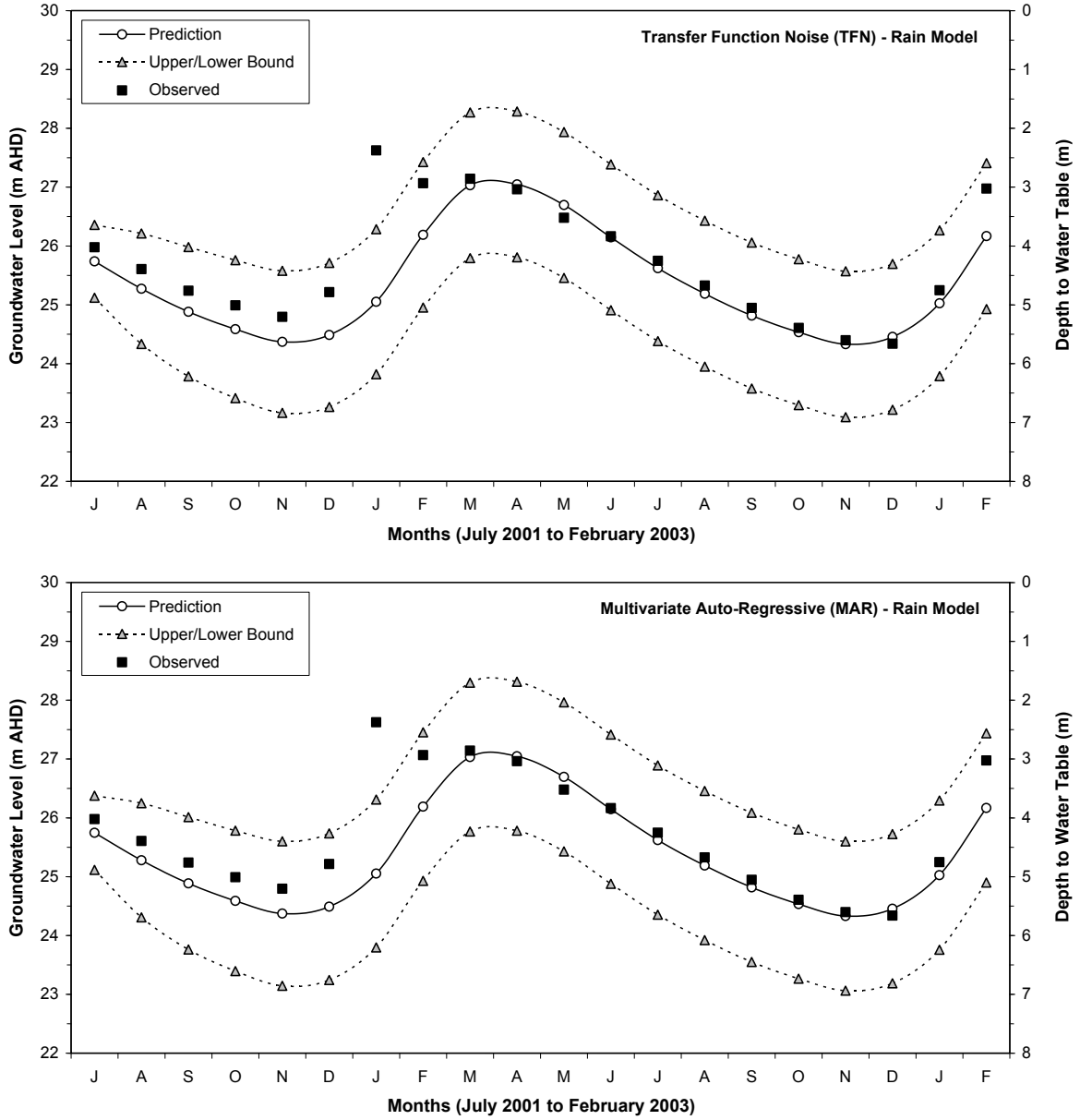

Figure 6.18 Result of rain-based TFN model (top) and MAR model (bottom)

6.7.2. Selection of Model Type

A decadal time scale is used for comparing the performance of the two models: the MAR model and the TFN model. The procedure consists of the differencing by lag of twelve time steps followed by the development of the MAR and TFN models for the monthly time step-based time series.

The commonly used performance criteria AICC statistic is the representation of both accuracy (goodness of fit) and parsimony (simplicity or computational efficiency) of the

models. In the computation of AICC, there are contribution from p, q and n of the model and data, as shown in Equation 6.9:

$$AICC = -2Log(Likelihood) + 2(p+q+1)n/(n-p-q-2) \qquad \text{Equation 6.9}$$

Maximisation of likelihood is equivalent to minimisation of -2Log (likelihood). The estimation of likelihood function is performed by considering the variance in such a way that the greater the value of variance, the less is the likelihood function. However, variance is a function of the estimated parameters coefficients (ϕ and θ) of auto regressive and moving average parts of the ARMA process. Based upon the information theory (Akaike 1972; Akaike 1973; Akaike 1974), the desirable attributes of the AICC are good statistical fit and model parsimony. The two terms on the right-hand side of the equation for estimation of AICC reflect these considerations respectively. The model that possesses the minimum value of the AIC should be selected. However, the question of interpretation of the relative differences in the values of the AICC for the various models that are fit to a specified data set need to be settled.

As shown by Akaike (1978), exp (-0.5AICC) is asymptotically a reasonable definition of the plausibility of a model specified by the parameters that are determined by the method of maximum likelihood. Consequently, the plausibility of model *m1 versus* model *m2* can be calculated using Equation 6.10:

$$Plausibility = \exp[0.5(AICC_{m1} - AICC_{m2})] \qquad \text{Equation 6.10}$$

where $AICC_{m1}$ is the value for AICC for the *m1* model and $AICC_{m2}$ is the AICC value for the *m2* model. As these difference increase, the plausibility decreases exponentially. However, all these criteria are used for deciding between the competing models of same class, not between different classes. Hence, some alternative criteria that are relatively common and simple have been identified to compare the models of different classes.

Alternative criteria for comparison between models of different type: To compare the statistical performance of the monthly-based models, the other criteria considered are root mean square error (RMSE), and square of correlation coefficient (R^2) for the models and

average range of confidence intervals of the predictions. Some validation tests of the data have been performed for the period November 2001 to October 2002 to examine the performances of the MAR model and the TFN model, as shown in Figures 6.19 and 6.20.

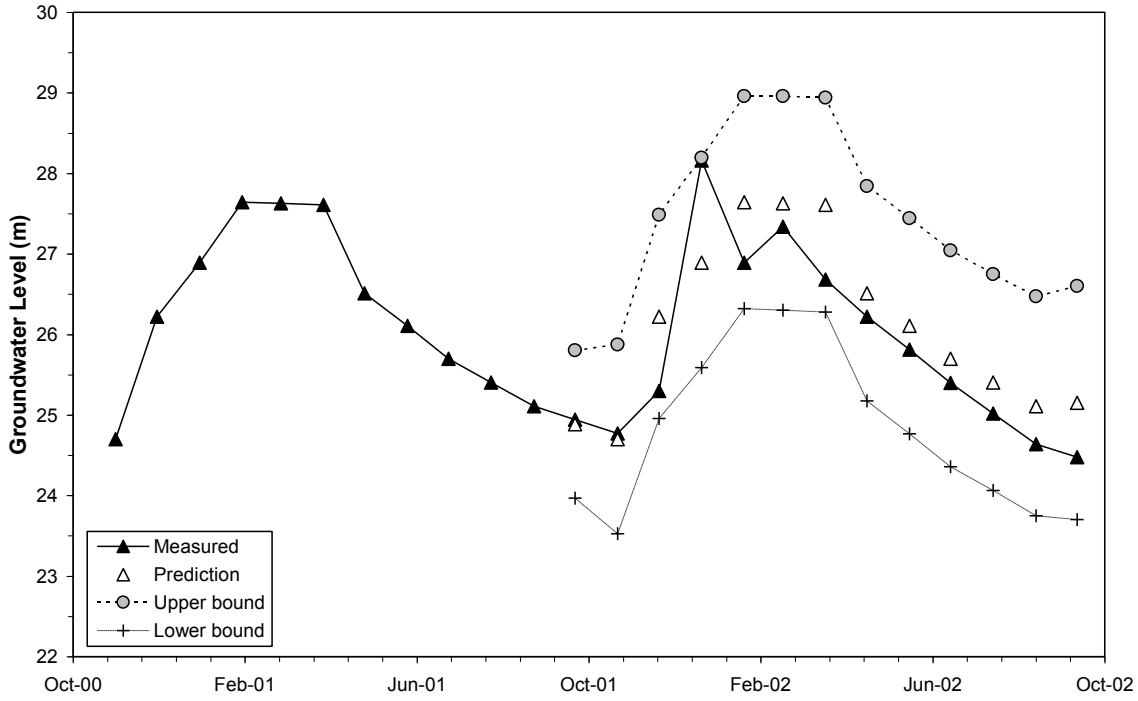

Figure 6.19 MAR validation

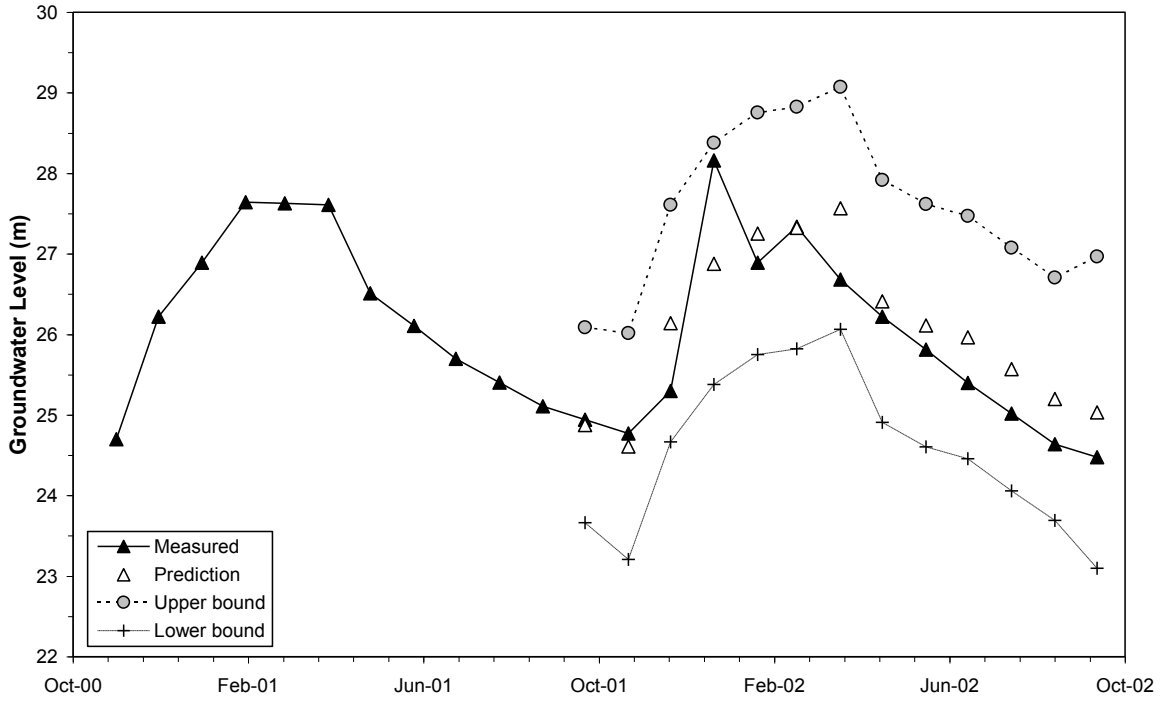

Figure 6.20 TFN validation

In Table 6.5, to compare the statistical performance of the monthly-based models, a number of criteria have been considered. Those are the AICC statistic, RMSE, square of correlation coefficient (R^2) and average range of 95% confidence interval for the models. It is found that the TFN Model performs better than the MAR Model with respect to RMSE and R^2; the reverse is true while AICC statistic and confidence limits are considered. AICC statistic is a standard criterion for model selection when the competing models are of the same type; however, it does not make sense when compared between two different types of models. Therefore, the TFN Model is better than the MAR Model. The detail analyses have been described in Kabir *et al*. (2008a).

Table 6.5 AICC, RMSE and R^2 of the models

Model Used	AICC	RMSE	R^2	Average range of confidence interval (m)
TFN Model	6698	0.166	0.761	2.94
AR Model	6585	0.173	0.760	2.56

The computational efficiency of the MAR model is much better that that of the TFN. The model fitness performance should not necessarily govern the model selection process, as indicated by many investigators. Franssen and Kinzelbach (2009) show that the group of models that perform comparably similarly with regard to model fitness but require widely varied CPU times should be treated reasonably. The model with less CPU time required is preferable for application.

It is found that the TFN model performs better than the AR model with respect to RMSE and R^2, while the reverse is true for the AICC statistic and average range of confidence interval; the differences are very small indeed. The AICC statistic is a standard selection criterion used when the competing models are of the same type, in which a minimum value indicates the best model. However, it does not make sense when comparing two different types of models. In this case, the TFN model is structurally different from the MAR model. From this basis, the TFN model is better than the MAR model with a better physical basis.

However, the other important practical consideration is the computational time in the environment of ITSM software. The time required for the MAR model is very small with

respect to TFN. Thus, for the forecasting of the centurial time scale of data, the MAR model is preferred.

6.8. Conclusion

The significance of unsaturated thickness in the relationship of groundwater-climate is a significant outcome of the exploratory analyses. This builds the scientific basis for considering the unsaturated flow model to be a better representation of the system. The scientific superiority and computational efficiency of the monthly TFN and multivariate AR model is well documented in this chapter. In addition, the competitive performance of the rain-based model and net flux-based model has been shown. Net flux has a physical process-based advantage over rainfall. Therefore, net flux is selected for long-term prediction. For the sake of computational efficiency, the multivariate AR model is considered preferable compared to the TFN for long-term simulation/prediction.

In the next chapter, the methodology for generating the future 100 years' replicates of climate data is described, considering climate change scenarios projected by General Climate Models (GCMs) and natural climatic variability. In the following chapter, the physically based model Seep/W (Krahn 2004b) for the site is developed, validated and the replicated climate data of 100 years is used to compute the GWLs for the site. The result of these representation and forecast are described in the 'Result' chapter.

7. Generation of Future Climate Replicates

This chapter presents the formulation of a method for predicting climatic variability, which is then combined with the climate change predictions for generating thousands of replicates of net flux. The generated net flux data are consequently used as boundary conditions to the unsaturated model. The climatic variability in the tropical region with intense monsoonal rains and extended dry seasons is thoroughly investigated. In order to predict future climatic variability, the current understandings of the influences of ENSO, La Nina, PDO or Interdecadal Pacific Oscillation (IPO) and Indian Ocean Dipole (IOD) (Chang et al. 2006) for the site are combined. Thus, the 'ENSO generation' program is developed to address the climatic variability of the region. This is a 'conditional/quasi' random process developed based on the latest understanding of the influences of the various ocean atmospheric circulations in the region. The past climatic variability is addressed by using Stochastic Climate Library (SCL) software (Srikanthan et al. 2005). The past climatic variability (SCL) replicates and future climatic variability (ENSO program) replicates are combined to generate thousands of future net flux data sets at the centurial scale. Finally, the trends of climate change projections for various emission scenarios of various GCMs are applied to those net flux data by multiplicative modification.

These net flux data are used as boundary conditions for the groundwater model. Using the unsaturated groundwater flow model, long-term impacts of climate on groundwater levels are predicted with a specific (68%) confidence interval by using the means and standard deviations in the next chapter.

7.1. Future Climate Models

The predictions performed by various GCMs for each of the SRES consist of a range of variations to the changes of the hydro-climatic variables such as precipitation, temperature and evapotranspiration. When plotted in time-based graphs, the predictions are regular, smooth curves of linear or parabolic shape. However, the real time historical time series data of rainfall, temperature are not smooth; they are rather irregular. Therefore, the combination of climate change prediction with natural climatic variability is another issue that needs to be addressed.

As a result of reduced precipitation and increased evaporation, water security problems are projected to intensify in southern and eastern Australia (Hennessy and Fitzharris 2007; Hennessy et al. 2007). However, there has been an increasing trend in rainfall over much of north and north-west Australia over recent decades, which has contrasted with decreases over the rest of the continent. It is argued that the trends in rainfall totals and average intensities are largely unrelated to trends in ENSO and most likely reflect the influence of other factors (Smith and Suppiah 2007). The possible factors could be associated with the observations and understandings related to ocean dynamics.

Climate variability in the Top End is related to the ENSO index, PDO and IOD (Chang et al. 2006; Cai 2007; Power et al. 2007). The ultimate effect of these three factors will give rise to the exaggerated climatic condition in two extreme directions. This will lead to a range of possibilities of high intensity rainfall during the wet season and longer spells of extreme temperature during summer (Watson et al. 1999). This conclusion (observation) is represented in the generated climatic variability such as using 99.99 percentile values in place of 99 percentile or so in the present research work. The percentile values are extracted by reviewing the indices of the Expert Team on Climate Change Detection and Indices (ETCCDI) (Alexander *et al.* 2006; Alexander *et al.* 2007). The details are provided in later sections.

7.2. Extraction of Climate Change Prediction Data from GCMs

While formulating the future climate data, the concept of climate change and climate variability as distinctly defined by the UNFCC (Houghton *et al.* 2001) is required to be reemphasised here. It can be recalled that climate change refers to a long-term phenomenon (multi-decadal to century time scale) that is especially perceived to be human-induced. Climatic variability is interannual to interdecadal and more closely related to naturally-induced phenomena. However, in the IPCC usage, ‘climate change’ refers to any change in climate over time, whether due to natural variability or as a result of human activity. This usage differs from that in the UNFCC. In the present research, the climate change predictions are the predictions induced by human activity and the climatic variability predictions are the predictions induced by natural phenomena such as ocean atmospheric circulations.

The influence of climate variability on the range of hydro-geologic processes is significantly important to address. The evidence of influence of climatic variability at a multi-annual and decadal time scale on the groundwater is established by many investigators. For example, Slimani et al. (2009) have shown the differential responses of piezometric levels in a chalk aquifer in France at various locations of the catchment during different spells of wet and dry years by using the historical data of groundwater monitoring bores.

The necessity of interpretation of future climate as a result of human-induced global warming and natural climatic variability is required to be argued with the current state of understanding. The latest report on *Climate change in Australia* (CSIRO 2007) states clearly that while there has been an increase in the frequency of El Nino events in recent years, there is no consensus amongst current climate models that global warming should cause an increase. Therefore, the increase might reflect naturally occurring variability (CSIRO 2007). The report is based upon international climate change research including conclusions from the IPCC's fourth assessment report. It also builds on a large body of climate research that has been undertaken for the Australian region in recent years.

The latest available understanding for the simulation of Australian climate and ENSO-related rainfall variability in GCMs, as reported by Rotstayn et al. (2010), is still in the process of development and requires sensitivity studies for increased confidence in their hypothesis. The work of Rotstayn et al. (2010) is an outcome of a combined program of the CSIRO and BoM and is not comparable to the scale of work of the present investigation. The GCM considered in their study is CSIRO Mk3.6, which is the latest versions of CSIRO Mk2, and includes an interactive aerosol scheme. The present study is being undertaken during the year of 2007; thus, the results from CSIRO Mk2 were used in combination with four other GCMs as will be detailed in a later section. The GCMs for this study have been selected from the recommendation of the latest available investigation by Hennessy et al. (2004) , specifically performed for the tropical region of NT, Australia.

The climate change predictions for the research site is addressed by using Ozclim data (CSIRO 2006). Ozclim uses scenarios for greenhouse gases and sulphate aerosols from the IPCC SRES (IPCC 2001a). Global warming projections derived from these scenarios in five-yearly intervals were sourced from the IPCC Third Assessment Report (Houghton *et*

al. 2001). These differ slightly to the global warming projections in the IPCC Fourth Assessment Report (Solomon *et al.* 2007), but the latest projections were not available during the time of data extraction from the Ozclim source (in September 2008), and the data needed to be generated by interactive procedure as could be found in CSIRO(2010). The output from Ozclim version 2.0.1 (CSIRO 2006), which uses the 25 km x 25 km grid for Australia with five-yearly intervals of climate variables, was available to be used in the study.

The hydro-climate data, namely rainfall and PPET, were extracted from GCMs and seven emission scenarios using the CSIRO's 'Ozclim' data tool. All PPET values were converted to AAET in order to calculate the hydrologic net flux used as the primary input for unsaturated flow modelling.

7.2.1. Review of GCM Performance for the Site

In 2004, a study was conducted by Hennessy et al. (2004) whereby a detailed performance evaluation of GCMs was undertaken for the NT, Australia. The latest IPCC report available during that time was Third Assessment Report 2001 and this 2004 report was based on the findings of IPCC 2001 report.

Since the third assessment report (TAR), there has been an improved understanding of projected patterns of precipitation. In the fourth report of the IPCC (2007), it has been found that increases in the amount of precipitation are very likely (>90% probability of occurrence) in high-latitudes, while decreases are likely (>66% probability of occurrence) in most subtropical land regions. The present research is concerned with a very localised area in relation to such a generalised summary statement. In addition, the IPCC WG1 Fourth Assessment Report did not reassess the emission scenarios of the IPCC SRES any further after 2001. Therefore, the more detailed and specific predictions of climatic data as available in the Ozclim, which incorporates a total of seven emission scenario groups (A2, A1B, B1, B2, A1F, A1T and IS92cc) were used. The descriptions of the SRES used are available in Appendix G.

In the summary of the policymakers' fourth assessment report of the IPCC (2007), values of relative changes in the per cent of precipitation for the period 2090–2099, relative to 1980–1999, are presented. The values are multi-model averages based on the SRES A1B

scenario. The project site is found to be in the area where less than 66% of the models agree in the sign (increase/decrease) of the change (change of precipitation in December-January-February). The models consist of a hierarchy of different models that encompass a simple climate model, several Earth Models of Intermediate Complexity (EMICs) and a large number of AOGCMs.

Some adjoining areas to the site lie in the range of -5 to +5% change of precipitation by the year 2099 relative to 1999. As the level of confidence is lower (such as 66% < 90%) for the site under consideration, all the scenarios with as many as five GCMs are considered in the study, as discussed in detail in the following section.

7.2.2. Selection of GCMs and Sensitivity Level

In order to select the reliable GCMs for the site from a range of as many as twelve GCMs as available in Ozclim source and climate sensitivity for the predicted data, a range of investigations from similar studies have been reviewed. After reviewing the contemporary works and considering the context of the present investigation with all its limitation of scope and available resources, the site-based previous investigation by Hennessy et al. (2004) has been selected as a reasonable reference for carrying on the work.

Some of the works broadly reviewed could be listed as follows:

- Hiscock et al. (2008) use four GCMs with four scenarios while studying the climate change impact on five locations of investigation under UNESCO's initiative GRAPHIC.
- Serrat-Capdevila et al. (2007) use four GCMs from an ensemble of seventeen GCMs and consider four scenarios in their modelling for climate change impact and uncertainty on the hydrologic system.
- Eckhardt and Ulbrich (2003) use five GCMs with two scenarios for their study of climate change impact.
- Herrera-Pantoja and Hiscock (2008) use a 'high' gas emission scenario (equivalent to A1F1 SRES) provided by HadCM3 GCM for three locations while studying the potential groundwater recharge as impacted by climate change. They use the Climate Research Unit (CRU) daily WGEN for generating other variables from precipitation. The precipitation is estimated by the Markov chain stochastic model and measured past data.

- Wilby et al. (2006b) use three GCMs, while Wilby and Harris (2006c) use four, CSIRO Mk2, ECHAM4, HadCM3 and CGCM2, with two scenarios, such as A2 and B2, while assessing the uncertainties in climate change impacts.
- Steele-Dunne et al. (2008) use ECHAM5 GCM and another RCM with A1B emission scenario for producing dynamically downscaled climate data.
- The other works in which one GCM with one scenario is considered are Basalirwa et al. (2008), Nyenje and Batelaan (2008), and Mileham et al. (2008). Providing Regional Climates for Impact Studies (PRECIS) of the UK Meteorological Office is used by some of these investigators for downscaling GCM data. Groves et al. (2008) use the decile concept to consider the probability density of predicted changes of climate by specific GCMs and scenario for a specific location in California.

There are a range of studies performed by recent investigators that are scientifically much more accurate in representing the physical processes. However, the scope of uncertainty also builds up in that proportion. In addition, the computational capability used for the studies are in the range of supercomputer (Groves *et al.* 2008; Lopez *et al.* 2009; Raje and Mujumdar 2009; Weng and Yu 2010). The present study is not of that scale but the incorporation of ocean atmospheric circulation when generating future climate variability, as is described in later sections, is a new contribution to the existing procedures of impact studies.

The traditional view of the scientific community involved in assessing climate change impacts is relatively narrow, while contribution from individual sources (such as choice of emission scenario) are considered and other components such as choice of climate model, downscaling methods and impact models are ignored (Wilby et al. 2006a). However, Manning et al. (2009) have demonstrated that different downscaling methods produce different flow predictions and those variations are partly attributable to potential evapotranspiration predictions. Qian et al. (2010) have shown the preference of regional models over GCMs in relation to the performance of the downscaling method. Holman et al. (2009) have shown that uncertainty related to the choice of downscaling method is greater than that of scenario selection, while Abbaspour et al. (2009) have shown that variation of flow for different hydrological models is greater than the variation of flow for different scenarios.

Although the issues and approaches for downscaling GCMs results to hydrological impact analyses are well known, and also reviewed by Prudhomme et al. (2002), there is no single appropriate downscaling approach (Holman 2006). Therefore, site-specific findings of the recent investigations in this regard are applied to address this issue. Hennessy et al. (2004) considered twelve GCMs' performance when simulating the current regional climate, such as average patterns of pressure, temperature and precipitation. However, future predictions were available for nine GCMs in the Ozclim data source, which was used in the research.

From the nine GCMs of Ozclim, the following five models, as described by Hennessy et al., (2004) were performing better for the region of NT:

- **CSIRO Mk2:** Australia, years 1881–2100, horizontal resolution 400 km, temporal resolution daily
- **CSIRO DARLAM:** Australia, years 1961–2100, horizontal resolution 125 km, temporal resolution daily
- **ECHAM4/OPY:** Germany, years 1860–2099, horizontal resolution 300 km, temporal resolution monthly
- **HadCM2:** UK, years 1861–2100, horizontal resolution 400 km, temporal resolution monthly
- **HadCM3:** UK, years 1861–2099, horizontal resolution 400 km, temporal resolution monthly

From the nine GCMs of Ozclim, the other four discarded models as described by Hennessy et al. (2004) are as follows:

- **CCM1:** Canada, years 1900–2100, horizontal resolution 400 km, temporal resolution monthly
- **GFDL:** US, years 1958–2057, horizontal resolution 500 km, temporal resolution monthly
- **ECHAM3:** Germany, years 1880–2085, horizontal resolution 600 km, temporal resolution monthly
- **NCAR:** US, years 1960–2099, horizontal resolution 500 km, temporal resolution monthly

After analysing that report and reviewing the Ozclim data source (CSIRO 2006) version 2.0.1 (which contains results of nine GCMs), five GCMs were selected for extracting future climate change data for the Ranger mine site. The available horizontal resolution of the Ozclim data source was 25 km and temporal resolution was monthly as used in the research.

Thus, to encompass the maximum possible range of long-term and best quality predictions as suggested by Hennessy et al. (2004) for the site, as many as five models are selected for the study. Of the three climatic sensitivity levels suggested by the CSIRO (2006), the medium sensitivity level is selected for the extraction of the projected data. The climate change projections are combined with climatic variability by representing the climate change projection by a set of multiplying factors (for twelve months of 100 years time) for each scenario of each GCM. These factors will increase for high sensitivity and reduced for low sensitivity. The multiplying factors used in the study are conceptually equivalent to the change factors as used by Kilsby et al. (2007). Chiew et al (2009) use a similar concept of 'seasonal scaling' or 'pattern scaling' factors for the downscaling of GCM data for the climate change impact study for south-east Australia. They state that this technique is followed from Mitchell (2003).

The climate data available from GCMs consists of rainfall and PPET. However, the required hydrologic variable for the groundwater model consists of rainfall and AAET. Therefore, it was necessary to convert PPET data to AAET data using some statistical methods as described in the following section.

The evidence of the influence of climatic variability at a multi-annual and decadal time scale on the groundwater has been established by many investigators. For example, Slimani et al. (2009) have demonstrated the differential responses of piezometric levels in a chalk aquifer of France at various locations of the catchment

7.2.3. Conversion of PPET of GCM to AAET for Net Flux Calculation

The climate data used in Seep/W modelling is net flux, which is the algebraic summation of rainfall and evapotranspiration. Therefore, the relevant data to be extracted from Ozclim were rainfall and evapotranspiration. However, the evapotranspiration data available in Ozclim were PPET (personal communication by email to Cher Page, CSIRO) and the

needed data was AAET, as used in the calculation of net flux. Therefore, by analysing the past 100 years of monthly AAET and PPET values for the site, the PPET of Ozclim were converted to AAET for use in the groundwater model. Goderniaux et al. (2009) use a similar concept of correlation for predicting potential evapotranspiration from the predictions of temperature as supplied by GCMs. They develop the correlation between potential evapotranspiration and temperature by using the calculated potential evapotranspiration, using Thornthwaite formula (Thornthwaite 1948), and measured potential evapotranspiration at a weather station. Moreover, they use a new model HydroGeoSphere (Therrien *et al.* 2009) in which actual evapotranspiration are calculated internally as a function of soil moisture. Their work is more accurate in terms of the scientific representation of the physical system. To perform this scale of work for the present study is far beyond the available resources. However, the present work considers the similar GCMs as used by Goderniaux et al. (2009) such as HadCM3, ECHAM4 and three other GCMs. In addition, they consider one emission scenario while the present study considers seven scenarios.

To identify the relationship between PPET and AAET, the monthly totals for the period of 1900 to 1999 have been estimated. Similarly, for the years 1970 to 2006, similar computations have been performed in parallel because the Jabiru East weather station commenced operation in 1970 and the data before 1970 had been interpolated from those of Darwin and Oenpelli by the BoM source. Linear correlation analyses between PPET and AAET have been performed for all twelve months.

From both results, it has been found that there is no significant difference between the pattern of variation of monthly PPET and AAET. Thus, the correlation is good for the four wet months (December to March) with positive correlation and moderate for the four dry months (June to September) with negative correlation. The remaining four months, consisting of two pre-monsoon transitional months and two post-monsoon transitional months (October to November and April to May) have little or no correlation. Cesanelli and Guarracino (2009) have shown a similar relationship between potential and actual evapotranspiration by numerical modelling in unsaturated flow conditions at a location in Buenos Aires, Argentina.

The annual pattern of variation of monthly PPET and AAET linear interpolation (for wet and dry months) and linear interpolation with a modification for the transitional months were used to convert the PPET of Ozclim to AAET for use in Seep/W. The details of the procedure can be found in Appendix G.

Analogy between downscaling and evapotranspiration variable conversion: The necessity of estimating AAET from PPET data was imperative in the context of the research. The analogy of downscaling hydrologic variables from GCMs to catchment scale analyses is used in this point of the problem. The concept of a synthetic WGEN is used in this regard. Synthetic WGENs are widely used in the context of climate change impact modelling, which can be found in a number of studies as stated below.

Dibike and Coulibaly (2005) have shown in their analyses that both 'downscaling techniques', which are statistical in nature, yield comparable results while used for GCMs output to be converted from a global to a local context. One of the techniques was stochastic, Long Ashton Research Station Weather Generator, LARS-WG (Semenov et al. 1998; Semenov and Barrow 2002). The other was a statistical downscaling model, SDSM (Wilby et al. 2002). In many instances, climate change scenarios are generated via SDSM, which is a hybrid of regression-based and stochastic WGEN downscaling methods (Wilby et al. 2006b). The use of SDSM and LARS-WG for the purpose of downscaling GCMs output to RCMs or catchment scale hydrologic models can be found in Scibek et al. (2006a; 2006b; 2008), and Appiah-Adjei and Allen (2008). Scibek et al. (2007) use PCA for the same purpose of downscaling, while Gurdak et al. (2007) use a singular spectrum analysis (SSA) method. Green et al. (2007a) use a modified WGEN model (Richardson and Wright 1984; Bates et al. 1994) and Fowler and Kilsby (2007) use monthly-based 'bias correction' on observed mean statistics of the hydrologic variables. Jyrkama and Sykes (2007) use a built-in WGEN in HELP3 to generate daily synthetic weather data in the study of spatially varying recharge in a large catchment.

All weather generators have certain limitations, such as their inability to reflect interdecadal climate variability sufficiently. They are also based on the assumption that the relationship between large-scale circulation and local weather remains the same in the future as for the period of historical measurements (Dibike and Coulibaly 2005; Herrera-Pantoja and Hiscock 2008).

All of the methods of generation are statistical in nature and their applicability has been decided based on the purpose of the modelling, fitness of the data and overall computational efficiency. The application of the correlation method for converting PPET to AAET is supported in a number of investigations such as Cesanelli and Guarracino (2009), and Goderniaux et al. (2009). The correlation method is a widely accepted method for converting potential evapotranspiration or pan evaporation to actual evapotranspiration or evaporation. Therefore, this analogy can be applied to the presently used method of conversion of PPET to AAET.

7.2.4. Sample Output of Ozclim

GCMs are used for future climate estimation incorporating the changes in the model atmosphere pertaining to the specific emission scenarios only and are not calibrated to reproduce the current climate. Therefore, the outputs of GCMs are always like linear long-term trends. Thus, the short-term climatic variability needs to be considered separately and combined thereafter. The PPET of GCMs is converted to AAET according to the procedure as stated above. The net flux is calculated as rainfall minus AAET. The annual net flux is the summation of the monthly net flux values. The annual net flux data for all seven IPCC scenarios from the HadCM3 model is illustrated in Figure 7.1 to indicate the pattern of average long-term trends of the predicted changes of climatic processes for the various emission scenarios.

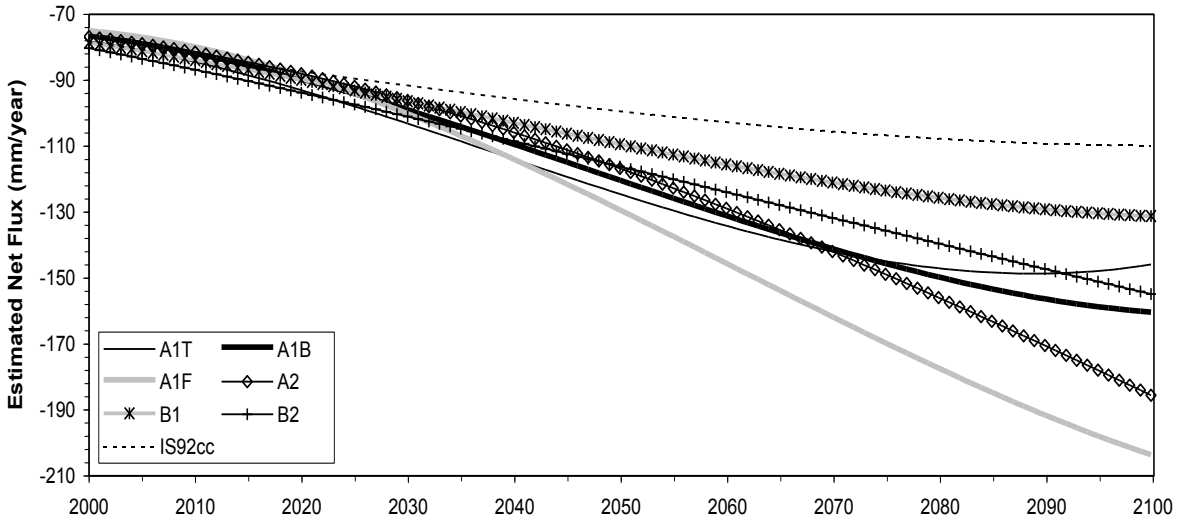

Figure 7.1 The annual net flux (Rainfall-AAET) estimated from rainfall and PPET of one GCM named HadCM3

7.3. Review of the Climatic Variability for the Site

Australia's climate is strongly influenced by the surrounding oceans. Key climatic features include tropical cyclones and monsoon in northern Australia, migratory mid-latitude storm systems in the south and the ENSO phenomenon, which causes floods and prolonged droughts, especially in eastern Australia (Watson et al. 1999). The wet season of the NT is strongly influenced by the summer monsoon, especially in the north where there are thunderstorms and occasional cyclones. The behaviour of the monsoon and the frequency of cyclones are affected by the ENSO. The El Nino phase tends to suppress monsoon and cyclone activity over the territory, while the La Nina phase tends to enhance the activity (Hennessy *et al.* 2004).

Average rainfall over the whole of the NT shows extremely dry years during 1901, 1904–1905, 1951, 1960, 1969, 1989, and 1991. There were extremely wet years during 1903, 1920, 1973–1975 and 1999–2000. The dry years tend to be El Nino years while the wet periods tend to be La Nina years (Chiew *et al.* 1995b; BoM 2004).

Limited confidence: The confidence limit of the predictions is relatively less in the tropical region compared to extra-tropical regions (IPCC 2007). The project site is found to be in the area where less than 66% of the models agree in the sign (increase/decrease) of the change (change of precipitation in December, January and February). There is an increasing recognition that rising temperature is exacerbating (increasing in severity) the impact of any rainfall reduction (Cai 2007). With regard to the global scale, Meehl et al. (1993; 1996) indicate that future seasonal precipitation extremes associated with a given ENSO event are likely to be more intense due to the warmer, more El Nino-like mean base state in a future climate. This means that for the tropical Pacific and Indian Ocean regions, anomalously wet areas could become wetter and anomalously dry areas could become drier during future ENSO events (Cubasch *et al.* 2001). Kundzewicz et al. (2008) have also indicated similar possibilities of variable responses of regions in wet tropics and dry tropics by the middle and end of this century. As a result of reduced precipitation and increased evaporation, water security problems are projected to intensify in southern and eastern Australia (Hennessy and Fitzharris 2007; Hennessy et al. 2007).

However, there has been an increasing trend in rainfall over much of north and north-west Australia over recent decades, which has contrasted with decreases over the rest of the continent. It is argued that the trends in rainfall totals and average intensities are largely unrelated to trends in ENSO and most likely reflect the influence of other factors (Smith and Suppiah 2007). The possible factors could be associated with the following observations and understandings.

7.3.1. Identification of the Relevant Natural Variability Factors for the Site

Regional climate patterns are largely driven by ocean states and associated atmospheric circulations, the modified through feedback from land surface conditions (Switanek and Troch 2007). The modelling of impact for climatic variability is a relatively newer challenge in comparison to that of climate change. The latest work to simulate and thus predict the ENSO-related rainfall variability of Australia in GCM is being performed by Rotstayn et al. (2010). Rotstayn et al. capture the variability of rainfall due to ENSO by incorporating empirical orthogonal teleconnections to consider interactive aerosol feedback in the GCM. The scientific basis of their work is far beyond comparison to the scope of present investigation in which an attempt is being undertaken to relate the ocean atmospheric circulations with climatic variability. Therefore, other similar studies undertaken at different regions of the world are also considered and the understanding of the possible association of surrounding ocean behaviour on the climatic variability of a particular region is obtained. The specific case of the region is then considered. Some of the examples in which SST indices are used for prediction of climatic variability at various time scales are cited below.

The pioneer investigators Madden and Julian (1971; 1972) have firstly investigated the tropical intraseasonal oscillation (ISO), which was recognised increasingly as the phenomena influencing the climate and weather in tropical regions (Weng and Yu 2010). Weng and Yu (2010) have demonstrated in their study the influence of central Pacific Ocean and Indian Ocean coupling on tropical ISO. They have considered both feedback processes, which consider the relationship of the various climatological variables such as wind, atmospheric pressure, temperature and sea surface temperature (SST). The feedback processes mainly considered were wind-evaporation-SST and cloud-radiation-SST.

Timilsena et al. (2009) have obtained the evidence of association of ENSO, Pacific Decadal Oscillation (PDO) (Mantua *et al.* 1997; Zhang *et al.* 1997; Mantua and Hare 2002) and Atlantic Multi-decadal Oscillation (AMO) events with the individual as well as coupled influences on hydrologic flows in the Colorado river basin. Gurdak et al. (2007; 2007) report the importance of interdecadal-climate cycles as controls on rates and mechanisms of climate-varying recharge and support the conclusion that understanding natural climate variability is a necessary step towards predicting groundwater response as a result of climate change. The relationship of climatic variability ranging from interannual to multi-decadal time scales with specific groundwater levels could be found in their work in which most of the variance in groundwater levels was correlated with PDO in climate for the site of the Southern High Plains aquifer in the US.

The methodology of relating the indices of circulation in the surrounding ocean with the natural climatic variability can be found in Fowler et al. (2003). They use a similar technique while formulating the climatic variability for northern England by using the relationship of North Atlantic Oscillation (NAO) with the regional climatic variability of the site. Similarly, Duah and Xu (2008) report evidence of the relationship between the interannual variability of winter rainfall in the southern Cape region of South Africa with SST of Southern Atlantic Ocean (SAO) and the large-scale ocean-atmosphere interaction in that region. Martinez et al. (2007) identify coupled modes of variability between Pacific and Atlantic SST with the monthly precipitation in south-west Florida while performing a hydrologic forecast to be used by the water supply managers. Switanek and Troch (2007) used time-lagged SST and Sea Level Pressure (SLP) of the Pacific Ocean to correlate with basin average precipitation and surface temperature in order to identify which regions of the Pacific Ocean have the most influence on the climatic variability of lower Colorado.

The climatic variability for the present research site is influenced by coupled ocean-atmosphere phenomena in the Pacific Ocean and Indian Ocean. The current understanding of the Pacific Ocean phenomena is based on ENSO, PDO and/or IPO (Power et al. 1999) while that of the Indian Ocean is based on the IOD as indicated by Chang et al. (2006). Kripalani et al. (2010) study the relationship of the IOD mode for east Asia-west Pacific monsoon rainfall and the possible mechanism is investigated. These understandings are in the process of development. Therefore, the factors influencing the multi-annual and

decadal variability of climate for the site are to be represented with due consideration for all possibilities.

ENSO is a global coupled ocean-atmosphere phenomenon relating to the temperature fluctuations in surface waters of the tropical eastern Pacific Ocean. The atmospheric signature, the Southern Oscillation (SO) reflects the monthly or seasonal fluctuations in the air pressure difference between Tahiti and Darwin. ENSO is associated with floods, droughts, and other disturbances in a range of locations around the world. These effects, and the irregularity of the ENSO phenomenon, make predicting it of high interest. ENSO is the most prominent known source of interannual variability in weather and climate around the world (approximately three to eight years), though not all areas are affected. ENSO has signatures in the Pacific, Atlantic and Indian Oceans.

The PDO is a pattern of Pacific climate variability that shifts phases on at least an interdecadal time scale, usually in the range of 20 to 30 years. The IOD is an oceanographic phenomenon affecting climate in the Indian Ocean region. The IPO or ID display similar SST and SLP patterns, with a cycle of 15–30 years, but affects both the north and south Pacific. The behaviour of all these phenomena are reviewed in light of existing literature and considered in the context of the project site of Ranger, NT in Australia.

The El Nino-rainfall and El Nino-stream flow teleconnections in Australia are amongst the strongest in the world (Chiew and Leahy 2003). A number of shifts in flood and drought risk in eastern Australia during 1945 and 1975 have been identified by many investigators (Erskine and Warner 1988; Franks 2002a; Verdon and Frank 2006b). The mid-1940s and mid-1970s correspond to the time periods of major changes in both SST anomalies and circulation patterns over the Pacific Ocean and Indian Ocean (Allan et al. 1995). These climate shifts are associated with variations in the large-scale climate modes known as the Pacific Decadal Oscillation (PDO) (Mantua *et al.* 1997; Zhang *et al.* 1997; Mantua and Hare 2002) and the Interdecadal Pacific Oscillation (IPO) (Power et al. 1999). Importantly, IPO and PDO time series are highly correlated and represent variable epochs of warming (positive phase) and cooling (negative phase) in both hemispheres of the Pacific Ocean (Mantua et al. 1997; Folland et al. 2002; Franks 2002b).

By reviewing the existing understanding of the ENSO, IPO, PDO, and IOD for global and local contexts, some conditional aspects of the random natural processes have been identified. Those understanding, observations and possibilities are translated in the algorithm for generating the spells of ENSO events for the site.

7.3.2. Interaction among ENSO, PDO and IOD

When assessing changes in ENSO, it must be recognised that an 'El Nino-like' pattern can apparently occur at a variety of time scales ranging from interannual to interdecadal (Zhang *et al.* 1997). These may occur either without any change in forcing or as a response to external forcing such as increased CO_2 (Meehl and Washington 1996; Knutson and Manabe 1998; Noda et al. 1999a; Noda et al. 1999b; Boer et al. 2000; Meehl et al. 2000). Making conclusions about 'changes' in future ENSO events will be complicated by these factors (Cubasch *et al.* 2001). The question of increased or decreased amplitude and/or frequency of El Nino variability has been addressed by a number of investigators through the use of climate models. The results were conflicting; a slight decrease in amplitude (Tett 1995; Knutson et al. 1997; Washington et al. 2000; Collins 2000b), and a small increase in amplitude (Timmermann et al. 1999; Collins 2000a) were reported. In addition, the increase in intensity (Collins 2000a), the skewness of variability in relation to cold *versus* dry events, shift of seasonal cycle of the events and changes in amplitude-frequency relationships were also reported by others. Therefore, in the present research, a conditional random data generation procedure is used for the incorporation of climatic variability into climate change predictions, assuming that the amplitude and frequency of future ENSO events will be occurring within the same limit of past extreme events.

Phase changes in the PDO have a propensity to coincide with changes in the relative frequency of ENSO events, in which the positive phase of the PDO is associated with an enhanced frequency of El Nino events. The negative phase is shown to be more favourable for the development of La Nina events (Verdon and Frank 2006a; Verdon and Frank 2006b).

As one goes from equator towards pole, the decadal time scale ENSO pattern, its activity and variability increase with respect to that of the interannual time scale ENSO (Power and Colman 2006b). Alternatively, decadal ENSO-like patterns have a broader meridional structure than interannual ENSO. One of the assumptions of this statement is that the

interannual ENSO activity is compared with decadal ENSO activity for a particular region (low latitude or extra-tropical). In addition, extents of interannual ENSO activity in the low latitude and extra-tropical region are not homogeneous. Therefore, the option of no PDO is available for the site, which is in a low-latitude region.

After the PDO value is selected, the frequency, amplitude and timing (months of a year) of the net flux (rainfall and AAET) are to be selected. In the context of the Australian climate, specifically the site, the existing observations of the past ENSO events are analysed and further decision rules are formulated in light of accepted understandings in this issue. Few fundamental issues are considered here in. The issues can be listed as the non-linearity in the strength of ENSO for Australia, occurrence of IOD in relation to ENSO for Australia, relationship between IOD and ENSO in Australia and uncertainty of future influence of IOD on ENSO of Australia. The interaction of ENSO events with the local climate of the site is represented into multiple numbers of replicates.

Non-linearity in the strength of ENSO for Australia: Non-linearity exists in the strength of the relationship of the climatic variability (ENSO events) in Australia also. The differences in the strength of relationship between El Nino (La Nina) and wet (dry) conditions can be described as follows.

The ENSO's impact on Australia is generally greatest during June–November (Power et al. 2006a). The timing of occurrence of impact of El Nino (La Nina) is recognised to be one of the key factors, which combines the influences of the Indian Ocean and the Pacific Ocean on the Australian climate. The IPO is computed from the average NINO3 indices from October to March of each year and +-0.5 is taken as a threshold value to distinguish from positive or negative (Power et al. 1999; Verdon and Wyatt 2004). Power et al. (1999) use a thirteen-year running block in the correlation analysis between rainfall and IPO indices.

The weak and strong relationship of ENSO events with the Australian climate can be explained with the consideration of the influence of the Indian Ocean in combination with the Pacific.

Occurrence of IOD in relation to ENSO for Australia: Being a typical tropical phenomenon, the evolution of IOD is strongly locked to the annual cycle; the phenomenon

develops during May/June, peaks in September/October, and diminishes in December/January (Chang et al. 2006) Table 7.1. Therefore, the IOD influences the SOI in the Pacific (Behera and Yamagata 2003) and the Australian winter climate (Ashok et al. 2003).

Table 7.1 The combination of the influences of global (IOD) and local (EL Nino/La Nina) phenomena related to natural climatic variability

J	F	M	A	M	J	J	A	S	O	N	D	J	F	M	A	M
				IOD start				IOD peak			IOD end					
				El Nino months												
								La Nina months								
Wet season				Dry season							Wet season					Dry

The El Nino events in Australia usually emerge in the March to June period and strongest influence occurs in the six months of June to November (BoM 2007a). The cooling of La Nina is relatively strongest during the October to March period (BoM 2007a). Not to mention El Nino and La Nina are mutually exclusive while they occur. Therefore, the overlapping of IOD with ENSO is more prevalent with El Nino than La Nina.

Relationship between IOD and ENSO in Australia: Saji and Yamagata (2003b) demonstrated that the IOD and El Nino have opposite influences in the eastern sector of IOD. Abram et al. (2007) also demonstrated the same dynamics in the eastern sector of IOD by coral records and model simulation. For the southern hemisphere in particular, Ashok et al. (2003), and Saji and Yamagata (2003a; 2003b) also report the impact of IOD to be remarkable in a band from the north-west shelf to south-eastern Australia. The IOD teleconnections in the winter is due to a Rossby wave train and its impact on the weather phenomenon (Chang et al. 2006).

Thus, the overlapping of IOD being greater (smaller) with El Nino (La Nina), the opposing influences of ENSO and IOD result in a weaker (stronger) relationship with the dry (wet) condition. Thus, the relationship between La Nina and wet conditions is also reported to be stronger than the strength of the relationship between El Nino and dry conditions (Power et al. 2006a). Similar findings are reported by Chiew et al. (1998), stating that the

teleconnections of ENSO with Australian rainfall, stream flow and drought is stronger in the latter part of the year, meaning stronger La Nina than El Nino.

Uncertainty of future influence of IOD on ENSO of Australia: However, this inverse relationship between IOD and ENSO has been reported to be broken/weakened in recent decades by Kumar et al. (1999), giving rise to the uncertain drought in the winter rainfall regions of Australia (Abram et al. 2007). The reason for the breaking of the link has been reported by Kumar et al. (1999) to be global warming. There is a possibility of rebuilding the relationship in the long-term if the reason was global warming and human response could stop it. Therefore, the range of possibilities needs to be addressed.

7.4. Algorithm of 'ENSO Generation' for Predicting Future Climatic Variability

With regard to the Ranger site, the El Nino events usually emerge in the March to June period and the strongest influence occurs in the six months of June to November (BoM 2007a). The dry season in our site occurs during May to October. Therefore, with regard to the site, the increased dry condition (caused by El Nino) occurs during the dry season of the year. The cooling is relatively strongest during the October to March period (BoM 2007a). The wet season at the site occurs during November to April. Therefore, with regard to the site, the increased wet condition (caused by La Nina) occurs during the wet season of the year.

Thus, if the influence of IOD with ENSO is not considered, the impact will be greater for both El Nino and La Nina. If the influence of IOD with ENSO is considered, the rainfall in the site being summer rainfall is not counteracted by IOD. Therefore, the wet season will still be unimpacted by IOD. Similar results have been reported by Bayliss et al (2007).

The predictability of the interdecadal changes is still an unexplored area. As shown by a series of decade-long perturbation experiments by Power et al. (2006a), the level of predictability of the relationship between ENSO and the Australian climate is low if the interdecadal changes are predictable. They have also shown that even IPO gives unpredictable, random changes in the relative frequency and magnitude of El Nino/La Nina events in a given interdecadal period; IPO can appear to modulate ENSO teleconnections, i.e. the response of rainfall and temperature to ENSO events.

Decision 1 for PDO: Random selection of PDO positive (El Nino enhanced), and PDO negative (La Nina enhanced) and PDO zero or transitional (both non-enhanced)

Decision 2 for IOD-ENSO relationship for Australia: La Nina is stronger than El Nino for Australia while IOD ENSO inverse relationship exists.

Decision 3 for IOD-ENSO relationship for site:

- Irrespective of the existence of the link between IOD and ENSO, the site wet season is supposed to be consistently and strongly influenced by La Nina.
- During the dry season, if the link (inverse relation between ENSO and IOD) remains broken, the El Nino will be stronger for the site.
- If the relation is again built then El Nino might become weakly related to dry condition for the site.

Therefore, there should be concern about the IOD-El Nino relationship for a future prediction algorithm but nothing for the IOD-La Nina relationship.

Ambiguity 1: The PDO duration to be from 20 to 40 years, randomly selected. The broad guideline comes from the studies based on the IPO during the past 100 years as performed by Verdon (2004).

Ambiguity 2: The randomly selected PDO duration is covered by selecting a random ENSO duration of zero to eight years. The guidelines for the selection of the frequency limit of ENSO events have been obtained by analysing the past 100-year's events in Australia (BoM 2005; BoM 2007a; BoM 2007b).

Ambiguity 3: The IOD El Nino inverse relationship can either exist or not exist.

Frequency of ENSO events: For positive or negative PDO, the cycle is selected to be zero to five years and for transitional PDO, the cycle is selected to be six to eight years.

Figure 7.2 shows the algorithm of the 'ENSO generation' program as developed on the basis of the aforementioned understanding, knowledge and ambiguities.

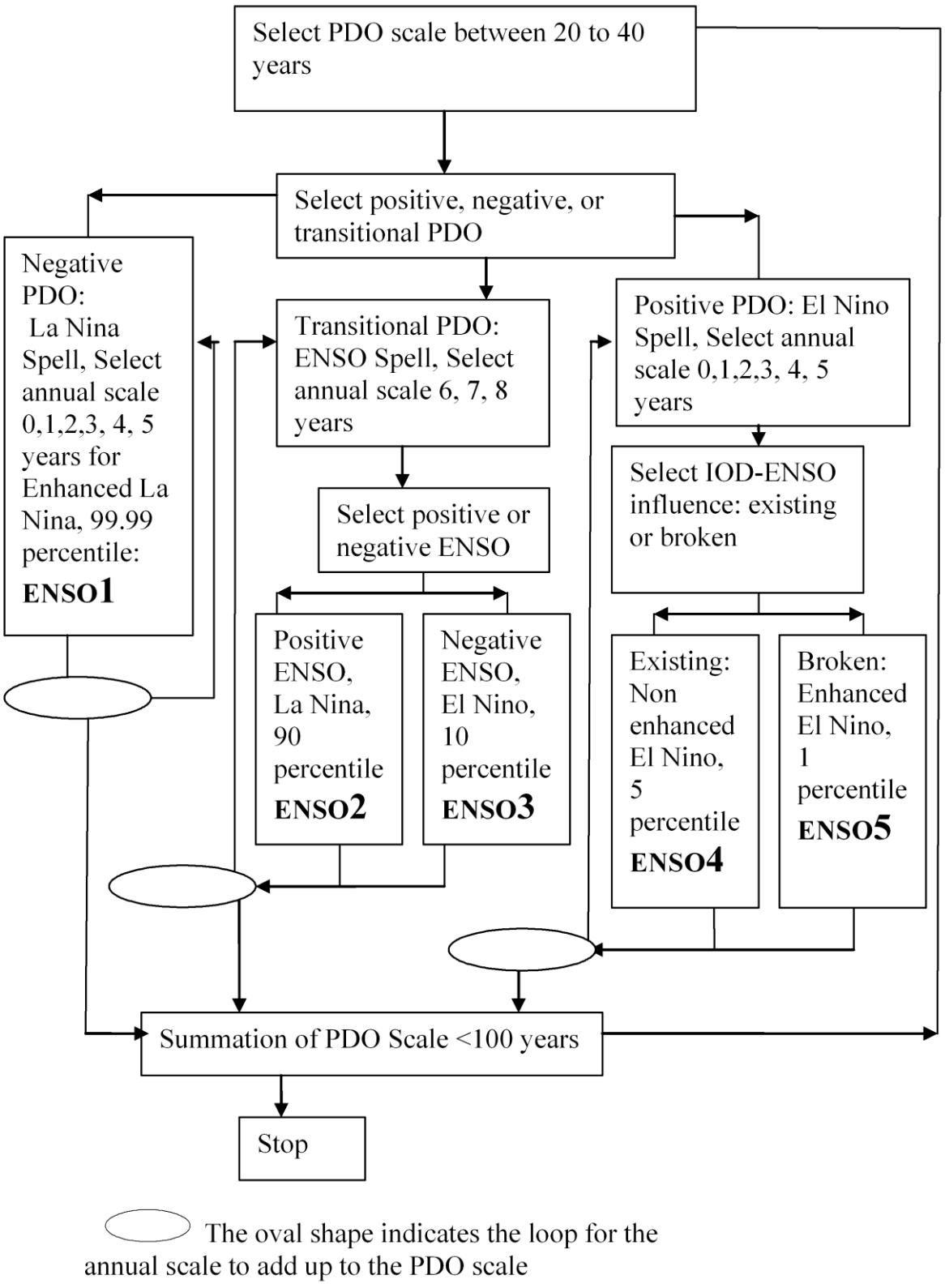

Figure 7.2 The flow chart for the 'ENSO generation' program for rainfall and AAET data for the Ranger site

7.4.1. Guidelines of ETCCDI for Amplitude of ENSO Events

The amplitude of ENSO events in the context of the present research relate to the rainfall and AAET values in the months of occurrence. During El Nino years, when rainfall is lower, it is assumed that AAET is also lower. During La Nina years, when rainfall is higher, AAET is also higher. However, practically this relationship is not linearly correlated for extrapolation meaning rainfall is unbounded while AAET is bounded, as suggested by Morton's equation. The historical percentile records of AAET are used to cut off the point of wet conditions AAET.

For the ENSO events, the ranking from ENSO1 to ENSO5 goes with 99.99, 90, 10, 5, 1 percentile value of rainfall and AAET. If PDO is for La Nina, it will always be enhanced (because it is independent of IOD), if PDO is for El Nino, it may be enhanced or may not be (it depends on IOD). For enhanced La Nina, the 99.99 percentile value of rainfall and AAET are used. For non-enhanced La Nina, 90 percentile values are used. For El Nino, 10, 5 and 1 percentile value of rainfall and AAET are used. The ranges of percentile values are extracted from reviewing the indices suggested by the ETCCDI (Alexander et al. 2006; Alexander et al. 2007). Goderniaux et al. (2009) also uses the concept of the quantile-based mapping approach to bias correction as referred by Wood et al. (2004b) and also used by Salathe' et al. (2007) for downscaling of RCM output. They use an empirical transfer function to force probability distribution of control simulation to match with observed distribution.

7.5. Combination of Past and Future Climatic Variability

In Figure 7.2, the algorithm for generation of rainfall and AAET data for future ENSO events are shown; this corresponds to future climatic variability. The net fluxes of the ENSO events are computed from rainfall and AAET. The ENSO years are those years with ENSO events, while non-ENSO years are the years with no ENSO events. The net flux for ENSO and non-ENSO years and months are combined to generate stochastically generated data at the centurial scale. The non-ENSO years net flux data are the output of SCL, which is generated from a fully stochastic process. In the time series of stochastically generated SCL replicates of net flux, the ENSO events' net fluxes are superimposed. Thus, the net flux of non-ENSO periods will have SCL values and those of ESNO periods will have the net flux from the 'ENSO generation' program.

7.5.1. Stochastic Generation of Net Flux by CRC-SCL

The available historical climate data was analysed by the SCL software (Srikanthan et al. 2005) to obtain a statistical description of climate variability, in order to facilitate a Monte Carlo approach to model a large number of replicates. To produce replicates of a future 100 years' (2001–2100) climate data, the past 100 years (1901–2000) climate data is analysed by using SCL. In SCL, the statistical summary for assessing the quality of the stochastically-generated monthly climate data consists of mean, standard deviation, coefficient of skewness, lag one autocorrelation coefficient, maximum, minimum and cross-correlation between climate variables such as rainfall, evapotranspiration and temperature (Srikanthan et al. 2005).

7.5.2. Quasi-stochastic Generation of Net Flux by 'ENSO Generation'

Given the 100-year timeframe under assessment, potential interdecadal factors such as PDO and IOD in climate variability are considered for the formulation of the algorithm named 'ENSO generation', which will be described in detail in this chapter. The generated net flux data (rainfall – AAET) for ENSO events as an output of this algorithm are then imposed on the stochastic replicates of SCL by overwriting the net flux values of selective periods of time in the range of 100 years.

7.5.3. Sample Output of 'ENSO Generation' Net Flux

The process of future climate replicate generation consists of the following steps such as the historical 100 years' monthly net flux time series being analysed using SCL. The graph of the time series of historical net flux is shown in Figure 7.3 and one sample of SCL replicates is given in Figure 7.4. The graph for the 'ENSO generation' program's output is shown in Figure 7.5. Finally, the graph for the combined SCL and ENSO is shown in Figure 7.6.

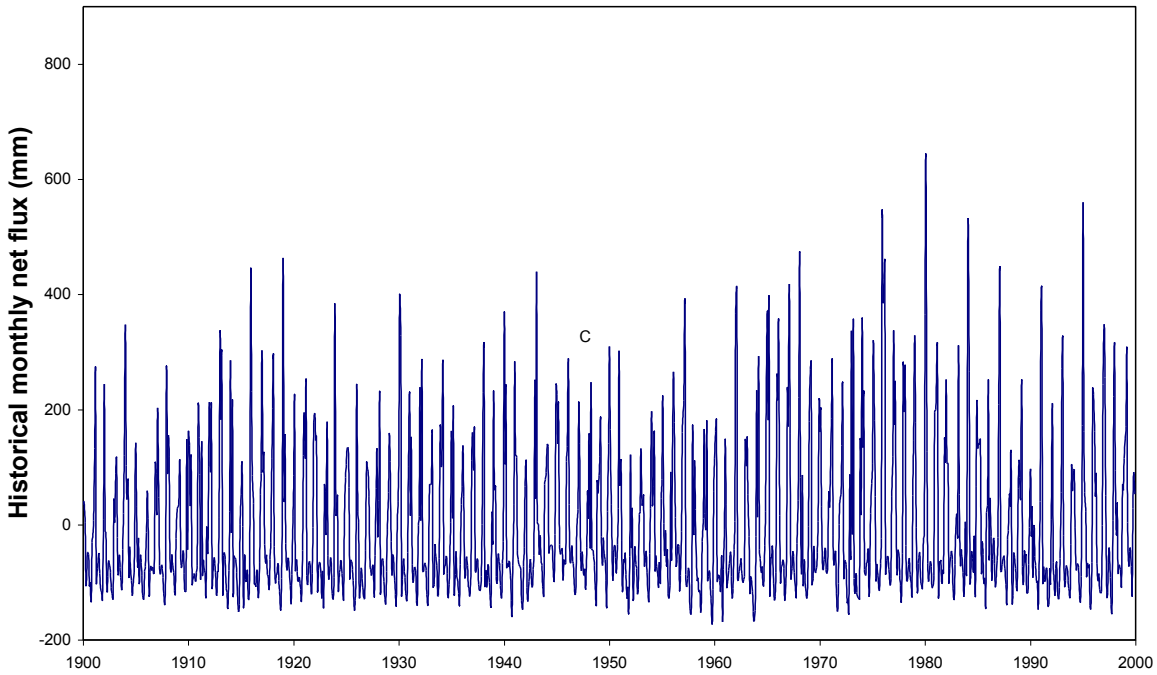

Figure 7.3 Historical monthly net flux from January 1900

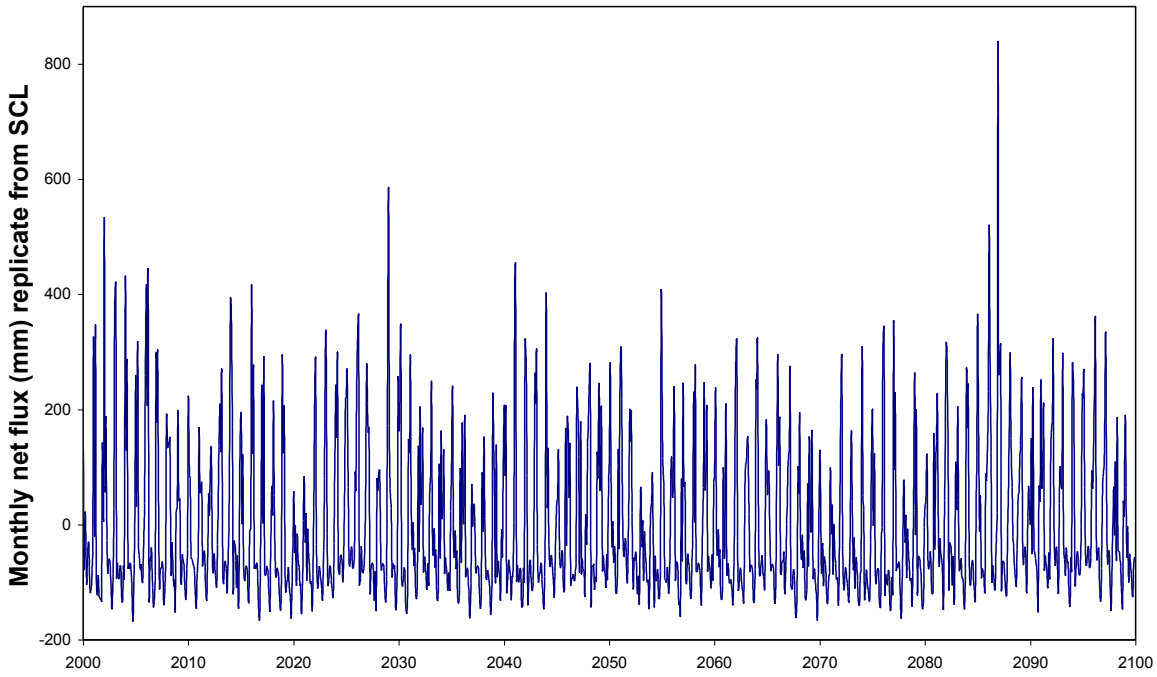

Figure 7.4 One sample of SCL replicate of monthly net flux from January 2001

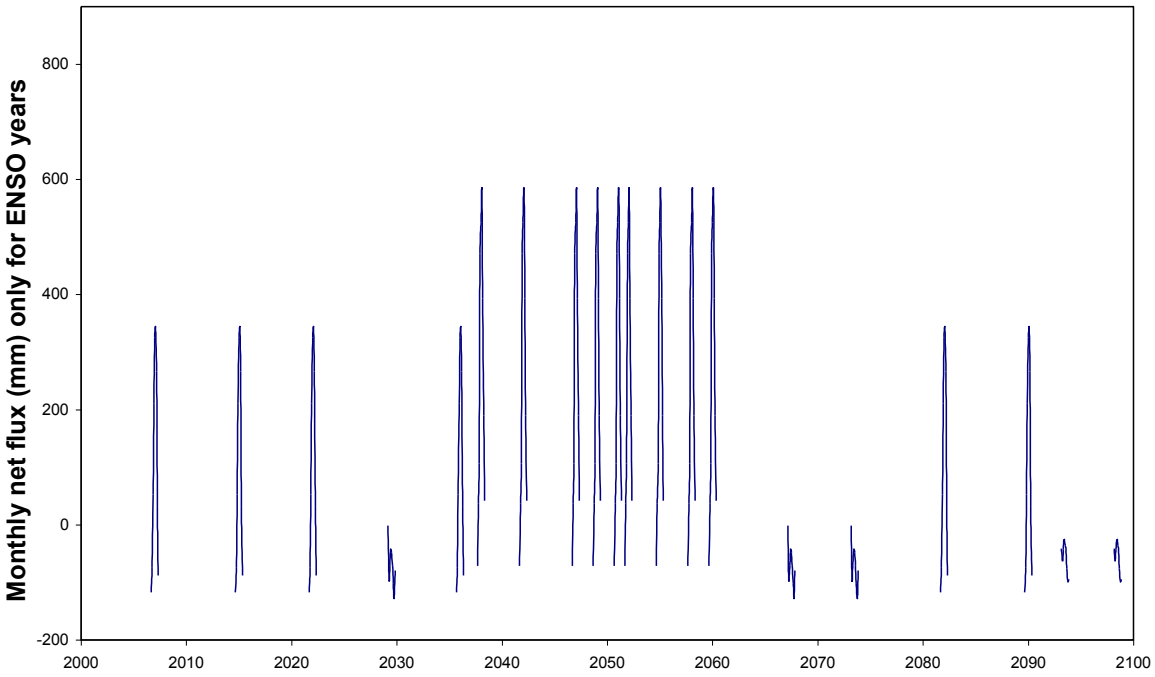

Figure 7.5 One sample of output of the program 'ENSO generation' for net flux of ENSO events

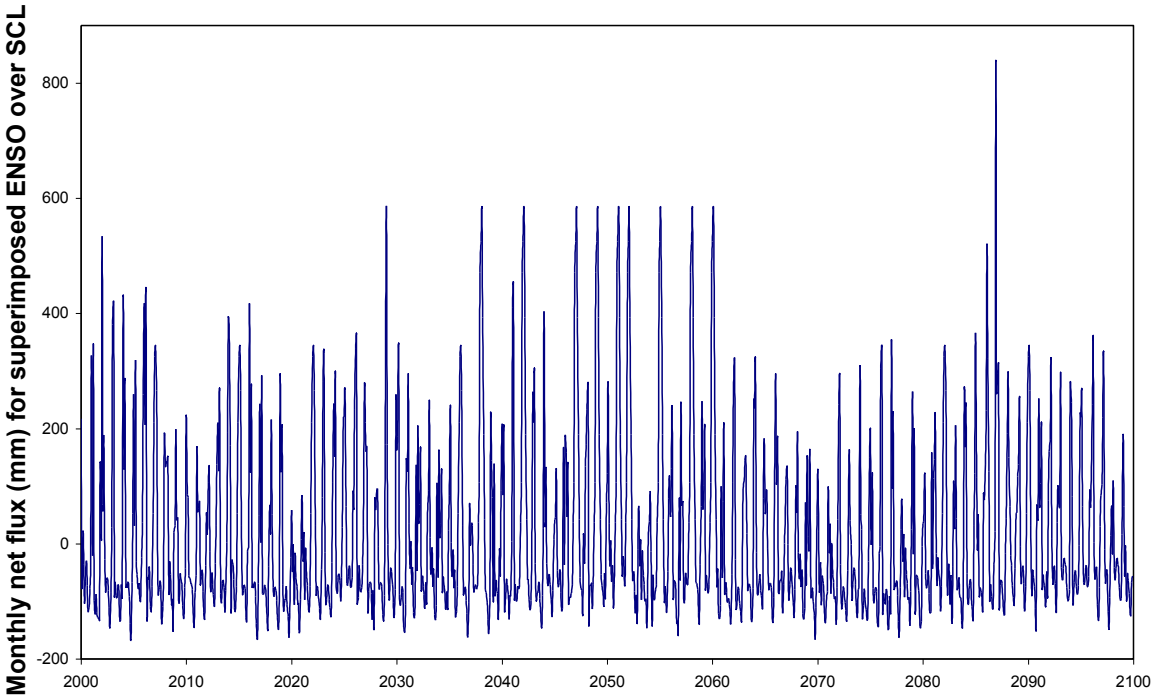

Figure 7.6 Net flux time series after combining the SCL and output of 'ENSO generation' program

7.5.4. Evaluation of Climatic Extremes and GWL Relationship for the Site

In context with the Ranger site, the extreme event relevant to surface water and groundwater is the tropical cyclone. Nott and Hayne (2001) determined a mean return

interval of 250 years for the most extreme tropical cyclones (super-cyclones) striking the east coast of Queensland, Australia based upon a 3000 to 5000 year record from seven separate sites. Assuming the same pattern of occurrence of extreme tropical cyclones for the Ranger site would not be unreasonable because the seven sites are located within a 1500 km distance and the Ranger area is located at about 1000 km north-west from the western site, Wallaby Islands of the same climatic zone of Australia.

Using the historical rainfall data from the site for the period of 1889 to 2006, analysed by the SCL (Srikanthan et al. 2005) monthly rainfall model, the rainfall for rank 1 of 250 year replicate, rank 2 of 500 year replicate, rank 3 of 750 year replicate and rank 4 of 1000 year replicate are estimated. The monthly rainfall values are in the range of 800 mm per month.

To consider the impact of tropical cyclone or any high intensity rainfall on the groundwater level, the rainfall and groundwater level data for the same time of record Table 7.2 are analysed. From 1982 to 2006, there is a record of three instances when the monthly rainfall is greater than 600 mm. However, in the record of subsequent groundwater levels, there is no significant change (rise). This reflects the fact that the flow of water in the soil is limited by the conductivity and soil storage capacity. The larger amount of rainfall in December produces fewer rises than the smaller amount of rainfall in the consecutive months. In fact, the response of December rainfall is transferred in January, taking approximately two months.

Table 7.2 The indifferent influence of high intensity rainfall in groundwater level

Month, Year	Rainfall (mm)	Change in Groundwater level (m)	Bore
February, 1984	645.4	1.7	OB21
January, 1995	704.0	1.7	OB21
December, 1995	**379.4**	**0.3**	OB21
January, 1996	**367.4**	**1.1**	OB21
February, 1996	**304.7**	**1.7**	OB21
January, 2001	619.3	1.7	OB21

The saturated hydraulic conductivity of clay (6 mm/month) and silt (2400 mm/month) are of a wide range of variation. Therefore, the conductivity is an uncertain issue to address. A more certain conclusion can be reached with regard to the occurrence of groundwater level at the ground surface. The flow of water above or below the soil surface is restricted by available soil storage capacity. Thus, the extreme climate would cause extreme flood, rather than groundwater response. It is obvious that when the GWL reaches the ground surface, it yields more runoff causing exaggerated flood downstream of the catchment. Therefore, the extreme climate event is not considered an influencing factor while predicting the inflow (net flux) in the groundwater modelling of the site.

7.6. Combining Deterministic Prediction (GCM) with Quasi-stochastic Predictions (SCL/ENSO/PDO/IOD)

To make scientifically justified use of the Ozclim data, the basic principle of generation of Ozclim data is investigated. The change factor used by previous investigators (Mitchell 2003; Chiew *et al.* 2009) is used in Ozclim in a similar fashion. The Ozclim data are estimated from the following relation (CSIRO 2006):

Baseline climatology + regional pattern from GCMs*global warming = result of Ozclim

Therefore, combining the natural climatic variability with the climate change predictions of Ozclim requires the multiplicative modification.

Mileham et al. (2007) have demonstrated that the calibration of hydrologic models driven by climate data derived from statistical downscaling of RCMs or GCMs remains largely

empirical due to the discrepancy between grided and locally-observed values of those data. Therefore, instead of calibrating the hydrologic model with the GCM data, it is calibrated with historical data. The multiplying factor from the GCMs is then applied to the quasi-stochastically generated climate data to represent the future replicates of climate.

Thus, to combine climate change predictions with natural climatic variability, multiplicative modification predicted by various emission scenarios of GCMs is applied to the quasi-stochastically generated replicates of climatic fluxes. The combined data of the stochastically generated net flux is indicated by $NF_{i,j}^{STO}$, meaning the net flux for i^{th} month of j^{th} year of any randomly generated century. A critical analysis has been performed for a sample set of predictions, as discussed in Table 7.3. The specific model and scenario in Table 7.3 predicts an increase in net flux for April and November and decrease in net flux for the remaining months. The monthly net flux changes -119% in March to +64% in April. A very wide range in the trends of the predictions in terms of magnitude and directions has been observed with all of the month's net flux for the selected five GCMs and seven scenarios.

Table 7.3 Example set of multiplying factors (climate change prediction trend) for HadCM3 GCM's A2 scenario

Months of the year	Years from 2000 to 2100					% change by 2100
	2000	2020	2050	2070	2100	
January	1	0.98	0.93	0.89	0.82	-18
February	1	0.99	0.98	0.96	0.94	-06
March	1	0.88	0.56	0.29	-0.19	-119
April	1	1.07	1.23	1.38	1.64	+64
May	1	0.98	0.93	0.89	0.81	-18
June	1	0.95	0.82	0.70	0.51	-49
July	1	0.96	0.86	0.76	0.60	-40
August	1	0.97	0.88	0.81	0.69	-31
September	1	0.98	0.94	0.90	0.83	-17
October	1	0.99	0.95	0.92	0.86	-14
November	1	1.03	1.10	1.16	1.25	+25
December	1	0.98	0.94	0.89	0.82	-18

Rainfall and PPET (converting to AAET) from five GCMs for seven scenarios are extracted and processed to determine the net flux as an algebraic summation of rainfall and AAET. Thus, 35 sets of net flux data are obtained for 100 years from 2000 to 2100. Using these 35 sets of 100 years net flux value, 35 sets of multiplying factor are computed as $NF_{i,2000+j}^{OZ(k)} / NF_{i,2000}^{OZ(k)}$

$NF_{i,2000+j}^{OZ(k)}$ is used to indicate the net flux for i^{th} month (i = 1 to 12) of j^{th} year (j = 0 to 100) predicted by Ozclim for the k^{th} set (k = 1 to 35). The representation of 'k' is described in Table 7.4. This multiplying factor is multiplied with the stochastically generated $NF_{i,j}^{STO}$ to obtain the $NF_{i,j}^{PRED(k)}$

$$NF_{i,j}^{PRED(k)} = NF_{i,j}^{STO} \times NF_{i,2000+j}^{OZ(k)} / NF_{i,2000}^{OZ(k)}$$

Table 7.4 The meaning of OZ(k) as k varies from 1 to 35, consisting of seven scenarios of five GCMs predictions provided by Ozclim data source

OZ(1) = CSIRO Mk2 A2	OZ(8) = DARLAM A2	OZ(15) = ECHAM4 A2	OZ(22) = HadCM2 A2	OZ(29) = HadCM3 A2
OZ(2) = CSIRO Mk2 A1B	OZ(9) = DARLAM A1B	OZ(16) = ECHAM4 A1B	OZ(23) = HADCM2 A1B	OZ(30) = HADCM3 A1B
OZ(3) = CSIRO Mk2 B1	OZ(10) = DARLAM B1	OZ(17) = ECHAM4 B1	OZ(24) = HadCM2 B1	OZ(31) = HadCM3 B1
OZ(4) = CSIRO Mk2 B2	OZ(11) = DARLAM B2	OZ(18) = ECHAM4 B2	OZ(25) = HadCM2 B2	OZ(32) = HadCM3 B2
OZ(5) = CSIRO Mk2 A1F	OZ(12) = DARLAM A1F	OZ(19) = ECHAM4 A1F	OZ(26) = HadCM2 A1F	OZ(33) = HadCM3 A1F
OZ(6) = CSIRO Mk2 A1T	OZ(13) = DARLAM A1T	OZ(20) = ECHAM4 A1T	OZ(27) = HadCM2 A1T	OZ(34) = HadCM3 A1T
OZ(7) = CSIRO Mk2 IS92cc	OZ(14) = DARLAM IS92cc	OZ(21) = ECHAM4 IS92cc	OZ(28) = HadCM2 IS92cc	OZ(35) = HadCM3 IS92cc

7.7. Appropriateness of Monte Carlo Method

Monte Carlo methods are a widely used class of computational algorithms used for simulating the behaviour of various physical and mathematical systems. Stochastic generation of random process is generally called the Monte Carlo method. Because of the repetition of algorithms and the large number of calculations involved, Monte Carlo is a

method suited to calculation using a computer, utilising many techniques of computer simulation. Monte Carlo simulations are distinguished from other simulation methods (such as molecular dynamics) by being stochastic, which are non-deterministic in some manner, usually by using random numbers (or, more often, pseudo-random numbers), as opposed to deterministic algorithms.

It may be recalled that the conditional random processes have been developed in this chapter to generate the future ENSO events at the centurial scale as described in the 'ENSO generation' program. The conditions of the random process have been developed from the knowledge and understanding from the literature data and possibilities of the behaviour of the climatic variability caused by ocean atmospheric circulations for the specific site. The use of Monte Carlo simulation in the predictive investigations is not new. For example, Aguilera and Murillo (2008) use probability distribution function for generating 100-year climate data while studying climate change and recharge relationship. Wilby and Harris (2006c) demonstrate the use of Monte Carlo simulations in generating the river flow data as an impact of climate change. However, the incorporation of certain ambiguities regarding future interactions of ocean atmospheric circulations in a specific location when generating various combinations of climatic variability are rarely found.

The computational effort on large models with many input parameters (or variables such as rainfall, evapotranspiration and net flux) can become extremely large in terms of time and data management. In the present context, stochastically generated data is employed to feed the physically based model Seep/W, which involves extensive computation. The output of the physically based model is monthly GWLs data at the centurial time scale, which is the target variable of the research.

Therefore, it is necessary to follow some guidelines for the number of replicates to be considered for each set of simulations. The guidelines of peer scientists such as Anderson and Bates (2001) in the realm of hydrological modelling are considered here.

7.7.1. Number of Replicates of Each Set of SRES of Each GCM

Monte Carlo-based techniques rely on the fact that variations in model inputs can generally be described as probability density functions. After specifying these distributions, sampling from these distributions is performed, resulting in a set of model inputs. All these inputs

are used to simulate the model output. Further analysis of the distributed modelling results, in terms of means, variances of the simulated outputs and correlation between model input and output, provides information on sensitivity and uncertainty of the model and its inputs (Booltink 2001).

In case of random sampling from the distributions, the number of samples to be taken should be larger than ten times the number of parameters included in the Monte Carlo analysis (Janssen *et al.* 1993). The conditional random generation of replicates of ENSO events is used in this research since there are three numbers of ambiguities and it is assumed that the three ambiguities can be analogous to three independent parameters.

Therefore, considering ten samples for each ambiguity should result in the total sample size to be 30 for each of the climate change scenarios of each of the GCMs. Holman et al. (2009) use 100 simulations for each hydrological year while they use the statistical properties from real time data of a limited number of hydrological years. They have shown that both 100 runs and 1000 runs produce similar variability while they preserve the relevant statistics of the real time data. Since the present method is not fully stochastic, it is reasonable to reduce the number of simulations to 30 as justified by Janssen et al. (1993). Since there are five GCMs with seven scenarios each, the total number of predicted data is therefore 1050 sets (35 sets X 30 samples). For each of the 35 sets of net flux data, the GWLs are computed using the Seep/W model. Uncertainty/reliability of the computed GWLs are analysed by performing some statistical analyses.

7.7.2. Confidence Limit

There could be a range of ways to examine the result of computed GWLs after 100 years time but at this stage of the work, it is preferable to select the most simple and commonly accepted computation for a randomly generated system. Normal probability distribution function is assumed valid for the computed GWLs by Seep/W as fed by the 30 replicates/samples of input, which are generated randomly as stated earlier. Therefore, the range ($\mu \pm \sigma$) of the time series of 100 years computed GWLs are computed. The estimate of a 68% confidence limit is ascertained.

It can be recalled that non-physical process-based models, i.e. the multivariate AR models are also used for the prediction of GWLs for 100-year periods, as decided in Chapter 6.

Therefore, the confidence limits for physical and non-physical models could be compared with Seep/W modelling as will be reported in Chapter 9.

7.8. Conclusion

The site-based understanding of the surrounding ocean circulations such as IOD, PDO or IDO, which influence the ENSO events, are analysed and reviewed. The Monte Carlo simulation is selected as a suitable method for the generation of the ENSO events, which are assumed to be a conditional, random process. The modelling of ENSO events for climatic variability is thus performed by developing the 'ENSO generation' program.

The SCL is used for the simulation of non-ENSO years. By combining ENSO years with non-ENSO years, the net flux data for baseline climate is formulated. Finally, multiplicative modification to the net flux data of baseline climate data is performed to consider the influence of climate change predictions by each of the seven emission scenarios of the five selected GCMs. Thirty replicates were generated for each scenario of each GCM.

Thus, 1050 sets of future net flux data replicates have been generated. The generated net flux data is used as input to the physically based unsaturated groundwater model Seep/W, as will be reported in Chapter 9. As a prerequisite of any predictive study, the physically based models need to be validated with historical monitored data. Therefore, the next chapter describes the parameter selection and validation of the Seep/W model with respect to historical monitored GWLs data.

8. Unsaturated Flow Modelling

Reviews of existing reports of previous investigations and laboratory-based investigations of soil samples of the site are performed to assess the range of soil property parameters that are required to represent the soil hydraulic property curves. The saturated hydraulic conductivity and porosity are the two key properties that are investigated. Based on the range of findings and calibration runs with a number of soil property functions, the modified functions of the Fredlund-Xing model are selected as the best for incorporating the range of historical net flux data and simulating observed GWLs with sufficient computational stability. For validation of the model with monitored GWLs, a wide range of statistical criteria is investigated, based on short-term and long-term performances and are applied to a number of bores. The most important criteria are selected from a number of considerations such as purpose of modelling, practical site conditions and limitations. The best performing bore is thus selected for the long-term prediction of GWLs for climate change.

8.1. Hydraulic Properties of Soil

For the representation of the behaviour of GWLs in the bores of the site, Seep/W modelling software (Krahn 2004b), the historical rainfall, AAET and GWLs are used by selecting appropriate boundary conditions and initial conditions. For simulation purposes, the soil hydraulic properties need to be defined for the bore soil. The past technical investigation reports are reviewed for the site to obtain some gross information in this regard. A number of soil samples from the site are also investigated in the laboratory to estimate the saturated hydraulic conductivity. Based on the collected soil property information, the past observed GWLs are validated with a range of values of saturated hydraulic conductivity and porosity for the long-term prediction of the GWLs response.

8.1.1. Hydrogeology of the Ranger Site

Although there have been numerous studies on the hydrogeology and water balance at Ranger, only a few have directly examined the relationship between groundwater and climate, especially rainfall-evaporation and recharge as in Vardavas (1993) and Woods (1994). A brief review of the hydrogeology is presented, followed by a justification of the modelling approach used for this work.

It has been reported in Chapter 3 that in the past, hydrogeology studies at Ranger have commonly focussed on water or tailings management issues. The hydrogeology is considered to comprise three principal aquifer types: alluvial sands and gravels (Type A); lateritic layers, clayey sands to weathered rocks (Type B); and fractured rocks (schists and dolomite) (Type C). These are demonstrated in Figure 3.5 (Ahmad and Green 1986; Woods 1994; Brown *et al.* 1998). The most important shallow aquifers are found as weathered and lateritic soils (by area), with annual variations in the water table being between 1 and 5 m. One example of the seasonal groundwater movement compared to cumulative net flux (rainfall – evapotranspiration) is given in Figure 5.11, showing annual variation along with long-term climatic variability (i.e. wetter *versus* dryer periods).

8.1.2. Soil Property

Saturated hydraulic conductivity was measured by Willett et al. (1993) over two depth intervals at each of the 10 locations within the central plot area of Magela Land Application Area (MLAA). Measurements were taken using the borehole permeameter technique of Talsma and Hallam (1980). The two depth intervals chosen to correspond to the natural soil A and B horizons were 3 to 33 cm and 33 to 63 cm. The decrease in mean hydraulic conductivity occurred from 33.6 metres per month (mpm) to 5.1 mpm with the increase in clay content in the B horizon. The unit of hydraulic conductivity used as mpm was chosen to facilitate modelling efficiency, which is discussed in a later section. 'Month' as used here refers to 30 days duration rather than the sequence of calendar months.

SHPA (Western and McKenzie 2004): Soil Hydrological Properties of Australia (SHPA) data source has been investigated for the region and the region has been found to be consisting of three soil landscape units with various solum depths and thicknesses of horizons A and B. The thickness of the horizons vary from 0.1 m to 1.1 m and their saturated hydraulic conductivity varies from 0.216 mpm to 216 mpm (Western and McKenzie 2004).

8.1.3. Measurement of Bore Soil Sample Properties in Laboratory

Disturbed soil samples from five locations (OB28, OB20, OB44, GC2 and OB27) in the mining site were analysed in the laboratory to determine the saturated hydraulic conductivity (K_{sat}) and grain size distribution curve (see Figure 8.1). The K_{sat} values varied widely, in the range of 0.006 to 1350 metre per month (mpm). The values were highly

sensitive to the compaction of the soil in the mould. A reasonable compaction procedure based on trial and error was developed to match the textbook values with the laboratory values for the whole range of soils, which varied from silty clay to gravel.

Table 8.1 Measured hydraulic conductivity of disturbed samples from different bores

Bore name	Generalised classification of bore soil based on sieve analysis	Hydraulic Conductivity K_{sat} (mpm)
OB28	coarse sand	1350
OB20	medium sand	360
OB44	medium to fine sand	75
GC2	fine sand	2.4
OB27	fine sand to silt	0.006

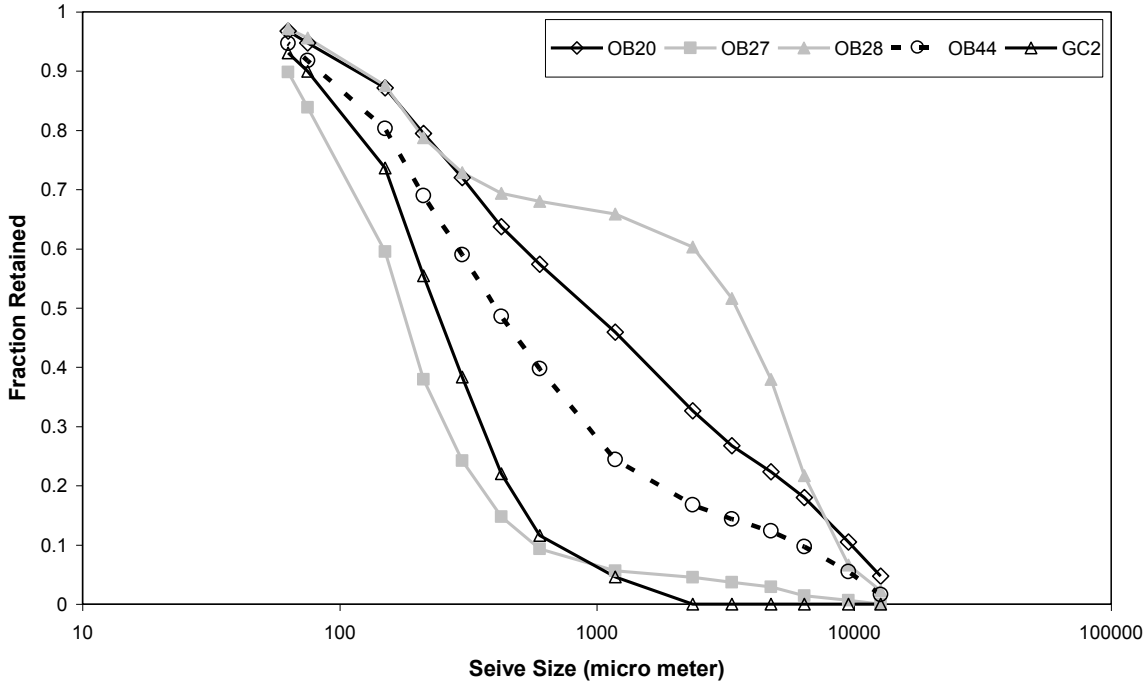

Figure 8.1 Grain size distribution curve of soil samples

Though these values were highly varied from the field observations performed by Willett et al. (1993), the grain size distribution curves of the soil samples from all these bores show consistency with the conductivity values.

For most practical problems, it has been found that approximate soil properties are adequate for analysis (Papagiannakis and Fredlund 1984). Hence, empirical procedures to estimate unsaturated soil parameters would be valuable (Fredlund and Xing 1994). Therefore, with this limited information on the soil property, we had to perform a large number of calibration runs of the model to simulate the past 26 years' real time groundwater level data of some of the monitoring bores that are relatively unimpacted by mining activities.

8.1.4. Comparison and Evaluation of Laboratory Result

The past field measurement values of saturated hydraulic conductivity (33.6 to 5.1 mpm) are within the range of measured values in the laboratory as performed for disturbed samples. The laboratory-measured values have limited acceptability because the samples were disturbed. As the site consists of very complex geology, we selected a range of values of saturated hydraulic conductivity and porosity for the selected bores OB1A, OB20, OB21A, OB27 and OB41. It should be mentioned here that the bores were selected for validation (OB1A, OB20, OB21A, OB27 and OB41) based on varied locations and longer periods of past data of GWLs. However, the samples were selected from the bore locations (OB28, OB20, OB44, GC2 and OB27) based on the present site situation and accessibility.

8.2. Seep/W Model Structure and Development

For modelling with Seep/W, the uncertainties with the highly variable hydraulic conductivity functions and soil water characteristics have been handled with the use of multiple numbers of standard equations, as suggested by Fredlund and Xing (1994), which are applicable for the whole range of soil in the model. The high degree of parameter uncertainty, as indicated by Scanlon et al. (2002), in the solution of RE is handled by fitting the modelled groundwater levels with measured groundwater levels of a number of monitoring bores by jointly calibrating the soil moisture characteristics curves. A wide range of statistical criteria has been considered in the selection of the most appropriate soil moisture characteristics curve for the long-term prediction of the system.

8.2.1. Model Structure

A one-dimensional conceptual model of groundwater-climate interaction was adopted (Type B). A homogenous vertical column was defined with no-flow boundaries on all sides except the surface, where net climate flux (rainfall – AAET) was applied at monthly time

steps (see Figure 8.2). The use of monthly time steps for any hydrological system is well accepted, such as Xu (1999), who uses monthly average flow as criteria for validation. The use of net flux as an indication of a climatic factor is also scientifically justified. For instance Knotters and Bierkens (2000) represent net flux as a climatic factor in their work. The detailed scientific basis for using monthly time steps in computation and using net fluxes for flow representation in the system has been provided in Chapters 2 and 4.

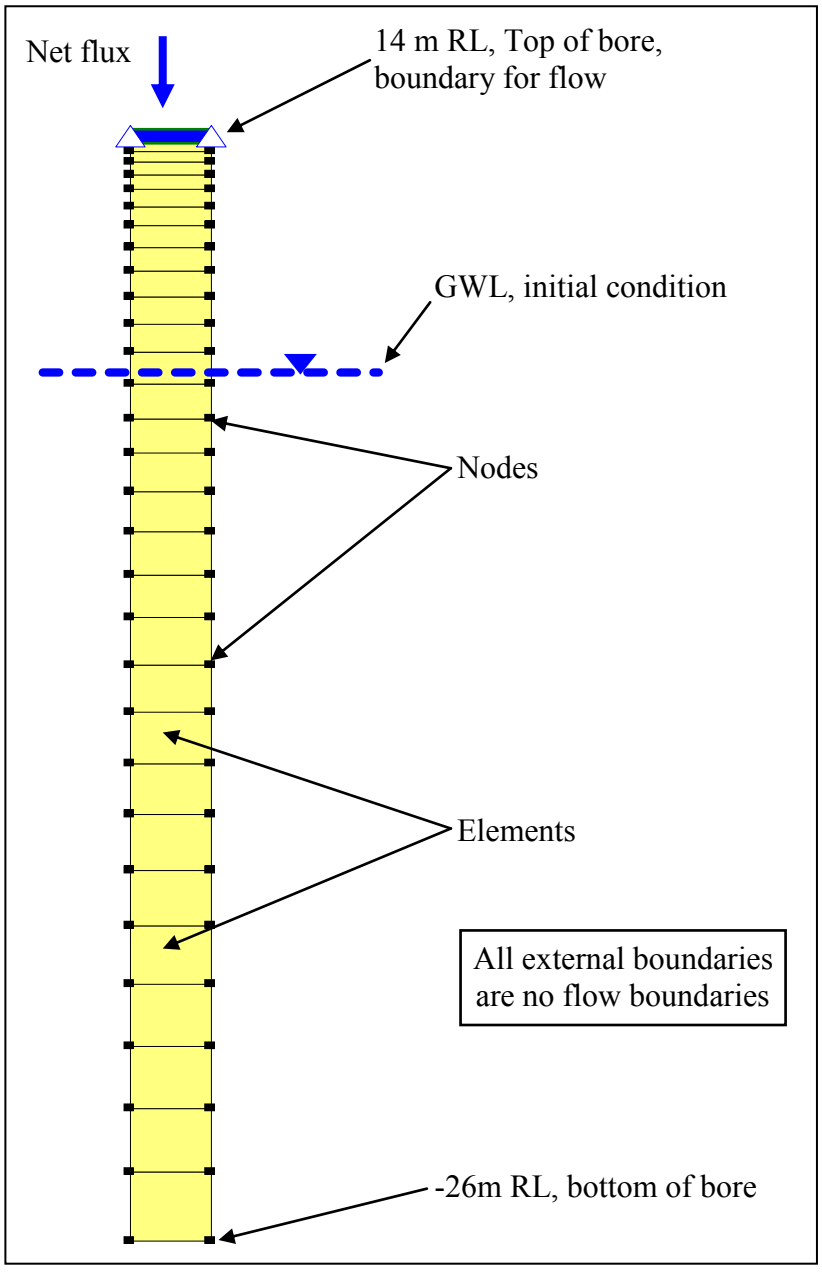

Figure 8.2 Schematic representation of the one-dimensional vertical flow column. The mesh resolution is finer at the top and gradually coarser at the bottom of the soil column

8.2.2. Soil Properties

Soil properties were based on previous work, such as porosity, saturated hydraulic conductivity and unsaturated moisture retention (characteristic) curve (Willett et al. 1993); (Willett *et al.* 1991); (Akber 1991). The unsaturated hydraulic conductivity function was defined from the Soil Water Characteristics Curves (SWCC) such as Van Genuchten or Fredlund-Xing models (Krahn 2004b). SWCC describe the variation of volumetric soil water content (VSWC) and hydraulic conductivity (HC) with respect to changing soil suction during the process of wetting and drying, meaning an unsaturated condition. The laboratory measurement of the properties at an unsaturated condition could not be conducted due to the high variability of the soil properties.

Laboratory studies have demonstrated a relationship between the soil-water characteristic curve for a particular soil and the properties of the unsaturated soil (Fredlund and Rahardjo 1993). A range of empirical equations (Fredlund and Xing 1994), computer programs using pedotransfer functions (Schaap *et al.* 2001), and data bases (Nemes *et al.* 2001) are developed to estimate the unsaturated soil property. Empirically predicting the permeability function for an unsaturated soil by using the saturated coefficient of permeability and soil water characteristic curve has become an acceptable procedure (Marshall 1958).

Therefore, a wide range of combinations of the various VSWC functions and HC functions were investigated to calibrate the most suitable set of coefficients. The observed GWLs were simulated by running the model with historical net flux data. The main criterion of the suitability was the numerical stability of the model runs since most of the model runs became unstable during the periods of dry years from 1985 to 1994. From the plot of accumulated net flux and observed GWLs graph, it can be seen that during this period, the GWLs had a falling trend due to stronger negative fluxes.

A systematic combination of model runs were tried to obtain a stable run for the whole range of historical net flux data and observed GWLs. Three types of HC functions and two types of VWC functions (Krahn 2004b) were investigated:

- Van Genuchten method (for VWC and then HC from the VWC)
- Fredlund and Xing method (for VWC and then HC from the VWC)

- Green and Corey method (for VWC only)

The three coefficients used to define the VWC function were ‘a’, ‘n’ and ‘m’. The coefficient ‘a’ relates to the air entry value of the soil, and is used with the unit of pressure in kPa. The coefficient ‘n’ relates to the slope of the VWC curve and the coefficient ‘m’ relates to the retention moisture or radius of curvature at the extreme dry condition when the graphs are plotted with log scale for soil suction and linear scale for VWC. The ‘n’ and ‘m’ are unit less coefficients. Detailed combinations are given in Table 8.2 for the Van Genuchten method. However, the Fredlund and Xing method performed better than the other two methods.

Table 8.2 Sample values of the coefficients as used for obtaining stable run and convergence of iterations

Van Genuchten	‘a’ = 500	‘n’ = 0.96	‘m’ = 0.29
	‘a’ = 50		
	‘a’ = 5		
	‘a’ = 0.5	‘n’ = 2.0	‘m’ = 0.5
		‘n’ = 1.5	
		‘n’ = 1.0	
	‘a’ = 2.5	‘n’ = 0.96	‘m’ = 0.8
			‘m’ = 0.4
			‘m’ = 0.2

Van Genuchten	‘a’ = 2.5	‘n’ = 0.96	‘m’ = 0.29
Fredlund and Xing	‘a’ = 2.5	‘n’ = 0.96	‘m’ = 0.29

After an extended set of combinations of the coefficients and careful judgement, the best result was obtained from the Fredlund-Xing method. The convergence of the solution is highly sensitive to the slope of the volumetric water content curve and hydraulic conductivity curve. The selection of hydraulic property coefficients (a, m, n) for defining the Fredlund-Xing model was accomplished by following a systematic calibration procedure for a range of combinations of the parameter values. Finally, the combination of the coefficients for generation of the volumetric water content curves was a = 2.0, n = 1.3 and m = 0.23 (see Figure 8.3). However, the hydraulic conductivity curves were modified from the generated Fredlund-Xing model to obtain the numerical stability and validation

with the monitored GWLs, especially for consecutive dry years such as from 1985 to 1994 (see Figures 8.4 and 8.5). In the earlier instances 'n' would mean the coefficient of SWCC as used by the investigators (Krahn 2004b) but the symbol *n* from here onwards refers to porosity.

As noted previously, the hydrogeology of the Ranger area is highly heterogeneous, leading to differing average responses of the water table to the annual wet season (annual fluctuation, or Δh, of 1–5 m). Obtaining reliable spatial data of all of the above properties is difficult and still includes residual uncertainty. As such, a range of Seep/W models was developed with varying soil parameters to assess this uncertainty. This allowed a choice of optimum properties for each bore to be used for assessing climate change impacts as could be found in Kabir *et al*. (2008b). In this work, saturated hydraulic conductivity (*K*, 0.3 to 30 mpm) and effective porosity (*n*, 2.5 to 20%) were varied. All model results were statistically evaluated using a range of statistical measures to ascertain the 'goodness of fit' for each model, as will be discussed in detail in a later section.

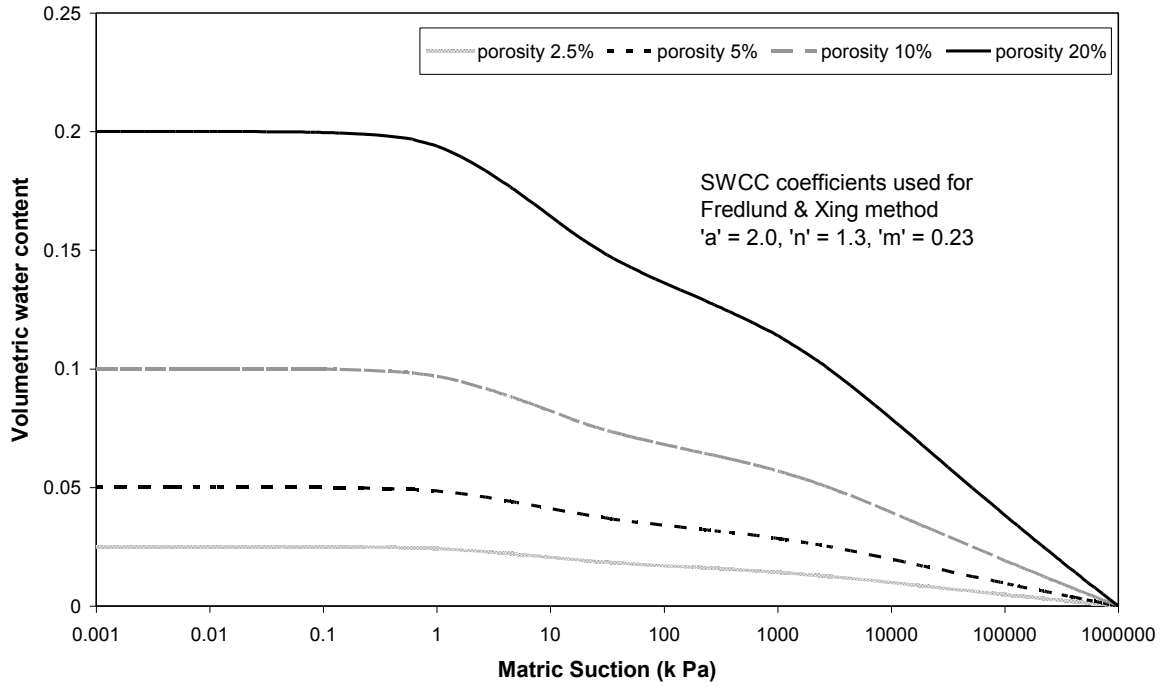

Figure 8.3 Volumetric water content curves generated by the Fredlund-Xing model used for the soil in Seep/W modelling

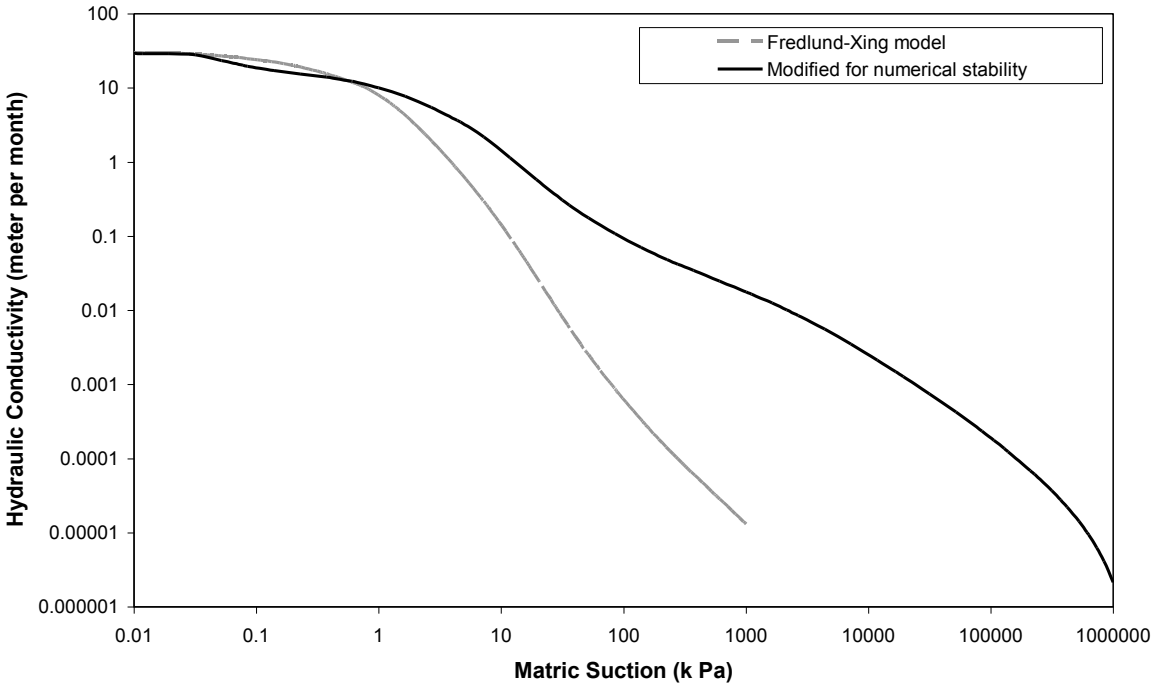

Figure 8.4 Modification of unsaturated hydraulic conductivity as obtained from the Fredlund–Xing equation. The objective was to provide a broader range of suction and corresponding hydraulic conductivity, similar to transformation from sand to clay

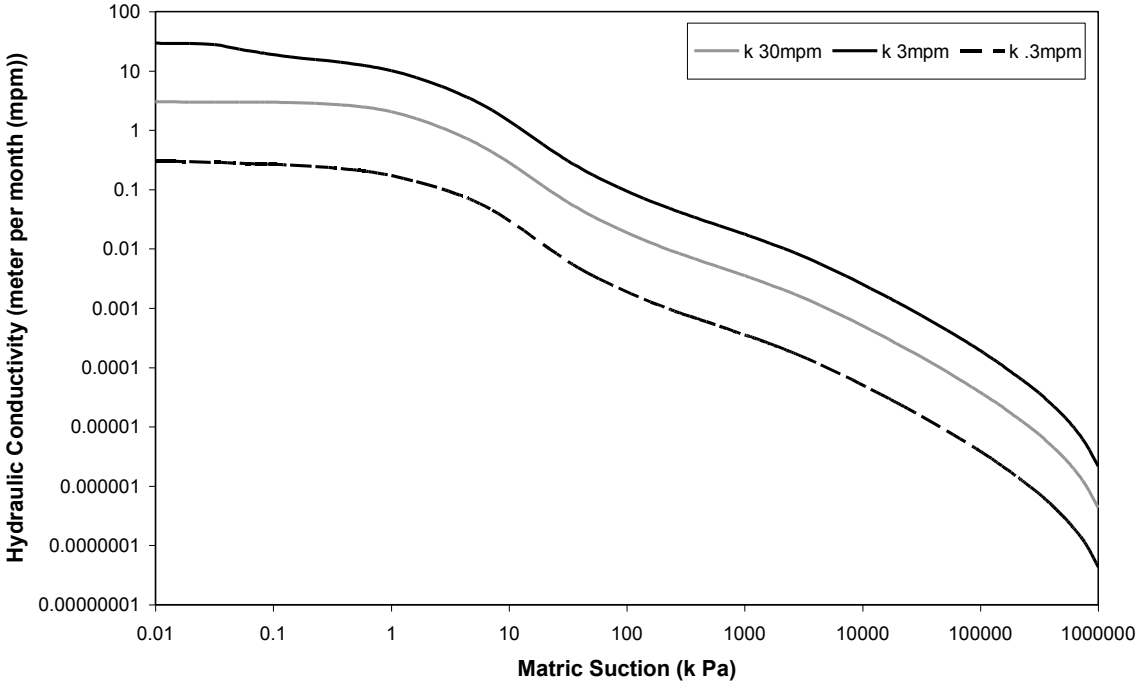

Figure 8.5 Unsaturated hydraulic conductivity curves used for the soil in Seep/W modelling

8.2.3. Boundary Condition

The net flux is used as the upper boundary flow, based on rainfall and AAET, with a one-dimensional model mesh to simulate the behaviour of a single groundwater monitoring bore.

Given the high variability of the near-surface geology, mainly due to complex weathering of underlying fractured metamorphic rocks, an idealised uniform shallow geology is adopted with a no-flow boundary at the base (i.e. a 'bathtub' type model). Based on a review of available shallow, unconfined monitoring bore data, several bores that were clearly unimpacted by mining activities were selected for Seep/W modelling. For each bore, a range of models was run based on varying hydraulic properties.

8.2.4. Initial Condition

The observed GWLs in the selected bore during the start of the validation period were assigned as the initial condition. Thus, the type of initial condition was initial groundwater level.

8.2.5. Selection of Time Step Duration

Any continuous process needs to be discretised for the sake of numerical computation (Von Asmuth *et al.* 2002). The daily time step based model is a discretised model but from the application perspective, the centurial time scale computation would have lead to extensive computational time. Therefore, efforts were conducted for more discretisation from daily to monthly bases. A trial run was conducted to compare the results for modelled GWLs using a daily time step and monthly time step. The results indicate little deviation between the two (see Figure 8.6). The ultimate purpose of the modelling is to predict the centurial scale response of GWLs with respect to climate change scenarios of IPCC. The thousands of replicates of the centurial time scale could be better handled with a monthly time step rather than daily. Therefore, a monthly time step is used to reduce computational intensity in the modelling work. Bidwell and Morgan (2002), and Bidwell (2005) use similar discretisation of daily data to monthly totals for similar modelling purposes.

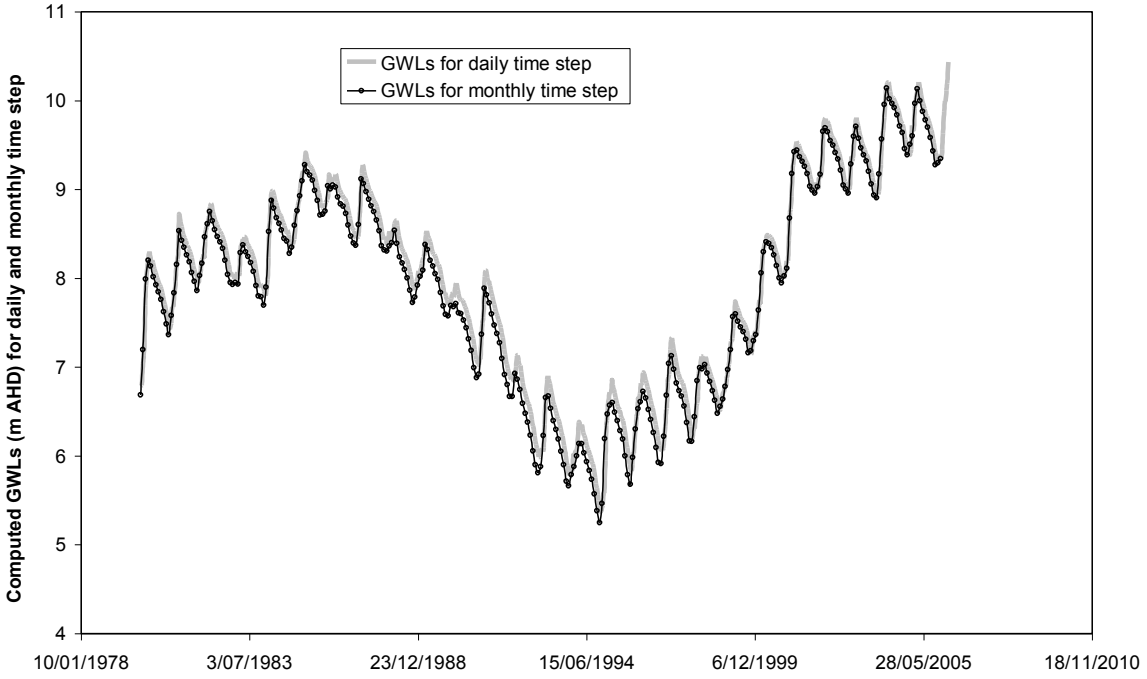

Figure 8.6 Comparison for the influence of time step duration on the computed GWLs

8.3. Selection of Bores for Validation

The total number of bores with available monitoring GW level data (1980 to 2006) was 21. As they were located in the surrounding of the mine site, most showed impact of seepage from retention ponds with a clear rising trend of GWLs, while others were influenced by open pits with a falling trend of GWLs (see Section 3.6).

There was also a long-term variability of net flux data during that period. The trend was not necessarily linear and the non-linearity could be explored while accumulated net flux is plotted in a simple scatter plot (see Figure 5.11). The accumulated net flux is supposed to be directly proportional to the groundwater level (storage state of water in the soil). This guideline is followed in selecting the bores, which are relatively unimpacted by mining activity and solely fed by climatic net flux. There are instances when the differentiated time series does not exactly show any trend but the integrated time series does show the trend. From a physical perspective, GWLs are related to accumulated net flux while monthly changes in groundwater levels are related to monthly net flux. For example, Ferdowsian et al. (2001) and Reid et al. (2006) use the integrated time series of deviations from average rainfall to represent inflow to the system while explaining groundwater hydrographs. The reverse technique of differencing transformation as described in

Brockwell and Davis (2002) is applied to non-stationary time series of accumulated net flux and modelled GWLs, which is described in Section 6.4.2.

From this perspective, initially seven bores were selected: OB1A, OB20, OB21A, OB27, OB38, OB41 and OB79_6. The bores were selected based on the varied topography and sparsely located conditions. Of these bores, OB38 and OB79_6 had to be excluded because they were open bores with no casing and extended up to a deep aquifer (at 150 m to 200 m depth) rather than being restricted to the shallow unconfined aquifer (at 30 m to 50 m depth). From these considerations, OB1A, OB20, OB21A, OB27 and OB41/OB43 bores were chosen for Seep/W validation.

8.3.1. Review of Model Fitness Criteria

The match between the model response and field observation may be examined qualitatively in the preliminary stages of the validation process, using such steps as visual comparison of contour maps of calculated and observed heads (Zheng and Bennett 1995). This approach refers to a larger scale of areal extent with a specific instant of time. The other practical condition may be a larger time scale and a specified location in space. Therefore, visual comparison is used to screen the best bores for simulation. However, to address the issue of missing data in some of the bores, more than one performance criteria are selected for assessing the model fitness.

Statistical measures of goodness of fit: The fitness performance of models has been evaluated using a range of criteria, some for short-term performance and others for long-term performance. The performance criteria selected for the purpose are listed in Table 8.3. When the time scale of the practical situation is important, this type of validation procedure is preferable over using single or similar criteria.

Of the five bores' responses to the range of porosity and conductivity values, the OB27 bore gives the best result with regard to long-term prediction. Overall, the validation procedure demonstrates some useful results in applying complex flow models using a simplified conceptual model framework.

Table 8.3 Statistical objective functions[a] used to assess model fit

Measure[b]	Expression[b]	Range	Decision Rule
E (Nash-Sutcliffe criterion)	$E = 1 - \frac{\sum_{t=1}^{T}(h_o^t - h_m^t)^2}{\sum_{t=1}^{T}(h_o^t - \overline{h_o})^2}$	-∝ to +1	+1 is desirable
r (linear correlation coefficient)	$r = \frac{\sum_{t=1}^{T}(h_m^t - \overline{h_m})(h_o^t - \overline{h_o})}{\sqrt{\sum_{t=1}^{T}(h_m^t - \overline{h_m})^2}\sqrt{\sum_{t=1}^{T}(h_o^t - \overline{h_o})^2}}$	-1 to 1	+1 is desirable, -1 is undesirable
Ratio	$Ratio = \overline{h_m} \,/\, \overline{h_o}$	0 to ∝	+1 is desirable
RMSE (root mean square error)	$RMSE = \sqrt{\sum_{t=1}^{T}(h_m^t - h_o^t)^2} \,\Big/\, T$	0 to ∝	0 is desirable
$\overline{d}$ (mean error)	$\overline{d} = \overline{h_m} - \overline{h_o}$ where $\overline{h_m} = \sum_{t=1}^{T} h_m^t \,\Big/\, T$	-∝ to +∝	0 is desirable
S_e (standard error)	$S_e = \sqrt{\frac{S^2}{T-1}}$ & $S^2 = \frac{\sum_{t=1}^{T}(d^t)^2}{T} - \overline{d}^2$	0 to ∝	0 is desirable
β	$\beta = \overline{d} \,\Big/\, \sqrt{S^2/(T-1)} = \overline{d} \,/ S_e$	0 to ∝	0 is desirable

[a] 'r' From Zheng and Bennett (1995) and Middlemis et al (2001), 'E' from Nash and Sutcliffe (1970).

[b] Primary variables are *h* head; *t* time step number (T total time steps); *d* model – measured difference; Subscript 'm' / 'o' – model / observed values; ¯ (overscore) average ($\overline{h_m}$ = average modelled head).

Note on missing data: It should be mentioned that the long-term (1980–2006) trend of mean annual GWL is not linear. It is similar to the trend of accumulated net flux values as shown in Figure 5.11. It can be stated to be consisting of approximately two convex profiles (1980–1987, 1995–2006) with a concave profile in the middle (1988–1994). Therefore, the missing data in the convex or concave section influences the average value of observed head ($\overline{h_o}$) differently. It should be noted that this is the most important parameter in the equations for most of the performance criteria. Missing data in the observed value also influences the modelled average value ($\overline{h_m}$).

Careful consideration should be given to the performance criteria such as the Nash-Sutcliffe efficiency of Nash (1970), the linear correlation coefficient 'r' of Zheng and

Bennett (1995) and the ratio of average. These are all influenced differently by the different sets of missing data. Only RMSE does not depend on the existence of missing data, as shown in the equations.

The Nash-Sutcliffe efficiency is one of the traditional criteria used by hydrologic modellers, while linear correlation coefficient 'r' of Zheng and Bennett (1995) is specifically suggested for GW modelling. However, the more commonly and widely used criteria for best fit is RMSE, as used by Mann (2004). Therefore, there are always strengths and weaknesses against selection of any particular criteria for decision-making. Thus, a more comprehensive framework of the various statistical criteria is developed and a consistent performance against multiple criteria is targeted rather than looking for best performance in a single criteria.

8.3.2. Calibration Performance of Selected Bores with Respect to Various Fitness Criteria and Soil Parameters

Nine models were developed with the combinations of K = 0.3, 3 and 30 mpm and n = 2.5, 5 and 10% for each of the bores of OB1A, OB20, OB21A, OB27 and OB41. After evaluating the results, some extra model runs were performed with n = 20% for some selected bores.

A graphical representation of an example of measured GWLs of bore OB1A with one of the selected models (K = 0.3 and n = 2.5) is shown in Figure 8.7. Other examples of measured *versus* modelled groundwater heads (bore OB21A) are graphed in Figure 8.8 with a range of values of porosity and saturated hydraulic conductivity. From Figure 8.8, the range of variation regarding the performance in terms of model fitness is visible. The variation of the model performance of this scale is generally acceptable as the hydrologic modellers report their investigations.

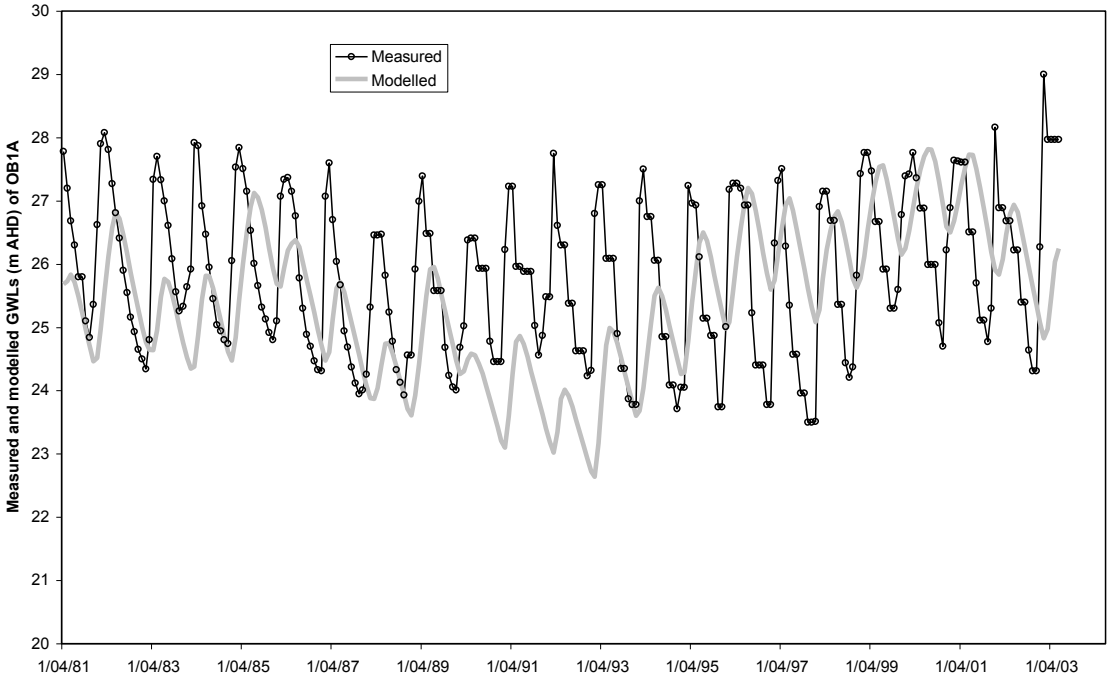

Figure 8.7 Observed *versus* modelled groundwater levels in bore OB1A

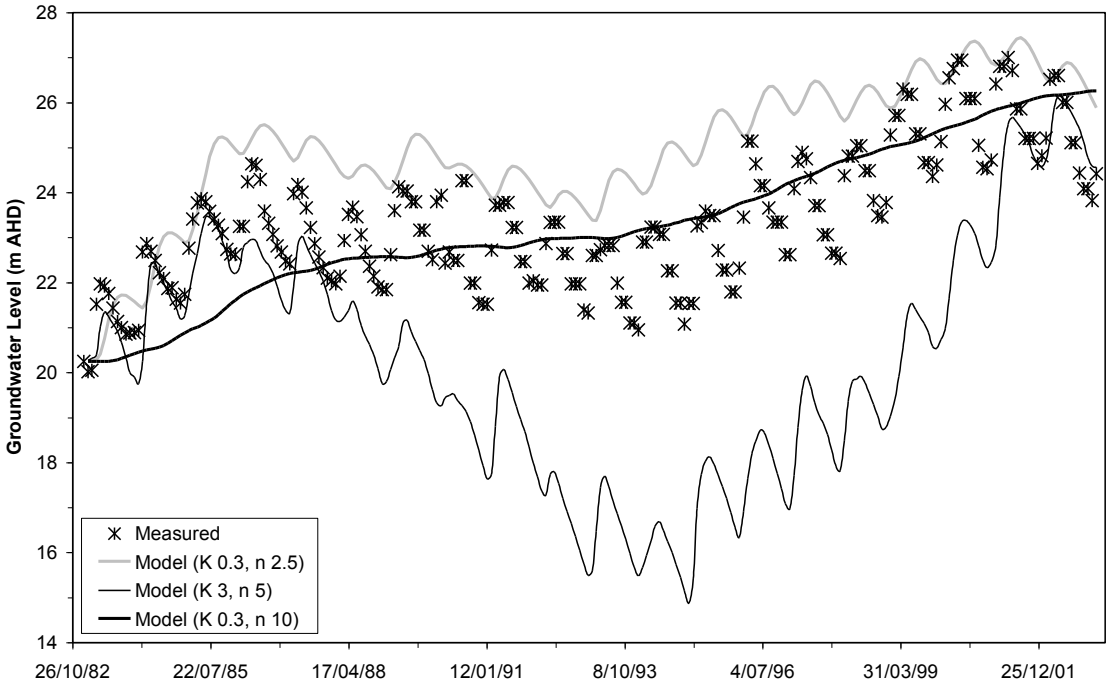

Figure 8.8 Observed *versus* modelled groundwater levels in bore OB21A

For example, in Aguilera and Murillo (2008) similar scatter with the observed and predicted groundwater levels has been reported, as shown in Figure 8.9, for natural water recharge to the four aquifers in south-east Spain. The soil hydraulic properties such as

hydraulic conductivity and porosity play a very significant role in estimated groundwater level, which is elaborated in the following sections. Misstear et al. (2009) conducted a similar groundwater level simulation by incorporating various methods of estimation of actual evapotranspiration, as shown in Figure 8.10.

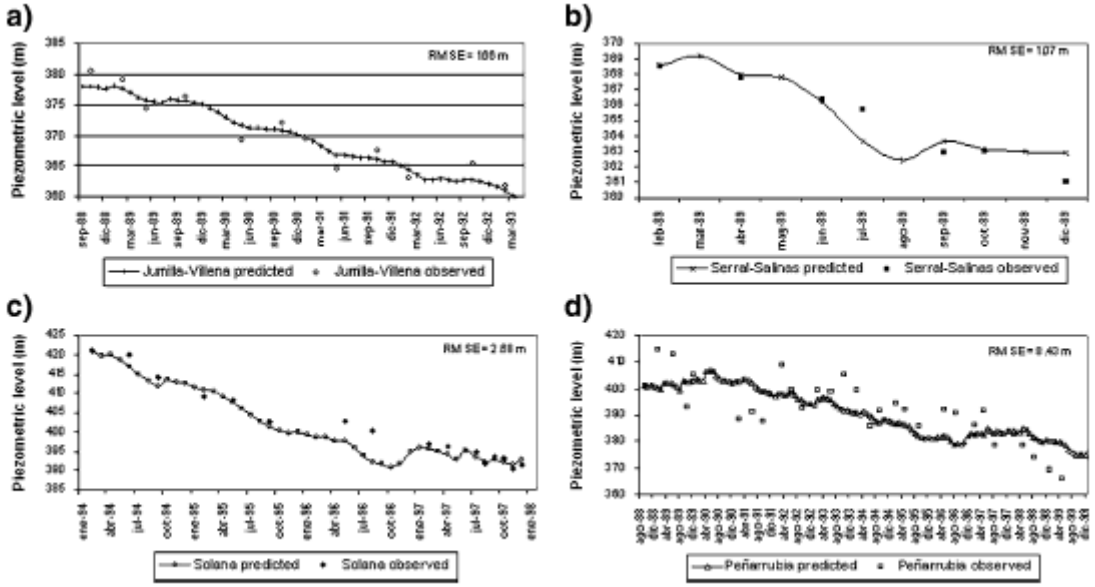

Figure 8.9 Observed and predicted piezometric levels for four aquifers named Jumilla-Villena (a), Solana (b), Serral-Salinas (c) and Penarrubia (d) at various time scale (Aguilera and Murillo 2008)

From visual judgement alone, it is difficult to justify the best model. Therefore, a number of standard criteria based on the statistics and physical processes are selected. A comprehensive analysis is conducted with due consideration of their relative significance to the context of the modelling objective.

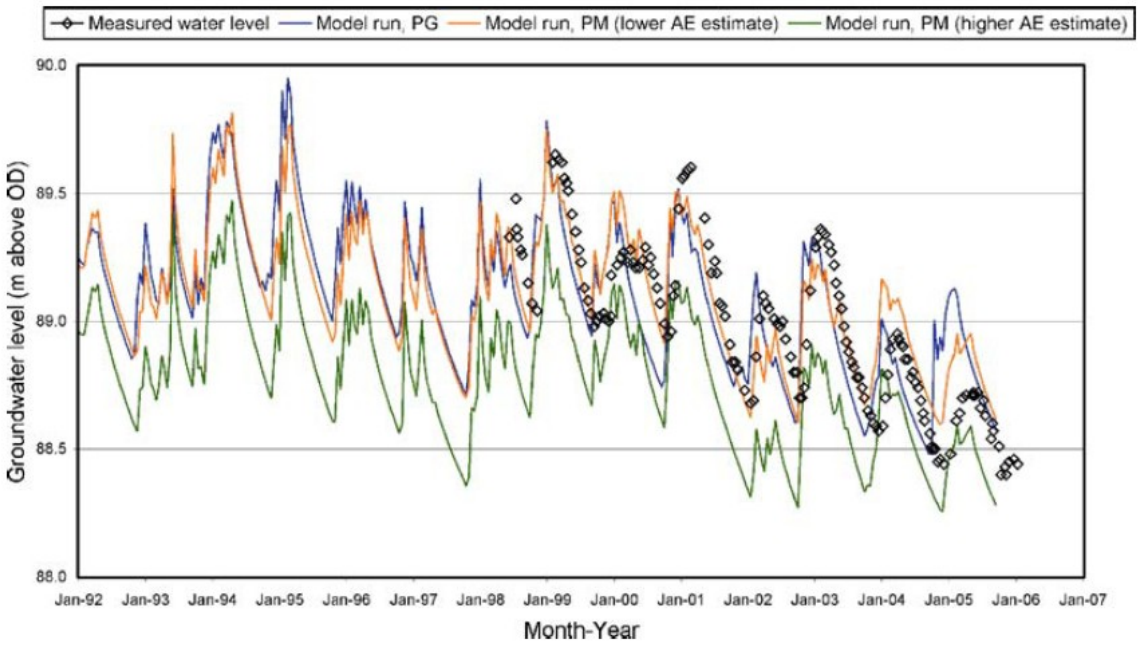

Figure 8.10 Simulated groundwater levels for different recharge estimates such as Penman-Grindley (PG), Penman-Monteith (PM) methods of estimation of actual evapotranspiration (Misstear et al. 2009)

Statistical evaluations of model runs with numerical values are given in Tables 8.4 and 8.5. Based on all of the results described above, the performance of the models for OB27 achieve the best result since this bore successfully includes the best *E* and *r* values in one combination of hydraulic conductivity and porosity. Another important aspect of the results is that the best model may not necessarily be unique; rather it corresponds to a range of parameter values for most of the bores. For example, with respect to the statistical evaluation of parameter combinations, OB41 demonstrates a large amount of scatter while OB27 shows a consistent parameter combination.

From Tables 8.4 and 8.5, optimum (desirable) values of criteria $\overline{h_m}$, *E*, *Ratio, RMSE,* β, $\bar{d}$, and S_e are found to be in one model combination, while criterion *r* is found to be in a different model run. However, the difference between *r*-values in these models is mostly marginal. To achieve better consistency between the criteria, runs are extended to additional set of combinations for n = 20%. The directions of changes of the criteria are again found to be mostly inconsistent. If the importance of all criteria in context to the primary objective of the modelling are analysed, the most important criterion is considered to be the *r* value as this deals with both the magnitude and direction of deviation whereas

Table 8.4 Statistical assessments[a] of Seep/W model runs *versus* soil parameters (K, n)

	$\overline{h_m}$	*E*	*r*	*Ratio*	*RMSE*	β	$\overline{d}$	S_e
Desired value	–	1	1	1	0	0	0	0
OB1A[b], $\overline{h_o}$ = 25.83 m, Δh = 3.17 m (*K* mpm, *n* %)								
K 0.3, n 2.5	25.43	-0.56	0.23	0.98	0.09	4.37	0.4	0.09
K 3, n 2.5	21.57	-30.2	***0.42***	0.84	0.42	12.94	4.26	0.33
K 30, n 2.5	1.83	-3781	0.3	0.07	4.62	5.47	24	4.39
K 0.3, n 5	25.69	-0.37	0.09	0.99	0.09	1.54	0.14	0.09
K 3, n 5	23.3	-11.07	0.33	0.9	0.26	11.99	2.53	0.21
K 30, n 5	22.01	-18.69	**0.35**	0.85	0.33	16.09	3.82	0.24
K 0.3, n 10	**25.82**	**-0.11**	0.16	**1**	**0.08**	**0.11**	**0.01**	**0.08**
K 3, n 10	23.94	-4.16	0.26	0.93	0.17	14.98	1.89	0.13
K 30, n 10	23.81	-0.12	0.33	0.92	0.17	16.75	2.02	0.12
K 0.3, n 20	***25.83***	***0.03***	0.21	***1***	***0.07***	***0.06***	***<0.01***	***0.07***
K 30, n 20	24.71	-0.99	0.3	0.96	0.11	13.9	1.12	0.08
OB20[b], $\overline{h_o}$ = 18.09 m, Δh = 1.67 m (*K* mpm, *n* %)								
K 0.3, n 2.5	16.82	-1.5	0.59	**0.93**	0.1	21.86	1.27	0.06
K 3, n 2.5	13.14	-42.81	***0.72***	0.73	0.41	18.18	4.94	0.27
K 30, n 2.5	9.76	-123.84	**0.63**	0.54	0.7	18.12	8.33	0.46
K 0.3, n 5	17.1	-0.67	0.59	***0.95***	0.08	19.12	0.99	***0.05***
K 3, n 5	14.39	-19.95	**0.63**	0.8	0.29	22.36	3.7	0.17
K 30, n 5	14.08	-23.53	0.61	0.78	0.31	22.49	4.01	0.18
K 0.3, n 10	***17.2***	***-0.42***	0.62	***0.95***	***0.07***	**17.79**	***0.88***	***0.05***
K 3, n 10	15.56	-7.28	0.54	0.86	0.18	30.49	2.53	0.08
K 30, n 10	15.14	-9.78	0.56	0.84	0.2	33.93	2.95	0.09
K 0.3, n 20	**17.17**	**-0.59**	0.6	***0.95***	**0.08**	***17.23***	**0.92**	0.05
K 30, n 20	16.09	-3.86	0.53	0.89	0.14	35.98	2	**0.06**
OB21A[b], $\overline{h_o}$ = 23.42 m, Δh = 2.14 m (*K* mpm, *n* %)								
K 0.3, n 2.5	24.98	-0.59	***0.75***	1.07	0.12	-22.7	-1.56	***0.07***
K 3, n 2.5	20.75	-8.13	0.66	0.89	0.29	11.34	2.67	0.24
K 30, n 2.5	17.14	-31.94	0.35	0.73	0.55	16.6	6.28	0.38
K 0.3, n 5	**24.62**	**-0.34**	0.7	**1.05**	**0.11**	**-14.97**	**-1.2**	**0.08**
K 3, n 5	20.24	-5.75	0.55	0.86	0.25	21.87	3.17	0.15
K 30, n 5	18.96	-11.53	0.34	0.81	0.34	24.09	4.45	0.18
K 0.3, n 10	***23.33***	***0.37***	**0.72**	***1***	***0.08***	***1.18***	***0.09***	**0.08**
K 3, n 10	19.86	-5.83	0.37	0.85	0.25	33.79	3.55	0.11
K 30, n 10	19.58	-7.05	0.24	0.84	0.27	32.97	3.84	0.12
K 0.3, n 20	21.77	-0.71	0.71	0.93	0.13	24.27	1.65	***0.07***
K 30, n 20	20.03	-5.05	0.34	0.86	0.24	36.91	3.39	0.09

[a] Best fits are highlighted in grey-shaded bold-italic text; next closest fits are bold only.
[b] Model runs with K 3 not performed based on previous outcome of model runs.

Table 8.5 Statistical assessments[a] of Seep/W model runs *versus* soil parameters (K, n)

	$\overline{h_m}$	*E*	*r*	*Ratio*	*RMSE*	β	$\overline{d}$	S_e
Desired value	–	1	1	1	0	0	0	0
OB27[b], $\overline{h_o}$ = 8.87 m, Δh = 2.00 m (*K* mpm, *n* %)								
K 0.3, n 2.5	10.15	-1.54	0.62	1.14	0.13	-20.57	-1.28	**0.06**
K 3, n 2.5	10.92	-5.37	0.77	1.23	0.2	-21.73	-2.05	0.09
K 30, n 2.5	11.09	-6.16	0.77	1.25	0.21	-23.58	-2.21	0.09
K 0.3, n 5	10.18	-2.1	0.42	1.15	0.14	-15.78	-1.31	0.08
K 3, n 5	10.69	-3.55	0.78	1.2	0.17	-27.86	-1.81	0.07
K 30, n 5	10.46	-2.82	**0.79**	1.18	0.15	-21.31	-1.58	0.07
K 0.3, n 10	9.92	-1.84	0.42	1.12	0.13	-10.71	-1.05	0.1
K 3, n 10	9.52	-0.04	0.72	1.07	0.08	-11.2	-0.65	**0.06**
K 30, n 10	9.42	0.23	0.77	1.06	0.07	-10.54	-0.54	***0.05***
K 3, n 20	***8.61***	**0.28**	0.62	**0.97**	0.07	***4.26***	***0.27***	**0.06**
K 30, n 20	**8.56**	***0.37***	***0.81***	**0.96**	***0.06***	**5.51**	**0.31**	**0.06**
OB41[b], $\overline{h_o}$ = 14.89 m, Δh = 1.69 m (*K* mpm, *n* %)								
K 0.3, n 2.5	12.24	-18.29	***0.55***	0.82	0.19	25.11	2.84	0.11
K 3, n 2.5	8.77	-168.18	**0.53**	0.59	0.57	15.74	9.43	0.6
K 30, n 2.5	-20.62	-26838	0.35	-1.38	7.21	***5.22***	65.38	12.54
K 0.3, n 5	12.59	-13.31	0.36	0.85	**0.17**	23.99	**2.44**	**0.1**
K 3, n 5	10.57	-69.46	0.42	0.71	0.37	21.34	6.39	0.3
K 30, n 5	9.97	-90.09	0.38	0.67	0.42	21.26	7.15	0.34
K 0.3, n 10	**12.92**	**-9.64**	0.21	**0.87**	***0.14***	21.71	2.05	***0.09***
K 3, n 10	12.08	-26.33	0.35	0.81	0.23	23.99	3.89	0.16
K 30, n 10	12.4	-21.75	0.39	0.83	0.21	23.92	3.57	0.15
K 0.3, n 20	***12.93***	***-5.53***	-0.24	**0.89**	0.18	19.29	***1.67***	***0.09***
K 30, n 20	12	-13.5	-0.01	0.82	0.27	24.29	2.6	0.11

[a] Best fits are highlighted in grey-shaded bold-italic text; next closest fits are bold only.

[b] Model runs with K 0.3-n 20 (OB27) and K 3-n 20 (OB41) not performed based on previous outcome of model runs.

other criteria deal with magnitude only (see (Middlemis *et al.* 2001). The best bore with consistent model parameter is OB27 with K 30 n 20.

8.3.3. Sensitivity Analyses

In Figure 8.11, it could be seen that the statistical performance of the model runs vary significantly with the variation of porosity and hydraulic conductivity. These variations are not only high in magnitude but also contrasting in direction. Hence, a change in the property improves a number of criteria and worsens other sets of criteria. Therefore, a very

careful assessment was performed to select the model values for future prediction of GWLs.

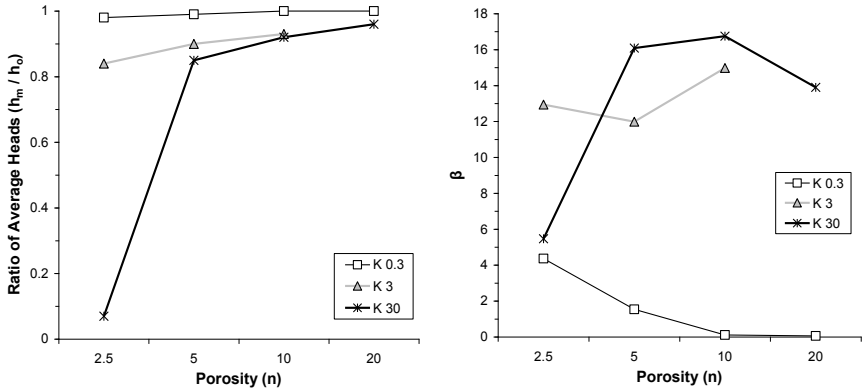

Figure 8.11 Example of the variation of selected statistical evaluations for bore OB1A

Sensitivity with porosity: The relative influence of porosity (*n*) on the annual average groundwater fluctuation (*Δh*) can be explored by comparing OB20 and OB21A, since they are in close proximity to each other. The model results show the importance of *n* in the amplitude of *Δh*. OB20 performs well with *n* of 10 to 20% and a measured average annual groundwater variation (*Δh*) of 1.67 m, whereas OB21A performs well with *n* of 5 to 10% with *Δh* of 2.14 m. This demonstrates that annual fluctuations are higher for lower porosity (all other factors remaining the same). The close-up view for two sample models runs are shown in Figure 8.12.

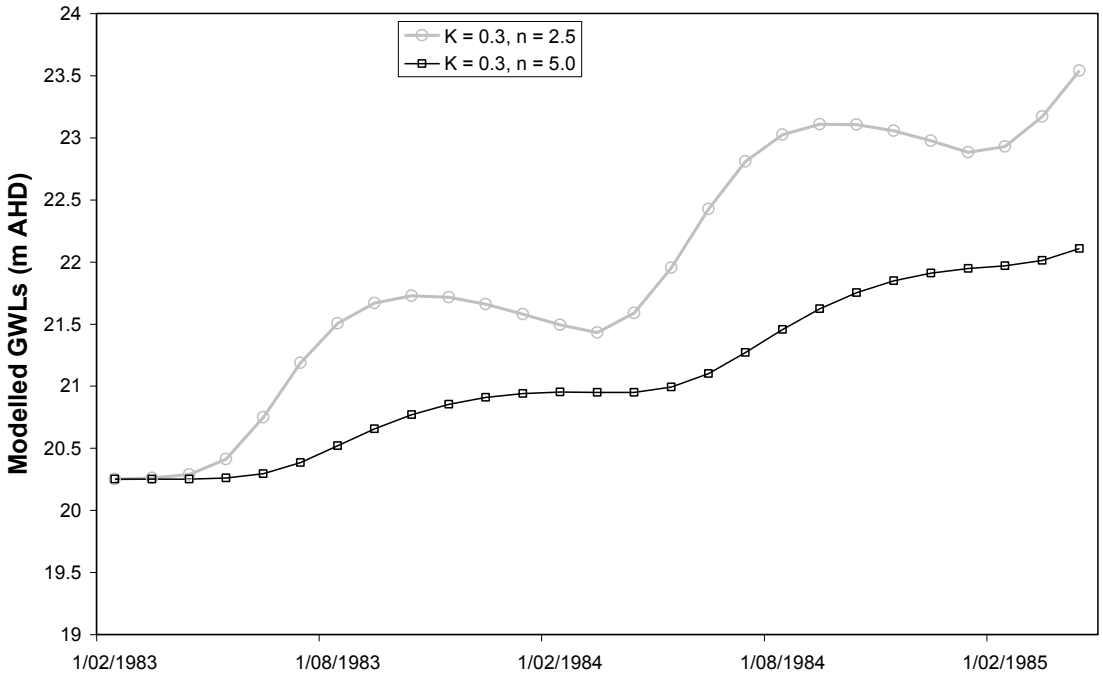

Figure 8.12 Sensitivity of computed GWLs for OB21A with different porosities

Sensitivity with hydraulic conductivity: The results also show that hydraulic conductivity is important in modelling the annual and longer-term response of groundwater (as should be expected). From the plot of time series of modelled GWLs and measured GWLs, it has been found that the time lag between modelled response and observed response changes with the change of hydraulic conductivity value and porosity. Figure 8.13 demonstrates a sample result of two sets of model runs to show the difference in response time for different hydraulic conductivity. In general, soil with higher conductivity causes quicker flow of water through it and *vice versa*.

Based on the fieldwork at Ranger (Willett *et al.* 1993); (Akber 1991), it is clear that the weathered near-surface geology and aquifers at the site are highly variable and heterogeneous. The approach adopted in this research is clearly a simplification, which allows for efficient modelling at the expense of more thorough discretisation of model parameters (K, n, others). As such, the approach adopted herein of using a simplified one-dimensional homogenous model appears reasonable.

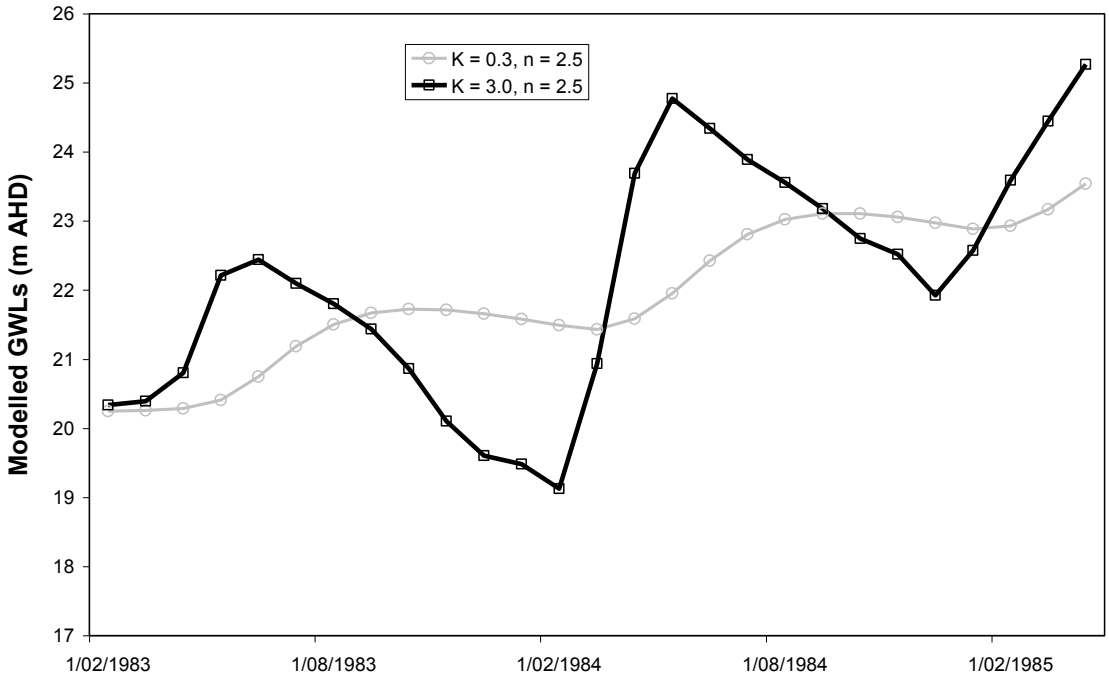

Figure 8.13 Sensitivity of computed GWLs for OB21A with hydraulic conductivities

8.4. Conclusions

This chapter presented the results of applying an unsaturated flow model (Seep/W) to observed historical groundwater-climate data at the Ranger uranium project. The approach adopted a one-dimensional groundwater-climate model to fit historical data for several bores, with varying values for hydraulic conductivity and porosity to assess uncertainty due to the heterogeneous geology of the area. All model runs were evaluated with a range of statistical measures for goodness of fit. In summary, the research approach utilised herein demonstrates that a simplified conceptual model implemented via an unsaturated flow model can achieve a robust model configuration with reasonable statistical confidence. The best bore with consistent model parameter turns out to be OB27 with saturated hydraulic conductivity K = 30 mpm and porosity n = 20 %.

9. Results: Groundwater-climate Change Predictive Modelling

In the previous chapters, the models for predicting the groundwater levels with the influence of climate change projections and natural climatic variability have been selected. The best conceptual model for the site considering the criteria of significant physical processes was selected. The framework of the physical process-based model has also been developed. The non-physical process-based time series model for representation and forecast of the combination of climate data and GWLs data has also been investigated.

The time series model prediction needed significant improvement and thereby detailed reporting is omitted in the thesis and recommended for further investigation with specific directives. The physical process based model result consists of climate replicates, and computed GWLs. The climate change predictions, as incorporated by multiplying factors, are described to demonstrate the relative influence of various GCMs and various scenarios with respect to base line climate of the year 2000. The influence of climatic variability is also shown by representing the ENSO events in a sample data set of net flux for the centurial scale. The predicted net fluxes at the centurial scale are calculated by combining SCL replicates, ENSO events and multiplying factors. The result of GWLs from the physical process-based model, fed with the predicted net flux data of the centurial scale is then presented. The result of 30 replicates is represented in terms of the mean ± standard deviation ($\mu \pm \sigma$) limits of the respective scenario of the respective GCM. The limitations with some GCMs net flux data are also described. The specific scopes of further investigations are also discussed.

9.1. Conceptual Model

The developed conceptual model considering the significant flow components has been described in detail in Chapter 5, consisting of a one-dimensional vertical flow model. The climatic variables have been accounted for by one single variable, named monthly 'net flux'. This is represented as the algebraic summation of monthly rainfall and AAET. The monthly value of net flux becomes positive or negative depending on the magnitude of the rainfall and evapotranspiration (that is, wet or dry season).

9.2. Time Series Model

In Chapter 6, the exploratory analyses of the monthly time series data of net flux, GWLs and changes of GWLs have been performed. Based on the result of ACF, CCF and classical decomposition, the applicability of the ARMA model has been established. Having tested a number of ARMA models, the TFN model and the multivariate AR model have been found to be equally good in terms of statistical performance. The physical basis of TFN is better while the computational time requirement is less for the multivariate AR model. As the best-fitting performances are almost the same, the multivariate AR model is recommended for the long-term representation and forecast of the GWLs of the system.

However, some of the limitations which are stated below have severely affected the scientific acceptance of the time series predictions.

The historical time series data range from 1980 to 2005, whereas future time series data range from 2001 to 2100. The time scale is decadal for historical time series and centurial for future time series.

The concept of stationarity varies with the time scale. With regard to the time scale of natural processes which are inherently non-stationary implies the greater the time span of the historical series, the greater the probability that the series will exhibit statistical characteristics that change with time. However, for relatively short time spans it is feasible to model approximately the given data using a stationary stochastic model. Nevertheless, the reverse position may seem just as plausible to other schools of thought. Apparent non-stationarity in a given time series may constitute only a local fluctuation of a process that is in fact stationary on a longer time scale (Hipel and McLeod 1994).

The time scale is not the only factor that makes the decision of stationarity. The type of variable analysed also makes a big difference to the same process. For instance, the monthly net flux data may be stationary while the accumulated net flux data is not. Similarly, when GWLs are non-stationary, the changes in GWLs' data might be stationary. The differencing is a very common transformation technique to convert a non-stationary time series into a stationary time series. Therefore, the entity of the variable under consideration is also an important factor that determines the stationarity of a process. Thus,

the selection of the variable and the model type of time series models, which rely on the stationarity, is always subject to the purpose (time scale of available data and required forecast) of the modelling work.

The preliminary modelling showed that time series forecast using multivariate AR model of GWL is comparable to Seep/W result of computed GWLs at centurial scale. However the result is not reported in the thesis because the time series modelling should implement TFN model also where the physical basis are stronger than that of multivariate AR model, to bring a scientific reason of comparison between the predicted GWLs by Seep/W. The TFN model needs significant amount of computational time which was not possible to be incorporated within the limited span of the research. This is recommended for further investigation.

9.3. Generated Future Climate Data

In Chapter 7, the decisions (methods) and ambiguities (assumptions) associated with generating thousands of replicates of the centurial time scale climate data have been described. In general, the process of generating data can be titled as a quasi-random process or conditional random process.

The net flux from the output of conditional random generated climatic variability, as resulted from the 'ENSO program', was combined with 35 sets of multiplying factors for each of the five GCMs and seven scenarios. The multiplying factors, as computed for each of the scenarios of each of the GCMs for monthly net flux are shown in the Figures 9.1, 9.2, and 9.3.

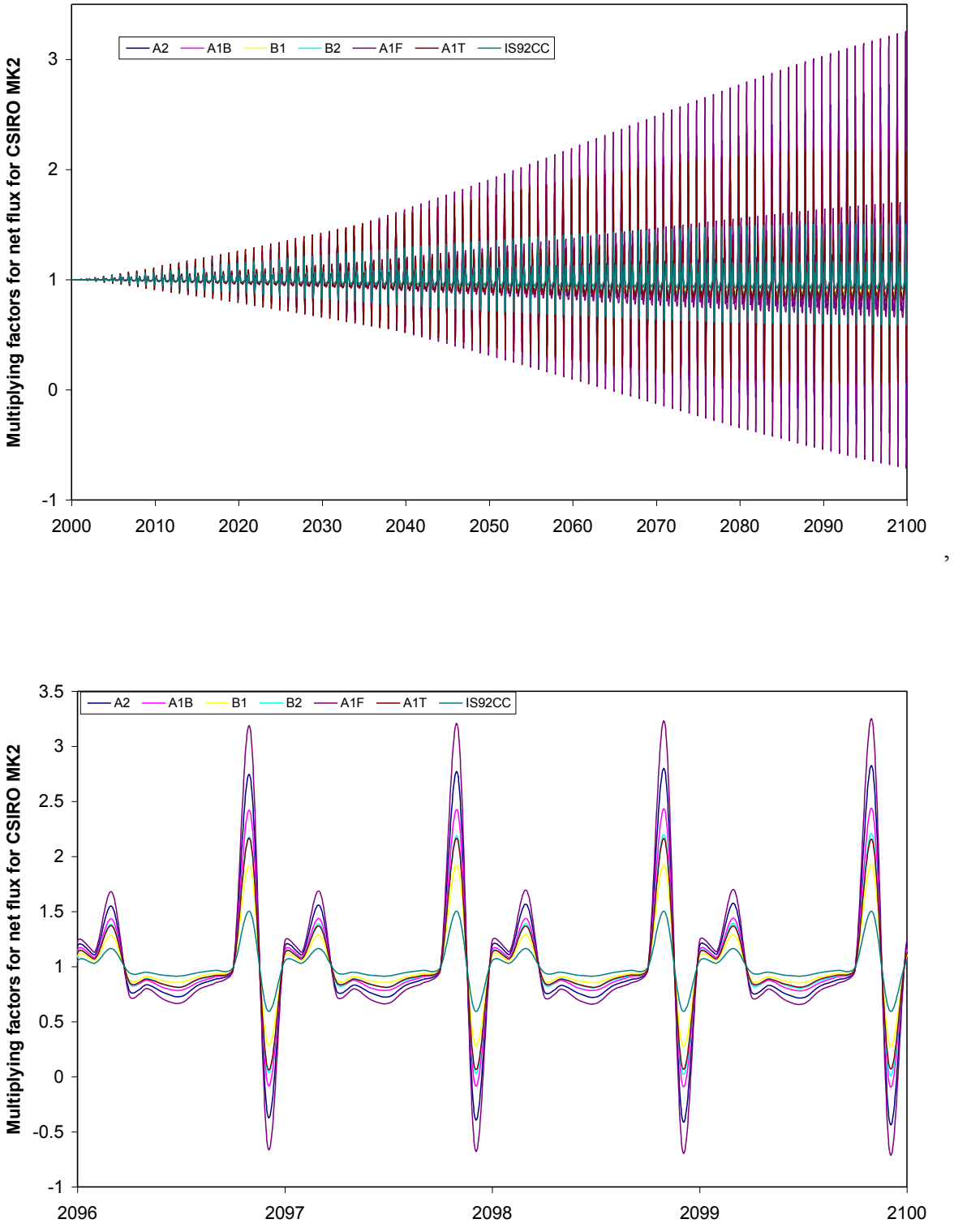

Figure 9.1 The monthly multiplying factors for 1200 months (100 years; 2001 – 2100) of seven scenarios (A2, A1B, B1, B2, A1F, A1T and IS92CC) of CSIRO Mk2 GCM (top) and for 2096 – 2100 (bottom)

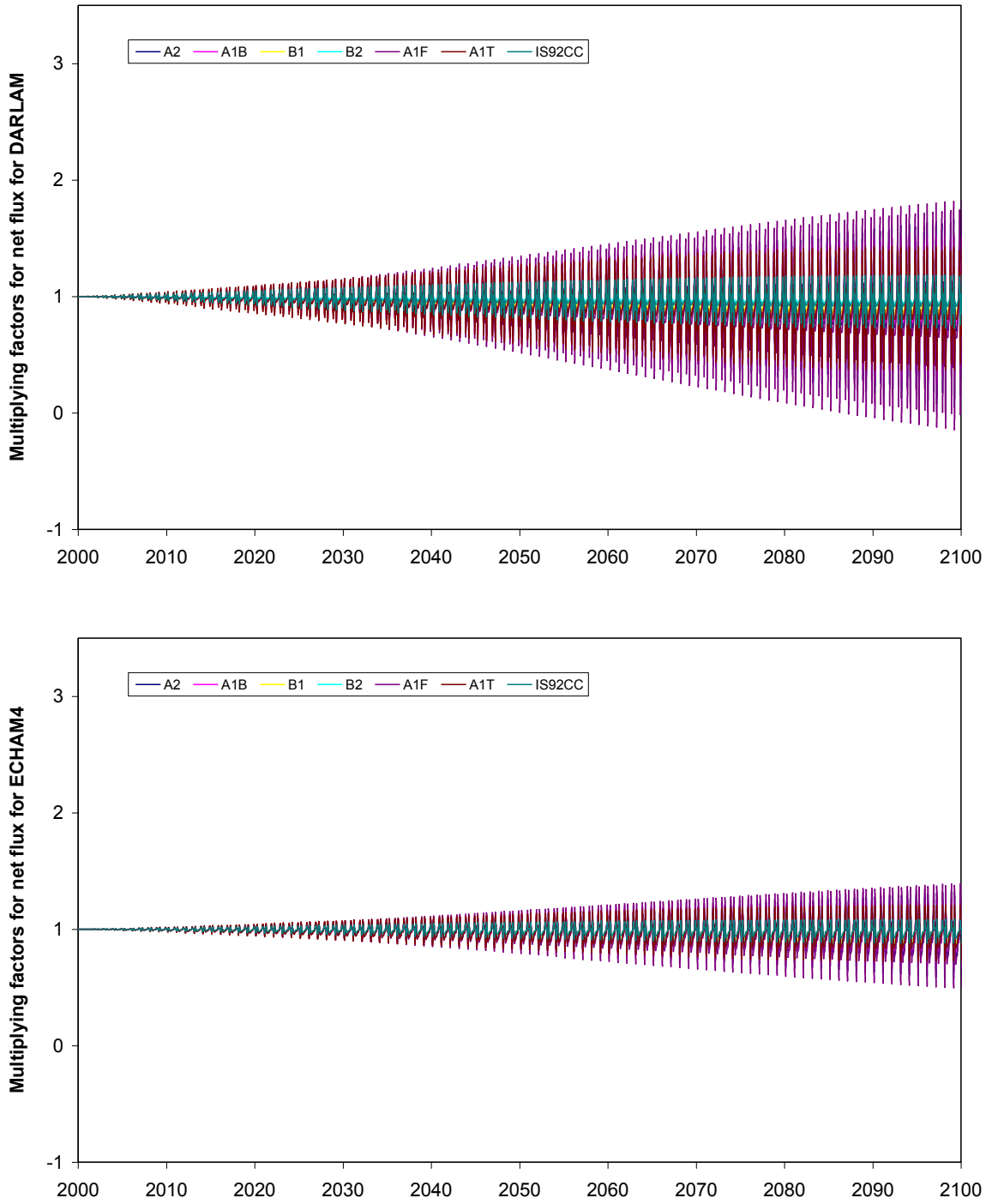

Figure 9.2 The monthly multiplying factors for 1200 months (100 years) of seven scenarios (A2, A1B, B1, B2, A1F, A1T and IS92CC) of DARLAM GCM (top) and ECHAM4 GCM (bottom)

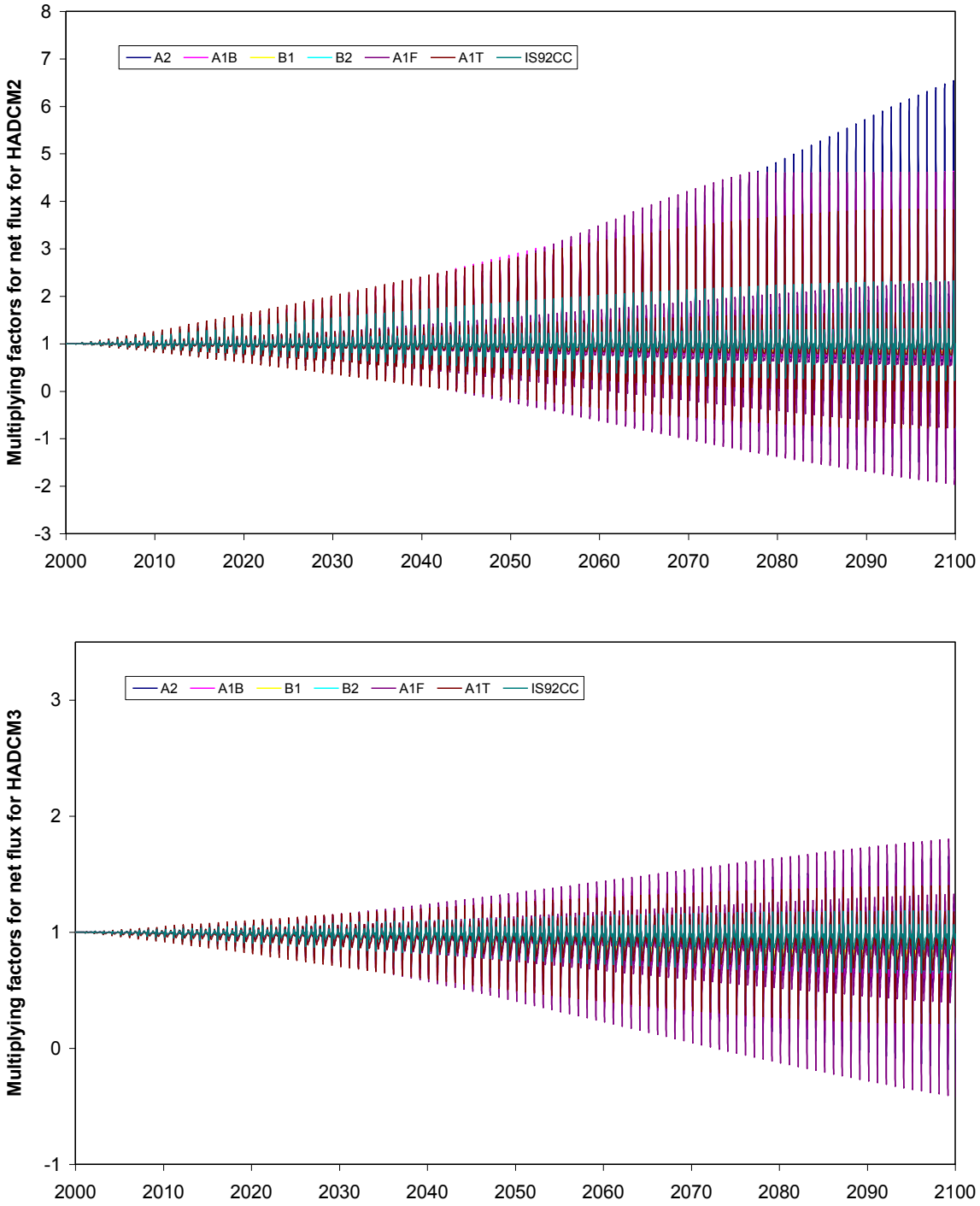

Figure 9.3 The monthly multiplying factors for 1200 months (100 years) of seven scenarios (A2, A1B, B1, B2, A1F, A1T and IS92CC) of HadCM2 GCM (note different scale) (top) and HadCM3 GCM (bottom)

9.3.1. Climate Change Prediction Trends

The multiplying factor is meant to indicate the ratio of predicted years value with respect to the year 2000 as indicated by $NF_{i,2000+j}^{OZ(k)}$ / $NF_{i,2000}^{OZ(k)}$. It is the prediction trend of monthly net flux values by various climate change prediction models (GCMs) and various emission scenarios. The value of k varies from 1 to 35 here as detailed in Table 7.3. The value of i varies from 1 to 12 for January to December and j varies from 1 to 100 for the years 2001 to 2100. The gradual change of each month's net flux values over the span of a 100-year period is demonstrated.

It should be noted that the multiplying factor comes from the ratio of net flux as predicted by various GCMs for a particular year to that of the year 2000, as indicated by [$NF_{i,2000+j}^{OZ(k)}$ / $NF_{i,2000}^{OZ(k)}$]. However, the net flux is not the direct output of GCMs. Rainfall and PPET values are extracted from GCMs and the PPET values are converted to AAET. The estimated net fluxes, as predicted by GCMs are then computed as algebraic summation of rainfall and AAET. The predicted rainfall and PPET are different for different GCMs and therefore the ratio of the final net flux (for the year 2100) to the base net flux (for the year 2000) (i.e. the multiplying factors) are different. The values of all the multiplying factors as calculated from the GCM output are provided in Appendix H.

It can be understood that the magnitude of the multiplying factors are different and this indicates the range of variation of predicted trends of net flux by various GCMs and their respective scenarios. The range of variation for ECHAM4 GCM is approximately 0.5 to 1.5, whereas for HadCM2 GCM, variations range from -2.0 to 6.0. Therefore, it is appropriate that a range of GCMs output has been considered in the present research.

9.3.2. Input Data Set of Net Flux

The five GCMs with seven scenarios consist of 35 sets of scenarios. For each of the 35 sets of scenarios the multiplying factors are computed. After that 30 replicates of generated net flux are considered for each of these 35 sets of multiplying factors. The generated net flux is the output of the conditional Monte Carlo process, which has been described in Chapter 7. By combining the replicates with multiplying factors the input data set of net flux are obtained. The input data of net flux for five GCMs and seven scenarios are given in

Appendix H. Some sample graphs of those input net flux data in the following figures are represented.

Figure 9.4 is from one GCM and Figure 9.5 is from one scenario. The graphical representations of maximum and minimum net flux of one GCM (named HadCM3) with all the seven scenarios are shown in Figure 9.4. Similarly, the graphical representations of maximum and minimum net flux of one scenario (named A2) with all the five GCMs are shown in Figure 9.5. From the visual assessment, there appears to be no significant difference between the maximums and minimums of the net flux values for various models and scenarios. However, if some cumulative time series graphs are plotted of the net flux data, then the existence of increasing or decreasing water balance in the system could be observed, which is elaborated in Section 9.6. The representation of the ENSO type of events can be found in some replicates, as shown in Figure 9.6.

ENSO type of events in net flux data: The generation of the conditional Monte Carlo process involves the consideration of natural variability such as ENSO events in conjunction with random process. The ENSO events occur with the frequency of interannual to decadal time scale. These phenomena are taken into consideration by considering the ocean circulations such as IOD and PDO for the region under consideration. Therefore, in the replicated net flux, there are evidences of such events as can be seen in the two sample replicates plotted in Figure 9.6. Chapter 7 describes how the ENSO events are incorporated in the climate flux replicates.

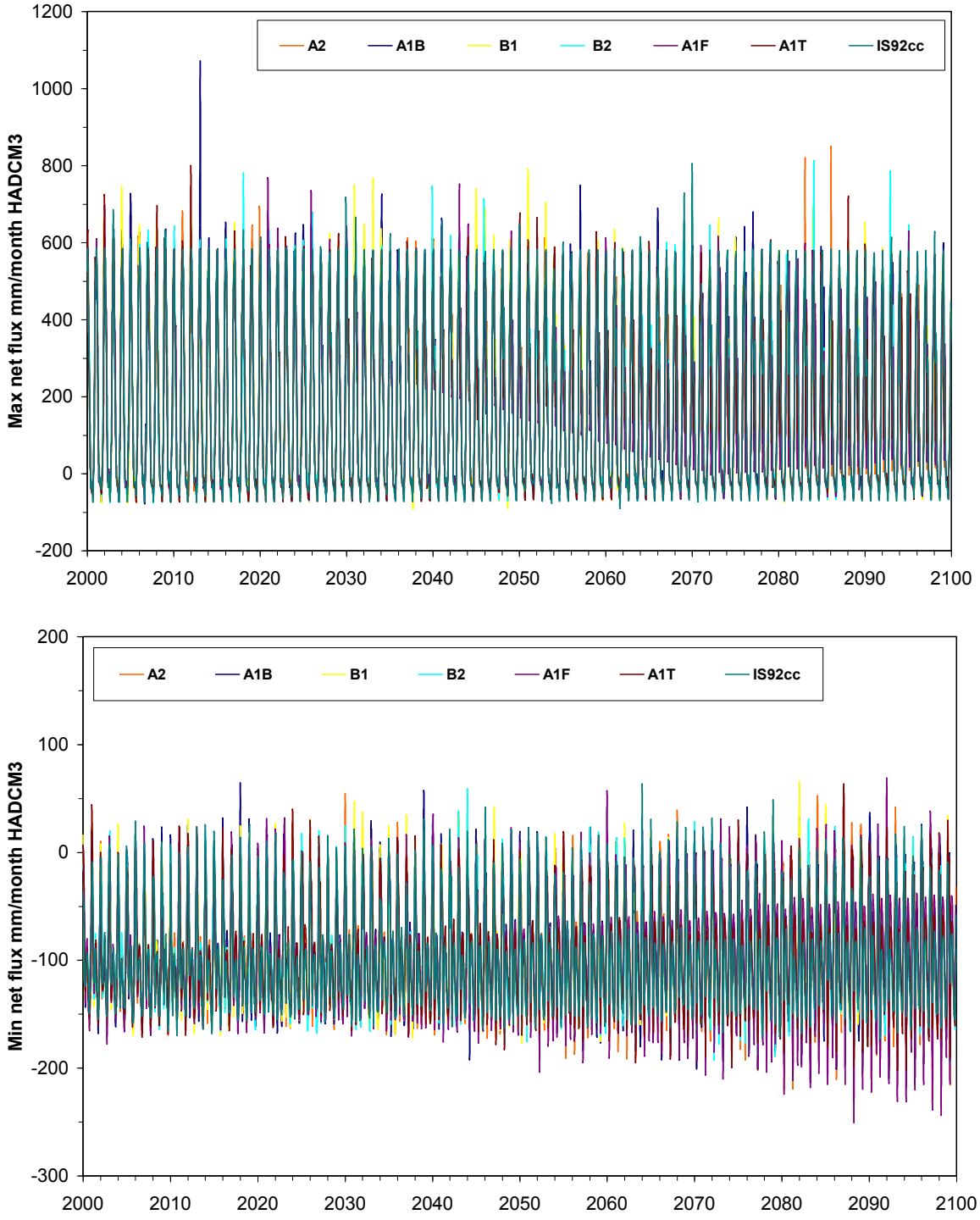

Figure 9.4 The maximum (top) and minimum (bottom) net flux values for each time step from the 30 replicates (HadCM3 GCM, seven scenarios)

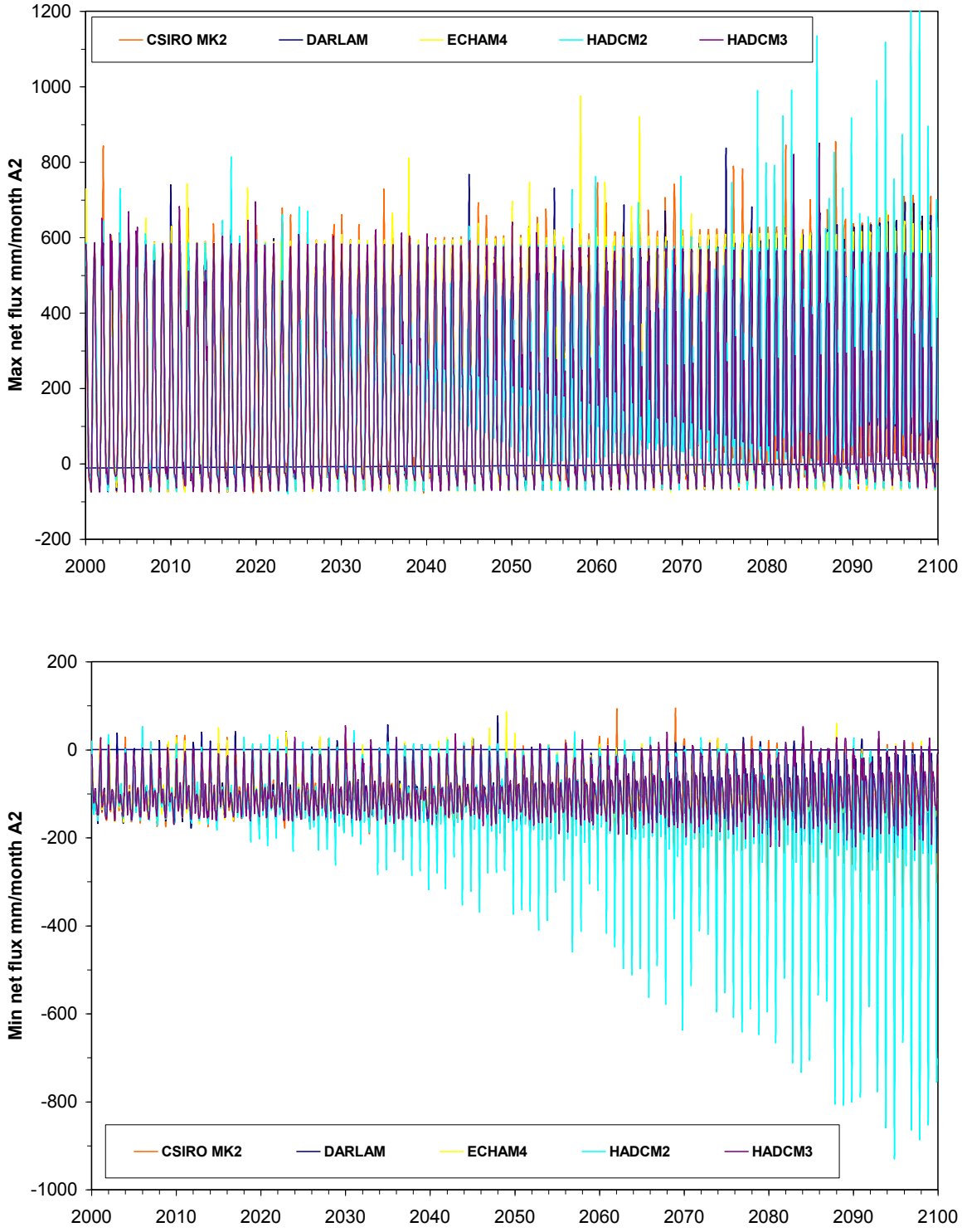

Figure 9.5 The maximum (top) and minimum (bottom) net flux values for each time step from the 30 replicates (A2 scenario, five GCMs)

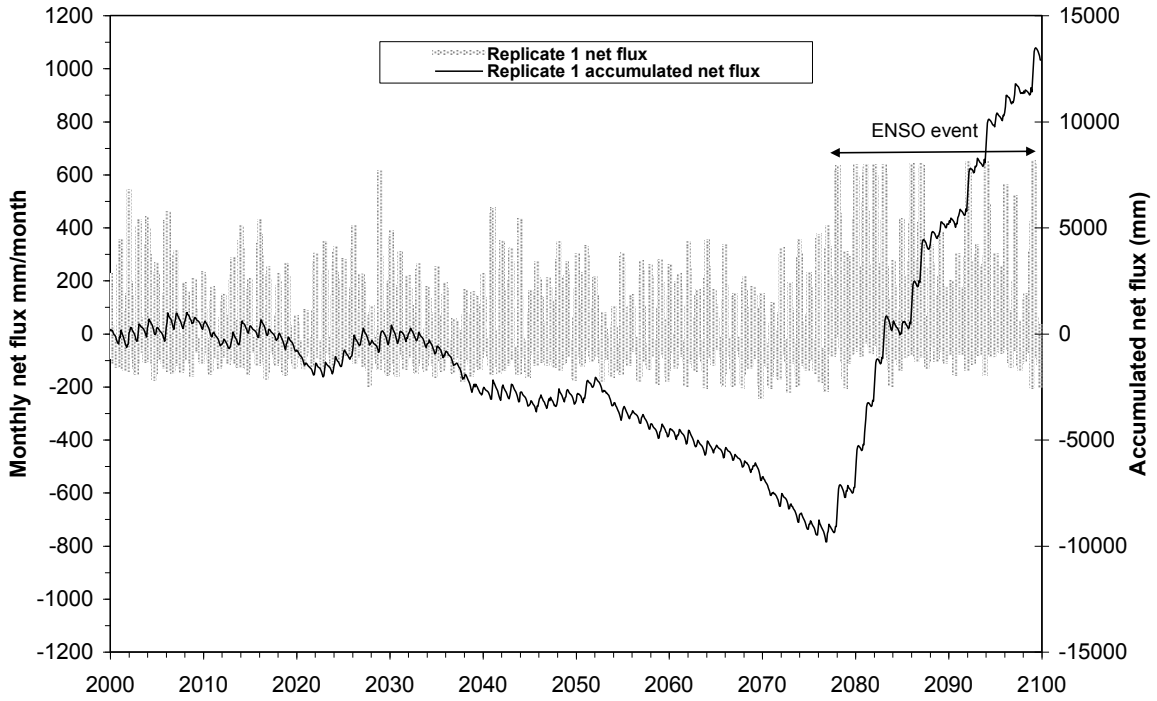

Figure 9.6 Example of net flux as used in Seep/W model for computation of GWLs at the centurial scale

Limitation of HadCM2 net flux data: The net flux of HadCM2, as shown in Figure 9.7, is very different from the other four GCMs. The reason behind this is the unavailability of the evapotranspiration variable in the output data of HadCM2. The evapotranspiration data (PPET) and thereby AAET of HadCM3 was used in the computation of net flux for HadCM2. It can be recalled that net flux is the algebraic summation of rainfall and AAET. Figure 9.8 illustrates the HadCM2 GCM's A1F scenario for the multiplying factors of monthly net flux. The HadCM2 A1F scenario has a maximum negative factor (-2) and the positive factor does not grow with the trend, it flattens in the last decades (after 2070) of predictions. That is why the net flux is increasingly negative in Figure 9.8; thus, the computed GWL goes far below and causes instability in the solution procedure of the Seep/W model. This issue will be discussed later in this chapter.

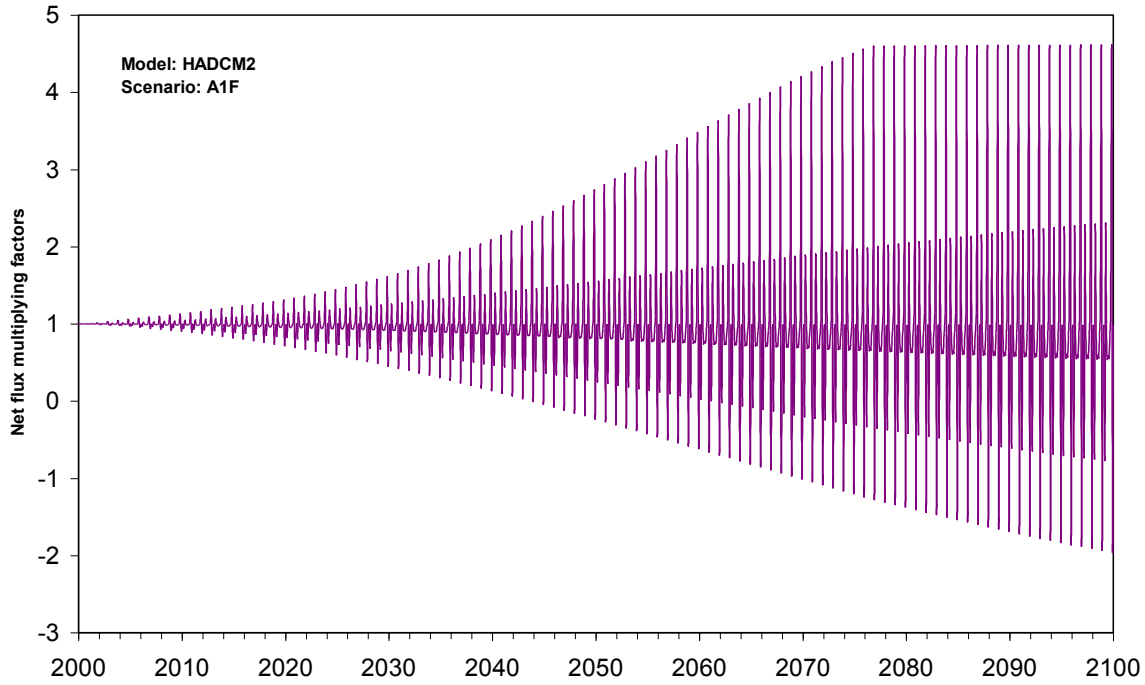

Figure 9.7 The multiplying factors for net flux of A1F scenario of HadCM2 GCM. The positive factors do not grow after 2070

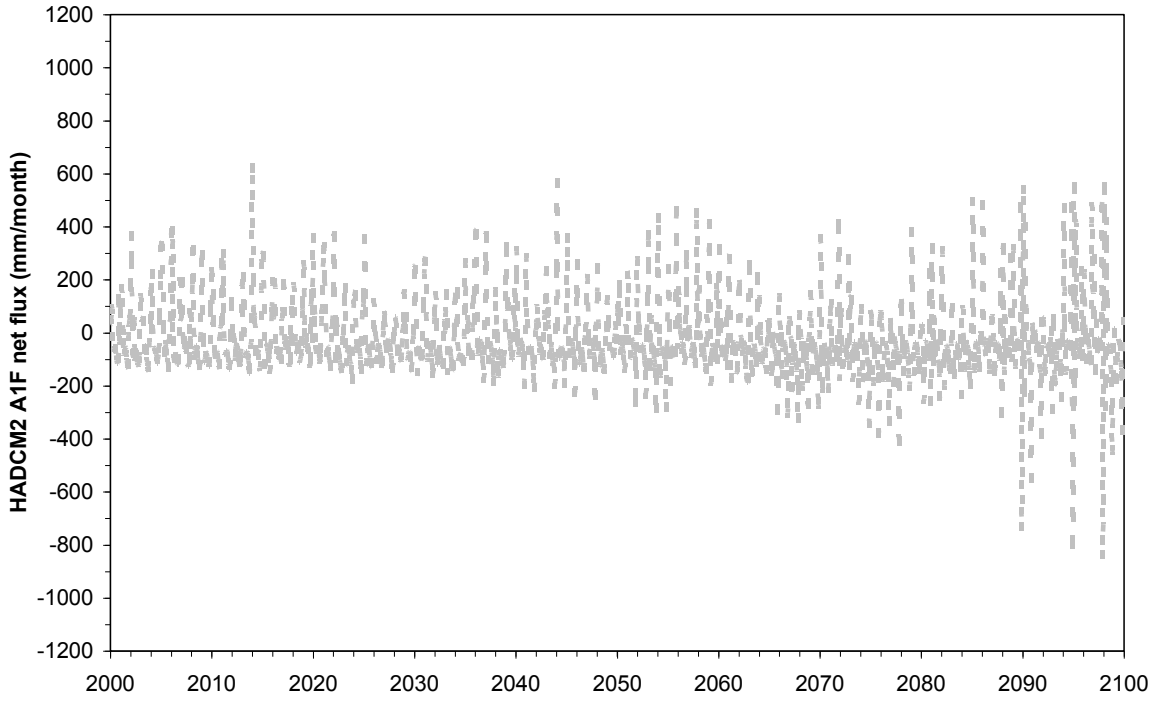

Figure 9.8 One sample net flux data for HadCM2 A1F scenario, negative flux increases significantly after 2070

9.4. Unsaturated Flow Model Prediction

As described in Chapter 8, a number of bores (OB1A, OB20, OB21A, OB27 and OB41) are selected for modelling by unsaturated flow model Seep/W to simulate the measured

GWLs. A combination of saturated hydraulic conductivity and porosity values were selected for assessing the best result in context with multiple numbers of statistical criteria for the period of the multi-decadal time scale. The bore OB27 was found to perform consistently better with respect to most of the statistical criteria. Therefore, this bore is selected for predicting the centurial time scale response of GWLs with respect to the thousands of replicates of climate data. One sample graph of 30 replicates for one scenario of one GCM is illustrated in Figure 9.9. The total of 35 graphs for all 1050 simulation of Seep/W model are given in Appendix I. The modelling shows that although the impact of climate change could be significant, it must be considered in the face of climate variability, as reported in the following section. An integrated description of the modelling for climate change and climate variability could be also found in Kabir *et al*. (2008c).

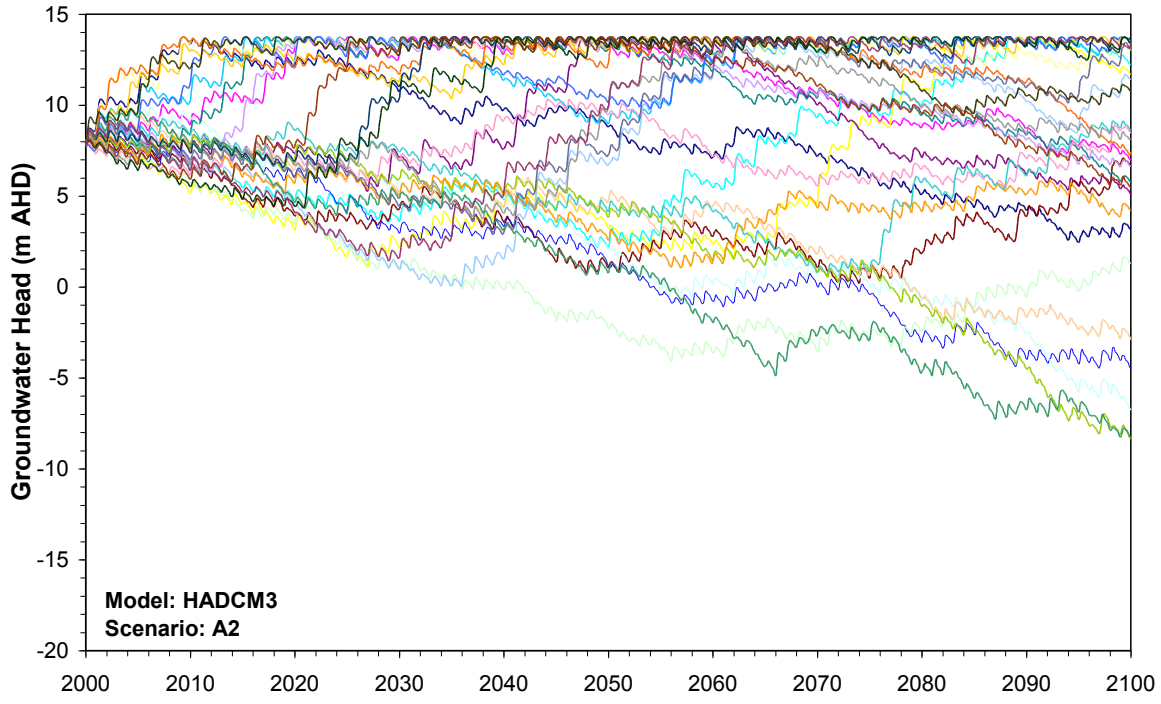

Figure 9.9 The 30 simulations of GWLs as computed by the Seep/W model. The input data to the Seep/W model was obtained from the output of HadCM3 GCM using A2 emission scenarios. The GWLs are controlled at an upper limit by the practical condition of runoff generation when GWLs reach ground surface at 14 m AHD (approximately)

9.4.1. Impact of Climate Change and Climatic Variability

It can be recollected that in the process of future climate data generation, the trend of climate change was represented by a change factor (multiplying factor). Climatic variability was represented by combining the data from the 'ENSO generation' program,

which is based on a conditional stochastic process, and SCL program, which is a random process based on historical data. The ENSO events are represented in the replicates by consecutive wet years or dry years, as could be easily differentiated from purely SCL replicates. The response of the groundwater system in relation to the range of climate data can be evaluated in terms of the gradual long-term trend of rising or falling, or stationary type and the sharp, short-term trend of rising or falling, indicated by a spell of a few years with ENSO events. There could be two possibilities, type 'a' and 'b':

Type 'a': The responses of GWLs are exactly similar to the variations of multiplying factors, which are gradual and unidirectional in nature.

Type 'b': The responses of GWLs are randomly influenced by sharp short-term rises and falls.

If the climate change impact were stronger than the impact of climatic variability, the responses of type 'a' would be more prominent. If the climatic variability impact were stronger, type 'b' would be more prominent. From the result of all the 1050 replicates (5 GCMs, 7 scenarios, 30 replicates) it can be easily seen that type 'b' responses are significantly more prominent than type 'a'. The relative influence of climate change indicated by a long-term trend and that of random variability indicated by a sharp and short spell of fluctuation could be statistically analysed to establish the conclusion with more confidence. This type of evaluation could be conducted by following a range of methods; therefore, it is excluded from this study. This could be a topic for further study in this field.

9.4.2. Long-term Response of GWL with Climate

The Seep/W result of the computed GWL for 1050 sets (5 GCMs, 7 scenarios, 30 replicates) of net flux are analysed for predicting the long-term response of groundwater to climate change. Of the five GCMs output, the HadCM2 has been identified with the weakness of inadequate climate variable. However, HadCM3 GCM has significant acceptance as it was found that Yohe et al. (2007) used this same GCM in the fourth assessment report of IPCC on the assessment of water resource availability in a global context. Therefore, in this analysis, all seven scenarios of HadCM3 GCM results are represented by plotting the time series of mean GWLs, mean plus standard deviation and mean minus standard deviation for each set of the 30 replicates, as shown in Figure 9.10. This demonstrates the result for HadCM3 GCM for all of the seven emission scenarios. HadCM3 is one of the five GCMs used for the analyses. It should be noted that the

probability distribution function (PDF) of stochastically-generated time series data can be adequately represented by the mean and standard deviation series as suggested by the Fokker-Plank equation (Risken and Frank 1989). In addition, the GWLs are not directly generated from the stochastic process; they are the output of the physically based model Seep/W.

The unsaturated flow model outputs of GWLs are plotted for the centurial scale and the corresponding confidence limit for 68% reliability is also computed. The mean (μ) and standard deviation (σ) of any data set can be combined to form the range of (μ + σ) to (μ - σ) data, which has the probability of occurrence of 68% for normally distributed data. It can be recalled that the confidence interval increases to 95% when the limit is chosen to be (μ ± 2σ). In consideration of all these issues, the 68% probability values are used, i.e. the (μ + σ) and (μ – σ) limit for all the time series of GWLs related to the net flux of all five GCMs and all seven scenarios.

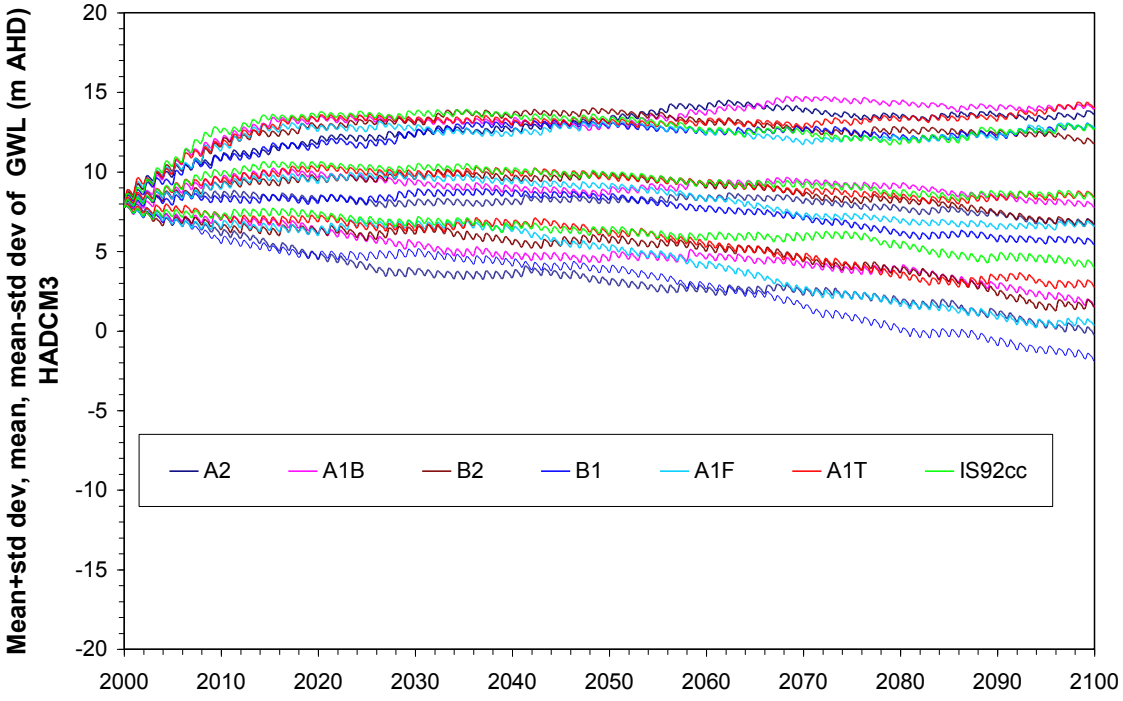

Figure 9.10 The HadCM3 GCMs A2, A1B, B1, B2, A1F, A1T and IS92cc emission scenarios mean with plus/minus standard deviations of GWL result from the year 2000 to 2100

The results of other GCMs are shown in the following figures such as Figures 9.11, 9.12, 9.13, 9.14 and 9.15, in the framework of the two bounds of uncertainty as μ ± σ. It should be noted that in evaluating the statistical performance of all five GCMs, the HADCM2

model runs, which are unstable and fall below -20 m RL are eliminated from the calculation as in Figure 9.14. The cause of unstable model runs is the severely dry conditions, which are found from HadCM2 trends and is explained in Section 9.4.3.

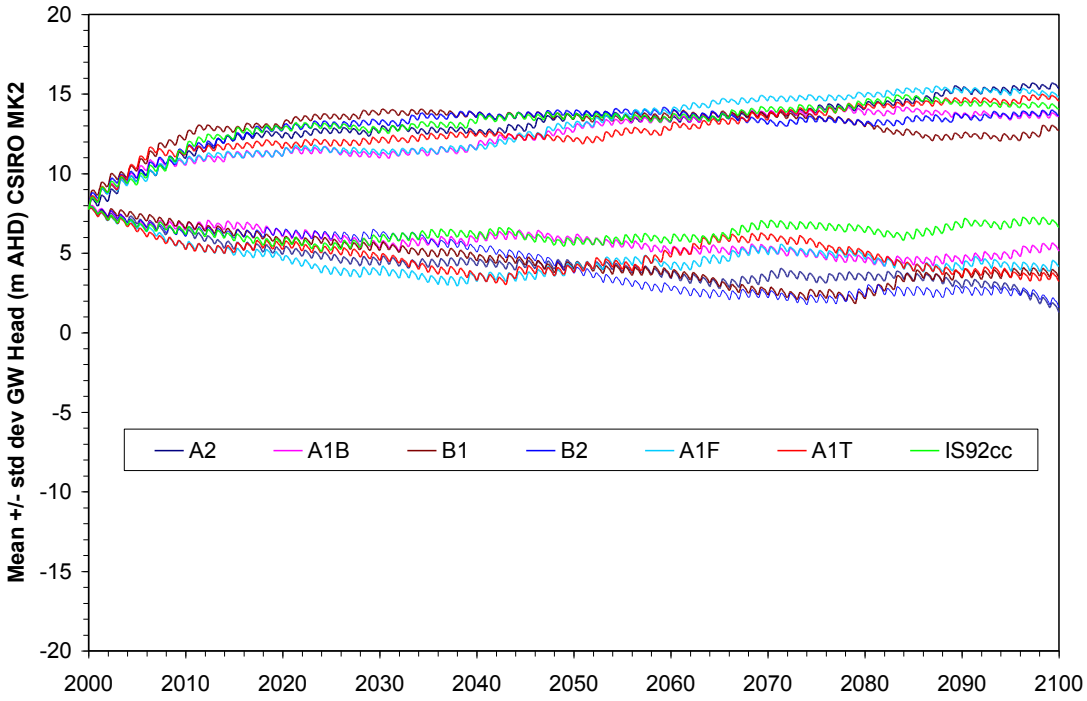

Figure 9.11 The CSIRO Mk2 GCMs A2, A1B, B1, B2, A1F, A1T and IS92cc emission scenarios mean plus/minus standard deviations, i.e. (μ + σ) and (μ – σ) limits of GWL result from the year 2000 to 2100

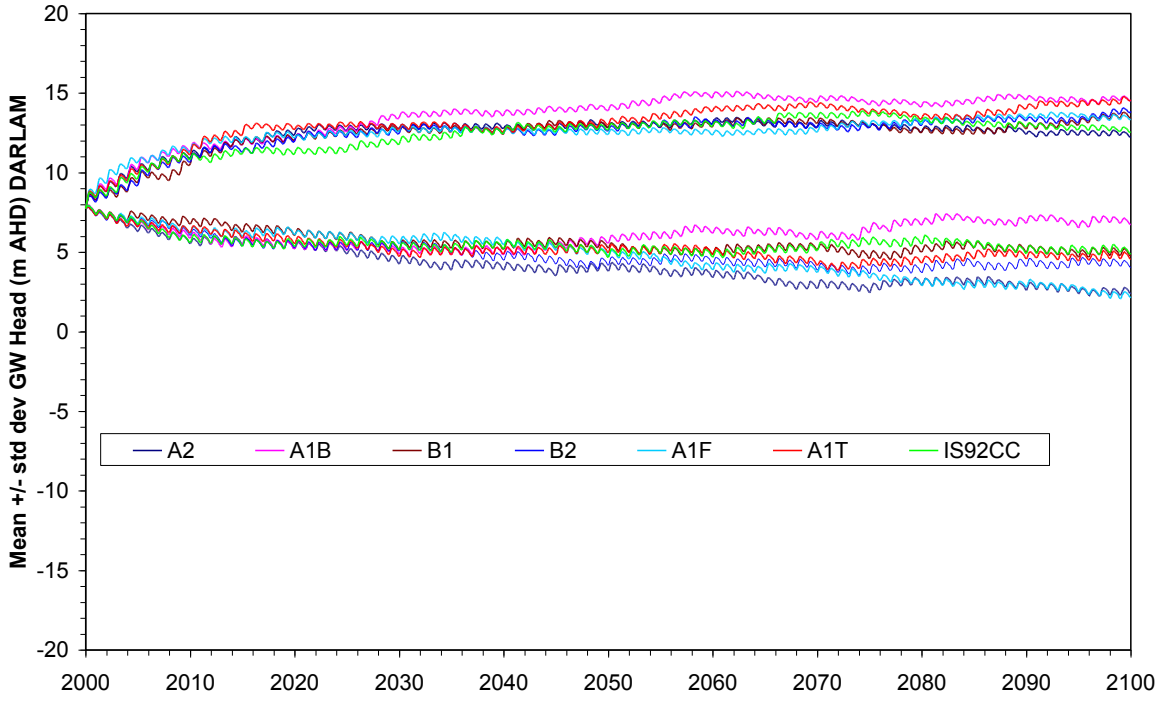

Figure 9.12 The DARLAM GCMs A2, A1B, B1, B2, A1F, A1T and IS92cc emission scenarios mean plus/minus standard deviations, i.e. (μ + σ) and (μ – σ) limits of GWL result from the year 2000 to 2100

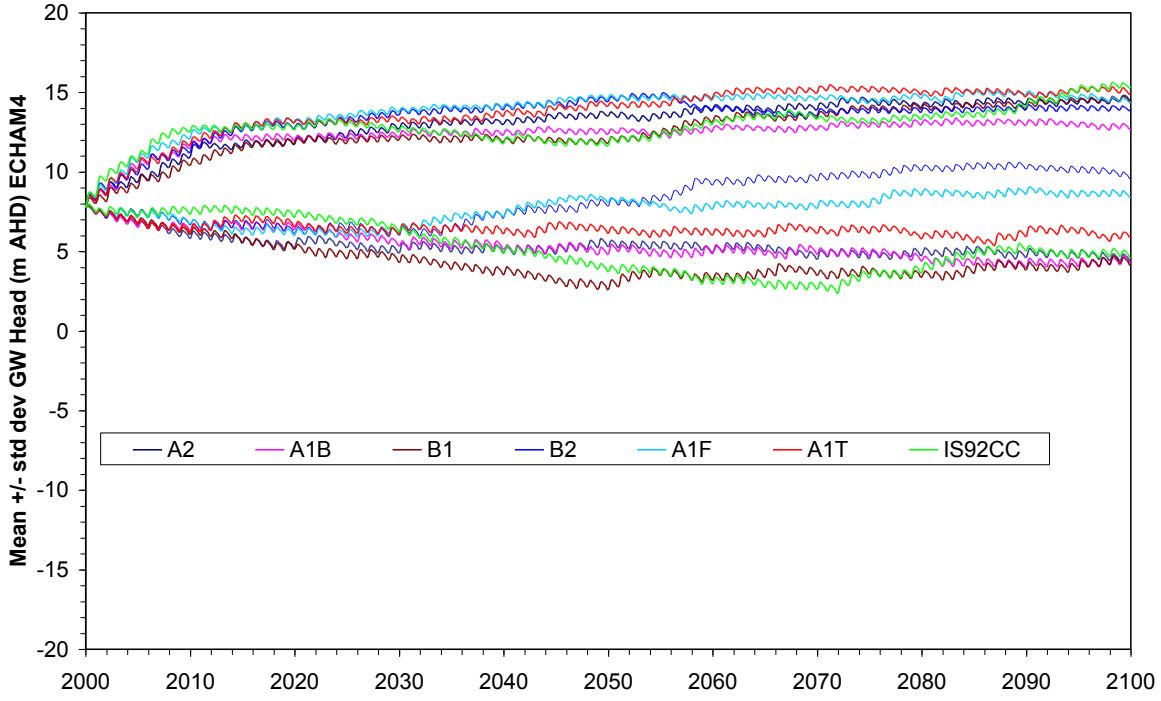

Figure 9.13 The ECHAM4 GCMs A2, A1B, B1, B2, A1F, A1T and IS92cc emission scenarios mean plus/minus standard deviations, i.e. (μ + σ) and (μ – σ) limits of GWL result from the year 2000 to 2100

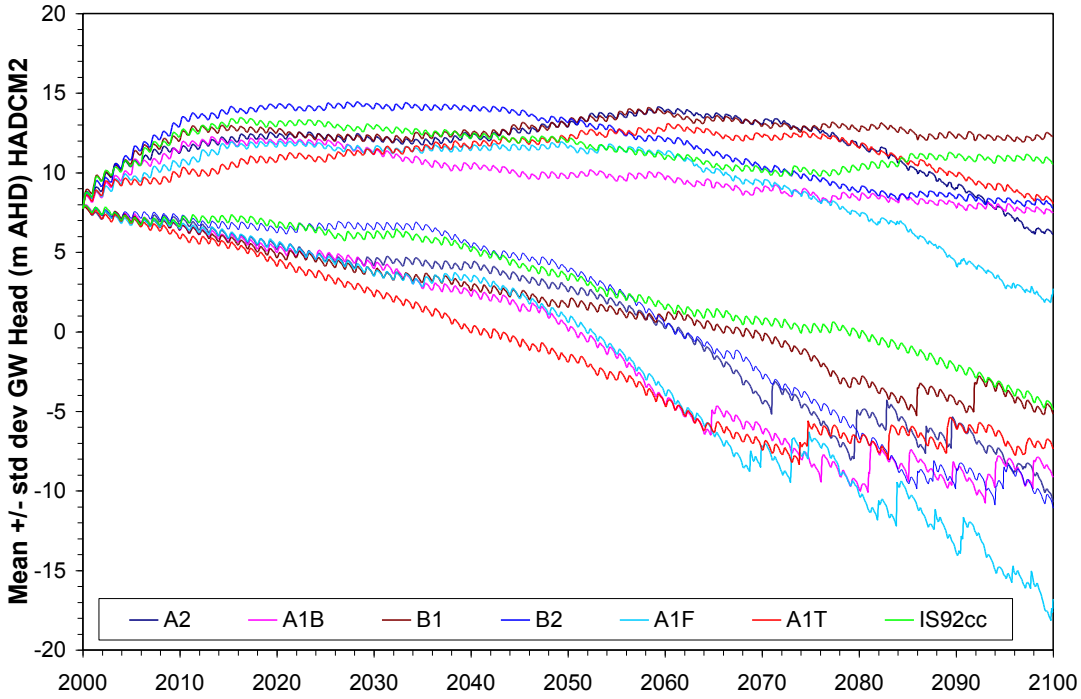

Figure 9.14 The HadCM2 GCMs A2, A1B, B1, B2, A1F, A1T and IS92cc emission scenarios mean plus/minus standard deviations, i.e. (μ + σ) and (μ – σ) limits of GWL result from the year 2000 to 2100

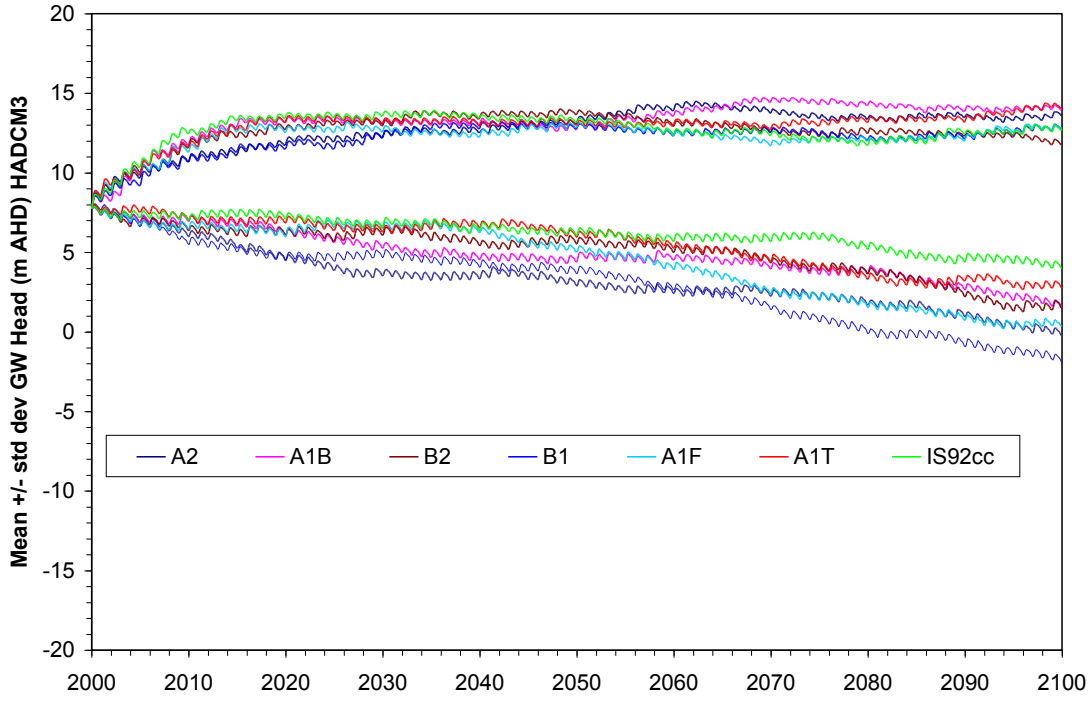

Figure 9.15 The HadCM3 GCMs A2, A1B, B1, B2, A1F, A1T and IS92cc emission scenarios mean plus/minus standard deviations, i.e. (μ + σ) and (μ – σ) limits of GWL result from the year 2000 to 2100

9.4.3. Numerical Instability with Some of the GCMs Data

The runs with unstable results were analysed to find the possible relationship between occurrences of instability and the underlying net flux data (boundary condition). When the accumulated net flux becomes negative, the GWL goes down. During the time steps of negative flux, the model uses the modifier function to handle the situation of extreme negative soil suction caused by negative flux. The modifier function converts the constant flux boundary (as used in the model runs) to constant head boundary and *vice versa* and checks with the water balance equation to achieve the convergence criteria in the cycle of each iteration (Krahn 2004b).

In cases of extreme dry conditions, while modifier functions are used for the satisfaction of water balance, the large negative head is computed, which does not necessarily signify any physical process. From observing some of the graphs of stable runs, such as in Figures 9.16 and 9.17, it can be easily seen that when the GWLs reach the ground surface (approximately +14 m AHD), with the increase of accumulated net flux, the excess water leaves the system by runoff. In defining the boundary condition of the model, it was selected that there would be no ponding of water at the top of the ground surface; excess water would be drained of by the surface runoff process. In the unstable run, as in Figure 9.18, it can be seen that when the GWL reaches the bottom of the model (at approximately -26 m AHD), the instability occurs.

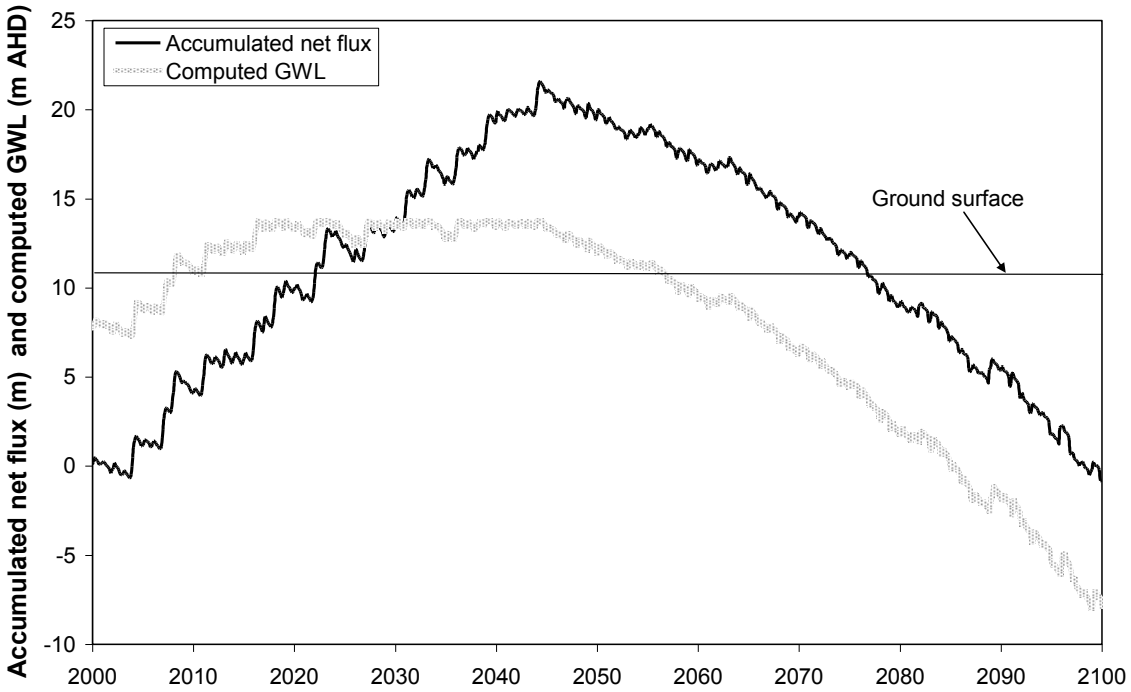

Figure 9.16 Stable run 1 with lowest GWL within -26 m AHD

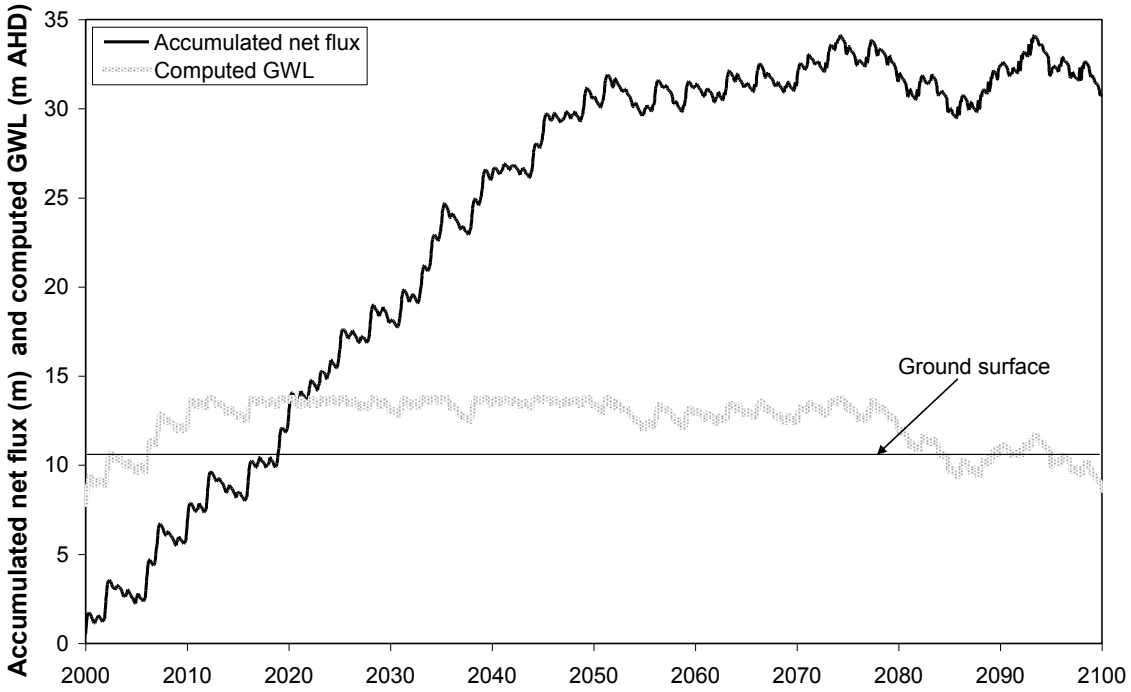

Figure 9.17 Stable run 2 with lowest GWL within -26 m AHD

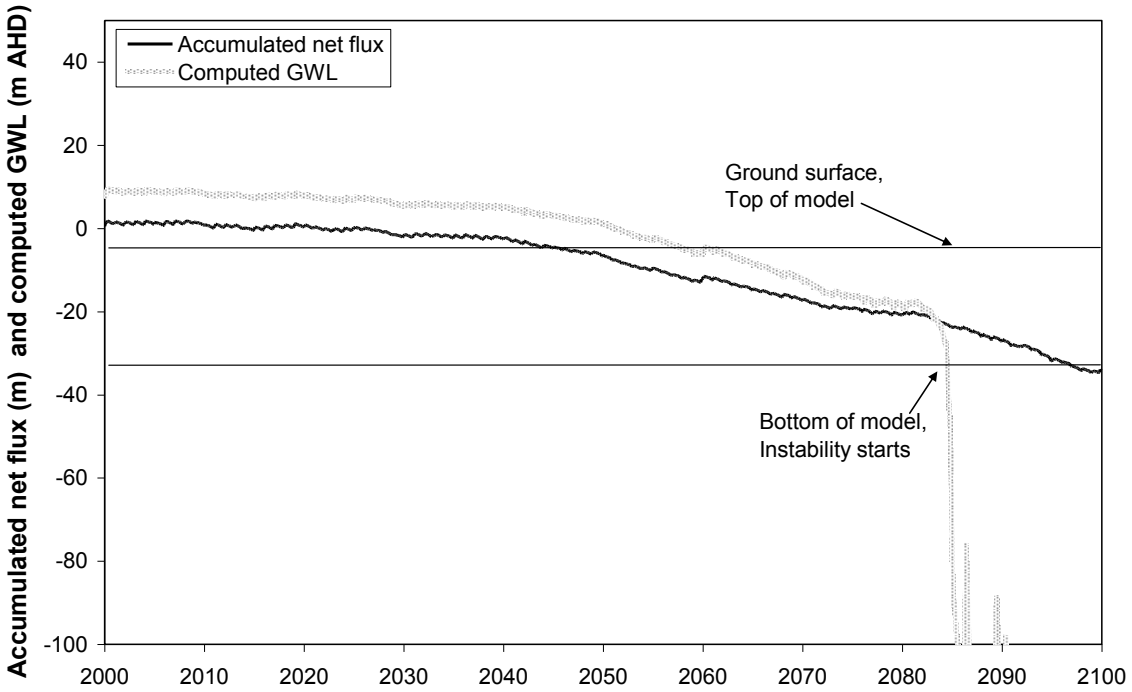

Figure 9.18 Instability of run 3 starts when the computed GWL goes below -26 m AHD

The values of GWL at -1000 m are theoretical, which are computed as the result of very dry conditions. Some more cases of unstable runs were investigated and it was concluded that when GWLs fall below approximately -26 m, the model becomes unstable. It should also be noted that the unstable runs occur only with the net flux predicted by the scenarios of HadCM2 GCM. The limitations of HadCM2 net flux data have already been discussed.

Thus, as a general conclusion for the statistical performance evaluation of the whole range of analyses, the unstable model runs results were excluded by considering them as outliers, which originate from deficiency of input data. The retention or deletion of any outlier can significantly affect the magnitude of statistical parameters especially when the sample size is small (Chow et al. 1988). Therefore, procedures for treating outliers require judgements in mathematics as well as the hydrological context. The occurrence of unstable runs is a distinct characteristic of the HadCM2 model net flux data. Although the number of data sets is only 30 for each scenario the runs with instability have been excluded from the analyses. Thus, the result of the HadCM2 model is analysed for the period of 2000 to 2100 for only stable runs.

Outliers in statistical analyses are sometimes not negligible when they signify some important phenomena that are significantly relevant to the research question. However, in this context, the outlier (i.e. unstable runs of Seep/W) is caused by the computational framework of the Seep/W model. It should be acknowledged that the numerical modelling of physical systems is always based on this type of compromise of the model representativeness with its computational accuracy and efficiency.

Instability as influenced by model depth: The depth of the model represented in the computation is 40 m from ground surface. The ground surface elevation is at +14 m RL and the bottom of the model is at -26 m RL. Therefore, with the range of net flux data, model runs that result in GWLs to fluctuate within a range of 40 m are considered only. 40 m depth is a reasonable compromise to encompass the range of future climate data. For HadCM2 model only the instability occurs and its inadequacy has already been discussed. The physical depth of OB27 is also in the range of 40 m.

The boundary condition used for the model is that no-flow boundaries exist along the bottom and the two lateral sides. Thus, when the computed GWL falls below the bottom of the bore, the instability occurs. Larger and smaller depths of model were experimented with and it was noted that the instability occurs when the computed GWL falls below the bottom of the model's bottom line. For deeper models, instability occurs at a later time step and for shallower models, instability starts at an earlier time step for the same set of net flux data. Hence, the gradual fall of GWL continues until it reaches the bottom of the model. For shallow models, that condition occurs earlier and therefore the instability starts earlier. In the representation of the graphs for the result, although the bottom level of the model indicates -26 m RL, most of the computed GWLs are found to be in the range of approximately -20 m RL. For closer assessment of results, -20 m RL (instead of -26 m RL) has been chosen for the graphs.

9.4.4. Uncertainty of the Work/Discussion

In the climate change impact study as performed by various investigators, it can be conceived that the sources of uncertainty typically originate from a number of steps of the modelling framework. The facets of uncertainty can be listed as follows:

1. The type of GCM
2. The emission scenario and climate sensitivity

3. The downscaling technique
4. The hydrogeologic model structure (with regard to groundwater impact)
5. The hydrogeologic model parameters

The aforementioned list of sources of uncertainty could be addressed in multiple ways while review of some relevant works are analysed. One of the most relevant investigations is the attempt to develop a probabilistic framework, as presented by Wilby and Harris (2006c) while combining information from GCMs, emission scenarios and downscaling techniques for modelling uncertainties regarding climate change impacts. They use four GCMs (HadCM3, ECHAM4, CSIROMk2 and CGCM2), two scenarios (A2 and B2), two statistical downscaling techniques, two hydrological model structures and two sets of hydrological model parameters. In the study by Wilby and Harris (2006c), it can be observed that they have used a limited number of all of the aforementioned sources of uncertainty in their analyses. With regard to the context of GCM and the emission scenario selection process, Giorgi and Mearns (2002) consider two 'reliability criteria': the performance of the model in reproducing the present day climate ('model performance' criterion) and the convergence of the simulated changes across models ('model convergence' criterion). These criteria are used to develop the 'reliability ensemble averaging' (REA) method for calculating average, uncertainty range and a measure of reliability of simulated climate changes at the sub-continental scale. Serrat-Capdevila et al. (2007) also use a similar approach to assess the performance of GCMs in their study. Whetton et al. (2005) suggest that the present day GCMs can simulate large-scale circulation features but they are unable to simulate local to small-scale circulation features that influence regional climate. Therefore, they suggest the necessity of joint probability consideration in quantifying the uncertainty. The study by Telbaldi et al. (2005) is an example of the probabilistic approach while predicting the regional climate.

In the present perspective, the selection of GCMs has been performed based on some recent investigations by Hennessy et al. (2004), as described in the Chapter 7. They applied statistical methods to verify the performance of each model in simulating the current climate. In their analyses, they have compared the observed and simulated patterns for 1961–1990 by calculating 'pattern correlation coefficient', which measures pattern similarity, and RMSE, which measures the magnitude of differences. Of the twelve GCMs, five selected to be considered in the study. The entire seven emission scenarios (A2, A1B,

B2, B1, A1F, A1T and IS92cc) are considered in this study. Medium climate sensitivity for all these scenarios is considered for the work. It should be mentioned that the SRES emissions scenarios are deliberately constructed in such a way that they are all equally plausible (Whetton et al. 2005). Therefore, it is reasonable to consider all the scenarios to capture the maximum range of possibility.

A downscaling technique is not required to obtain the regional climate data from GCMs as the data source 'Ozclim' of CSIRO (2006) was available based on the IPCC Third Assessment Report series. The spatial resolution is a 25 km grid and the climate data available is at the monthly time step. It should be noted that the then available resource of climate data 'Ozclim' is no longer freely available in the website and needs to be calculated with prescribed procedures for a specific set of particulars of the GCMs and variable under consideration.

The hydrogeologic model structure was selected by considering a number of conceptual model studies as discussed in Chapter 5. The best representation of the problem was determined in consideration to the significant flow processes and available data. The representation of climate by the variable 'net flux' as the algebraic summation of rainfall and evapotranspiration (AAET) has been used by many investigators. For example, Wilby and Harris (2006c) use 'effective rainfall' and Xu (1999) uses 'active rainfall' to represent the similar hydrologic input. A detailed discussion of this topic has been given in Chapter 5.

The selection of hydrogeologic model parameters in the groundwater study mostly relates to the HC and soil moisture content or porosity of soil. The unsaturated flow model has additional complexity due to the variable flow and storage characteristics with soil suction. With the historical climate data, the Seep/W model runs were made numerically stable by calibrating the volumetric water content function and hydraulic conductivity function. Next, to validate the measured groundwater levels in some of the selected bores, a range of statistical criteria were considered. In validating the measured groundwater level data with the modelled data, the saturated hydraulic conductivity and porosity values were selected by considering the most important statistical criteria for the problem in the context. The detailed result is presented in Chapter 8. The selected soil properties were consistent with the field measurements, laboratory measurements and SHPA sources. With regard to the

present research, the frequency distribution function analyses are performed to assess the outcome of the result.

The Seep/W model approach used herein, while representing the climate with net flux as a boundary condition of the system, is a simplification of the real processes of soil water interaction. A certain amount of water is forced to flow out of the system, namely AAET, which sometimes may not be practical. The AAET is computed from GCMs trends and local scale stochastic processes (as discussed in Chapter 7). In reality, the negative flux might not be large enough to pull the GWLs that low, as shown in some of the simulations. This is a big limitation of this work. However, since the purpose of the modelling is to develop the framework for the impact study, future research could be extended to build a more realistic groundwater model that would compute the climate flux based on climatic processes and observed climate data and thus represent the system in an improved way.

9.4.5. Physical Significance of Frequency Distribution

The cumulative frequency distribution function or probability density functions analyses give relatively better quantifications of the uncertainty in relation to the representation of mean and variance (Tartakovsky *et al.* 2009). Therefore, a sample analysis of this kind is provided here as a sample result. Detailed analyses could be conducted in a similar fashion but are avoided for brevity of the chapter. The frequency of occurrence of GWL at a certain depth and at a certain instant in time indicates the probability of the soil at that depth to be in a saturated condition, which is the prerequisite of safe containment of tailing waste. Therefore, the 210 simulations are considered, i.e. all seven scenarios and each of the 30 sets of data of the HADCM3 model-based net flux fed Seep/W model runs results. By integrating the frequency distribution curve, the cumulative frequency distribution function is estimated.

The cumulative frequency distribution of various unsaturated soil thicknesses during a particular time of the 100-year span (i.e. in 2050) for all seven emission scenarios of a specific GCM (HadCM3) is shown in Figure 9.19. Clearly, the more frequent occurrence of GWL at ground surface is caused by the fact that excessive rainfall, in excess of the soil's infiltration capacity, causes the fully saturated condition. The ponding is not allowed in the Seep/W model; therefore, the rise of GWL is limited to the ground surface. There is a sharp rise of frequency at that level of ground surface because of the no ponding situation.

The symmetry of the distribution of frequency is thereby distorted. Symmetry of frequency distribution is a prerequisite for the validity of the decision that a 68% confidence interval should be attained by μ±σ bound, 95% confidence by μ±2σ bound and 99.7 % confidence by μ±3σ bound (Kerr et al. 2002). There are methods that deal with skewed distribution, but those are not employed here as the skewness of the data is the outcome of the modelling framework that is accepted for some practical reason. The physically significant part of the result is the conclusion about the relative frequency of level of saturation at the various depths and the geometry of the cumulative frequency curve, which can be adequately described with a parabolic equation. The μ value of the distribution is 8.94 m and σ value of the distribution is 4.13 m. The range of 68% prediction bound at 2050 is therefore 8.26 m

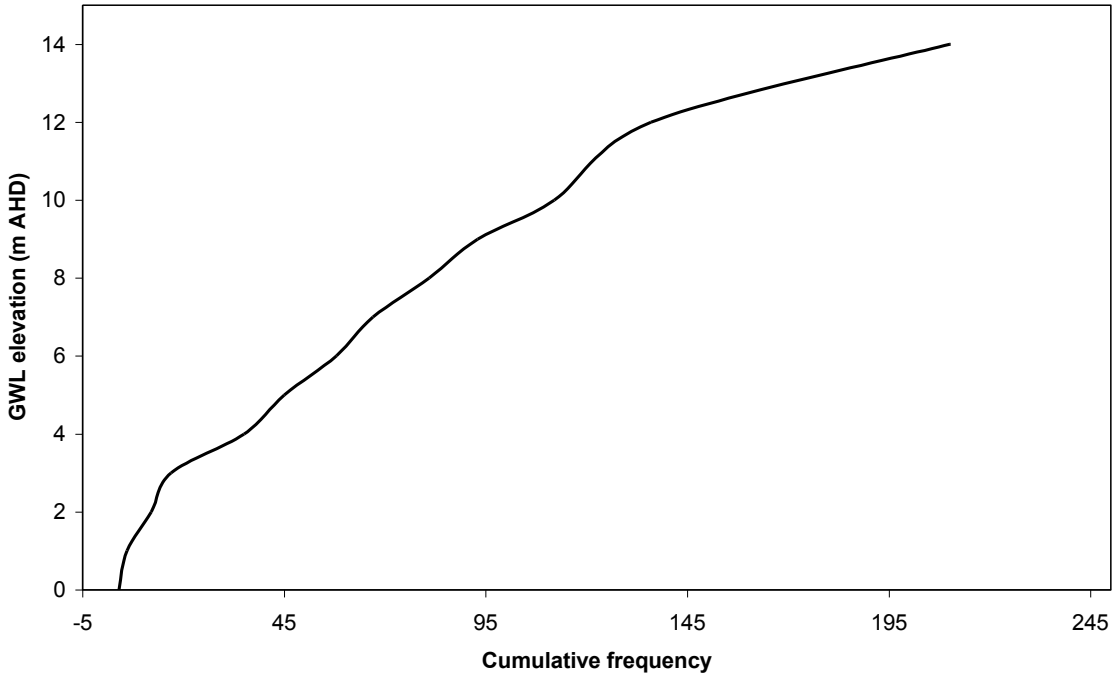

Figure 9.19 Cumulative frequency distribution of GWLs at various depths for 210 simulations of HadCM3 GCM during January 2050. The ground surface is at 14 m AHD, the mean value is 8.84 m, standard deviation value is 4.125 m

9.5. Integration of Physical and Non-physical Models

The objective of the research is the prediction of groundwater level; the recharge process causes the variation of groundwater level. Therefore, the detailed modelling work targets the estimation of recharge at the catchment scale. The review of key climate feedbacks,

which are related to groundwater recharge or hydrologic processes, suggests that to manage the complex interaction between climate and groundwater recharge, the development of a balanced modelling framework is necessary.

As stated by Carter et al. (2007), two common terms can be used to describe assessment types: 'top-down' and 'bottom-up'. These address the issues of scale, subject matter (from physical to socio-economic) and policy (global or local) (Dessai *et al.* 2004). However, it is realised that assessment of impact has become increasingly complex, and combining elements of top-down and bottom-up approaches is preferable (Dessai *et al.* 2005).

It is clear that the precise implications of a given climate change scenario for the volume, timing and quality of groundwater and stream flows in a catchment will depend very much on the physical, chemical and biological characteristics of the catchment. It is difficult to generalise in quantitative terms. All the assessments of the potential effect of climate change on hydrological systems have only considered the effects of a change in mean climate. Climate change is also likely to affect relative variability, at all time steps, and this variability is a key characteristic of hydrological behaviour in a catchment. Unfortunately, scenarios of possible changes in climatic variability are difficult to define, and the potential effects of climate change on the key modes of climatic variability, such as ENSO, are currently very uncertain (Arnell 2002). The CSIRO (2007) specifically addresses this issue for Australia. Some new work is still being conducted regarding the incorporation of the climatic variability of Australia in some selected GCMs, as indicated by Rotstayn et al. (2010). In physically based modelling, the incorporation of climate change and climatic variability has been considered in a relatively logical way. In time series modelling, the prediction has been made based purely on the stationarity assumption. However, the prediction of 100 years of data from the model developed with less than 30 years of real time data possesses significant uncertainty and that is comparable to the uncertainty of the physically based modelling.

One of the important limitations of the study is that it does not consider the real time climate data to be embedded in the climate change prediction time series when examining the representativeness of the GCMs. However, this has already been performed for the NT by Hennessy et al. (2004) and the result of their work is used here. It has been established that the HadCM3 model is the best in many regards, as described in Section 8.4.1.

HadCM3 is one of the four GCMs used by Wilby and Harris (2006c). Yohe et al. (2007) also use the water availability assessment by using the result of this model after the Fourth Assessment Report. Therefore, the HadCM3 GCM prediction range result is compared with the time series prediction by the multivariate AR model.

9.6. Integrated/Differenced Time Series for Long-Term Prediction

One sample set of data of net flux has been plotted in Figure 9.20. The climatic variability shows that during the last two decades (2080 to 2100), there are spells of wet years in comparison to previous dry years. The accumulated net flux (integrated time series of net flux) is also computed to assess the influence of wet and dry spells of net flux. From the accumulated net flux plot, the sharp change in the long term trend is distinct. This is result of climate variability rather than climate change.

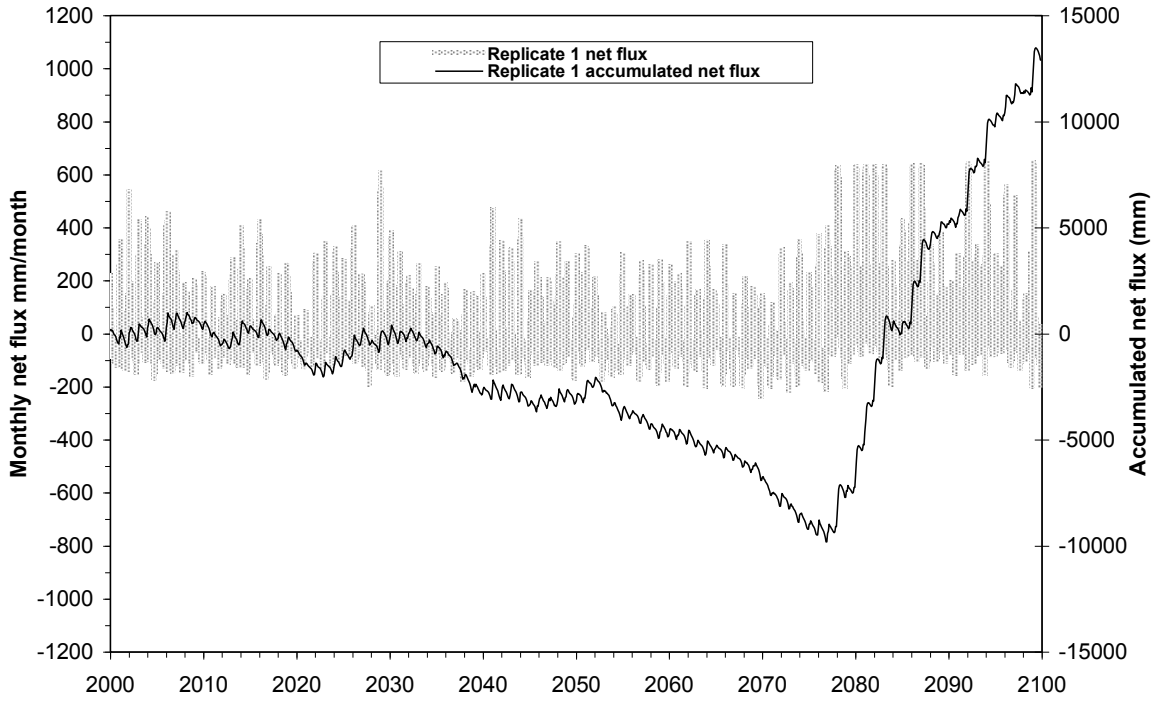

Figure 9.20 A sample graph of generated monthly flux and accumulated values (pareto) of that monthly flux

When applying the visual assessment of the data by considering the Seep/W results at random, as described in Chapter 8, it is found that most of the computed GWLs have long-term trends. The unsaturated flow model results of GWLs are consistent with the integrated time series of net flux. Figure 9.21 has been plotted to demonstrate the differences in the

resulting water balance of the system that is subjected to two different set of net flux (replicate 1 and 2).

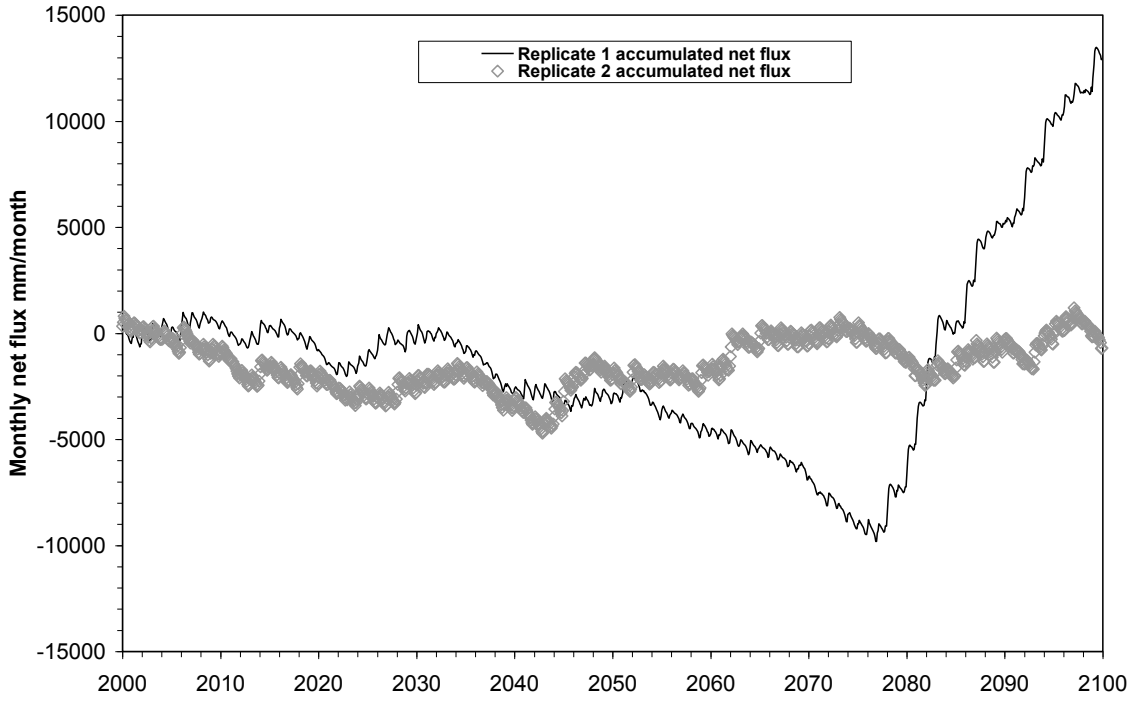

Figure 9.21 Accumulated net flux of replicate 1 and 2

However, after the application of the differencing technique to the GWLs data, the series could be made stationary. The physical significance of differenced GWLs data can be derived from the following discussion. The concept of mass balance for a control volume of soil mass can be considered.

Inflow – Outflow = *f* (rate of change of storage). There may be two forms of this equation, one in terms of rate of flow and another in terms of total volume of flow. The volume-based representation of the system in performing time series analyses can be found in Duah and Xu (2008). They use Cumulative Rainfall Departure (CRD) and Cumulative groundWater level Departure (CWD) in a similar study that analyses the impact of climate variability in an aquifer.

The graphical representation of total volume is shown in Figure 9.22 and that of rate of flow is shown in Figure 9.23.

Net flux per month = f (change of GWLs) (see Figure 9.23)

Summation of net fluxes = f (GWLs) (see Figure 9.22)

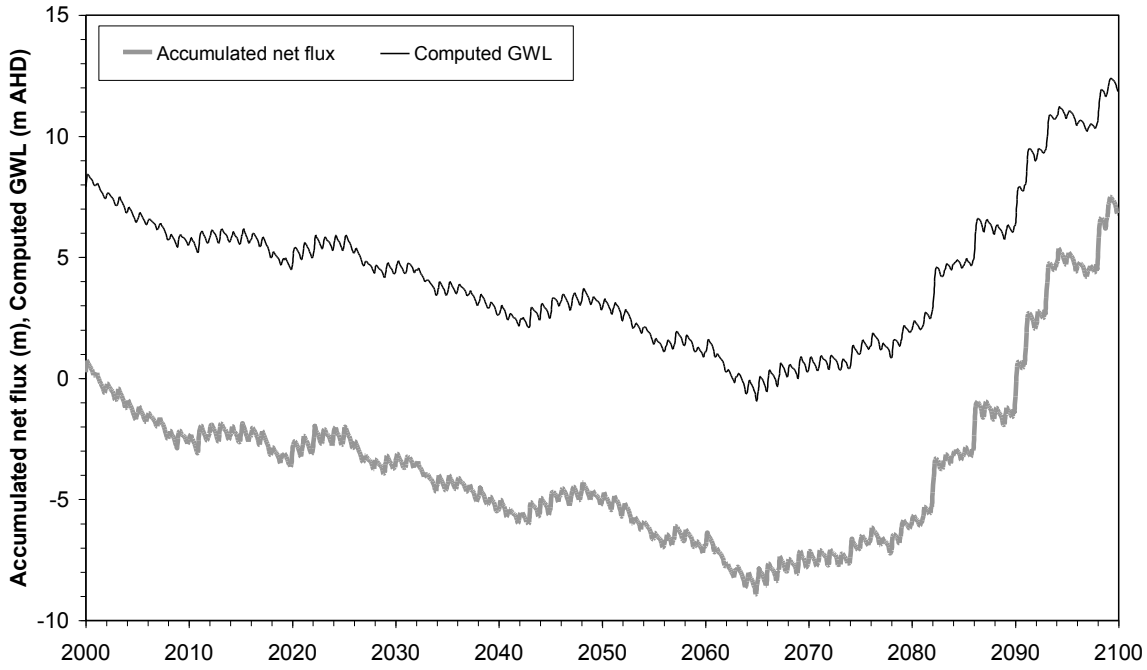

Figure 9.22 Generated replicates of net flux data summarised to estimate the accumulated net flux, which is plotted parallel to computed GWLs

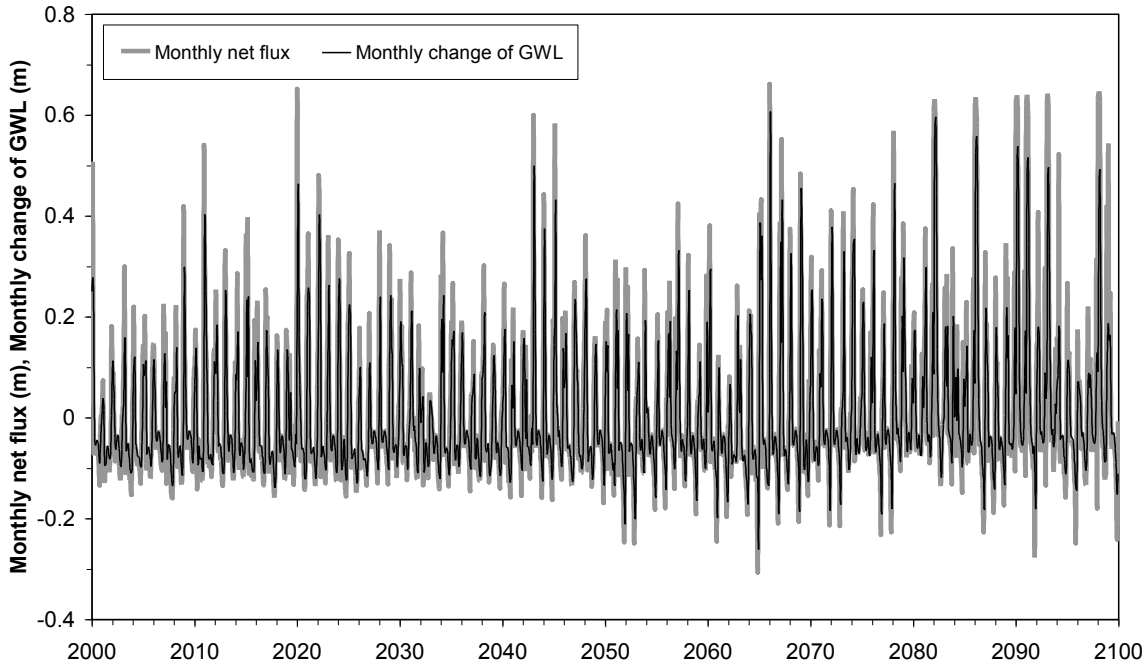

Figure 9.23 Trends of accumulated net flux and GWLs are eliminated by differencing

Therefore, in Figure 9.23, generated replicates of net flux data are used to estimate the accumulated net flux for 100 years. The computed GWLs and accumulated net flux are found to be of a similar trend which is logical and expected.

The incorporation of integration and differentiation for handling the problem of nonstationarity in the climate and GWLs time series should be used with utmost care and judgement for obtaining a scientifically acceptable prediction of the long-term response. Some attempts have been conducted in this area of investigation but the findings needed to be more in depth investigation and understanding. Therefore this has been recommended for the further extensive research.

9.7. Conclusion

The results of the analyses are evaluated in terms of the processes of calculation and their limitation with regard to the various assumptions. The future replicates of time series data of net flux are generated by incorporating climate variability and climate change projection scenarios. Significant achievements have been attained in the formulation of a modelling framework for the long-term impact study but a more realistic groundwater model needs to be incorporated for further advancement of the research. Natural climate variability is strong enough to influence the groundwater flow in the shallow unconfined aquifer and comparable to the influence of climate change trends.

10. Conclusion and Recommendations

The groundwater hydrograph has a clear interaction with the climate and more specifically, with the annual rainfall hyetograph. The extent of this relationship depends on the characteristics of the catchments and distribution of rainfall in time and space. In order to study this problem, the field site of the Ranger uranium project in the Kakadu region of northern Australia was chosen, since it is required to demonstrate that solutes derived from its radioactive mill tailings 'will not result in any detrimental environmental impacts for at least 10,000 years'. A key rehabilitation issue, therefore, is to understand and predict this rise and fall of the groundwater with respect to the climate system, including both climate variability and climate change, since it is relative groundwater levels which will control flow rates, direction and thus solute transport.

To study this challenging groundwater-climate problem, this thesis has undertaken a stepwise approach, from theoretical reviews, site review, development of conceptual hydrological and hydrogeological models, and quantitative physical and statistical modelling to characterise the Ranger site. Given the critical importance of climate change and variability in making projections of 100 years, a complex methodology was developed to assess the potential impacts of this on groundwater levels at the Ranger mine. Based on the five GCMs, seven emission scenarios and the inclusion of climate variability using conditional stochastic replicates, more than 1000 model runs were completed to assess the long-term impacts of both climate change and climate variability. The results of the climate were then used to project groundwater levels in the site over this 100-year timeframe.

Overall, this has allowed an assessment of the potential future groundwater levels to be generated based on climate change and variability. The development of such methodology for the rehabilitation of uranium mill tailings is believed to be the first such example worldwide, and should make planning for safe rehabilitation design more rigorous and thorough. This represents a significant contribution to new knowledge in this area, and should provide a model for similar problems around the world.

10.1. Summary of Scientific Achievements

- The historical hydro-climatic data and groundwater level data have been analysed from a number of methods including four different types of conceptual models and various time series models.
- The most appropriate conceptual model has been established for representing the groundwater flow system in the shallow unconfined aquifer of the site.
- The groundwater-monitoring bore data have been used for validation of the established physically based model by calibrating the soil hydraulic characteristic curves for the site under saturated-unsaturated flow conditions.
- Natural climatic variability has been replicated with the help of recently obtained scientific knowledge regarding the ocean-atmospheric circulation surrounding the investigation site. Starting with climate change predictions by a number of GCMs for multiple emission scenarios and combining them with the climatic variability for the site, thousands of replicates of climate data are generated.
- The physically based groundwater model has been run with the thousands of predicted climate replicates and corresponding GWLs are analysed for the possible ranges of long-term fluctuations.
- The methodology for the prediction of groundwater level as impacted by climate change and variability at the 100-year time scale has been developed.

Climatic variability, as indicated by the conditional stochastic process, is predicted using the current understanding of the various relevant phenomena related to the site, such as ENSO (El Nino/La Nina), PDO and IOD. The climate change predictions are obtained from the results of various IPCC emission scenarios of GCMs. These two predictions are combined to generate thousands of replicates of climatic flux to feed the physically based unsaturated groundwater flow model. The results of the unsaturated flow model are then analysed by using the probability distribution function of stochastically generated time series data to demonstrate the ranges of variation of the GWL in a 100-year period.

10.1.1. Summary of Results

Overall, the results show the critical importance of climate variability as well as climate change. During extended wet periods, groundwater levels are predicted to rise significantly, while major declines are expected under lengthy dry climatic periods. The modelling shows that although the impact of climate change could be significant, it must also be considered in the face of climate variability. Therefore, the research provides a sound methodology and scientific basis upon which it is possible to understand the potential impacts of climate change and variability on different uranium mine rehabilitation approaches in a wet-dry tropical climate surrounded by a region of very high conservation and cultural values. This is believed to be the first such rigorous methodology developed to address such a challenging problem anywhere in the world, and represents a significant scientific advance on current approaches and knowledge.

10.2. Recommendations for Further Investigations

Multiple ranges of known and unknown aspects relevant for predicting future ENSO events for the site have been considered in the generation of replicates of future climate. This method can be updated accordingly with new knowledge of influencing events such as ocean circulation phenomena, global greenhouse gas emissions, new GCM data, and so on. In addition, the methodology could be further enhanced in the following areas – (i) application to and optimisation of rehabilitation designs; (ii) expanded model scope and complexity, such as density-driven effects, regional scales or longer time periods (eg. 1,000 to 10,000 years); solute transport in conjunction with flow modelling; (iii) improved comparison of statistical and physical modelling approaches; (iv) application of stochastic modelling methods to more explicitly account for uncertainty; and (v) updating model runs with the latest GCM data and other scientific studies for climate change and variability.

10.2.1. Application to Rehabilitation Design

The application of the knowledge regarding the predicted long-term GWLs in the research site is targeted for establishing guidelines for the design range of fluctuation of saturated-unsaturated zone in the rehabilitation structure. After the closure of the mine site, the rehabilitation structure will be built in such a way that the groundwater divide will be built along the ridgeline of the elevated regions. The physical dimension and orientation of the unsaturated zone, as modelled in the present work, should be changed and the condition of no ponding of runoff at the top of the ground surface should be in existence. In this

situation, the probability of the propagation of contaminant from the tailing dam would be equivalent to the probability of the event of reaching GWL at the surface.

From point to region: The influence of the spatial variability of the catchment's physical characteristics should be combined with the temporal variability of the hydrologic processes for the long-term impact study of climate change on groundwater (Jyrkama and Sykes 2007). Kocher and Reichert (2008) identify a progressive approach to develop a groundwater model starting from a sub-catchment of approximately 30 km^2 and then a second step that involves a regional scale with 14,500 km^2 for the same catchment. The impact modelling starts from one single bore and then it should be extended for a wider area and more complex geological heterogeneity.

Design of rehabilitation structure by varying models: The practical design of the rehabilitation structure could be conducted with the help of various programming software such as the HELP (Schroeder *et al.* 1994) model and the Vadose/W (Krahn 2004a) model. The HELP model is a quasi-two-dimensional, deterministic, water-routing model for determining water balances. This program is used for conducting water balance analyses of landfills, cover systems and other solid waste containment facilities. The interaction between different layers (liner systems consisting of vegetation, cover soils, waste cells, lateral drain layers, low permeability barrier soils and synthetic geomembrane liners) and different processes (surface storage, snowmelt, runoff, infiltration, evapotranspiration, vegetative growth, soil moisture storage, lateral subsurface drainage, leachate recirculation, unsaturated vertical drainage, leakage through soil, geomembrane and composite liners) are represented by a number of empirical and semi-empirical equations. Pre-defined criteria are used for ascertaining the logical interaction between those processes. The Vadose/W model is a much more data-intensive model in which the net flux is computed from the measured climate variables such as rainfall, humidity, wind speed, temperature, solar radiation and duration of sunlight hours. It is a finite element model and involves extensive computation. This model can also be used for designing the rehabilitation structures.

Benson (2007) modelled the unsaturated flow and atmospheric interaction by using four codes: HYDRUS (Simunek *et al.* 1996), SVFLUX (Thode 2009), UNSAT-H (Fayer 2000) and VADOSE/W (Krahn 2004a). Wang and Murray (2005) used SoilCover (GeoAnalysis

2000) software and Seep/W software to design a soil cover system by simulation of the infiltration rate and estimation of groundwater level in a gold mine closure site in Canada. Kowalewski (1999) used both the HELP model and the SoilCover (GeoAnalysis 2000) model to compare the percolation rates for arid climate data. Similar analyses could be performed for this study to explain the outcome in a more comprehensive way.

Integrated water management issue: In climate change studies, the integration of other changes such as demography, land cover and land use, economy, technology and overall human activity should also be considered in a pragmatic way for practical needs (Varis et al. 2004). Understanding the regional groundwater flow for safety of geological disposal, as indicated by Toth and Sheng (1996), may serve one way of designing the rehabilitation structures safely to achieve low long-term environmental impacts.

10.2.2. Density Driven Flow Modelling and Solute Transport modelling

Flow dynamics change when there is a high concentration of salts present in water – making the saline water more dense than fresh water (eg. seawater has a typical density of 1.03 kg/L). The process water at the Ranger mine is typically saline (Ferguson and Mudd 2010) and thus in modelling regional scales density-driven effects would be important to address. Furthermore, it would be necessary to include solute transport in such modelling, as this is crucial in predicting long-term behaviour of tailings-derived solutes with respect to the 10,000 year rehabilitation goal.

10.2.3.Comparison of Statistical and Physical Modelling Approaches

The time series forecast using multivariate AR model, TFN model could be more thoroughly developed and thereby compared with physical process based modelling. Some initial investigations on this issue showed that incorporation of TFN model requires larger computational time and therefore it could be investigated under new initiative. The physical basis of TFN is stronger while the simplicity of multivariate AR model is an advantage for long-term modelling. Therefore this area remains to be investigated

Improved TFN representation: Significant improvement of the time series prediction could be achieved by investigating the optimum complicated model (in terms of the number of inputs) for optimum lead time (forecast time) (Tankersley and Graham 1994). The incorporation of unsaturated thickness as a second input function together with net

flux as the first input function can be used in double-input TFN. Goor et al. (2006) predict recharge as a function of dam water release and rainfall using the double-input TFN. In addition, there could be multiple-input TFN. Liu and Hanssens (1982), Edlund (1984), Liu (1986) and Edlund (1988) developed methods for the estimation of multiple-input TFN using the theory based on multiple regression, and considering the multi-colinearity of input data and auto-correlated residuals.

10.2.4.Stochastic Modelling

Extensive stochastic modelling would result in more explicit quantification of the uncertainty of this investigation. Very preliminary stage of analyses associated with the net flux data has been performed but the other factors could be addressed in conjunction with net flux.

Sources of uncertainty: In this study, there are multiple areas of uncertainty related to a range of issues. The future long-term climate flux, the interaction among the physical, chemical, biological and environmental processes and the future mode of human activities in response to the scientific development are some examples. In terms of modelling perspective, these could be categorised in many ways. For instance, in a study that evaluated the uncertainties specifically related to regional groundwater flow around a nuclear waste disposal site, Ijiri et al. (2009) have demonstrated that uncertainty for porous media heterogeneity is more influential than uncertainty for modelling approaches or scenario development. The Ranger area certainly exhibits considerable heterogeneity, which has been addressed in this thesis through calibration of historical data for each groundwater bore. Similar investigations could be performed for the Ranger site to identify the most vulnerable area of uncertainty.

Generation of climate variability: There are other possible methods to generate climate variability which could be further explored. For example, Singular Spectrum Analysis (SSA) has been applied extensively to the study of paleo-climatic time series, interdecadal climate variability, interannual and interseasonal oscillations in geophysical time series (Allen and Smith 1996; Gurdak *et al.* 2007). The work of Ghil et al. (2002) could be further investigated to explore the possibility of generating future climatic variability using other techniques such as the Blackman-Tukey method and the Multitaper Method of advanced spectral analyses for the site.

Larger time scale: Goodess et al. (1990) have employed a number of methodologies for assessing the probable ranges, successions and durations of major climate states that are likely to occur over a time scale of 10^6 years for the design of a radioactive waste repository in the UK. One of the methods includes the empirical analysis of the long-term reconstructed climate record, as we have used with SCL in this work. However, the current status of GCM's prediction is not reliable a time scale of thousands of years.

The application of the Milankovitch Theory for analysing changes in global climate over a million-year time scale was another method used by Goodess et al. (1990). Similarly, Stothoff (2007) estimated a million-year average of deep percolation from estimates of two independent climate sequences based on the correlation between past climate during glacial cycles and orbital characteristics of the Earth to project orbital characteristics into the future. This can be applied to the Ranger mine site for the estimation of longer time scale impacts, such as the 10,000 year rehabilitation criteria.

10.2.5. Updating Model Runs

The Ozclim data used in the study are derived from the Third Assessment Report. The data based of Fourth Assessment Report is now available. There is slight variation with the climate data among Third and Fourth Assessment Reports. The incorporation of Fourth Assessment Report based data will improve the scientific basis of this modelling.

10.3. Final Comments

The thesis addresses all relevant scientific issues which are to be considered for impact study of climate change and natural climatic variability on the shallow unconfined groundwater system. Some of the issues are explicitly incorporated while others are mentioned to be scope for further investigated. This approach can be applied for any other hydro-climatic system in any location for the long-term impact study of climate. The incorporation of prediction of the future climate variability is one of the most significant contribution to the existing methods followed in these type of investigations. The other significant contributions consist of application of statistics for understanding the physical processes, thorough investigation on the performances of various statistical models, detailed comparison of the various fitness criteria for validation of the physical process based groundwater model. Therefore the piece of work should be regarded as a significant new contribution to the knowledge in the existing state of the art in this field of science and its application.

11. References

Abbaspour, K. C., M. Faramarzi, S. S. Ghasemi and H. Yang (2009). Assessing the impact of climate change on water resources in Iran. Water Resources Research. 45**:** W10434, doi: 10.1029/2008WR007615.

Abbott, M. B., J. C. Bathurst, J. A. Cunge, P. E. O'Connel and J. Rasmussen (1986). An introduction to the European Hydrological System - Systeme Hydrologique Europeen, SHE, 2: Structure of a physically-based, distributed modeling system. Journal of Hydrology 87(1-2): pp 61 - 77.

Abram, N. J., M. K. Gagan, Z. Liu, W. S. Hantoro, M. T. McCulloch and B. W. Suwargadi (2007). Seasonal characteristics of the Indian Ocean Dipole during the Holocene epoch. Nature 445: pp 299 - 302.

Adam, J. C., A. F. Hamlet and D. P. Lettenmaier (2009). Implications of global climate change for snowmelt hydrology in the twenty first century. Hydrological processes 23: pp 962 - 972.

Adamowski, K. and T. Hamory (1983). A stochastic systems model of groundwater level fluctuations. Journal of Hydrology 62: pp 129-141.

Aeby, P. G. (1998). Quantitative fluorescence imaging of tracer distributions in soil profiles. Zurich, Swiss Federal Institute of Technology. Ph D**:** 77 p.

Aguilera, H. and J. M. Murillo. (2008). The effect of possible climate change on natural groundwater recharge based on a simple model: a study of four karstic aquifers in SE Spain. Environmental Geology, doi: 10.1007/s00254-00801381-2.

Ahmad, M. and D. C. Green (1986). Groundwater Regimes and Isotopic Studies, Ranger Uranium Mine Area, Northern Territory, Australia. Australian Journal of Earth Sciences 33: pp 391 - 399.

Ajami, H., J. Hogan, T. Maddock and T. Meixner (2007). Application of GIS Based Tools for Groundwater Recharge and Evapotranspiration Estimation: Arc-Recharge and RIPGIS-NET. American Geophysical Union, Fall Meeting 2007**:** Abstract H11F-0845.

Akaike, H. (1969). Fitting autoregressive models for prediction. Annals of the Institute of Statistical Mathematics 21: pp 243-247.

Akaike, H. (1972). Use of an information theoretic quantity for statistical model identification. 5th Hawaii International Conference on Systems Sciences, North Hollywood, California.pp 249-250.

Akaike, H. (1973). Information theory and an extention of the maximum likelihood principle. 2nd International Symposium on Information Theory, Budapest, Akademial Kiado.pp 267 - 281.

Akaike, H. (1974). A new look at the statistical model identification. IEEE Transactions on Automatic Control 19: pp 716 - 723.

Akaike, H. (1978). On the likelihood of a time series model. Journal of the Royal Statistical Society. Series D (The Statistician) Vol. 27, No. 3/4, Partial Proceedings of the 1978 Institute of Statisticians Annual Conference on Time Series Analysis (and Forecasting) (Sep. - Dec., 1978): pp 217 - 235.

Akber, R. I. (1991). Proceedings of the Workshop on Land Application of Effluent Water from Uranium Mines in the Alligator Rivers Region. Jabiru, NT, Australian Government Publishing Service, Canberra 1992, 11-13 September 1991; 355 p.

Alexander, L. V., P. Hope, D. Collins, B. Trewin, A. Lynch and N. Nicholls (2007). Trends in Australia's climate means and extremes: a global context. Australian Meteorological Magazine 56: pp 1 - 18.

Alexander, L. V., X. Zhang, T. C. Peterson, J. Caesar, B. Gleason, A. M. G. Klein Tank, M. Haylock, D. Collins, B. Trewin, F. Rahimzadeh, A. Tagipour, K. R. Kumar, J. Revadekar, G. Griffiths, L. Vincent, D. B. Stephenson, J. Burn, E. Aguilar, M. Brunet, M. Taylor, M. New, P. Zhai, M. Rusticucci and J. L. Vazquez-Aguirre (2006). Global observed changes in daily climate extremes of temperature and precipitation. Journal of Geophysical Research 111(D05109): pp 1 - 22.

Allan, R. J., J. A. Lindesay and C. J. C. Reason (1995). Multidecadal variability in the climate system over the Indian Ocean region during the austral summer. Journal of Climate 8(7): pp 1853 - 1873.

Allen, D. M. and M. W. Toews (2007). Modeling Spatial Recharge in the Arid Southern Okanagan Basin and Impacts of Future Predicted Climate Change. American Geophysical Union, Fall Meeting 2007**:** Abstract H11F-0841.

Allen, M. R. and L. A. Smith (1996). Monte Carlo SSA: Detecting irregular oscillations in the presence of colored noise. Journal of Climate 9: pp 3373 - 3404.

Allen, R. G., T. A. Howell, W. O. Pruitt, I. A. Walter and M. E. Jensen (1991). Lysimeters for evapotranspiration and environmental measurements International Symposium on Lysimetry New York, American Society of Civil Engineers**:** 444 p.

Allen, R. G., L. S. Pereira, D. Raes and M. Smith (1998). Crop evapotranspiration-Guidelines for computing crop water requirements, Food and Agriculture Organization of the United Nations, Paris; 300 p.

Alley, W. M., T. E. Reilly and O. L. Franke. (1999). Sustainability of Ground-Water Resources. Denver, Colorado, USA, U.S. Geological Survey.USGS Circular 1186; 86 p.

Allison, G. B. and M. W. Hughes (1977). The histry of Tritinium fallout in southern Australiaas inferred from rainfall and wine sample. Earth Planer Science Letter 36: pp 334 - 340.

Anderson, M. G. and P. D. Bates, Eds. (2001). Model Validation: Perspectives in Hydrological Science, John Wiley & Sons Ltd.500 p.

Appiah-Adjei, E. K. and D. M. Allen (2008). Quantifying the impact of predicted climate change on groundwater recharge to fractured rock aquifers. Groundwater and Climate in Africa: an international conference, 24 to 28 June, 2008. Kampala, Ministry of Water and Environment, The Republic of Uganda**:** 64 p.

Armstrong, D. and K. Narayan (1998). Using Groundwater Responses to Infer Recharge. The basics of recharge and discharge. L. Zhang and G. Walker (Editors), CSIRO Division of Land and Water 5: pp 1 - 13.

Arnell, N. (2002). Hydrology and Global Environmental Change. London, Prentice Hall.364 p.

Arnell, N. W. (1998). Climate Change and Water Resources in Britain. Climatic Change 39(1): pp 83-110.

Arnell, N. W. and N. S. Reynard (2000). Climate change and UK hydrology. The Hydrology of the UK: A Study of Change. M. C. Acreman (Editor), Routledge, London: pp 3 - 29.

Arnold, J. G., R. Srinivasan, R. S. Muttiah and J. R. Williams (1998). Large Area Hydrologic Modeling and Assessment. Part I: Model Development. Journal of American Water Resources Association 34(1): pp 73 - 89.

ARRI (1991). Environmental Modelling Alligator Rivers Region Research Institute Annual Research Summary 1988-89. S. S. f. t. A. R. Region (Editor), Australian Government Publishing Service Canberra 1991: pp 140-156.

Ashok, K., Z. Guan and T. Yamagata (2003). Influence of the Indian Ocean Dipole on the Australian winter rainfall. Geophysical Research Letters. 30 (15)**:** 1821, doi:10.1029/2003GL017926. .

Athavale, R. N. and R. Rangarajan (1988). Natural recharge measurements in the hard-rock regions of semi-arid India using Tritinium injection - a review. Estimation of Natural Groundwater Recharge, Reidel, Dordrecht.pp 175 - 195.

Bartlett, M. S. (1935). Stochastic Processes. London, Cambridge University Press.

Basalirwa, C., G. Sabiiti, R. Taylor, A. W. Majugu and C. Tindimugaya (2008). Assessing the impacts of climate change and variability on water resources in Uganda: developing an integrated approachat the sub-regional scale. Groundwater and Climate in Africa: an international conference, 24 to 28 June 2008. Kampala, Ministry of Water and Environment, The Republic of Uganda**:** 64 p.

Bates, B. C., S. P. Charles, N. R. Sumner and P. M. Fleming (1994). Climate change and its hydrological implications for South Australia. Transactions of the Royal Society of South Australia 118: pp 35 - 43.

Bayliss, P., R. J. Wasson and R. Bartolo (2007). Decadal trends in rainfall, streamflow and aquatic ecosystems in the wet-dry tropics of the Northern Territory: influence of the ENSO-IPO interaction**:** (personal communication) Kabir, M.

Becker, A. (1995). Problems and progress in macroscale hydrological modelling. Space and Time Scale Variability and Interdependencies in Hydrological Processes. R. A. Feddes (Editor), Cambridge University Press: pp 135 - 144.

Behera, S. K. and T. Yamagata (2003). Influence of the Indian Ocean Dipole on the Southern Oscillation. Journal of the Meteorological Society of Japan 81(1): pp 169 - 177.

Belan, R. A. and G. W. Matlock (1973). Groundwater recharge from a portion of the Santa Catalina Mountains. proc Meeting Hydrology and Water Resources in Arizona and the Southwest. Tucsin, Arizona, Americam Water Works Association and Arizona Academy of Science**:** pp 33-40.

Benson, C. H. (2007). Modeling Unsaturated Flow and Atmospheric Interactions. Theoreritical and Numerical Unsaturated Soil Mechanics, Springer Proceedings in Physics, 2007, Berlin Heidelberg. Volume 113, Part III.pp 187 - 201.

Berendrecht, W. L. (2004). State space modelling of groundwater fluctuations, Delft University of Technology. Ph. D.

Beven, K. (1995). Linking parameters across scales: subgrid parameterizations and scale dependent hydrological models. Hydrological Processes 9: pp 507-525.

Bidwell, V. J. (2005). Realistic forecasting of groundwater level, based on the eigenstructure of aquifer dynamics. Mathematics and Computers in Simulation 69: pp 12 - 20.

Bidwell, V. J. and M. J. Morgan (2002). The eigenvalue approach to groundwater modelling for resource evaluation at regional scale. ModelCARE 2002, 4th International Conference on Calibration and Reliability in Groundwater Modelling. Prague, Czech Republic.

Bloschl, G. and M. Sivapalan (1995). Scale issues in hydrological modelling: a review. Hydrological Processes 9: pp 251 - 290.

Boer, G. J., G. Flato and D. Ramsden (2000). A transient cliamte change simulation with greenhouse gas and aerosol forcing: projected climate for the 21st century. Climate Dynamics 16: pp 427 - 450.

BoM (2004). Annual Australian Climate Summary 2003. http://www.bom.gov.au/climate/annual_sum/2003/index.shtml, Bureau of Meteorology.

BoM (2005). El Nino, La Nina and Australia's Climate. http://www.bom.gov.au/info/leaflets/nino-nina.pdf, Commonwealth of Australia: 6 p.
BoM (2007a). ENSO Wrap-Up. http://www.bom.gov.au/climate/enso/, Commonwealth of Australia.
BoM (2007b). El Nino - Detailed Australian Analysis. http://www.bom.gov.au/climate/enso/enlist/index.shtml, Commonwealth of Australia.
Booltink, H. W. G. (2001). Soil Water Relations. Model Validation: Perspectives in Hydrological Science. M. G. Anderson and P. D. Bates (Editors), John Wiley & Sons, Ltd: pp 195-232.
Bornhoft, D. (1994). A Simulation Model for the Description of the One - Dimensional Vertical Soil Water Flow in the Unsaturated Zone. Ecological Modelling 75 - 76: pp 269 - 278.
Bouchet, R. J. (1963). E´vapotranspiration re´elle et potentielle, signification climatique. General Assembly Berkeley, International Association for Hydrological Sciences, Gentbrugge, Belgium. Publ 62.pp 134–142.
Boughton, W. C. (2002). AWBM Catchment water balance model - calibration and operation manual, Version 4.0, unpublished report.
Bouraoui, F., G. Vachaud, L. Z. X. Li, H. Le Treut and T. Chen (1999). Evaluation of the impact of climate changes on water storage and groundwater recharge at the watershed scale. Climate Dynamics 15: pp 153 - 161.
Box, G. E. P. and G. M. Jenkins (1976). Time Series Analysis: Forecasting and Control. San Fransisco, Holden-Day.575 p.
Brockwell, P. J. and R. A. Davis (2002). Introduction to Time Series and Forecasting, Springer-Verlag New York.434 p.
Brouyere, S., G. Carabini and A. Dassargues (2004). Climate Change Impacts on Groundwater Resources: modelled deficits in a chalky aquifer in Geer Basin, Belgium. Hydrogeology Journal 12(2): pp 123-134.
Brown, P. L., M. Guerin, S. I. Hankin and R. T. Lowson (1998). Uranium and other contaminant migration in groundwater at a tropical Australian Mine. Journal of Contaminant Hydrology 35: pp 295-303.
Brundtland, G. H., M. Khalid, S. Agnelli, S. A. Al-Athel, B. Chidzero and Others (1987). Our Common Future: The World Commission on Environment and Development - Commission for the Future Oxford University Press Australia.416 p.
Brutsaert, W. (1982). Evaporation into the Atmosphere, Theory, History and Applications (Environmental Fluid Mechanics). Reidel, London.316 p.
Brutsaert, W. and H. Stricker (1979). An advection-aridity approach to estimate actual regional evapotranspiration. Water Resources Research 15(2): pp 443 - 450.
Buckingham, E. (1907). Studies on the movement of soil moisture. Washington DC, USA, US Department of Agriculture Bureau of Soils. Bulletin 38.
Cai, W. (2007). What will happen to future Australian rainfall? Greenhouse2007: The latest science and technology. Sydney, NSW, Australia.
Carabin, G. and A. Dassargues (1999). Modeling groundwater with ocean and river interaction. Water Resources Research 35(8): pp 2347–2358.
Carter, T. R., R. N. Jones, X. Lu, S. Bhadwal, C. Conde, L. O. Mearns, B. C. O'Neill, M. D. A. Rounsevell and M. B. Zurek (2007). New Assessment Methods and the Characterisation of FutureConditions. Climate Change 2007: Impacts, Adaptation and Vulnerability. Contribution of Working Group II to the Fourth Assessment Report of the Intergovernmental Panel on Climate Change. M. L. Parry, O. F.

Canziani, J. P. Palutikof, P. J. Van der Linden and C. E. Hanson (Editors), Cambridge, UK., Cambridge University Press: pp 133 - 171.
Cartwright, N., P. Nielsen and P. Perrochet (2009). Behavior of a shallow water table under periodic flow conditions. Water Resources Research. 45**:** W03416, doi:10.1029/2008WR007306.
Cesanelli, A. and L. Guarracino (2009). Estimation of actual evapotranspiration by numerical modelling of water flow in the unsaturated zone: a case study in Buenos Aires, Argentina. Hydrogeology Journal 17: pp 299 – 306.
Chang, P., T. Yamagata, P. Schopf, S. K. Behera, J. Carton, W. S. Kesslet, G. Meyers, T. Qu, F. Schott, S. Shetye and S.-P. Xie (2006). Climate fluctuations of tropical coupled systems - the role of ocean dynamics. Journal of Climate - Special Section 19: pp 5122 - 5174.
Chartres, C. J., P. H. Walker, I. R. Willett, T. J. East, R. F. Cull, T. Talsma and W. J. Bond (1991). The soils and hydrology of two sites at the Ranger Uranium Mine and their suitability for land application of retention pond water. I. Site and soil properties. Supervising Scientist for the Alligator Rivers Region,Technical Memorandum 34, Australian Govenment Publishing Service, Canberra.
Chen, J. Y., C. Y. Tang, Y. J. Shen, Y. Sakura, A. Kondoh and J. Shimada (2003). Use of water balance calculation and tritium to examine the dropdown of groundwater table in the piedmont of the North China Plain (NCP). Environmental Geology 44: pp 564 - 571.
Chen, Z., S. E. Grasby and K. G. Osadetz (2002). Predicting average annual groundwater levels from climatic variables: an empirical model. Journal of Hydrology 260: pp 102 - 117.
Chen, Z., S. E. Grasby and K. G. Osadetz (2004). Relation between climate variability and groundwater levels in the upper carbonate aquifer, southern Manitoba, Canada. Journal of Hydrology 290: pp 43-62.
Cheng, X., M. Reid, M. Cotter and A. Terry (2006). Analysis of groundwater response to climatic variation in the south west Goulburn region in nothern Victoria. 10th Murray-Darling Basin Groundwater Workshop, September-2006. Canberra.
Chiew, F., Q. J. Wang, F. McConachy, R. James, W. Wright and G. deHoedt (2002). Evapotranspiration Maps for Australia. Hydrology and Water Resources Symposium, Melbourne, Australia, Institute of Engineers. CDROM (ISBN 0-8582-5778-5).pp 1 - 10.
Chiew, F. H. S., N. N. Kamaladasa, H. M. Malano and T. A. McMahon (1995a). Penman-Monteith, FAO-24 reference crop evapotranspiration and class-A pan data in Australia. Agricultural Water Management 28: pp 9-21.
Chiew, F. H. S. and C. P. Leahy (2003). Comparison of Evapotranspiration Variables in Evapotranspiration Maps for Australia with Commonly Used Evapotranspiration Variables. Australian Journal of Water Resources 7(1): pp 1-11.
Chiew, F. H. S. and T. A. McMahon (1991). The Applicability of Morton's and Penman's Evapotranspiration Estimates in Rainfall-Runoff Modelling. Water Resources Bulletin, American Water Resources Association 27(4): pp 611- 620.
Chiew, F. H. S. and T. A. McMahon (1992). An Australian Comparison of Penman's Potential Evapotranspiration Estimates and Class A Evaporation Pan Data. Australian Journal of Soil Research 30: pp 101 - 112.
Chiew, F. H. S., T. C. Piechota, J. A. Dracup and T. A. McMahon (1998). El Nino/Southern Oscillation and Australian rainfall, streamflow and drought: Links and potential for forecasting. Journal of Hydrology 204: pp 138 - 149.

Chiew, F. H. S., J. Teng, J. Vaze, D. A. Post, J. M. Perraud, D. G. C. Kirono and N. R. Viney (2009). Estimating climate change impact on runoff across southeast Australia: Methods, results and implications of the modeling method. Water Resources Research. 45**:** W10414, doi:10.1029/2008WR007338.

Chiew, F. H. S. and Q. J. Wang (1999). Hydrological analysis relevant to surface water storage at Jabiluka, Commonwealth Department of the Environment and Heritage, Canberra.Supervising Scientist Report 142; 35 p.

Chiew, F. H. S., P. H. Whetton, T. A. McMahon and A. B. Pittock (1995b). Simulation of the impacts of climate change on runoff and soil moisture in Australian catchments. Journal of Hydrology 167: pp 121 - 147.

Chow, V. T., D. R. Maidment and L. W. Mays (1988). Applied Hydrology, McGraw-Hill International Editions.572 p.

Christian, C. S. and J. M. Aldrick (1975). Alligator Rivers Study - A Review Report of the Alligator River Region Environmental Fact Finding Study, Commonwealth Department of the Northern Territory and the Australian Mining Industry Council; 187 p.

Cohen, D., M. Person, R. Daannen, S. Locke, D. Dahlstrom, V. Zabielski, T. C. Winter, D. O. Rosenberry, H. Wright, E. Ito, J. L. Nieber and W. J. J. Gutowski (2006). Groundwater-supported evapotranspiration within glaciated watersheds under conditions of climate change. Journal of Hydrology 320(3-4): pp 484 - 500.

Collins, M. (2000a). The El-Nino Southern Oscillation in the second Hadley Centre coupled model and its response to greenhouse warming. Journal of Climate 13: pp 1299 - 1312.

Collins, M. (2000b). Understanding uncertainities in the response of ENSO to greenhouse warming. Geophysical Research Letters 27: pp 3509 - 3512.

Collison, A., S. Wade, J. Griffiths and M. Dehn (2000). Modelling the impact of predicted climate change on landslide frequency and magnitude in SE England. Engineering Geology 55: pp 205 - 218.

Constantz, J., C. L. Thomas and G. Zellweger (1994). Influence of diurnal variations in stream temperature on streamflow loss and groundwater recharge. Water Resources Research 30: pp 3253 - 3264.

Cook, P. G., T. J. Hatton, D. Pidsley, A. L. Herczeg, A. Held, A. O'Grady and D. Eamus (1998). Water balance of a tropical woodland ecosystem, Northern Australia: a combination of micro-meteorological, soil physical and groundwater chemical approaches. Journal of Hydrology 210: pp 161 - 177.

Cook, P. G., A. L. Herczeg and K. L. McEwan (2001). Groundwater recharge and stream baseflow, Atherton Tablelands, Queensland. CSIRO Land and Water Technical Report 08/01, April 2001**:** 84 p.

Cooper, D. M. and E. F. Wood (1982). Parameter estimation of multiple input-output time series models: Application to rainfall-runoff processes. Water Resources Research 18: pp 1352 - 1364.

Cooper, J. D., C. M. K. Gardner and N. MacKenzie (1990). Soil controls on recharge to aquifers. Journal of Soil Science 41: pp 613 - 630.

CRCCH. (2005). General approaches to modelling and practical issues of model choice. Series on Model Choice, from http://www.toolkit.net.au/modelchoice.

Cresswell, R., J. Wischusen, G. Jacobson and K. Fifield (1997). Assessment of recharge to groundwater systems in the arid southwestern part of Northern Territory, Australia, using chlorine-36. Hydrogeology Journal 7: pp 393 - 404.

Croley II, T. E. and C. L. Luukkonen (2003). Potential Effects of Climate Change on Groundwater in Lansing , Michigan. Journal of the American Water Resources Association 39(1): pp 149 - 163.
CSIRO (2006). Ozclim. http://www.cmar.csiro.au/ozclim/index.html, CSIRO Australia 1997-2005, Updated 10/01/06
CSIRO. (2007). Technical Report 2007: Climate Change in Australia. Accessed on 12/07/2008, from http://www.climatechangeinaustralia.gov.au/documents/resources/TR_Web_FrontmatterExecSumm.pdf.
CSIRO (2010). OZCLIM - Climate Change Scenario Generator. http://www.csiro.au/ozclim/home.do, Accessed on 19/09/2010, CSIRO Australia.
Cubasch, U., G. A. Meehl, G. J. Boer, R. J. Stouffer, M. Dix, A. Noda, C. A. Senior, S. Raper and K. S. Yap (2001). Projections of Future Climate Change. Climate Change 2001: The Scientific Basis. J. T. Houghton, Y. Ding, D. J. Griggs, M. Noguer, P. J. Linden, X. Dai, K. Maskell and C. A. Johnson (Editors), Cambridge University Press, UK: pp 525 - 582.
Cushman, J. H. (1984). Unifying the concepts of scale, instrumentation, and stochastics in the development of multiphase transport theory. Water Resources Research 20: pp 1668 - 1676.
Cushman, J. H. (1987). More on stochastic models. Water Resources Research 23: pp 750 - 752.
Dahe, Q., L. Shiyin and L. Peiji (2006). Snow cover distribution, variability and response to climate change in Western China. Journal of Climate 19: pp 1820 - 1833.
Darcy, H. (1856). Les fontaines publiques de le ville de Dijon. Dalmont, Paris.647 p.
Dawes, W. R. and D. L. Short (1993). The efficient numerical solution of differential equations for coupled water and solute dynamics: the WAVES model. Technical Memorandum 93- 18, Division of Water Resources, CSIRO.
Deen, A. R. (1983a). Water Divisions Rainfall Network in the Alligator Rivers Region. Environmental Protection in the Alligator River Region, Jabiru, Northern Territory, Supervising Scientist for the Alligator River Region. 1.pp (13-1) - (13-7).
Deen, A. R. (1983b). Surface Hydrology. Environmental Protection in the Alligator River Region, Jabiru, NorthernTerritory, Supervising Scientist for the Alligator River Region. 1.pp (14-) - (14-11).
Dessai, S., W. N. Adger, M. Hulme, J. R. Turnpenny, J. Kohler and R. Warren (2004). Defining and experiencing dangerous climate change. Climatic Change 64: pp 11 - 25.
Dessai, S., X. Lu and J. S. Risbey (2005). On the role of climate scenarios for adaptation planning. Global Environmental Change 15(2): pp 87 - 97.
Devore, J. L. (1999). Probability and Statistics for Engineering and the Sciences. California, Brooks/Cole Publishing Company.750 p.
Dibike, Y. B. and P. Coulibaly (2005). Hydrologic impacts of climate change in the Saguenay watershed: comparison of downscaling methods and hydrologic models. Journal of Hydrology 307: pp 145 - 163.
Doble, R. C., C. T. Simmons and G. R. Walker (2009). Using MODFLOW 2000 to Model ET and Recharge for Shallow Ground Water Problems. Ground Water 47(1): pp 129 - 135.
Dooge, J. C. I. (1982). Parameterization of hydrologic processes. Land Surface Processes in Atmospheric General Circulation Models. P. S. Eagleson (Editor), Cambridge University Press, London: pp 243-288.

Dooge, J. C. I. (1986). Looking for hydrologic laws. Water Resources Research 22: pp 46S-58S.
Dooge, J. C. I. (1995). Scale problems in surface fluxes. Space and Time Scale Variability and Interdependencies in Hydrological Processes. R. A. Feddes (Editor), Cambridge University Press: pp 21 - 32.
Doorenbos, J. and W. O. Pruitt (1977). Guidelines for Predicting Crop Water Requirements, Food and Agriculture Organization of the United Nations; 156 p.
Doyle, P. (1990). Modelling catchment evaporation: an objective comparison of the Penman and Morton's approaches. Journal of Hydrology 121: pp 257 - 276.
Duah, A. and Y. Xu (2008). Climate variability and its impact on the Table Mountain aquifers in South Africa. Groundwater and Climate in Africa: an international conference, 24 to 28 June, 2008. Kampala. Uganda, Ministry of Water and Environment, The Republic of Uganda. Session 4**:** 49.
Duan, Q. (1994). The SCE-UA Method. Journal of Hydrology 158: pp 265 - 284.
Earman, S. (2007). Climate Influences on Groundwater Recharge: Implications for Western Groundwater and Surface Water Resources in the Face of Climate Change. American Geophysical Union, Fall Meeting 2007**:** Abstract H14E-04.
Eckhardt, K. and U. Ulbrich (2003). Potential impacts of climate change on groundwater recharge and streamflow in a central European low mountain range. Journal of Hydrology 284: pp 244 - 252.
Edlund, P. (1984). Identification of Multi-input Box-Jenkins Transfer Function Model. Journal of Forecasting 3: pp 297 - 308.
Edlund, P. (1988). On identification of transfer function models by biased regression methods. Journal of Statistical Computation and Simulation 31: pp 131 - 148.
Edmunds, W. M. and S. W. Tyler (2002). Unsaturated zones as archives of past climates: toward a new proxy for continental regions. Hydrogeology Journal 10: pp 216 - 228.
Egboka, B. C. E., J. A. Cherry, R. N. Farvolden and F. E. O (1983). Migration of contaminants in groundwater at a landfill : A case study: 3. Tritinium as an indicator of dispersion and recharge. Journal of Hydrology 63: pp 51 - 80.
El-Shaarawi, A. H. and S. R. Esterby, Eds. (1981). Time Series Methods in Hydrosciences. Developments in Water Science, Elsevier Scientific Publishing Company.614 p.
Engle, R. F. and C. W. J. Granger (1987). Co-integration and error correction: representation, estimation, and testing. Econometrica 55(2): pp 251 - 276.
ERA. (2005, 15/04/2005). Energy Resources of Australia, Ltd. Retrieved 26/07/05, 2005, from http://www.energyres.com.au/ranger/ore.shtml.
ERA (var.-a). Annual Report. Darwin, NT, Australia, Energy Resources of Australia (ERA). Years 1981 to 2008, (Photo is 2008 years).
ERA (var.-b). Ranger Uranium Mine - Annual Environmental Management Report. Jabiru NT, Australia, Energy Resources of Australia (ERA). Years 1995 to 2008, (Photo is 2008 years).
Erskine, W. D. and R. F. Warner (1988). Geomorphic effects of alternating flood and drought dominated regimes on a NSW coastal river. Fluvial Geomorphology of Australia. R. F. Warner (Editor), San Diego, California, Academic: pp 223 - 242.
Eupene, G. S., P. H. Fee and R. G. Colville (1975). Ranger One Uranium Deposits. Economic Geology of Australia and Papua New Guinea. C. L. Knight (Editor), Australasian Institute of Mining and Mettalurgy. Monograph No 5: pp 308 - 317.
Faye, S., M. Diaw, S. Ndoye, R. Malou and A. Faye (2008). Groundwater recharge and salinization in coastal areas of Senegal: impacts of climate change Groundwater and Climate in Africa: an international conference, 24 to 28 June, 2008. Kampala.

Uganda, Ministry of Water and Environment, The Republic of Uganda. Session 4**:** 49.
Fayer, M. J. (2000). UNSAT-H Version 3.0: Unsaturated soil -water and heat flow model, theory, user manual, and examples. Hanford, Washington Battle Pacific Northwest Laboratory; 184 p.
Feddes, R. A., Ed. (1995a). Space and Time Scale Variability and Interdependencies in Hydrological Processes. International Hydrology Series, Cambridge University Press.193 p.
Feddes, R. A. (1995b). Remote sensing - inverse modelling approach to determine large scale effective soil hydraulic properties in soil-vegetation-atmosphere systems. Space and Time Scale Variability and Interdependencies in Hydrological Processes. R. A. Feddes (Editor), Cambridge University Press: pp 33 - 42.
Feddes, R. A., P. J. Kowalik and H. Zaradny (1978). Simulation of Field Water Use and Crop Yield, Wiley, New York.188 p.
Fendekova, M. (1999). Quantitative aspects of groundwater regime. Acta Geologica Universitatis comenianae 54: pp 27 - 52.
Fendekova, M. and M. Fendek (2006). Factors affecting the groundwater regime in the High Tarta Mountains. Fifth FRIEND World Conference - *Climate Variability and Change-Hydrological Impacts*, Havana, Cuba, November 2006, IAHS Publ. 308.pp 617 - 622.
Ferdowsian, R., D. J. Pannell, C. McCarron, A. Ryder and L. Crossing (2001). Explaining groundwater hydrographs: separating atypical rainfall events from time trends. Australian Journal of Soil Resources 39: pp 861 - 875.
Ferguson, B. and G. M. Mudd (2010). Water Quality, Water Management and the Ranger Uranium Project: Guidelines, Trends and Issues. Water, Air and Soil Pollution**:** doi:10.1007/s11270-010-0592-9.
Flint, A. L., L. E. Flint, E. M. Kwicklis, J. T. Fabryka-Martin and G. S. Bodvarsson (2002). Estimating Recharge at Yacca Mountain, Nevada, USA: comparison of methods. Hydrogeology Journal 10(1): pp 180 - 204.
Flury, M., H. Fluhler, W. A. Jury and J. Leuenberger (1994). Susceptibility of soils to preferential flow of water: a field study. Water Resources Research 30: pp 1945 - 1954.
Folland, C. K., J. A. Renwick, M. J. Salinger and A. B. Mullan (2002). Relative influences of the Interdecadal Pacific Oscillation and ENSO on the South Pacific Convergence Zone. Geophysical Research Letters 29(13): pp (21-1) - (21-4)
Forrer, T., R. Kasteel, M. Flury and H. Fluhler (1999). Longitunidal and dispersion in unsaturated field soil. Water Resources Research 35(10): pp 3049 - 3060.
Fowler, H. J. and C. G. Kilsby (2007). Using regional climate model data to simulate historical and future river flows in northwest England. Climatic Change 80(3 - 4): pp 337 - 367.
Fowler, H. J., C. G. Kilsby and P. E. O'Connell (2003). Modelling the impacts of climate change and variability on the reliability, resilience, and vulnerability of a water resource system. Water Resources Research. 39 (8)**:** doi:10.1029/2002WR001778, 2003.
Fox, R. W., G. G. Kellehar and C. B. Kerr (1976). Ranger uranium environmental inquiry; 213 p.
Fox, R. W., G. G. Kellehar and C. B. Kerr (1977). Ranger uranium environmental inquiry; 425 p.
Franks, S. W. (2002a). Identification of a change in climate state using regional flood data. Hydrology and Earth System Sciences 6(1): pp 11-16.

Franks, S. W. (2002b). Assessing hydrological change: deterministic general circulation models or spurious solar correlations? Hydrological Processes 16(2): pp 559 - 564.
Franssen, H. J. H. and W. Kinzelbach (2009). Ensemble Kalman filtering versus sequential self-calibration for inverse modelling of dynamic groundwater flow systems. Journal of Hydrlogy 365: pp 261 - 274.
Fredlund, D. G. and H. Rahardjo (1993). Soil mechanics for unsaturated soils, John Willey & Sons, Inc.544 p.
Fredlund, D. G. and A. Xing (1994). Equations for the Soil - Water Characteristics Curve. Canadian Geotechnical Journal 31(3): pp 521 - 532.
Gaspar, E. (1984). Time Series Methods in Hydrosciences. Journal of Hydrology 73: pp 399 - 400.
Gates, J. B., E. W. M., J. Ma, Scanlon and B. R. (2008). Estimating groundwater recharge in a cold desert environment in nothern China using chloride. Hydrogeology Journal 16(5): pp 893 - 910.
Gavigan, J., M. Cuthbert and R. Mackay (2008). Climate change impacts on the groundwater recharge in northeaster Uganda and potential role of groundwater development in livelihood adaptation and peace building. Groundwater and Climate in Africa: an international conference, 24 to 28 June 2008. Kampala. Uganda, Ministry of Water and Environment, The Republic of Uganda. Session 3**:** 43.
Gehrels, J. C., F. C. van Geer and J. J. de Vries (1994). Decomposition of groundwater level fluctuations using transfer modelling in an area with shallow to deep unsaturated zones. Journal of Hydrology 157(1 - 4): pp 105 - 138.
GeoAnalysis (2000). SoilCover Version 4.01 Software User's Manual. Unsaturated Soils Group. Department of Civil Engineering, University of Saskatchewan, Saskatoon, Canada, GeoAnalysis 2000 Ltd.
Gerhart, J. M. (1986). Ground-water Recharge and its effect on nitrate concentrations bebeath a manured field site in Pennsylvania. Ground Water 24(4): pp 483 - 389.
Ghil, M., M. R. Allen, M. D. Dettinger, K. Ide, D. Kondrashov, M. E. Mann, A. W. Robertson, A. Saunders, Y. Tian, F. Varadi and P. Yiou (2002). Advanced spectral methods for climatic time series. Reviews of Geophysics 40(1): pp (3-1) - (3-41).
Giorgi, F. and L. O. Mearns (2002). Calculation of Average, Uncertainty Range, and Reliability of Regional Climate Changes from AOGCM Simulations via the "Reliability Ensemble Averaging" (REA) Method Journal of Climate 15: pp 1141 - 1158.
Glassley, W. E. (2003). The impact of climate change on vadose zone pore waters and its implication for long-term monitoring. Computers and Geosciences 29(3): pp 399 - 411.
Goderniaux, P., S. Brouyere, H. J. Fowler, S. Blenkinsop, R. Therrien, P. Orban and A. Dassargues (2009). Large scale surface-subsurface hydrological model to assess climate change impacts on groundwater reserves. Journal of Hydrology 373: pp 122 - 138.
Goodess, C. M., J. P. Palutikof and T. D. Davies (1990). A first approach to assessing future climate states in the UK over very long timescales: Input to studies of the integretity of radioactive waste repositories. Climatic Change 16: pp 115 - 140.
Goor, Q., E. Persoons and M. Vanclooster (2006). A linear transfer function model to predict groundwater recharge in the valley of the Draa (South-Morocco). Geophysical Research Abstracts, European Geosciences Union 2006.
Gordon, N., T. McMahon, B. Finlayson, C. Gippel and R. J. Nathan. (2006). AQUAPAK. Sinclair Knight Merz Pty Ltd. Retrieved 20/08/2007, from

http://www.skmconsulting.com/Markets/environmental/resource_management/AQUAPAK_Download.htm.
Granger, R. J. and D. M. Gray (1990). Examination of Morton's CRAE model for estimating daily evaporation from field-sized areas. Journal of Hydrology 120: pp 309 - 325.
Grayson, R. and G. Bloschl (2000a). Summary of pattern comparison and concluding remarks. Spatial Patterns in Catchment Hydrology: Observations and Modelling. R. Grayson and G. Bloschl (Editors), Cambridge, UK, Cambridge University Press: pp 355 - 367.
Grayson, R. and G. Bloschl, Eds. (2000b). Spatial Patterns in Catchment Hydrology: Observations and Modelling. Cambridge, UK, Cambridge University Press.432 p.
Grayson, R. B., R. M. Argent, R. J. Nathan, T. A. McMahon and R. G. Mein (1996). Hydrological Recipes: Estimation Techniques in Australian Hydrology, Cooperative Research Centre for Catchment Hydrology.134 p.
Green, T. R., B. C. Bates, S. P. Charles and E. Fathelrahman (2008). Global analogues of climate change effects on agriculture and groundwater between hydrologically similar regions of the world. Groundwater and Climate in Africa: an international conference, 24 to 28 June, 2008. Kampala, Uganda, Ministry of Water and Environment, The Republic of Uganda. Session 4**:** 47.
Green, T. R., B. C. Bates, S. P. Charles and P. M. Fleming (2007a). Physically Based Simulation of Potential Effects of Carbon Dioxide-Altered Climates on Groundwater Recharge. Vadose Zone Journal 6(3): pp 597 - 609.
Green, T. R., M. Taniguchi and H. Kooi (2007b). Potential Impacts of Climate Change and Human Activity on Subsurface Water Resources. Vadose Zone Journal 6(3): pp 531 - 532.
Grigor'ev, A. S. and Y. A. Trapenznikov (2002). Level of Lake Ladoga at Possible Climate Changes. Water Resources Research 29(2): pp 155 - 159.
Groves, D. G., D. Yates and C. Tebaldi (2008). Developing and applying uncertain global climate change projections for regional water management planning. Water Resources Research. 44**:** W12413, doi:10.1029/2008WR006964.
Gupta, V. K., I. Rodriguez-Iturbe and E. F. Wood, Eds. (1986). Scale Problems in Hydrology: Runoff Generation and Basin Response (Water Science and Technology Library), Springer.260 p.
Gurdak, J. J. (2007). Recharge response to natural climate variability on interannual to multidecadal timescales. American Geophysical Union, Fall Meeting 2007**:** abstract # H14E-08.
Gurdak, J. J., R. T. Hanson, P. B. McMahon, B. W. Bruce, J. E. McCray, G. D. Thyne and R. C. Reedy (2007). Climate Variabilty Controls on Unsaturated Water and Chemical Movement, High PLains Aquifer, USA. Vadose Zone Journal 6(Special Section: Groundwater Resources Assessment under the Pressures of Humanity and Climate Change): pp 533 - 547.
Halford, K. J. and G. C. Mayer (2000). Problems associated with estimating ground water discharge and recharge from stream-dis-charge records. Ground Water 38: pp 331 - 342.
Hall, D. W. and D. W. Risser (1993). Effects of agricultural Nutrient Management on nitrogen fate and transport in Lancaster county. Water Resources Bulletin 29(1): pp 55 - 76.
Hanson, R. T. and M. D. Dettinger (2005). Ground water/surface water responses to global climate simulations, Santa Clara-Calleguas Basin, Ventura, California. Journal of the American Water Resources Association 41(3): pp 517 - 536.

Hart, B. T., E. M. Ottaway and B. N. Noller (1987a). Magela Creek System, Northern Australia. I. 1982-83 Wet-season Water Quality. Australian Journal of Marine Freshwater Research 38(2): pp 261 - 288.
Hart, B. T., E. M. Ottaway and B. N. Noller (1987b). Magela Creek System, Northern Australia. II. Material Budget for the Floodplain. Australian Journal of Marine Freshwater Research 38(6): pp 861 - 876.
Hatton, T. (1998). Catchment Scale Recharge Modelling. The Basics of Recharge and Discharge. L. Zhang. Melbourne, CSIRO Publishing. 4.
Hatton, T. J., W. R. Dawes and R. A. Vertessy (1995). The importance of landscape positionin scaling SVAT models to catchment scale hydroecological prediction. Space and Time Scale Variability and Interdependencies in Hydrological Processes. R. A. Feddes (Editor), Cambridge University Press: pp 43 - 54.
Haugh, L. D. and G. E. P. Box (1977). Identification of dynamic regression (distributed lag) models connecting two time series. Journal of American Statistical Association 72(357): pp 121 - 130.
Healy, R. W. and P. G. Cook (2002). Using ground-water levels to estimate recharge. Hydrogeology Journal 10(1): pp 91 - 109.
Healy, R. W. and P. C. Mills (1991). Variability of an unsaturated sand unit underlying a radioactive-waste trench. Soil Science Society of America Journal 55(4): pp 899 - 907.
Healy, R. W. and A. Ronan (1996). Documentation of computer program VS2DH for simulation of energy transport in variably saturated porous media - modification of the U.S. Geological Survey's computer program VS2DT. http://pubs.er.usgs.gov/pubs/wri/wri964230, U.S. Geological Survey Water-Resources Investigations Report 96-4230**:** 36.
Henderson-Sellers, A., K. McGuffie and T. B. Durbidge (1995). Modelling the hydrological response to large scale land use change. Space and Time Scale Variability and Interdependencies in Hydrological Processes. R. A. Feddes (Editor), Cambridge University Press: pp 63 - 88.
Hennessy, K. and B. Fitzharris (2007). Australian climate change impacts, adaptation and vulnerability. Greenhouse2007:The Latest Science and Technology Sydney, NSW, Australia.
Hennessy, K., B. Fitzharris, B. C. Bates, N. Harvey, S. M. Howden, L. Hughes, J. Salinger and R. Warrick (2007). IPCC 2007: Australia and New Zealand. Climate Change 2007: Impacts, Adaptation and Vulnerability. Contribution of Working Group II to the Fourth Assessment Report of the Itergovernmental Panel on Climate Change. M. L. Parry, O. F. Canziani, J. P. Palutikof, P. J. van der Linden and C. E. Hanson (Editors), Cambridge, UK, Cambridge University Press: pp 507 - 540.
Hennessy, K., C. Page, K. Walsh, B. Pittock, J. Bathols and R. Suppiah (2004). Climate Change in the Northern Territory. CSIRO Consultancy report for the Northern Territory Department of Infrastructure , Planning and Environment, CSIRO; 64 p.
Herrera-Pantoja, M. and K. M. Hiscock (2008). The effects of climate change on potential groundwater recharge in Great Britain. Hydrological processes 22(1): pp 73 - 86.
Herrmann, A., M. Schoniger and S. Schumann (2006). A new, physically-based, numerical runoff generation model system for study of surface-shallow groundwater relationships and system reactions to environmental changes. Fifth FRIEND World Conference: Climate Variability and Change - Hydrological Impacts, Havana, Cuba, November 2006, IAHS Publ. 308.pp 623 - 628.
Herrmann, F., C. Jahnke, F. Jenn, R. Kunkel, H. Voigt, J. Voigt and F. Wendland (2009). Groundwater recharge rates for regional groundwater modelling: a case study using

GROWA in the Lower Rhine lignite mining area, Germany. Hydrogeology Journal 17(8): pp 2049 - 2060.
Hildebrand, D. K., J. D. Laing and H. Rosenthal (1977). Prediction Analysis of Cross Classifications. New York, John Wiley & Sons.311 p.
Hinzman, L. D., N. D. Bettez, W. R. Bolton, F. S. Chapin, M. B. Dyurgerov, C. L. Fastie, B. Griffith, R. D. Hollister, A. Hope, H. P. Huntington, A. M. Jensen, G. J. Jia, T. Jorgenson, D. L. Kane, D. R. Klein, G. Kofinas, A. H. Lynch, A. H. Lloyd, A. D. McGuire, F. E. Nelson, W. C. Oechell, T. E. Osterkamp, C. H. Racine, V. E. Romanovsky, R. S. Stone, D. A. Stow, M. Sturm, C. E. Tweedie, G. L. Vourlitis, M. D. Walker, P. J. Webber, J. M. Welker, K. S. Winker and K. Yoshikawa (2005). Evidence and implications of recent climate change in northern Alaska and other Arctic regions. Climatic Change 72: pp 251 - 298.
Hipel, K. W. and A. I. McLeod (1994). Time Series Modelling of Water Resources and Environmental Systems. Amsterdam, Elsevier.1013 p.
Hipel, K. W., A. I. McLeod and W. K. Li (1985). Causal and dynamic relationships between natural phenomena. Time Series Analysis: Theory and Practice. O. D. Anderson, J. K. Ord and E. A. Robinson (Editors), North-Holland, Amsterdam: pp 13 - 34.
Hipel, K. W., A. I. McLeod and E. A. McBean (1977). Stochastic modelling of the effects of reservoir operation. Journal of Hydrology 32(1 - 2): pp 97 - 113.
Hipel, K. W., A. I. McLeod and D. J. Noakes (1982). Fitting dynamic models to hydrological time series. Time Series Methods in Hydrosciences. A. H. El-Shaarawi and S. R. Esterby (Editors), Amsterdam, Elsevier: pp 110 - 129.
Hirsch, R. M. (1983). The use of transfer function models in estimating river quality variables. Transactions of the American Geophysical Union 64: pp 708 - 718.
Hiscock, K. M., R. Sparkes, A. Hodgson, J. L. Martin and M. Taniguchi (2008). Evaluation of future climate impacts in Europe on potential groundwater recharge. Geophysical Research Abstracts. 10**:** EGU2008-A-10211.
Hobbins, M. T., J. A. Ramirej, T. C. Brown and L. H. J. M. Claessens (2001). The complementary relationship in estimation of regional evapotranspiration: The Complementary Relationship Areal Evapotranspiration and Advection-Aridity models. Water Resources Research 37(5): pp 1367 - 1387.
Holman, I. P. (2006). Climate change impacts on groundwater recharge - uncertainty, shortcomings, and the way forward? Hydrogeology Journal 14(5): pp 637 - 647.
Holman, I. P., D. Tascone and T. M. Hess (2009). A comparison of stochastic and deterministic downscaling methods for modelling potential groundwater recharge under climate change in East Anglia, UK: implications for groundwater resource management. Hydrogeology Journal 17(7): pp 1629 - 1941.
Houghton, J. T., Y. Ding, D. J. Griggs, M. Noguer, P. J. Linden, X. Dai, K. Maskell and C. A. Johnson, Eds. (2001). Climate Change 2001: The Scientific Basis. Contribution of Working Group I to the Third Assessment Report of the Intergovernmental Panel on Climate Change. Cambridge, Cambridge University Press.873 p.
Hsieh, P. A., W. Wingle and R. W. Healy (2000). VS2DI - a graphical software package for simulating fluid flow and solute or energy transport in variably saturated porous media, US Geological Survey Water-Resources Investigation Report 99 - 4130; 16 p.
Hull, J. (2005). Properties of Lognormal Distribution. Options, Futures, and Other Derivatives, Prentice Hall**:** 720 p.

Hunt, R. J., D. E. Prudic, J. F. Walker and M. P. Anderson (2008). Importance of Unsaturated Zone Flow for Simulating Recharge in a Humid Climate. Ground Water 46(4): pp 551 - 560.
Hutley, L. B., A. P. O'Grady and D. Eamus (2000). Evapotranspiration from Eucalypt open - forest savanna of Northern Australia. Functional Ecology 14(2): pp 183 - 194.
Hutton, J. T. (1976). Chloride in rainfall in relation to distance from coast. Search 7: pp 207 - 208.
IAEA (1981). Current Practices and Options for Confinement of Uranium Mill Tailings. Vienna, Austria, September 1981; 110 p.
IAEA (1992). Current Practices for the Management and Confinement of Uranium Mill Tailings. Vienna, Austria, June 1992; 149 p.
Ijiri, Y., H. Saegusa, A. Sawada, M. Ono, K. Wantanabe, K. Karasaki, C. Doughty, M. Shimo and K. Fumimura (2009). Evaluation of uncertainties originating from the different modeling approaches applied to analyze regional groundwater flow in the Tono area of Japan. Journal of Contaminant Hydrology 103: pp 168 - 181.
IPCC (2001a). IPCC Special Report on Emissions Scenarios. IPCC Special Report on Climate Change. N. Nakicenovic and R. Swart. http://www.grida.no/publications/other/ipcc_sr/, GRID-Arendal, Accessed on 26/05/2010.
IPCC (2001b). Climate Change 2001: Impacts, Adaptation and Vulnerability. Summary for Policymakers, Cambridge University Press: Cambridge.
IPCC (2007). Summary for Policy Makers. In: Climate Change 2007: The Physical Science Basis. Contribution of Working Group I to the Fourth Assessment Report of the Intergovernmental Panel on Climate Change. S. Solomon, D. Qin, M. Manning,Z. Chen, M. Marquis, K.B. Averyt, M.Tignor and H.L. Miller (Editor), Cambridge University Press, Cambridge, United Kingdom and New York, NY, USA: pp 1 - 18.
Issar, A. S. (2008). A tale of two cities in ancient Canaan: how the groundwater storage capacity of Arad and Jericho decided their history. Climate Change and Groundwater. W. Dragoni and B. S. Sukhija (Editors), The Geological Society of London. Geological Society Special Publication No. 288: pp 137 - 143.
Jakeman, A. J., C. R. Dietrich and G. A. Thomas (1989). Solute transport in a stream-aquifer system. 2. Application of model identification to the River Murray. Water Resources Research 25(10): pp 2177 - 2185.
Jakeman, A. J., I. J. Littlewood and P. G. Whitehead (1990). Computation of instantaneous unit hydrograph and identifiable component flows with application to two small upland catchments. Journal of Hydrology 117(1 - 4): pp 275 - 300.
Janssen, P. H. M., P. S. C. Heuberger and R. Sanders (1993). UNSCAM 1.1: A Software Package for Sensitivity and Uncertainty Analysis, Manual. RIVM Report No. 959101004. RIVM, Bilthoven, The Netherlands.
Jeffrey, S. J., J. O. Carter, K. B. Moodie and A. R. Beswick (2001). Using spatial interpolation to construct a comprehensive archive of Australian climate data. Environmental Modelling & Software 16: pp 309 - 330.
Jiang, X., G. Niu and Z. Yang (2009). Impacts of vegetation and groundwater dynamics on warm season precipitation over the Central United States. Journal of Geophyisical Research. 114 (D06109)**:** doi:10.1029/2008JD010756.
Jimenez-Martinez, J., T. H. Skaggs, M. T. van Genucgten and L. Candela (2009). A root zone modelling approach to estimating groundwater recharge from irrigated areas. Journal of Hydrology 367(1- 2): pp 138 - 149.

Johnston, A. and R. S. Needham (1999). Protection of the environment near the Ranger uranium mine. Canberra, Commonwealth Department the Environment and Heritage.SSR 139; 39 p.
Jong, C., D. Lawler and R. Essery (2009). Mountain Hydroclimatology and Snow Seasonality- Perspectives on climate impacts, snow seasonality and hydrological change in mountain environments. Hydrological processes 23: pp 955 - 961.
Jyrkama, M. I. and J. F. Sykes (2004). Response of Groundwater Recharge to Potential Future Climate Change in the Grand River Watershed. American Geophysical Union, Fall Meeting 2004**:** abstract # H23E-03.
Jyrkama, M. I. and J. F. Sykes (2007). The impact of climate change on spatially varying groundwater recharge in the grand river watershed (Ontario). Journal of Hydrology 228(3 - 4): pp 237 - 250.
Kabir, M., K. Hamza, G. M. Mudd and A. R. Ladson (2008a). Groundwater-Climate Relationships, Ranger Uranium Mine, Australia: 1. Time Series Statistical Analyses. Uranium, Mining and Hydrogeology - 5th International Conference, September 2008, Freiberg, Germany.pp 365 - 374.
Kabir, M., G. M. Mudd and A. R. Ladson (2007). Understanding the inconsistencies between two different sources of Morton's AAET data for Ranger Uranium Mine site, Northern Territory, Australia Victorian Universities Earth and Environmental Science Conference. La Trobe University, Bundoora Campus Geological Society of Australia. Abstract No 86.
Kabir, M., G. M. Mudd and A. R. Ladson (2008b). Groundwater-Climate Relationships, Ranger Uranium Mine, Australia: 2. Validation of Unsaturated Flow Modelling. Uranium, Mining and Hydrogeology - 5th International Conference, September 2008, Freiberg, Germany.pp 375 - 382.
Kabir, M., G. M. Mudd and A. R. Ladson (2008c). Groundwater-Climate Relationships, Ranger Uranium Mine, Australia: 3. Predicting Climate Change Impacts. Uranium, Mining and Hydrogeology - 5th International Conference, September 2008, Freiberg, Germany.pp 383 - 392.
Kashyap, R. L. and A. R. Rao (1976). Dynamic Stochastic Models from Empirical Data. New York, Academic Press, Inc.334 p.
Kates, R. W., W. C. Clark, R. Corell, J. M. Hall, C. C. Jaeger, I. Lowe, J. J. McCarthy, H. J. Schellnhuber, B. Bolin, N. M. Dickenson, S. Faucheux, G. C. Gallopin, A. Grubler, B. Huntly, J. Jager, N. S. Jodha, R. E. Kasperson, A. Mabogunje, P. Matson, H. Mooney, B. Moore III, T. O'Riordan and U. Svedlin (2000). Environment and Development: Sustainability Science. Science 292(5517): pp 641 - 642.
Kendall, C. J. (1990). Ranger Uranium deposits. Geology of Mineral Deposits of Australia and Papua New Guinea F. E. Hughes (Editor), Australasian Institute of Mining and Metallurgy, Monograph No. 14. Vol. 1: pp 799 - 805.
Kerr, A. W., H. K. Hall and S. A. Kozub (2002). Doing Statisitics with SPSS, SAGE Publications.238 p.
Kilsby, C. G., P. D. Jones, A. Burton, A. C. Ford, H. J. Fowler, C. Harpham, P. James, A. Smith and R. L. Wilby (2007). A daily weather generator for use in climate change studies. Environmental Modelling & Software 22(12): pp 1705 - 1719.
Kim, C. P., J. N. M. Stricker and P. Torfs (1996). An anlytical framework for the water budget of the unsaturated zone. Water Resources Research 32(12): pp 3475 - 3484.
Kirk, S. and A. W. Herbert (2002). Assessing the impact of groundwater abstractions on river flows. Sustainable Groundwater Development. Geological Society, London, Special Publications K. M. Hiscock, M. O. Rivett and R. M. Davison (Editors), The Geological Society of Lopndon 2002. 193: pp 211 - 233.

Kirshen, P. H. (2002). Potential impacts of global warming on groundwater in Eastern Massachusetts. Journal of Water Resources Planning and Management 128(3): pp 216 - 226.
Kite, G. W. (1995). The SLURP model. Computer models of watershed hydrology. V. P. Singh (Editor), Highlands Ranch, Colorado: pp 521 - 562.
Klaasen, B. and D. H. Pilgrim (1975). Hydrograph Recession Constants for New South Wales Streams. Civil Engineering Transactions CE17: pp 43 - 49.
Kleeberg, H.-B., Ed. (1992). Regionalisierung in der Hydrologic. DFG-Mitt, XI, VCH Verl. ges. Weinheim.444 p.
Klemes, V. (1978). Physically based stochastic hydrologic analysis. Advances in Hydroscience, New York, Academic Press. 11.pp 285 - 356.
Knotters, M. and F. P. Bierkens (2000). Physical basis of time series models for water table depths. Water Resources Research 36(1): pp 181 - 188.
Knutson, T. R. and S. Manabe (1998). Model assessment of decadal variability and trends in the tropical Pacific ocean. Journal of Climate 11(9): pp 2273 - 2296.
Knutson, T. R., S. Manabe and D. Gu (1997). Simulated ENSO in a global coupled ocean-atmosphere model: multidecadal amplitude modulation and CO_2-sensitivity. Journal of Climate 10(1): pp 138 - 161.
Kocher, A. and B. Reichert (2008). Progressive approach for groundwater model development as a water management tool under climate change in Benin. Groundwater and Climate in Africa: an international conference, 24 to 28 June, 2008. Kampala, Uganda, Ministry of Water and Environment, The Republic of Uganda. Session 4**:** 48.
Kowalewski, P. E. (1999). Design and evaluation of engineered soil covers for infiltration control in heap leach closure. Closure, Remediation & Managemnet of Precious Metals Heap Leach Facilities '99, Reno, Nevada.pp 21 - 28.
Kraatz, D. B. (1977). Irrigation canal lining, FAO Land and Water Development Series 1; 199 p.
Krahn, J. (2004a). Vadose Zone Modelling with VADOSE/ W: An Engineering Methodology. http://www.geo-slope.com, GEO-SLOPE International Ltd. Accession Date 12/06/2005.
Krahn, J. (2004b). Seepage Modelling with Seep/W. http://www.geo-slope.com, GEO-SLOPE International Ltd. Accession Date 12/06/2005.
Kripalani, R. H., J. H. Oh and H. S. Chaudhari (2010). Delayed influence of the Indian Ocean Dipole mode on the East Asia-West Pacific monsoon: possible mechanism. International Journal of Climatology 30(2): pp 197 - 209.
Kruger, A., U. Ulbrich and P. Speth (2001). Groundwater recharge in Northrhine-Westfalia predicted by a statistical model for greenhouse gas scenarios. Physics and Chemistry of the Earth, Part B: Hydrology, Oceans and Atmosphere 26(11 - 12): pp 853 - 861.
Krysanova, V., F. Hattermann and A. Habeck (2005). Expected changes in water resources availability and water quality with respect to climate change in the Elbe River basin (Germany). Nordic Hydrology 36(4 - 5): pp 321 - 333.
Kumar, K. K., B. Rajagopalan and M. A. Cane (1999). On the weakening Relationship Between the Indian Monsoon and ENSO. Science 284(5423): pp 2156 - 2159.
Kundzewick, Z. and P. Doll (2008). Will groundwater ease the freshwater stress under climate change? Groundwater and Climate in Africa: an international conference Kampala, Uganda, Ministry of Water and Environment, The Republic of Uganda**:** 26.

Kundzewicz, Z. W., L. J. Mata, N. W. Arnell, P. Doll, B. Jimenez, K. Miller, T. Oki, Z. Sen and I. Shiklomanov (2008). The implication of projected climate change for freshwater resources and their management. Hydrological Sciences Journal 53(1): pp 3 - 10.

Kung, K.-J. S. (1990). Influence of plant uptake on the performance of bromide tracer. Soil Science Society of America Journal 54(4): pp 975 - 979.

Ladson, A. (2008). Hydrology: An Australian Introduction. Melbourne, Australia, Oxford University Press.326 p.

Lapham, W. W. (1989). Use of temperature profiles beneath streams to determine rates of vertical groundwater flow and vertical hydraulic conductivity. US Geological Survey Water Supply Paper No 2337: pp 1 - 35.

Lappala, E. G., R. W. Healy and E. P. Weeks (1987). Documentation of the computer program VS2D to solve the equations of fluid flow invariably saturated porous media, US Geological Survey Water-Resources Investigations Report; 184 p.

Lautz, L. K. (2008). Estimating groundwater evapotranspiration rates using diurnal water-table fluctuations in a semi-arid riparian zone. Hydrogeology Journal 16(3): pp 483 - 497.

Lawrence, D. (2000). Kakadu : The Making of a National Park. Melbourne, VIC, The Miegunyah Press, Melbourne University Press.401 p.

Leavesley, G. H. and L. G. Stannard (1995). The precipitation-runoff modeling system - PRMS. Computer models of watershed hydrology. V. P. Singh (Editor), Highlands Ranch, Colorado: pp 281 - 310.

Lee, D. R. and J. A. Cherry (1978). A field exercise on groundwater flow using seepage meters and mini-piezometers. Journal of Geological Education 27(1): pp 6 - 10.

Leggett, J., W. J. Pepper and R. J. Swart (1992). Emissions Scenarios for IPCC: An Update. Climate Change 1992: The Supplementary Report to the IPCC Scientific Assessment. J. T. Houghton, B. A. Callander and S. K. Varney (Editors), Cambridge University Press, Cambridge, UK: pp 69 - 95.

Lerner, D. N. (1997). Groundwater recharge. Geochemical processes, weathering and groundwater recharge in catchments. S. O. M and d. C. P (Editors), Rotterdam, AA Balkema: pp 109 - 150.

Lerner, D. N., A. S. Issar and I. Simmers (1990). Groundwater recharge, a guide to understanding and estimating natural recharge. Kenilworht, International Association of Hydrogeologists; 345 p.

Li, Z., W. Liu, X. Zhang and F. Zheng (2009). Impacts of land use change and climate variability on hydrology in an agricultural catchment on the Loess Plateau of China. Journal of Hydrology 377(1 - 2): pp 35 - 42.

Liu, L.-M. (1986). Multivariate Time Series Analysis Using Vector ARMA Models, Scientific Computing Associates.80 p.

Liu, L.-M. and D. M. Hanssens (1982). Identification of Multiple-Input Transfer Function Model. Communications in statistics: theory and methods 11(3): pp 297 - 314.

Loaiciga, H. A. (2003). Climate change and groundwater. Annals of the Association of American Geographers 93(1): pp 30 - 41.

Lopez, A., F. Fung, M. New, G. Watts, A. Weston and R. L. Wilby (2009). From climate model ensembles to climate change impacts and adaptation: A case study of water resource management in the southwest of England. Water Resources Research. 45**:** doi:10.1029/2008WR007499.

Lubczynski, M. W. (2006). Fluxes, numerical models and sustainability of groundwater resources. Sustainability of Groundwater Resources and its Indicators. B. Webb, R. Hirata, E. Kruse and J. Vrba (Editors), IAHS 2006. 302: pp 67 - 77.

Ludwig, F., S. P. Milroy and S. Asseng (2009). Impacts of recent climate change on wheat production systems in Western Australia. Climatic Change 92(3 - 4): pp 495 - 517.
Ma, Z., S. Kang, L. Zhang, L. Tong and X. Su (2008). Analysis of impacts of climate variability and human activity on streamflow for a river basin in arid region of northwest China. Journal of Hydrology 352(3 - 4): pp 239 - 249.
Mackay, R., A. Montenegro, S. Montenegro and J. V. Wonderen (2006). Alluvial aquifer indicators for small-scale irrigation in northern Brazil. Sustainability of Groundwater Resources and its Indicators. B. Webb, R. Hirata, E. Kruse and J. Vrba (Editors), IAHS 2006. 302: pp 117 - 125.
Madden, R. A. and P. R. Julian (1971). Detection of a 40-50 day oscillation in the zonal wind in the tropical Pacific. Journal of Atmospheric Sciences 28(5): pp 702 - 708.
Madden, R. A. and P. R. Julian (1972). Description of global-scale circulation cells in the tropics with a 40-50 day period. Journal of Atmospheric Sciences 29(6): pp 1109 - 1123.
Maidment, D. R., Ed. (1993). Handbook of Hydrology. NewYork, McGraw - Hill Inc p.
Maidment, D. R., S.-P. Miaou and M. M. Crawford (1985). Transfer function models of daily urban water use. Water Resources Research 21(4): pp 425 - 432.
Mann, M. E. (2004). On smoothing potentially non-stationary climate time series. Geophysical Research Letters. 31(L07214)**:** doi:10.1029/2004GL019569.
Manning, L. J., J. W. Hall, H. J. Fowler, C. G. Kilsby and C. Tebaldi (2009). Using probabilistic climate change information from a multimodel ensemble for water resources assessment. Water Resources Research. 45(W11411)**:** doi:10.1029/2007WR006674.
Mantua, N. J. and S. R. Hare (2002). The Pacific Decadal Oscillation. Journal of Oceanography 58(1): pp 35 - 44.
Mantua, N. J., S. R. Hare, Y. Zhang, J. M. Wallace and R. C. Francis (1997). A Pacific interdecadal climate oscillation with impacts on salmon production. Bulletin of the American Meteorological Society 78(6): pp 1069 - 1079.
Marshall, T. J. (1958). A relation between permeability and size distribution of pores. European Journal of Soil Science 9(1): pp 1 - 8.
Martinez, C. J., M. A. Newman, M. A. Newman, J. W. Jones, W. D. Graham and W. D. Graham (2007). Coupled Modes of Variability between Pacific and Atlantic Sea Surface Temperatures and Monthly Precipitation in Southwest Florida. American Geophysical Union, Fall Meeting 2007**:** Abstract H23F-1677.
Mau, D. P. and T. C. Winter (1997). Estimating grounewater recharge from streamflow hydrographs for a small mountain watershed in a temperate humid climate, New Hampshire, USA. Ground Water 35(2): pp 291 - 304.
Mayer, T. D. and R. D. Congdon (2007). Evaluating climate variability and pumping effects in statistical analyses. Ground Water 46(2): pp 212 - 227.
Mc Quade, C. V. (1991). Hydrology of Ranger Land Application Area. Land Application of Effluent Water from Uranium Mines in the Alligator Rivers Region, Jabiru, Australian Government Publishing Service.pp 70-78.
McDonald, M. G. and A. W. Harbaugh (1988). A Modular Three - Dimensional Finite - Difference Ground - Water Flow Model. Techniques of Water - Resources Investigations of the United States Geological Survey. Washington, USGS. Book 6, Chapter A1**:** 586 p.
McGuffie, K., P. L. Airey, A. Henderson-Sellers, C. V. Tadros and D. M. Stone (2004). Stable Isotopes in Precipitation and Groundwater as Tracers for Climate Change in Central Australia. American Geophysical Union, Fall Meeting 2004**:** abstract # C51B-1029.

Meehl, G. A., G. W. Branstator and W. M. Washington (1993). Tropical Pacific interannual variability and CO_2 climate change. Journal of Climate 6(1): pp 42 - 63.
Meehl, G. A., W. Collins, B. Boville, J. T. Kiehl, T. M. L. Wigley and J. M. Arblaster (2000). Response of the NCAR Climate System Model to increased CO_2 and the role of physical processes. Journal of Climate 13(11): pp 1879 - 1898.
Meehl, G. A., T. F. Stocker, W. D. Collins, P. Friedlingstein, A. T. Gaye, J. M. Gregory, A. Kitoh, R. Knutti, J. M. Murphy, A. Noda, S. C. B. Raper, I. G. Watterson, A. J. Weaver and Z.-C. Zhao (2007). Global climate projections. Climate Change 2007: The Physical Science Basis. Contribution of Working Group I to the Fourth Assessment Report of the Intergovernmental Panel on Climate Change. S. Solomon, D. Qin, M. Manning, Z. Chen, M. Marquis, K. B. Averyt, M. Tignor and H. L. Miller (Editors), Cambridge University Press, Cambridge, United Kingdom and New York, NY, USA: pp 748 - 845.
Meehl, G. A. and W. M. Washington (1996). El Nino-like climate change in a model with increased atmospheric CO_2-concentrations Nature 382: pp 56 - 60.
Mein, R. (1993). Flood Hydrology, May 1993. Catchword, Cooperative Centre for Catchment Hydrology, Monash University, Clayton, Victoria.
Meinzer, O. E. and N. D. Stearns (1929). A study of groundwater in the Pomperaug Basin, Connecticut: with special reference to Intake and Discharge. US Geological Survey Water-Supply Paper.
Merz, R. and G. Bloschl (2009). A regional analysis of event runoff coefficients with respect to climate and catchment characteristics in Australia. Water Resources Research. 45 (W01405)**:** doi:10.1029/2008WR007163.
Merz, R., G. Bloschl and J. Parajka (2006). Spatio-temporal variability of event runoff coefficients. Journal of Hydrology 331(3 - 4): pp 591 - 604.
Merz, R., J. Parajka and G. Bloschl (2009). Scale effects in conceptual hydrological modeling. Water Resources Research. 45 (W09405)**:** doi:10.1029/2009WR007872.
Meyboom, P. (1961). Estimating groundwater recharge from stream hydrographs. Journal of Geophysical Research 66(4): pp 1203 - 1214.
Michaud, Y., C. Rivard, J. Marion, A. Rivera and R. Lefebvre (2004). Groundwater Resources and Climate Change: Trends from Eastern Canada. American Geophysical Union, Fall Meeting 2004**:** abstract # H23E-02.
Middlemis, H., N. Merrick and R. J (2001). Murray - Darling Basin Commission Groundwater Flow Modelling Guideline, Aquaterra Consulting Pty Ltd; 133 p.
Miguel, G., L. Rebollo and M. Martin-Loeches (2008). Episodic recharge to the Quelo-Luanda aquifer: anticipating the impacts of climate change. Groundwater and Climate in Africa: an international conference, 24 to 28 June, 2008. Kampala. Uganda, Ministry of Water and Environment, The Republic of Uganda. Session 4**:** 50.
Miguez-Macho, G., H. Li and Y. Fan (2008). Simulated water table and soil moisture climatology over North America. Bulletin of the American Meteorological Society 89: pp 663 - 672.
Mileham, L., R. Taylor, J. Thompson, M. Todd and C. Tindimugaya (2007). Impact of rainfall distribution on the paramterisation of a soil-moisture balance model of groundwater recharge in equatorial Africa. American Geophysical Union, Fall Meeting 2007**:** Abstract H11F-0848.
Mileham, L., R. Taylor, M. Todd, J. Thompson and C. Tindimugaya (2008). The impact of climate change on groundwater recharge and runoff in a humid, equatorial catchment of Uganda. Groundwater and Climate in Africa: an international

conference, 24 to 28 June 2008. Kampala. Uganda, Ministry of Water and Environment, The Republic of Uganda. Session 3**:** 40.
Misstear, B. D. R., L. Brown and P. M. Johnston (2009). Estimation of groundwater recharge in a major sand and gravel aquifer in Ireland using multiple approaches. Hydrogeology Journal 17: pp 693 – 706.
Mitchell, T. (2003). Pattern Scaling - An Examination of the Accuracy of the Technique for Describing Future Climates. Climatic Change 60(3): pp 217 - 242.
Mondal, M. S. and S. A. Wasimi (2005). Periodic Transfer Function-Noise Model for Forecasting. Journal of Hydrologic Engineering 10(5): pp 353 - 362.
Mondal, M. S. and S. A. Wasimi (2006). Generating and forecasting monthly flows of the Ganges river with PAR model. Journal of Hydrology 323(1 - 4): pp 41 - 56.
Montanari, A. and G. Grossi (2008). Estimating the uncertainty of hydrological forecasts: A statistical approach. Water Resources Research. 44 (W00B08)**:** doi:10.1029/2008WR006897.
Monteith, J. L. (1980). The developement and extention of Penman's evaporation formula. Applications of Soil Physics. D. Hillel (Editor), Orlando, Academic Press: pp 247 - 253.
Morabito, J. A., E. P. Querner and D. Tozzi (2006). Using performance indicators for the analysis of water use in the Mendoza irrigated area. Sustainability of Groundwater Resources and its Indicators. B. Webb, R. Hirata, E. Kruse and J. Vrba (Editors), IAHS 2006. 302: pp 126 - 133.
Morel-Seytoux, H. J. (2001). Groundwater. Model Validation: Perspectives in Hydrological Science M. G. Anderson and P. D. Bates (Editors), John Wiley & Sons, Ltd: pp 293 - 323.
Morris, B. L., A. R. L. Lawrence, P. J. C. Chilton, B. Adams, C. R. C and B. A. Klinck (2003). Groundwater and its Susceptibility to Degradation: A Global Assessment of the Problem and Options for Management. Nairobi, Kenya, United Nations Environment Programme.Early Warning and Assessment Report Series, RS. 03-3; 140 p.
Morton, F. I. (1983). Operational estimates of areal evapotranspiration and their significance to the science and practice of hydrology. Journal of Hydrology 66(1 - 4): pp 1 - 76.
Morton, R. D. (1976). The Western and North Australian Uranium Deposits - Exploration Guides or Exploration Deterrants for Saskatchewan? Uranium in Saskatchewan Symposium, Saskatoon, Saskatchewan, Canada, Saskatchewan Geological Society. Special Publication No. 3 pp 211 - 254.
Mudgway, L. B., R. J. Nathan, T. A. McMahon and H. M. Malano (1997). Estimating salt loads in high water table areas. I. Identifying processes Journal of Irrigation and Drainage Engineering 123(2): pp 79 - 90.
Mulvaney, J. and J. Kamminga (1999). Prehistory of Australia St Leonards, NSW, Australia, Allen & Unwin Pty Ltd.480 p.
Mutiibwa, R. (2008). An assessment of the response time of groundwater levels to climate change and abstraction. Groundwater and Climate in Africa: an international conference, 24 to 28 June 2008. Kampala. Uganda, Ministry of Water and Environment, The Republic of Uganda. Session 3**:** 44.
Nash, J. E. (1989). Potential evaporation and "The Complementary Relationship". Journal of Hydrology 111(1 - 4): pp 1 - 7.
Nash, J. E. and J. Sutcliffe (1970). River flow forecasting through conceptual models, Part 1, A discussion of principles. Journal of Hydrology 10(3): pp 282 - 290.

Nathan, R. J. and T. A. McMahon (1990). Evaluation of Automated Techniques for Base Flow and Recession Analyses. Water Resources Research 26(7): pp 1465 - 1473.
Nativ, R., E. Adar, O. Dahan and M. Geyh (1995). Water recharge and solute transport through the vadose zone of fractured chalk under desert conditions. Water Resources Research 31(2): pp 253 - 261.
Naumburg, E., R. Mata-Gonzalez, R. G. Hunter, T. Mclendon and D. W. Martin (2005). Phreatophytic Vegetation and Groundwater Fluctuations: A Review of Current Research and Application of Ecosystem Response Modeling with an Emphasis on Great Basin Vegetation. Environmental Management 35(6): pp 726 - 740.
Needham, R. S. (1988). Geology of the Alligator Rivers Uranium Field, Northern Territory. Department of Primary Industries and Energy, Bureau of Mineral Resources, Geology and Geophysics, Australian Government Publishing Service. Canberra 1988**:** 96.
Nelson, E. J. (2001). WMS v6.1 HTML Help Document Environmental Modelling Research Laboratory, Bringham Young University: Provo, UT.
Nemes, A., S. M. G, F. J. Leij and J. H. M. Wosten (2001). Description of the Unsaturated Soil Hydraulic Database UNSODA version 2.0. Journal of Hydrology 251(3 - 4): pp 151 - 162.
Nimmo, J. R., D. A. Stonestrom and K. C. Akstin (1994). The feasibility of recharge rate determinations using the steady-state centrifuge method. Soil Science Society of America Journal 58: pp 49 - 56.
Noda, A., K. Yoshimatsu, A. Kitoh and H. Koide (1999a). Relationship between natural variability and CO_2-induced warming pattern: MRI coupled atmosphere/mixed-layer (slab) ocean GCM (SGCM) Experiment. 10th Symposium on Global Change Studies, Dallas, Texas, American Meteorological Society, Boston, Mass.pp 355 - 358.
Noda, A., K. Yoshimatsu, S. Yukimoto, K. Yamaguchi and S. Yamaki (1999b). Relationship between natural variability and CO_2-induced warming pattern: MRI AOGCM Experiment. 10th Symposium on Global Change Studies, Dallas, Texas, American Meteorological Society, Boston, Mass.pp 359 - 362.
Noller, B. N. and N. A. Currey (1990). Chemical composition and acidity of rainfallin the Alligator Rivers Region, Northern Territory, Australia. The Science of the Total Environment 91(February 1990): pp 23 - 28.
Nott, J. and M. Hayne (2001). High frequency of 'super-cyclones' along the Great Barrier Reef over the past 5,000 years. Nature 413: pp 508 - 512.
Nyenje, P. M. and O. Batelaan (2008). Estimating effects of climate change on groundwater : case of Ssezibwa catchment in Uganda. Groundwater and Climate in Africa: an international conference, 24 to 28 June 2008. Kampala. Uganda, Ministry of Water and Environment, The Republic of Uganda. Session 3**:** 40.
O'Kane, M., B. Ayres, D. Christensen and G. Meiers (2002). CANMET – CETEM Manual on Cover System Design for Reactive Mine Waste. Saskatoon, Canada, O'Kane Consultants Inc; 160 p.
Ogden, F. L. (2000). CASC2D Reference Manual, Version 2.0, Department of Civil and Environmental Engineering, Universirt of Connecticut: Storrs, CT.
Ogden, F. L. and J. P. Y (2002). CASC2D : A two-dimensional, physically-based, Hortonian, hydrologic model. Mathematical Models of Small Watershed Hydrology and Applications. V. Singh and D. Freverts (Editors): pp 69 - 112
OSS (var.). Annual Report. Sydney, NSW / Darwin, NT, Australia, Office of the Supervising Scientist (OSS). Years 1978 to 2009.

Ostrom, C. W. J. (1990). Time Series Analysis Regression Techniques. Newbury Park, Sage Publications, Inc.95 p.
Panagoulia, D. and G. Dimou (1996). Sensitivities of Groundwater-streamflow Interaction to Global Climate Change. Hydrological Sciences Journal 41(5): pp 781 - 796.
Pankratz, A. (1991). Forecasting with Dynamic Regression Models. New York, John Wiley & Sons Inc.386 p.
Papagiannakis, A. T. and D. G. Fredlund (1984). A steady state model for flow in saturated-unsaturated soils. Canadian Geotechnical Journal 21: pp 419 - 430.
Parlange, M. B., G. G. Katul, R. H. Cuenca, M. L. Kavvas, D. R. Nielson and M. Mata (1992). Physical Basis for a Time Series Model of Soil Water Content. Water Resources Research 28(9): pp 2437 - 2446.
Penman, H. L. (1948). Natural evaporation from open water, bare soil, and grass. Proceedings of the Royal Society of London. Series A, Mathematical and Physical Sciences 193(1032): pp 120 – 145.
Person, M. A., T. C. Winter, D. O. Rosenberry, H. Cohen, W. J. Gutowski, D. Dahlstrom, P. Roy, I. Emi, V. Zabielski, H. Wright, J. Nieber and R. Daannen (2004). Groundwater Supported Evapotranspiration within Glaciated Watersheds under Conditions of Climate Change. American Geophysical Union, Fall Meeting 2004**:** abstract # H23E-01.
Pilgrim, D. H. (1983). Some problems in transferring hydrological relationships between small and large drainage basins and between regions. Journal of Hydrology 65: pp 49-72.
Pillai, M. (2005). Hydrogeological Review of Recharge and Discharge Mechanisms in the Ranger Mine Site Catchment, ERA Limited; 9 p.
Podger, G. (2004). Rainfall Runoff Library User Guide, Catchment modelling toolkit, CRC for Catchment Hydrology, Accessed on 23/09/2006 http://www.toolkit.net.au/rrl; 110 p.
Portniaguine, O. and D. K. Solomon (1998). Parameter estimation using groundwater age and head data, Cape Cod, Massachusetts. Water Resources Research 34(4): pp 637 - 645.
Power, S., T. Casey, C. Folland, A. Colman and V. Mehta (1999). Inter-decadal modulation of the impact of ENSO on Australia. Climate Dynamics 15(5): pp 319 - 324.
Power, S. and R. Colman (2006b). Multi-year predictability in a coupled general circulation model. Climate Dynamics 26(2 - 3): pp 247 - 272.
Power, S., M. Haylock, R. Colman and X. Wang (2006a). The Predictability of Interdecadal Changes in ENSO Activity and ENSO Teleconnections. Journal of Climate 19(19): pp 4755 - 4771.
Power, S., I. Smith, A. Morgan, A. Moise, S. Grainger and M. Reeder (2007). How will the impact of El Nino and La Nina on Australia change under global warming. Greenhouse2007: The latest science and technology. Sydney, NSW, Australia.
Prasad, P. R., C. S. Rao and N. V. B. S. S. Prasad (2006). Analysis of NO_3-N pollution with a distributed groundwater quality model. Sustainability of Groundwater Resources and its Indicators: IAHS proceedings and reports. B. Webb, R. Hirata, E. Kruse and J. Vrba (Editors), IAHS 2006. 302: pp 172 - 183.
Prathapar, S. A., W. S. Meyer, S. Jain and A. van der Lelij (1994). SWAGSIM: a soil water and groundwater simulation model. Divisional Report 94/3, CSIRO, Division of Water Resources.

Press, T., D. Lea, A. Webb and A. Graham (1995). Kakadu Natural and Cultural Heritage and Management, Darwin, Australian Nature Conservation Agency & North Australia Research Unit, ANU, 1995: pp 94 - 126.
Price, M. (1998). Water Storage and Climate Change in Great Britain: the Role of Groundwater. Proceedings of the Institute of Civil Engineers. Water, maritime and energy 130(1): pp 42 - 50.
Priestley, C. H. B. and R. J. Taylor (1972). On the assessment of surface heat flux and evaporationusing large-scale parameters. Monthly Weather Review 100(February 1972): pp 81 - 92.
Prudhomme, C., N. Reynard and S. Crooks (2002). Downscaling of global climate models for flood frequency analysis: where are we now? Hydrological processes 16(6): pp 1137 - 1150.
Qian, Y., S. J. Ghan and L. R. Leung (2010). Downscaling hydroclimatic changes over the Western US based on CAM subgrid scheme and WRF regional climate simulations. International Journal of Climatology 30(5): pp 675 - 693.
Rajasooriyar, L., V. Mathavan, H. A. Dharmagunawardhane and V. Nandakumar (2002). Groundwater quality in the Valigamam region of the Jaffna Peninsula, Sri Lanka. Sustainable Groundwater Development. Geological Society, London, Special Publication. K. M. Hiscock, M. O. Rivett and R. M. Davison (Editors), The Geological Society of London 2002. 193: pp 181 - 197.
Raje, D. and P. P. Mujumdar (2009). A conditional random field-based downscaling method for assessment of climate change impact on multisite daily precipitation in the Mahanadi basin. Water Resources Research. 45 (W10404)**:** doi:10.1029/2008WR007487.
Ranjan, S. P., S. Kazama and M. Sawamoto (2006a). Effects of climate and land use changes on groundwater resources in coastal aquifers. Journal of Environmental Management 80: pp 25 - 35.
Ranjan, S. P., S. Kazama and M. Sawamoto (2006b). Effects of climate change on coastal fresh groundwater resources. Global Environmental Change 16(4): pp 388 - 399.
Rasmussen, W. C. and G. E. Andreasen (1959). Hydrologic Budget of the Beaverdam Creek Basin, Maryland, USA. US Geological Survey Water-Supply Paper 1472**:** 106 p.
Refsgaard, J. C. (2001). Discussion of Model Validation in Relation to the Regional and Global Scale. Model Validation: Perspectives in Hydrological Science M. G. Anderson and P. D. Bates (Editors), John Wiley & Sons, Ltd: pp 461 - 483.
Reid, M., X. Cheng and C. Huggins (2006). Using groundwater responses to improve understanding of climate variation impacts and salinity risk. 10th Murray-Darling Basin Groundwater Workshop, September 2006. Canberra.
Reilly, T. E., L. N. Plummer, P. J. Philips and E. Busenberg (1994). The use of simulationand multiple environmental tracers to quantify groundwater flow in a shallow aquifer. Water Resources Research 30(2): pp 421 - 433.
Rennolls, K., R. Carnell and V. Tee (1980). A descriptive model of the relationship between rainfall and soil water table. Journal of Hydrology 47(1 - 2): pp 103 - 114.
Richards, L. A. (1931). Capilary conduction of liquids through porous medium. Physics 1: pp 318-333.
Richardson, C. W. and D. A. Wright (1984). WGEN: A model for generating daily weather variables. ARS-8. USDA-ARS, Washington, DC.
Risbey, J. S., M. Kandlikar and D. J. Karoly (2000). A protocol to articulate and quantify uncertainties in climate change detection and attribution. Climate Research 16(1): pp 61 - 78.

Risken, H. and T. Frank (1989). The Fokker-Planck Equation: Methods of Solutions and Applications. Berlin, Springer-Verlag.474 p.
Risser, D. W., W. J. Gburek and G. J. Folmer (2009). Comparison of recharge estimates at a small watershed in east-central Pennsylvania, USA. Hydrogeology Journal 17: pp 287 – 298
Robertson, W. D. and J. A. Cherry (1989). Tritium as an indicator of recharge and dispersion in a groundwater system in central Ontario. Water Resources Research 25(6): pp 1097 - 1109.
Robins, N. S., K. J. Griffiths, P. D. Merrin and W. G. Darling (2002). Sustainable groundwater resources in a hard-rock island aquifer - the Channel Island of Guernsey. Sustainable Groundwater Development. Geological Society, London, Special Publications. K. M. Hiscock, M. O. Rivett and R. M. Davison (Editors), The Geological Society of London 2002. 193: pp 121 - 132.
Ronan, A. D., D. E. Prudic, C. E. Thodal and J. Constantz (1998). Field study and simulation of diurnal temperature effects on infiltration and variably saturated flow beneath an ephemeral stream. Water Resources Research 34(9): pp 2137 - 2153.
Rorabough, M. I. (1964). Estimating change in bank storage and groundwater contribution to streamflow. International Association of Scientific Hydrology Publication 63: pp 432 - 441.
Rosenberg, N. J., D. J. Epstein, D. Wang, L. Vail, R. Srinivasan and J. G. Arnold (1999). Possible Impacts of Global Warming on the Hydrology of the Ogallala Aquifer Region. Climatic Change 42(4): pp 677 - 692.
Rosenzweig, C., G. Casassa, D. J. Karoly, A. Imeson, C. Liu, A. Menzel, S. Rawlins, T. L. Root, B. Seguin and P. Tryjanowski (2007). Assessment of observed changes and responses in natural and managed systems. Climate Change 2007: Impacts, Adaptation and Vulnerability. Contribution of Working Group II to the Fourth Assessment Report of the Intergovernmental Panel on Climate Change. M. L. Parry, O. F. Canziani, J. P. Palutikof, P. J. van der Linden and C. E. Hanson (Editors), Cambridge, UK, Cambridge University Press: pp 79 - 131.
Rotstayn, L. D., M. A. Collier, M. R. Dix, Y. Feng, H. B. Gordon, S. P. O'Faffell, I. N. Smith and J. Skytus (2010). Improved simulation of Australian climate and ENSO-related rainfall variability in a global climate model with an interactive aerosol treatment. International Journal of Climatology 30(7): pp 1067 - 1088.
RUM (1974). Environmental Impact Statement, Ranger Uranium Mines Pty Ltd. February 1974.
Rushton, K. (1997). Recharge from permanent water bodies. Recharge of pheatic aquifers in (semi) arid areas. I. Simmers (Editor), Rotterdam, AA Balkema: pp 215 - 255.
Rutledge, A. T. (1997). Model-estimated ground-water recharge and hydrograph of ground-water discharge to a stream. US Geological Survey Water Resources Investigation Report.
Saji, N. H. and T. Yamagata (2003a). Structure of SST and surface wind variability during Indian Ocean dipole mode events: COADS observations. Journal of Climate 16(16): pp 2735 - 2751.
Saji, N. H. and T. Yamagata (2003b). Possible impacts of Indian Ocean Dipole Mode events on global climate. Climate Research 25(2): pp 151 -169.
Salama, R. and G. Foley (1997). Ranger Regional Hydrogeology Conceptual Model. Report prepared for ERA Ranger Mine, CSIRO.Report No 97/65; 48 p.
Salama, R., P. Kin, D. Pollock, D. Ellerbroek and G. Foley (1998). Groundwater Interaction with Magela Creek. Report prepared for ERA Ranger Mine, CSIRO.Report No 98/18; 22 p.

Salama, R. B., P. Farrington, G. A. Battle and G. D. Watson (1993). Distribution of recharge and discharge areas in a first-order catchment as interpreted from water level patterns. Journal of Hydrology 143(3 - 4): pp 259 - 277.
Salas, J. D. and R. A. Smith (1981). Physical Basis of Stochastic Models of Annual Flows. Water Resources Research 17(2): pp 428 - 430.
Salathe', E. P., P. W. Mote and M. W. Wiley (2007). Review of scenario selection and downscaling methods for the assessment of climate change impacts on hydrology in the United States Pacific Northwest. International Journal of Climatology 27(12): pp 1611 - 1621.
Sammis, T. W., D. D. Evans and A. W. Warrick (1982). Comparison of methods to estimate deep percolation rates. Journal of the American Water Resources Association 18(3): pp 465 - 470.
Scanlon, B. R., R. W. Healy and P. G. Cook (2002). Choosing Appropriate Techniques for Quantifying Recharge. Hydrogeology Journal 10: pp 18 - 39.
Scanlon, B. R., D. G. Levitt, R. C. Reedy, K. E. Keese and M. J. Sully (2005). Ecological controls on water-cycle response to climate variability in deserts. Proceedings of the National Academy of Sciences (PNAS) 102(17): pp 6033 - 6038.
Schaap, M. G., F. J. Leij and M. T. van Genuchten (2001). ROSETTA: A Computer Program for Estimating Soil Hydraulic Parameters with Heirarchical Pedotransfer Functions. Journal of Hydrology 251(2001): pp 163 - 176.
Schaffranek, R. W., Ed. (1981). A model for simulation of flow in singular and interconnected channels. Techniques of Water-Resources Investigations of the USGS. Book 7.110 p.
Schaffranek, R. W. (1987). Flow model for open-channel reach or network, US Geological Survey Professional Paper 1384; 11 p.
Schmidt, S., B. Weber and M. Winiger (2009). Analysis of seasonal snow disappearance in an alpine valley from micro- to meso-scale (Loetschental, Swiitzerland). Hydrological processes 23: pp 1041 - 1051.
Schoner, W., I. Auer and R. Bohm (2009). Long term trend of snow depth at Sonnblick (Austrian Alps) and its relation to climate change. Hydrological processes 23: pp 1052 - 1063.
Schroeder, P. R., T. S. Dozier, P. A. Zappi, B. M. McEnroe, J. W. Sjostrom and R. L. Peyton (1994). The Hydrologic Evaluation of Landfill Performance (HELP) Model, Engineering Documentation for Version 3. Cincinnati, Ohio, US Environment Protection Agency.
Schwarz, G. (1978). Estimating the dimension of a model. Annals of Statistics 6(2): pp 461 - 464.
Schymanski, S. J., M. Sivapalan, M. L. Roderick, L. B. Hutley and J. Beringer (2009). An optimality-based model of the dynamic feedbacks between natural vegetation and the water balance. Water Resources Research 45: pp W01412, doi:10.1029/2008WR006841.
Scibek, J. and D. M. Allen (2006a). Comparing modelled responses of two high-permeability, unconfined aquifers to predicted climate change. Global and Planetary Change 50(1 - 2): pp 50 - 62.
Scibek, J. and D. M. Allen (2006b). Modeled impacts of predicted climate change on recharge and groundwater levels. Water Resources Research. 42 (W11405)**:** doi:10.1029/2005WR004742.
Scibek, J., D. M. Allen, A. J. Cannon and P. H. Whitfield (2007). Groundwater-surface water interaction under scenarios of climate change using a high-resolution transient groundwater model. Journal of Hydrology 333(2 - 4): pp 165 - 181.

Scibek, J., D. M. Allen, P. Whitfield and M. Wei (2004). Linking Climate, Hydrology and Groundwater in High-Resolution Transient Groundwater Flow Models: a Case Study For a Climate Change Impacts Assessment in Grand Forks, BC. American Geophysical Union, Fall Meeting 2004**:** abstract # H23E-04.

Scibek, J., D. M. Allen and P. H. Whitfield (2008). Quantifying the impacts of climate change on groundwater in an unconfined aquifer that is strongly influenced by surface water. Geological Society, London, Special Publications 288: pp 79 - 98.

Seiler, K.-P., W.-Z. Gu and W. Stichler (2008). Transient response of groundwater systems to climate changes. Climate Change and Groundwater. W. Dragoni and B. S. Sukhija (Editors), The Geological Society of London. Geological Society Special Publication No. 288: pp 111 - 119.

Semenov, M. A. and E. M. Barrow (2002). LARS-GW: A Stochastic Weather Generator for the Use in Climate Impact Studies - Developed by Mikhail A. Semenov - Version 3.0 User Manual. Hertfordshire, UK.

Semenov, M. A., R. J. Brooks, E. M. Barrow and C. W. Richardson (1998). Comparison of the WGEN and LARS-WG stochastic weather generators for diverse climate. Climate Research 10: pp 95 - 107.

Senate, C. (2003). Regulating the Ranger, Jabiluka, Beverly and Honeymoon uranium mines. C. Environment, Information Technology and the Arts References Committee. Canberra, Commonwealth of Australia.

Serrat-Capdevila, A., J. B. Valdes, J. G. Perez, K. Baird, L. J. Mata and T. Maddock III (2007). Modeling climate change impacts - and uncertainty - on the hydrology of a riparian system: The San Pedro Basin (Arizona/Sonora). Journal of Hydrology 347(1 - 2): pp 48 - 66.

Serreze, M. C., J. E. Walsh, F. S. Chapin III, T. Osterkamp, M. Dyurgerov, V. Romanovsky, W. C. Oechel, J. Morison, T. Zhang and R. G. Barry (2000). Observational evidence of recent change in the northern-high latitude environment Climatic Change 46: pp 159 - 207.

Sharma, M. L., M. Bari and J. Byrne (1991). Dynamics of seasonal recharge beneath a semiarid vegetation on the gnangara mound, Western Australia. Hydrological Processes 5(4): pp 383 - 398.

Sherif, M. M. and V. P. Singh (1999). Effect of climate change on sea water intrusion in coastal aquifers. Hydrological Processes 13(8): pp 1277 - 1287.

Sibanda, T., J. C. Nonner and S. Uhlenbrook (2009). Comparison of groundwater recharge estimation methods for the semi-arid Nyamandhlovu area, Zimbabwe. Hydrogeology Journal 17(6): pp 1427 - 1441.

SILO (2006). SILO Meteorology for the Land, Climate Variability in Agriculture R&D Program (CVAP). Queensland Department of Natural Resources. Accessed on 13/07/2007, http://www.nrme.qld.gov.au/silo.

SILO (2009). SILO PPD and DD. http://www.longpaddock.qld.gov.au/silo/, Queensland Department of Natural Resources.

Simmons, C. S. and P. D. Meyer (2000). A simplified model for the transient water budget of a shallow unsaturated zone. Water Resources Research 36(10): pp 2835 - 2844.

Simunek, J., M. Sejna and M. T. Van Genuchten (1996). Hydrus-2D: simulating water flow and solute transport in two-dimensional variably saturated media, International Groundwater Modelling Centre, Colorado School of Mines, Golden, Colorado.

Simunek, J., M. T. van Genucgten and M. Sejna (2005). The HYDRUS-1D Software Package for Simulating the Movement of Water, Heat, and Multiple Solutes in

Variably Saturated Media, Version 3.0, Department of Environmental Sciences, University of California Riverside, Riverside, California, USA; 270 p.
Simunek, J., M. T. van Genucgten and M. Sejna (2008). Development and applications of the HYDRUS and STANMOD software packages and related codes. Vadose Zone Journal 7(2): pp 587 - 600.
Sivapalan, M., G. Bloschl, L. Zhang and R. A. Vertessy (2003). Downward approach to hydrological prediction. Hydrological Processes 17(11): pp 2101 - 2111.
Sivapalan, M. and J. D. Kalma (1995). Scale problems in hydrology: Contributions of the Robertson Workshop. Hydrological processes 9: pp 243 - 250.
Slimani, S., N. Massei, J. Mesquita, D. Valdes, M. Fournier, B. Laignel and J. Dupont (2009). Combined climatic and geological forcings on the spatio-temporal variability of piezometric levels in chalk aquifer of Upper Normandy (France) at pluridecennal scale. Hydrogeology Journal 17(8): pp 1823 - 1832.
Smerdon, B. D., D. M. Allen, S. E. Grasby and M. A. Berg (2009). An approach for predicting groundwater recharge in mountainous watersheds. Journal of Hydrology 365(3 - 4): pp 156 - 172.
Smith, I. and R. Suppiah (2007). Characteristics of the northern Australian rainy season. Greenhouse2007: The Latest Science and Technology. Sydney, NSW, Australia.
Solomon, S., D. Qin, M. Manning, Z. Chen, M. Marquis, K. B. Averyt, M. Tignor and H. L. Miller, Eds. (2007). IPCC, 2007: Climate Change 2007: The Physical Science Basis. Contribution of Working Group I to the Fourth Assessment Report of the Intergovernmental Panel on Climate Change Cambridge, United Kingdom and New York, NY, USA Cambridge University Press.996 p.
Somura, H., A. Goto, H. Matsui, E. A. Musa and M. Mizutani (2006). Analysis of NO_3-N pollution with a distributed groundwater quality model. Sustainability of Groundwater Resources and its Indicators. B. Webb, R. Hirata, E. Kruse and J. Vrba (Editors), IAHS 2006. 302: pp 158 - 171.
Sophocleous, M. (2004). Climate Change: Why Should Water Professionals Care? Ground Water 42(5): pp 637.
Sophocleus, M. and S. P. Perkins (2000). Methodology and application of combined watershed and ground-water models in Kansas. Journal of Hydrology 236(3 - 4): pp 185 - 201.
Srikanthan, S., F. Chiew and A. Frost (2005). SCL Stochastic Climate Library. User Guide CRC for Catchment Hydrology.Accessed on 17/07/2007 http://www.toolkit.net.au/scl; 55 p.
Srinivasan, R., J. G. Arnold, R. S. Muttiah, C. Walker and P. T. Dyke (1993). Hydrologic Unit Model for the Unites States (HUMUS). Proceedings of Advances in Hydro-science and Engineering. CCHE, School of Engineering, University of Mississippi, Oxford, MS.
Stallman, R. W. (1964). Multiphase fluid flow in porous media - a review of theories pertinent to hydrology studies. US Geological Survey Professional Paper, US Geological Survey.
Steele-Dunne, S., P. Lynch, R. McGrath, T. Semmler, S. Wang, J. Hanafin and P. Nolan (2008). The impacts of climate change on hydrology in Ireland. Journal of Hydrology 356(1 - 2): pp 28 - 45.
Stephens, D. and L. Coons (1994). Landfill performence assessment at a semi-arid site: modeling and validation. Ground Water Monitoring and Remediation 14(1): pp 101 - 109.
Stephens, D. and R. J. Knowlton (1986). Soil water movement and recharge through sand at a semiarid site in New Mexico. Water Resources Research 22(6): pp 881 - 889.

Stothoff, S. A. (1995). BREATH Version 1.1- coupled flow and energy transport in porous media, simulator description and user guide. Publ NUREG/CR-6333. Washington, DC, US Nuclear Regulatory Commission.
Stothoff, S. A. (2007). Million-Year Estimates of Net Infiltration at Yucca Mountain, Nevada. American Geophysical Union, Fall Meeting 2007**:** Abstract H11F-0842.
Strack, O. D. L. (1989). Groundwater Mechanics. New Jersey, Prentice Hall Englewood Cliffs.732 p.
Stuyfzand, P. J. (1989). Hydrology and water quality aspects of Rhine bank groundwater in The Netherlands. Journal of Hydrology 106(3 - 4): pp 341 - 363.
Switanek, M. and P. A. Troch (2007). Quantifying the Hydrologic Effect of Climate Variability in the Lower Colorado Basin. American Geophysical Union, Fall Meeting 2007**:** Abstract H23F-1675.
Szabo, Z., D. E. Rice, L. N. Plummer, E. Busenberg, S. Drenkard and P. Schlosser (1996). Age dating of shallow groundwater with chloroflourocarbons, tritiunm/helium 3, and flow path analysis, southern New Jersey coastal plain. Water Resources Research 32(4): pp 1023 - 1038.
Szilagyi, J., F. E. Harvey and F. Ayers (2003). Regional Estimation of Base Recharge to Ground Water Using Water Balance and a Base-Flow Index. Ground Water 41(4): pp 504 - 513.
Talsma, T. and P. M. Hallam (1980). Hydraulic conductivity measurement of forest catchments. Australian Journal of Soil Research 18(2): pp 139 - 148.
Tan, B. Q. and K. M. O'Connor (1996). Application of an empirical infiltration equation in the SMAR conceptual model. Journal of Hydrology 185 (3 - 4): pp 275 - 295.
Tang, Q., H. Hu and T. Oki (2006). Hydrological processes within an intensively cultivated alluvial plain in an arid environment. Sustainability of Groundwater Resources and its Indicators. B. Webb, R. Hirata, E. Kruse and J. Vrba (Editors), IAHS 2006. 302: pp 134 - 144.
Taniguchi, M., A. Aureli and J. L. Martin (2008). GRAPHIC: Groundwater resources assessment under the pressures of humanity and climate change. Groundwater and Climate in Africa: an international conference, 24 to 28 June 2008. Kampala. Uganda, Ministry of Water and Environment, The Republic of Uganda. Plenary Opening Session**:** 27.
Tankersley, C. D. and W. D. Graham (1993). Comparison of univariate and transfer function models of groundwater fluctuations. Water Resources Research 29(10): pp 3517 - 3533.
Tankersley, C. D. and W. D. Graham (1994). Development of an optimal control system for maintaining minimum groundwater levels. Water Resources Research 30(11): pp 3171 - 3181.
Tartakovsky, D. M., M. Dentz and P. C. Lichtner (2009). Probability density functionsfor advective-reactive transport with uncertain reaction rates. Water Resources Research. 45 (W07414)**:** doi: 10.1029/2008WR007383.
Taylor, C. B., L. G. Brown, J. J. Cunliffe and P. W. Davidson (1992). Environmental tritium and O^{18} applied in a hydrological study of the Wairau Plain and its contributing mountain catchments, Marlborough, New Zealand. Journal of Hydrology 138(1 - 2): pp 269 - 319.
Taylor, C. B., D. D. Wilson, L. G. Brown, M. K. Stewart, R. J. Burden and G. W. Brailsford (1989). Sources and flow of North Cantebury Plains groundwater. Journal of Hydrology 106(3 - 4): pp 311 - 340.
Taylor, R. and C. Tindimugaya (2008). Groundwater and Climate in Africa: an international conference Groundwater and Climate in Africa: an international

conference, 24 to 28 June 2008. Kampala, Uganda Ministry of Water and Environment, The Republic of Uganda**:** 63.
Telbaldi, C., R. Smith, D. Nychka and L. O. Mearns (2005). Quantifying uncertainty in projections of regional climate change: A Bayesian Approach to the analysis of multimodel ensembles Journal of Climate 18: pp 1524 - 1540.
Tett, S. F. B. (1995). Simulation of El Nino-Southern Oscillation-like variability in a global coupled AOGCM and its response to CO_2-increase. Journal of Climate 8(6): pp 1473 - 1502.
Theis, C. V. (1937). Amount of ground-water recharge in the Southern High Plains. American Geophysical Union Transactions 18th Annual Meeting**:** 564 - 568 pp.
Therrien, R., R. G. McLaren, E. A. Sudicky and S. M. Panday (2009). HydroGeoSphere: A three-dimensional numerical model describing fully-integrated subsurface and surface flow and solute transport., Groundwater Simulations Group, University of Waterloo**:** 366 p.
Thode, R. (2009). SVFLUX^{Tm} 2D /3D Seepage modelling software M. Fredlund, http://www.soilvision.com/subdomains/svflux.com/index.shtml**:** Soilvision Systems Ltd.
Thompstone, R. M., K. W. Hipel and A. I. McLeod (1985). Forecasting Quarterly-Monthly Riverflow. Water Resources Bulletin 21(5): pp 731 - 741.
Thornthwaite, C. W. (1948). An approach toward a rational classification of climate. Geographical Review 38(1): pp 55 - 94.
Thornthwaite, C. W. and B. Holzman (1939). The determination of evaporation from land and water surfaces. Monthly Weather Review 67(1): pp 4 - 11.
Tilahun, K. and B. J. Merkel (2009). Estimation of groundwater recharge using a GIS-based distributed water balance model in Dire Dawa, Ethiopia. Hydrogeology Journal 17(6): pp 1443 - 1457.
Timilsena, J., T. Piechota, G. Tootle and A. Singh (2009). Associations of interdecadal/interannual climate variability and long-term colorado river basin streamflow. Journal of Hydrology 365(3 - 4): pp 289 - 301.
Timmermann, A. J., J. Oberhuber, A. Bacher, M. Esch, M. Latif and E. Roeckner (1999). Increased El Nino frequency in a climate model forced by future greenhouse warming. Nature 398: pp 694 - 696.
Tindall, J. A. and J. R. Kunkel (1999). Unsaturated Zone Hydrology for Scientists and Engineers. New Jersy, Prentice-Hall, Inc.624 p.
Todd, D. K. (1980). Groundwater Hydrology, John Wiley & Sons.535 p.
Tong, H. (1990). Non-linear Time Series: A Dynamical System Approach (Oxford Statistical Science Series, 6). New York, Oxford University Press.564 p.
Toth, J. and G. Sheng (1996). Enhancing safety of nuclear waste disposal by exploring regional groundwater flow: The recharge area concept. Hydrogeology Journal 4(4): pp 4 - 25.
Tukey, J. W. (1977). Exploratory Data Analysis, Addison-Wesley Publishing Company.688 p.
Turc, L. (1954). Colcul du bilan de l'eou evaluation en function des precipitations et des temperatures. des i/Association International d'Hydrology, Assemblte Gtnrale de Rome, Tome III. 37.pp 188 - 202.
Tuteja, N. K., J. Vaze, B. Murphy and G. Beale (2004). CLASS - Catchment scale multiple-landuse atmosphere soil water and solute transport model, Department of Infrastructure, Planning and Natural Resources, New South Wales, Australia.04/12, July 2004; 63 p.

Twarakavi, N. K. C., J. Simunek and S. Seo (2008). Evaluating Interactions between Groundwater and Vadose Zone Using the HYDRUS-Based Flow Package for MODFLOW. Vadose Zone Journal 7(2): pp 757 - 768.
Vaccara, J. J. (1992). Sensitivity of groundwater recharge estimates to climate variability and change, Columbia Plateau, Washington. Journal of Geophysical Research 97 (D3): pp 2821-2833.
Van Bavel, C. H. M. (1966). Potential evaporation: the combination concept and its experimental verification. Water Resources Research 2(3): pp 455 - 467.
van der Kamp, G., H. Maathuis and A. Pietroniro (2004). Climate Change and Groundwater in the Northern Prairies of Northern America. American Geophysical Union, Spring Meeting 2004**:** abstract #H31C-01.
van Geera, F. C. and P. R. Defize (1987). Detection of natural and artificial causes of groundwater fluctuations. IAHS Publ: pp 597 - 606.
van Geera, F. C. and A. F. Zuur (1997). An extension of Box-Jenkins transfer/noise models for spatial interpolation of groundwater head series. Journal of Hydrology 192(1 - 4): pp 65 - 80.
van Roosmalen, L., B. S. B. Christensen and T. O. Sonnenborg (2007). Regional Differences in Climate Change Impacts on Groundwater and Stream Discharge in Denmark. Vadose Zone Journal 6(3): pp 554 - 571.
van Roosmalen, L., T. O. Sonnenborg and K. H. Jensen (2009). Impact of climate and land use change on the hydrology of a large-scale agricultural catchment. Water Resources Research. 45 (W00A15)**:** doi:10.1029/2007WR006760.
Vandaele, W. (1983). Applied Time Series and Box-Jenkins Models, Academic Press, Inc.417 p.
Vardavas, I. M. (1987). Modelling the seasonal variation of net all-wave radiation flux and evapotranspiration in a tropical wet-dry region. Ecological Modelling 39: pp 247-268.
Vardavas, I. M. (1988). A Simple Water Balance Daily Rainfall - Runoff Model with Application to the Tropical Magela Creek Catchment. Ecological Modelling 42(3 - 4): pp 245 - 264.
Vardavas, I. M. (1989). A Water Budget Model for the Tropical Magela Floodplain. Ecological Modelling 46(3 - 4): pp 165 - 194.
Vardavas, I. M. (1992). Annual rainfall statistics for stations in the Top End of Australia: normal and log-normal distribution analysis, Supervising Scientist for the Alligator Rivers Region.Technical Memorandum 27; 35 p.
Vardavas, I. M. (1993). A Simple Groundwater Recharge - Depletion Model for the Tropical Magela Creek Catchment. Ecological Modelling 68(3 - 4): pp 147 - 159.
Vardavas, I. M. and L. M. Cannon (1991). A simple expression for estimating monthly runoff for catchments in the East Alligator River system. Alligator Rivers Region Research Institute Annual Research Summary for 1988-89,Supervising Scientist for the Alligator Rivers Region, Australian Government Publishing Service Canberra 1991**:** 144 - 156.
Varis, O., T. Kajander and R. Lemmela (2004). Climate and water: from climate models to water resources management and vice versa. Climatic Change 66: pp 321 - 344.
Vaze, J., N. K. Tuteja and J. Teng (2005). CLASS Unsaturated Moisture Movement Model-1D User Guide 2.0.1, CRC for Catchment Hydrology; 41 p.
Vecchia, A. V. (1985). Periodic Autoregressive-moving average (PARMA) modelling with Applications to Water Resources. Water Resources Bulletin 21(5): pp 721 - 730.
Verburg, K., P. J. Ross and K. L. Bristow (1996). SWIMv2.1 User Manual. CSIRO Division of Soils, CSIRO Australia.Divisional Report No 130; 107 p.

Verdon, D. C. and S. W. Frank (2006a). Long-term behaviour of ENSO: Interactions with the PDO over the past 400 years inferred from paleoclimate records. Geophysical Research Letters 33(L06712): pp 1 - 5.
Verdon, D. C. and S. W. Frank (2006b). Long Term Drought Risk Assessment in the Lachlan Catchment - A Paleoclimate Perspective. 30th Hydrology and Water Recources Symposium, Launceston, Tasmania.pp 486 - 491.
Verdon, D. C. and A. M. Wyatt (2004). Multidecadal variability of rainfall and streamflow: Eastern Australia. Water Resources Research 40(W10201): pp 1 - 8.
Viswanathan, M. N. (1984). Recharge characteristics of an unconfined aquifer from the rainfall-water table relationship. Journal of Hydrology 70(1 - 4): pp 233 - 250.
Von Asmuth, J. R., M. F. P. Bierkens and K. Maas (2002). Transfer function-noise modeling in continuous time using predefined impulse response functions. Water Resources Research 38 (12): pp 23.1 - 23.12.
Von Asmuth, J. R. and M. Knotters (2004). Characterising groundwater dynamics based on a system identification approach. Journal of Hydrology 296(1 - 4): pp 118 - 134.
Vries, J. J. and I. Simmers (2002). Groundwater Recharge: an Overview of Processes and Challenges. Hydrogeology Journal 10(1): pp 5 - 17.
Walker, G. R. (1998). Using Soil Water Tracers to Estimate Recharge. The Basics of Recharge and Discharge. L. Zhang and G. R. Walker, CSIRO Publishing. 7.
Walker, G. R., L. Zhang, T. W. Ellis, T. J. Hatton and P. C (2002). Towards a predictive framework for estimating recharge under different land uses: review of modelling and other approaches appropriate for management of dryland salinity. Hydrogeology Journal 10(1): pp 68 - 90.
Walker, T. A. and T. H. F. Wong (1999). Effectiveness of Street Sweeping for Stormwater Pollution Control.Technical Report 99/8, December 1999; 43 p.
Wang, B. and L. Murray (2005). An unsaturated soil seepage analysis for design of a soil cover system to reduce oxidation of a mine tailing deposit. Unsaturated Soils: Numerical and Theoretical Approaches T. Schanz (Editor), Springer: pp 359 - 368.
Wang, J., E. Wang, Q. Luo and M. Kirby (2009b). Modelling the sensitivity of wheat growth and water balance to climate change in Southeast Australia. Climatic Change 96(1 - 2): pp 79 - 96.
Wang, Q. J., F. L. N. McConachy, F. H. S. Chiew, R. James, G. C. de Hoedt and W. J. Wright (2002). Climatic Atlas of Australia: Maps of Evapotranspiration, Bureau of Meteorology; 4 p.
Wang, T., V. A. Zlotnik, J. Simunek and M. G. Schaap (2009a). Using pedotransfer functions in vadose zone models for estimating groundwater recharge in semiarid regions. Water Resources Research. 45 (W04412) doi:10.1029/2008WR006903.
Washington, W. M., J. W. Weatherly, G. A. Meehl, A. J. Semtner Jr, T. W. Bettge, A. P. Craig, S. J. W. G., J. M. Arblaster, V. B. Wayland, R. James and Y. Zhang (2000). Parallel climate model (PCM) control and transient simulations. Climate Dynamics 16(10 - 11): pp 755 - 774.
Wasson, R. J. (1992). Modern Sedimentation and Late Quaternary Evolution of the Magela Creek Plain, Canberra, ACT, Office of the Supervising Scientist; 349 p.
Watson, R. T., M. C. Zinyowera and R. H. Moss, Eds. (1999). Australasian impacts of climate change: an assessment of vulnerability : extracted from The regional impacts of climate change: an assessment of vulnerability. Canberra, Published for IPCC.98 p.
Wellman, T. P. and E. P. Poeter (2005). Estimating spatially variable representative elementary scales in fractured architecture using hydraulic head observations. Water Resources Research 41(W03001): pp 1 - 13.

Welsh, D. R. and D. B. Stewart (1991). A Transfer Function Modelling Approach to Understanding the Turbidity of a Lake Australian Journal of Marine and Freshwater Research 42(3): pp 219 - 239.
Weng, S. and J. Yu (2010). Impacts of Pacific and Indian Ocean coupling on wintertime tropical intraseasonal oscillation: a basin-coupling CGCM study. International Journal of Climatology 30(3): pp 359 - 371.
Western, A. and N. McKenzie (2004). Soil Hydrological Properties of Australia: User Guide, CRC for Catchment Hydrology, Accessed on 19/09/2006, http://www.toolkit.net.au/shpa; 21 p.
Whetton, P. H., K. L. McInnes, R. N. Jones, K. J. Hennessy, R. Suppiah, C. M. Page, J. Bathols and P. J. Durack (2005). Australian climate change projections for impact assessment and policy application: A review, CSIRO Electronic Edition 2005; p.
White, I., A. C. Falkland, T. Metutera, E. Metai, M. Overmars, P. Perez and A. Dray (2007). Climatic and human influences on groundwater in low atolls. Vadose Zone Journal 6(3): pp 581 - 590.
Whitehead, B. R. (1980). A Compilation and Interpretation of Hydrogeological Data, Ranger on Site Area. Northern Territory Geological Survey Technical Report, Department of Mine and Energy.
Whitehead, P. G., C. Neal, S. Seden- Perriton, N. Christophersen and S. Langan (1986). A time series approach to modelling stream acidity. Journal of Hydrology 85(3 - 4): pp 281 - 303.
Wilby, R. L., C. W. Dawson and E. M. Barrow (2002). SDSM - a decision support tool for the assessment of regional climate change impacts. Environmental Modelling Software 17(2): pp 145 - 157.
Wilby, R. L. and I. Harris (2006c). A framework for assessing uncertainties in climate change impacts: Low-flow scenarios for the River Thames, UK. Water Resources Research. 42 (W02419)**:** doi:10.1029/2005WR004065
Wilby, R. L., H. G. Orr, M. Hedger, D. Forrow and M. Blackmore (2006a). Risks posed by climate change to the delivery of Water Framework Directive objectives in the UK. Environment International 32(8): pp 1043 - 1055.
Wilby, R. L., P. G. Whitehead, A. J. Wade, D. Butterfield, R. J. Davis and G. Watts (2006b). Integrated modelling of climate change impacts on water resources and quality in a lowland catchment: River Kennet, UK. Journal of Hydrology 330(1 - 2): pp 204 - 220.
Wilby, R. L. and T. M. L. Wigley (1997). Downscaling general circulation model output: a review of methods and limitations. Progress in Physical Geography 21(4): pp 530 - 548.
Willett, I. R., W. J. Bond, R. A. Akber, D. J. Lynch and G. D. Campbell (1993). The fate of water and solutes following irrigation with retention pond water at Ranger Uranium Mine, Supervising Scientist for the Alligator Rivers Region.Research Report 10; 122 p.
Willett, I. R., C. J. Chartres and W. J. Bond (1991). Soils and Hydrology of the Ranger Uranium Mine Land Application Site. Land Application of Effluent Water from Uranium Mines in the Alligator Rivers Region, Jabiru, NT, Australian Government Publishing Service, Canberra 1992.pp 25 - 42.
Wilson, G. W. (1990). Soil evaporative fluxes for geotechnical problems. Department of Civil Engineering. Saskatoon, Canada, University of Saskatchewan. Ph D Thesis.
Wolaver, B. D. (2007). Groundwater Recharge Evaluation in Semi-Arid Northeast Mexico in Response to Projected Climate Change. American Geophysical Union, Fall Meeting 2007**:** Abstract H14E-05.

Woldeamlak, S. T., O. Batelaan and F. De Smedt (2007). Effects of climate change on the groundwater system in the Grote-Nete catchment, Belgium. Hydrogeology Journal 15: pp 891 - 901.
Wood, A. W., L. R. Leung, V. Sridhar and D. P. Lettenmaier (2004b). Hydrologic implications of dynamical and statistical approaches to downscaling climate model outputs. Climatic Change 62(1): pp 189 - 216.
Wood, E. F. (1995). Heterogeneity and scaling land-atmospheric water and energy fluxes in climate systems. Space and Time Scale Variability and Interdependencies in Hydrological Processes. R. A. Feddes (Editor), Cambridge University Press: pp 3 - 20.
Wood, E. F., M. Silvapalan, K. Beven and L. Band (1988). Effects of spatial variability and scale with implications to hydrologic modeling. Journal of Hydrology 102(1 - 4): pp 29 - 47.
Woods, P. H. (1994). Likely recharge to permanent groundwater beneath future rehabilitated landforms at Ranger uranium mine, Northern Austalia. Australian Journal of Earth Sciences 41(5): pp 505 - 508.
Woods, R. (2002). Seeing catchments with new eyes. Hydrological processes 16(5): pp 1111-1113.
Woodward, W. A. and H. L. Gray (1993). Global Warming and the Problem of Testing for Trend in Time Series Data. Journal of Climate 6(5): pp 953 - 962.
Wu, J., R. Zhang and J. Yang (1996). Analysis of rainfall-recharge relationships. Journal of Hydrology 177(1 - 2): pp 143 - 160.
Xu, C. (1999). Operational testing of a water balance model for predicting climate change impacts. Agricultural and Forest Meteorology 98 - 99(December 1999): pp 295 - 304.
Yakirevich, A., V. Borisov and S. Sorek (1998). A quasi threedimensional model for flow and transport in unsaturated and saturated zones: 1. Implementation of the quasi two-dimensional case. Advances in Water Resources 21(8): pp 679 – 689.
Yeh, P. J.-F. and J. S. Famiglietti (2009). Regional Groundwater Evapotranspiration in Illinois. Journal of Hydrometeorology 10(2): pp 464 - 478.
Yesertener, C. (2005). Impacts of climate, land and water use on declining groundwater levels in the Gnangara Groundwater Mound, Perth, Australia. Australian Journal of Water Resources 8(2): pp 143 - 152.
Yohe, G. W., R. D. Lasco, Q. K. Ahmad, N. W. Arnell, S. J. Cohen, C. Hope, A. C. Janetos and R. T. Perez (2007). Perspectives on climate change and sustainability. Climate Change 2007: Impacts, Adaptation and Vulnerability. Contribution of Working Group II to the Fourth Assessment Report of the Intergovernmental Panel on Climate Change. M. L. Parry, O. F. Canziani, J. P. Palutikof, P. J. van der Linden and C. E. Hanson (Editors), Cambridge, UK, Cambridge University Press: pp 811 - 841.
Young, M. H., P. J. Wierenga and C. F. Mancino (1996). Large Weighing lysimeters for water use and deep percolation studies. Soil Science 161(8): pp 491 - 502.
Zhang, L., W. R. Dawes and T. J. Hatton (1996). Modelling hydrologic processes using a biophysically based model: Application of WAVES to FIFE and HAPEX-MOBILHY. Journal of Hydrology 185(1 - 4): pp 147 - 169.
Zhang, L., G. R. Walker and M. Fleming (1998). Surface Water Balance for Recharge Estimation. The Basics of Recharge and Discharge. R. B. Salama (Editor), CSIRO publishing. 9: pp 1 - 20.
Zhang, Y., J. M. Wallace and D. S. Battisti (1997). ENSO-like interdecadal variability: 1900-93. Journal of Climate 10(5): pp 1004 - 1020.

Zheng, C. and G. D. Bennett (1995). Applied Contaminant Transport Modeling: Theory and Practice. New York, Van Nostrand Reinhold.440 p.
Zheng, H., L. Zhang, R. Zhu, C. Liu, Y. Sato and Y. Fukushima (2009). Responses of streamflow to climate and land surface change in the headwaters of the Yellow River Basin. Water Resources Research. 45 (W00A19)**:** doi:10.1029/2007WR006665.

Appendix A: Steps for estimation of Morton's Areal Actual Evapotranspiration

The steps for estimation of Morton's Areal Actual Evapotranspiration have been sourced from the paper (Morton 1983). Monthly AAET as estimated for a specific location is described first. Then the daily values of AAET are estimated from monthly AAET retaining the monthly structure of AAET.

It should be mentioned that in the present research the monthly values of AAET are computed from daily AAET as supplied by SILO (SILO 2009) and used in the estimation of climate flux which is the algebraic summation of monthly rainfall (measured) and monthly AAET (estimated).

The operations performed for a particular station involves the following steps.

1. Estimation of zenith value of dry-season snow-free clear-sky albedo for the station location.

$$\frac{p}{p_s} = \left[\frac{288 - 0.0065H}{288}\right]^{5.256}$$

$$a_{zd} = 0.26 - 0.00012\, P_A \left(\frac{p}{p_s}\right)^{0.5} \left[1 + \left|\frac{\phi}{42}\right| + \left(\frac{\phi}{42}\right)^2\right]$$

$$0.11 \le a_{zd} \le 0.17$$

a_{zd}	Zenith value of dry-season snow-free clear-sky albedo
p	Atmospheric pressure at the station (m bar)
p_s	Atmospheric pressure at sea level (m bar)
ϕ	Latitude (degree), negative for southern hemisphere
P_A	Average annual precipitation (mm)
H	Altitude above sea level (m)

The operations performed for a particular month involves the following steps.

2. Development of saturation vapour pressure-temperature curve and estimation of slope of the curve at the average air temperature (for the month).

$$v_D = 6.11e^{\left[\frac{17.27T_D}{T_D+237.3}\right]}$$

$$v = 6.11e^{\left[\frac{\alpha T}{T+\beta}\right]}$$

$$\Delta = \frac{dv}{dT} = \frac{\alpha\beta v}{(T+\beta)^2}$$

v	Saturation vapour pressure at temperature T
α, β	Constants used in estimating vapour pressures- change at below-freezing temperatures
T	Average air temperature or average of maximum and minimum values at instrument level
v_D	Atmospheric vapour pressure at instrument level or saturation vapour pressure at T_D (m bar)
T_D	average dew-point temperature at instrument level (^oC)
Δ	Slope of saturation vapour pressure curve at temperature T (m bar/^oC)

3. Estimation of extra-atmospheric global radiation (for the month)

$$\theta = 23.2\sin(29.5i - 94)$$

$$\cos Z = \cos(\phi - \theta)$$

$$\cos Z \geq 0.001$$

$$\cos\omega = 1 - \frac{\cos Z}{\cos\phi.\cos\theta}$$

$$\cos\omega \geq -1$$

$$\cos z = \cos Z + \left[\frac{\left(\frac{180}{\pi}\right)\sin\omega}{\omega} - 1 \right] \cos\phi.\cos\theta$$

$$\eta = 1 + \left(\frac{1}{60}\right)\sin(29.5i - 106)$$

$$G_E = \left(\frac{1354}{\eta^2}\right)\left(\frac{\omega}{180}\right)\cos z$$

θ	Declination of sun
i	Month number
Z	Noon angular zenith distance of sun
ω	Angle the earth rotates between sunrise and noon
z	Average angular zenith distance of sun
G_E	Extra-atmospheric global radiation (W/m^2)
η	Radius vector of the sun

4. Estimation of clear sky albedo (for the month)

$$a_{zz} = a_{zd}$$

$$0.11 \le a_{zz} \le 0.5\left(0.91 - \left(\frac{v_D}{v}\right)\right)$$

$$c_o = v - v_D$$

$$0 \le c_o \le 1$$

$$a_z = a_{zz} + (1 - c_o^2)(0.34 - a_{zz})$$

$$a_o = \frac{a_z\left(e^{1.08} - \left(\left(2.16\cos\frac{Z}{\pi}\right) + \sin Z\right)e^{0.012Z}\right)}{1.473(1-\sin Z)}$$

a_{zz}	Zenith value of snow-free clear-sky albedo
a_z	Zenith value of clear-sky albedo
a_o	Clear-sky albedo
c_o	Constrained variable (m bar) used in longer equations

5. Estimation of precipitable water vapour and turbidity coefficient (for the month)

$$W = \frac{v_D}{\left(0.49 + \frac{T}{129}\right)}$$

$$c_1 = 21 - T$$

$$0 \le c_1 \le 5$$

$$j = \left(0.5 + 2.5\cos^2 z\right)e^{\left[c_1\left(\frac{p}{p_s}\right)-1\right]}$$

c_1	Constrained variable (^{o}C) used in longer equations
j	Turbidity coefficient
W	Precipitable water vapour (mm)

6. Estimation of the transmittancy of clear skies to direct beam solar radiation and the part of transmittancy that is result of absorption (for the month)

$$\tau = e^{\left[-0.089\left(\frac{\left(\frac{p}{p_s}\right)}{\cos z}\right)^{0.75} - 0.083\left(\frac{j}{\cos z}\right)^{0.90} - 0.029\left(\frac{W}{\cos z}\right)^{0.60}\right]}$$

$$\tau_a = e^{\left[-0.0415\left(\frac{j}{\cos z}\right)^{0.90} - 0.0029^{0.5}\left(\frac{W}{\cos z}\right)^{0.30}\right]}$$

$$\tau_a \geq e^{\left[-0.0415\left(\frac{j}{\cos z}\right)^{0.90} - 0.029\left(\frac{W}{\cos z}\right)^{0.60}\right]}$$

τ_a	part of τ that is the result of absorption
τ	transmittancy of clear skies to direct beam solar radiation

7. Estimation of clear-sky global radiation, incident global radiation and average albedo (for the month)

$$G_o = G_E \tau \left[1 + \left(1 - \frac{\tau}{\tau_a}\right)(1 + a_o \tau)\right]$$

$$G = SG_o + (0.08 + 0.30S)(1 - S)G_E$$

$$a = a_o\left[S + (1 - S)\left(1 - \frac{Z}{330}\right)\right]$$

S	Ratio of observed to maximum possible sunshine duration
a	albedo
G	Incident global radiation (W/m^2)
G_o	Clear-sky global radiation (W/m^2)

8. Estimation of proportional increase in atmospheric radiation due to clouds (for the month)

$$c_2 = 10\left(\frac{v_D}{v} - S - 0.42\right)$$

$$0 \le c_2 \le 1.0$$

$$\rho = 0.18\left[(1-c_2)(1-S)^2 + c_2(1-S)^{0.5}\right]\frac{p_s}{p}$$

c_2	Constrained variable used in longer equations
ρ	Proportional increase in atmospheric radiation due to cloud

9. Estimation of the net long-wave radiation loss for soil-plant surfaces at air temperature (for the month)

$$B = \in \sigma(T+273)^4\left[1 - \left(0.71 + 0.007 v_D \frac{p}{p_s}\right)(1+\rho)\right]$$

$$B \ge 0.05 \in \sigma(T+273)^4$$

B	Net long-wave radiation loss with the surface at air temperature (W/m^2)
$\in$	Surface emissivity
σ	Stefan-Boltzmann constant ($W/m^2\ K^4$)

10. Estimation of the net radiation for soil-plant surfaces at air temperature, the stability factor, the vapour transfer coefficient and the heat transfer coefficient (for the month)

$$R_T = (1-a)G - B$$

$$R_{TC} = R_T$$

$$R_{TC} \ge 0$$

$$\frac{1}{\zeta} = 0.28\left(1 + \frac{v_D}{v}\right) + \frac{\Delta R_{TC}}{\left[\gamma p\left(\frac{p_s}{p}\right)^{0.5} b_o f_Z(v - v_D)\right]}$$

$$\frac{1}{\zeta} \leq 1$$

$$f_T = \left(\frac{p_s}{p} \right)^{0.5} \frac{f_Z}{\zeta}$$

$$\lambda = \gamma p + \frac{4 \in \sigma (T + 273)^3}{f_T}$$

ζ	Stability factor
f_Z	Constant (W/(m^2 .m bar)) used in estimating f_T – changes at below-freezing temperatures
f_T	Vapour transfer coefficient (W/(m^2 .m bar)) between surface and instrument level
γ	Psychrometric constant- changes at below freezing temperature (/^{o}C)
b_o	constant
R_{TC}	R_T with $R_{TC} \geq 0$
R_T	Net radiation for soil-plant surfaces at air temperature (W/m^2)
λ	Heat transfer coefficient (m bar/^{o}C)

11. Iterative solution of vapour transfer and energy balance equation for estimation of equilibrium temperature (for the month)

$$[\delta T_P] = \frac{\left[\frac{R_T}{f_T} + v_D - v'_P + \lambda (T - T'_P) \right]}{\Delta'_P + \lambda}$$

$$T_P = T'_P + [\delta T_P]$$

$$v_P = 6.11 e^{\frac{\alpha T_P}{T_P + \beta}}$$

$$\Delta_P = \frac{\alpha\beta v_P}{(T_P + \beta)^2}$$

v'_P	Trial value of v_P in iteration process
v_P	Saturation vapour pressure at T_P
Δ'_P	Slope of saturation vapour pressure curve at T'_P
Δ_P	Slope of saturation vapour pressure curve at T_P
T'_P	Trial value of T_P in iteration process
T_P	Potential evapotranspiration equilibrium temperature
$[\delta T_P]$	Correction to T'_P in iteration process

12. Estimation of potential evapotranspiration, the net radiation for soil-plant surfaces and wet environment areal evapotranspiration at equilibrium temperature (for the month)

$$E_{TP} = R_T - \lambda f_T(T_P - T)$$

$$R_{TP} = E_{TP} + \gamma p f_T(T_P - T)$$

$$E_{TW} = b_1 + b_2\left(1 + \frac{\gamma p}{\Delta_P}\right)^{-1} R_{TP}$$

$$\frac{1}{2}E_{TP} \le E_{TW} \le E_{TP}$$

R_{TP}	Net radiation for soil-plant surfaces at potential evapotranspiration equilibrium temperature (W/m^2)
b_1	Constant (W/m^2)
b_2	Constant
E_{TW}	Wet-environment areal evapotranspiration (W/m^2)
E_{TP}	Potential evapotranspiration (W/m^2)

13. Estimation of areal evapotranspiration from complementary relationship (for the month)

$$E_T = 2E_{TW} - E_{TP}$$

E_T	Areal evapotranspiration (W/m^2) as indicated as areal actual evapotranspiration (AAET)

The latent heat of vaporization or sublimation is used for converting the evapotranspiration from the power units to depth unit.

As stated earlier, this monthly values are then converted to daily values by retaining the monthly structure of AAET.

Appendix B: Types of time series model and some relevant concepts

Time series models can be classified according to the number of variables included in the model. A time series model consisting of just one variable is called a *univariate* time series model. A univariate time series model will use only current and past data on one variable. Implicit in the formulation of such a model is the assumption that factors which influence the variable have not changed or are not expected to change sufficiently to warrant introducing these explicitly into the model (Vandaele 1983).

A time series model, which makes explicit use of other variables to describe the behaviour of the desired series, is called a *multivariate* time series model. The model expressing the dynamic relationship between these variables is called *transfer function noise model.* The terms transfer function noise model and multivariate time series model are sometimes used interchangeably but in this work we indicate transfer function model as the model, which have a dependent variable, and one or more explanatory variable. On the other hand in multivariate time series model, there may be a system of simultaneous regression models where the relationship between input and output consists of time–lagged input (exogenous variable) as well as time-lagged output (endogenous variable) (Ostrom 1990).

A transfer function noise model is related to the standard regression model (Hildebrand et al. 1977) in that both have a dependent variable and one or more explanatory variable. But a transfer function model can allow for a richer dynamic structure in the relationship between the dependent variable, and each explanatory variable, and between the error term (Vandaele 1983).

Regression models with time-lagged inputs are called *distributed lag* models. The word "rational" here refers to a mathematical *ratio* (Pankratz 1991). This model is named as *multiple regression* model. The representation of GWL as a dynamic regression of rainfall has been done by (Haugh and Box 1977; Adamowski and Hamory 1983; Viswanathan 1984). Similar type of representation done for snow cover as a function of precipitation, temperature etc. by Dahe et al. (2006) by using multiple regression models. Thus many investigators have used the technique of using multiple regression and Auto Regressive Moving Average (ARMA) model since the introduction of time series in hydrologic data analysis (Kerr *et al.* 2002; Dahe *et al.* 2006).

In multiple regression, $Y= a+ b_1X_1+b_2X_2+b_3X_3$ type of equation is developed, where the X's are independent variables (IVs) and Y is the dependent variable (DV). The strength and weakness of various independent variables are indicated by the coefficients and Beta values whereas the quality of fit is indicated by R^2 as well.

The scale upon which the IVs were measured influences the slope, indicated by the values of (b_1, b_2 …). As different IVs may be measured on scales of very different units, it is very difficult to compare their relative importance. The use of standardised regression coefficient 'Beta' allows meaningful comparisons regarding the degree of predicted change on the DV associated with changes in a number of IVs. The variable with the largest 'Beta' will have the most relative influence on the DV (Kerr *et al.* 2002).

Auto Regressive Moving Average (ARMA (p,q)) model

In an ARMA model, the series to be forecast is expressed as a function of both previous values of the series (auto-regressive terms, *p*) and previous error values from forecasting (the moving average terms, *q*). Let us assume $\{X_t\}$ is an ARMA *(p,q)* process if $\{X_t\}$is stationary and if for every *t*,

$$X_t - \phi_1 X_{t-1} - .... - \phi_p X_{t-p} = Z_t + \theta_1 Z_{t-1} + ...\theta_q Z_{t-q}$$

where, $\{Z_t\} \sim WN(0,\sigma^2)$ and the polynomials $(1 - \phi_1 z - \ldots - \phi_p z^p)$ and $(1 + \theta_1 z + \ldots \theta_q z^q)$ have no common factors.

A first-order autoregressive model was used to describe the response of the water table in a borehole to a series of rainfall events (Rennolls et al. 1980; Parlange et al. 1992). ARMA models are investigated in this work as univariate process and multivariate AR (MAR) process. The transfer function noise (TFN) models are also investigated, developed and compared for the prediction performances for the site. The comparative analyses of the performance of MAR and TFN is also detailed in chapter 6.

Relation between multivariate MA prediction and multiple regressions

The multivariate prediction analysis methods are analogues of conventional regression – correlation methods with important differences and Hildebrand (1977) explains the contrasts in detail. It refers to two basic components of multivariate prediction analysis such as prediction rule and a prediction success measure whereas the conventional model

represented by prediction equation determined by multiple regression and an evaluation of the prediction being given by the R^2 value in multiple regression.

The contemporaneous ARMA or CARMA, family of models is designed for modelling two or more time series that are statistically related to one another only because they represent the processes of same time i.e.; simultaneous processes (Hipel and McLeod 1994). The groundwater fluctuation in a number of bores located at the unconfined shallow aquifer system or partially confined system surrounding the Ranger site should be represented as the CARMA model in the current research. For example the selected bores for the present research such as OB1A, OB20, Ob43 and OB27 form CARMA model for the site as described in chapter 6.

Some relevant concepts for time series

Coefficient of correlation

While linear relationship is considered between two variables such as net flux (X) and GWL (Y), the relationship can be represented with equation of linear regression, the equation structure being Y = bX + a. To assess the predictive value of the regression line a measure of the strength of the relationship between the two variables is necessary. The nature of the relationship is represented by correlation coefficient (r). One way of obtaining a measure of r is

$$r = \mathrm{cov}\,ariance(X,Y)/([\mathrm{var}\,iance(X)][\mathrm{var}\,iance(Y)])^{1/2}$$

The estimation of variance and covariance for the set of X and Y values can be found from any text book of statistics. The value of r varies between -1 to +1. The signs indicate the direction of relationship; positive sign indicates the two variables covary in the same direction. 0 values indicate there is no correlation between the two variables. r^2 value multiplied by 100 is called coefficient of determination. It expresses the amount of the variance on one dimension that can be explained or accounted for by the variance on the other dimension.

Autocorrelation and cross correlation

Autocorrelation: This term is used to describe the association or mutual dependence between values of the time series at different time periods. It is similar to correlation, but relates the series for different time lags. Auto covariance function, and autocorrelation

function (ACF) (Brockwell and Davis 2002) is always related to a specific time lag and the pattern of variation of ACFs are plotted graphically for different time lags to assess the important statistical characteristics of the time series process such as to identify whether or not seasonality is present in a given time series and the length of that seasonality, to identify appropriate time-series models for specific situations, and to determine the stationarity in the data (Makridakis and Wheelwright 1978).

Partial autocorrelation: The partial autocorrelation function (PACF) is a measure of correlation which is used to identify the extent of relationship between current values of a variable with earlier values of that same variable (values for various time lags) while holding the effects of all other time lags constant (Brockwell and Davis 2002).

Cross correlation: The cross correlation function (CCF) perform the same function in multivariate time-series analysis as auto-correlation performs for univariate time-series analysis. The estimations of ACF and PACF of univariate analyses and CCF in multivariate analyses are done for innovating appropriate class and type of model (Box and Jenkins 1976; Welsh and Stewart 1991).

Stationarity

Stationarity of a stochastic process can be qualitatively interpreted as a form of statistical equilibrium. Therefore, the statistical properties of the process are not a function of time. Stationarity is analogous to the concept of isotropy within the field of physics. In order to be able to derive physical laws that are deterministic, it is often assumed that the physical properties of a substance are the same regardless of the direction or location of measurement (Hipel and McLeod 1994). Similarly for our purpose a stationary process is one whose *mean, variance* and *autocorrelation function* are constant through time. Our notion of stationarity is a *weak* form. There is also a *strong* form, which requires that, the entire probability distribution function for the process is independent of time. For practical reasons it is common to work with the weak form. If the random shocks are normally distributed, then the two forms are identical (Pankratz 1991).

Some researchers believe that natural processes are inherently nonstationary and therefore the greater the time span of the historical series, the greater is the probability that the series will exhibit statistical characteristics which change with time. However, for relatively short time spans it is feasible to approximately model the given data using a stationary stochastic model. Nevertheless, the reverse position may seem just as plausible to other scientists.

Apparent nonstationarity in a given time series may constitute only local fluctuation of a process that is in fact stationary on a longer time scale (Hipel and McLeod 1994). Therefore, to encompass both of the viewpoints, a combination of model (TFN Model 1, TFN Model 2 and AR Model 3) has been developed. When dealing with yearly hydrological and other kinds of natural time series of moderate time spans, it is often reasonable to assume that the process is approximately stationary (Yevjevich, 1972, page 68 of (Hipel and McLeod 1994)).

Whiteness of residual

The comparison of the performance of a number of models is usually done by looking at the residual variances. Model with least residual variance represents best fit. To compare the models, it is convenient to work with whitened process for two reasons. The structure of the model (such as AR model, integrated autoregressive IAR model, model with log transformed values etc) influences the residual variances. Hence inferences based on a model with incorrect structure can be only of dubious value. Secondly the regression theory and the associated statistics are valid only if independent and identically distributed observations are used for both regressed and regressor variables (Kashyap and Rao 1976).

The white noise components as assumed to be independently distributed, a recommended procedure for checking the whiteness assumption is to examine a plot of the residual ACF along with confidence limits (Hipel and McLeod 1994; Brockwell and Davis 2002). The plot of residual ACF is the best whiteness test to use as described in (Brockwell and Davis 2002). Hence finally residual correlations and cross-correlations are computed for model checking by performing the ACF plot.

Cointegration and others

Cointegration is an econometric technique for testing the correlation between non-stationary time series variables. If two or more series are themselves non-stationary, but a linear combination of them is stationary, then the series are said to be cointegrated. Spurious correlation occurs when the sample size is small, and the R^2 metric is misleading i.e. there is a high likelihood that the fit occurred purely by chance. Hence to handle the concept of cointegration with caution, we apply appropriate transformation for converting any non stationarity for instance in the hundred years monthly time series, because there

are serious obligations imposed to identify cointegration before doing the multivariate time series analyses (Engle and Granger 1987).

The other relevant and important concepts include *causality* (Cromwell et al. 1994) and *invertibility* of ARMA representation (Kashyap and Rao 1976), *feedback* check of univariate ARMA representation (Pankratz 1991), *parsimony* of model (Vandaele 1983), *stability* of system (Kaplan 1962), detecting *chaos* and *nonlinearity* of past data (Kaplan and Glass 1995), using *physical approach* to suggesting useful interesting statistical models (Tong 1990). Most of these concepts are taken care by applying the knowledge of the physical laws and practical information instead of performing traditional statistical tests or diagnostic checks as applicable for data with least information about the attributes to the system.

Appendix C: SILO climate data

See the attached CD

Appendix D: Ranger bore data

See the attached CD

Appendix E: Australian Water Balance Model (AWBM)

The conceptual framework of AWBM consists of the following system of representation of the hydrologic system of a catchment.

1. Rainfall – Evapotranspiration = Effective rainfall (deterministic)
2. Effective rainfall = Surface Storage (function of A1, A2, A3 and C1, C2, C3) + Excess
3. Excess = Surface Runoff + Base flow Recharge (function of BFI)
4. **Base flow Recharge** = Base flow + Base flow Store (function of K_{base})
5. Total runoff = Base flow + Surface Runoff (function of K_{surf})

The rainfall excess produced from surface stores is splitted and routed as either surface flow or base flow and then combined together to form total runoff Figure 1. The following equations describe the procedure. Moisture in surface storages are represented as a combination of three different storage capacities per unit area (C1, C2 and C3) and three proportions (A1, A2 and A3) of areal extents respectively.

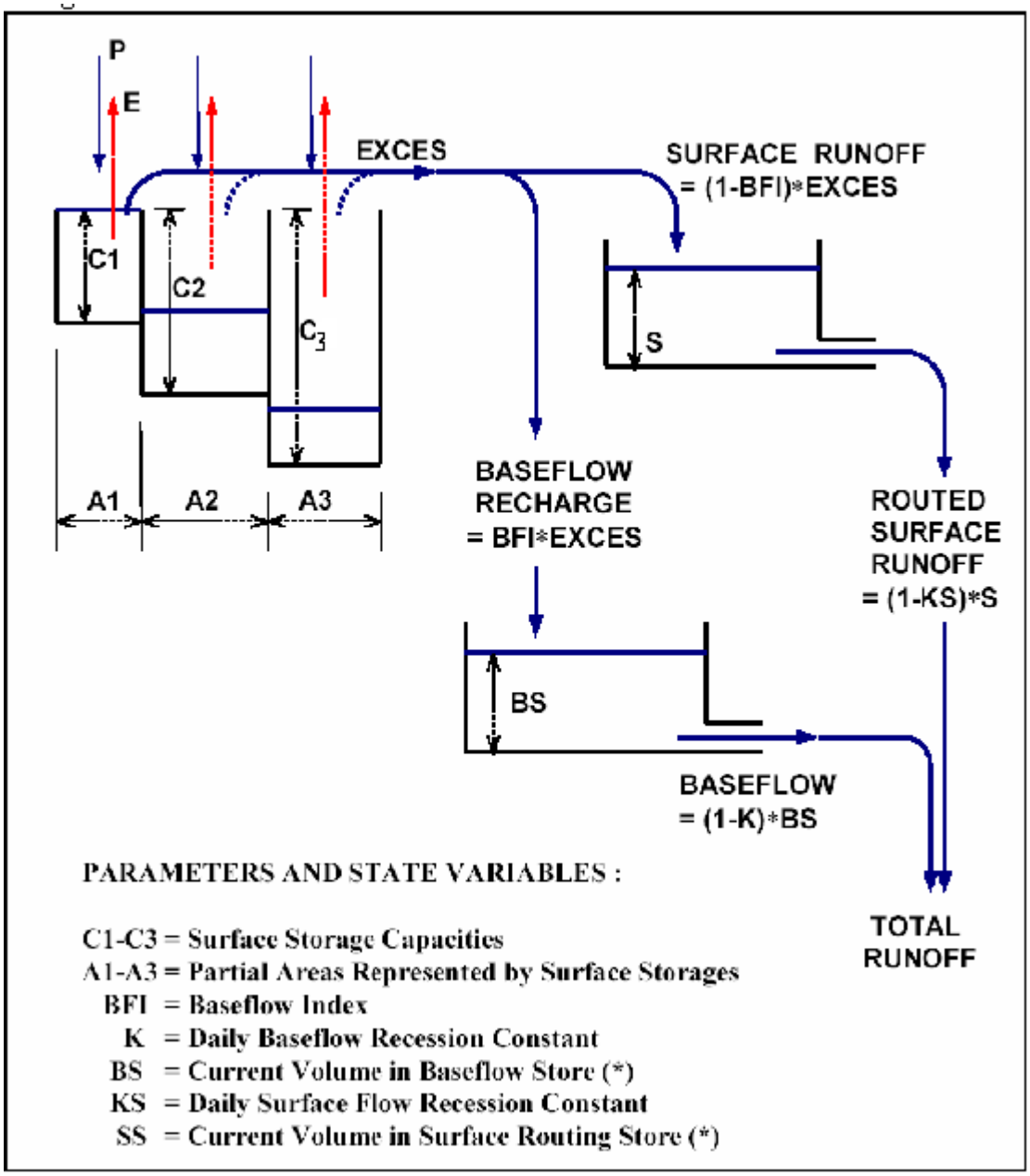

Figure 1 Conceptual diagram of the Australian Water Balance Model (AWBM) (Podger 2004)

Selection of calibration procedure: The AWBM framework provides both manual and automatic procedures for model calibration. In manual calibration, the number of parameters is eight (A1, A2, BFI, C1, C2, C3, $K_{base,}$ K_{surf}). The sensitivity of one particular parameter depends on the values of the remaining parameters making the calibration procedure quite complex (Podger 2004). Thus the non-linear relation between the substantial numbers of calibration parameter is the major disadvantage of manual calibration. This disadvantage is reduced in the automatic calibration procedure. Hence the automatic calibration procedure is preferred for the study.

In automatic calibration procedure, there are two options such as

1. Custom calibration
2. Generic calibration.

Custom calibration: The AWBM Custom calibration is a specific facility written to automatically calibrate the AWBM model. The automatic calibration procedure follows predefined optimisation method and it consists of two step computations. In the first step preset values of BFI, K_{base} and K_{surf} are used and the average surface store capacity C_{ave} is verified by trial and error until the modelled runoff closely matches with observed runoff. In the second step, the parameters BFI, K_{base} and K_{surf} are optimised using the specific objective function (Boughton 2002). The record of daily rainfall, evapotranspiration and runoff being available, the objective function adequately utilizes the available data for model fitting indeed.

Based on the knowledge gained from many previous AWBM applications, the automatic calibration procedure incorporates fixed proportion of area as A1: A2: A3 as 0.134: 0.433: 0.433 and fixed proportion of surface store capacities as C1: C2: C3 as 0.075: 0.762: 1.524 (Podger 2004).

Generic calibration: The Generic calibration procedure gives options for seven different optimisation algorithms. From the seven different optimisation algorithm, Shuffled Complex Evolution (SCE-UA) method of optimisation is selected as this is a combination of deterministic and probabilistic approaches (Duan 1994; Podger 2004). There are also options for two objective functions, one to be selected from 8 primary objective functions and another to be selected from 4 secondary objective functions in Generic calibration procedure.

From the observation of the 8 primary objective functions, the Nash-Sutcliffe criterion is selected to be best to fulfil the purpose of modelling. The other objective functions do not consider the mean observed value of runoff in the expression of the function. The significance of considering mean observed flow in the expression of objective function is discussed later. The objective function such as Nash-Sutcliffe Criterion (E) for model calibration is expressed in the following equation.

$$E = 1 - \frac{\sum_{i=1}^{t}\left((x_i obs - x_i sim)^2\right)}{\sum_{i=1}^{t}\left((\bar{x} obs - x_i obs)^2\right)}$$

x_i obs= observed value

x_i sim=simulated value

$\bar{x}$ obs = mean observed value

a) Selection of primary objective function: Considering the flow distribution of the site, it can be seen that the runoff in Magela creek is very much uneven throughout the year. The typical wet season is from November to April and Magela creek starts to flow after 200mm of rainfall. The annual average rainfall is 1548mm (1971 to 2005). It can be also found from the Figure 2 that the flow in the Magela creek at the station GS821009 is highly fluctuating with no flow during the dry season, mean observed flow 1.65 mm/day and peak values up to more than 100 mm/day. The flow distribution of observed runoff has high kurtosis value 113 indicating sharp peak and flat tail. Kurtosis characterizes the relative peaked ness or flatness of a distribution compared with the normal distribution. Positive kurtosis indicates a relatively peaked distribution. Negative kurtosis indicates a relatively flat distribution.

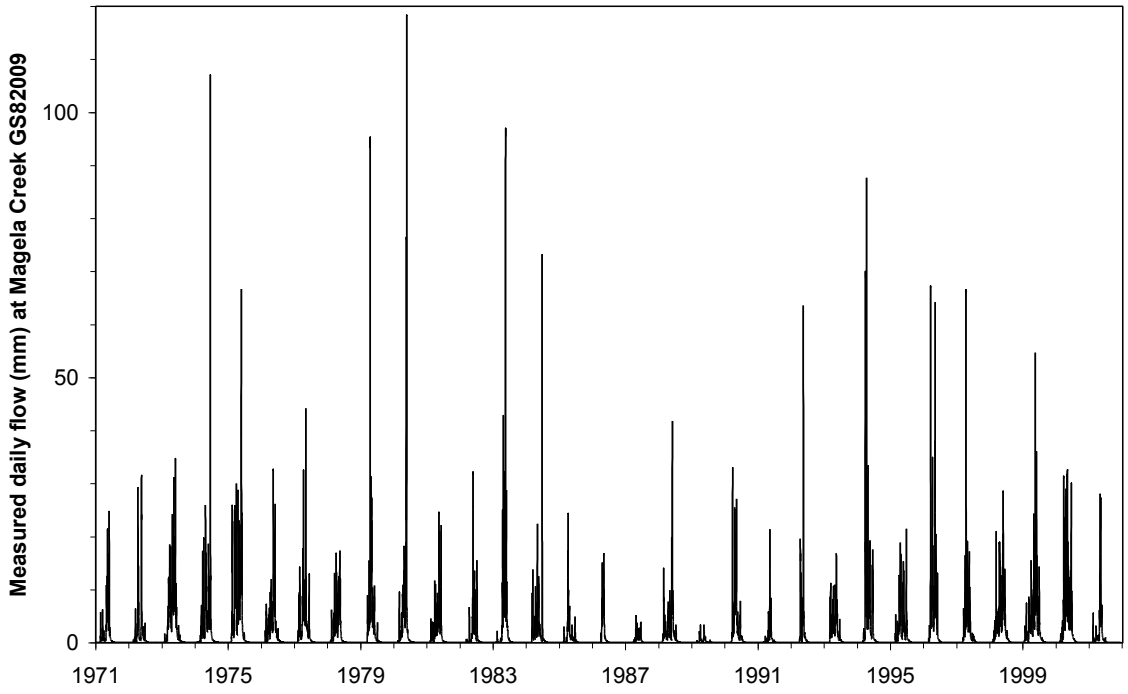

Figure 2 Flow variation in the Magela creek.

Hence the consideration of mean observed flow value in the calibration function such as Nash-Sutcliffe to represent a flow which is very much different from even distribution in time domain, will eventually give more weighage to smaller flow than larger flow indeed. It is also stated by Boughton (2002) that the **automatic calibration procedure** places more weight on smaller flow values as the Nash- Sutcliffe criterion is the only available calibration function in there.

b) Selection of secondary objective function: The prime objective of water balance modelling is the computation of base flow recharge which is generated from base flow as shown in the structure of AWBM. Hence the secondary objective function is selected to be the Base flow Method 2 which has been described in (Grayson et al. 1996).

Conclusion of selection of calibration procedure: There had been a number of model runs with different set of input data, different calibration methods and different objective functions for optimisation. While using the generic calibration considering the secondary objective function as Base flow Method 2 (Grayson et al. 1996) , the Nash Sutcliffe criteria improves very little (from 0.55 to 0.56, 0.57. 0.58) but the relative difference in flow between observed and calculated value increases from 0.61% to 28.1%. Some of the results are shown in Table 1.

Table 1 Selection criteria for automatic calibration method

Method of calibration	Objective function	Nash-Sutcliffe Criteria	Flow Difference	Correlation
Custom Calibration (AWBM auto calibration)	Nash-Sutcliffe Criteria	.55	0.61 %	.74
Generic Calibration	Nash-Sutcliffe Criteria and Baseflow method 2	.56-.58	28.1 %	.75-.76

From the modelling experience the best-suited method of calibration was selected as the AWBM auto calibration. The criteria of selection were, higher value of Nash-Sutcliffe criterion, minimum error with the observed and computed runoff, and eventually all other

water balance components. Moreover the auto calibration was faster than the other calibration methods. Hence auto calibration method was selected finally.

Data requirement for AWBM: As shown in the structure of AWBM, the input data required in running the model are three set of flow data such as daily rainfall, daily evapotranspiration, and daily runoff. No monthly scaling factor is used to either rainfall or evapotranspiration estimates as daily Areal Actual Evapotranspiration (AAET) is used rather than using pan factor and pan evaporation data. It should be mentioned that if the evapotranspiration are potential values, then the scaling factors are used to convert them into actual values, but if the evapotranspiration are actual values then scaling factors are not required. When the flow values are in volume per unit time, then area of catchment is required to convert those into depth per unit time values. The time series flow data are available in terms of depth per unit time and therefore the catchment area is not required.

Representation of Evapotranspiration across the catchment: The options for representing the catchment evapotranspiration by combining the concepts of scale factors of AWBM with the earlier available techniques such as to monthly values of pan factors (Chow et al. 1988; Chiew and Wang 1999) and "ET ratio" used in this study is investigated. The "ET ratio" as used in this thesis is the ratio between the areal value of actual and potential evapotranspiration. In Table 2, the numerical values of pan factors i.e. "Pan Coefficient or Pan Factor" for Jabiluka site used by Chiew and Wang (1999) has been compared to the ET ratio for Ranger site. The data from "Evapotranspiration map of Australia" i.e., Wang et al (2002) has been used to obtain the values of ET ratio. Various ET variables are available for the whole Australia in the source of Wang et al (2002) and those are long term monthly averages.

From the table below, it is clear that these two methods are giving comparable but different estimation of open water evaporation (column 4) and areal actual evapotranspiration (column 5) and as a third choice considered is the latest available Morton's areal actual evapotranspiration data available in (SILO 2006) with no scaling factor. A comparison have been performed between this average monthly ET data of (Wang *et al.* 2002) and the average monthly ET data for the site obtained from (SILO 2006) which has already been discussed in earlier section of this chapter and also in (Kabir *et al.* 2007). Based on these three alternative set of data as evaporation (one set) and evapotranspiration (two sets)

the latest available Morton's areal actual ET (AAET) is selected which is daily time series data to compute the water balance components for the site by using AWBM.

Table 2 Numerical comparison of monthly ET ratio and Pan Coefficient for Ranger

Month	Observed Pan Evaporation (mm) (Chiew and Wang 1999)	Pan Coefficient for converting Pan Evaporation to Open Water Evaporation (Chiew and Wang 1999)	Open Water Evaporation = Observed Pan Evaporation x Pan Coefficient (mm)	Average Areal Actual Evapo-transpiration (mm)(Wang et al. 2002)	Average Areal Potential Evapo-transpiration (mm)(Wang et al. 2002)	ET ratio for converting Potential ET to Actual ET
Col (1)	Col (2)	Col (3)	Col (4) = Col (2) x Col (3)	Col (5)	Col (6)	Col (7) = Col (5) / Col (6)
January	184	0.92	169.28	120.6	210	0.57
February	156	0.92	143.52	96.9	165	0.59
March	175	0.95	166.25	133.8	225	0.59
April	203	0.77	156.31	94.9	180	0.53
May	216	0.7	151.2	68.4	150	0.46
June	204	0.7	142.8	51.4	135	0.38
July	216	0.66	142.56	46	130	0.35
August	247	0.64	158.08	61.2	150	0.41
September	268	0.66	176.88	79	180	0.44
October	288	0.66	190.08	96.9	210	0.46
November	244	0.75	183	97.5	195	0.50
December	212	0.84	178.08	117	220	0.53

Input data: The analysis by the use of AWBM was performed using three different sets of data. With the three daily time series data such as rainfall, runoff and evapotranspiration, various sources of data have been considered. The daily rainfall and AAET data are available from Jabiru Airport Station 14198 of BoM. The daily runoff is available from the gauge station GS821009 in the catchment of Magela creek.

A brief outline is given in the Table 3.

Table 3 Input data description of the model runs by AWBM

	Rainfall and runoff data	Evapotranspiration data and scaling factor	Comments on catchment and unit of data
Model run 1	Existing data of RRL (Podger 2004)	Daily potential evapotranspiration (Podger 2004) and ET ratio (Wang *et al.* 2002)	Catchment area 260 Km^2 with gauging station at GS821007, Rainfall, ET and Runoff in mm/d
Model run 2	Rainfall data from Jabiru Airport (SILO 2005) and runoff data from station GS821009	Daily pan evaporation (SILO 2005) and monthly pan factor (Chiew and Wang 1999)	Catchment area 600 Km^2 with gauging station at GS821009, Rainfall and ET in mm/d, Runoff in cumec
Model run 3	Same as above	Daily Morton actual evapotranspiration (SILO 2006) and no scaling factor	Same as above

The data used for long-term average computation consist of daily rainfall (mm/day), daily AAET (mm/day), daily-observed runoff (mm/day). The period of data analysed is from 25/09/1971 to 13/03/2005 in Model run 3. By comparing the model performances of these three runs in terms of calibration criteria, the numerical performance of the Model run 3 by the AWBM is reported finally. The calibration period is from 16/04/1972 to 24/09/2002 and verification period is 10/03/2003 to 13/03/2005. The calibration result is used for developing the conceptual model of the site.

Appendix F: GWL Charts for the monitoring bores

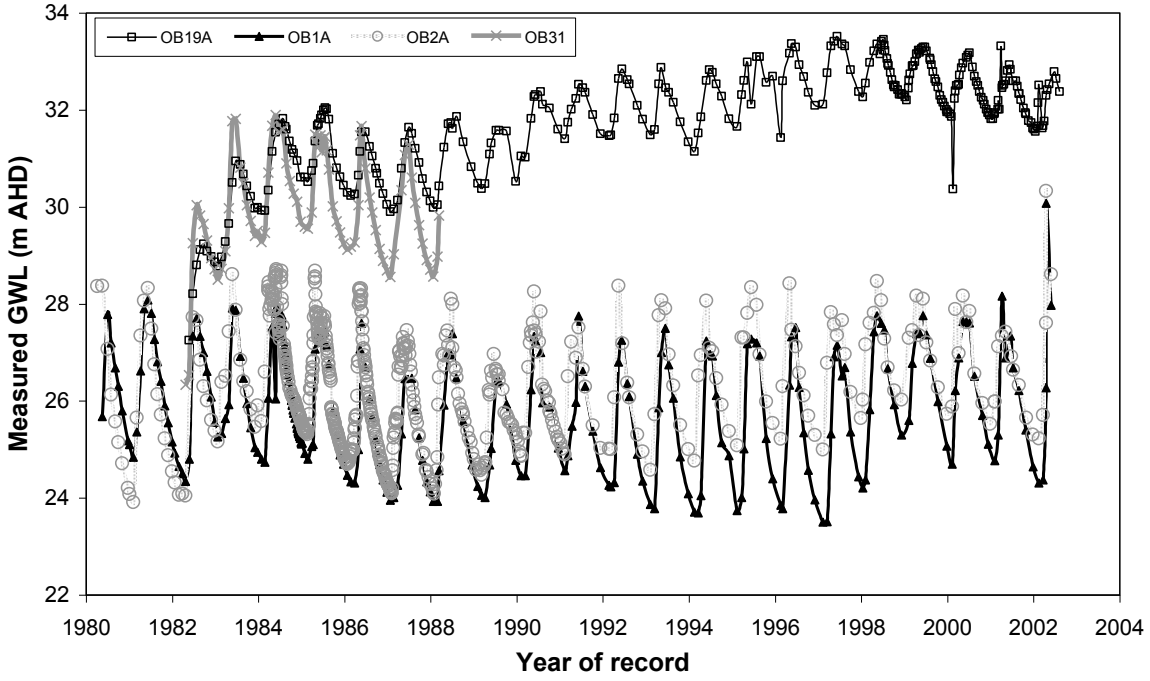

Figure 1. Measured GWL (m AHD) for bores OB19A, OB1A, OB2A and OB31

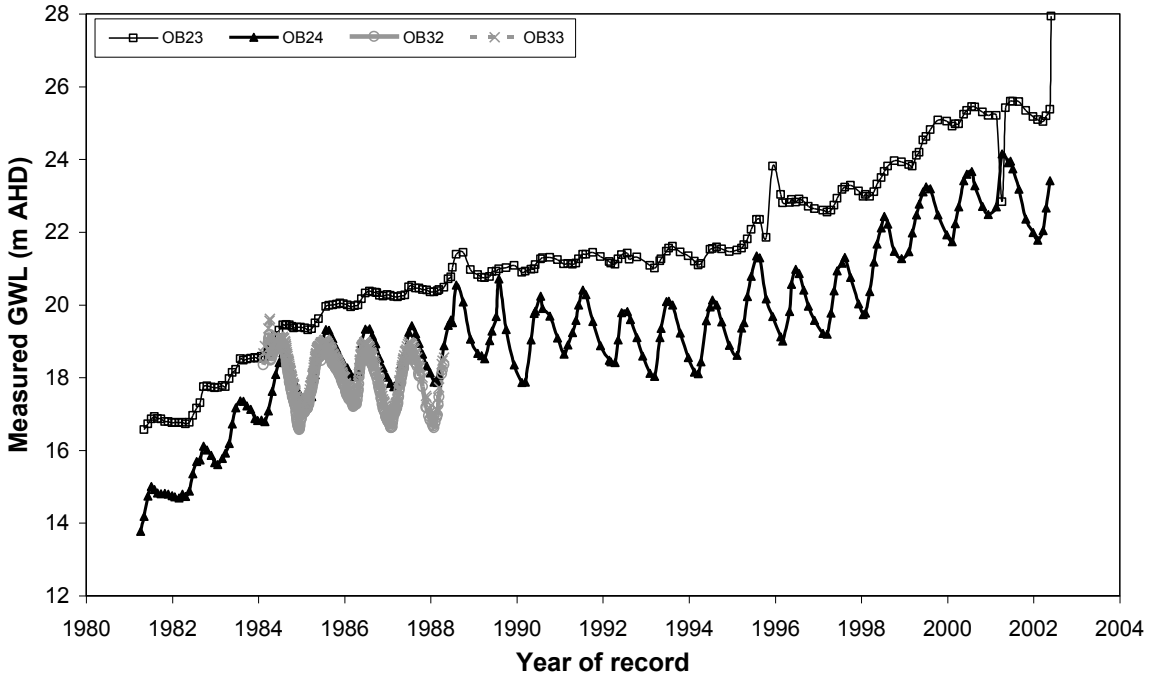

Figure 2. Measured GWL (m AHD) for bores OB23, OB24, OB32 and OB33

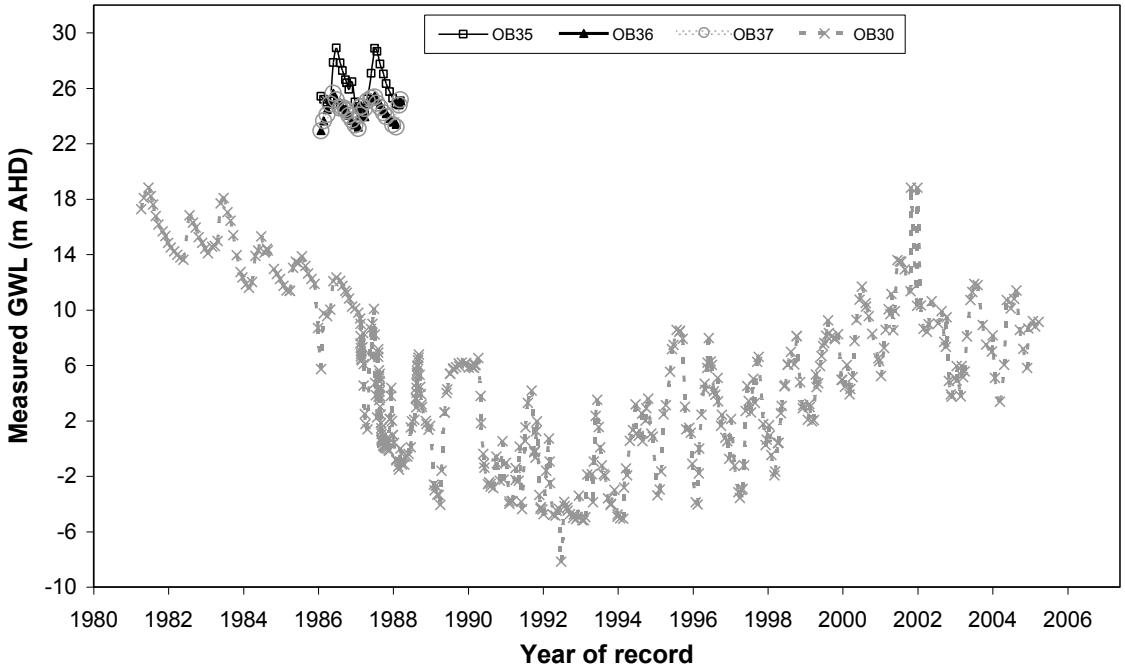

Figure 3. Measured GWL (m AHD) for bores OB35, OB36, OB37 and OB30

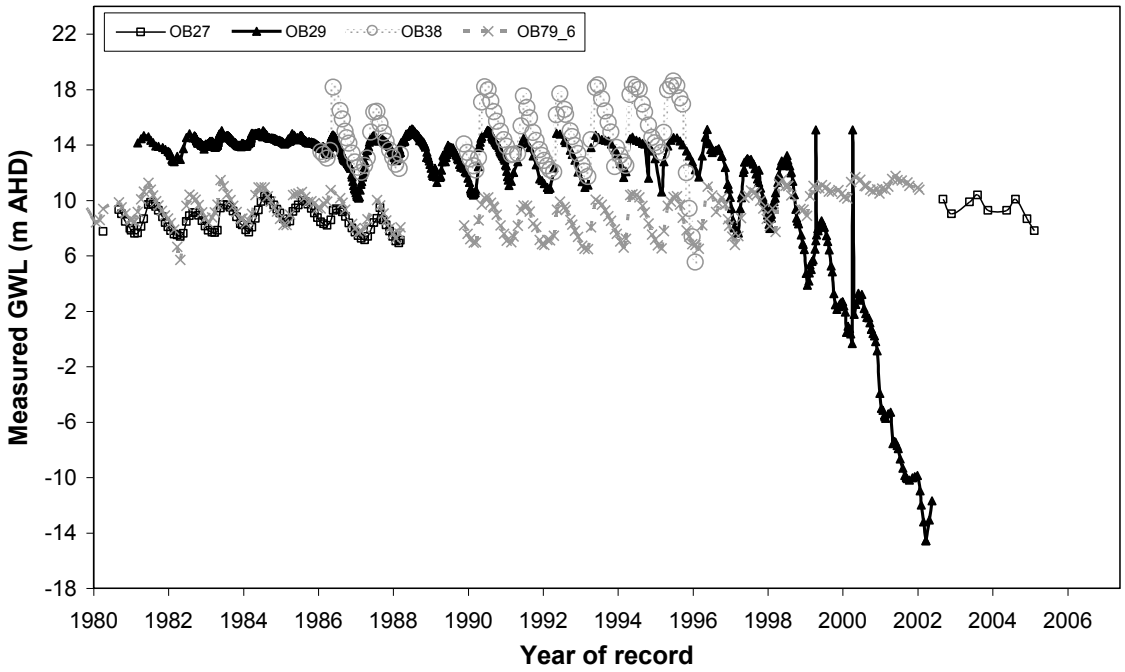

Figure 4. Measured GWL (m AHD) for bores OB27, OB29, OB38 and OB79_6

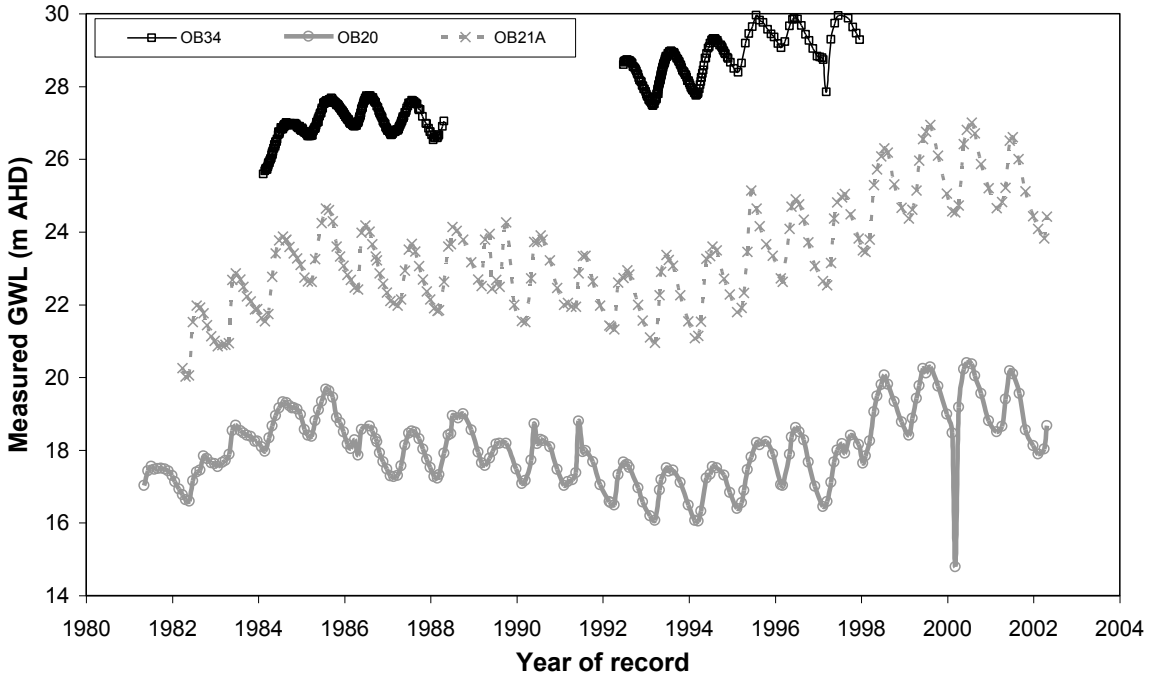

Figure 5. Measured GWL (m AHD) for bores OB34, OB20 and OB21A

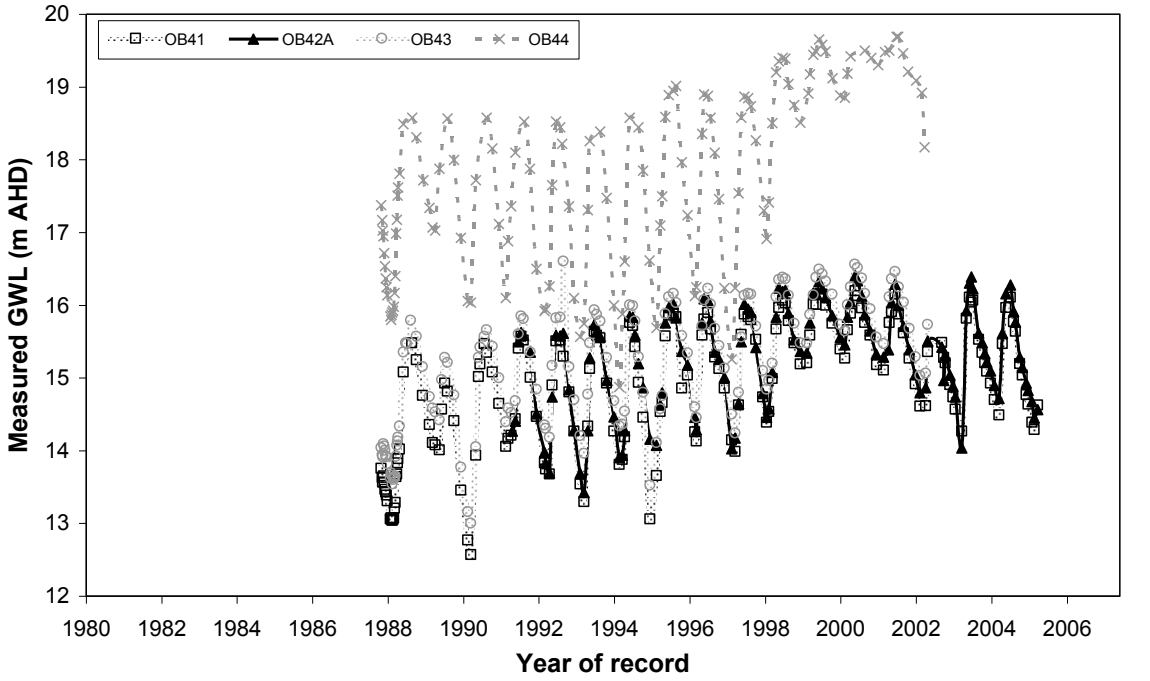

Figure 6. Measured GWL (m AHD) for bores OB41, OB42A, OB43 and OB44

Appendix G: Emission scenarios and evapotranspiration data for GCMs

Emission scenarios (IPCC 2001a)

The following descriptions about the emission scenarios are copied from (IPCC 2001a).In 1992 the Intergovernmental Panel on Climate Change (IPCC) released six emissions scenarios (Leggett *et al*., 1992) providing alternative emissions trajectories spanning the years 1990 through 2100 for greenhouse-related gases, Carbon dioxide (CO_2), carbon monoxide (CO), methane (CH_4), nitrous oxide (N_2O), nitrogen oxide (NO_x), and sulfur dioxide (SO_2). These scenarios were intended for use by atmospheric and climate scientists in the preparation of scenarios of atmospheric composition and climate change. The work updated and extended earlier work prepared for the IPCC first assessment report. These six scenarios are referred to as the IS92 scenarios.

These scenarios have been widely used in the analysis of possible climate change, its impacts, and options to mitigate climate change. In 1995, the IPCC 1992 scenarios were evaluated. The evaluation recommended that significant changes (since 1992) in the understanding of driving forces of emissions and methodologies should be addressed. These changes in understanding relate to, e.g., the carbon intensity of energy supply, the income gap between developed and developing countries, and to sulphur emissions. This led to a decision by the IPCC Plenary in 1996 to develop a new set of scenarios named as Special Report on Emissions Scenarios (SRES).

The **SRES Marker Scenario A1 storyline and scenario family** describes a future world of very rapid economic growth, global population that peaks in mid-century and declines thereafter, and the rapid introduction of new and more efficient technologies. Major underlying themes are convergence among regions, capacity building, and increased cultural and social interactions, with a substantial reduction in regional differences in per capita income. The A1 scenario family develops into three groups that describe alternative directions of technological change in the energy system.

The **A1B group** is based on the **A1 storyline and scenario family** but describes a balance across all energy sources.

The **A1FI group** is based on the **A1 storyline and scenario family** but describes an alternative direction of technological change in the energy system by emphasizing fossil-fuel intensity.

The **A1T group** is also based on the **A1 storyline and scenario family** but emphasizes predominately non-fossil energy resources.

The **SRES Marker Scenario A2 storyline and scenario family** describes a very heterogeneous world. The underlying theme is self-reliance and preservation of local identities. Fertility patterns across regions converge very slowly, which results in continuously increasing global population. Economic development is primarily regionally oriented and per capita economic growth and technological change is more fragmented and slower than in other storylines.

The **SRES Marker Scenario B1 storyline and scenario family** describes a convergent world with rapid change in economic structures, "dematerialization" and introduction of clean technologies. The emphasis is on global solutions to environmental and social sustainability, including concerted efforts for rapid technology development, dematerialization of the economy, and improving equity.

The **SRES Marker Scenario B2 storyline and scenario family** describes a world in which the emphasis is on local solutions to economic, social, and environmental sustainability. It is a world with continuously increasing global population at a rate lower than A2, intermediate levels of economic development, and less rapid and more diverse technological change than in the B1 and A1 storylines. While the scenario is also oriented toward environmental protection and social equity, it focuses on local and regional levels.

Evapotranspiration data for GCMs: Estimating AAET from PPET

The Ozclim source as used during the period of the intended research (2006-07) had the various hydrologic variables. The rainfall and evapotranspiration data were needed and those data are used to estimate the net flux. By email correspondence with CSIRO, it was learned that the evapotranspiration data as supplied by Ozclim was point potential evapotranspiration (PPET or M_{pot}) while the estimation of net flux requires areal actual evapotranspiration (AAET or M_{act}). Therefore it was necessary to estimate the AAET data for net flux calculation from the available PPET of Ozclim.

A number of exploratory data analyses procedures were investigated to identify the most appropriate relationship between these two variables (PPET and AAET) as found from the historical data set of SILO. It was found that the correlation between the past data of AAET and PPET as available in SILO PPD source could be used for the estimation of AAET. The description of the two sources such as SILO PPD and Ozclim, the two ET variables such as PPET and AAET and two periods of availability such as past and future are given in Table 1. It can be seen that both the past AAET and PPET data are available in SILO PPD for the site. The data are tabulated with the variable name as M_{act} and M_{pot} respectively as used in the SILO database. But only PPET data is available in Ozclim for the future and future AAET data were needed for net flux calculation.

Table 1 Description of ET variables of Morton as available in SILO PPD and OZCLIM

ET variable	Source of data	Period of analyses
Mact = Morton areal actual evapotranspiration over land = AAET	SILO PPD available	(1900 – 1999)
	Required to be estimated for Ozclim	(2000 - 2100)
Mpot = Morton point potential evapotranspiration over land = PPET	SILO PPD available	(1900 – 1999)
	Available in Ozclim	(2000 – 2100)

Method of past data analysis: To investigate the relationship between PPET and AAET, the monthly totals for 1900 to 1999 year have been computed. The linear correlation analyses between PPET along X-axis and AAET along Y-axis have been performed for all the twelve months. The correlation is good only for four wet months (December-J-F-March). The remaining eight months have little or no correlation Figure 0.

Similarly for 1970 to 2006 year have been computed in parallel Figure 2 because the Jabiru airport weather station started to operate in 1970 and the data before 1970 had been interpolated from those of Darwin and Oenpelli by the BoM source. All the results of the slope, intercepts and R^2 for the lines of correlation are presented in Table 2. From the result it has been found that there is no significant difference between the pattern of variation of monthly PPET and AAET. Thus the correlation is good for four wet months (Dec-Mar) with positive correlation and moderate for four dry months (Jun-Sep) with negative

correlation. The remaining four months, consisting of two pre monsoon transitional months and two post monsoon transitional months (Oct-Nov, Apr-May) have little or no correlation.

The equations of the lines of correlation for the twelve months have been analysed and the Figure 3 and Figure 4 show the typical variation in the coefficients (slopes and intercepts) of the equation Y=slope*X + Intercept. Figure 5 showing the variation of the coefficients for different months. The twelve months have been classified into wet, post monsoon, dry, and pre monsoon periods of the year.

Table 2 Y is the actual ET and X is the PPET of Morton for 1970 to 2006.

Months	Y=slope*X + Intercept		R^2
	Slope	Intercept	
Jan	0.68	15.38	0.63
Feb	0.68	20.78	0.82
Mar	0.71	7.80	0.74
Apr	0.18	82.43	0.05
May	-0.44	193.62	0.14
Jun	-0.69	213.45	0.34
Jul	-0.60	204.25	0.34
Aug	-0.87	315.24	0.67
Sep	-0.46	243.14	0.26
Oct	-0.10	170.82	0.02
Nov	0.13	108.45	0.07
Dec	0.40	59.07	0.54

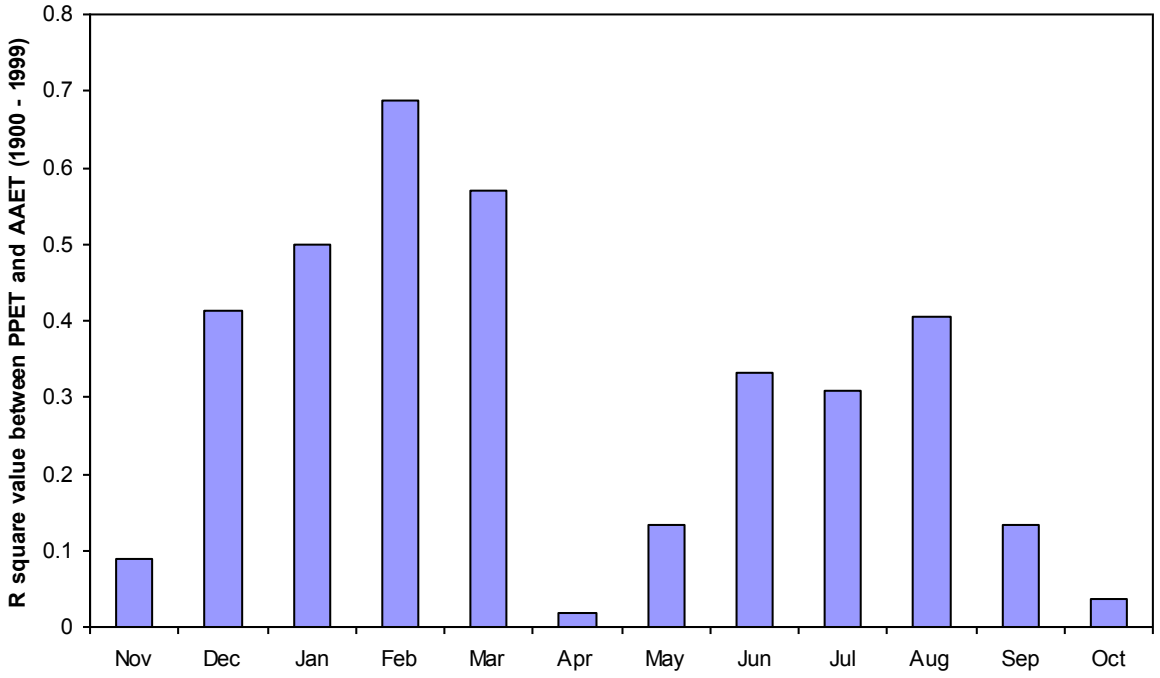

Figure 0. wet months (DEC_MAR) have positive correlation, dry months (JUN_SEPT) have negative correlation, pre and post monsoon months have little correlation between PPET and AAET (1900 – 1999).

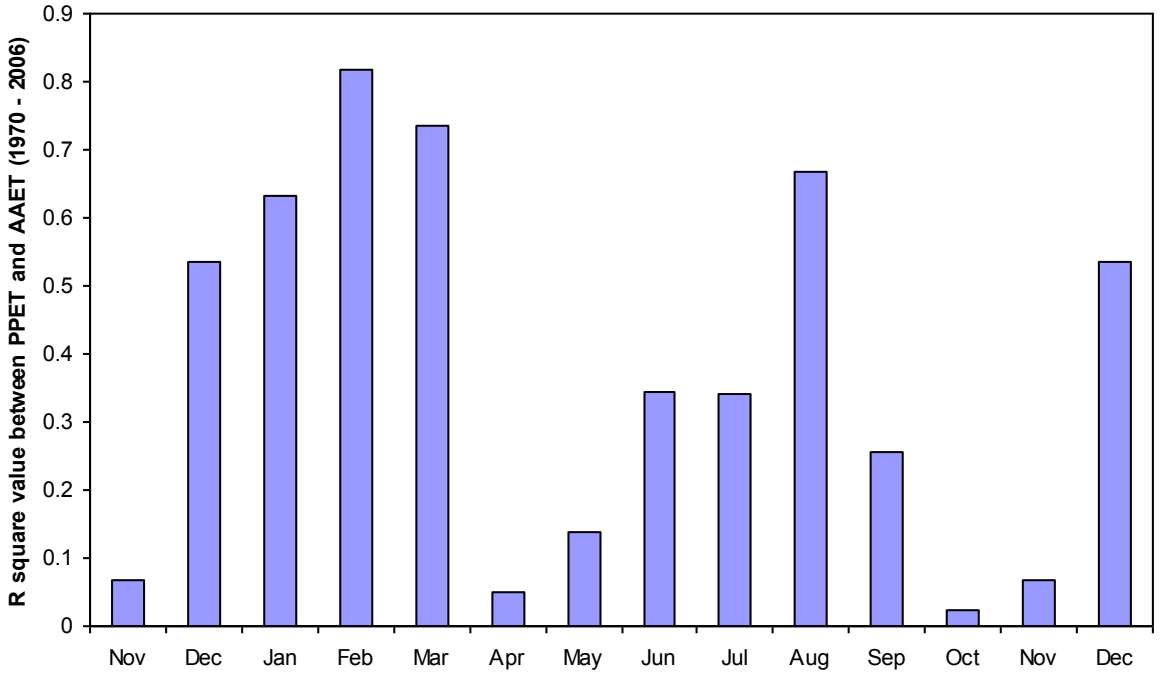

Figure 2. wet months (DEC_MAR) have positive correlation, dry months (JUN_SEPT) have negative correlation, pre and post monsoon months have little correlation between PPET and AAET (1970 – 2006).

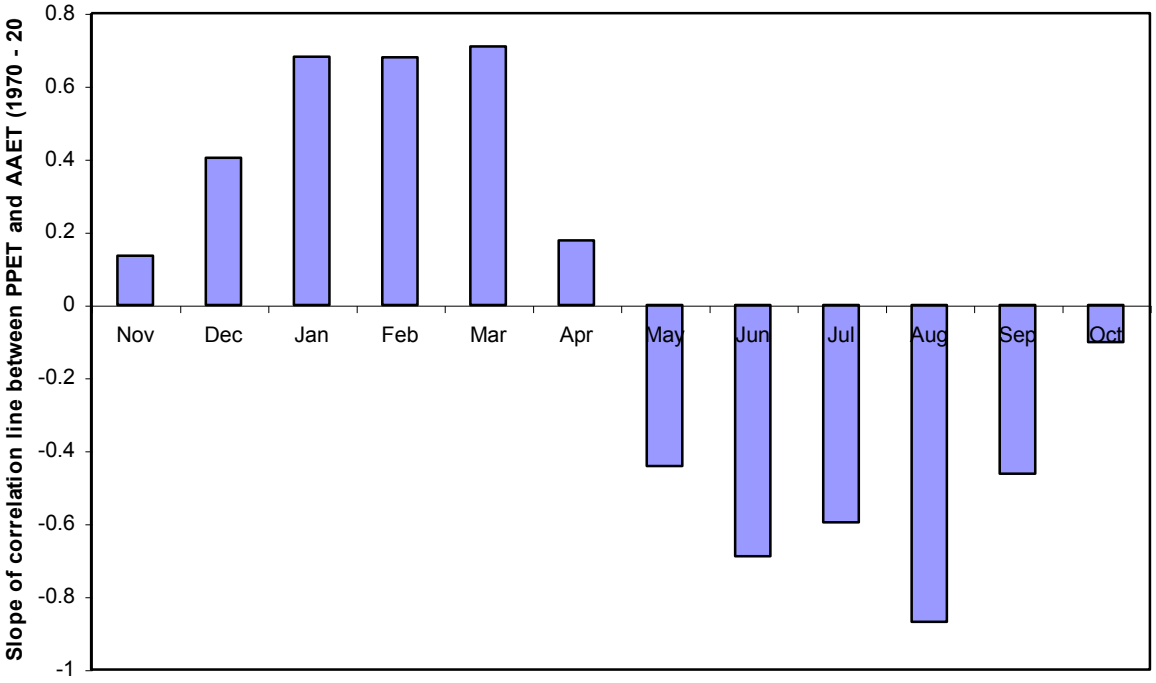

Figure 3. the slope changes from positive to negative with wet to dry season

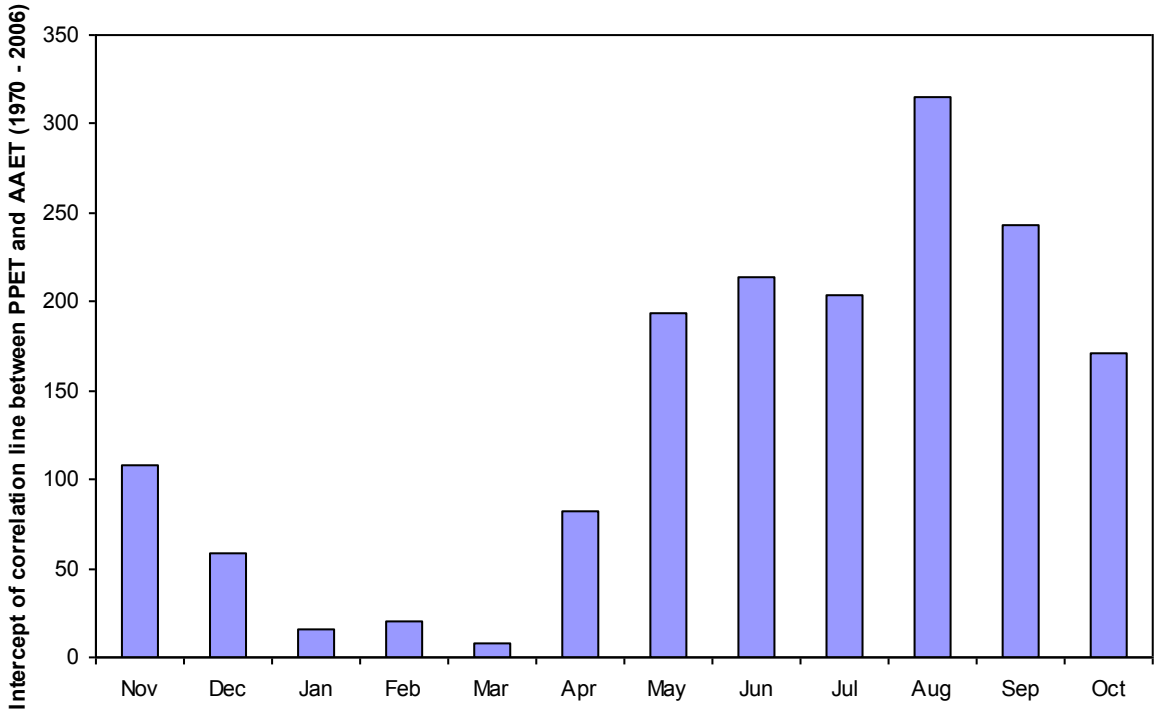

Figure 4. the intercept is minimum with highest positive slope and maximum with highest negative slope

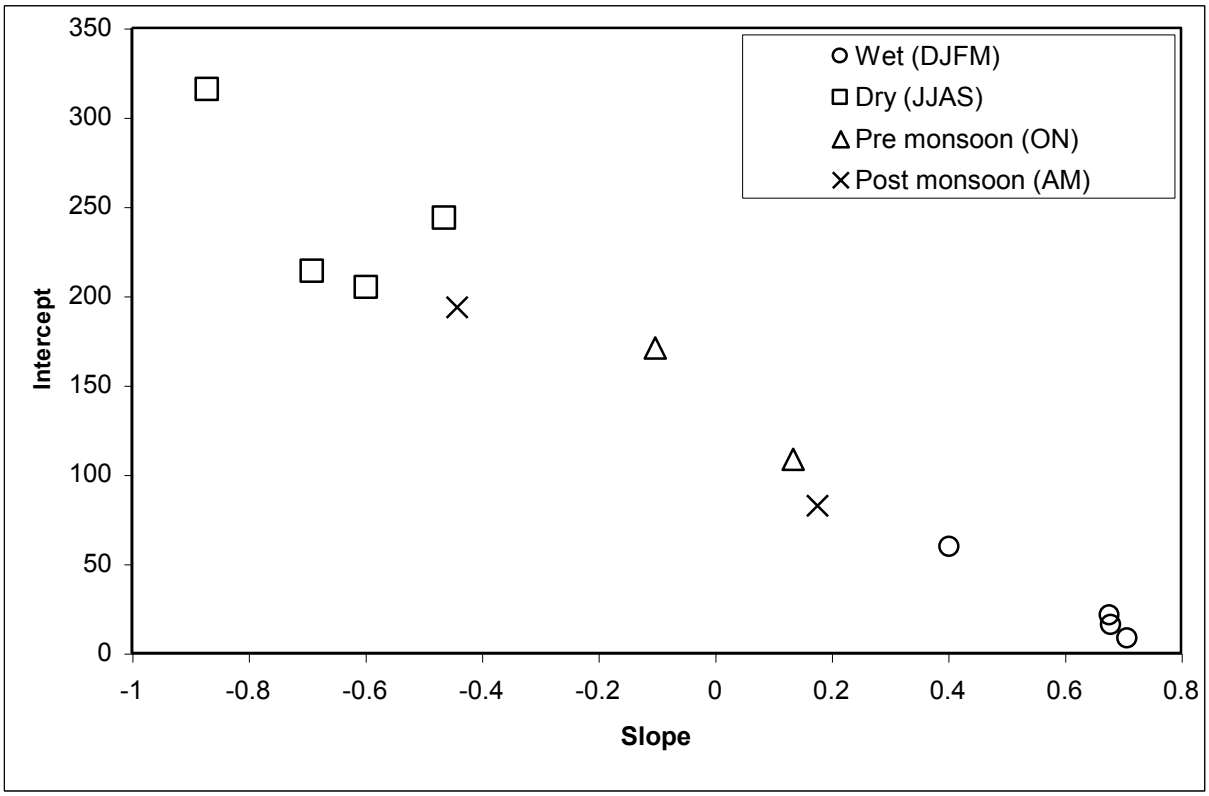

Figure 5. The slope and intercepts of the lines of correlation between PPET and AAET for the seasons. DJFM (Dec – Mar) and JJAS (Jun – Sep), ON (Oct – Nov) and AM (Apr – May)

Analysis of result: The R^2 value indicates the relation between PPET and AAET is not uniform for all months. To analyse the variation of the relations, further considerations have been given to the other parameters such as slope and intercept of the line of correlation. These are some qualitative measures of the relationship. The slope indicates the strength of X to influence Y and the intercept indicates the degree of constancy of Y.

Smaller slope (absolute value) indicates weaker influence of X values on Y and larger slope indicates stronger influence. Thus during wet and dry season the equation of correlation was used to estimate actual ET and during transitional months various ways were investigated.

The concept of linear interpolation: For the time of 1970 to 2006, the average monthly PPET and average monthly AAET values are given in Table 3 and plotted in Figure 6 with the months January to December along X axis. The figure shows that for April and May the AAET values can be easily interpolated from AAET of March and June. But the AAET values of October and November will be slightly underestimated if interpolation is done

for the AAET of September and December. Thus linear interpolation in this case will underestimate the AAET value indeed.

Table 3 the monthly average rainfall, AAET and PPET for the climate data of Jabiru weather station for 1970 to 2006

	Monthly Rainfall(mm)	Aerial Actual ET (mm)	Point Potential ET(mm)	Percentage for conversion of Oct/Nov ET
Jan	368	149	193	0.762978
Feb	369	134	165	0.80569
Mar	257	154	205	0.748954
Apr	78	123	224	0.553499
May	10	90	239	0.380968
Jun	1	61	225	0.276172
Jul	2	63	239	0.267431
Aug	0	85	266	0.343084
Sep	7	117	278	0.429714
Oct	37	140	298	0.47891
Nov	135	146	263	0.556564
Dec	234	150	224	0.67042

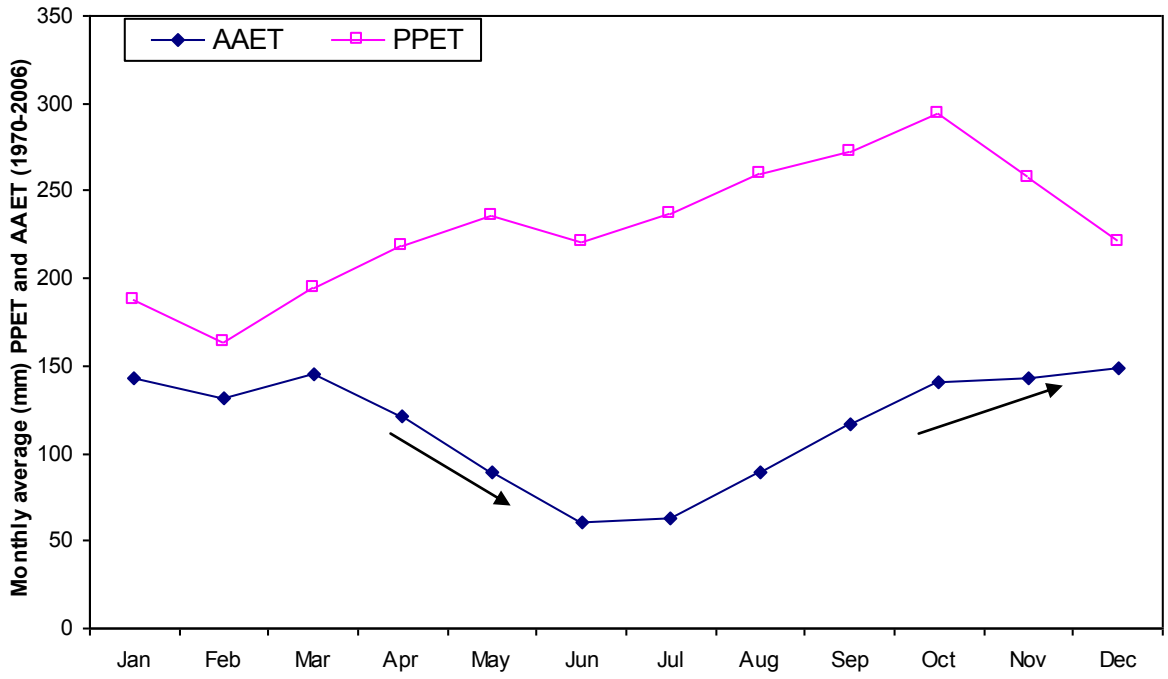

Figure 6 monthly average AAET and PPET values for 1970 to 2006

If the option of y = c was considered to be the compromise between lower intercept with positive slope (for wet months, y = +mx + c) and higher intercept with negative slope (for

dry months, y = -mx +c). However that does not consider the changes in the prediction of PPET values as y = c is a line with constant value of y and it does not change with x. Thus the percentage of PPET as the AAET is more logical than the consideration of the wet dry transition. Assuming the AAET for the October and November as a certain percentage of PPET of those months may be a reliable option though it only indicates y = +mx type of equation. It has been found that the assumption of linear correlation between AAET and PPET is untrue for these transitional months.

However, the percentage rule is nothing but simplest correlation as stated earlier. Therefore finally percentage rule is not used for October and November. Linear interpolation with a modification, which is described herein, is applied.

The concept of fitting polynomial for interpolation: It is assumed that the AAET of the months with good correlation are already available. Using those values a polynomial can be fitted J, F, M, _, _, J, J, A, S, _, _, D. The missing points in the polynomial will be indicated for April, May, October and November. The equations of the polynomials will be varied for various GCMs and various scenarios. Therefore, for each GCM and each scenario, it would be required to use different equation.

Conversion of PPET to AAET: Therefore it is established that the underlying rules are different for wet/dry months and transitional months.
FOR WET /DRY MONTHS: The correlation between PPET and AAET of 1970 to 2007 monthly values for wet (December to March) or dry (June to September) months are used for converting PPET of Ozclim to AAET for Ozclim. The equations for the wet months (Dec to Mar) are given in the respective columns of Table 4. Similarly those of dry months (Jun to Sep) are also given. For the rest of the months such as Apr, May, Oct and Nov which are termed as *transitional* months the following replacement of the correlation method are applied.

FOR TRANSITIONAL MONTHS: The linear interpolation between AAET of the March and June is used for AAET of April and May. Similarly September and December month's values are used for estimating AAET of October and November. The AAET changes from March to June following a straight line but it is not straight line for September to December as shown with the arrows Figure 6. Therefore, additional terms are used for the

estimation of October and November. The additional terms are found out by using the straight-line equation between September and December as shown in Figure 7. and Table 5. The equations for all months are given in Table 4.

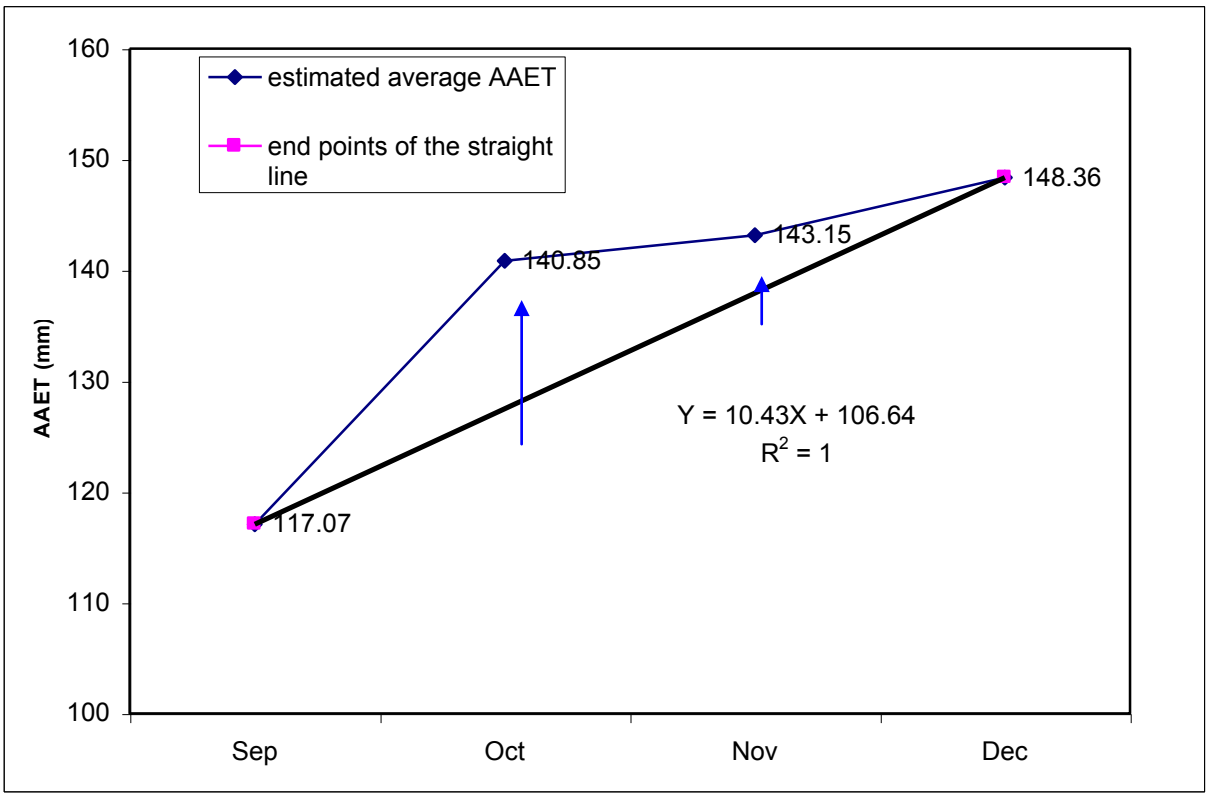

Figure 7. The blue arrows indicate the additional terms (13.35 for October, 5.22 for November)

Table 4 Equations of correlation, and interpolation for the estimation of AAET from PPET for all months

Eq^{n}. of corr^{n} bet^{n} AAET and PPET	Jan	Feb	Mar	Apr	May	June	July	Aug	Sep	Oct	Nov	Dec
	AAET = 0.68* PPET + 15.38	AAET = 0.68* PPET + 20.78	AAET= 0.71* PPET + 7.80	Interpolated between Mar and Jun: Apr = Mar – (Jun – Mar)/3 May = Mar – 2(Jun – Mar) /3		AAET= -0.69* PPET + 213.45	AAET= -0.60* PPET + 204.25	AAET= -0.87* PPET + 315.24	AAET= -0.46* PPET + 243.14	Interpolated between Sep and Dec: Oct = Sep + (Dec – Sep)/3 + additional term for Oct Nov = Sep + 2(Dec – Sep) /3 + additional term for Nov		AAET= 0.40* PPET + 59.07

Table 5 Computation of the additional terms for Oct and Nov as used in Table 4

	Estimated average AAET (mm) (1970 - 2006) *Col II*	Equation of the line connecting September to December is {Y = 10.43X + 106.64} (Fig 7)	*The points on the straight line (mm) Col IV*	*Col II – Col IV*	Additional terms for Oct and Nov
Sep	117.07	X= 1, Y = 117.07	117.07	0	
Oct	140.85	X = 2, Y = 10.43 * 2 + 106.64	127.50	140.85-127.50 = 13.35	13.35
Nov	143.15	X = 3, Y = 10.43 * 3 + 106.64	137.93	143.15 - 137.93 = 5.22	5.22
Dec	148.36	X = 4, Y = 148.36	148.36	0	

For the time of 1970 to 2006, the average monthly PPET and average monthly AAET have been plotted in Figure 8 with the monthly average rainfall along X-axis. The natures of the curves are very similar to Morton's basic equation of evapotranspiration variables. This data representation indicates that the wet season has got maximum positive correlation and dry season has got the maximum negative correlation. Therefore the transitional months fill the gap between these two extreme cases of correlation as well.

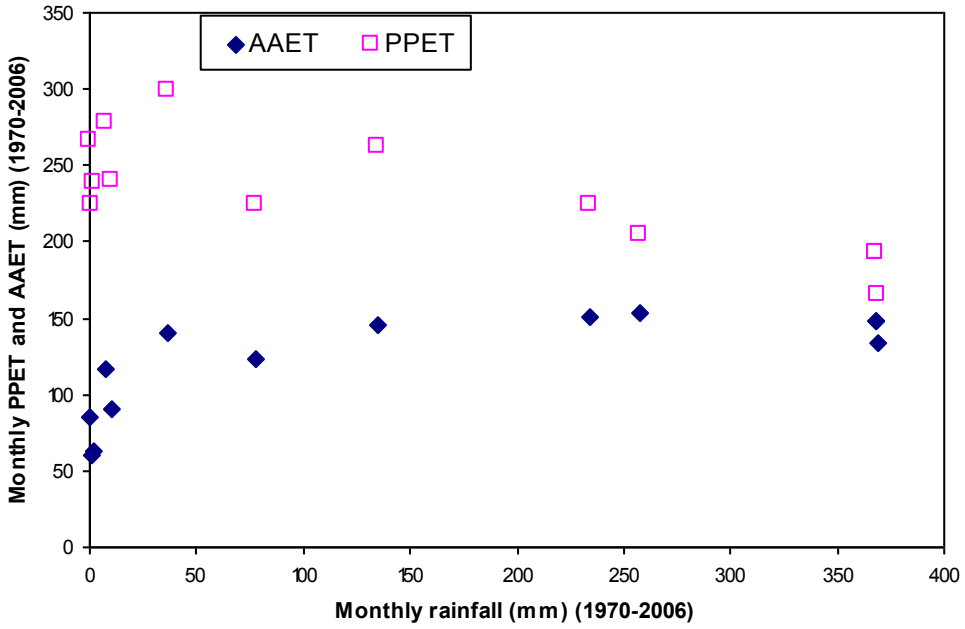

Figure 8. The result for 1970 to 2006 monthly average AAET and PPET data along y-axis and rainfall along x-axis. Dry months (rainfall 0 to 50mm) have negative correlation and wet months (rainfall 250 to 400mm) have positive correlation.

Reliability: During wet season the AAET is influenced by PPET in a stronger way. The physical factors governing evapotranspiration process also indicate that water availability is one important factor and energy gradient is one of the others. The dry season ET is influenced by energy gradient as well.

Thus all these results indicate that to estimate the AAET from PPET, the wet season values are more reliable, and the reliability decreases in dry seasons and is least during the transitional months.

Use of AAET data of GCMs: Historical data of SILO PPET and AAET are thus used for developing the relationship between the PPET and AAET. Following this relationship, AAET data of GCMs were estimated by using the extracted PPET data for 1200 time steps (12 month and 100 year) for all the seven scenarios of each of the five GCMs. After estimating AAET, the projected net flux values were computed by subtracting AAET from rainfall. Using the projected values of net flux the multiplying factors (change factors) for climate change were found out with respect to the net flux of the base year 2000. From 2001 to 2100 the multiplying factors were estimated for 1200 time steps for seven scenarios and five GCMs. These multiplying factors were used with the SCL and ENSO generated net flux to obtain the generated net flux to be used as input to the groundwater model Seep/W. The 1050 sets (30 replicates of 5 GCMs and 7 scenarios) net fluxes are given in Appendix H. The computed groundwater heads for the net fluxes are given in Appendix I.

Appendix H: Replicates of net flux

See attached CD

Appendix I: Results for 1050 runs

See the following pages

Appendix I: Result for 1050 runs (Sheet 1 of 5)

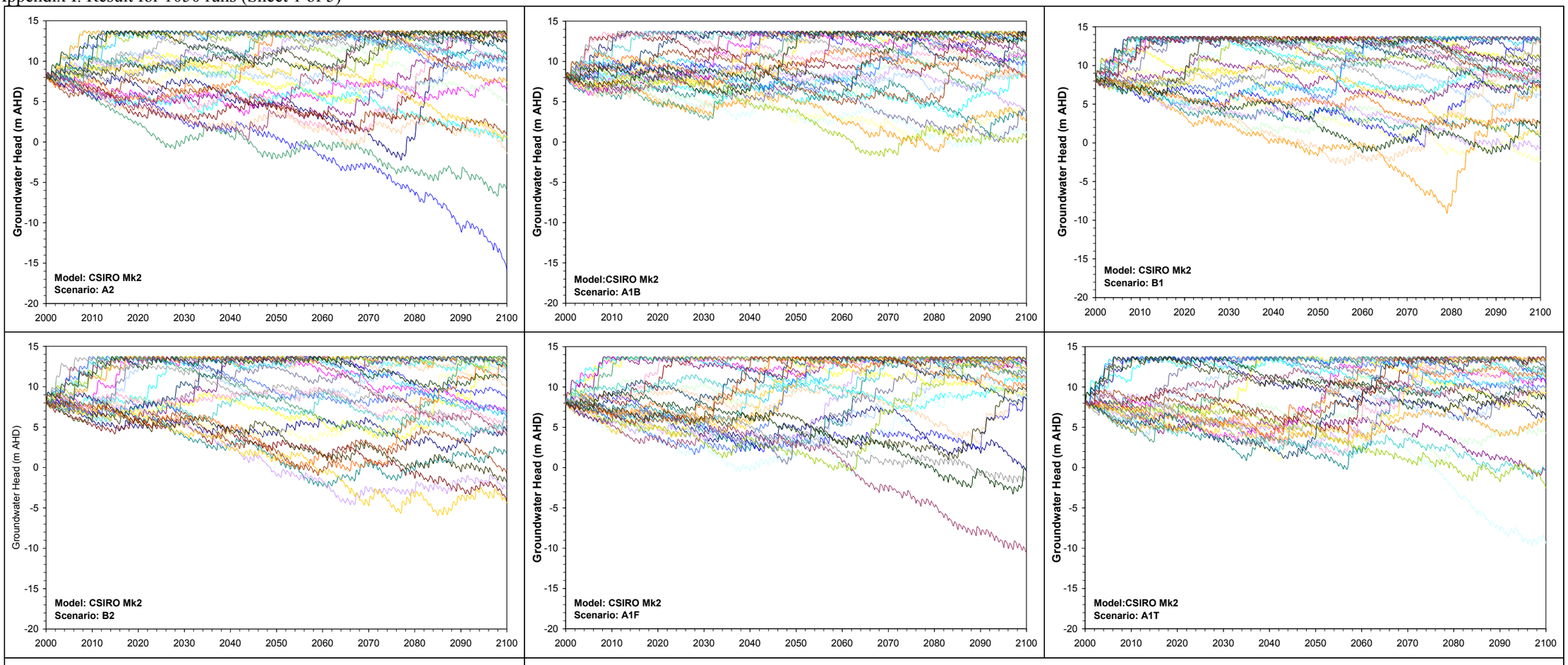

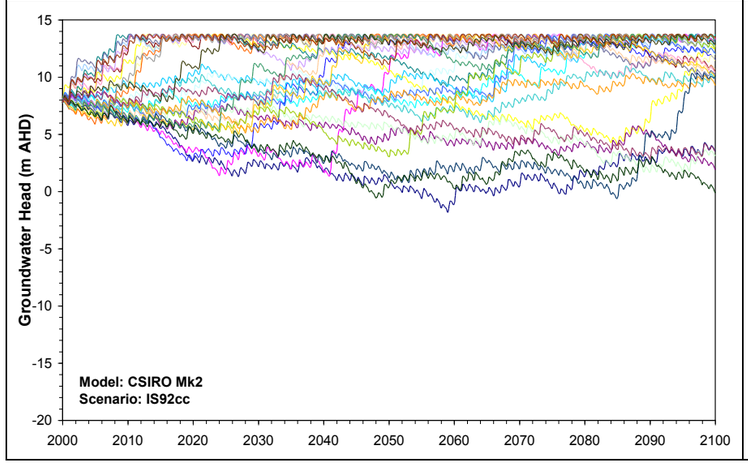

CSIRO Mk2: The Seep/W result for computed groundwater head for 100 year (from 2001 to 2100) net flux data derived from CSIRO Mk2 GCM. The seven figures are for the seven emission scenarios as indicated in the figures. The groundwater head fluctuation is forced to be bounded by the ground surface (14 m AHD) at the highest and base of the bore at the lowest levels.

Appendix I: Result for 1050 runs (Sheet 2 of 5)

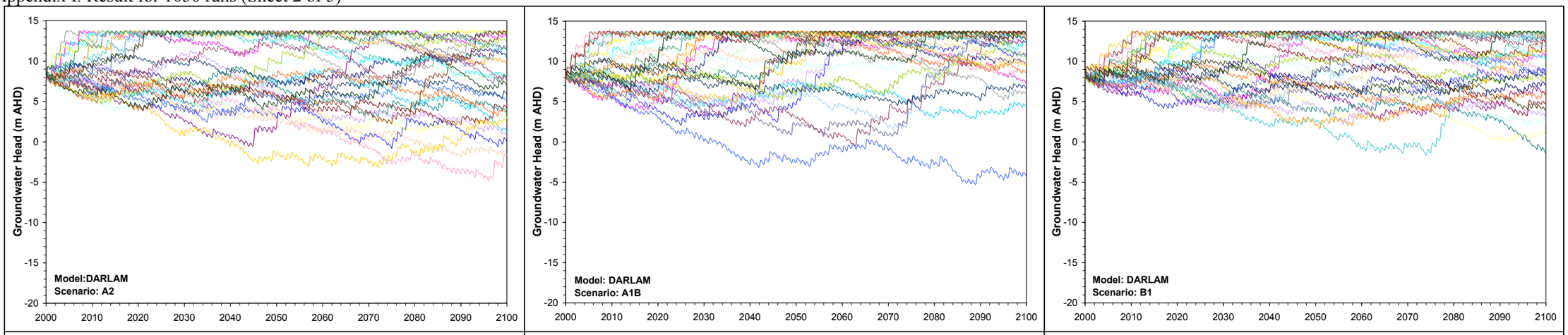

DARLAM: The Seep/W result for computed groundwater head for 100 year (from 2001 to 2100) net flux data derived from DARLAM GCM. The seven figures are for the seven emission scenarios as indicated in the figures. The groundwater head fluctuation is forced to be bounded by the ground surface (14 m AHD) at the highest and base of the bore at the lowest levels.

Appendix I: Result for 1050 runs (Sheet 3 of 5)

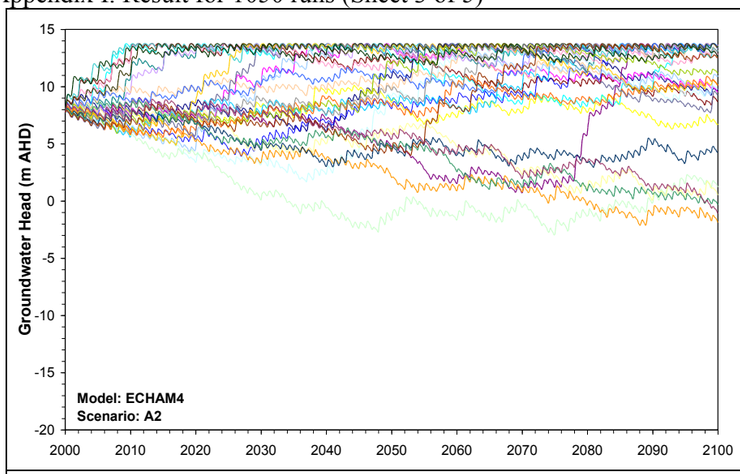

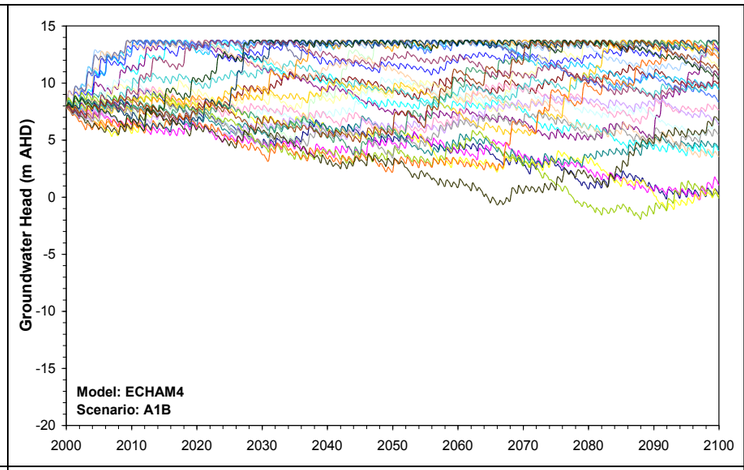

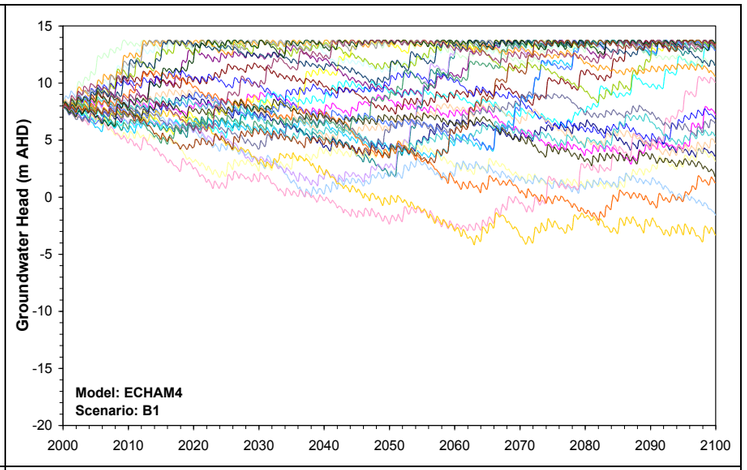

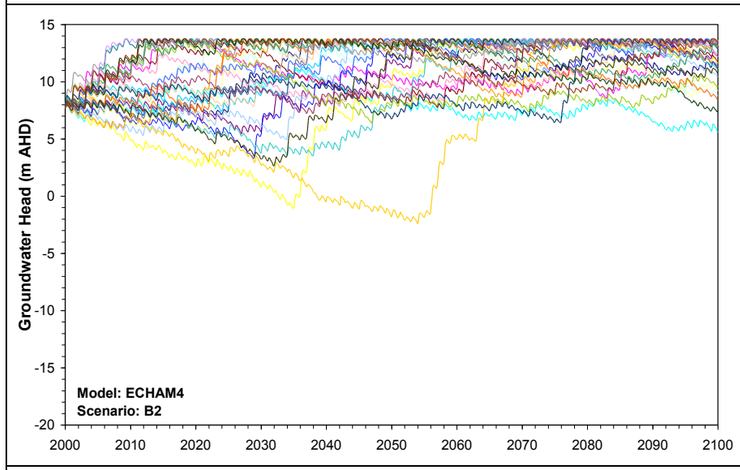

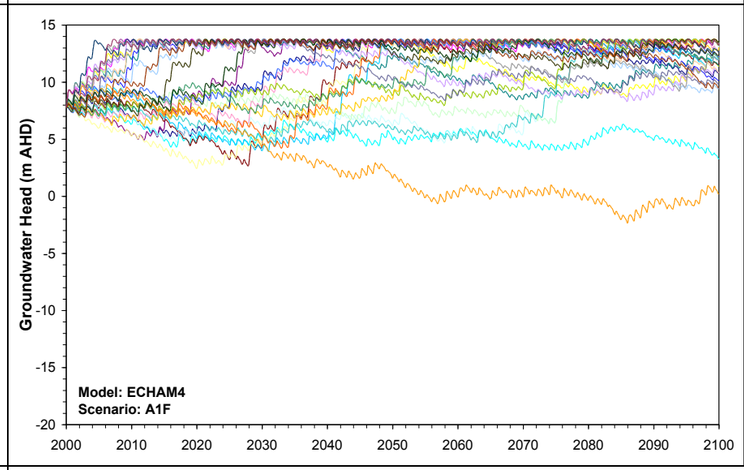

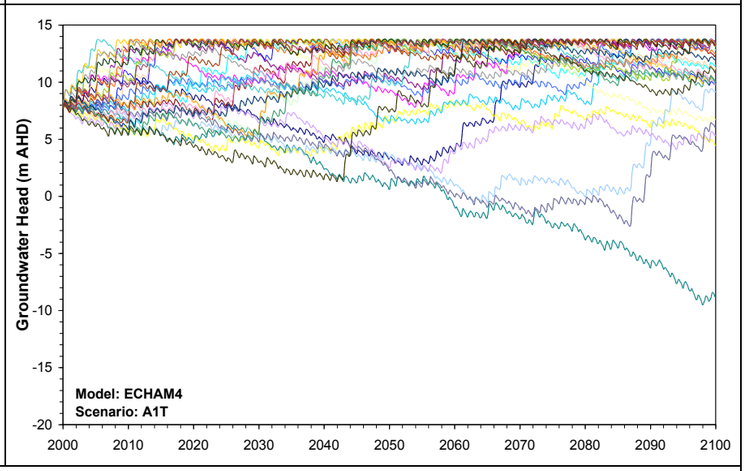

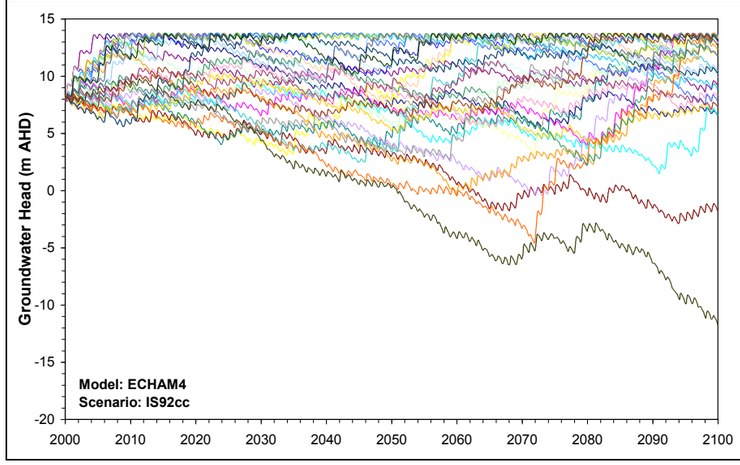

ECHAM4: The Seep/W result for computed groundwater head for 100 year (from 2001 to 2100) net flux data derived from ECHAM4. The seven figures are for the seven emission scenarios as indicated in the figures. The groundwater head fluctuation is forced to be bounded by the ground surface (14 m AHD) at the highest and base of the bore at the lowest levels.

Appendix I: Result for 1050 runs (Sheet 4 of 5)

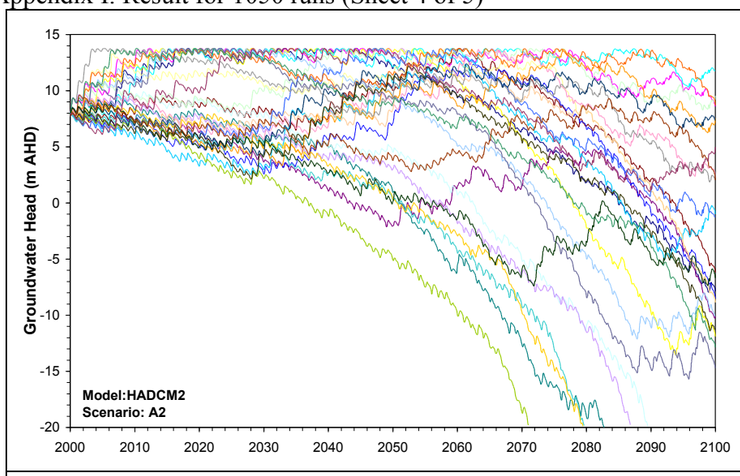

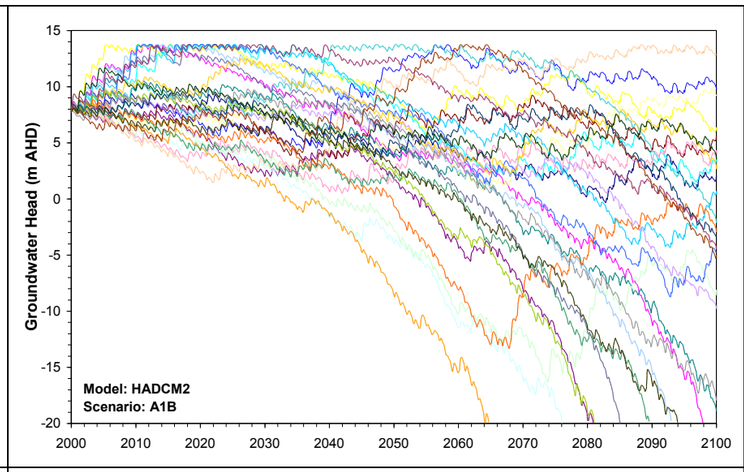

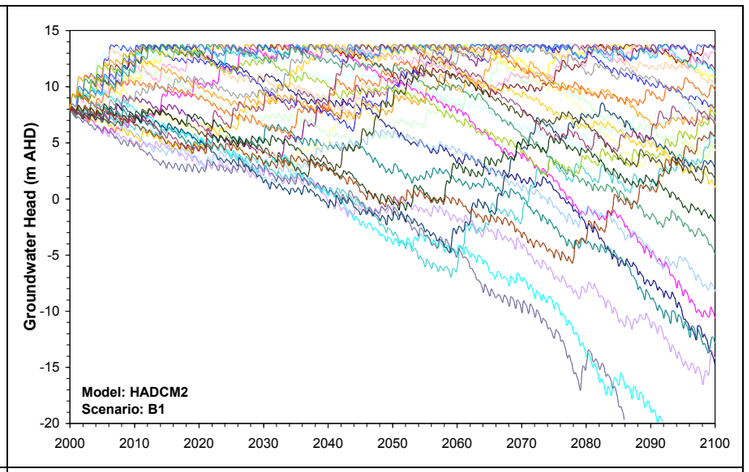

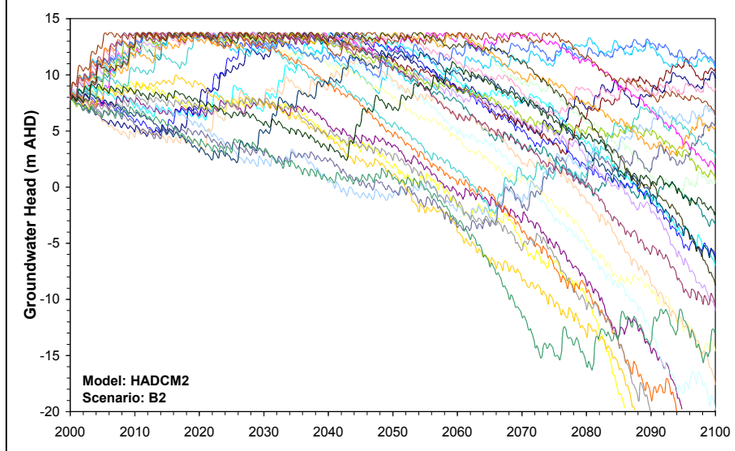

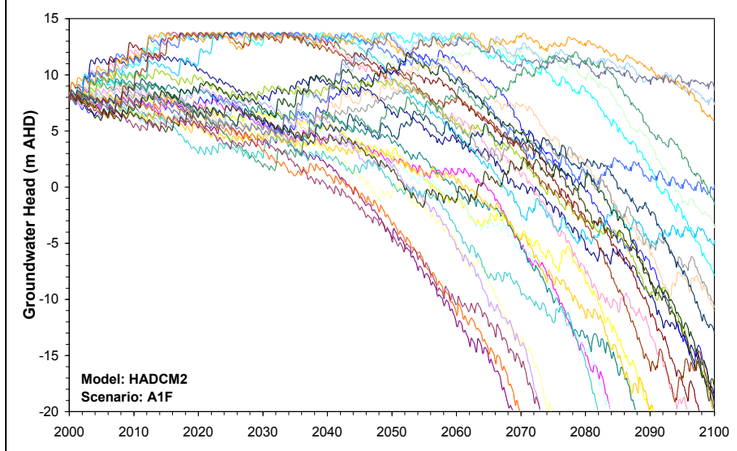

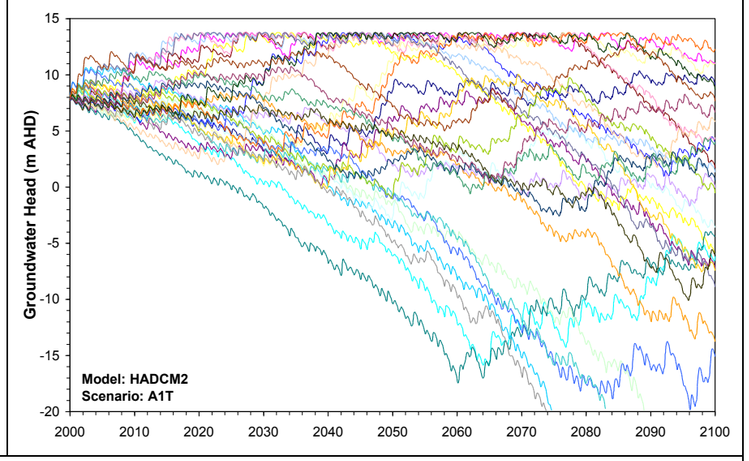

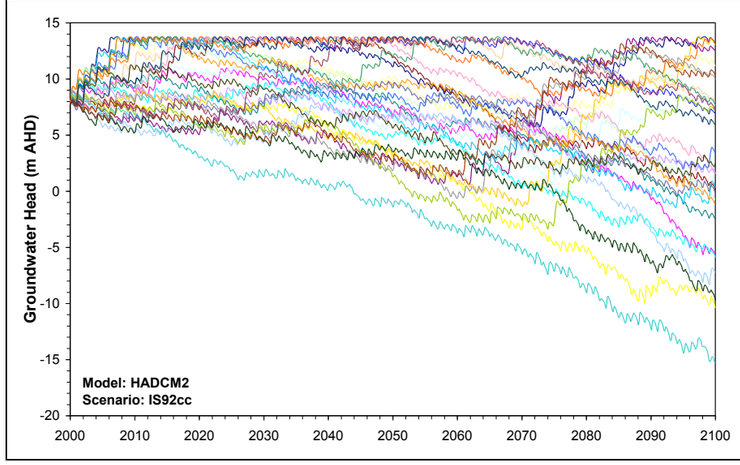

HadCM2: The Seep/W result for computed groundwater head for 100 year (from 2001 to 2100) net flux data derived from HadCM2 GCM. The seven figures are for the seven emission scenarios as indicated in the figures. The groundwater head fluctuation is forced to be bounded by the ground surface (14 m AHD) at the highest and base of the bore at the lowest levels. The curves have been truncated at -20 m AHD for better resolution. Those runs were numerically unstable.

Appendix I: Result for 1050 runs (Sheet 5 of 5)

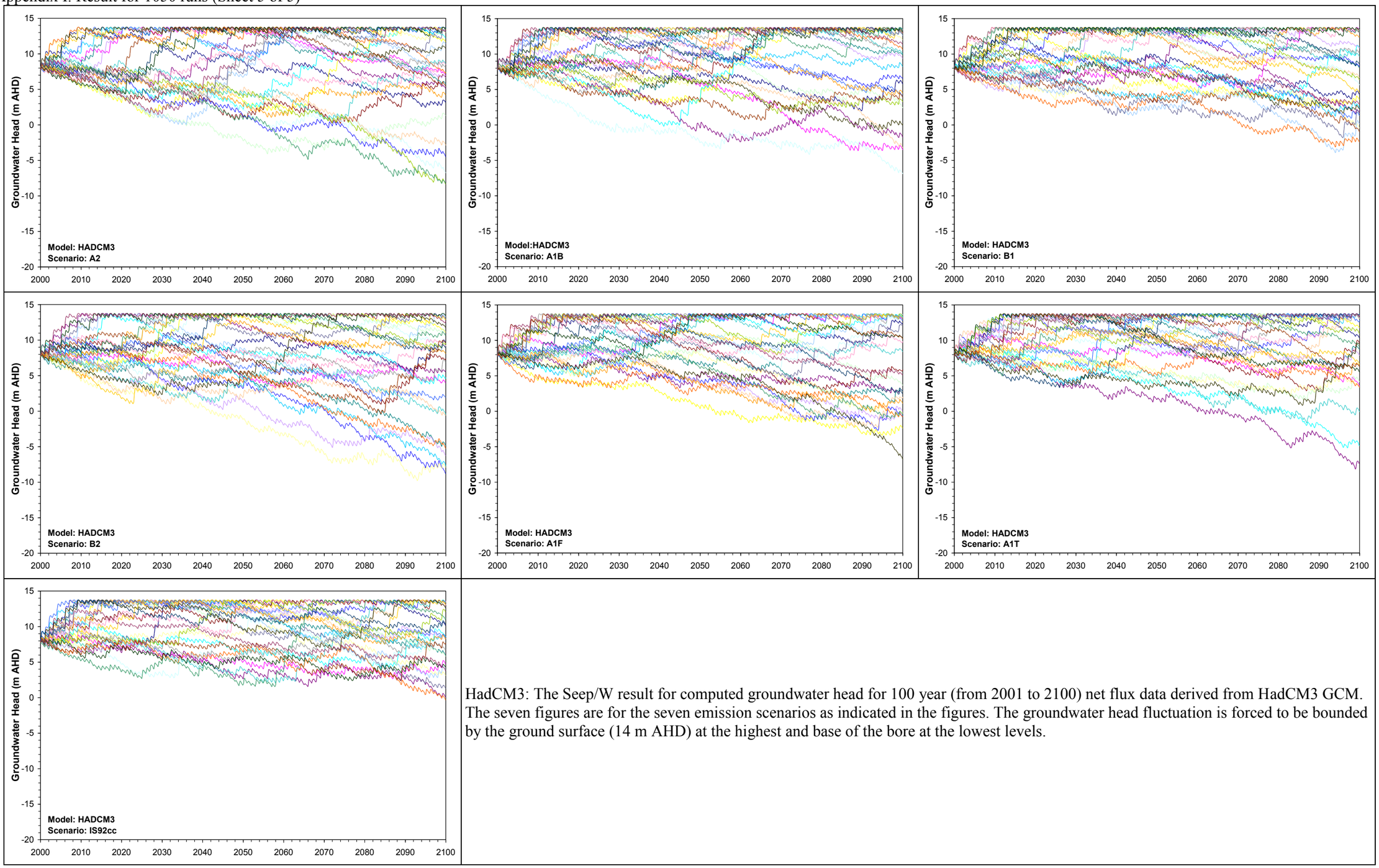

HadCM3: The Seep/W result for computed groundwater head for 100 year (from 2001 to 2100) net flux data derived from HadCM3 GCM. The seven figures are for the seven emission scenarios as indicated in the figures. The groundwater head fluctuation is forced to be bounded by the ground surface (14 m AHD) at the highest and base of the bore at the lowest levels.

Appendix J: Publications

See the following pages

Inaugural Australasian Hydrogeology Research Conference

University College,
Melbourne, Australia

December 2-3, 2004

MODELLING LONG-TERM GROUNDWATER REBOUND AND RECHARGE AT RANGER URANIUM MINE, KAKADU NATIONAL PARK

Mobashwera Kabir: Institute for Sustainable Water Resources, Department of Civil Engineering, Monash University, Clayton 3800, Australia.
Gavin M Mudd: Institute for Sustainable Water Resources, Department of Civil Engineering, Monash University, Clayton 3800, Australia.

Overview

The Kakadu National Park is a World Heritage-listed property in the 'Top End' of the Northern Territory of Australia, shown in Figure 1. It comprises some 20,000 km^2 of high conservation value wilderness, including Ramsar wetlands, sandstone heathlands, open woodland, floodplains, seasonal watercourses and permanent billabongs (OSS, 1991). The region also contains some major uranium deposits excised from the park, namely Ranger, Jabiluka and Koongarra. These areas, although not part of the national park, are completely surrounded by it. Thus the mining leases are intimately linked with the important ecological and cultural values of Kakadu. For example, Magela Creek flows through Kakadu into the Ranger Project Area and then back into the wetlands of Kakadu. It is therefore important to evaluate both existing and potential future impacts from mining in this environmentally sensitive region (Ko, 2004).

According to current regulatory requirements, the rehabilitation of the Ranger mine site must ensure that tailings and associated contaminants are effectively contained for a period of at least 10,000 years. The long-term rebound and behaviour of groundwater following mining and milling is therefore a fundamental issue to address, necessitating a thorough application of numerical models and hydrological-hydrogeological knowledge. The primary objective of this study is to develop a physically-based modelling technique which can be used to assess the long-term groundwater recharge (infiltration) at the Ranger site under varying climatic conditions over the long-term (ie. 10,000 years), thus providing a more realistic basis for assessing the environmental performance of the rehabilitation of the Ranger site.

Climate, Hydrology and Hydrogeology

The Kakadu region has a monsoon-like climate cycle involving an extended dry season followed by an intense wet season. The average annual rainfall of about 1,500 mm occurs almost entirely between November to March, while average annual pan evaporation is about 2,650 mm, shown in Figure 2 (Kinhill, 1996). With October and April as transitional months, the dry season lasts from May to September. The evaporation generally exceeds rainfall, leading to an overall negative water balance, though during the wet season there is generally a positive water balance. This leads to strong groundwater recharge during the wet season with evapotranspiration during the dry season, thereby creating a seasonal cycle in the position of the water table. A typical example is shown in Figure 3. The hydrogeology is best described as consisting of three formations - alluvial sands and gravels ('Type A'), weathered soils ('Type B') and fractured rocks ('Type C'), shown in Figure 4 (Ahmad and Green, 1986).

There are several permanent wetlands adjacent to Ranger at Georgetown, Coonjimba and Djalkmarra Billabongs. Some of the major wetlands of Kakadu are downstream of the Ranger site in the Magela Creek floodplain, and thus are important to protecting the Ramsar and World Heritage values of the region. Given the closeness of these to the disturbed mining region, it is critical to understand and quantify the long-term potential for solute migration to these surface water ecosystems.

Some Previous Studies

There have been some limited studies on quantifying and modelling the seasonal groundwater recharge processes in the northern Kakadu region. A climatically-based water balance-depletion model for the Magela Creek catchment was developed by Vardavas (1992). The main processes considered

were seasonal variation of the water table as a function of infiltration and evapotranspiration. A review of mine rehabilitation with regards to long-term infiltration to groundwater was given by Woods (1994), though this was largely conceptual and contained no modelling of the links between climate and groundwater recharge. At the Ranger mine, some field and modelling studies have been conducted to date on the hydrogeology, largely related to tailings management (Whitehead 1980; Ahmed and Green 1986; Salama and Foley 1997; Salama et al. 1998). Collectively, these studies have shown the importance of local geological features as preferential flowpaths, such as fault zones, high permeability weathered zones, and fractured rocks (though not all fracture zones are permeable). In general, the various studies have only focused on the shallow and deeper aquifers in relation to contaminant sources (eg. tailings) and not on seasonal recharge behaviour. For many of the modelling studies a constant rate of recharge is assumed.

After rehabilitation, the rate of recharge will be critical in determining the potential for solute migration in the shallow aquifers (as well as driving heads for deeper aquifers). Experience at other mine sites in the Top End has shown that predicting recharge is difficult, with Rum Jungle, for example, showing increasing infiltration over only 15 years following rehabilitation (Pidsley, 2002).

The primary driver for any solute migration will be the degree of infiltration through the rehabilitated Ranger mine site and the resulting shape of the water table. The degree of infiltration will be governed by the unsaturated conditions of the surface soils, the balance of rainfall and evapotranspiration, and the final rehabilitated form of the landscape. An important issue in this regard is that of climate change (Quinn et al., 2001), especially with respect to the important wetlands of the region (van Dam et al., 1999) – the long-term patterns of rainfall, storm intensity, temperature and evapotranspiration. Thus, in order to predict solute migration over a time-scale of some 10,000 years, a theoretically rigorous approach to modelling groundwater behaviour linked to the climate and hydrological cycle is clearly required.

Selection of Models to Assess Long-Term Groundwater Recharge

There are two principal types of models which can be used to assess infiltration or groundwater recharge – water balance models (eg. HELP, PRZM-2, SESOIL) or unsaturated zone models based on Richard's equation (eg. VS2DT, HYDRUS-1D, SoilCover) (Gogolev, 2002). Coupled models are also becoming more widely used, such as SMILE and CLASS (Beverly et al., 1999; Tuteja et al., 2004 respectively), which couple one-dimensional unsaturated flow within a three-dimensional saturated flow (groundwater) model. As noted by Vries (2002), however, estimation of groundwater recharge is an iterative process, highly dependent on climate, surface and sub-surface conditions. A relatively new model which couples unsaturated flow to climatic conditions is VADOSE/W (Geo-Slope, 2002), although it is exceedingly numerically intensive and is likely to be impractical for modelling variable conditions over a period of some 10,000 years.

This project will review all available models, including saturated, unsaturated and coupled models, with a view to developing a theoretically robust and computationally efficient technique designed to address long-term groundwater recharge under variable climatic conditions.

Main Outcomes

The principal outcome from this research project is expected to be a major contribution to the understanding and modelling of groundwater recharge processes in the wet-dry tropics of northern Australia. The ability to predict long-term groundwater behaviour is a key issue for both mine rehabilitation and climate change and the possible extent of environmental impacts on important wetlands and ecosystems. The project should also contribute to improved minesite rehabilitation design based on a more rigourous approach to hydrogeological issues.

References

Ahmad M and Green D C (1986) Groundwater regimes and isotopic studies, Ranger mine area, Northern Territory, Austr J Earth Sci 33: 391-399

Beverly C R, Nathan R J, Malafant K W J and Fordham D P (1999) Development of a simplified unsaturated module for providing recharge estimates to saturated groundwater models, Hydrol Proc 13: 653-675

De Vries J J, Simmers I (2002) Groundwater recharge: an overview of processes and challenges , Hydrogeo J 10: 5-17

ERA (2000) ERA Ranger mine – annual environmental management report, Energy Resources of Australia Ltd (ERA), Jabiru, NT, October

Geo-Slope (2002), VADOSE/W User's Guide, Geo-Slope International Pty Ltd, Calgary, Alberta, Canada

Gogolev K I (2002) Assessing groundwater recharge with two unsaturated zone modeling technologies, Env Geol 42: 248-258

Kinhill (1996) The Jabiluka Project- draft environmental impact statement, Kinhill Engineers Pty Ltd and ERA Environmental Services Pty Ltd, Milton, QLD, October

Ko J (2004) Modelling groundwater recharge in the wet-dry tropics, Final Year Environmental Engineering Research Project, Department of Civil Engineering, Monash University, Clayton, VIC

OSS (1991) Proceedings of the workshop on land application of effluent water uranium mines in the Alligator Rivers Region Jabiru, 11-13 September, Office of the Supervising Scientist (OSS), Jabiru NT, Australia, pp 5-13

Pidsley S M (Editor), (2002) Rum Jungle Rehabilitation Project Monitoring Report 1993-1998. NT Department of Infrastructure Planning and Environment (NTDIPE), Technical Report Number 01/2002, Darwin, NT

Quinn N W T, Miller N L, Dracup J A , Brekke L and Grober L F (2001) An integrated modeling system for environmental impact analysis of climate variability and extreme weather events in the San Joaquin Basin, California Adv Env Rese 5(4): 309-317

Salama R, Foley G (1997) Ranger regional hydrogeology conceptual model, CSIRO Land and Water Report No 97/65

Salama R, Kin P, Pollock D, Ellerbroek Dand Foley G (1998) Groundwater interaction with Magela Creek, CSIRO Land and Water Report No 98/18

Tuteja N K, Vaze J, Murphy B and Beale G (2004) Catchment scale multiple-landuse atmosphere soil water and solute transport model, Department of Infrastructure, Planning and Natural Resources, NSW

van Dam R A, Finlayson, C M and Watkins, D (Editors) (1999) Vulnerability assessment of major wetlands in the Asia-Pacific region to climate change and sea level rise. Office of the Supervising Scientist (OSS), Supervising Scientist Report 149, Darwin, NT

Vardavas I M (1992) A simple groundwater recharge – depletion model for the tropical Magela Creek catchment, Ecol Mod 68: 147-159

Whitehead B R (1980) A compilation and interpretation of hydrogeological data, Ranger site area, NT Geological Survey Technical Report 80/33

Woods, P H (1994) Likely Recharge to Permanent Groundwater Beneath Future Rehabilitated Landforms at Ranger Uranium Mine, Northern Australia. Austr J Earth Sci 41: 505-508.

Figure 1 – Location of Kakadu National Park and the Ranger uranium mine, Northern Territory, Australia (top right) (Courtesy: Scott Ludlam)

Figure 2 – Kakadu climate : monthly rainfall and pan evaporation (centre) (Data courtesy OSS, ERA)

Figure 3 – Typical water table fluctuation around the Ranger mine region (bottom) (ERA, 2000)

Figure 4 – Conceptual hydrogeology of Kakadu National Park, Northern Territory, Australia (below) (Ahmed and Green 1986)

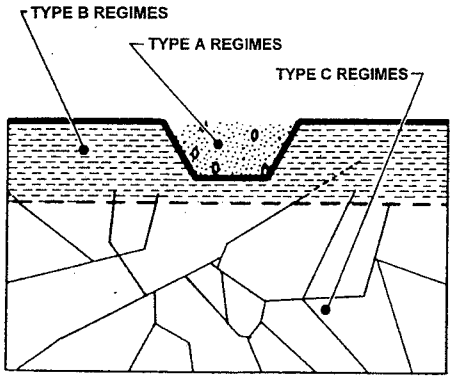

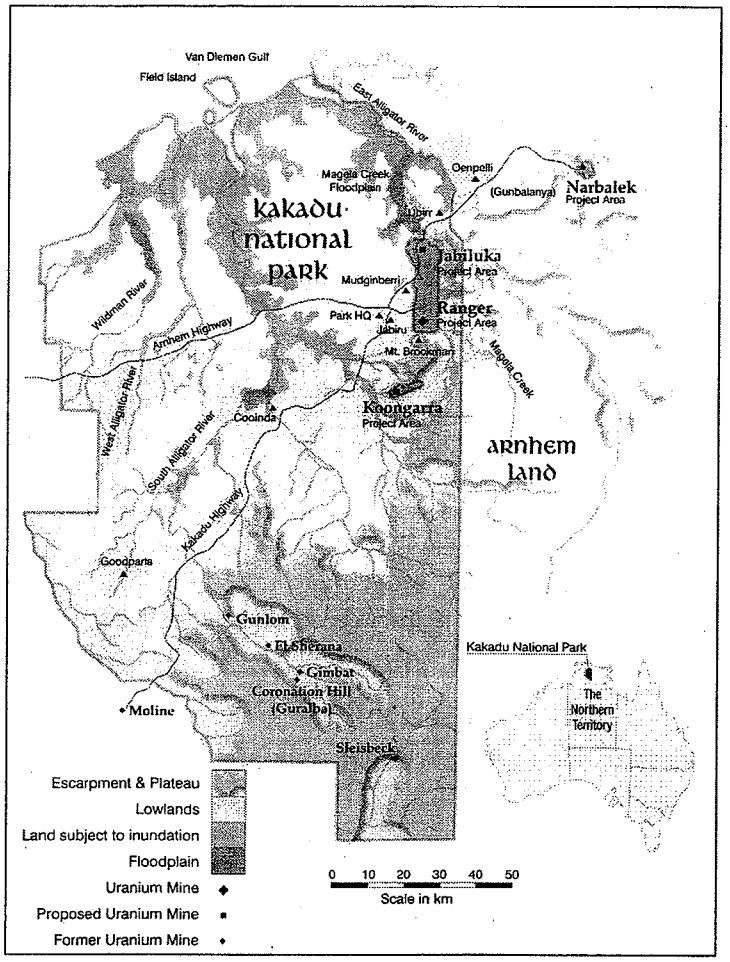

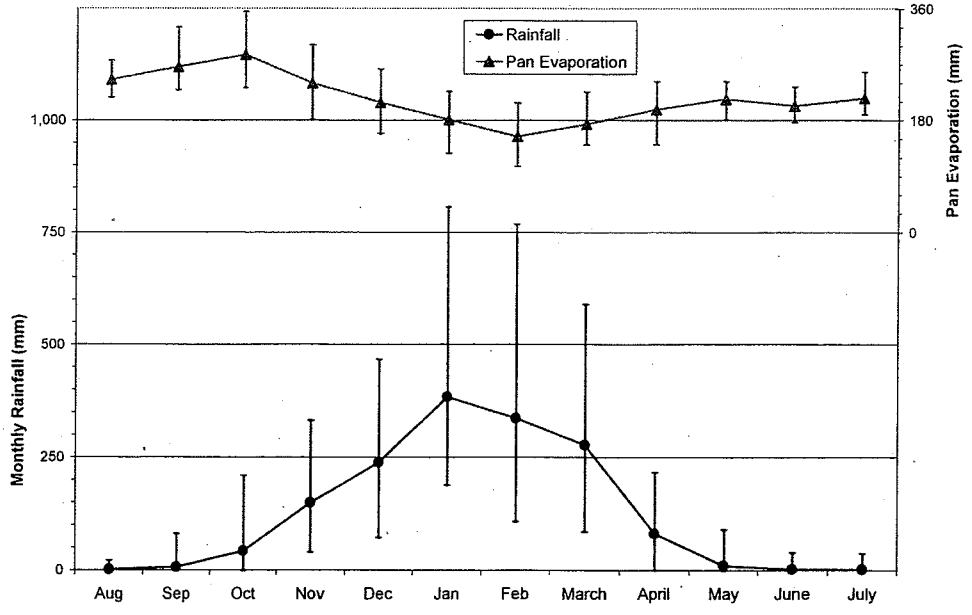

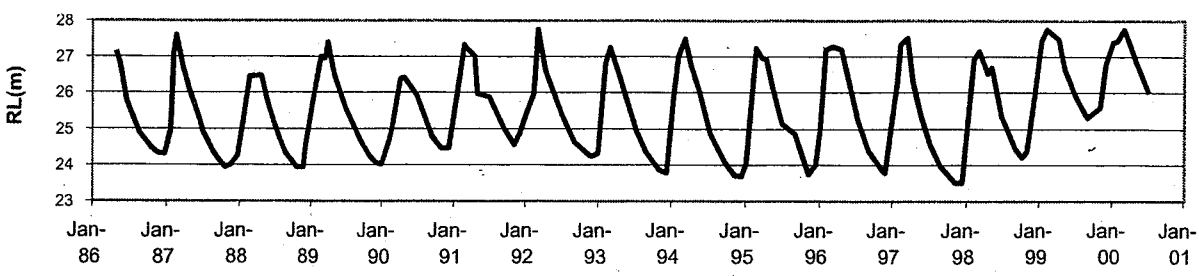

The Application of Time Series Techniques to Groundwater Level and Climate Relationships

Mobashwera KABIR[1], Gavin M. MUDD and Anthony R. LADSON

[1]Institute for Sustainable Water Resources, Department of Civil Engineering, Monash University, VIC 3800, Australia; e-mail:Mobashwera.Kabir@eng.monash.edu.au

Introduction:
The response of the groundwater table (GWT) to climate variability depends on a complex combination of geology, topography, vegetation, soil type and moisture status. To predict future behaviour of the GWT with respect to climate, it is important to analyse historical GWT and climate data. The primary driver for groundwater recharge or changes in the GWT is the net flux – or the difference between rainfall and actual evapotranspiration (ET).

For this project, a number of methods have been utilised for estimating the correlation between the net flux and groundwater recharge. Traditional statistical techniques produced poor correlations, and hence time series techniques were adopted for more realistic representation of the ongoing hydrologic processes (Berendrecht 2004) . A class of time series models called transfer function-noise (TFN) models have become popular for describing dynamic causal relationships between time series. The TFN model is a combination of stochastic and deterministic components.

This paper will summarise the results to date in the application of time series techniques to understanding groundwater and climate variability towards formulating the stochastic part of the intended TFN model. The study site is the Ranger uranium project, surrounded by Kakadu National Park, Northern Territory.

Methodology:
We have existing data on rainfall and ET from nearby weather station Jabiru, and GWT elevations in the surrounding bores for 1980 to 2005. The times series techniques applied in this research consists of estimation of auto correlation function (ACF), partial auto correlation function (PACF), cross correlation function (CCF), seasonality and trend components, auto regressive moving average (ARMA) models and prediction by ARMA model (Brockwell and Davis 2002).

To undertake a robust statistical technique for analysing the hydrologic data, which relates to time series process, such as rainfall, ET, stream flow runoff, groundwater recharge, time series analyses have been employed in the study. The estimation of ACF is used to identify seasonality in climate and GWT data. The CCF assesses the statistically significant time lag between the responses (GWT) and cause (climate) which has been utilised in a companion conference paper to (Kabir et al. 2006). Classical decomposition technique is used to identify the seasonal component of the GWT elevation. The trend component has been calculated and was found to be approximately quadratic (concave) with a minimum caused by dry period between 1987-1991.

The wide range of variation of the annual maximus and minimus is handled with the incorporation of suitable ARMA models. Separation of seasonality from the non-stationary data has been done by using monthly data of climate and GWT for 20 to 25 years duration. The residuals have been checked for randomness and after that the values of ACF and PACF have been used in the preliminary estimation of the orders (p, q) of suitable ARMA model. The respective estimated ARMA models have been used for the prediction of future values of climate flux and GWT of the bores with specified prediction bounds (Figure 2).

Result:
The ACF of climate fluxes and GWT of the selected bores showed the seasonality with a cycle of 12 months. The cross correlation between monthly flux and corresponding change in GWT for the bores

showed that up to a maximum lag of two month was statistically significant to influence current months GWT (Figure 1). By comparing the unsaturated thickness of the selected bores, it was found that the lag was more with the bores that had greater thickness of unsaturated soil. The bores analysed result a maximum of two month and minimum of one-month lag to be significant.

An ARMA model forecast of the GWT for bore OB27 is given in Figure 2. This predicted range is within previous GWT fluctuations, and future research is planned to utilise unsaturated flow models for more rigorous modelling of moisture movement.

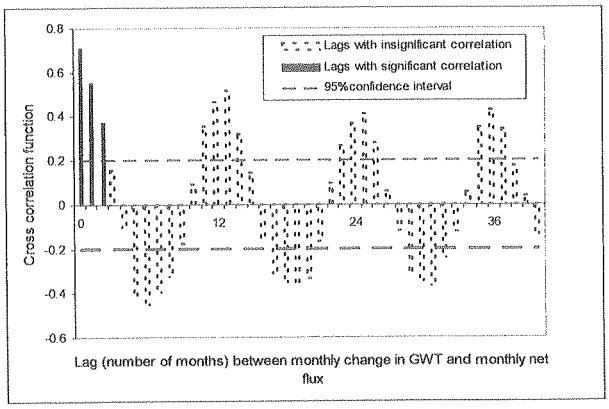

Figure 1 CCF for monthly change in GWT as response to monthly net flux for bore OB27 for 1981 to 1988

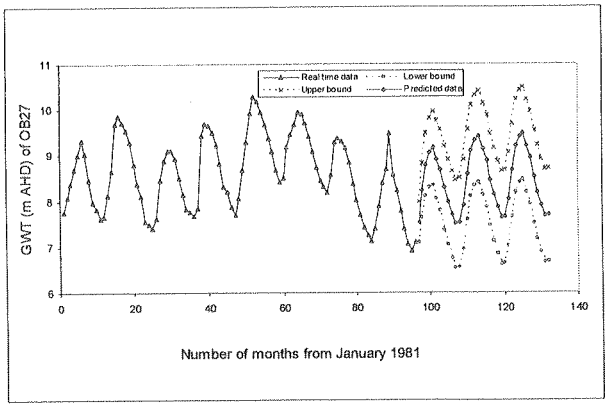

Figure 2 ARMA forecast for GWT of OB27 with 95% prediction bounds, real time data for 1981 to1988

Conclusion:

The ability to predict the future behaviour of the GWT with respect to climate is important. To date, applying univariate time series statistical techniques has shown good results in auto-correlating key variables. In future, multi-variate time series techniques are planned to be investigated. The outputs from these statistical analyses are useful in quantifying past relationships as a basis to undertake more deterministic modelling of the hydrologic cycle of climate, soils and groundwater recharge.

References:

Berendrecht, W. L. (2004). State space modelling of groundwater fluctuations, Delft University of Technology. Ph. D.

Brockwell, P. J. and R. A. Davis (2002). Introduction to Time Series and Forecasting, Springer-Verlag New York.

Kabir, M., G. M. Mudd and T. Ladson (2006). Understanding the groundwater recharge process with climate-GWT data. Joint Congress of: 9th Australasian Environmental Isotope Conference and 2nd Australasian Hydrogeology Research Conference. Adelaide, South Australia, Centre for Groundwater Studies.

Joint Congress of:

9th Australasian Environmental Isotope Conference
and
2nd Australasian Hydrogeology Research Conference

Integrating Research and Innovation

Wednesday 13th – Friday 15th December 2006

Concurrent Conferences

Stamford Grand Hotel

Moseley Square, Glenelg Beach, ADELAIDE, South Australia, AUSTRALIA

Centre for
Groundwater Studies

Understanding the Groundwater Recharge Process near the Ranger Mine in the Northern Territory

Mobashwera KABIR[1] Gavin M. MUDD, Anthony R. LADSON

[1]Institute for Sustainable Water Resources, Department of Civil Engineering, Monash University, VIC 3800, Australia; email:Mobashwera.Kabir@eng.monash.edu.au

Introduction

It is important to understand the processes of groundwater recharge near the Ranger mine to predict the likely impact of climate change on ground water table elevations and hence to quantify the risks to long term containment of mine tailings.

Methodology

With the daily rainfall, evapotranspiration and groundwater table (GWT) data for the period 1980 to 2005, statistical analyses have been used to test and quantify conceptual models of expected recharge processes. The simplest technique to obtain correlation between climate data and change in GWT is based on calculations of net flux, which is the difference between rainfall and evapotranspiration (ET) (Armstrong and Narayan 1998). This analysis was then extended by considering the influence of unsaturated soil thickness and the monthly net flux series with statistically significant lags as detailed in another accompanying paper (Kabir et al. 2006) The influence of these variables was quantified by the Beta values calculated from multiple regression and R^2 values (Kerr et al. 2002; Dahe et al. 2006). The Beta value represents the degree to which the independent variables are related, with a higher value showing a more important relationship.

The bores chosen for detailed analyses were those that were clearly unimpacted from mining-related activities so that the changes observed in the GWT were related to climate only.

Result:

The GWT varies significantly both in space and time over the Ranger project area and shows a distinct seasonal cycle in GWT levels. Net flux explained about 50% of the variance in GWT elevation (Figure 3). In the multiple regression analyses for selected bores, the influence of unsaturated zone thickness has been realised as a barrier to recharge. Based on the Beta values obtained for the selected bores (Figure 4), the importance of unsaturated thickness decreased in comparison to the climate as the unsaturated zone thickness increases. From the multiple regression, bore OB27, having highest R^2 value of 0.646, was selected for correlation analysis to investigate the relative influence of rainfall and ET on the recharge.

Discussion & Conclusion:

There is a significant difference in the response of GWT to positive and negative flux through saturated and unsaturated soil as it is observed that the maximum monthly rainfall is much greater than maximum monthly ET (Figure 3). The reasons behind this variation may be mentioned as firstly the availability (storage) of water and secondly the saturated hydraulic conductivity, which is many times greater than that of unsaturated soil The infiltration into and evaporation of moisture from soils is a complex process (as shown by the scatter in Figure 3). The thickness of the unsaturated zone is clearly an important factor identified by this analysis, as it influences recharge both through storage and unsaturated hydraulic conductivity. In terms of potential climate change impacts on groundwater recharge in the Kakadu region, the net effect of changes in rainfall and evapotranspiration need to be considered jointly with unsaturated soil behaviour.

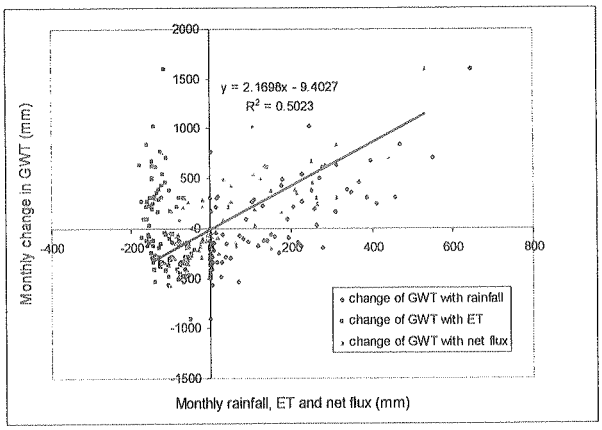

Figure 3 The monthly change of GWT of OB27 during 1981 to 1988 with the monthly rainfall, ET and net flux.

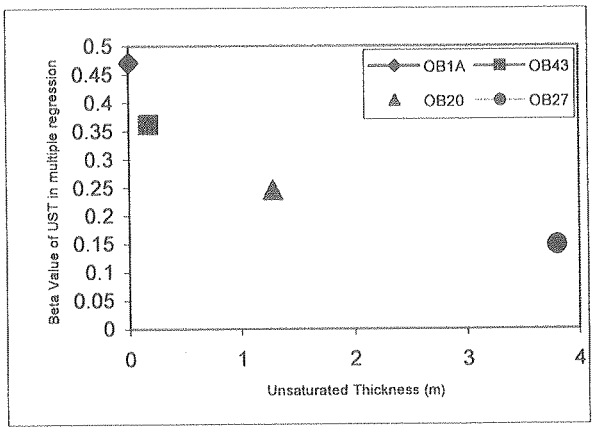

Figure 4 The Beta value of unsaturated thickness of four selected bores as computed in multiple regression.

References:
Armstrong, D. and K. Narayan (1998). Using Groundwater Responses to Infer Recharge. The basics of recharge and discharge. L. Zhang and G. Walker, CSIRO Division of Land and Water. 5: 13.
Dahe, Q., L. Shiyin and L. Peiji (2006). "Snow cover distribution, variability and response to climate change in Western China." Journal of Climate 19: 1820-1833.
Kabir, M., G. M. Mudd and T. Ladson (2006). The application of time series techniques to groundwater and climate relationships. Joint Congress of: 9th Australasian Environmental Isotope Conference and 2nd Australasian Hydrogeology Research Conference. Adelaide, South Australia, Centre for Groundwater Studies.
Kerr, A. W., H. K. Hall and S. A. Kozub (2002). Doing Statisitics with SPSS, SAGE Publications.

Joint Congress of:

9th Australasian Environmental Isotope Conference
and
2nd Australasian Hydrogeology Research Conference

Integrating Research and Innovation

Wednesday 13th – Friday 15th December 2006

Concurrent Conferences

Stamford Grand Hotel

Moseley Square, Glenelg Beach, ADELAIDE, South Australia, AUSTRALIA

Centre for
Groundwater Studies

UNDERSTANDING THE INCONSISTENCIES BETWEEN TWO DIFFERENT SOURCES OF MORTON'S AAET DATA FOR RANGER URANIUM MINE SITE, NORTHERN TERRITORY, AUSTRALIA

M. Kabir[1], G. M. Mudd[1] and A. R. Ladson[1]

[1]Institute for Sustainable Water Resources, Department of Civil Engineering, Monash University, Australia

To understand the relationship between the climate and groundwater levels in shallow unconfined aquifers, the historical data of rainfall and evapotranspiration (Morton's Actual Areal Evapotranspiration, AAET) and groundwater level data have been analysed. The site studied is the Ranger uranium mine, Northern Territory, Australia. Of the three main hydrologic variables, rainfall and groundwater level data are measured whereas evapotranspiration data are estimated. As the process of evapotranspiration estimates involves a lot of climatic variables, which vary significantly in time and space, there was a need to investigate the available methods and sources for estimating evapotranspiration (ET) data.

The two principal sources of ET data are the Bureau of Meteorology ET map data and SILO Patched Point Data (PPD). The ET map of Australia is developed based on long-term averages (1961-1990) for the monthly values of a year. The SILO data provides daily values of estimated evapotranspiration. We select the AAET from both sources for our analysis. We estimate the monthly AAET of SILO data by summing up the daily values, with SILO data obtained in 2006 being for the period 1980-2005. Both of these sources have used the Morton equations in the estimation of AAET. We compare the annual AAET of these two sources in view of their performance in the annual water balance for the Ranger site.

The average annual Morton's AAET from SILO is 1414 mm whereas the AAET for the same site from the ET map gives 1064 mm. The ET map is based on the period of 1961 to 1990. Therefore we find the average annual Morton's AAET from SILO 2006 source for the Jabiru site for the same period (1961 to 1990) also and it is 1361 mm. Thus the SILO data source of Morton's AAET is consistently higher then the ET map. The consideration of annual runoff in the water balance fits better with ET map data in comparison to SILO; ie. Runoff (514 mm) + AAET (1064 mm) = Rain (1498).

Though both are ideally supposed to be the same estimates, the reason for inequality may be attributed to the fact that after estimation of AAET, the values of map were adjusted for the regional water balance by the investigators.

Therefore two sets of conceptual models need to be considered to demonstrate the validity of both of the AAET estimates. For AAET estimates of SILO, we should consider (Rain = wet season AAET + runoff) and (runoff = dry season AAET). That means, the runoff is a sink for wet season rainfall and source for dry season evapotranspiration in the form of soil moisture. This is valid where the catchments under consideration generates and absorbs the runoff within itself.

For AAET estimates from ET map data we should consider Rain = Runoff + AAET. This is valid when the runoff is a one-way flow; it is generated from rainfall and not absorbed within the catchments boundary for recycling in dry season.

In summary, it is critical to check and cross-correlate AAET data for hydrologic catchments, especially in the context of regional water balances.

Key words: Morton's AAET, SILO Patched Point Data, evapotranspiration map data, Ranger uranium mine

Email: Mobashwera.Kabir@eng.monash.edu.au

21st Victorian Universities Earth and Environmental Sciences Conference

Geological Society of Australia Abstracts Number 86

Editors: Sarah Hagerty
Dale McKenzie
Yohannes Yihdego

ISSN: 0729 011X

Preferred citation for this volume:
Hagerty, S.H., McKenzie, D.S. and Yihdego, Y. (editors). 21st Victorian Universities Earth and Environmental Sciences Conference, September 2007, Geological Society of Australia Abstracts No **86.**

Example citation for papers in this volume
Hart, C.V., 2007 Surface and groundwater interactions of the Glenelg River, western Victoria, Australia. In: Hagerty, S.H., McKenzie, D.S. and Yihdego, Y. (editors). 21st Victorian Universities Earth and Environmental Sciences Conference, September 2007, Geological Society of Australia Abstracts No **86.**

Copies of this publication may be obtained from:

The Business Manager
Geological Society of Australia Incorporated
Suite 706 Thakral House, 301 George Street
Sydney NSW 2000 Australia

Groundwater-climate relationships, Ranger uranium mine, Australia: 1. Time series statistical analyses

Mobashwera Kabir[1], Kais Hamza[2], Gavin M. Mudd[1,*] and Anthony R. Ladson[1,3]

[1]Institute for Sustainable Water Resources, Department of Civil Engineering, Monash University, VIC 3800 Australia (* Gavin.Mudd@eng.monash.edu.au)
[2]School of Mathematics, Monash University, VIC 3800 Australia
[3]Presently SKM Consulting Pty Ltd, Melbourne, VIC Australia

Abstract. This paper presents the results of applying specific time series statistical techniques to observed historical groundwater-climate data at the Ranger uranium project. By developing and applying existing statistical techniques, rarely used in mining studies, improved confidence about the understanding of the groundwater-climate relationship at the Ranger uranium project is obtained. This forms a sound basis upon which future climate scenarios can be used to predict the response of the groundwater after rehabilitation and into the long-term, especially with respect to potential climate change impacts.

Introduction

The relationship between groundwater and climate is critical to understand in the design of uranium mine rehabilitation, especially in tropical regions with intense monsoonal rains and extended dry seasons. The Ranger uranium mine is located in the wet-dry tropics of northern Australia and is surrounded by the world heritage-listed Kakadu National Park (Fig. 1) – making it imperative to understand the groundwater-climate relationship to ensure that appropriate rehabilitation designs are implemented upon mine closure.

There are a variety of techniques which can be used to model the relationship between groundwater and climatic conditions. The complex geology, topography and climatic variability of the Ranger project area makes a deterministic process-based model a challenging task. For a simpler approach, this paper presents the application of time series statistical techniques, an approach rarely used in mining projects (companion conference papers present physical modelling approach).

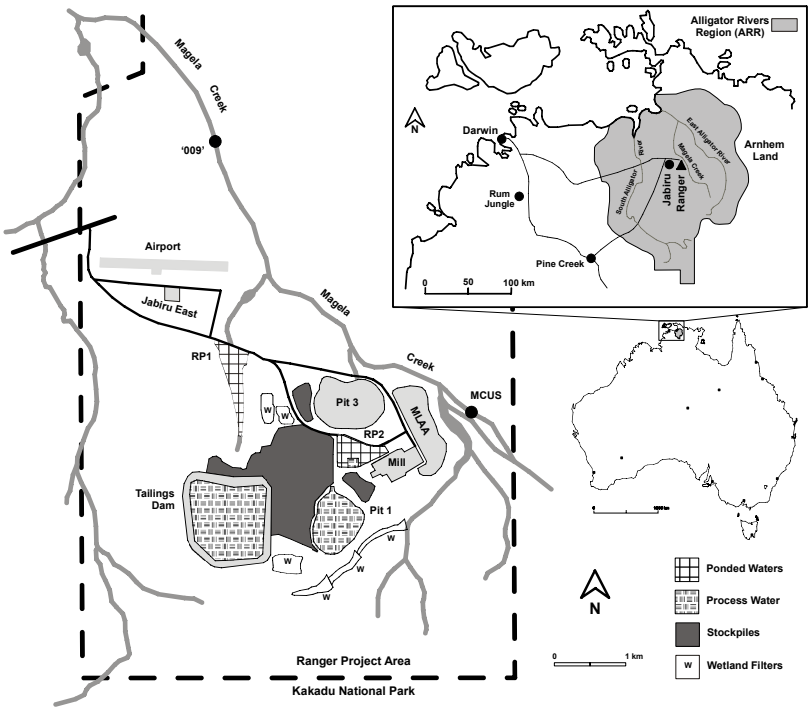

Fig.1. Location and outline of the Ranger uranium project, Northern Territory, Australia.

Ranger uranium project, Northern Territory, Australia

The Ranger uranium deposits were first discovered and 1969, and after extended controversy and debate, was approved for development in 1977. Production began in August 1981, and is currently at 5,000 t U_3O_8/year via open cut mining and a conventional mill. At present, mining is scheduled to be completed in 2012, with milling of ore stockpiles to be completed by 2020. The site is located on freehold indigenous land, controlled by the Mirarr traditional owners.

The Ranger project is located in the Alligator Rivers Region and is surrounded by the world-heritage listed Kakadu National Park (Fig. 1). The area has a wet-dry monsoonal climate, with average annual rainfall of ~1,450 mm and pan evaporation of ~2,500 mm. Virtually all rainfall occurs during the monsoonal months of December to March, leading to a strongly positive water balance over this time.

After completion of mining and milling, the Ranger site will be rehabilitated, and a key legal criterion for tailings is that they "will not result in any detrimental environmental impacts for at least 10,000 years" (Senate 2003). As groundwater is the key driver for long-term migration, it is therefore critical to understand groundwater-climate relationships (especially in light of potential climate change

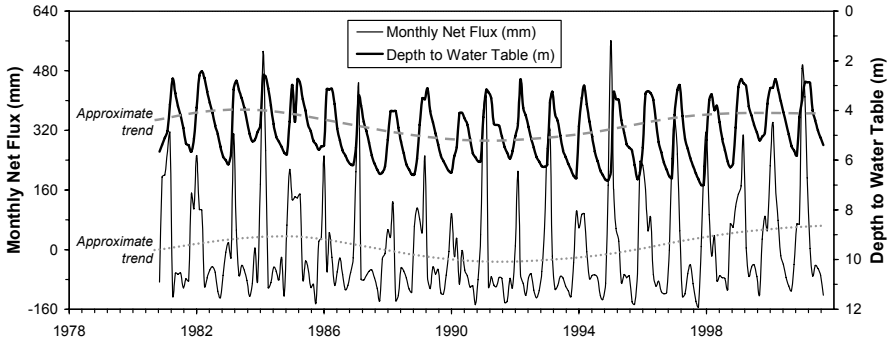

Fig.2. Monthly net flux (rainfall minus estimated evapotranspiration) versus groundwater response, Ranger site. Note both annual variation plus longer term decadal variation.

impacts). Given Ranger's location, there is a range of climate and groundwater monitoring data which can be analysed, with an example shown in Fig. 2.

Methodology and approach

Conceptual hydrologic model

The groundwater behaviour at the Ranger site is treated as a one-dimensional and effectively vertical flow system, based on the large head changes each wet season relative to minor lateral flow. In this manner, the recharge of groundwater during the wet season causes a rise in the water table, while the negative flux during the dry season (due to both soil evaporation and vegetative transpiration) leads to a subsequent decline in the water table. The monthly climatic flux is shown in Fig. 3. The extent of this annual cyclical movement of groundwater is dependent on soil types, underlying geology and relatively flat topography (see Kabir et al 2008). The groundwater bores chosen for analysis were screened based on long-term trends and no evidence of direct mining impacts on head levels (eg. seepage).

All data is obtained from monitoring of groundwater and climate (rainfall, pan evaporation) at the Ranger site, courtesy of Energy Resources of Australia Ltd (ERA, mine owner) or the Office of the Supervising Scientist (OSS, Federal agency) (further details are given in Kabir, 2008).

Time series statistical techniques – brief review

Although times series statistical techniques (TSST) methods are widely used in other disciplines (e.g. economics, hydrology), they have seen little application in groundwater studies(e.g. Fig. 2). Only a brief review is possible herein; for a more thorough treatment see Brockwell and Davis (2002).

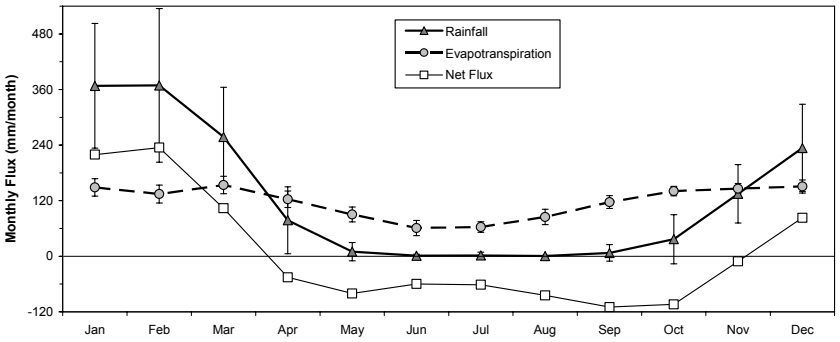

Fig.3. Monthly rainfall, estimated evapotranspiration and net flux.

At its simplest conceptual basis, time series techniques involve developing a statistical relationship between an independent variable (e.g. climate data as cause) and a dependent variable (e.g. groundwater response as effect).

In this study, exploratory data analysis was undertaken to examine seasonality, trends and random noise (e.g. Fig. 2). Classical decomposition techniques were used to address this, and represents a univariate time series model, given as (Brockwell and Davis 2002):

$$X_t = m_t + s_t + A_t \qquad \text{(Eq.1)}$$

$$\text{and} \qquad EA_t = 0,\ s_{t+d} + A_t \qquad \text{and} \sum_{j=1}^{d} s_j = 0 \qquad \text{(Eq.2)}$$

where X_t is the dependent variable at time t (ie. groundwater), m_t is the long-term trend component, s_t is the seasonal component, A_t is the random noise component (a zero-mean stationary process), EA_t is the expected value of A_t, and d is the period of seasonal components.

The seasonal component is calculated such that the period length (d) ensures the values are the same. For example, a period of 12 is used for monthly data. The algebraic sum of the 12 months seasonal components should equal zero (*Eq. 2*). The seasonal components of the net flux and groundwater level are given in Fig. 3.

A univariate autoregressive moving average (ARMA) model could explain the time series of climate and groundwater data of four selected bores, however, the causal relationship between climate and groundwater levels requires multivariate analyses. Therefore two specific TSST methods, namely the transfer function noise (TFN) model and the multivariate autoregressive (MA) model, were used for modelling the groundwater-climate data.

The first TSST model applied in this paper is the TFN model, and involves transforming data to generate zero-mean stationary data sets. The TFN model can then be represented as (Brockwell and Davis 2002):

$$Y(t) = T(B).X(t) + N(t) \qquad \text{(Eq.3)}$$

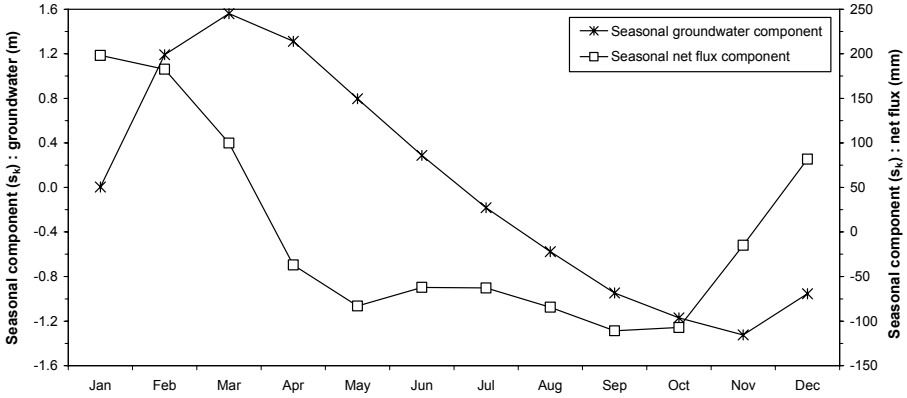

Fig.4. Seasonal components of climatic net flux and groundwater level data.

where *Y(t)* is the dependent variable (ie. groundwater), *X(t)* is the independent variable (climate), *T(B)* is a causal time-invariant linear filter, B is back shift operator and *N(t)* is a zero-mean stationary process (uncorrelated with *X(t)*).

The second TSST model developed is a Yule-Walker multivariate autoregressive (MA) model using monthly data.

Further theoretical discussion, development and references for both TSST models can be found in Brockwell and Davis (2002).

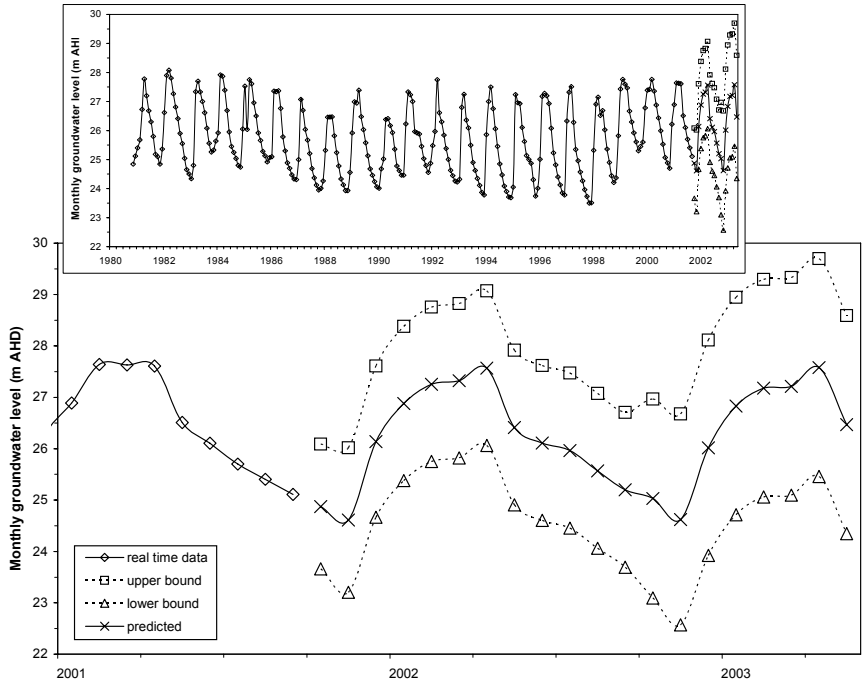

Fig.5. Predictions of groundwater level by the transfer function noise (TFN) model.

Results

Monthly groundwater levels have been predicted for twenty months by analysing twenty two years monthly data (Fig. 5) by TFN model. The monthly net flux and monthly groundwater levels have been predicted for twenty years by analysing twenty-two years monthly data, shown in (Fig. 6) by MA model.

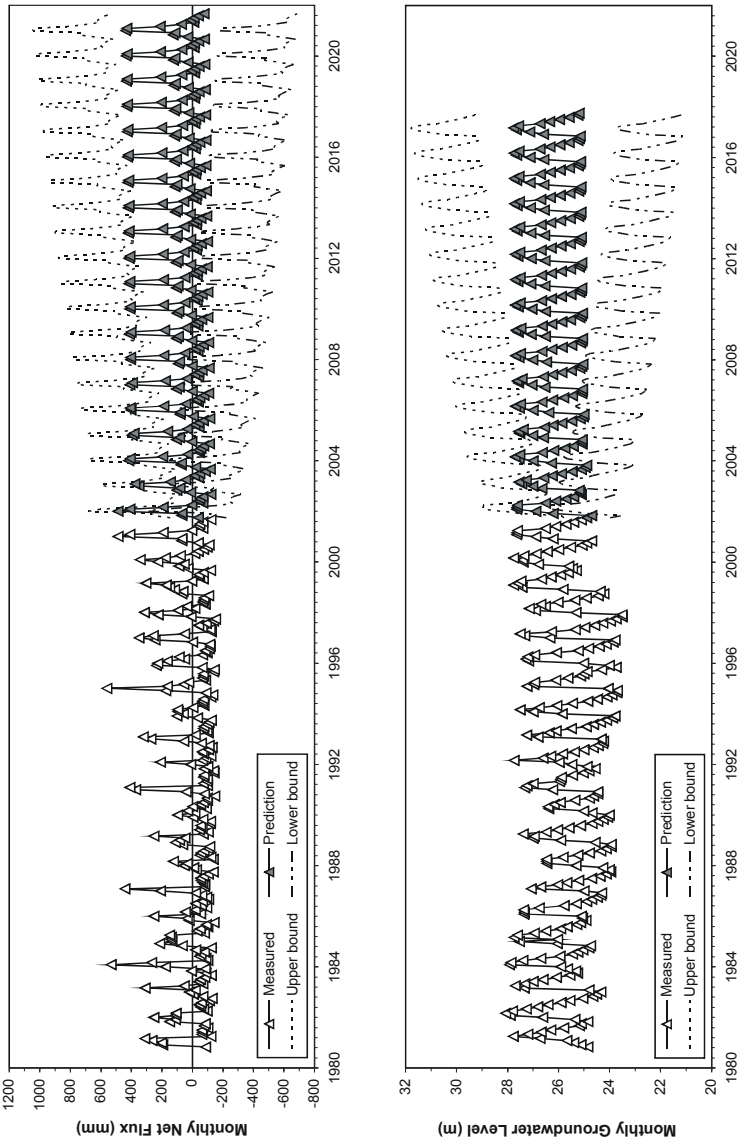

Fig.6. Predictions of monthly net flux (left) and groundwater levels (right) by multivariate autoregressive (MA) model.

The TFN model is represented by:

$$\text{Input} \quad X(t) = -0.012\,X(t-1) + 0.121\,X(t-2) + 0.266\,X(t-3) - 0.201\,X(t-4) - 0.551\,X(t-5) + Z(t) + 0.190\,Z(t-1) - 0.367\,Z(t-2) - 0.438\,Z(t-3) + 0.276\,Z(t-4) + 0.935\,Z(t-5) \quad \text{(Eq.4)}$$

$$\text{Transfer} \quad T(B) = 1.7\,B / (1 - 0.283\,B) \quad \text{(Eq.5)}$$

$$\text{Noise} \quad N(t) = W(t) + 0.5135W(t-1) + 0.336W(t-2) + 0.2365W(t-3) \quad \text{(Eq. 6)}$$

Model performance was evaluated in the light of existing statistical criteria, such as model simplicity, model fitness and the Akaike Information Criterion with Correction AICC (Akaike 1969), combined with the appropriateness of the physical basis of the two methods. In Table 2, to compare the statistical performance of the monthly-based models, a number of criteria have been considered. These are the AICC statistic, root mean square error (RMSE), and square of correlation coefficient (R^2) for the models. It is found that the TFN model performs better than the AR model with respect to RMSE and R^2, while the reverse is true for the AICC statistic. The AICC statistic is a standard selection criterion when the competing models are of the same type, where a minimum value indicates the best model, but it does not make sense when comparing two different types of models. In this case, the TFN model is structurally different from the MA model. From this basis, the TFN model can be said to be better than the AR model.

The groundwater levels are predicted by the monthly TFN and MA models for the period November 2001 to October 2002 and compared to measured values (ie. a model validation test). The results are shown in Fig. 7 and confidence intervals are compared in Table 2. In the validation test the two models are similar.

Table 1. Statistical evaluation and comparison of TFN and MA models.

Model	AICC	RMSE	R^2
Transfer function noise (TFN)	6698	0.166	0.761
Multivariate autoregressive (MA)	6585	0.173	0.760

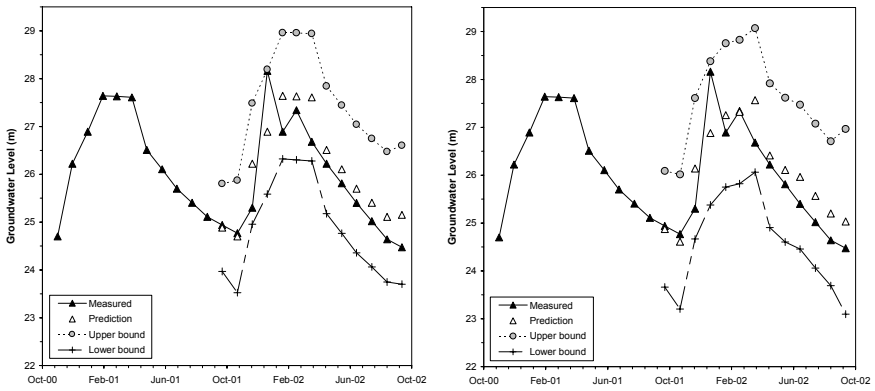

Fig.7. Validation of TFN model (left) and MA model (right) for Nov. 2001 to Oct. 2002.

Table 2. Average confidence interval range for TFN and MA models, Nov. 2001 to Oct. 2002 validation.

Model	Average range of confidence interval (m)
Transfer function noise (TFN)	2.94
Multivariate autoregressive (MA)	2.56

Technically, TFN models are superior to MA models in explaining the groundwater-climate relationship. The theory of MA model considers the mutual dependence of all the series of the process. For instance, the net flux at time t+1 is represented as function of net flux at t, t-1, t-2 … together with groundwater level at t, t-1, t-2 … as well and a noise component. However, in the TFN model, the previous values of the groundwater level series are not considered explicitly. From the scientific point of view, there does exist a strong causal relationship between net flux and groundwater level, but the relationship is not two way. That means net flux influences groundwater level but groundwater level does not influence net flux to any significant extent (ie. the influence is effectively one way). Although the evaporative flux depends on soil moisture content, which in turn is influenced by the nearness of groundwater level to the surface, the importance of this variable is much less than other factors such as intensity and duration of radiative energy, relative humidity, temperature gradient, soil thermal conductivity, vegetation type, wind speed, etc., which influence the evaporation and transpiration process. The statistical fits and confidence intervals of both models, however, are comparable. Therefore, the TFN model is more acceptable than the MA model in representing the system and predicting future groundwater levels.

Discussion

To select the appropriate method of analysis of the groundwater-climate relationship, reviews of the various classes of models were performed. The three basic features, useful for distinguishing approaches to modelling are (CRCCH 2005):

- the nature of the basic algorithms (empirical, conceptual or process-based);
- whether a statistical or deterministic approach is taken to input or parameter specification;
- whether the spatial and temporal representation is lumped or distributed.

The review of key climate feedbacks which are related to groundwater recharge and hydrologic processes suggests that to manage the complex interaction between climate and groundwater recharge, the development of a balanced modelling framework is necessary. Data-based statistical techniques are more preferable than deterministic models when the latter requires too much simplification of the complex system. Comprehensive modelling of groundwater-climate relationships could go to the ultimate extent of including a variety of processes, such as heat flow, groundwater flow and pumping, vapour fluxes, cloud cover, vegetative transpiration, soil evaporation, variable geology and soils, and so on. However, such complexity is clearly unrealistic given the large spatial and temporal uncertainties involved in all of these aspects and processes.

Climatic conditions and variability undoubtedly govern or contribute to shallow groundwater levels (e.g. Fig. 2) (see also Alley 2001; Glassley 2003; Loáiciga 2003; Michaud et al 2004), yet a complete process representation is computationally and physically unrealistic given the complex variability of processes and inter-dependence of many factors. This is not to ignore the value of sound physical or process-based models, but it highlights that different approaches such as time series statistics can be used to compliment such models and analyses, often providing efficient numerical techniques which effectively combine the complexity of natural processes into functional statistical relationships.

Conclusions

Groundwater levels will be the major driver for the potential transport of solutes from a rehabilitated Ranger uranium mine, especially levels relative to non-mine areas. To ensure that the rehabilitation achieves its legal obligations to protect the surrounding water resources and ecosystems for 10,000 years from tailings, it is vital to understand and be able to model the groundwater-climate relationship. This is a fundamental objective to ensure a sustainable post-mining land use and protection of the recognised world-heritage values of the region.

To bridge the gap between the observation scale (~monthly data) and modelling scale (long-term prediction) (Bloschl and Sivapalan 1995), we have used common time series statistical techniques. These methods identify the underlying patterns and the qualitative description of the groundwater-climate relationship, such as seasonal variability or long-term trends.

The application of a classical decomposition model to the groundwater-climate data for Ranger was used first to gain an understanding of the relationship. The timing of the peak and trough between the two seasonal data sets indicates that the lag between them is less (2 months) during high groundwater levels (wet season) and much more (4 to 5 months) during low groundwater levels (dry season). Hence the process has a variable lag throughout the year.

Thus, for improved understanding of the physics with the help of statistics, a classical decomposition model has been used with historical net flux and groundwater level data for the Ranger uranium mine site. A transfer function noise (TFN) model and multivariate autoregressive (MA) model were then developed by using the net flux and groundwater level data to predict the future groundwater level. Some of them have been found to be numerically efficient and others have the quality of best fit.

Finally the statistical performance is almost equal for both the TFN model and MA model but the physical representation is better in TFN than MA. Therefore a monthly-based TFN should be the recommended model for the prediction purpose in future research.

References

Akaike H (1969) Fitting autoregressive models for prediction. Annals of the Institute of Statistical Mathematics, 21, pp 243-247

Alley WM (2001) Ground Water and Climate. Ground Water, 39(2), pp 161

Bloschl G and Sivapalan M (1995) Scale issues in hydrological modelling: a review. Hydrological Processes 9, pp 251-290

Brockwell PJ and Davis RA (2002) Introduction to time series and forecasting. Springer-Verlag, New York, USA

CRCCH (2005) General approaches to modelling and practical issues of model choice. Cooperative Research Centre for Catchment Hydrology, Series on Model Choice, see http://www.toolkit.net.au/modelchoice/

Glassley WE (2003) The impact of climate change on vadose zone pore waters and its implication for long-term monitoring. Computers and Geosciences 29(3), pp 399-411

Kabir M (2008) Modelling groundwater-climate relationships at the Ranger uranium mine, Australia. PhD Thesis (In Preparation), Dept. of Civil Eng., Monash University

Kabir M, Mudd GM and Ladson AR (2008) Groundwater-climate relationships, Ranger uranium mine, Australia : 2 validation of unsaturated flow modelling. Proc. “Uranium mining and hydrogeology V”, Freiberg, Germany, September 2008

Loáiciga HA (2003) Climate change and groundwater. Annals of the Association of American Geographers 93(1), pp 30-41

Michaud YC, Rivard et al. (2004) Groundwater resources and climate change: Trends from eastern Canada. American Geophysical Union, Spring Meeting 2004.

Senate (2003) Regulating the Ranger, Jabiluka, Beverley and Honeymoon uranium mines. Environment, Communications, Information Technology and the Arts References Committee, Australian Senate, Canberra, Australia, 355p

Groundwater-climate relationships, Ranger uranium mine, Australia: 2. Validation of unsaturated flow modelling

Mobashwera Kabir[1], Gavin M. Mudd[1,*] and Anthony R. Ladson[1,2]

[1]Institute for Sustainable Water Resources, Department of Civil Engineering, Monash University, VIC 3800 Australia (*Gavin.Mudd@eng.monash.edu.au)
[2]Presently SKM Consulting Pty Ltd, Melbourne, VIC Australia

Abstract. This paper presents the results of applying an unsaturated flow model to observed historical groundwater-climate data at the Ranger uranium project, Northern Territory, Australia. Based on observed data, a one-dimensional model was developed to fit historical data for several bores. Statistical evaluation of varying porosity and hydraulic conductivity was undertaken, thereby giving a reasonable model configuration. The model is thus confirmed as suitable for predicting the impacts of future climate change scenarios on water table fluctuations.

Introduction

The relationship between groundwater and climate is critical in the design of uranium mine rehabilitation, especially in tropical regions with intense monsoonal rains and extended dry seasons. The Ranger uranium mine is located in the wet-dry tropics of northern Australia and is surrounded by the world heritage-listed Kakadu National Park (Fig. 1). It is imperative to understand the groundwater-climate relationship to ensure that appropriate rehabilitation designs are implemented upon mine closure (see also companion paper Kabir et al 2008).

A variety of techniques can be used to model groundwater fluctuations as a function of climatic conditions. The complex geology and climatic variability of the Ranger region makes a deterministic, detailed process-based model a difficult task. For an alternative viable approach, this paper uses the unsaturated flow model Seep/W (Krahn 2004) based on a one-dimensional conceptual model of the groundwater-climate system. Given the relatively flat topography and large annual fluctuations in the water table versus minor lateral flows, the flow system can be simplified as effectively vertical, thereby allowing direct implementation in Seep/W. The refined model can then be used for a variety of purposes.

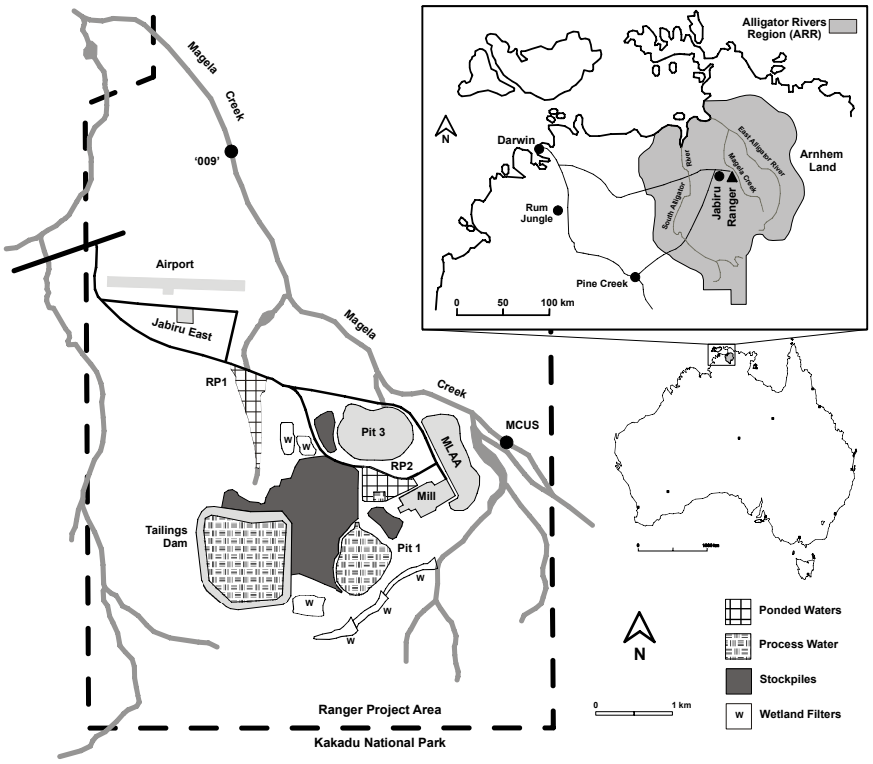

Fig.1. Location and outline of the Ranger uranium project, Northern Territory, Australia.

Hydrogeology of the Ranger site

The Ranger uranium project was briefly described in the companion paper Kabir et al (2008). Although there have been numerous studies on the hydrogeology and water balance at Ranger, only a few have directly examined the relationship between groundwater and climate, especially rainfall-evaporation and recharge (e.g. Vardavas, 1993; Woods 1994). A brief review of the hydrogeology is presented, followed by a justification of the modelling approach used for this work.

In the past, hydrogeology studies at Ranger have commonly focussed on water or tailings management issues. The hydrogeology is considered to comprise three principal aquifer types – alluvial sands and gravels (Type A), lateritic layers, clayey sands to weathered rocks (Type B), and fractured rocks (e.g. schists, dolomite) (Type C), shown in Fig. 2 (Ahmad and Green 1986; Woods 1994; Brown et al 1998). The most important shallow aquifers are found as weathered and lateritic soils (by area), with annual variations in the water table being between 1 to 5 m.

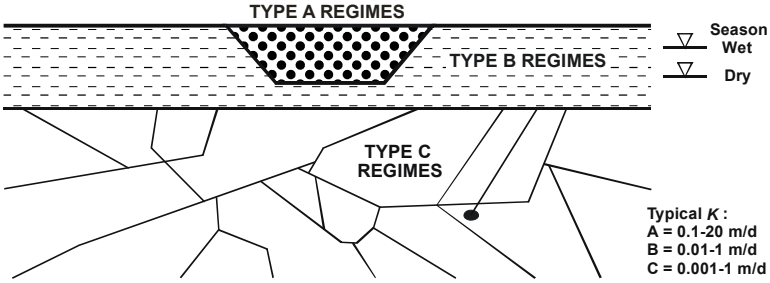

Fig.2. Conceptual hydrogeology of Ranger, including approximate wet and dry season position of the water table (adapted from Ahmad and Green 1986; Woods 1994).

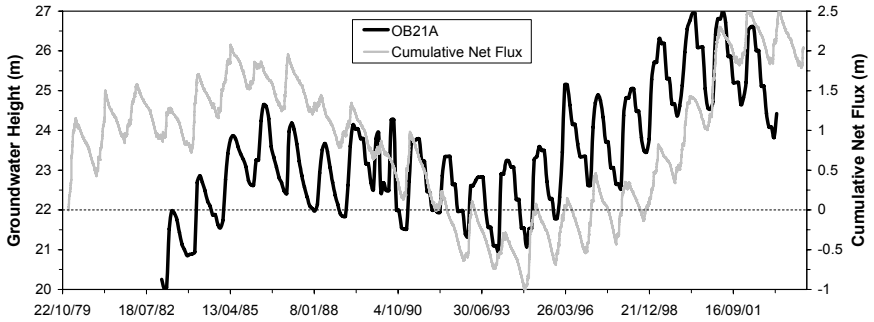

Fig.3. Variation of groundwater (bore OB21A) and cumulative climatic net flux.

One example of the seasonal groundwater movement compared to cumulative net flux (rainfall – evapotranspiration) is given in Fig. 3, showing annual variation along with long term climatic variability (ie. wetter versus dryer periods).

Seep/W model structure and development

A one-dimensional conceptual model of groundwater-climate interaction was adopted (e.g. Type B). A homogenous vertical column was defined with no-flow boundaries on all sides except the surface where net climate flux was applied (rainfall – evapotranspiration) at monthly time steps. Soil properties were based on previous work, such as porosity, saturated hydraulic conductivity and unsaturated moisture retention (characteristic) curve (e.g. Willett et al 1993; Akber 1991), while the unsaturated hydraulic conductivity function was defined from the characteristic curve (e.g. van Genuchten or Fredlund-Xing models, see Krahn 2004).

As noted above, the hydrogeology of the Ranger area is highly heterogeneous, leading to differing average responses of the water table to the annual wet season (e.g. annual fluctuation, or Δh, of 1-5 m). Obtaining reliable spatial data on all of the above properties is difficult and still includes residual uncertainty. As such a range of Seep/W models were developed with varying soil parameters to assess this uncertainty. This allowed a choice of optimum properties for each bore to be

used for assessing climate change impacts (see Kabir et al 2008b). In this work, saturated hydraulic conductivity (*K*, 0.3 to 30 m/30 days) and effective porosity (*n*, 2.5% to 20%) were varied. All model results were statistically evaluated using the measures in Table 1, to ascertain the 'goodness of fit' for each model.

Table 1. Statistical objective functions[a] used to assess model fit.

Measure[b]	Expression[b]	Range	Decision Rule
E (Nash-Sutcliffe criterion)	$E = 1 - \frac{\sum_{t=1}^{T}(h_o^t - h_m^t)^2}{\sum_{t=1}^{T}(h_o^t - \overline{h_o})^2}$	-∝ to +1	+1 is desirable
r (linear correlation coefficient)	$r = \frac{\sum_{t=1}^{T}(h_m^t - \overline{h_m})(h_o^t - \overline{h_o})}{\sqrt{\sum_{t=1}^{T}(h_m^t - \overline{h_m})^2}\sqrt{\sum_{t=1}^{T}(h_o^t - \overline{h_o})^2}}$	-1 to 1	+1 is desirable, -1 is undesirable
Ratio	$Ratio = \overline{h_m} \,/\, \overline{h_o}$	0 to ∝	+1 is desirable
RMSE (root mean square error)	$RMSE = \sqrt{\sum_{t=1}^{T}(h_m^t - h_o^t)^2} \Big/ T$	0 to ∝	0 is desirable
$\overline{d}$ (mean error)	$\overline{d} = \overline{h_m} - \overline{h_o}$ where $\overline{h_m} = \sum_{t=1}^{T} h_m^t \Big/ T$	-∝ to +∝	0 is desirable
S_e (standard error)	$S_e = \sqrt{\frac{S^2}{T-1}}$ & $S^2 = \frac{\sum_{t=1}^{T}(d^t)^2}{T} - \overline{d}^2$	0 to ∝	0 is desirable
β	$\beta = \overline{d} \Big/ \sqrt{S^2/(T-1)} = \overline{d} \Big/ S_e$	0 to ∝	0 is desirable

[a] From Zheng and Bennett (1995), Middlemis et al (2001), Nash and Sutcliffe (1970).
[b] Primary variables are *h* head; *t* time step number (T total time steps); *d* model – measured difference; Subscript 'm' / 'o' – model / observed values; ¯ (overscore) average (e.g. $\overline{h_m}$ = average modelled head).

Results

Nine model were developed with the combinations of K=0.3, 3 and 30 m/30days and n=2.5, 5 and 10%. Statistical evaluations of model runs are given in Tables 2 and 3, with an example in Fig. 4. An example of measured versus modelled groundwater heads (bore OB21A) is graphed in Fig. 5.

From Tables 2 and 3, optimum (desirable) values of criteria $\overline{h_m}$, *E*, *Ratio, RMSE,* β, $\overline{d}$, and S_e are found to in one model combination, while criterion *r* is found to be in a different model run. The difference, however, between *r* values in these models is mostly marginal. To achieve better consistency between the criteria, runs are extended to additional set of combinations for n=20%. The direction

of changes of the criteria are again found to be mostly inconsistent. The best bore with consistent model parameter comes out to be OB27 with K 30 n 20.

Table 2. Statistical assessments[a] of Seep/W model runs versus soil parameters (K, n).

	$\overline{h_m}$	*E*	*r*	*Ratio*	*RMSE*	β	$\overline{d}$	S_e
Desired value	–	1	1	1	0	0	0	0
OB1A[b], $\overline{h_o}$ = 25.83 m, Δh = 3.17 m (*K* m/30 days, *n* %)								
K 0.3, n 2.5	25.43	-0.56	0.23	0.98	0.09	4.37	0.4	0.09
K 3, n 2.5	21.57	-30.2	***0.42***	0.84	0.42	12.94	4.26	0.33
K 30, n 2.5	1.83	-3781	0.3	0.07	4.62	5.47	24	4.39
K 0.3, n 5	25.69	-0.37	0.09	0.99	0.09	1.54	0.14	0.09
K 3, n 5	23.3	-11.07	0.33	0.9	0.26	11.99	2.53	0.21
K 30, n 5	22.01	-18.69	**0.35**	0.85	0.33	16.09	3.82	0.24
K 0.3, n 10	**25.82**	**-0.11**	0.16	**1**	**0.08**	**0.11**	**0.01**	**0.08**
K 3, n 10	23.94	-4.16	0.26	0.93	0.17	14.98	1.89	0.13
K 30, n 10	23.81	-0.12	0.33	0.92	0.17	16.75	2.02	0.12
K 0.3, n 20	***25.83***	***0.03***	0.21	***1***	***0.07***	***0.06***	***<0.01***	***0.07***
K 30, n 20	24.71	-0.99	0.3	0.96	0.11	13.9	1.12	0.08
OB20[b], $\overline{h_o}$ = 18.09 m, Δh = 1.67 m (*K* m/30 days, *n* %)								
K 0.3, n 2.5	16.82	-1.5	0.59	**0.93**	0.1	21.86	1.27	0.06
K 3, n 2.5	13.14	-42.81	***0.72***	0.73	0.41	18.18	4.94	0.27
K 30, n 2.5	9.76	-123.84	**0.63**	0.54	0.7	18.12	8.33	0.46
K 0.3, n 5	17.1	-0.67	0.59	***0.95***	0.08	19.12	0.99	***0.05***
K 3, n 5	14.39	-19.95	**0.63**	0.8	0.29	22.36	3.7	0.17
K 30, n 5	14.08	-23.53	0.61	0.78	0.31	22.49	4.01	0.18
K 0.3, n 10	***17.2***	***-0.42***	0.62	***0.95***	***0.07***	**17.79**	***0.88***	***0.05***
K 3, n 10	15.56	-7.28	0.54	0.86	0.18	30.49	2.53	0.08
K 30, n 10	15.14	-9.78	0.56	0.84	0.2	33.93	2.95	0.09
K 0.3, n 20	**17.17**	**-0.59**	0.6	***0.95***	**0.08**	***17.23***	**0.92**	0.05
K 30, n 20	16.09	-3.86	0.53	0.89	0.14	35.98	2	**0.06**
OB21A[b], $\overline{h_o}$ = 23.42 m, Δh = 2.14 m (*K* m/30 days, *n* %)								
K 0.3, n 2.5	24.98	-0.59	***0.75***	1.07	0.12	-22.7	-1.56	***0.07***
K 3, n 2.5	20.75	-8.13	0.66	0.89	0.29	11.34	2.67	0.24
K 30, n 2.5	17.14	-31.94	0.35	0.73	0.55	16.6	6.28	0.38
K 0.3, n 5	**24.62**	**-0.34**	0.7	**1.05**	**0.11**	**-14.97**	**-1.2**	**0.08**
K 3, n 5	20.24	-5.75	0.55	0.86	0.25	21.87	3.17	0.15
K 30, n 5	18.96	-11.53	0.34	0.81	0.34	24.09	4.45	0.18
K 0.3, n 10	***23.33***	***0.37***	**0.72**	***1***	***0.08***	***1.18***	***0.09***	**0.08**
K 3, n 10	19.86	-5.83	0.37	0.85	0.25	33.79	3.55	0.11
K 30, n 10	19.58	-7.05	0.24	0.84	0.27	32.97	3.84	0.12
K 0.3, n 20	21.77	-0.71	0.71	0.93	0.13	24.27	1.65	***0.07***
K 30, n 20	20.03	-5.05	0.34	0.86	0.24	36.91	3.39	0.09

[a] Best fits are highlighted in grey shaded bold-italic text; next closest fits are bold only.
[b] Model runs with K 3 not available.

Table 3. Statistical assessments[a] of Seep/W model runs versus soil parameters (K, n).

	$\overline{h_m}$	*E*	*r*	*Ratio*	*RMSE*	β	$\overline{d}$	S_e
Desired value	–	1	1	1	0	0	0	0
OB27[b], $\overline{h_o}$ = 8.87 m, Δh = 2.00 m (*K* m/30 days, *n* %)								
K 0.3, n 2.5	10.15	-1.54	0.62	1.14	0.13	-20.57	-1.28	**0.06**
K 3, n 2.5	10.92	-5.37	0.77	1.23	0.2	-21.73	-2.05	0.09
K 30, n 2.5	11.09	-6.16	0.77	1.25	0.21	-23.58	-2.21	0.09
K 0.3, n 5	10.18	-2.1	0.42	1.15	0.14	-15.78	-1.31	0.08
K 3, n 5	10.69	-3.55	0.78	1.2	0.17	-27.86	-1.81	0.07
K 30, n 5	10.46	-2.82	**0.79**	1.18	0.15	-21.31	-1.58	0.07
K 0.3, n 10	9.92	-1.84	0.42	1.12	0.13	-10.71	-1.05	0.1
K 3, n 10	9.52	-0.04	0.72	1.07	0.08	-11.2	-0.65	**0.06**
K 30, n 10	9.42	0.23	0.77	1.06	0.07	-10.54	-0.54	***0.05***
K 3, n 20	***8.61***	**0.28**	0.62	**0.97**	0.07	***4.26***	***0.27***	**0.06**
K 30, n 20	**8.56**	***0.37***	***0.81***	**0.96**	***0.06***	**5.51**	**0.31**	**0.06**
OB41[b], $\overline{h_o}$ = 14.89 m, Δh = 1.69 m (*K* m/30 days, *n* %)								
K 0.3, n 2.5	12.24	-18.29	***0.55***	0.82	0.19	25.11	2.84	0.11
K 3, n 2.5	8.77	-168.18	**0.53**	0.59	0.57	15.74	9.43	0.6
K 30, n 2.5	-20.62	-26838	0.35	-1.38	7.21	***5.22***	65.38	12.54
K 0.3, n 5	12.59	-13.31	0.36	0.85	**0.17**	23.99	**2.44**	**0.1**
K 3, n 5	10.57	-69.46	0.42	0.71	0.37	21.34	6.39	0.3
K 30, n 5	9.97	-90.09	0.38	0.67	0.42	21.26	7.15	0.34
K 0.3, n 10	**12.92**	**-9.64**	0.21	**0.87**	***0.14***	21.71	2.05	***0.09***
K 3, n 10	12.08	-26.33	0.35	0.81	0.23	23.99	3.89	0.16
K 30, n 10	12.4	-21.75	0.39	0.83	0.21	23.92	3.57	0.15
K 0.3, n 20	***12.93***	***-5.53***	-0.24	**0.89**	0.18	19.29	***1.67***	***0.09***
K 30, n 20	12	-13.5	-0.01	0.82	0.27	24.29	2.6	0.11

[a] Best fits are highlighted in grey shaded bold-italic text; next closest fits are bold only.
[b] Model runs with K 0.3-n 20 (OB27) and K 3-n 20 (OB41) not available.

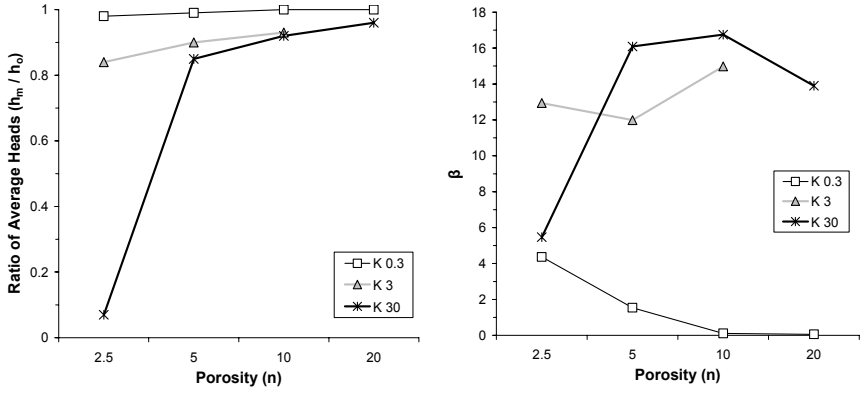

Fig.4. Example of the variation of selected statistical evaluations for bore OB1A.

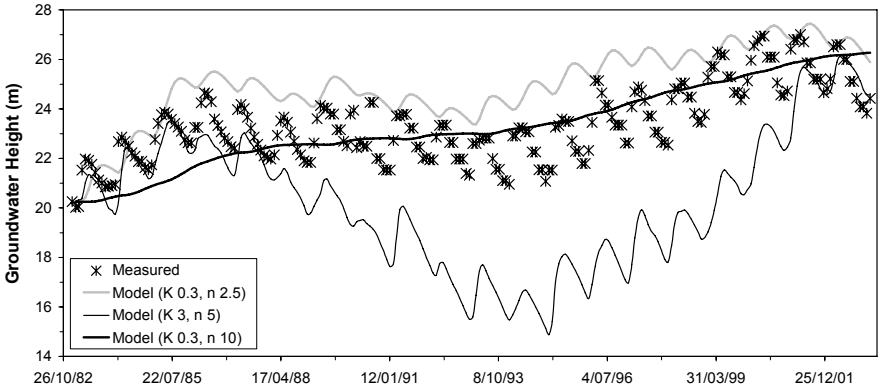

Fig.5. Observed versus modelled groundwater levels in bore OB21A.

Discussion

Based on all results above, the performance of the models for OB27 achieves the best result since this bore successfully includes the best E and r values in one combination of hydraulic conductivity and porosity. Another important aspect of the results is that the best model may not necessarily be unique, rather it corresponds to a range of parameter values for most of the bores. For example, with respect to the statistical evaluation of parameter combinations, OB41 shows a lot of scatter while OB27 shows a consistent parameter combination.

If we analyse the importance of all criteria in context to the primary objective of the modelling, the most important criterion is considered to be the r value as this deals with both the magnitude and direction of deviation whereas other criteria deal with magnitude only (see Middlemis et al. 2001).

The relative influence of porosity (n) on the annual average groundwater fluctuation (Δh) can be explored by comparing OB20 and OB21A, since they are close to each other. The model results show the importance of n in the amplitude of Δh. OB20 performs well with n of 10% to 20% and a measured average annual groundwater variation (Δh) of 1.67m, whereas OB21A performs well with n of 5% to 10% with Δh of 2.14m. This shows that annual fluctuations are higher for lower porosity (all other factors remaining the same).

The results also show that hydraulic conductivity is important in modelling the annual and longer term response of groundwater (as should be expected). Based on field work at Ranger (e.g. Willett et al 1993; Akber 1991), it is clear that the weathered near surface geology and aquifers at Ranger are highly variable and heterogeneous. The approach adopted in this paper is clearly a simplification which allows for efficient modelling at the expense of more thorough discretisation of model parameters (K, n, others). As such, the approach adopted herein of using a simplified one-dimensional homogenous model appears reasonable.

Conclusions

This paper presented the results of applying an unsaturated flow model (Seep/W) to observed historical groundwater-climate data at the Ranger uranium project. The approach adopted a one-dimensional groundwater-climate model to fit historical data for several bores, with varying values for hydraulic conductivity and porosity to assess uncertainty due to the heterogeneous geology of the area. All model runs were evaluated with a range of statistical measures for goodness of fit. In summary, the research approach utilised herein demonstrates that a simplified conceptual model implemented via an unsaturated flow model can achieve a robust model configuration with reasonable statistical confidence.

References

Ahmad M and Green DC (1986) Groundwater regimes and isotopic studies, Ranger mine area, Northern Territory. Australian Journal of Earth Sciences, 33, pp 391-399

Akber RA and Harris F (1991) Proc. of the workshop on land applications of effluent water from uranium mines in the Alligator Rivers Region. Office of the Supervising Scientist, Jabiru, Australia, September 1991, 360p

Brown PL, Guerin M, Hankin SI and Lowson RT (1998) Uranium and other contaminant migration in groundwater at a tropical Australian uranium mine. Journal of Contaminant Hydrology, 35, pp 295-303

Kabir M, Hamza K, Mudd GM and Ladson AR (2008a) Groundwater-climate relationships, Ranger uranium mine, Australia : 1 time series statistical analyses. Proc. "Uranium mining and hydrogeology V", Freiberg, Germany, September 2008.

Kabir M, Mudd GM and Ladson AR (2008b) Groundwater-climate relationships, Ranger uranium mine, Australia : 3 predicting climate change impacts. Proc. "Uranium mining and hydrogeology V", Freiberg, Germany, September 2008.

Krahn, J (2004) Seepage modelling with SEEP/W. Geo-Slope International Ltd, Canada

Middlemis H, Merrick N and Ross J (2001) Groundwater flow modelling guideline. Prepared by Aquaterra Consulting Pty Ltd for the Murray-Darling Basin Commission, Canberra, Australia, January 2001, 133p

Nash JE and Sutcliffe J (1970) River flow forecasting through conceptual models, Part 1, A discussion of principles. Journal of Hydrology, 10, pp 282-290

Vardavas IM (1993) A simple groundwater recharge-depletion model for the tropical Magela Creek catchment. Ecological Modelling, 68, pp 147-159

Willett IR, Bond WJ, Akber RA, Lynch DJ and Campbell GD (1993) The fate of water and solutes following irrigation with retention pond water at Ranger uranium mine. Office of the Supervising Scientist, Sydney, Australia, Research Report 10, 132p

Woods PH (1994) Likely recharge to permanent groundwater beneath future rehabilitated landforms at Ranger uranium mine, Northern Australia. Australian Journal of Earth Science 41, pp 505-508

Zheng C and Bennett GD (1995) Applied contaminant transport modeling: theory and practice. Van Nostrand Reinhold, New York

Groundwater-climate relationships, Ranger uranium mine, Australia: 3. Predicting climate change impacts

Mobashwera Kabir[1], Gavin M. Mudd[1,*], Anthony R. Ladson[1,2] and Edoardo Daly[1]

[1]Institute for Sustainable Water Resources, Department of Civil Engineering, Monash University, VIC 3800 Australia (*Gavin.Mudd@eng.monash.edu.au)
[2]Presently SKM Consulting Pty Ltd, Melbourne, VIC Australia

Abstract. This paper presents the results from using a validated unsaturated flow model to predict groundwater response to climate variability and climate change at the Ranger uranium project, Northern Territory, Australia. A Monte Carlo-style approach was adopted, with 30 statistically generated replicates for each of the 5 models and 7 scenarios from the IPCC climate change projections, giving 1050 model runs in total. The results are presented in terms of predicted groundwater levels to 2100. The paper demonstrates the usefulness of this modelling approach in understanding the future impacts from climate change on groundwater levels.

Introduction

The relationship between groundwater and climate is critical in the design of uranium mine rehabilitation, especially in tropical regions with intense monsoonal rains and extended dry seasons. The Ranger uranium mine is located in the wet-dry tropics of northern Australia and is surrounded by the world heritage-listed Kakadu National Park (see companion paper, Kabir et al 2008, for location map).

Given that climate change is predicted to lead to significant hydrologic changes across northern Australia (e.g. Hennessy et al. 2007), such as changing rainfall and evapotranspiration, it is critical to use the available data to best understand what this means for groundwater recharge, levels and therefore minesite rehabilitation.

This paper develops an approach to model the potential impacts of climate change and climate variability on groundwater levels through a Monte Carlo technique. The unsaturated flow model used is taken from Kabir et al (2008), and compliments other methods to model groundwater-climate relationships such as time series statistical techniques.

Climate variability and climate change

For this research work, the processes of climate variability and climate change need to be carefully defined, followed by a brief review of northern Australia.

According to the UN Framework Convention on Climate Change (UNFCCC), climate change refers to long-term processes occurring over several decades or centuries which leads to changes in average climatic conditions, and includes both anthropogenic and natural causes (Houghton et al 2001). Climate variability is considered to range from inter-annual to inter-decadal and is related to natural phenomena. However, the Intergovernmental Panel of Climate Change (IPCC) definition of climate change means any change in climate over time, whether due to natural variability or as a result of human activity – different to the UNFCCC.

There is an abundance of literature on the processes and controls on climatic conditions across northern Australia. The most common indices used in this area include sea surface temperature (SST) differences between certain regions, such as the Southern Oscillation Index (SOI) to predict El Nino (dry, leading to 'ENSO') or La Nina (wet) climatic periods, Indian Ocean Dipole (IOD) (Ashok et al. 2003; Chang et al 2006), Pacific Decadal Oscillation (PDO) (Mantua et al 1997; Zhang et al 1997; Mantua and Hare 2002; Verdon and Frank 2006a,b) and Interdecadal Pacific Oscillation (IPO) (Power et al 1999). In general, they describe whether climatic conditions are more likely to be warm/ cool, or wet/dry, based on differential SST's between particular regions. They are commonly correlated to major continental regions, such as eastern Australia or western Americas, occur on different cycles (e.g. annual to decadal or longer) and widely used to predict likely climatic conditions. Northern Australia is influenced by the variable combination of all of these indices (with PDO perhaps being the least important).

The models used by the IPCC to predict climate change are not consistent in tropical northern Australia (Alley et al 2007), meaning for the Ranger mine site there is uncertainty regarding the nature and magnitude of change. Less than 66% of models agree on the sign of the change (increase/decrease of precipitation in Dec-Jan-Feb), and is probably related to complex interaction of multiple factors.

There is an increasing recognition that rising temperature is exacerbating the impact of any rainfall reduction (Cai 2007). As a result of reduced precipitation and increased evaporation, dryer periods are projected to intensify in southern and eastern Australia (Hennessy and Fitzharris 2007; Hennessy et al. 2007). But there has been an increasing trend in rainfall over much of north and northwest Australia over recent decades, which has contrasted with decreases over the rest of the continent. Also, Smith and Suppiah (2007) argue that the trends in rainfall totals and average intensities in northern Australia are largely unrelated to trends in ENSO and most likely reflect the influence of other factors.

The degree to which climate change will impact on the frequency or magnitude of all of the above indices and processes remains uncertain and difficult to predict. For example, ENSO events will still occur without any climate change or they may alter due to climate change, with different climate models predicting variable changes such as intensity, duration, wet/dry, warm/cool and so on (see Knutson et al 1997; Timmermann et al 1999; Collins 2000a,b; among others).

Although periods of flood and drought risk in eastern Australia have been correlated to the PDO and IPO, they appear to have minimal influence in northern tropical Australia. However, due to their importance in overall climatic conditions across Australia, they are retained in algorithms to generate net flux data sets.

A number of fundamental issues need to be considered. The non-linearity in the strength of ENSO for Australia, the occurrence of IOD in relation to ENSO for Australia, the relationship between IOD and ENSO in Australia, the uncertainty of future influence of IOD on ENSO of Australia, and the interaction of ENSO events with local climate of the Kakadu region.

There exists non-linearity in the strength of ENSO events in Australia. The differences in the strength of relationship between El Nino (La Nina) with wet (dry) condition can be described as follows.

As a typical tropical phenomenon, the evolution of the IOD is strongly linked to the annual seasonal cycle – the phenomenon develops during May/June, peaks in September/October, and diminishes in December/January (Chang et al 2006). Therefore the IOD influences the Australian winter climate (Ashok et al. 2003). The El Nino events in Australia usually emerge in the March to June period and strongest influence occurs in the six months of June to November (BoM 2007a). The cooling of La Nina is relatively strongest during October to March period (BoM 2007a). Therefore the overlapping of IOD with ENSO is more prevalent with El Nino than La Nina. However, the link between IOD and ENSO has been reported to be have been broken or weakened by climate change (Kumar et al 1999), giving rise to further uncertainty in winter climate conditions in Australia.

The increased dry conditions caused by El Nino occur during the dry season, compared to the increased wet conditions caused by La Nina which occur during the wet season. Therefore if we do not consider the influence of IOD with ENSO, the impact will be greater for both El Nino and La Nina. If we do consider the IOD influence with ENSO, the rainfall in the site being summer rainfall, it is not counteracted by IOD, thus the wet season will still be unimpacted by IOD. Similar results have been recognised by others (Bayliss, pers. comm., 2007). A tabular representation of the links between IOD and ENSO is shown in Table 1.

The predictability of interdecadal climate events remains an area of uncertainty. By reviewing the existing understanding of the ENSO, IPO, PDO, and IOD events, some conditional aspects of these natural processes have been identified. We translate this understanding, observations and possibilities into our algorithm for generating the spells of ENSO events for the Ranger site and combine this with IPCC predicted climate data to generate net flux data sets for modelling.

Table 1. Annual links between ENSO and IOD events.

J	F	M	A	M	J	J	A	S	O	N	D	J	F	M	A	M
				IOD start				IOD peak			IOD end					
			El Nino months													
								La Nina months								
Wet season				Dry season						Wet season						Dry

Modelling methodology

A Monte Carlo-style approach is adopted to generate multiple replicates of input data for numerous model runs. A multi-step algorithm is developed to generate a series of net flux data, incorporating average climate data, predicted climate change trends from IPCC global climate models (GCMs), ENSO and IOD events.

Climate change models and predicted data

The IPCC make the output data from GCMs available, and in Australia this is from the CSIRO through the OzClim software (CSIRO 2006). The OzClim data used for this report is from the Third Assessment report series, as the 2007 reports and data were not yet available.

The GCMs hydro-climate data available from OzClim were rainfall and point potential evapotranspiration (PPET). For application in flow models, however, PPET needs to be converted to areal actual evapotranspiration (AAET). All PPET data was converted to AAET based on standard methods (e.g. Morton 1983).

In 2004, Hennesy et al (2004) undertook a detailed performance evaluation of 12 GCMs for the Northern Territory, Australia, in simulating the current regional climate. Based on this study, other IPCC reports and related literature, five GCMs were selected for extracting future climate change data for the Ranger mine site, namely the CSIRO: Mk2, HadCM2, HadCM3, ECHAM4/OPY and CSIRO: DARLAM 125km GCMs. Further to the physical models, IPCC use six future emission scenarios as inputs to the various GCMs, called A1B, A1FI, A1T, A2, B1 and B2, and they have remain unchanged from the Third to Fourth Assessment reports. An additional scenario, IS92cc, was also available from OzClim, giving a total of seven scenarios for each of the five GCMs. Further details regarding all GCMs and emissions scenarios is available in the varous IPCC literature. Annual net flux data for all 7 IPCC scenarios from the HadCM3 model is shown in Fig. 1.

Climate variability algorithm

We summarise the findings of the literature review and translate these into decision rules and address ambiguity in generating the conditional random process.

Decision for PDO: Random selection of PDO positive (El Nino enhanced), and

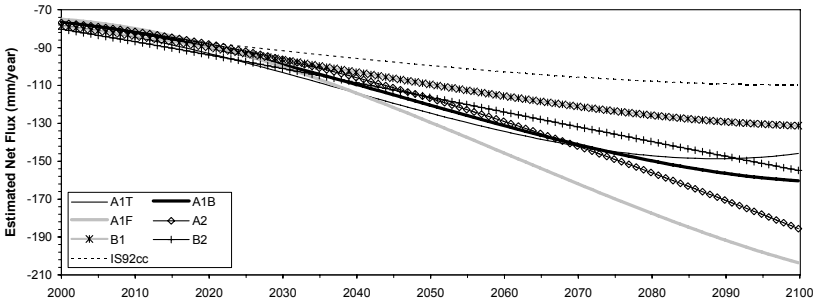

Fig.1. Estimated net flux for all scenarios (HadCM3 GCM)

PDO negative (La Nina enhanced) and PDO zero (both non enhanced)

Decision for IOD-ENSO relationship for Australia: La Nina is stronger than El Nino for Australia while IOD ENSO inverse relationship exists.

Decision for IOD-ENSO relationship for site:

- Irrespective of the existence of the link between IOD and ENSO, the site wet season is supposed to be consistently and strongly influenced by La Nina.
- With the dry season, if the link (inverse relation between ENSO and IOD) remains broken then the El Nino will be stronger for the site.
- And if the relationship is again established then the El Nino might become weakly related to dry condition for the site.

There could be concern for the IOD-El Nino relationship in future predictions but nothing for the IOD-La Nina relationship.

Ambiguity 1: PDO duration is to be randomly selected from 20 to 40 years. This broad guideline comes from the studies based on the IPO during past hundred years (e.g. Verdon and Wyatt 2004).

Ambiguity 2: The randomly selected PDO duration is covered by selecting random ENSO duration of 0 to 8 years. The guidelines for selection of frequency limit of ENSO events have been obtained by analysing the past 100 year's events in Australia (BoM 2005; BoM 2007a,b). For positive or negative PDO the cycle is selected to be 0 to 5 years and for transitional PDO the cycle is selected to be 6 to 8 years.

Ambiguity 3: The IOD-El Nino inverse relationship can exist or not.

The amplitude of ENSO events in the context of present research relate to the rainfall and AAET in ENSO months. We assume during El Nino years that when rainfall is less, AAET is also less. During La Nina years, when rainfall is more, then AAET is also more. But practically, however, this relationship is not linearly correlated, meaning rainfall is unbounded while AAET is bounded as suggested by Morton's equation (Morton 1983). We use the historical percentile records of AAET to cut off the point of wet conditions' AAET.

For the ENSO events, the ranking from ENSO1, ENSO2 … to ENSO5 goes with the 99.99, 90, 10, 5, 1 percentile values of rainfall and AAET. If PDO is for La Nina, it will be always enhanced (because it is independent of IOD), if PDO is for El Nino, it may be enhanced or not (because it depends on IOD). For enhanced La Nina we use the 99.99 percentile value, and for non-enhanced La Nina we use 90 percentile values. For El Nino we use 10, 5 and 1 percentile values. The ranges of percentile values are extracted from reviewing the indices of Expert Team on Climate Change Detection and Indices (ETCCDI) (Alexander et al. 2006, 2007).

Combining climate change and variability

We combine the net flux for ENSO and non-ENSO years and months to generate stochastically generated data. The combined data of the stochastically generated net flux is indicated by NFi,jSTO, meaning the net flux for ith month of jth year of any randomly generated century. We obtain 35 sets of net flux data from OzClim for 100 years from 2000 to 2100 and 35 sets of multiplying factors are computed as NFi,2000+jOZ(k) / NFi,2000OZ(k), where NFi,2000+jOZ(k) is used to indicate

the net flux for ith month (i = 1 to 12) of jth year (j = 0 to 100) predicted by Oz-Clim for the kth set (k = 1 to 35). Therefore, the predicted data NFi,jPRED(k) is as follows:

$$NF_{i,j}^{PRED(k)} = NF_{i,j}^{STO} \times NF_{i,2000+j}^{OZ(k)} / NF_{i,2000}^{OZ(k)} \quad \text{(Eq.1)}$$

The number of replicates is selected as 30, based on the guideline of Janssen et al (1993), where it is stated that for random sampling the number of samples to be taken should be larger than ten times the number of parameters included in the Monte Carlo analysis. We use three numbers of ambiguities, leading to 30 replicates. The overall algorithm for conditional random generation of ENSO events is shown in Fig. 2. The total number of sets of $NF_{i,j}^{PRED(k)}$ is therefore 1050 (35 GCM-scenario combinations and 30 replicates).

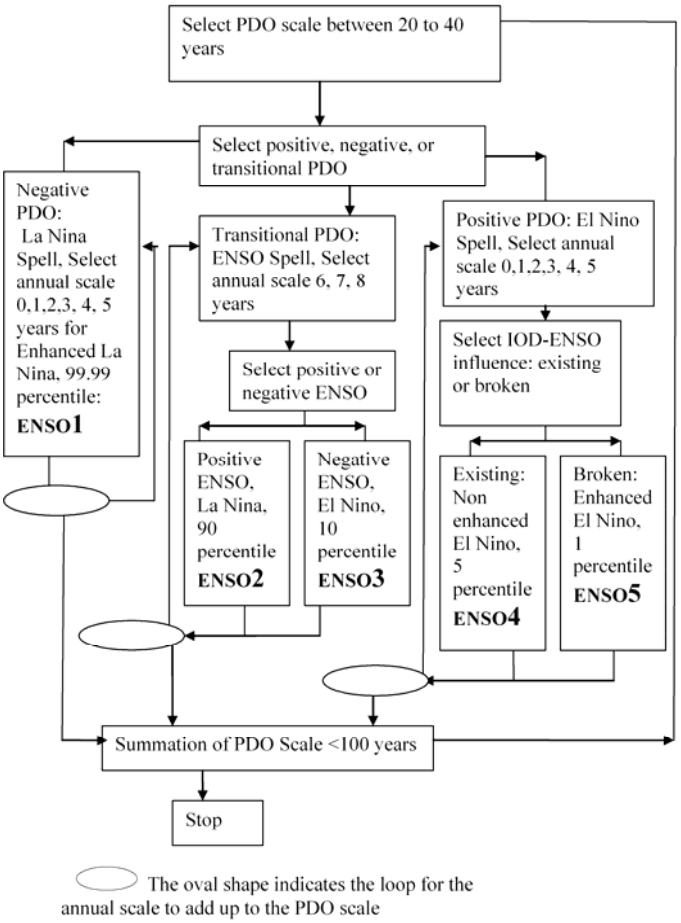

Fig.2. Algorithm flow chart for the generation of ENSO rain and AAET data (climate change and natural climatic variability) for the Ranger site

A major issue not addressed by the above approach and algorithm is extreme events such as tropical cyclones. In reality, such severe events would cause intense flooding rather than an extreme rise of the groundwater level (Kabir 2008). Therefore, in the monthly-based time series data, we neglect tropical cyclone events whose duration is normally 3 to 5 days only.

Results

One sample set of net flux data is shown in Fig. 3. The cumulative net flux was also computed to assess the influence of wet and dry periods on net flux, which can not be seen from the monthly net flux data. The SeepW model result of the computed groundwater level for that net flux is also shown in Fig. 3.

The aggregrate results from all 30 replicates and 7 scenarios of the HadCM3 GCM are shown in Fig. 4, giving mean (μ) groundwater level for each scenario and the maximum/minimum mean plus/minus standard deviation (±σ). Yohe et al (2007) used HadCM3 in IPCC's Fourth Assessment report in the assessment of global water resource availability. Complete results are given in Kabir (2008).

The results of groundwater levels in Fig's 3 and 4 establishes two key findings. Firstly, that longer term trends in climatic conditions are indeed critical in shaping overall groundwater levels (e.g. Fig. 3). Secondly, despite all 7 IPCC scenarios predicting a long-term decline in net flux and dryer overall hydrologic conditions, climate variability, giving rise to extended wetter or dryer periods, can achieve major rises or declines in groundwater levels which appear to outweigh the trends predicted under climate change scenarios.

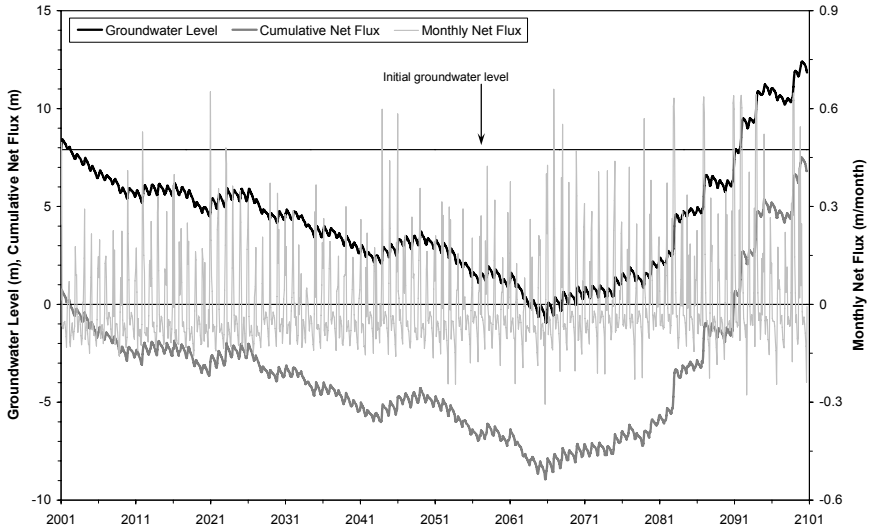

Fig.3. Generated monthly net flux, cumulative net flux and modelled level response (bore OB27, CSIRO MK2, Scenario A2).

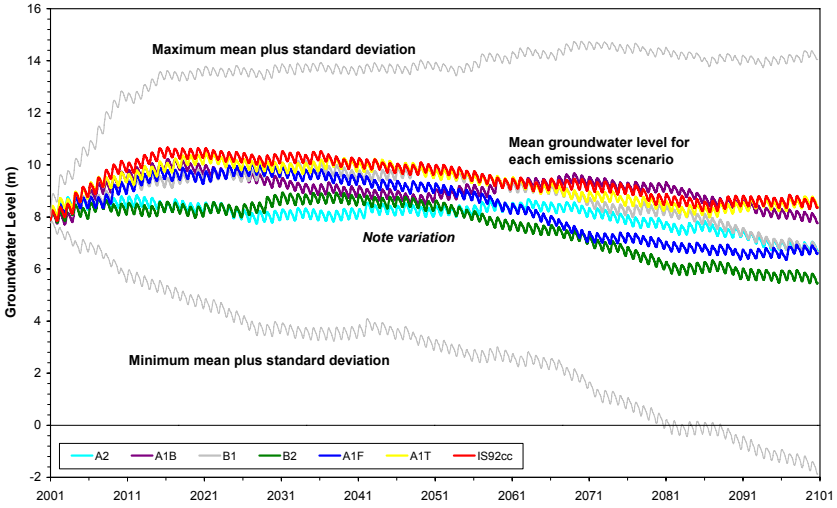

Fig.4. Modelled mean groundwater levels (bore OB27), HadCM3 GCM and A2, A1B, B1, B2, A1F, A1T and IS92cc emission scenarios; max/min mean ± standard deviation

Conclusions

This paper sought to build on previous modelling work by developing a methodology to assess the impacts on groundwater levels from potential climate change scenarios and climate variability.

Climate variability was predicted by combining the current understanding of important climate indices such as El Nino/La Nina, IPO, PDO and IOD into a stochastic algorithm for generating climate data. Data for climate change predictions were obtained from IPCC global climate models and future emissions scenarios. These two components were then combined to produce an input data set of net flux for use in the previously validated unsaturated flow model for the Ranger site. Summary results were then presented in terms of mean groundwater level over time under each scenario for the HadCM3 GCM, including maximum/minimum ± standard deviation groundwater level at each time step from all model runs. The algorithms incorporate current climate knowledge, and can be updated as new knowledge or udnerstanding comes to light.

Overall, the results show the critical importance of climate variability as well as climate change. Under extended wet periods, groundwater levels are predicted to rise significantly, while the major declines are expected under lengthy dry climatic periods. The modelling shows that although the impact of climate change could be significant, it must also be considered in the face of climate variability. The paper, combined with the two concurrent papers, therefore provides a sound basis and methodology upon which to understand the potential impacts of climate change and climate variability on groundwater levels. This, in turn, is critical with respect

to different uranium mine rehabilitation approaches in a wet-dry tropical climate surrounded by a region of very high conservation and cultural values.

References

Alexander LV, Hope P et al (2007) Trends in Australia's climate means and extremes: a global context. Australian Meteorological Magazine, 56, pp 1-18

Alexander LV, Zhang X et al (2006) Global observed changes in daily climate extremes of temperature and precipitation. Journal of Geophysical Research, 111(D05109), pp 1-22

Alley R, Berntsen T et al. (2007) Climate change 2007: The physical science basis. Intergovernmental Panel of Climate Change, Cambridge University Press, UK

Ashok K, Guan Z et al (2003) Influence of the Indian Ocean Dipole on the Australian winter rainfall. Geophysical Research Letters, 30(15), doi:10.1029/2003GL017926

Bayliss P (2007) Personal communication. Office of the Supervising Scientist, May 2007

BoM (2005) El Nino, La Nina and Australia's climate. Bureau of Meteorology, Commonwealth of Australia, Accessed 31 July 2007, http://www.bom.gov.au/lam/epage.shtml

BoM (2007a) ENSO wrap-up. Bureau of Meteorology, Commonwealth of Australia, Accessed 31 July 2007, http://www.bom.gov.au/climate/enso/index.shtml#impacts

BoM (2007b) El Nino – Detailed Australian analysis. Bureau of Meteorology, Commonwealth of Australia, Accessed 31 July 2007, http://www.bom.gov.au/climate/enso/australia_detail.shtml

Cai W (2007) What will happen to future Australian rainfall? Proc. "Greenhouse 2007: The latest science and technology", Sydney, Australia, October 2007

Chang P, Yamagata T et al (2006) Climate fluctuations of tropical coupled systems - the role of ocean dynamics. Journal of Climate – Special Section, 19, pp 5122-5174

Collins M (2000a) The El-Nino Southern Oscillation in the second Hadley Centre coupled model and its response to greenhouse warming. Journal of Climate, 13, pp 1299-1312

Collins M (2000b) Understanding uncertainities in the response of ENSO to greenhouse warming. Geophysical Research Letters, 27, pp 3509-3512

CSIRO (2006) Ozclim – Climate change data (Version 2.0.1), CSIRO Australia (website: http://www.csiro.au/ozclim/home.do)

Hennessy K and Fitzharris B (2007) Australian climate change impacts, adaptation and vulnerability. Proc. "Greenhouse 2007: The latest science and technology", Sydney, Australia, October 2007

Hennesy K, Page C et al (2004) Climate change in the Northern Territory. CSIRO Consultancy report for the NT Department of Infrastructure, Planning and Environment.

Hennessy K, Fitzharris B et al (2007) Australia and New Zealand. In "Climate change 2007: Impacts, adaptation and vulnerability", Working Group II, Intergovernmental Panel on Climate Change, Cambridge University Press, UK, pp 507-540

Houghton JT, Ding Y et al (Eds.) (2001) Climate change 2001: The scientific basis. Working group I, Intergovernmental Panel on Climate Change, Cambridge University Press, UK

Janssen PHM, Heuberger PSC et al (1993) UNSCAM 1.1: A software package for sensitivity and uncertainty analysis. RIVM Report 959101004, Bilthoven, The Netherlands

Kabir M (2008) Modelling groundwater-climate relationships at the Ranger uranium mine, Australia. PhD Thesis (In Preparation), Dept. of Civil Eng., Monash University

Kabir M, Mudd GM and Ladson AR (2008) Groundwater-climate relationships, Ranger uranium mine, Australia : 2. Validation of unsaturated flow modelling. Proc. "Uranium mining and hydrogeology V", Freiberg, Germany, September 2008

Knutson TR, Manabe S et al (1997) Simulated ENSO in a global coupled ocean-atmosphere model: multidecadal amplitude modulation and CO2-sensitivity. Journal of Climate, 10, pp 138-161

Kumar KK, Rajagopalan B et al (1999) On the weakening relationship between the Indian monsoon and ENSO. Science, 284, pp 2156-2159

Mantua NJ and Hare SR (2002) The Pacific Decadal Oscillation. Journal of Oceanography, 58, pp 35-44

Mantua NJ, Hare SR et al (1997) A Pacific interdecadal climate oscillation with impacts on salmon production. Bulletin of the American Meteorological Society, 78(6), pp 1069-1079

Morton FI (1983) Operational estimates of areal evapotranspiration and their significance to the science and practice of hydrology. Journal of Hydrology, 66, pp 1-76

Power S, Casey T et al (1999) Interdecadal modulation of the impact of ENSO on Australia. Climate Dynamics, 15, pp 319-324

Smith I and Suppiah R (2007) Characteristics of the northern Australian rainy season. Proc. "Greenhouse 2007: The latest science and technology", Sydney, Australia, October 2007

Timmermann AJ, Oberhuber J et al (1999) Increased El Nino frequency in a climate model forced by future greenhouse warming. Nature, 398, pp 694-696

Verdon DC and Frank SW (2006a) Long-term behaviour of ENSO: Interactions with the PDO over the past 400 years inferred from paleoclimate records. Geophysical Research Letters, 33(L06712), pp 1-5

Verdon DC and Frank SW (2006b) Long term drought risk assessment in the Lachlan catchment – A paleoclimate perspective. Proc. "30th Hydrology and Water Resources Symposium", Engineers Australia, Launceston, Australia, December 2006

Verdon DC and Wyatt AM (2004) Multidecadal variability of rainfall and streamflow: eastern Australia. Water Resources Research 40(W10201), pp 1-8

Yohe GW, Lasco RD et al (2007). Perspectives on climate change and sustainability. In "Climate change 2007: Impacts, adaptation and vulnerability", Working Group II, Intergovernmental Panel on Climate Change, Cambridge University Press, UK, pp 811-841

Zhang Y, Wallace JM et al (1997) ENSO-like interdecadal variability. Journal of Climate, 10, pp 1004-1020

Under the Auspices of

Saxon State Ministry of Environment and Agriculture

Uranium Mining and Hydrogeology V

14.9.-18.9.2008 Freiberg / Germany

Broder J. Merkel, Andrea Hasche-Berger
(Editors)

in cooperation with

supported by

Forschungszentrum Dresden Rossendorf

Deutsche Forschungsgemeinschaft DFG

This page has been added to the PDF for completeness only.

Publishing details for UMH-V are:

Editors: Prof. Broder J Merkel, Andrea Hasche-Berger

Title: Uranium, Mining & Hydrogeology – 5th International Conference
Freiberg, Germany
14-18 September 2008

Publisher: Springer-Verlag, Heidelberg, Germany © 2008

ISBN: 978-3-540-87745-5

e-ISBN: 978-3-540-87746-2